60th HIGHWAY GEOLOGY SYMPOSIUM

www.HighwayGeologySymposium.org

BUFFALO, NEW YORK
September 29 - October 1, 2009

PROCEEDINGS

HOSTED BY:
NEW YORK STATE THRUWAY AUTHORITY
NEW YORK STATE DEPARTMENT OF TRANSPORTATION
NEW YORK STATE MUSEUM

TABLE OF CONTENTS

PROCEEDINGS PAPERS

60th ANNUAL HIGHWAY GEOLOGY SYMPOSIUM

BUFFALO, NEW YORK

September 29 – October 1, 2009

Local Organizing Committee

Mike Vierling	New York State Thruway Authority
Steve Sweeney	New York State Canal Corporation
Matt Podniesinski	New York State Dept. of Environmental Conservation
Douglas Hadjin	New York State Department of Transportation
Verne McGuffy	Consultant (Retired NYSDOT)
Tom Eliassen	Vermont Agency of Transportation
Steve Senior	Ministry of Transportation
Eileen Litts	Writing Resources
Peter Ingraham	Golder Associates
Mark Telesnicki	Golder Associates
Jay Smerekanicz	Golder Associates

Special Thanks To

Tom Van Splunder	New York State Department of Transportation
Barry Virgillo	State Park Program Staff
David Giambra	State Park Program Staff

Field Trip Speakers

Brent Black	Scoby Hill Landslide
Tom Van Splunder	Rte. 219 over Cattaraugus Creek
Park Guides	Devil's Hole and Whirlpool Gorge

Hosted by

New York State Thruway Authority
New York State Department of Transportation
New York State Museum

HIGHWAY GEOLOGY SYMPOSIUM
NATIONAL STEERING COMMITTEE OFFICERS   2009

Michael Vierling - **(CHAIRMAN)**
Term: 9/2006 until 2009
(YAA) Engineering Geologist
Canal Design Bureau
New York State Thruway Authority
200 Southern Blvd
Albany, NY 12209
E-Mail: michael_vierling@thruway.state.ny.us
Phone: 518-471-4378
Fax: 518-436-3060

Jeff Dean - **(VICE-CHAIRMAN)**
Term: 9/2006 until 2009
Oklahoma DOT
200 NE 21st St.
Oklahoma City, OK 73105
Ph: (405)522-0988
Fax: (405)522-4519
Email: jdean@odot.org

Vanessa Bateman - **(SECRETARY)**
Term: 9/2006 until 2009
Tennessee Department of Transportation
Geotechnical Engineering Section
Address: 6601 Centennial Blvd.
Nashville, TN 37243-0360
Phone: (615) 350-4133
Fax: (615) 350-4128
Email: vanessa.bateman@state.tn.us

Russell Glass - **(TREASURER)**
(Publications & Proceedings)
Retired NCDOT 100 Wolf Cove
Asheville, NC 28804
Ph: (828) 252-2260
Email: frgeol@aol.com

HIGHWAY GEOLOGY SYMPOSIUM 2009
NATIONAL STEERING COMMITTEE MEMBERS

Ken Ashton (Membership)
West VA Geological Survey
P.O. Box 879
Morgantown, WV 26507-0879
Ph: (304)594-2331
Fax: (304)594-2575
ashton@geosrv.wvnet.edu

Vanessa Bateman (Secretary)
Tennessee Department of Geotechnical
Engineering Section
Address: 6601 Centennial Blvd.
Nashville, TN 37243-0360
Phone: (615) 350-4133
Fax: (615) 350-4128
vanessa.bateman@state.tn.usTransportation

Richard Cross
Golder Associates
RD 1 Box 183A
Solansville, NY 12160
Ph: (518)868-4820
Cell: (603)867-4191
dick_Cross@juno.com

John D. Duffy
50 Higuera St.
San Luis Obispo, CA 93401
Ph: (805)527-2275
Fax: (805)549-3297
John_D_Duffy@dot.ca.gov

Jeff Dean(Vice-Chairman)
Oklahoma DOT
200 NE 21st St.
Oklahoma City, OK 73105
Ph: (405)521-2677 or (405)522-0988
Fax: (405)522-4519
jdean@odot.org

Tom Eliassen - Transportation Geologist
State of Vermont, Agency of Transportation
Materials & Research Section
National Life Building, Drawer 33
Montpelier, VT 05633 Ph: 802-828-2516
fax: 802-828-2792
tom.eliassen@state.vt.us

Marc Fish
Engineering Geologist
WSDOT Geotechnical Division
Environmental & Engineering Programs
Materials Laboratory
PO Box 47365

Olympia, WA 98504-7365
360-709-5498 (office)
360-485-5825 (cell)
fishm@wsdot.wa.gov

Russell Glass (Treasurer)
(Publications & Proceedings)
NCDOT (Retired)
100 Wolf Cove
Asheville, NC 28804
Ph: (828) 252-2260
frgeol@aol.com

Bob Henthorne - Chief Geologist
Materials and Research Center
2300 Van Buren
Topeka, KS 66611-1195
Phone 785-291-3860
Fax 785-296-2526
roberth@ksdot.org

Peter Ingraham
Golder Associates
540 North Commercial Street, Suite 250
Manchester, New Hampshire 03101-1146
Ph: (603)668-0880
Fax: (603)668-1199
pingraham@golder.com

Daniel Journeaux
Janod Inc.
34 Beeman Way
P.O. Box 2487
Champlain, NY 12919
Phone: (518) 298-5226
Fax: (450) 424-2614
info@janod.biz

Richard Lane
NHDOT, Bureau of Materials & Research
5 Hazen Drive, Concord
New Hampshire 03301
Phone: (603) 271-3151
Fax: (603) 271-8700
dlane@dot.state.nh.us

Henry Mathis - (By-Laws)
H.C. Nutting A/ Terracon Co.
561 Marblerock Way
Lexington, KY 40503 Office: (859)296-5664
Cell: 859-361-8362
Office: 859-455-8530
Fax: 859-455-8630
hmathis@iglou.com

Harry Moore - (Historian, Appt.)
Tenn. DOT (retired)
Golder Associates
Senior Consultant
3730 Chamblee Tucker Rd.,
Atlanta, GA 30341
Atlanta Office phone: 770-496-1893
HLMoore@golder.com

John Pilipchuk
NCDOT Geotechnical Engineering Unit
5253 Z-Max Blvd
Harrisburg, NC 28075
Ph: 704-455-8902
Fax: 704-455-8912
jpilipchuk@dot.state.nc.us

Nick Priznar - Sr. Eng. Geologist
Arizona D.O.T.
121 N. 21st Ave. 068R
Phoenix AZ, 85009 Ph: (602)712-8089
Fax: (602)712-8138
npriznar@azdot.gov

Erik Rorem
Geobrugg North America, LLC
551 W. Cordova Road, PMB 730
Santa Fe, NM 87505 Phone: 505-438-6161
Fax: 505-438-6166
erik.rorem@geobrugg.com

Christopher A. Ruppen (YAA)
Michael Baker Jr., Inc.
4301 Dutch Ridge Rd.
Beaver, PA 15009-9600
Ph: (724)495-4079
Fax: (724)495-4017
Cell: (412)848-2305
cruppen@mbakercorp.com

Stephen Senior
Ministry of Transportation, Ontario
Soils and Aggregates Section
1201 Wilson Ave.
Rm 220, Building C
Downsview, ON M3M IJ6
Canada Ph: (416)235-3743
Fax: (416)235-4101
stephen.senior@mto.gov.on.ca

Michael P. Schulte, P.G.
Terry West (Medallion, Emetrius)
Earth and Atmospheric Science Dept.
Purdue University West Lafayette, IN
47907-1297 Ph: (765)494-3296
Fax: (765)496-1210
trwest@cas.purdue.edu

WYDOT Geology Program
5300 Bishop Blvd.
Cheyenne, WY 82009-3340
Office: (307) 777-4222
Cell: (307) 287-2979
Fax: (307) 777-3994
Mike.Schulte@dot.state.wy.us

Jim Stroud (Appt)
Vulcan Materials Company
Manager of Geological Services
4401 Patterson Ave.
PO Box 4239 Winston-Salem, NC 27105
Office 336-744-2940
Fax 336-744-2018
336-416-3656 (M)
stroudj@vmcmail.com

Steven Sweeney
NYS Canal Corporation
Phone: (518) 334-2511
Email: ssweeney2@nycap.rr.com

John F. Szturo R.G.
HNTB Corporation
KC Office
715 Kirk Drive
Kansas City, MO 64105
Direct Line 816 527-2275
Fax 816 472-5013
Cell 913 530-2579
jszturo@hntb.co

Robert Thommen
Rotec International, LLC
P.O.Box 31536
Sante Fe, NM 87594-1536
Ph: 505-989-3353
Fax: 505-984-8868
thommen@www.rotecinternational-usa.com

Michael P. Vierling (Chairman)
(YAA) Engineering Geologist
Canal Design Bureau
New York State Thruway Authority
200 Southern Blvd
Albany, NY 12209
michael_vierling@thruway.state.ny.us
Phone: 518-471-4378
Fax: 518-436-3060

9

HIGHWAY GEOLOGY SYMPOSIUM

HISTORY, ORGANIZATION AND FUNCTION

Established to foster a better understanding and closer cooperation between geologists and civil engineers in the highway industry, the Highway Geology Symposium (HGS) was organized and held its first meeting on March 14, 1950, in Richmond, Virginia. Attending the inaugural meeting were representatives from state highway departments (as referred to at the time) from Georgia, South Carolina, North Carolina, Virginia, Kentucky, West Virginia, Maryland and Pennsylvania. In addition, a number of federal agencies and universities were represented. A total of nine technical papers were presented.

W.T. Parrott, an engineering geologist with the Virginia Department of Highways, chaired the first meeting. It was Mr. Parrott who originated the Highway Geology Symposium.

It was at the 1956 meeting that future HGS leader, A.C. Dodson, began his active role in participating in the Symposium. Mr. Dodson was the Chief Geologist for the North Carolina State Highway and Public Works Commission, which sponsored the 7th HGS meeting.

Since the initial meeting, 60 consecutive annual meetings have been held in 32 different states. Between 1950 and 1962, the meetings were held east of the Mississippi River, with Virginia, West Virginia, Ohio, Maryland, North Carolina, Pennsylvania, Georgia, Florida and Tennessee serving as host state.

In 1962, the Symposium moved west for the first time to Phoenix, Arizona where the 13th annual HGS meeting was held. Since then it has alternated, for the most part, back and forth from the east to the west. The Annual Symposium has moved to different locations as follows:

List of Highway Geology Symposium Meetings

No.	Year	HGS Location	No.	Year	HGS Location
1st	1950	Richmond, VA	2nd	1951	Richmond, VA
3rd	1952	Lexington, VA	4th	1953	Charleston, W VA
5th	1954	Columbus, OH	6th	1955	Baltimore, MD
7th	1956	Raleigh, NC	8th	1957	State College, PA
9th	1958	Charlottesville, VA	10th	1959	Atlanta, GA
11th	1960	Tallahassee, FL	12th	1961	Knoxville, TN
13th	1962	Phoenix, AZ	14th	1963	College Station, TX
15th	1964	Rolla, MO	16th	1965	Lexington, KY
17th	1966	Ames, IA	18th	1967	Lafayette, IN
19th	1968	Morgantown, WV	20th	1969	Urbana, IL
21st	1970	Lawrence, KS	22nd	1971	Norman, OK
23rd	1972	Old Point Comfort, VA	24th	1973	Sheridan, WY
25th	1974	Raleigh, NC	26th	1975	Coeur d'Alene, ID
27th	1976	Orlando, FL	28th	1977	Rapid City, SD
29th	1978	Annapolis, MD	30th	1979	Portland, OR
31st	1980	Austin, TX	32nd	1981	Gatlinburg, TN
33rd	1982	Vail, CO	34th	1983	Stone Mountain, GA
35th	1984	San Jose, CA	36th	1985	Clarksville, IN

37th	1986	Helena, MT	38th	1987	Pittsburgh, PA
39th	1988	Park City, UT	40th	1989	Birmingham, AL
41st	1990	Albuquerque, NM	42nd	1991	Albany, NY
43rd	1992	Fayetteville, AR	44th	1993	Tampa, FL
45th	1994	Portland, OR	46th	1995	Charleston, WV
47th	1996	Cody, WY	48th	1997	Knoxville, TN
49th	1998	Prescott, AZ	50th	1999	Roanoke, VA
51st	2000	Seattle, WA	52nd	2001	Cumberland, MD
53rd	2002	San Luis Obispo, CA	54th	2003	Burlington, VT
55th	2004	Kansas City, MO	56th	2005	Wilmington, NC
57th	2006	Breckenridge, CO	58th	2007	Pocono Manor, PA
59th	2008	Santa Fe, NM	60th	2009	Buffalo, NY

Unlike most groups and organizations that meet on a regular basis, the Highway Geology Symposium has no central headquarters, no annual dues, and no formal membership requirements. The governing body of the Symposium is a steering committee composed of approximately 20-25 engineering geologists and geotechnical engineers from state and federal agencies, colleges and universities, as well as private service companies and consulting firms throughout the country. Steering committee members are elected for three-year terms, with their elections and re-elections being determined principally by their interests and participation in and contribution to the Symposium. The officers include a chairman, vice chairman, secretary, and treasurer, all of whom are elected for a two-year term. Officers, except for the treasurer, may only succeed themselves for one additional term.

A number of three-member standing committees conduct the affairs of the organization. The lack of rigid requirements, routing, and relatively relaxed overall functioning of the organization is what attracts many of the participants.

Meeting sites are chosen two or four years in advance and are selected by the Steering Committee following presentations made by representatives of potential host states. These presentations are usually made at the steering committee meeting, which is held during the Annual Symposium. Upon selection, the state representative becomes the state chairman and a member protem of the Steering Committee.

The symposia are generally for two and one-half days, with a day-and-a-half for technical papers and a full day field trip. The Symposium usually begins on Wednesday morning. The field trip is usually Thursday, followed by the annual banquet that evening. The final technical session generally ends by noon on Friday. In recent years this schedule has been modified to better accommodate climate conditions and tourism benefits.

The field trip is the focus of the meeting. In most cases, the trips cover approximately from 150 to 200 miles, provide for six to eight scheduled stops, and require about eight hours. Occasionally, cultural stops are scheduled around geological and geotechnical points of interest. To cite a few examples: in Wyoming (1973), the group viewed landslides in the Big Horn Mountains; Florida's trip (1976) included a tour of Cape Canaveral and the NASA space installation; the Idaho and South Dakota trips dealt principally with mining activities; North Carolina provided stops at a quarry site, a dam construction site, and a nuclear generation site; in Maryland, the group visited the Chesapeake Bay hydraulic model and the Goddard Space Center; The Oregon trip included visits to the Columbia River Gorge and Mount Hood; the Central Mineral Region was visited in Texas; and the Tennessee meeting in 1981 provided stops at several repaired landslides in Appalachia regions of East Tennessee.

In Utah (1988) the field trip visited sites in Provo Canyon and stopped at the famous Thistle Landslide, while in New Mexico in 1990 the emphasis was on rockfall treatment in the Rio Grande River canyon and included a stop at the Brugg Wire Rope headquarters in Santa Fe.

Mount St. Helens was visited by the field trip in 1994 when the meeting was in Portland, Oregon, while in 1995 the West Virginia meeting took us to the New River Gorge bridge that has a deck elevation 876 feet above the water.

In Cody, Wyoming the 1996 field trip visited the Chief Joseph Scenic Highway and the Beartooth uplift in northwestern Wyoming. In 1997 the meeting in Tennessee visited the newly constructed future I-26 highway in the Blue Ridge of East Tennessee. The Arizona meeting in 1998 visited Oak Creek Canyon near Sedona and a mining ghost town at Jerrome, Arizona.

At the technical sessions, case histories and state-of-the-art papers are most common; with highly theoretical papers the exception. The papers presented at the technical sessions are published in the annual proceedings. Some of the more recent proceedings may be obtained from the Treasurer of the Symposium.

Banquet speakers are also a highlight and have been varied through the years.

A Medallion Award was initiated in 1970 to honor those persons who have made significant contributions to the Highway Geology Symposium. The selection was and is currently made from the members of the national steering committee of the HGS.

A number of past members of the national steering committee have been granted Emeritus status. These individuals, usually retired, resigned from the HGS Steering Committee, or are deceased, have made significant contributions to the Highway Geology Symposium. A total of 30 persons have been granted the Emeritus status. Ten are now deceased.

Several Proceedings volumes have been dedicated to past HGS Steering Committee members who have passed away. The 36th HGS Proceedings were dedicated to David L. Royster (1931-1985, Tennessee) at the Clarksville, Indiana Meeting in 1985. In 1991 the Proceedings of the 42nd HGS meeting held in Albany, New York was dedicated to Burrell S. Whitlow (1929-1990, Virginia).

HIGHWAY GEOLOGY SYMPOSIUM

EMERITUS MEMBERS OF THE STEERING COMMITTEE

Emeritus Status is granted by the Steering Committee

R.F. Baker*

John Baldwin

David Bingham

Virgil E. Burgat*

Robert G. Charboneau*

Hugh Chase*

A.C. Dodson*

Walter F. Fredericksen

Brandy Gilmore

Robert Goddard

Joseph Gutierrez

Charles T. Janik

John Lemish

Bill Lovell

George S. Meadors, Jr.*

Willard McCasland

David Mitchell

W.T. Parrot*

Paul Price*

David L. Royster*

Bill Sherman

Willard L. Sitz

Mitchell Smith

Steve Sweeney

Sam Thornton

Berke Thompson*

Burrell Whitlow*

W. A. "Bill" Wisner

Earl Wright

Ed J. Zeigler

John Baldwin

Robert Goddard

Richard Humphries

*(*Deceased)*

HIGHWAY GEOLOGY SYMPOSIUM
MEDALLION AWARD WINNERS

The Medallion Award is presented to individuals who have made significant contributions to the Highway Geology Symposium over many years. The award, instituted in 1969, is a 3.5-inch medallion mounted on a walnut shield and appropriately inscribed. The award is presented during the banquet at the annual Symposium.

Hugh Chase*	**1970**
Tom Parrott*	**1970**
Paul Price*	**1970**
K.B. Woods*	**1971**
R.J. Edmonson*	**1972**
C.S. Mullin*	**1974**
A.C. Dodson*	**1975**
Burrell Whitlow*	**1978**
Bill Sherman	**1980**
Virgil Burgat*	**1981**
Henry Mathis	**1982**
David Royster*	**1982**
Terry West	**1983**
Dave Bingham	**1984**
Vernon Bump	**1986**
C.W. "Bill" Lovell	**1989**
Joseph A. Gutierrez	**1990**
Willard McCasland	**1990**
W.A. "Bill" Wisner	**1991**
David Mitchell	**1993**
Harry Moore	**1996**
Earl Wright	**1997**
Russell Glass	**1998**
Harry Ludowise*	**2000**
Sam Thornton	**2000**
Bob Henthorne	**2004**
Mike Hager	**2005**
Joseph A. Fischer	**2007**
Ken Ashton	**2008**
A. David Martin	**2008**

*(*Deceased)*

HIGHWAY GEOLOGY SYMPOSIUM

Future Symposia Schedule and Contact List

YEAR	STATE	HOST COORDINATOR	TELEPHONE	EMAIL
2010	Oklahoma	Jeff Dean	405-522-0988	jdean@odot.org
2011	Kentucky	Henry Mathis	859-455-8530	hmathis@iglou.com
2012	California	Bill Webster	916-227-1041	Bill_Webster@dot.ca.gov
2013	OPEN	Mike Vierling Chairman HGS	518-436-3197	Michael_vierling@thruway.state.ny.us

60th HIGHWAY GEOLOGY SYMPOSIUM

SPONSORS

The following companies have graciously contributed toward sponsorship of the Symposium. The HGS relies on sponsor contributions for refreshment breaks, field trip lunches and other activities. We want these sponsors to know that their contributions are very much appreciated.

Janod Inc.

Gebrugg

American Mountain Management

HITECH Rockfall Construction

Maccaferri

Golder

Michael Baker

60th HIGHWAY GEOLOGY SYMPOSIUM

EXHIBITORS

Thanks to all participating exhibitors.
Booths are in the Pavilion Exhibit Hall

TABLE	COMPANY
1	Michael Baker
2	Dataforensics
3	Golder Associates
4	Fisher & Strickler Rock Engineering
5	Maccaferri
6	Geo-Instruments
7	Monotube Pile Corporation
8	Hayward Baker, Inc
9	Hager-Richter Geoscience, Inc.
10	AIS Construction Co.
11	L.G. Hetager Drilling, Inc
12	HITECH Rockfall Construction
13	Layne GeoConstruction
14	McMahon & Mann Consulting Engineers
15	Geobrugg North America
16	American Mountain Management
17	Janod Inc.
18	Central Mine Equipment Company
19	open
20	Pacific Blasting & Demolition LTD
21	Acker Drill Company, Inc.
22	Geokon
23	61th HGS Host
24	SIMCO Drilling Equipment
25	Expanded Shale Clay and Slate Institute
26	Tencate Geosynthetics N. A.

60ᵗʰ HIGHWAY GEOLOGY SYMPOSIUM
AGENDA

60ᵗʰ ANNUAL HGS Buffalo, NY 2009 – AGENDA	
Monday, September 28ᵗʰ, PM	**11:00 AM – Registration Open - Grand Ballroom Foyer**
	8:00 AM to 5:00 PM Exhibitor Setup Time- **Regency Ballroom**
	1:00 PM to 3:10 PM – Transportation Research Board Session *Long-Term Performance of Geotechnical Infrastructure* Grand Ballroom E
	3:10 PM to 3:30 PM – BREAK
	3:30 PM to 5:05 PM – TRB Session Continues
	6:30 PM to 8:30 PM – Welcome Reception **Ice Breaker in the Grand Ballroom Foyer** **Bar Sponsored by JANOD** **Food Sponsored by AMERICAN MOUNTAIN MANAGEMENT**
Tuesday, September 29ᵗʰ	**6:30 AM to 8:00 AM – BREAKFAST on Own**
	7:00 AM – Registration is Open - Grand Ballroom Foyer

	9:30 AM to 4:00 PM – Guest Tour of Art Gallery and Erie Canal Cruise	
Session	**8:00 AM to 8:20 AM – Welcome- Grand Ballroom B - C**	
1 **NY Geology,** **Landslides** *Moderator:* **Nick Priznak**	*Title* – Author	
	8:20 – 8:40 *Overview of NY Geology* – Dr. Andy Kozlowski, NY State Geological Survey	
	8:40 – 9:00 *High Bridge Area Roadway Slide, Letchworth State Park, Portageville, New York* - Nichols	
	9:00 – 9:20 *Remediation Of The SR 15 Welcome Center Landslide* - Scherer	
	9:20 – 9:40 *Rio Blanco Landslide Failure between Rifle and Meeker Colorado - Investigation, Design and Emergency Mitigation using Lightweight Expanded Polystyrene Fill* - Arndt	
	9:40 AM to 10:15 AM – BREAK Regency Room Sponsored by HITECH	
2 **Rock Slope Stabilization and Mitigation** *Moderator:* **Bob Henthorne**	10:15 – 10:35 *Innovations in Rockfall Barriers and the New European Standard ETAG 027* – Amend	
	10:35 – 10:55 *Controlling Large Rockfalls on Steep Slopes, the Kama Bluffs Experience* – Wood	
	10:55 – 11:15 *Ring Net Drapery for Rockfall Protection: Installation Observations* – Fish	
	11:15 – 11:35 *Protection from High Energy Rockfall Impacts using Terramesh Embankments: Design and Experiences* - Brunet	
	11:35 – 11:55 *Post Foundations for Flexible Rockfall Fences* - Turner	
	11:55 AM to 1:15 PM – LUNCH Grand Ballroom A Sponsored by JANOD	
3 **Rock Slope Stabilization and**	1:15 – 1:35 *Role of Stratigraphy in Cut Slope Design for Horizontally-Bedded Sequences of Competent and Incompetent Rocks of Eastern Ohio* - Admassu	
	1:35 – 1:55 **Green River Bridge Pier 1 Landslide, KingCounty, Washington** – Badger	

	Mitigation **Slope Designs** *Moderator:* *John Szturo*	1:55 – 2:15 *Getting it Right the Third Time - Reconstruction of Interstate 476 over Unstable Karst in Plymouth Meeting, PA* – Shelly
		2:15 – 2:35 *US-50 Big Horn Sheep Canyon, Fremont County, Colorado - A Rockfall Mitigation Case Study* - Lukkarila
		2:35 – 2:55 *Colorado Rockfall Simulation Program Version 5.0* - Bartingale
Tuesday, September 29th	**2:55 PM to 3:15 PM – BREAK Regency Room Sponsored by Maccaferri**	
	4 **Karst,** **Field Trip Overview** *Moderator:* *Pete Ingraham*	3:15 – 3:35 *A Proactive Approach To Limit Potential Impacts from Blasting to Drinking Water Supply Wells, Windham, New Hampshire* – Pelham
		3:35 – 3:55 *Remediation of Soft Clay Utilizing the "Dry Mix Method"* Logan
		3:55 – 4:15 *Load-Settlement Model of Rock Sockets from O-Cell Testing* Turner
		4:15 – 5:00 *Field Trip Overview – Scoby Hill Landslide – Route 219* Black - Machan
	ADJOURN FOR THE DAY – 5:00 PM	
	HGS National Steering Committee Meeting **5:00 PM to 6:30 PM Board Room**	
Wednesday, September 30th	**6:15 AM to 7:00 AM – BREAKFAST – Dining Room open early – On Own**	
	7:00 AM to 5:00 PM – HIGHWAY GEOLOGY FIELD TRIP **Lunch Dinosaur BBQ Sponsored by Geobrugg** **Drinks Sponsored by Golder**	
	6:00 PM to 7:00 PM – SOCIAL HOUR **Grand Ballroom Foyer** **Bar Sponsored by AMERICAN MOUNTAIN MANAGEMENT**	
	7:00 PM to 10:00 PM – BANQUET- Grand Ballroom **Cash bar**	

Thursday, October 1st, AM		**6:30 AM to 8:00 AM – BREAKFAST Dinning Room On Own**
	5 **Case Histories** *Moderator:* *Dick Cross*	8:00 – 8:20 *The Practical Solution for a Cave Located on a School Campus in Central Kentucky* – Wilson
		8:20 – 8:40 *Some Notes on the Geotechnical Investigation Process* - McGuffey
		8:40 – 9:00 *High Energy Rockfall Embankment Constructed using a Freestanding Woven Wire Mesh Reinforced Soil Structure Recent Experience in British Columbia, Canada* - Simmons
		9:00 – 9:20 *SH 20 Keetonville Hill Landslide Repair Rogers County, Oklahoma* - Nevels
		9:20 – 9:40 *Review of Bridge Sites Visited for NCHRP Project 24-29: Scour at Bridge Foundations on Rock* – Keaton
	9:40 AM to 10:00 AM – BREAK Regency Room Sponsored by Michael Baker Jr.	
	6 **Design Considerations** *Moderator:* *Tom Eliassen*	10:00 – 10:20 *Condition Assessment of Earth Reinforcements for Asset Management* – Fishman
		10:20 – 10:40 *Rock Slope Stabilization Projects Letchworth State Park Portageville, New York* - Mann
		10:40 – 11:00 *Rock Slope Stabilization Using Spider System* - Bigger
		11:00 – 11:20 *Terrain Reconnaissance at New York State Department of Transportation* – Hadjin
		11:20 – 11:40 *The Use of Time Domain Reflectometry (TDR) to Monitor an Active Landslide* - Neely
	WRAP-UP, ADJOURN – 12:00 PM	

1.1

HIGH BRIDGE AREA ROADWAY SLIDE

LETCHWORTH STATE PARK
PORTAGEVILLE, NEW YORK

INTRODUCTION

Letchworth State Park is located along the Genesee River about 35 miles south of Rochester, New York. The Genesee River has carved a gorge up to 550 feet deep through this area and plummets over three separate waterfalls as it flows northward towards Lake Ontario. Letchworth State Park is operated by the Office of Parks, Recreation and Historic Preservation (OPRHP).

Norfolk Southern operates a rail line that crosses about 230 feet above the Genesee River near the town of Portageville, the southern entrance to the park. The present bridge is a steel structure that replaced what at one time was the longest and highest wooden bridge in the country. This bridge is referred to as the High Bridge.

The Portageville park entrance provides important access for large trucks and busses that support park inns and restaurants. The entrance allows tourists access to two major waterfalls in that area. Figure 1 shows the location of the roadway, gorge, railroad and additional site features. The Portageville entrance road circles around and about 100 feet below the western abutment of the high bridge and has experienced subsidence for many years requiring numerous pavement repairs. By 2007 the slope conditions had deteriorated to the point where it was difficult to maintain traffic on the road. Vehicles rounding the curve beneath the bridge were encountering a pavement dip that was nearly 3 feet in depth. Approximately 150 feet of the road was severely cracked and showed signs of significant movement.

In response to the deteriorating slope and road conditions the OPRHP commissioned an engineering study to determine the cause of the subsidence and to formulate a plan to remediate slope movements. This paper describes the subsurface explorations conducted to evaluate the conditions and the subsequent design and construction to remediate the area.
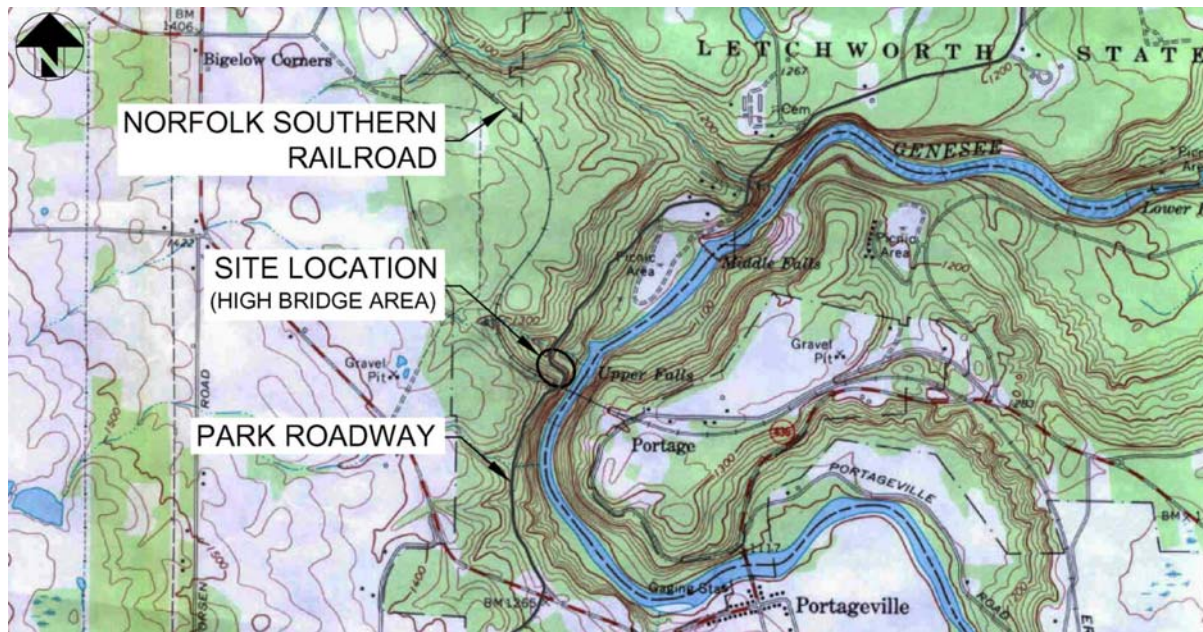
FIGURE 1

SUBSURFACE EXPLORATIONS

In 2007 Earth Dimensions, Inc. (EDI) drilled borings to rock and installed instrumentation to monitor slope movements and groundwater conditions. The site generally consists of glacially deposited surficial soils overlying sandstone and shale bedrock. A review of surficial geology maps indicates that the soils are either lacustrine or till in nature. Bedrock is of the Nunda Formation, which is part of the West Falls Group, formed during the Paleozoic Upper Devonian period.

Seven test borings were advanced to rock to characterize the soils at this site at the locations shown on Figure 2. Asphalt thickness varied from 0.1 feet to 1.7 feet between boring locations. Soils consist of a shallow layer of sand and gravel fill, approximately 3 feet in depth. From approximately 3 feet to 10 feet a "water sorted" glacial deposit exists and consists of a mixture of sand, silt and clay and layers of sand and sandy silt. The density of this zone varies from loose to dense based on Standard Penetration Test (SPT) N-values that vary from 5 to 36. Below this layer from approximately 10 feet to 35 feet is a "clayey lake sediment" consisting of clayey silt or silty clay. The consistency of this layer ranges from stiff to hard based on SPT N-values that vary from 10 to 33. The clayey silt soil contains vertical, silt-filled desiccation cracks, extending to a depth of approximately 16 feet with horizontal silt lenses noted in the clayey silt deposit in Boreholes 1–07 and 2-07. The silt lenses are prevalent in Borehole 2-07 from a depth of 14 feet to 18 feet and in Borehole 1-07 from 16 to 22 feet deep, where they were observed to be greater than 1 inch thick. The silt seams are described as extremely moist and are subject to "liquefaction" when disturbed. A glacial till layer approximately 10 feet in thickness consisting of gravel, sand, silt and clay is below the "clayey lake sediment" and extends to the top of rock. The glacial till is hard based on SPT N-values that exceed 30. Borehole 4-07 was extended into the underlying bedrock, which was classified as a sandstone or siltstone, moderately soft to medium stiffness. The 10-foot rock core from Borehole 4-07 indicates excellent recovery percentages with a poor rock quality designation due to the soft and highly fractured bedrock.

EDI installed an inclinometer in Borehole 1-07 to monitor the amount and direction of slope movement. Data is first collected for two orthogonal axes, and then the vector sum of the measured displacements is calculated to determine the magnitude and direction of the movement. Data collected for over an approximately four-month period (Figure 3 below), indicated the slope moved approximately 0.5 inches and was occurring at a depth of approximately 16 feet. Laboratory tests on sample S9 from Borehole 1-07 (silt lens at 16 feet), indicates that the natural water content is 29.5 percent and the liquid limit is 26 percent.

EDI also installed standpipe piezometers in Boreholes 2-07 and 3-07. The piezometer in Borehole 3-07 screens the upper "water sorted" glacial deposit and the piezometer in Borehole 2-07 screens the lower "clayey lake sediment" intersecting the silt lenses. The groundwater level in both piezometers was lowest in late summer and in both cases was at or near the bottom of the piezometers. After approximately six months of monitoring the piezometers and with the lack of significant groundwater data, we recommended installing vibrating wire piezometers to attempt to measure pore pressure in the silt lenses. EDI installed vibrating wire piezometers in Boreholes 6-07 and 7-07 within zones of saturated silt lenses in the "clayey lake sediment". Data from these piezometers indicates that the pore water pressure in the silt lenses at times was above the ground surface. We believe that the high pore pressure in the silt lenses reduces the soil strength of these layers providing a weak zone along which slope movement occurs.
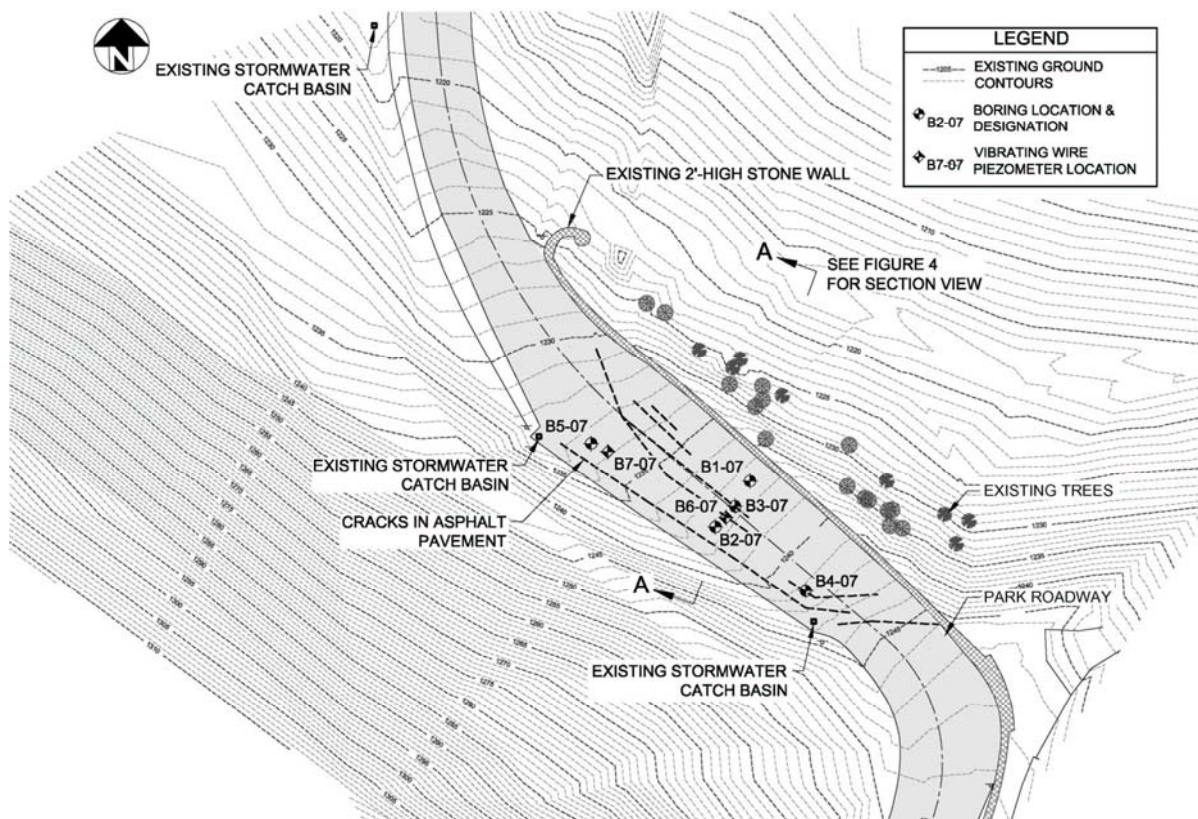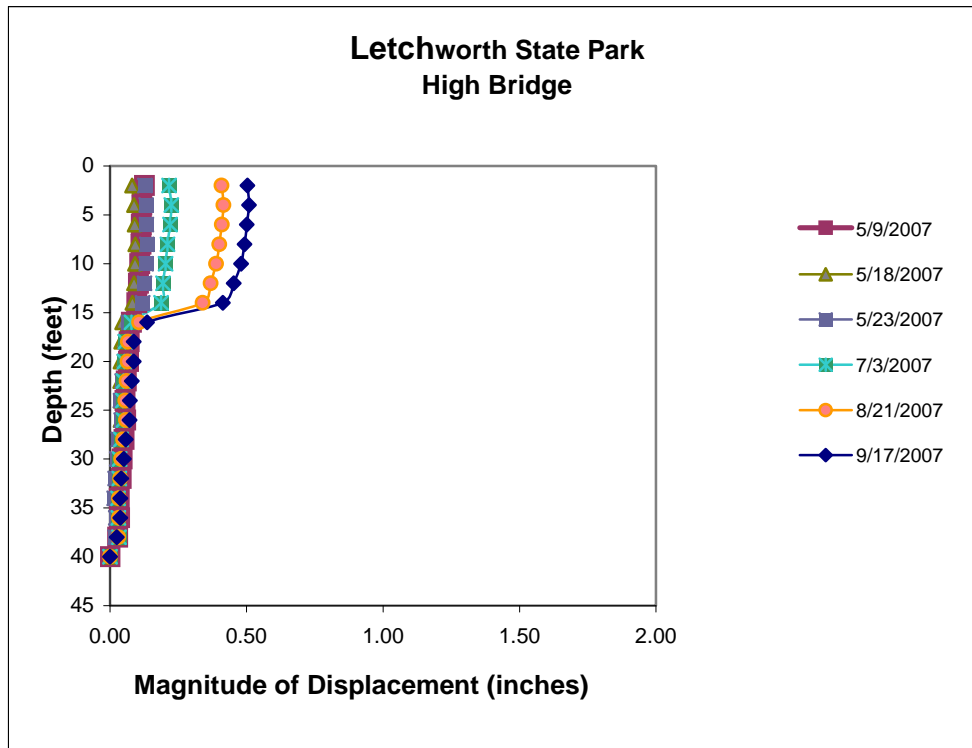

FIGURE 2

FIGURE 3

Figure 4 depicts data from Boreholes 1-07, 2-07 and 3-07 and the location of the theoretical failure plane in section view.
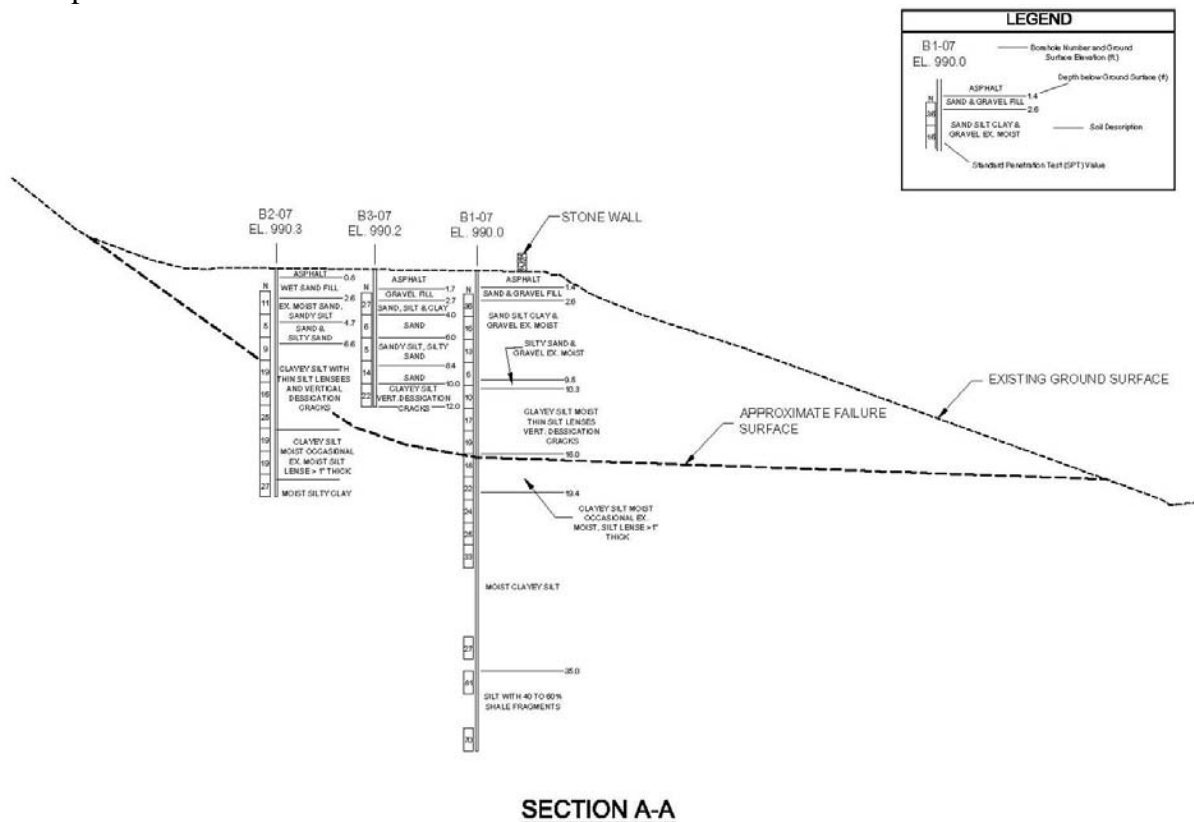

SECTION A-A

FIGURE 4

EVALUATIONS AND RECOMMENDATIONS

Traditional stabilization methods that involve lowering the top of the slope, flattening the slope or adding a buttress at the toe of the slope were not feasible here given that the road location and elevation cannot vary significantly from its current configuration. Furthermore, 20 feet of excavation to remove saturated silt lenses was also not considered a feasible option, as this could destabilize the Norfolk Southern Railroad track. Because of the site constraints, we recommended a two-step approach using anchored reaction blocks and drainage to improve slope stability and reduce the effect of future slope movements on the road.

We used PCSTABL6H, a slope stability program developed by Purdue University, to complete an analysis of the existing conditions and then to evaluate the benefit associated with adding normal force to the failure zone using reaction blocks and ground anchors. Both analyses were completed using the soil and groundwater data that had been collected, including a weak silt layer with high pore pressure to represent the silt lenses observed in the clayey lake sediment. The strength of the silt layer was estimated assuming a factor of safety of 1.0 for the existing conditions. The remediated conditions analysis was then completed using these same strength values and applying a normal force necessary to achieve a calculated factor of safety of 1.5.

We considered the factor of safety for the existing and remediated conditions to be benchmark values that show relative improvement to the slope offered by the selected remediation method. These values however do not address slope movements before or after remediation.

REMEDIAL DESIGN

Our design includes nine ground anchors and reaction blocks installed below the road. The blocks provide a stabilizing force that increases normal stress on the failure zone to resist future slope movement. Figure 5 shows the reaction blocks and ground anchors in plan and Figure 6 shows them in section view. The reaction blocks and ground anchors could be drilled and grouted into the hillside from a bench area below the road. We also recommended lowering the groundwater level using a series of subsurface drains to provide a pathway for the silt lenses to drain during and after the ground anchors are tensioned.
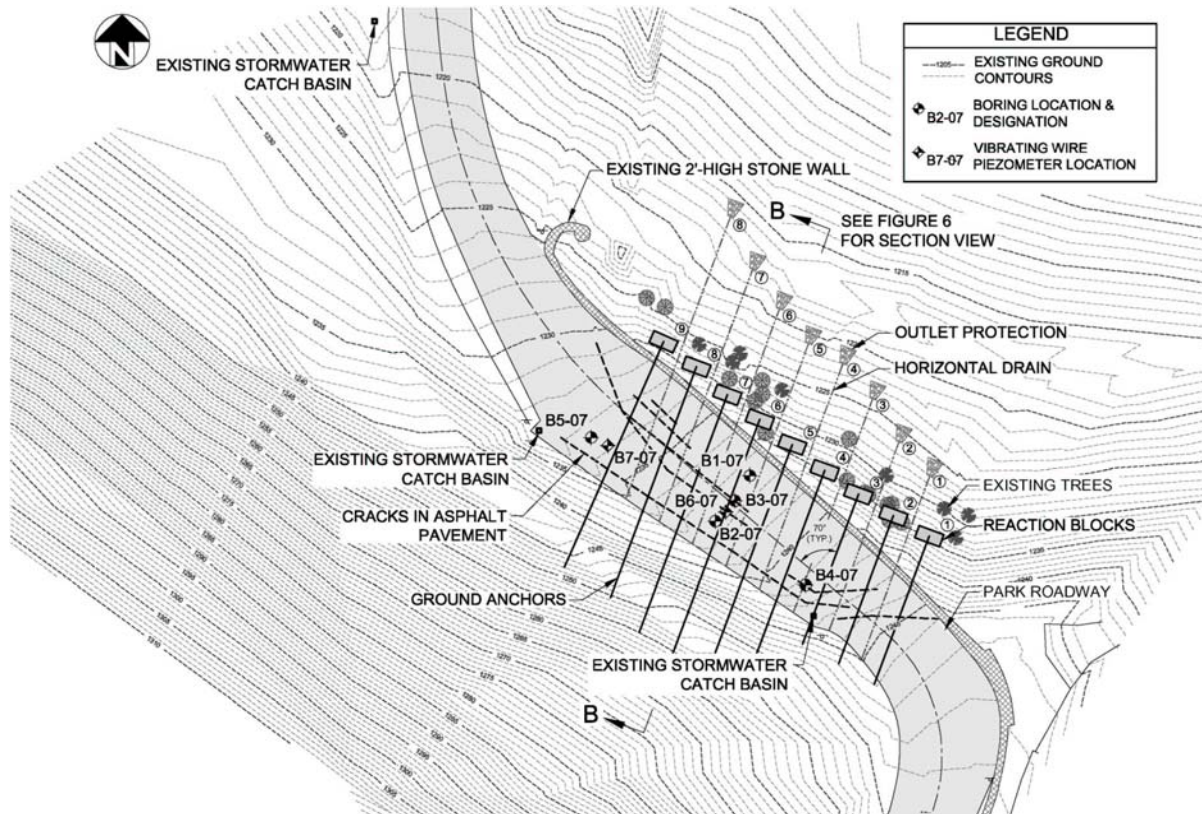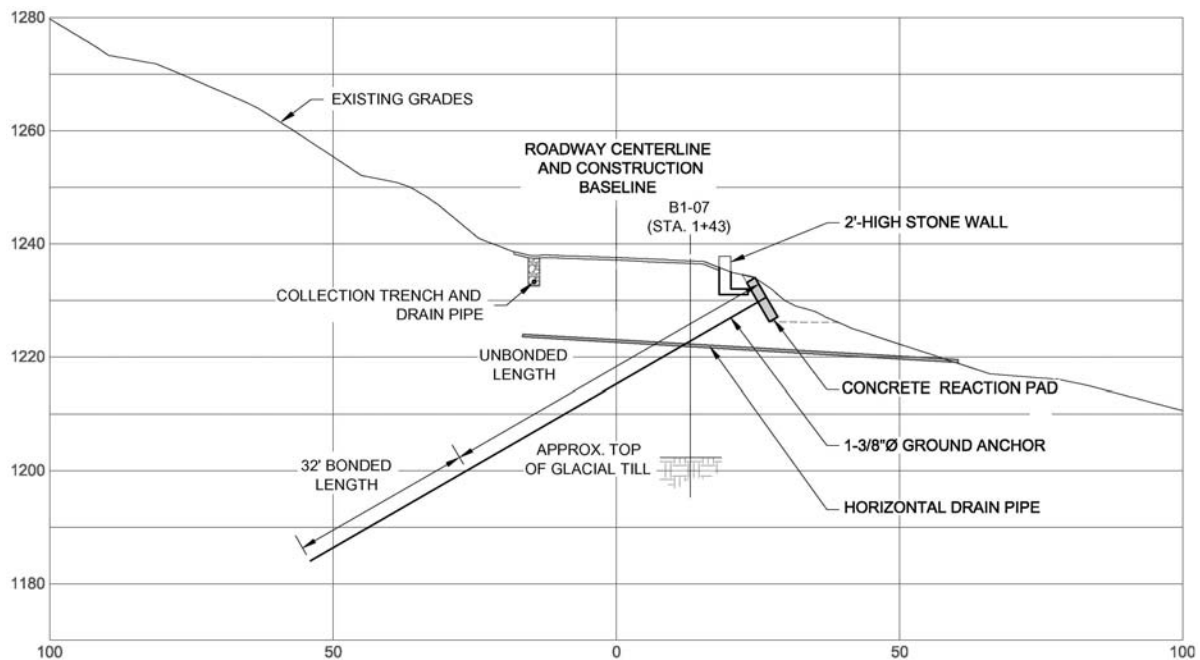
FIGURE 5

SECTION B-B

FIGURE 6

1-3/8 inch high strength (150 kips per square inch) steel bars for the ground anchors, each designed to carry a design load of 142.2 kips were specified. The bonded zone was specified to

be 32 feet long and to be installed completely beyond the theoretical failure zone. The bond would be developed in either glacial till or bedrock depending on location. The unbonded length for each ground anchor varied between 60 and 100 feet, based on its location and observed ground conditions. Dual corrosion protected (DCP) bars were specified to maximize service life of the anchors.

The reaction blocks are reinforced concrete and are 8 feet by 8 feet, 21 inches thick and spaced approximately 12 feet on center. The ground anchors extend through the reaction blocks and are locked off at the face using base plates and nuts. This system allows the ground anchor force to be transmitted into the reaction block, which in turn exerts a uniform pressure on the surface of the slope. This pressure is then translated into a stabilizing force on the failure surface.

The design includes two types of drainage systems. A drainage trench approximately 4 feet deep with a perforated pipe surrounded in clean stone is included along the upslope side of the roadway. The purpose of the trench is to collect groundwater from the upper zones of soil and reduce recharge to the silt lenses. Eight horizontal drains that are designed to intercept groundwater in the deeper silt lenses were also included to provide a drainage pathway for the silt lenses during and after tensioning of the ground anchors. The horizontal drains consist of 6-inch diameter slotted drainpipes placed directly in contact with the native site soils. See Figure 6 for the location of the drains in section view.

CONSTRUCTION

OPRHP contracted with Keeler Construction Company, Inc. (Keeler) in the spring of 2008 to reconstruct the roadway and remediate the slope remediation discussed above. Keeler subcontracted with Berkel and Company Contractors, Inc. (Berkel) to construct and install the ground anchors and horizontal drains. BVR Construction Company, Inc. (BVR) was subcontracted to install the reaction blocks. Figure 7 shows the condition of the roadway prior to construction.

FIGURE 7

Keeler began construction by removing the existing road surface and fill materials that had been placed over the years as the road had continued to move. The upslope subsurface drainage was installed along with new surface water catch basins and outlet pipes. The road sub base was then regraded and compacted using a 2-inch minus crushed stone material. The work progressed down slope of the road by clearing and removing the existing trees and vegetation to allow for installation of the ground anchors and horizontal drains.

Berkel was then mobilized to the site to install the ground anchors and horizontal drains. The subcontractor utilized a horizontal rotary air powered drill rig to drill boreholes to the design lengths shown and advanced steel casing pipe to create a 5-1/4 inch diameter hole to bedrock. Boreholes were advanced without the casing into the bedrock resulting in a 4-1/2-inch diameter hole. Prior to drilling, a cross section at each ground anchor was plotted and the previously collected boring data superimposed. Based on these sections, it was expected that some of the bonded lengths might be partially in glacial till and bedrock. During ground anchor installation, it was found that bedrock was present at shallower depths than had been expected, which allowed for the bonded zone of all the ground anchors to be in bedrock. Upon completing each borehole, the DCP bar was inserted and grouted into place. Figure 8 is a photo of the drill rig installing the ground anchors.

FIGURE 8

Upon completing the ground anchors, Berkel proceeded down slope to the horizontal drain outlet locations. The drain holes were installed using the same drill rig. Upon finishing each borehole, the 6 inch slotted pipe was inserted to the design length and the casing was then removed. The last 10 feet of each pipe was installed without slots and was completed with the installation of an animal guard outlet and riprap apron. Figure 9 is a photo of the drill rig installing the horizontal drains.

FIGURE 9

BVR was then mobilized to the site to construct the reaction blocks. The design had specified that the reaction blocks be cast in place concrete formed by using shotcrete. This method was chosen to enable the concrete to be placed in intimate contact with the ground surface and constructed without the use of forms.

Prior to placing the shotcrete, BVR installed two mats of reinforcing steel and a protective pipe sleeve to allow the ground anchor to pass through the reaction block. The shotcrete was then installed to the specified thickness with the surface of the blocks troweled to allow for placement of the ground anchor base plate and nut. Figure 10 is a photo of the shotcrete installation.

FIGURE 10

After the reaction block concrete reached its specified compressive strength, Berkel returned to test and tension the ground anchors. Each anchor was then tested to 133 percent of the design load. The first ground anchor was performance tested, which is a cyclic test of loading and unloading, followed by all of the other ground anchors being proof tested, which is a single cycle test. The results show that all the anchors exhibited the expected elongations during testing. After completing the testing, all nine of the ground anchors were locked off at the design load. Berkel installed load cells on three of the ground anchors for future monitoring.

The load cells are an open steel cylinder installed between two base plates, which are locked off with a nut. The load cells each contain three vibrating wire strain gauges that are activated when read. During ground anchor lock off, the load cells and jack pressure were compared to check that the correct design load was applied. The intent of installing the load cells was to enable a recheck of the ground anchors over time to watch for loss in ground anchor tension.

Once the ground anchors were tested and locked off, Keeler installed protective caps over the ground anchor head assemblies and backfilled around the reaction blocks. The backfilling was to create a gradual down slope area adjacent to the road that could be revegetated. Keeler then

repaved the roadway and applied topsoil and seed to the completed slope. Figure 11 shows the condition of the roadway at the end of construction.

FIGURE 11

MONITORING

Instrumentation included an inclinometer, two vibrating wire piezometers, two monitoring wells and three load cells.

The vibrating wire piezometers and both monitoring wells were destroyed during removal of the pavement. The inclinometer survived the construction phase and continues to be monitored to check the effectiveness of the remediation. Inclinometer measurements taken shortly after pavement removal showed large deflections near the surface, probably associated with the construction. We collected a new baseline measurement after construction was completed and have made several additional measurements. To date, approximately one year after construction, inclinometer measurements have shown little to no movements.

Additionally, the horizontal drainpipes could be monitored visually to view if they were actively draining water from the subsurface soils. Upon completing the installation, the westerly drains (drains 5 through 8 shown on Figure 5) began draining water immediately and have continued following ground anchor tensioning. The easterly drains (drains 1 through 4 shown on Figure 5) have not been observed to drain water to date.

The load cells were installed on three of the anchors near the end of construction and also been monitored since the design load was applied. To date, the cells have lost approximately 12 to 25 percent of their pretension load. Figure 12 is a plot of the load cell data.
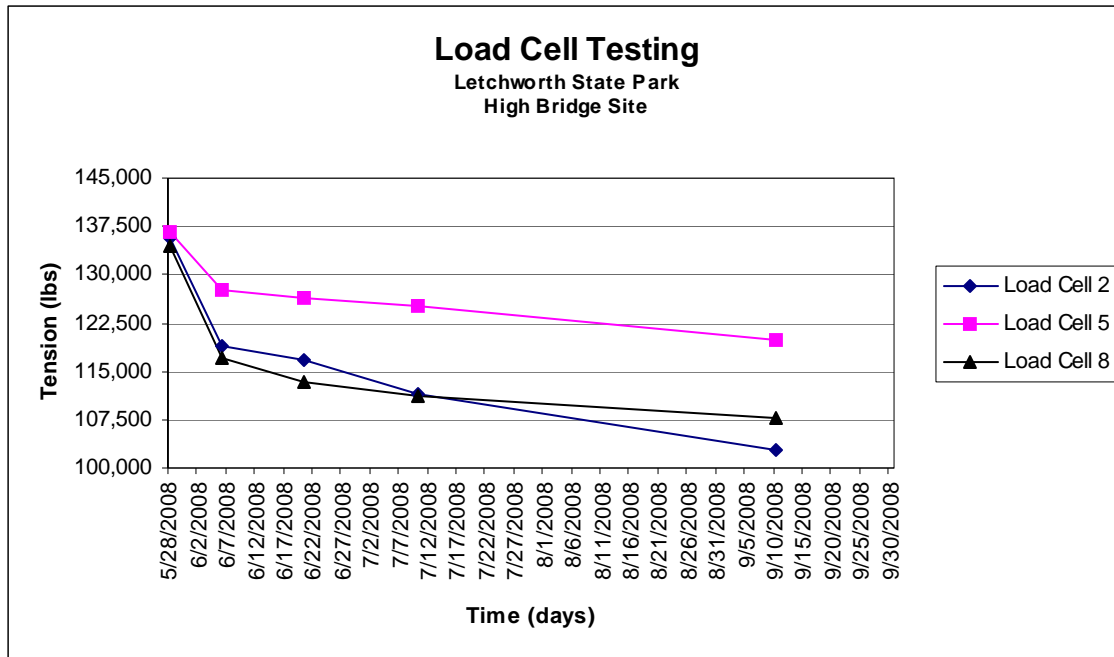
FIGURE 12

SUMMARY

The Portageville entrance road to Letchworth State Park had experienced subsidence for many years requiring numerous pavement repairs. By 2007 approximately 150 feet of the road was severely cracked and showed signs of significant movement. The slope conditions had deteriorated to the point where it was difficult to maintain traffic on the road.

An engineering study commissioned by OPRHP identified movement occurring at a depth of approximately 16 feet below the road. The movement was occurring through a zone of saturated silt lenses confined between layers of clay.

Traditional methods to stabilize the slope were considered but found impractical when considering the site conditions. A non-traditional approach utilizing reaction blocks and ground anchors was selected to improve the stability of the road and slope. The design included nine reaction blocks and ground anchors to provide a stabilizing force to the moving soil mass. Additionally, a trench drain on the uphill side of the road and horizontal drains below the road were added to the design. The upslope drain would minimize the water entering the soils below the road and the lateral drains would remove existing water trapped within the silt lenses and allow for water to be released during reaction block loading.

Inclinometer readings indicate that no detectable movement has occurred since construction was completed in the spring of 2008. The ground anchor load cell monitoring data shows some loss of pretension, however the data indicates that the loss of pretension is slowing. Visual observations of the lateral drains indicate that water is slowly draining from the slope. It is anticipated that monitoring of the inclinometer, load cells and lateral drains will continue for several more years.

PAPER AUTHORS:

Andrew J. Nichols, P.E.
Project Engineer
McMahon & Mann Consulting Engineers, P.C.
2495 Main St., Suite 432
Buffalo, New York 14214
(716) 834-8932
anichols@mmce.net

James Bojarski, P.E.
Project Engineer
McMahon & Mann Consulting Engineers, P.C.
2495 Main St., Suite 432
Buffalo, New York 14214(716) 834-8932
jbojarski@mmce.net

1.2

## REMEDIATION OF THE SR 15 WELCOME CENTER LANDSLIDE

David R. Scherer, P.E.[1], Robert E. Johnson, P.E.[2], Paul J. Lewis, P.E.[3]

ABSTRACT

In 2004 a landslide resulted in the closure of the southbound lanes of SR 15 in northern Tioga County approximately one half mile north of the Pennsylvania Welcome Center and 6 miles south of the New York State border. The landslide measured approximately 800 feet along the head scarp and 400 feet from the head scarp to the toe. Total vertical displacement at the head scarp was approximately 20 feet. Forty-four borings were drilled to investigate the subsurface conditions in the area of the landslide. Soil samples collected from the borings were tested in the laboratory to estimate the engineering properties of the site soils. The tests included direct and triaxial shear. Inclinometer casing was installed in 13 of the borings, and piezometers were constructed in 12 of the borings. The computer program PASTABL was used to perform the slope stability analyses. Numerous alternatives were considered to remediate the landslide. The selected alternative included: realignment of SR 15 and Park Hill Road, load reduction (excavation) at the landslide head, construction of a soil berm at the toe, and placement of a chimney (blanket) drain behind the toe berm. Construction was completed in 2007 for a cost of approximately 3 million dollars. Inclinometer readings continue to be obtained to monitor the area.

INTRODUCTION

In the fall of 2004 a landslide resulted in the permanent closure of the two southbound lanes of SR 15, Section 037 in northern Tioga County approximately six miles south of the New York and Pennsylvania state line, and one half mile north of the Pennsylvania Welcome Center. Maps showing the location of the landslide are provided in Figures 1 and 2.
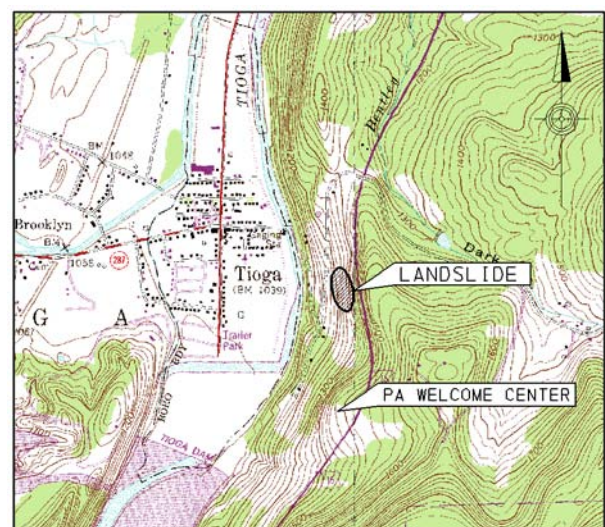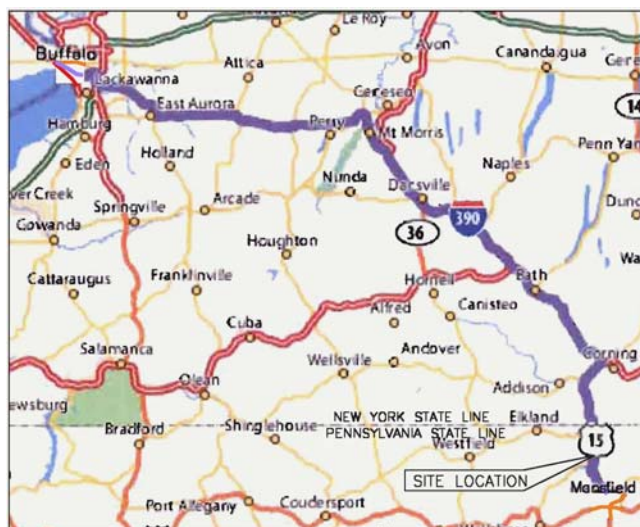
The landslide measured approximately 800 feet along the head scarp and 400 feet from the head scarp to the toe. Total vertical displacement at the head scarp was approximately 20 feet (see Photo 1). The toe of the landslide was located just above Park Hill Road (T-667). Periodic clean-up of soil off Park Hill Road was required to keep it in service. Landslide remediation was completed in the summer of 2007.

Photo 1: Head Scarp along SR15 Southbound

ROUTE 15 PROJECT HISTORY

Route 15 was originally located in the valley along the Tioga River. In 1975 the two lane roadway was relocated to the hillside prior to construction of the Tioga-Hammond Reservoir. At this same time the majority of the fill was placed for two future southbound lanes. The two lanes constructed in 1975 carried one lane of northbound and southbound traffic. Ultimately, the two lanes constructed in 1975 would carry northbound traffic after completion of the southbound lanes. The natural ground sloped generally 2H:1V in the area of the landslide, but varied from 4H:1V at the toe to 1.5H:1V at the head. The embankment placed in 1975 was sloped 2H:1V.

In 2002 the southbound lanes were completed by adding approximately 25 feet of fill and bituminous pavement. This fill was placed with a 1.5H:1V side slope. These lanes were opened to traffic in the fall of 2002. A crack extending across the southbound travel lanes and into the median was

observed in the spring of 2003, and the area was monitored through the fall of 2004. In the fall of 2004 the southbound lanes were closed due to continued movement, and traffic was shifted to a northbound lane.

FIELD RECONNAISSANCE

Field reconnaissance of the project area was done in February 2006. Trees in the landslide toe area were distorted and numerous wet areas were also observed near the toe. Throughout the landslide mass the ground was extremely hummocky. In addition to the main scarp, numerous "secondary" scarps and toes were observed.

REVIEW OF AVAILABLE INFORMATION

Several Pennsylvania Bureau of Topographic and Geologic Survey publications were reviewed. The "Atlas of Preliminary Geologic Quadrangle Maps of Pennsylvania" indicated that the contact between the Catskill (Dck) and Lock Haven (Dlh) Formations traverses the site. Rock of the Catskill Formation is exposed in the SR 15 cut directly above the landslide, and rock of the Lock Haven Formation is exposed below and just to the north where Park Hill Road crosses SR 15. The Catskill Formation is a complex unit consisting of grayish-red sandstone, siltstone, and shale generally in a fining upward sequence. The Lock Haven Formation consists of interbedded light-olive-gray, very fine grained, fossiliferous sandstone, siltstone and shale.

Aerial photos taken between 1952 and 2002 were reviewed. The photographs from 1952 show the presence of a "suspicious" area within the limits of the slide area. An area within or in close proximity to the footprint of the slide displayed an irregular pattern of trees, possibly disturbed trees, suggesting the area is poorly drained or that slope movement occurred in the area. The most prominent feature in the recent photos was the presence of a seep or spring. The seep was located approximately in the middle (length) of the landslide and approximately one third of the slope height above the toe.

SUBSURFACE INVESTIGATION

Forty-four (44) borings were drilled to investigate the subsurface conditions and for installation of inclinometer casing and piezometers in the area of the landslide between August of 2003 and July of 2006. A Boring Location Plan is shown in Figure 4, and a typical subsurface cross-section is shown in Figure 5.

Figure 4: Boring Location Plan

The borings indicated similar subsurface conditions throughout the project area. The overburden generally consisted of reddish brown sand and gravel with silt and clay (sm and gm). Local materials were used to construct the embankment; therefore, it was difficult to discern between fill and the in-situ soil. The in-situ soils were believed to be colluvium and glacial till. Standard Penetration Test (SPT) N-values recorded in the borings indicated that the soils were generally medium dense to very dense.

Bedrock from both the Catskill and Lock Haven Formations was cored. The Catskill Formation was encountered in the borings drilled in the upper part of the landslide; the Lock Haven Formation was encountered in the borings drilled in the middle and lower part of the landslide. The bedrock was generally described as sandstone, but layers of siltstone and shale were occasionally encountered.

LABORATORY TESTING

Soil samples collected from the borings were tested in the laboratory. Tests performed included: sieve analysis, Atterberg limit, natural moisture content, unit weight, and direct and triaxial shear. The soils generally classified as silty, clayey sands and gravels, (GC, GM, SC, SM). A few of the soil samples classified as silt and clay (ML, CL). The natural moisture contents measured in the laboratory typically ranged from 4.5 to 14.3 percent, and the dry unit weights typically ranged from 109.9 to 121.5 pcf.

Seven (7) direct shear tests, 4 residual direct shear tests and a triaxial shear test were performed on Shelby tube and remolded samples to estimate the shear strength of the soil. Plots of peak and residual shear strength test results are shown in Figures 6 and 7, respectively.
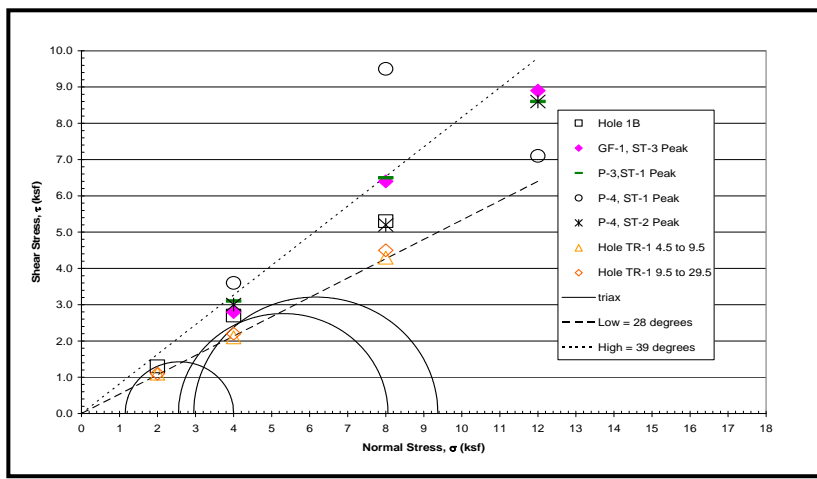
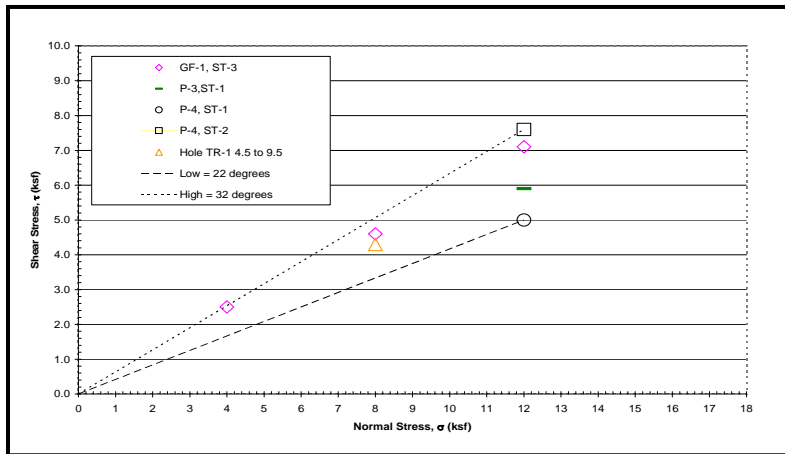Figure 6: Plot of peak shear strength laboratory test results

Figure 7: Plot of residual shear strength laboratory test results

INSTRUMENTATION

Inclinometer casing (2.75-inch diameter) was installed in 13 of the borings. Seven of these borings were located within the landslide and 6 were located outside of the landslide. Inclinometer readings were obtained until excessive movement of the casing prevented the probe from being lowered to the bottom of the hole. A typical inclinometer plot is shown in Figure 8.
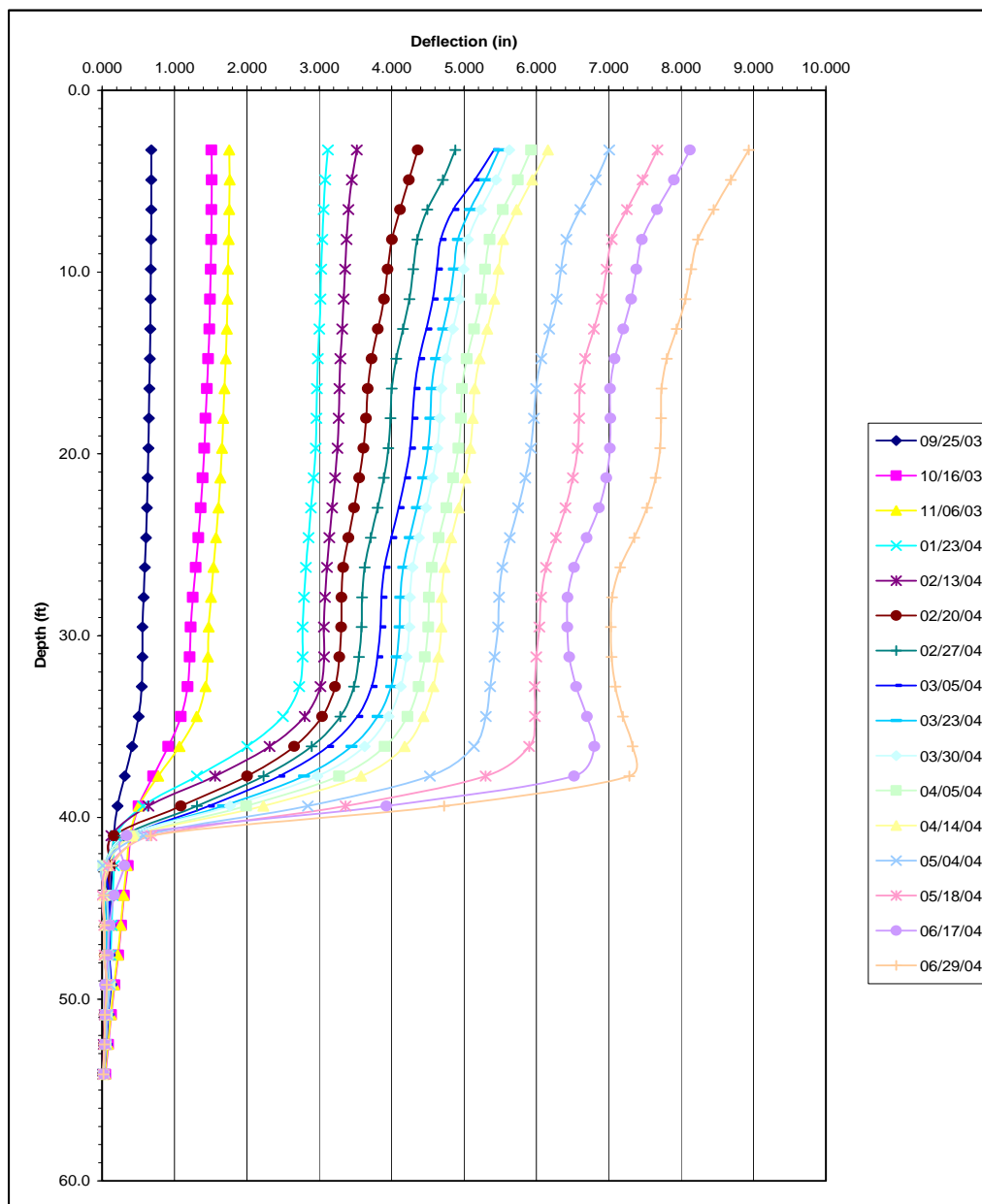
Figure 8: Inclinometer 1T was located within Welcome Center Landslide near the head scarp.

Twelve (12) standpipe (Casagrande) piezometers were constructed in borings drilled throughout the landslide area, and automated transducers were placed in some of the piezometers to monitor long term groundwater levels. Based on piezometer readings the depth to water varied from approximately 12 feet below ground surface at the toe of the landslide to approximately 60 feet below ground surface near the middle of the landslide.

LANDSLIDE TRIGGER MECHANISMS

It is believed that several factors triggered the Welcome Center landslide. The main cause was most likely elevated water levels within the lower portion of the embankment. Field observations indicated numerous seeps and wet areas in the embankment, and review of aerial photographs dating back to the early 1950's revealed the presence of seeps in this area. It is believed that either no measures were taken during construction to outlet the seeps, or the measures that were taken were

ineffective. Another cause of elevated water levels was believed to be the contact between the two geologic formations in the upper portion of the slope. Formation contacts are often extremely fractured and thus more permeable compared to the surrounding bedrock; therefore, subsurface water is likely being channeled to the slide area through this geologic feature. An annotated aerial photograph with the geology, head scarp and seep is shown in Photo 2.
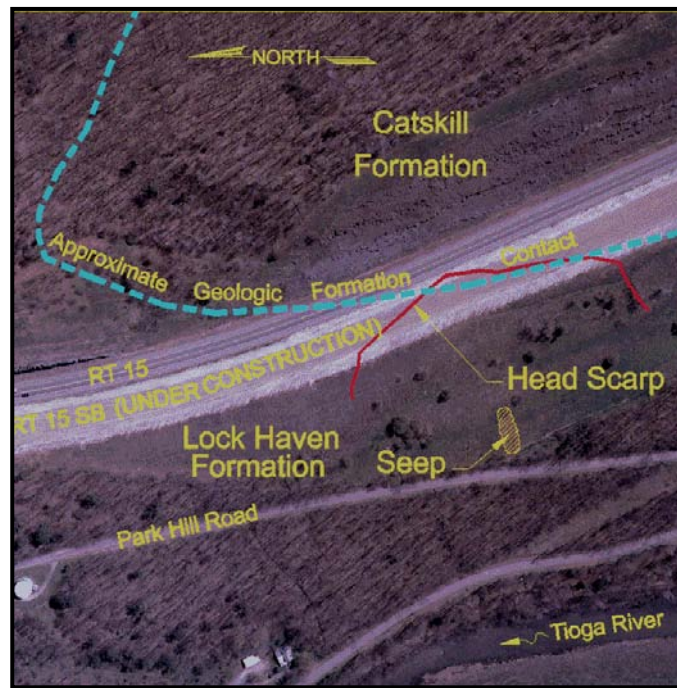
Another possible contributor to the landslide was the shear strength of the foundation soils. The borings indicated that the foundation soils were predominantly granular but did contain a considerable amount of silt and clay. The presence of coarse material in the soil made shear strength difficult to estimate in the laboratory with the commonly available testing apparatus. Laboratory test results indicated the internal soil friction angle of the material could have been as low as 28°, but based on material gradation and density, published data suggested that the internal soil friction angle of this material was at least 32°.

A third factor that may have contributed to the landslide was the construction techniques used to build the embankment in the 1970's. Original ground slope in the area was 2H:1V. Current embankment construction practices would include stripping vegetation, constructing longitudinal bonding benches, and removing wet or unsuitable material prior to fill placement. It is possible that some or all of these practices were not employed when this fill was constructed.

SLOPE STABILITY ANALYSES

The computer program PASTABL was used to analyze the stability of the slope before and after construction of the southbound lanes in 2002. "Back analyses" were done to assess the parameters used in the stability analyses and to validate the PASTABL model, which would eventually be used to

design a remediation.   A cross-section in the middle of the landslide (Station 814+00) was used for these analyses. Inclinometer data and visual landslide features (head scarp and toe) were used to model the location of the landslide failure plane. Borings and laboratory test results were used to estimate soil and rock strata and properties.

The location of the groundwater was believed to be the least defined parameter in the stability model. Initially, static groundwater levels indicated by the borings were used. Subsequent analyses with elevated groundwater levels were used to achieve stability safety factors representative of the condition analyzed (i.e., safety factor greater than 1 for stable slope and less than 1 for failed slope).

The first analysis performed modeled the embankment shortly after construction of the southbound lanes when the landslide was observed (Spring 2003). This analysis modeled a saturated embankment to Elevation 1210 feet. This groundwater level was the approximate elevation of the seep estimated from aerial photograph, and appeared reasonable based on field observations of seeps and wet areas on the embankment. This stability model resulted in a safety factor of 1.0, and had failure plane entry and exit points in the general area of the head scarp and toe observed in the field. Based on these results the PASTABL model appeared reasonable. A plot of this analysis from PASTABL is shown in Figure 9.
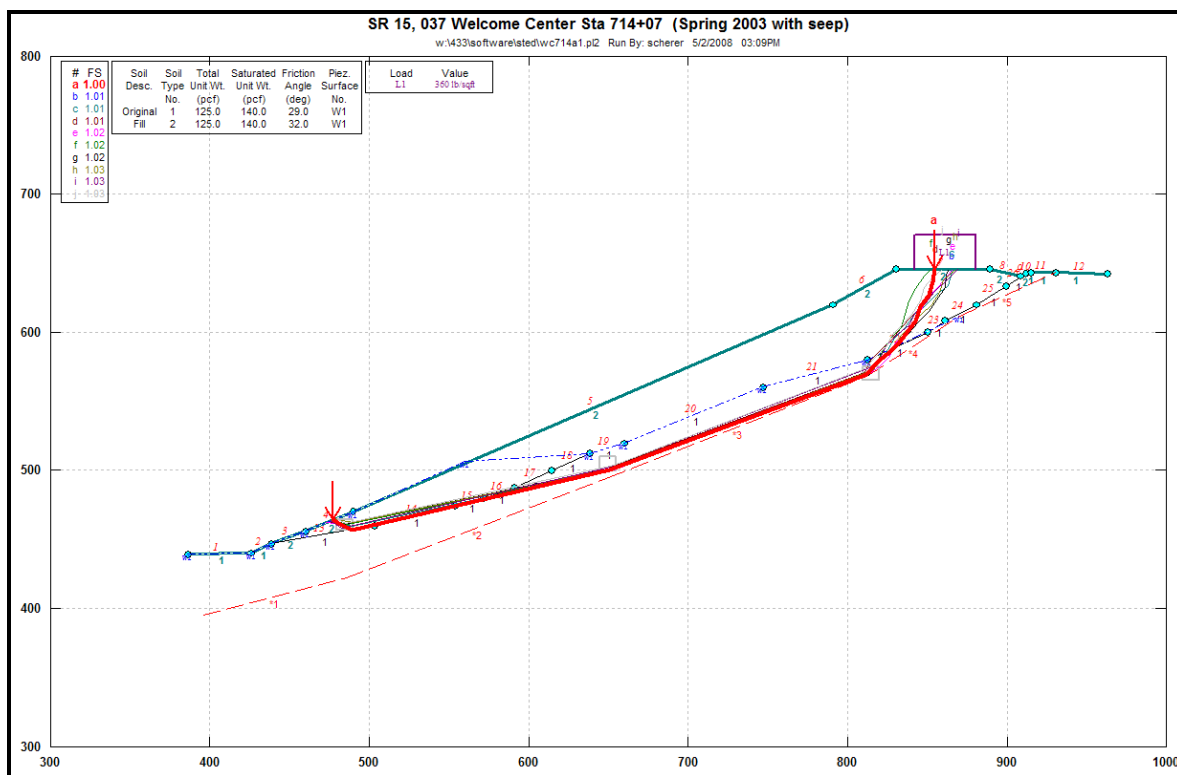

Figure 9: PASTABL model for conditions at time of failure in 2003.

The second analysis modeled conditions prior to construction in 2002 when the embankment appeared stable. This model used identical subsurface conditions to the first analysis, and yielded a safety factor of 1.1. The safety factor of 1.1 indicated that the embankment was stable, as evidenced by

no observed signs of slope movement, but most likely only marginally stable prior to additional fill placement in 2002. This analysis also indicated that the slope stability model was reasonable.

The third analysis modeled conditions in 2006. At this time the landslide was active, and ground at the head of the landslide was approximately 40 feet below the 2002 ground line because of landslide movement and regrading. Residual soil strength was used in the analysis since the landslide was active for several years and significant movement had occurred along the landslide failure plane. A residual shear strength of 23°, which was reasonable based on laboratory test results and published data, resulted in a safety factor of 1.0. This safety factor indicated an unstable slope condition, which agreed with the continued slope movement observed in the field. Based on these three back analyses it appeared that the subsurface conditions were reasonably modeled, and that this slope stability model was appropriate for landslide remediation design.

LANDSLIDE REMEDIATION ALTERNATIVES

Prior to remediation of the landslide, the SR 15 alignment was permanently shifted into the hillside (i.e., east) so that all travel lanes would be founded on bedrock, and the landslide would have little likelihood of affecting the roadway in the future. Therefore, the landslide remediation focused on maintaining traffic on Park Hill Road, which is at the toe of the landslide. Remediation alternatives considered included: load reduction (excavation), earth berms, horizontal drains, piles and rock anchors, and no-build. Combinations of these alternatives were also considered. A table with the pros and cons of the alternative considered is provided below. The load reduction and toe berm alternative was considered the most desirable and selected to remediate the landslide.

Landslide Remediation Alternatives Pros and Cons

Remediation Alternative	Pros	Cons
Load Reduction and Toe Berms	• Excavated material could be used to build berms • No maintenance and indefinite life • Designed using PASTABL • Specialty contractor not needed	• Required relocating Park Hill Road • Required ROW acquisition and environmental clearance
Horizontal Drains	• Lower groundwater • No impact to Park Hill Road	• Drains alone not sufficient • Long term maintenance required • Requires specialty contractor
Piles and Rock Anchors	• No impact to Park Hill Road • High Level of success	• Long (70ft) piles with several rows required • Need to be socketed into rock • Rock anchors needed to restrain top of pile • Cast-in-place concrete cap required • Requires specialty contractor
No-build	• Inexpensive in short term	• Continual maintenance to maintain Park Hill Road • Continued movement at head scarp could impact Rt 15

LANDSLIDE REMEDIATION DESIGN

The computer program PASTABL was used to design the load reduction and berm remediation. The subsurface model developed during the back analyses, which was discussed earlier, was used for remediation design, including residual strengths for the in-situ soil in the area of the failure plane. A friction angle of 34° was used for the proposed berms since the material was granular and was required to be placed and compacted in lifts.

The analyses indicated that excavation of approximately 40 feet of material at the head of the landslide, and a berm 80 feet high extending 50 feet beyond the existing toe of slope was needed. A typical section of the remediated slope is shown in Figure 10.
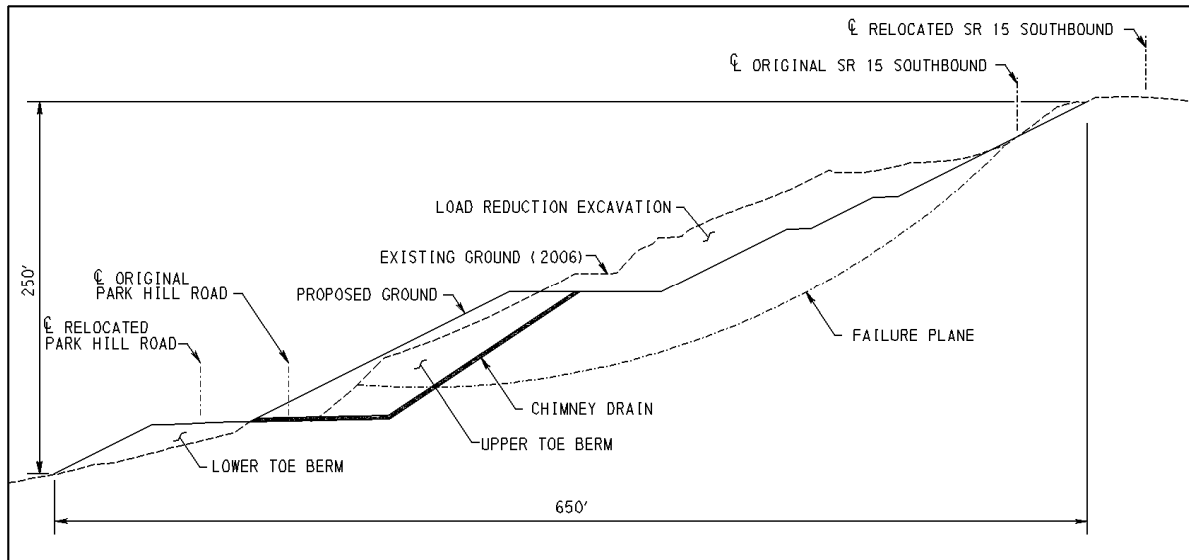

Figure 10: Typical section of remediated slope

In order to lower the water level in the bottom portion of the embankment, excavation of this material for placement of a chimney (blanket) drain was required. The chimney drain consisted of a 2-foot-thick layer of free-draining aggregate wrapped in geotextile. The chimney drain was placed beneath the toe berm and extended up the 1.5H:1V toe berm backslope. Perforated longitudinal and transverse drainage pipes were included in the aggregate for an added drainage measure. A lower secondary berm was needed to provide stability for the main/upper berm. This lower berm also served as an embankment for the realignment of Park Hill Road. Based on the analyses this remediation provided a slope stability safety factor of 1.3.

Glen O. Hawbaker submitted the low bid of approximately $3.2 million and was awarded the landslide remediation contract in the late summer of 2006. Remediation of the landslide was completed in September 2007. Photo 3 was taken during remediation construction.

Photo 3: Placement of stone blanket/chimney drain during toe berm construction.

One unforeseen condition was encountered during construction. Excavation at the toe of the landslide for construction of the chimney drain encountered trees at several locations. It appeared that the trees had been pushed into piles, set fire and then buried during embankment construction in the 1970's. Where encountered, the trees were removed and stockpiled outside of the work area. A few of the borings recovered pieces of tree limbs in the split-spoon sampler near original ground line, but the large quantity of trees encountered in the excavations was not anticipated. Photos 4 shows the trees encountered during construction.

Photo 4: Stockpile of trees encountered in chimney drain excavation

March 2008 and June 2009 Inclinometer Readings

Inclinometers installed during remediation construction have been monitored several times after completion of construction in September 2007. Readings were obtained in March 2008, and a plot of Inclinometer 5 is shown below in Figure 11. Inclinometer 5 was located at the top of the excavation slope that was made to install the blanket drain. As seen by the plot, approximately 1.25 inches of movement occurred during construction in the area of the failure surface (i.e., depth of approximately

45 feet). Since the completion of construction in September 2007 through March 2008 the inclinometers indicated minimal movement has occurred. Readings taken since March 2008 indicate that no movement has occurred at 4 of the inclinometer locations, and less than 0.25 inch of movement has occurred at the 2 inclinometers immediately above the chimney drain.
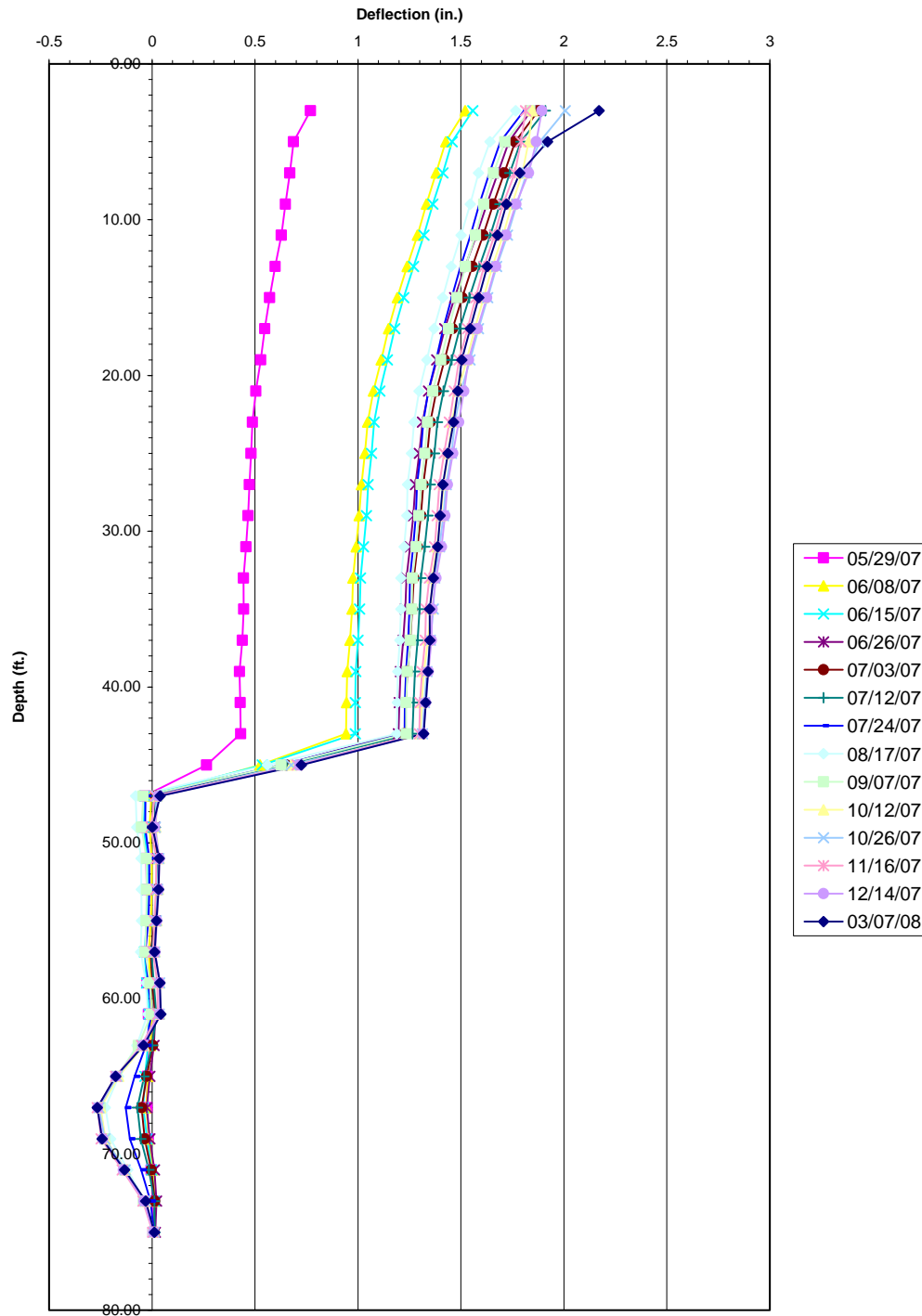

Figure 11: Plot of Inclinometer I-5 from May 2007 to March 2008

August 2008 Field View

       A field view of the remediated landslide was conducted in August 2008, approximately a year after the completion of construction. Based on visual observations the remediation appears to be performing well. No cracks in the pavement were noted, and the alignment of the guiderail was good. The cracks in the load reduction excavation slope and at the top of the toe berm that were observed in September 2007 were not visible. The swale along Park Hill had intermittent pools of water, indicating the chimney drain was functioning. In general the project area was well vegetated, and particularly at the base of the toe berms. No signs of movement were observed in either SR 15 or Park Hill Road. Photos 7, 8, and 9 were taken during the field view.

Photo 7: View from top of toe berm looking toward load reduction slope. SR 15 is at top of slope

Photo 8: View from toe of toe berm looking north along Park Hill Road

Photo 9: Aerial view of remediated landslide; Park Hill Road at bottom and SR 15 at top.

Rio Blanco Landslide Failure Between Rifle and Meeker Colorado
Investigation, Design and Emergency Mitigation using Lightweight Expanded Polystyrene Fill

Ben Arndt, P.E., P.G. *(Presenter)*
Yeh and Associates, Inc.
5700 East Evans Ave
Denver, CO 80222
(barndt@yeh1.net)

Pete Mertes, P.E.
Colorado Department of Transportation - Region 3
222 South 6th Street, Room 100
Grand Junction, CO 81501
(pete.mertes@dot.state.co.us)

Bahram Seifipour, P.E.
HDR Engineering, Inc.
303 East 17th Avenue, Suite 700
Denver, Colorado, 80203
(bahram.seifipour@hdrinc.com)

ABSTRACT

The Rio Blanco landslide is located on State Highway (SH) 13, between the semi-rural towns of Rifle, Colorado and Meeker, Colorado. A roadside embankment composed of fill began to fail in March of 2008, which initiated an emergency response. The failure was approximately 800 feet in length along a section of roadway with a 6 percent climbing grade. The existing embankment fill is comprised of low to moderate plasticity clays and silty clay material that was borrowed from native soils in the project area. Unfortunately, the native clay soils lose cohesive strength when saturated and are prone to surficial slope failures. The embankment fill had been placed into a deeply incised drainage channel creating fill depths greater than 110 feet from the top of the roadway to the underlying claystone bedrock.

The geotechnical investigation indicated this section of roadway had two modes of failure: oversteepened embankment slopes and deep seated instability of the filled area. The embankment fill slopes were placed at slope angles ranging from 2:1 to 1:1 (H:V). Periodic failure has been observed on these slopes when the ground is saturated. There was also a deep-seated global failure mechanism that caused settlement, consolidation, and bearing failure of the entire embankment fill section. Inclinometer data indicated a deep-seated, relatively flat-lying failure surface was located between 30

and 40 feet below the base of the embankment fill and approximately 30 to 40 feet above the top of the bedrock.

During the spring of 2008, the roadway distress became so great that vertical and lateral movement of the landslide required nearly constant maintenance by the Colorado Department of Transportation (CDOT). On occasion, the roadway would experience vertical displacements from 2 to 6 inches a day. This presentation addresses the geotechnical investigation, design, and construction of the emergency repair which subsequently occurred.

INTRODUCTION

The project is located along SH 13 in northwestern Colorado on a two-lane roadway with an approximate 6 percent grade climbing to the north. The roadway was originally constructed as three lanes (2 lanes uphill and 1 lane downhill), but slope instabilities and resulting loss of embankment reduced the roadway width to two lanes. Deep embankment fills support the roadway in this section. These embankment fill slopes range from 2:1 to 1:1 (H:V) have maximum thicknesses greater than 110 feet from roadway elevation to underlying claystone bedrock. The depth to bedrock is deepest in the center sections of the embankment where fill had been placed over a deeply incised stream channel. A culvert underdrain had been installed but seemed to be located well above the pre-existing channel elevation. Slope movement on both the east and west embankment slopes has been documented since the 1990's and had been the subject of several previous studies by CDOT. Figure 1 depicts the project site location.
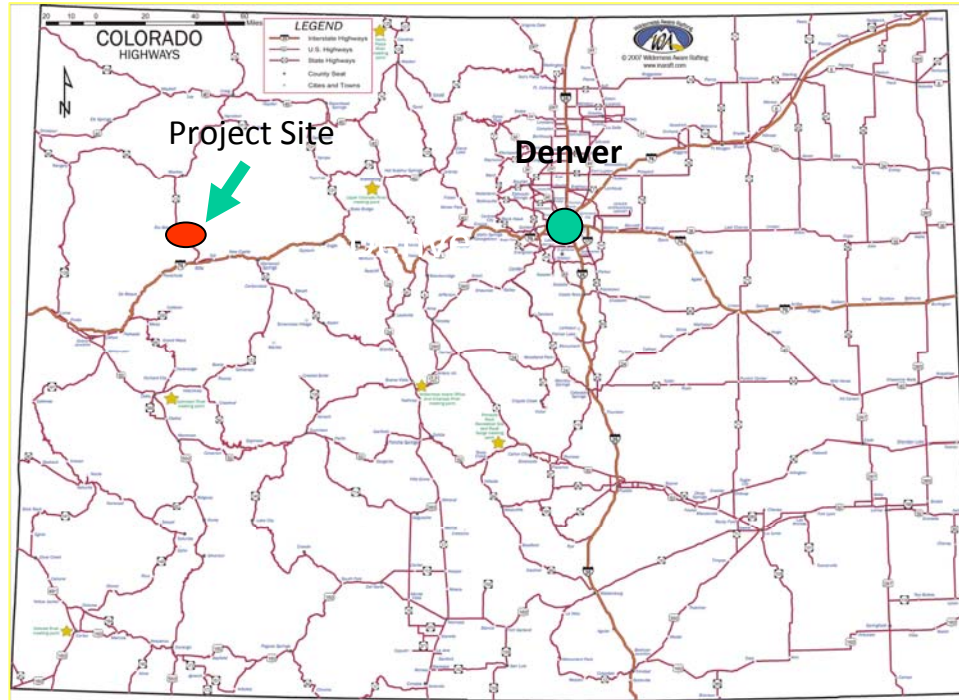
Figure 1. General location of the project area

SITE GEOLOGY

The project area lies along the Grand Hogback on the western flank of the White River Uplift. The geologic materials at the project site consist of native sandy and/or silty clays overlying moderately weathered claystone, siltstone, and sandstone of the Wasatch Formation (Tertiary age). The embankment fill lies on the native clays that overlay the Wasatch Formation. The embankment fill consists of low to moderate plasticity clays and sandy or silty clay material, borrowed from the native soils in this area.

The embankment fill section of the roadway had been placed over a deeply incised drainage bottom. Figure 2 depicts the general site layout looking south along SH 13. Figure 3 depicts the roadway and guardrail distress.

Figure 2. Aerial Photograph of the Project Site (Prior to Emergency Repair) - Looking South. Red Oval Indicates Section of Embankment Fill. Red Arrow Depicts Active Failure Section.

Figure 3. View Looking South Depicting Roadway Distress.

ANALYSIS OF THE EMBANKMENT LANDSLIDE

Subsurface Investigation

Yeh and Associates, Inc were contracted as a sub-consultant under an HDR Engineering, Inc. task order with CDOT. The geotechnical investigation was undertaken to provide long-term mitigation options to CDOT and supplemented previous geotechnical investigations conducted by CDOT Geotechnical Program. The drilling investigation within the project area took place between January 22, 2007 and August 23, 2007 (one sequence in right of way (ROW) and another sequence outside of ROW) utilizing a track mounted CME 55 drill rig. A total of 23 geotechnical and pavement borings were advanced to varying depths.

A total of 40 soil/bedrock samples were tested to determine the classification and engineering characteristics of the on-site materials. Laboratory tests performed included sieve analysis, Atterberg limits, natural moisture content, in-situ dry density, swell/consolidation, unconfined compression, R-value, direct shear, water-soluble sulfates, and pH.

The laboratory classifications indicated the subsurface materials at the site consist of silty and sandy clays (CL), silty sands (SM), clayey sands (SC) and sandy silt (ML) according to the Unified Soil Classification System (USCS), or A-2 to A-7 materials based on the American Association of State Highway Transportation Officials (AASHTO) classifications. The subsurface materials displayed non-plastic to moderate plasticity characteristics.

Inclinometers

Previous to the Yeh and Associates, Inc geotechnical investigation, CDOT Geotechnical had installed three inclinometers, designated INC-1, INC-2, and INC-3, in March of 2006. INC-1 was installed on the east side of the roadway at an approximate elevation of 7320 feet to a depth of 74 feet, INC-2 was installed on the west side of the roadway at an approximate elevation of 7314 feet to a depth of 74 feet, and INC-3 was installed at the base of the west embankment at an approximate elevation of 7274 feet to a depth of 68 feet. INC-1 showed no signs of movement, INC-2 sheared at a depth of 45 feet (elevation 7269) by April 20, 2006, and INC-3 sheared at a depth of 38 feet (elevation 7236) by May 16, 2006. Figure 4 depicts the general locations of the inclinometers.

Figure 4. Approximate Inclinometer Locations Installed by CDOT.

Based on the inclinometer readings from CDOT and subsequent inclinometer instrumentation by Yeh and Associates, Inc, it appeared that at least two separate failure mechanisms were present at the site:

1. Shallow embankment fill failures slumping off oversteepened embankment slopes. This was triggered by the presence of surface and sub-surface water decreasing the slope stability.
2. Deep seated embankment failures due to the inherently unstable foundation soils underneath the embankment fill.

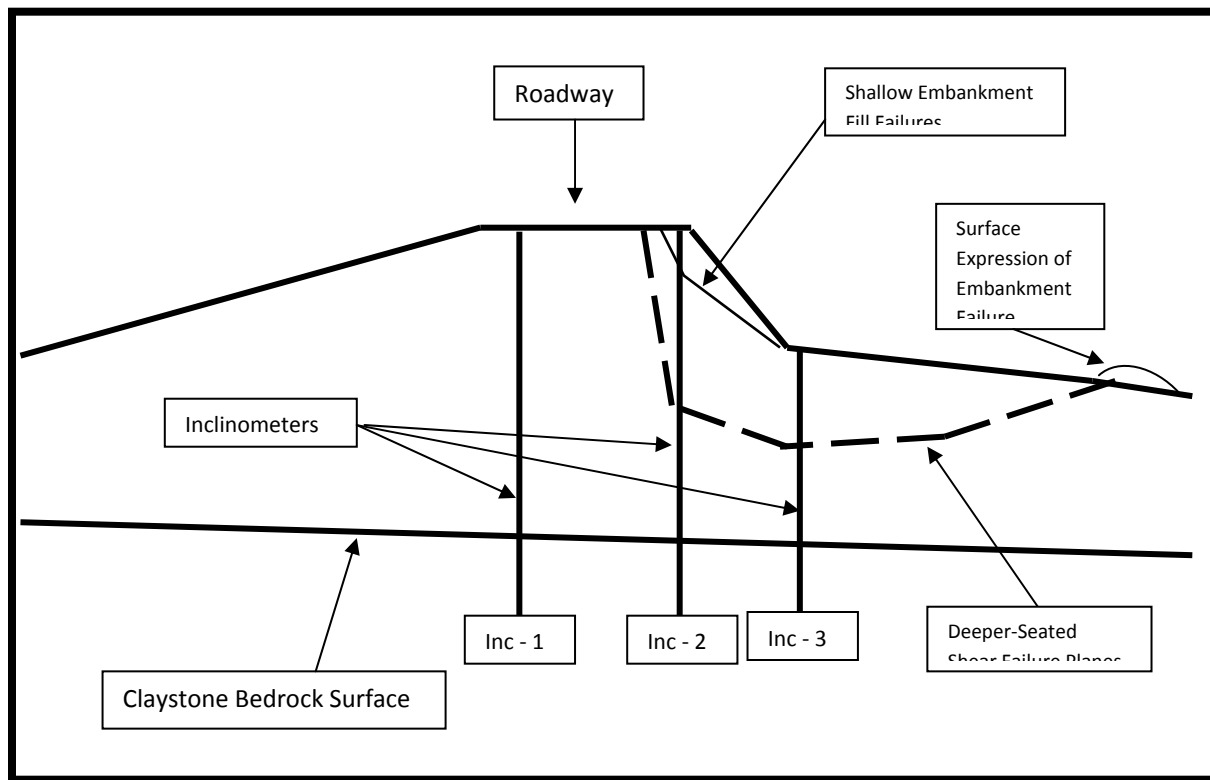Figure 5 depicts a generalized cross section of the failure mechanisms.

Figure 5. Generalized Cross Section Looking South Through The Embankment Fill Failure.

During March of 2008, CDOT maintenance crews reported pavement cracking that formed a "half-moon" shape with displacements that ranged from 3 to 12 inches horizontally and vertically. The "half-moon" shape was much larger and more extensive than any other previous failures that had occurred in previous spring runoff seasons. Vertical displacements on the order of feet per day were occurring. Figure 6 depicts the filled in half moon section with asphalt. Figure 7 depicts the vertical displacement that the roadway section was subjected to. Figure 8 depicts the surface expression of the deep seated shear failure.

Figure 6. Depicts The Use of Asphalt To Fill In The Half-Moon Section of Roadway.

Figure 7. Vertical Displacement of Pavement Section – Approximately 2 Feet Within A Few Weeks.

Figure 8. Surface Expression of The Deep Seated Shear Failure.

At this point, the investigation undertaken by Yeh and Associates, Inc became an emergency repair project. Based on the results of our geotechnical investigation, previous CDOT geotechnical investigations and evaluation of the embankment failure, Yeh and Associates, Inc recommend that the failed embankment be replaced with lightweight expanded polystyrene (EPS) fill. Based on the analysis, a global factor of safety between 1.20 and 1.30 could be achieved using this mitigation method. Successful use of the lightweight EPS fill occurred at four locations in Colorado between Durango and Mancos along US 160. These designs were done by Yeh and Associates, Inc and constructed by CDOT.

The proposed EPS fill was designed with a density of 1.15 pcf, minimum compressive strengths of 5.8 psi and 16.0 psi at 1% and 10% deformation respectively, and maximum water absorption of 3%. The EPS section was also designed to replace a minimum of 10 vertical feet of roadway fill with a concrete cap and an impervious liner was also placed on top of the EPS to prevent petroleum products from affecting the EPS material. One very important aspect of the design was to include a free-draining system for subsurface water behind and underneath the proposed EPS material. The EPS was also tapered on both sides of the excavation cut to reduce the potential for differential settlements to occur in the roadway between the EPS and fill.

CONSTRUCTION - EXPANDED POLYSTYRENE FILL

Based on the recommendations above, an Emergency Mitigation Project was undertaken by CDOT to stabilize the embankment fill failure. At the request of CDOT, HDR and Yeh and Associates provided a construction advertisement package within a few weeks. Construction and placement of the EPS was done between April and June of 2008. Figures 9 to 13 depict a summary of the construction sequence.

Figure 9. Start of Emergency Project – Looking South (Note deformed guardrail alignment).

Figure 10. Excavation of Site – Looking South.

Figure 11. Placement of EPS Blocks In Excavation.

Figure 12. Completion of Project June 2008.

Summary

The project was completed over four weeks at an approximate total cost of $2 million for 300 linear feet of EPS stabilization. EPS costs were approximately $80 per cubic yard. It was necessary to run traffic in one lane for approximately 2 weeks of the construction effort. Geologic and geotechnical assessment of the site and geo-structural designs were integral to completion of the project.

Overall, the wall systems appear to be performing as they were designed. It was imperative to have the geotechnical/geo-structural designer involved in both the design and the construction process since a multitude of construction issues arose during the construction. Communication between the Owner, Contractor, Subcontractors and Designer of Record was imperative for the successful completion of this project. Figure 16 depicts the project approximately one year after completion following a heavy spring runoff.

Figure 13. Status of Project Site After Construction in May 2009 – One Year Later.

2.1

Innovations in Rockfall Barriers
and the New European Standard ETAG 027

Frank Amend (author/presenter)
Regional Sales Manager, Southeastern United States
Geobrugg North America, LLC, PO Box 7453
Rocky Mount, NC 27804-0453
frank.amend@geobrugg.com

ABSTRACT

Current rockfall mitigation designs and techniques span preventing the rocks from becoming loose on a rock face/slope to catching them as they near a pre-selected area at the slope's bottom. Many different types of barrier material have been employed to entrap the rocks as well. To design and approve the barriers, previously different testing techniques were utilized with different test site geometries and procedures. This resulted in data that was not easily comparable across testing protocols. The recent endorsement by EOTA (European Organization for Technical Approvals) of an ETAG (European Technical Approval Guideline) for testing and assessing the acceptance for rockfall barriers will soon bring about changes to the marketplace and could influence the American Association of State Highway and Transportation Officials (AASTHO) guideline in the United States. This paper will address the new guideline and present new barrier designs that will incorporate the most recent barrier innovations.

Figure 1: Rockfall Barrier during Installation

INTRODUCTION

Two (2) types of rockfall protection methods have been employed to mitigate rockfall:

- Active Systems like TECCO mesh with soil nailing to prevent the blocks from breaking off the rock walls
- Passive Systems: Drapes, ditches, rockfall shelters, ground embankments, and net barriers which control, intercept or deviate the blocks during their movement down the slope

In the past history of rockfall barrier design, no testing was used to derive energy ratings and early testing to verify design was by full-scale, drop testing. There were approval processes and guidelines put in place: most notably BAFU, the Swiss guideline, and AASHTO (proposed but never adopted), for the United States. The following contains comparisons of these to the present EOTA guidelines:

Criteria	Europe (EOTA)	Swiss (BAFU)	US (AASHTO)
Test angle	0 – 90°	90° only	0 – 90°
Small blocks	No	Yes	Yes
Pre-test	2 x 33%	1 x 50 %	1 x 50 %
Main test	1 x 100 %	1 x 100 %	1 x 100 %
Residual height	Cat. A, B ,C	> 50 %	> 60 %
Deflection	Declared only	Limited	Limited
Test heights	Indirectly defined	Exactly defined	Exactly defined
Cable forces	Evaluated	Evaluated	Evaluated
Baseplate Forces	Not evaluated	Not evaluated	Evaluated
Tolerances	+/- 7 % (energy)*	None	None
Maintenance	Not evaluated	Evaluated	Evaluated

It can be argued that the vertical tests are the most comprehensive as all forces can be directly measured. Therefore the Swiss guideline would be the most restrictive and a general argument could be made to primarily accept vertical tests and with EOTA category A residual height. Furthermore it must be noted that a weakness of the EOTA guideline is that maintenance is not assessed at all.

Analytical methods for the mathematical determination of the rockfall phenomenon have been set up by several researchers, almost all in the last twelve years, and they allow the statistical forecast of the block trajectories – most notably the Colorado Rockfall Simulation Program (CRSP). When height of the trajectory and the energy to be absorbed can be calculated, the correct barrier can be chosen and designed.

With reference to rockfall barriers, many tests were carried out in the past by some manufacturers and research institutions, but each of them followed a different standard and the results were not easily comparable. For this reason the EOTA (European Organization for Technical Approvals) recently endorsed the new ETAG 027 (European Technical Approval Guideline) where the testing procedure for CE marking of a rockfall barrier is settled. According to the Construction Products Directive 89/106/EEC, the European Technical Approval (ETA) is a harmonized technical specification and is considered as a favorable assessment of a product for its intended use. The ETA provides the basis for the certification procedure to award the CE approval marking to the product and its basic tenets are as follows:

- It is not just one full-scale test
- Manufacturer must submit application to an approval body
- Full-scale tests by a notified test institute (accredited by European Commission for ETAG 027) must be conducted
- Individual identification tests of components used in 1:1 test must be performed
- Factory production control FPC (initial and continuous) must be conducted
- European Technical Approval ETA (circulated to all approval bodies for review) must be obtained
- CE Marking is then awarded and applied to the product

This guideline will influence the approval for rockfall barriers: the producers must certify their products follow the described test procedure to sell them in Europe. Furthermore the designers must take this data into account for a correct choice and design evaluation (i.e. energy that can be absorbed under safe conditions, maximum displacement during the impact, forces acting on the foundations).

CONTENTS OF THE ETAG 027

General Aspects

A rockfall barrier is comprised of the following elements: interception structure (usually a metallic net), a support structure (posts), and connection components (ropes and energy dissipating devices), which are secured to foundations buried in the ground.

Barrier Elements

Main Parts	Components	Function
Interception Structure	Principal net; comprised of cables, wires and/or bars (i.e. cable nets joined with clamps, submarine nets, or ring nets - for the last two the rings forming the net are connected to each other). A mesh backing is usually attached to the principal net to catch smaller rocks.	Bears the direct impact of the rockfall event, deforms elastically and/or plastically, and transmits the stresses to the connection components, the support structure, and the foundations.
Support Structure	Posts which may be fabricated from different materials, geometries, and lengths (i.e. pipes, structural components, etc.) and which may be directly buried into the ground or mounted on a pedestal.	Provides the barrier's overall height. Can be connected to the Interception Structure directly or via the Connection Components.
Connection Components	Ropes, steel cables, junctions, clamps, and energy dissipating devices (i.e. brake rings which disperse energy and/or allow a controlled displacement when stressed).	Transmits the stresses to the foundation structure during impact and/or maintains Interception Structure in position.
Foundation	Not part of the ETAG – to be designed by the engineer based upon technical data.	Transmits the forces from the impact to the ground.

Figure 2: Post

To correctly size the rockfall barriers, the following parameters should be known: maximum energy which can be absorbed in safe conditions and the maximum displacement of the interception structure considering the design energy and the loads acting on the foundations and the structural elements during the impact. The only way to validate these parameters and the barrier is to conduct full scale testing.

Barrier Classification

In the guideline, the parameters useful to determine the barrier fitness are defined. The barrier fitness means that the product can satisfy the essential requirements. For rockfall barriers the fitness assessment includes the energy absorption of the assembled system when a regular block impacts the barrier. Two energy levels are defined: SEL "Service Energy Level" and MEL "Maximum Energy Level".

The tests are fully described in the guideline. The barrier must be tested with both energy levels to obtain CE marking. The table below classifies the rockfall barriers taking into account the energy level:

Rockfall Barrier Classification

Energy Level Classification	0	1	2	3	4	5	6	7	8
SEL (kJ)	-	85	170	330	500	660	1000	1500	>1500
MEL (kJ) ≥	100	250	500	1000	1500	2000	3000	4500	>4500

Test Procedure

The tests are carried out by impacting the rockfall barriers with a regular block (all net barriers must be impacted in the central zone of a three zone barrier. The maximum block size shall be 3 times smaller than the nominal height of the barrier and the average speed of the block shall be greater or equal to 25 m/s.

Characteristics of the initial type testing are:

- 1:1 full-scale test with at least 25 m/s
- No ground contact allowed for all tests
- Energy classes 0-8 (100 kJ to >4500 kJ)
- SEL: Service Energy Level (2 x 33%)
- No maintenance in between the two SEL tests
- Residual height after the first SEL test of at least 70%
- MEL: Maximum Energy Level (100%)
- Residual height: Category A (>50%), B (>30%) or C
- Identification tests of the tested components

The Service Energy Level (SEL) test is carried out with two launches of a block into the rockfall barrier at the same kinetic energy. The test is passed if:

- after the first launch, the block is stopped by the barrier, there are not ruptures in the connection components, the opening of the mesh are smaller than two times the initial size of the mesh and the barrier's residual height after the impact (the minimum distance between the lower and the upper rope, measured orthogonally to the reference slope after the test without removing the block) is equal to or greater than 70% of the nominal height of the barrier before the test
- after the second launch the block is stopped by the barrier.

The MEL test is carried out with one single launch of a block into the rockfall barrier. The rockfall barrier passes the MEL test if the rockfall barrier stops the block and the block does not touch the ground until the barrier reaches the maximum elongation during the test. During MEL testing the maximum displacement of the structure should be measured, but it should not have a limited value.

Product Characterization

The materials used to build the test barrier should be the same used for the final barrier design. In addition the corrosion protection for the ropes, nets, and posts shall be evaluated. These checks verify that the tested barrier is the same one as described in the design documents and will be installed on a job site.

Conformity Verification

In the CE marking process for a rockfall barrier, the verification of conformity requires the manufacturer to employ factory production control (FPC) and provide further factory sample testing in accordance with a prescribed test plan as described here:

- FPC must be made by an accredited body
- Initial inspection of factory must be made before issuing ETA
- Continuous surveillance (once a year) must be conducted

- Control plan must be developed and implemented based on the specifications in ETAG 027
- Component tests of produced components must be done
- Results should be compared to the results of identification tests
- Material certificates of purchased materials must be obtained
- ISO 9001 is recognized as a good technical basis but is not sufficient to comply with ETAG 027

The directions for installing the rockfall barriers shall be obtained from the manufacturer's installation guide. The Approval Body shall verify the quality and sufficiency of the installation guide (i.e. regarding clamp bolt torque, the number and type of clamps to be used for connecting the ropes, the foundation types [for posts and cables], and/or the installation procedure of the energy dissipating devices). The guide shall contain drawings to show the standard geometry of the barrier and the installation scheme as well as the technical specifications for all the components.

The height of the barrier cannot be reduced in comparison with the tested kit and its height cannot be raised up of more than 1m for tested height superior or equal to 4m and 0.5m for tested height less than 4m. The manufacturer shall provide geometric tolerances in the installation guide with special references to the spacing of the posts and the inclination of the main ropes.

If it is necessary to have a different geometry from the test site one due to local geology, a specific design shall be provided. Forces acting in the structure should be evaluated to demonstrate the fitness for verification of the final rockfall barrier design.
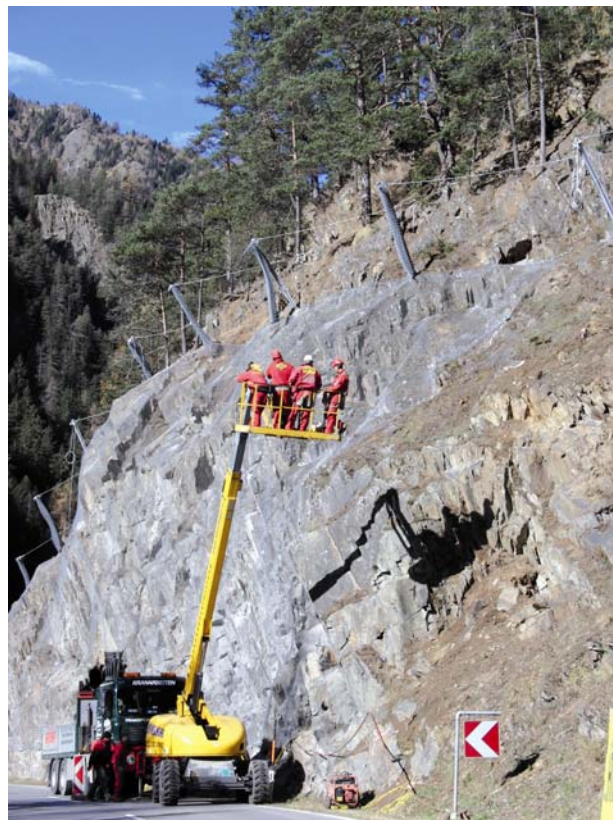
Figure 3: Overview of Installation Site

GUIDELINE LIMITATIONS

- Barrier heights: wide parameters (+0.5/+1.0m higher than tested) will result in many required tests which will increase costs
- Test heights are not clearly defined and will vary from supplier to supplier
- Small blocks not considered which could lead to big net apertures
- Maintenance not considered which could lead to system which are expensive to maintain
- Since residual height for Category B and C often have unacceptable residual heights, Category A has the greatest chance for success
- Deflection only declared
- ETAG 027 will serve as basis for the standardization of rockfall barriers - ETAs are required for such barriers and "certificates", "test reports", etc. alone are not adequate to compare the different products
- First barriers with ETAs can be expected in 2009
- It is recommended that purchasing agencies should wait for products to be awarded ETAs before using the ETAG 027 as a purchasing criterion - Even then engineering know-how and knowledge of the product is essential for non-standard applications

DESIGN PARAMETERS CHOOSING A ROCKFALL BARRIER

To establish the optimal rockfall barrier requires a determination if the eventual event will likely be either a single block fall or a bevy of rocks and if the rockfall event will occur during a single time interval or repeated ones at the same area. In case of repeating events with high energy levels and distinct time domain, the barrier(s) should be designed with reference to the Maximum Energy Level (MEL) while applying a suitable safety factor.

The Service Energy Level SEL verifies the effectiveness of the restraining system to control minor events, which might occur on a more frequent basis. In this case it is not necessary to proceed with repair or maintenance after each event.

In the case of slopes subjected to frequent falls of little to average blocks occurring along the same alignment, it is possible to undertake two different design methods: two alignments of MEL-based design restraining nets or an alignment of SEL-based design restraining nets, which must be able to control the maximum energy which the blocks may develop.

The choice of the which rockfall barrier to use should be based on an ultimate limit state design (MEL approach), applying suitable safety factors to the actions characteristic values determined by the trajectories analysis and to the effective energy level attested by the European Commission. The determination may also instead utilize the service limit state (SEL approach) applying suitable safety factors to the actions.

The determination must take into account:

- the energy that can be dissipated by the rockfall barriers in safe condition is greater than design energy of the application, that is the project energy of the block, which moves with the calculated velocity
- the interception height, which is the barrier height, to the average slope in the installation zone is greater than the design interception height
- the barrier maximum deformation, when it is subjected to a MEL impact, multiplied by a safety factor must be smaller than the design distance between the area that must be protected and the rockfall barriers

CONCLUSIONS

While the Swiss BAFU guideline was the first of its kind in Europe, the EOTA guideline is recognized as the first one accepted and approved by all of Europe. The new ETAG 027 on rockfall barriers and its application will be important in the future of rockfall protection devices, since it defines a uniform international testing standard thus permitting the comparison of the various products based upon the energy levels they can absorb. Furthermore, other significant information for designers, like maximum elongation of the rockfall barriers and forces applied to the foundations, are provided by the full scale tests and will permit improvement of a barrier's design and quality.

Figure 4: Hybrid Barrier Design

2.2

Controlling Large Rockfalls on Steep Slopes, the Kama Bluffs Experience

David Wood, David F. Wood Consulting Ltd., Sudbury, Ontario, Canada
        (705) 673-8080 info@dfwood.com
Peter McKenna, Engineering Northwest Ltd., Thunder Bay, Ontario, Canada
        (807) 623-3449 pmckenna@enl-tbay.com
Derek Daneff, Ministry of Transportation, Thunder Bay, Ontario, Canada
        (807) 473-2153 derek.daneff@ontario.ca
Stephen Senior, Ministry of Transportation, Downsview, Ontario, Canada0
        (416) 253-3743 stephen.senior@ontario.ca

Abstract

Over the last few decades Ministry of Transportation personnel had observed sporadic, large scale rockfall events originating from an igneous rock mass forming pronounced bluffs above the TransCanada Highway near Kama, Ontario, Canada. A preliminary design agreement was entered into to evaluate the potential rockfall hazard and to recommend a range of solutions. A subsequent agreement was let for the detailed design of site-specific remediation of the lower, highway cut incorporating machine scaling and trim blasting followed by ditch clean out, as well as for the design of a high energy rockfall catchment fence to be installed along the crest of the lower slope to protect the highway from blocks of rock originating hundreds of metres above the highway.

A 200 metre long, 2000 kJ system was installed in 20 panels, each 10 metres long with 21 base plates, 22 upslope anchors connecting the cables to the fence posts and 16 lateral anchors dividing the overall fence into 4 independent sections. Construction for this project was deferred to allow nesting peregrine falcons the opportunity to raise their young without interruption and was completed within budget in the fall of 2008. The system was designed to restrain a 10,000 kg block of rock falling from the upper bluff, striking the talus pile below the rock face and then travelling downslope towards the highway. Block speeds of approximately 20 metres per second can be handled with the system as-designed.

This paper reviews the rockfall hazard potential, the remediation design process and the construction details of the final mitigation measures installed at the site.

Introduction

This paper describes the evaluation of rockfall hazards alongside TransCanada Highway 17 at Kama Hill in Northwestern Ontario, Canada, as well as the design and construction of a high energy rockfall catchment fence at the site. The project is located to the north side of the highway approximately 21km east of the intersection of Highways 11 and 17 at Nipigon, Ontario, see Figure 1. This stretch of highway has been identified as having high rockfall hazard potential and a number of rockfall events have occurred here in the recent past.

The design process included a site investigation program, an analysis and comparison of the various benefit and risk strategies including cost estimates, limitations and constructability issues associated with different options for rock slope rockfall hazard reduction, including tunnelling, realignment, cover and/or catchment, for the mitigation of rockfall hazards originating from within the upper rock bluffs at the site. Both preliminary and detailed design studies were carried out by David F. Wood Consulting Ltd., Sudbury, Ontario.

Figure 1. Site location map

Site Geology and Geomorphology

Adjacent to Highway 17, approximately 21 km east of the Highway 11/17 junction, Nipigon, the Kama Hill bluffs form high, towering escarpments along the eastern shores of Kama Bay where they rise more than 200m above Lake Superior, Figure 2. These mesas comprise the eroded remnants of thick diabase sills of the Upper Keweenawan Supergroup (Mesoproterozoic ~1100Ma) intruded into the metasedimentary rocks of the Sibley Group (Lower Keweenawan Supergroup ~1339Ma). The massive diabase sheets are broken by numerous vertical joints that result in the formation of a natural sheer cliff rock face. The underlying Sibley rocks consist of bright red to purple mudstones and impure shaley dolostones and dolomitic limestones with

interbedded sandstone. In locations, they are injected by thin, fine-grained diabase sills that pinch out abruptly.

The Sibley Group can be divided into the arenaceous to clayey dolomites of the Rossport Formation which is exposed in the 8-12 m high rock cut at road level, and the red to purple mudrocks of the Kama Hill Fm. that slope back above the rock cut crest forming part of the talus and the base of the natural cliff face. At the road level, differential erosion of interbedded fine-grained beds within the Rossport Fm. leads to periodic failure of overlying blocks. Spalling of smaller rock fragments along the rock face is also common. The lower portion of the natural cliff face (from 42m to 55m above road level) is composed of the horizontally bedded rocks of the Kama Hill Fm.

The Upper Sibley Gp. rocks have been intruded by a thick sequence of Nipigon diabase sills that rise up to 120 m above road level. The sills are quasi-conformable with the Kama Hill Fm. There are various, small natural benches within the cliff that separate the sedimentary rocks from the diabase, and that separate different parts of the intrusive flows. These benches are characterized by local talus accumulation and tree growth.

Figure 2 Overall site image with major features highlighted

Rock Mass Conditions

The rock mass conditions alongside Highway 17 in this area are atypical of those found elsewhere in Northwestern Ontario in the Precambrian Canadian Shield. The rock mass of the Rossport Formation is *moderately weathered, bedded and blocky, dark red to yellowish red to grey, medium-grained*, and *medium strong*. The rock types are of interbedded sedimentary rocks with low-grade metamorphism, originally sandstone, siltstone and dolostone with one diabase sill to 1.5 metres wide, horizontally bedded with poorly developed bedding plane separations. Rossport Fm. blocks are in the 15 cm size range, while the diabase sill has blocks in the 30 to 60 cm size range. Some well developed sub-vertical joints lead to toppling potential as well as local sliding on very steeply inclined base planes.

The rock mass of the Kama Hill Formations is *slightly weathered, bedded and massive, dark brownish red to dark greenish red, fine-grained*, and *medium strong*. The rock types are low- to medium grade metamorphic equivalents of interbedded mudrocks (siltstones and claystones predominantly) with weakly developed bedding plane partings, and strongly developed columnar jointing.

The rock mass of the Upper Keweenawan Supergroup diabase sills is interpreted from a close examination of blocks in the talus slope and at the highway level, together with information gathered during the helicopter inspection. This rock mass is *fresh, dark greenish grey, massive to columnar, coarse-grained*, and *very strong*. The rock type is most commonly described as diabase, although no detailed thin section analysis has been carried out.

Local rockfall hazards are commonly caused when intersecting rock mass discontinuities isolate rock blocks that are able to slide, roll, fall or topple from their *in situ* location. The severity of the hazard is a function of the size, shape and location of the rock fall material as well as the geometry of the slope and the alignment of highway at the toe of the rock slope. For the purposes of this study, rockfalls may be expected from the Rossport Fm. highway rock cut as well as from the Upper Keweenawan bluffs. Both styles of rockfall may produce a high hazard, and both should be addressed in a detailed design study for this area.

Helicopter Inspection

A series of passes was made from west to east at different elevations in order to gain different perspectives of the cliff area. The results were astonishing. The exact source locations for two rockfall events could be determined; these are believed to relate to the two anecdotal events in October 1996 and August 2003. Further, there were many occurrences of potentially unstable blocks and wedges, up to a column of rock estimated to be 15 metres high, 5 metres across and about 3 metres deep that has already toppled some 3-4 metres before becoming 'stable' again, see Figure 3.

The debris field of diabase material originating from the upper bluffs extends at least to the shoreline of Lake Superior. From the helicopter, one very large block of diabase can be seen near the CPR track that is estimated to be almost 100 cubic metres in size (250 tonnes). Another, similar sized, block can be seen between the railway and highway slightly to the east of this area. It has been incorporated into the drystone wall constructed above the railway tracks probably in the 1880s. In the vicinity of Station 19+095 to 19+115 there is a group of about seven, similar-

sized blocks in the 150-200 tonne range that originated from the Keweenawan Supergroup bluffs when a column of rock collapsed at some unknown time in the past. These types of extreme events are thought to represent 1 in 1,000 year occurrence. If it were necessary to control against this type of failure in the current design program, then the only solution would be to tunnel through the Kama Hill bluffs.
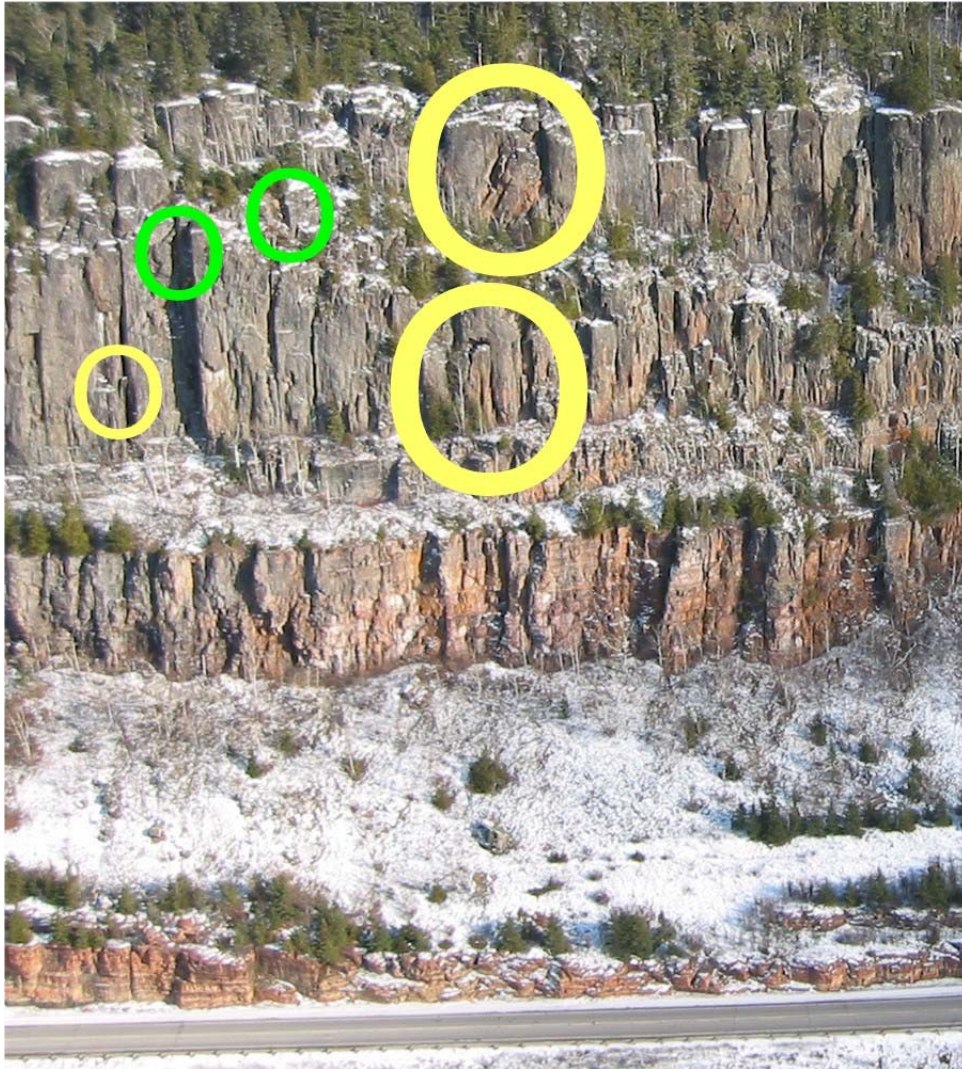

Figure 3.Worst area of Upper Keweenawan diabase, Station 18+925 to 19+950

Evaluation and Investigation of the Talus Slope Area

A specific terrain evaluation survey and preliminary subsurface investigation of the talus slope area above the highway rock cut was carried out and all geological and geotechnical engineering parameters related to slope stability assessment of this area were identified. This study was carried out in November, 2003. The principal considerations for this part of the study included:

- Determining the angle of the surface of the talus in different locations to compare the slope to the "angle of repose" of rock blocks;

- Evaluating the different materials making up the talus – Kama Hill Fm. metasediments and Keweenawan Supergroup diabase;
- Evaluating the weathering and alteration of rock materials on the surface of the talus to determine different levels of activity;
- Assessing the evidence for impact craters within the talus as indicative of rockfall activity from above and the influence this may have on stability of the talus; and
- Evaluating the vegetation within the talus slope as an indicator of long-term stability conditions.

Large diabase blocks were identified at the crest of the Rossport Fm. in the rudimentary chain link mesh fence, Figure 4.. Blocks measured to be 0.5 to over 4 m^3 in size, weighing an estimated 1,300 to 12,500 kg. Crest angle from here to Keweenawan crest is 64°. Limited evidence of such large falls to west. The talus is reasonably uniform with a 37° slope.

Figure 4. Large diabase block in chain link mesh fence, Station 18+891

The large blocks found across the talus are exclusively diabase and it appears that if the originating block is massive and elongate it strikes the talus and slides into it, coming to rest within the talus. For roughly equidimensional blocks, it appears that the block is probably rotating as it falls and when it strikes the talus it is more likely to bounce, possibly more than once as it makes its way downslope, see Figures 5 and 6. The talus slope is reasonably uniform at 37°.

Figure 5. Diabase block embedded in talus, Station 18+970

Figure 6. Strike mark in talus, Station 18+965

Computer Rockfall Simulation

The software package "RocFall", distributed by Rocscience Inc. of Toronto was used to carry out a risk analysis of falling rocks from the upper bluffs at the Kama Hill site. The actual sections selected for study were taken from those provided by the MTO Geomatics section, and based on the results of the field review. The intent was to identify optimum design parameters related to the installation of a rockfall catchment system within the talus slope area above the highway rock cut. Discussions with various manufacturers of catch fences also took place.

The historical reports regarding the rockfall events that have happened at this site, and the field evidence of rockfall material observed during the site investigation program indicated that the "design event" for a return period of around 50 years is probably a block approximately 3.5 cubic metres in size. This corresponds to a rock block approximately 10,000 kg in weight. This was the size of block used in the RocFall simulation runs. It is quite likely that blocks of rock that are larger than this do become unstable from time to time, but they break up when striking either the lower bluffs or the talus pile such that the rock blocks that do become a hazard (i.e. reach the travelled portion of the highway) are in the design size range.

At this preliminary design stage of the project, it is considered appropriate to use the results of the simulations to evaluate rockfall catch fences that would restrain and contain 10,000 kg blocks. Base on an assumed installation location near to the crest of the Rossport Fm., at the toe of the main talus slope, a fence in the 2,000 kJ energy absorption range would protect against some 95% of the blocks falling in the most challenging locations, around Stations 18+900 to 18+925. The program allows the user to "drop" a number of rocks from the source location and have then bounce and roll according to coefficients of restitution input by the user and based on suggestions and recommendations in the software package. Most of the input parameters are given a standard distribution rather than a single value, so each run can give slightly different results even if the input parameters remain unchanged, see Table 1.

Table 1   Input parameters for RocFall simulation

Material type	Coefficient of normal restitution (Rn)	Coefficient of tangential restitution (Rt)	Angle of internal friction (Phi)	Slope Roughness over friction angle
Diabase	0.40	0.85	30	3
Kama Hill Fm.	0.35	0.80	30	0
Rossport Fm.	0.35	0.80	30	2
Talus cover (def)	0.32	0.82	30	0
Talus slope	0.37	0.75	37	0
Soil w. veg (def)	0.30	0.80	30	0
Asphalt (def)	0.40	0.90	30	0

Notes: (def) are default values used in RocFall. Other values selected based on a tutorial and tables provided with the software. The coefficient of normal restitution (Rn) is used with a standard deviation of 0.04 and tangential restitution (Rt) has a standard deviation of 0.02. The friction angle is used with a standard deviation of 2 degrees, except for the talus slope that is used with a single value. The various parameters used were selected after a process of parametric sensitivity to 'calibrate' the model by attempting to duplicate the observed rockfall events and the final location of rockfall material from the anecdotal evidence.

The results of the simulation also show that the velocity of the falling rocks, and therefore the kinetic energy of the blocks is lowest right at the crest of the Rossport Fm slope. This then would be the most efficient place to locate a catch fence. It is also the most accessible part of the talus slope area when considering small equipment that may be needed for the project. Two different rockfall catchment fence-manufacturing companies have been approached regarding this project and both believe that this alternative is constructible. Costs have been estimated, see Subsection 5.4 below. Examples of RocFall runs are shown in Figure 7.
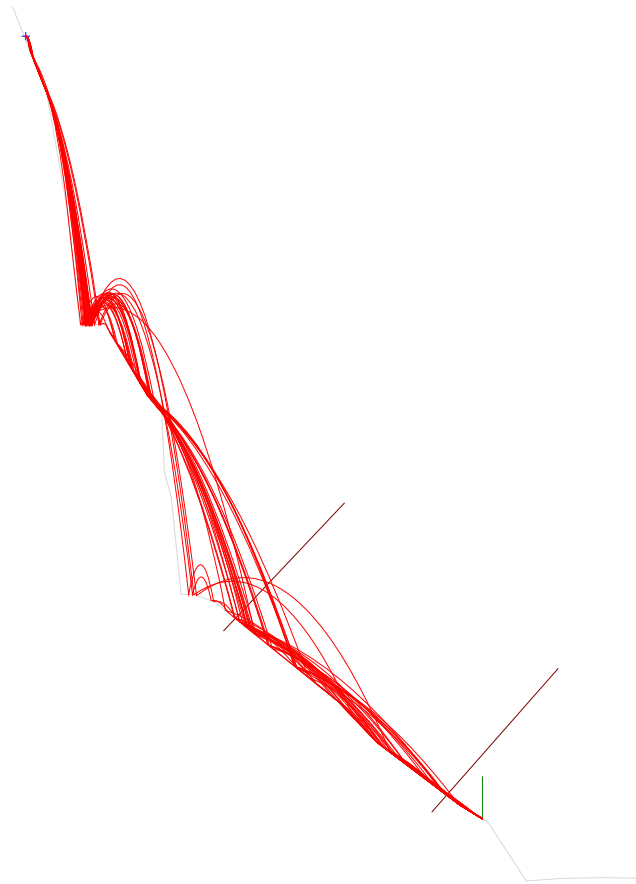

Figure 7. Station 18+925, example of RockFall output with 50 rocks

Analysis and Comparison of Benefit and Risk Strategies

The basic premise for this study is to carry out an investigation into the potential rockfall hazard a) from the Rossport Fm. rock cut adjacent to the highway and b) from the upper bluffs, predominantly the Upper Keweenawan diabase sills, and to evaluate the various strategies that may be considered to mitigate the hazard. It is again noted that this was to be a preliminary evaluation and that detailed design would follow in a separate study.

The following paragraphs consider different strategies in terms of benefit, residual risk, constructability, cost, and impact. Some treatments would have to be considered in combination with others, some would be sufficient on their own. The hazard exists because of potentially loose rock in a location that will allow it to fall and reach the highway.

- The loose rock can be dislodged intentionally to be brought down to highway level under control, or at least at a known time.
- The loose rock can be pinned in place using rock bolts or cables to prevent it from falling.
- The loose rock can be allowed to fall as and when nature dictates provided that there is a safe place to fall that does not constitute a rockfall hazard.
- The loose rock can be allowed to fall and measures are taken to prevent there being a rockfall related accident.

In this way, hazard mitigation can be subdivided into four categories: remove, reinforce, contain and protect. The results are presented in Table 2.

Cost Estimate

Cost estimates for the proposed work at the Kama Hill site were developed during the detailed design phase in 2007 and are included in Table 3.

Item	Base Cost	Unit	Required amount	Estimated Cost ($)
Highway Rock Cut - Remove				
Scale Rossport Fm	$700.00	$/hr	40	$28,000.00
Trim blast Rossport	$295.00	$/m	160	$47,200.00
Ditch clean out	$700.00	$/hr	20	$14,000.00
HERCF - Contain				
Trumer TS-2000-ZD*	$570.00	$/m	200	$114,000.00
Ancillary components**		Lump sum		$50,000.00
Mob-Demob		Lump sum		$20,000.00
Construction, labour	$4,500	$/day	45	$202,500.00
Ancillary equipment***		Lump sum		$80,000.00
Traffic Control		Lump sum		$30,000.00
Contingency		Lump sum		$60,000.00
Construction Cost				**$645,700.00**
Administration****			20% of construction	**$129,140.00**
Total Estimated Costs				**$774,840.00**
* baseplates, posts, post heads, net, bearing ropes, retaining ropes, braking elements, wire rope clips, shackles and shipping included in estimate				
** supplementary mesh netting, anchors for base plates, micropile tubes, concrete, side anchors, upslope anchors included in estimate				
*** crawler drill, crane and loader included in estimate				
**** contract administration, QA/QC, environmental and maintenance included in estimate				

Table 3. Costs estimates for rockfall hazard reduction measures planned (CDN$).

Concept	Item	Source	Base Cost	Unit	Cost CDN$/m	Required amount	Estimated Cost (CDN$)	Installation/ Comment	Potential Success	Residual Risk	Construction Disruption
Remove	Scale upper face	Estimate	$3,000	CDN$/day	$600	500	$300,000	Ass. 5 m/day	Low	Moderate	High
	Excavate talus	Estimate	$30	CDN$/cu. m	$900	500	$450,000	Ass. 30 cu. m/m	Moderate	Low	Low
	Scale Rossport	Estimate	$450	CDN$/hr		50	$22,500	Ass. 50 hr	High	Low	Moderate
	Trim Rossport	Estimate	$325	CDN$/hr		90	$29,273	Est. 90 m	High	Low	Moderate
Reinforce	Bolt/cable face	CPR	$150	CDN$/m		1450	$250,000	Per 72.92 HeBa	Low	Moderate	V Low
	Buttresses	CPR	$1,500	CDN$/cu. m		65	$97,500	Per 73.14 HeBa	Moderate	Low	Low
Contain	Brugg RX-300-10	Geobrugg	$1,115	US$/m	$1,505	300	$451,575	$72,000	High	Low	Low
	Brugg RX-300-8	Geobrugg	$1,224	US$/m	$1,652	300	$495,720	$72,000	High	Low	Low
	Mountain 2000 kJ	Mountain	$75,000	US$/100m	$1,012	300	$303,750	$72,000	High	Low	Low
	Mountain 3000 kJ	Mountain	$87,000	US$/100m	$1,174	300	$352,350	$72,000	High	Low	Low
Protect	Rock shed	CPR	$3,000,000	CDN$/174m	$17,241	300	$5,172,413	Per 31.1 Mntn	High	V Low	V High
	Tunnel	Hoek	$12,000	US$/m	$16,200	1,500	$24,300,000	Average cost	V High	V Low	Low
	Silver Creek Cliff	Internet	$15,000,000	US$/1400ft	$35,142	1,500	$52,714,285	1994-1995 cost			
	Signage	Estimate		Lump sum			$10,000		Moderate	High	V Low
	SBGR barrier	MTO	$120	CDN$/m	$120	300	$36,000		Moderate	High	Low
	Realign highway	Estimate	Elevated		$15,000	500	$7,500,000		Moderate	Low	V High

Table 2. Comparison of Mitigation Measures

Construction

The Contract was awarded with a fixed completion date of October 31, 2008. Work in the field began on September 4, 2008 with all operations ending on September 30, 2008. Contract administration was provided by Engineering Northwest Ltd.

Pacific Blasting and Demolition Ltd., Burnaby, B.C. was awarded this contract. The work included placing a high energy rockfall catchment fence in the designed location, trim blasting then machine scaling the rock face along the highway to mitigate local rockfall hazard, ditch cleanout under the rock face area, and providing appropriate traffic control for public safety.

Pacific Blasting contracted Trumer Schutzbauten Canada Ltd, Vancouver, B.C. to supply the catchment fence, posts, and all required fasteners. The catchment fence is an imported product from Switzerland and has a number of advantages over the traditional fences used. All catchment fences are designed with the understanding that after active use the fence needs to be inspected and any damage to the fence repaired. Unlike other fences the Trumer fence is designed to be placed in sections with an anchorage system provided for each section. In the event that the fence is used to stop a large rock, the potential maintenance or repair to the fence is limited to the damaged fence section rather than the whole fence.

The fence placed on this contract is currently the longest fence of this type in Canada providing a kinetic energy impact resistance of 2000 KJ. The Kama Hill fence is made up of 20 x 10m sections for a total length of 200m. There are 21 anchor base plates for the fence posts to be mounted on and each base plate has two anchors. There are also 22 upslope anchors connected with cables to the fence posts and 16 lateral anchors breaking the fence into 4 independent sections acting as intermediate retention anchors, see Figure 8.
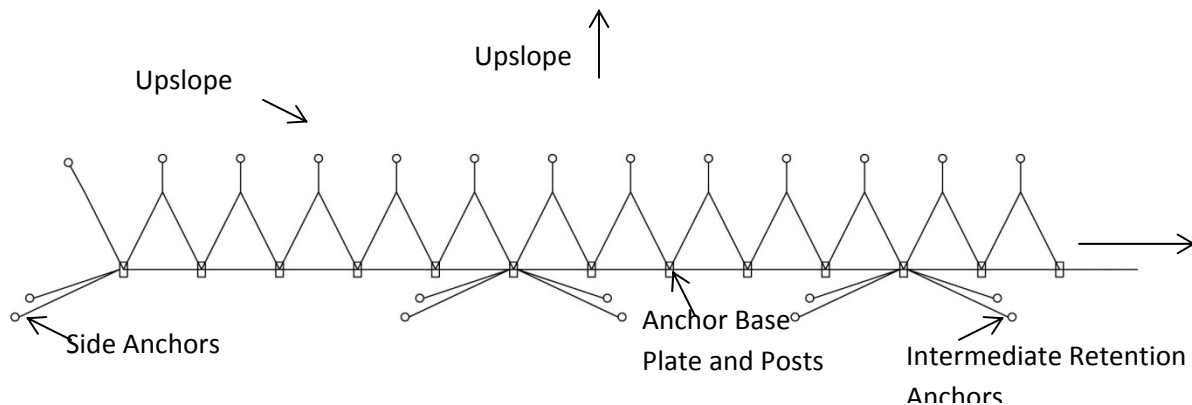

Figure 8: Top View of Fence (2 Sections)

The anchors were grouted in place as they were being drilled to the designed depths. Each of the base plate anchors were drilled and grouted into solid rock. The upslope anchors were drilled

and grouted to the required depths into the talus material on the slopes. Each of the base plate anchors was pull-tested by the contractor and witnessed by the on site consultant inspector.

Pacific Blasting arrived on site September 4, 2008 and began construction. The Contractor used a Komatsu 135 backhoe to construct an access road to the plateau where the fence was to be located. Once the area for the fence was cleared and levelled, the locations of the posts were marked out and materials were brought up. 21 concrete blocks were dug into place to provide a level surface for the base plates and posts to sit on, Figure 9. The areas around the concrete pads were filled in and compacted. Each concrete block arrived on site with existing holes in the correct locations for the anchors.

Figure 9. Preparing talus for installation of concrete bases for steel posts.

Once the concrete pads were in place an Air Track 750 drill was used to install the anchors, see Figure 10. A grout mix was pumped to the drill and fed through the anchor rods during the drilling process. This ensured that the anchors were held securely in place and also provided a form of lubricant to facilitate the drilling. Grout cubes were cast for 7-day, 14-day and 2 at 28-

days to ensure that the strength of the grout met with the manufacturers' specifications, which they did.

Figure 10. Drilling base plate anchors.

After the anchors were placed the base plate anchors were tested in tension. The required hydraulic pressure for the pull test was 60 kip or 4600 psi, and each anchor passed, see Figure 11. The Contractor then used the Komatsu backhoe to erect the fence and posts while the anchor cables were placed to support the complete system, Figures 12 and 13. The Contractor completed the erection of the 200m fence in 6 days.

Figure 11. Pull-test apparatus on base plate.

Figure 12. Erecting fence and cables.

Figure 13. Erected fence.

Another component of this contract was trim blasting and machine scaling of the rock face adjacent to the highway. The Contractor found that trim blasting was not necessary and using a Volvo EC 360 backhoe on the rock face was appropriate to remove the potential hazard, Figure 14. Following behind the backhoe, which was used to remove the large rock blocks, the Contractor had two scalers tied off to ropes remove the smaller rocks using 4-foot pry bars, Figure 15.

Conclusion

Over the period from late 2003 to 2007 a preliminary investigation was carried out, initial designs were completed and a detailed design agreed to. Finalization of a contract package took place in early 2008 for construction during the 2008 working season. The actual construction activities were delayed for environmental reasons (there are nesting peregrine falcons at this site) and construction was carried out during September 2008.

The project was completed on time and under budget for a total cost of CDN$703,000.

Figure 14. Machine scaling.

Figure 15. Manual scaling.

2.3

Ring Net Drapery for Rockfall Protection: Installation Observations

M. Fish[1], T.C. Badger[1], S.M. Lowell[1], and D. Journeaux[2]

ABSTRACT

To evaluate cost- and performance-competitive materials to cable net drapery, WSDOT proposed a study of ring nets to the FHWA as an Experimental Feature on a federally-funded rockfall mitigation project. At the time of the study, only one manufacturer was producing ring nets that could meet Buy-America steel requirements. To compare attributes and performance of various ring nets, a Buy-America steel waiver was concurrently sought from and granted by FHWA to allow foreign sources of ring nets. The project entailed covering a 300-ft-high slope, consisting of large diameter columnar to blocky basalt, with both standard unsecured and post-supported (hybrid) drapery. Four different ring nets were specified that included bound wire loops and wire rope rings utilizing either 4:1 or 6:1 weaves. Control sections of cable nets were incorporated to compare performance.

Results indicate that the ring nets with 4:1 weaves and wire rope rings had the greatest tendency to contract in width when lifted. In comparison, lightweight 6:1-weave ring nets and cable nets exhibited virtually no contraction. Pre-attachment of wire mesh to the ring nets that were prone to excessive contraction led to the widespread failure of the fasteners and the detachment of the wire mesh. Panel contraction resulted in greater effort to vertically seam adjacent panels. Material shortages were encountered due to the Contractor's (Janod) difficulty in stretching the contracted panels. Also, the considerable slope height resulted in some permanent ring deformation.

INTRODUCTION

The Washington State Department of Transportation (WSDOT) has used double-twisted hexagonal wire mesh and wire rope cable nets for several decades as slope protection to control rockfall initiating from slopes along state highways. Double-twisted hexagonal wire mesh has generally been applied to slopes with rock blocks less than 2 ft in diameter, while wire rope cable nets have been employed where larger blocks, typically up to 4-5 ft in diameter, are expected. In recent years, ring nets have been increasingly used for slope protection (drapery), mostly outside North America, to control large-sized rockfalls.

Because of the reported high strength of ring nets and the need to examine cost-competitive alternatives to cable nets, WSDOT proposed to evaluate ring nets for slope protection on a Federally-

---

[1] Washington State Department of Transportation, P.O. Box 47365, Olympia, WA 98504-7365; 360.709.5461.; fishm@wsdot.wa.gov; badgert@wsdot.wa.gov; lowells@wsdot.wa.gov

[2] Janod Ltd, 34 Beeman Way, P.O. Box 2487 Champlain, NY 12919; 518-298-5226; Daniel@janod.biz

funded rockfall mitigation project. A study of ring nets was proposed to the Federal Highway Administration (FHWA) as an Experimental Feature in August 2007, which was accepted and approved by FHWA in September 2007. At the time the study was proposed and approved, only one manufacturer was producing ring nets that could meet Buy-America steel requirements. To compare attributes and performance of various ring nets from known manufacturers producing ring nets outside the US, a Buy-America steel waiver was concurrently sought from and granted by FHWA to use these ring nets from foreign manufacturers.

The study was incorporated into a rockfall mitigation project (*Contract #7450 State Route 28 Rock Island – Rock Slope Nettings*) located in central Washington State about 12 miles east of Wenatchee on State Route 28. The project was to address rockfall hazards from a 300-foot-high natural/cut slope approximately 700 feet in length (Fig. 1). The north and south ends of the slope are near vertical. The middle portion includes an intermediate slope about 80 feet in width and inclined ~45º beneath a large overhang that extends back into the slope about 20 feet. Above the overhang the rock slope rises another 100 feet vertically to the crest of the slope. A soil nail wall was constructed beyond the rock slope crest as part of previously planned, but currently unfunded, highway widening project. The rock slope is composed of columnar to hackly basalt with typical block sizes ranging from 2 to 6 feet in diameter. The slope frequently produced rockfalls, some of which would reach the shoulder and travel lanes. The project entailed some initial safety scaling to remove large strained blocks/masses, and then a drape of ring net slope protection.

FIGURE 1. The 300-foot-high basalt slope consists of near vertical, northern and southern sections, a middle section with a prominent intermediate slope and overhang, and a soil nail wall beyond the slope crest.

DESIGN AND CONTRACT AWARD

During the project design phase, four ring net manufacturers, all that possessed a U.S. market presence, were identified and solicited to provide product information for potential inclusion in the contract. Based on product availability and the documentation provided, four types of ring nets, one from each of the manufacturers, were specified to cover an equal portion of the slope. These included two 4:1 and two 6:1 weaves, referring to how many rings are woven into each ring. The specified products included:

- Geobrugg: 300 mm diameter – 3 mm galvanized wire – 5 wires – 4:1 weave
- IGOR: 300 mm diameter – 2 mm galvanized wire – 7 wires – 6:1 weave
- Maccaferri: 300 mm diameter – 3.5 mm galvanized wire – 6 wires – 4:1 weave
- ROTEC International: 12 in diameter – 5/16 in wire rope – 6:1 weave

Because the study was intended to compare the performance of ring nets to cable nets, we attempted to select ring nets that were close in strength and weight to cable nets. The selected Geobrugg, IGOR, and ROTEC ring nets were thought to be close in this regard; however, Maccaferri only offered the heavier and stronger ring nets at the time of the contract preparation and award.

The slope protection was designed to include both a standard installation, which is secured along the slope crest to a top horizontal support rope that lies on the ground, and a modified (hybrid) installation, which lifts the top of the slope protection off the ground with steel posts to intercept rockfalls originating upslope of the installation. The standard slope protection was specified for the entire southern and northern sections, and the upper portion of the middle section. A section of modified slope protection was specified for the intermediate bench. All ring nets and cable nets incorporated double-twisted wire mesh on the outside to prevent smaller rocks from passing through the larger openings.

The coverage area for the slope protection was estimated using a digital terrain model (DTM) created with traditional survey and ground-based light detection and ranging (LIDAR) data. Using a geographical information system (GIS), we estimated the coverage area for the standard slope protection to be about 166,000 ft^2 and the modified section to be 59,000 ft^2, which included a 20% contingency to account for slope irregularities, necessary panel overlaps, and other uncertainties. The quantity estimates planned for the slope protection to extend to within 5 feet of the ditch line and 15 feet beyond the slope crest. A 20-foot-long tail was specified to cover the upper portion of the intermediate bench. The slope areas to be covered with standard and modified slope protection were divided into equal areas with approximately 52,000 ft^2 specified for each type of ring net (Fig. 2). In addition, two control sections of cable nets were included for approximately 16,000 ft^2 of coverage area. Total plan quantity for slope protection materials was 224,664 ft^2.
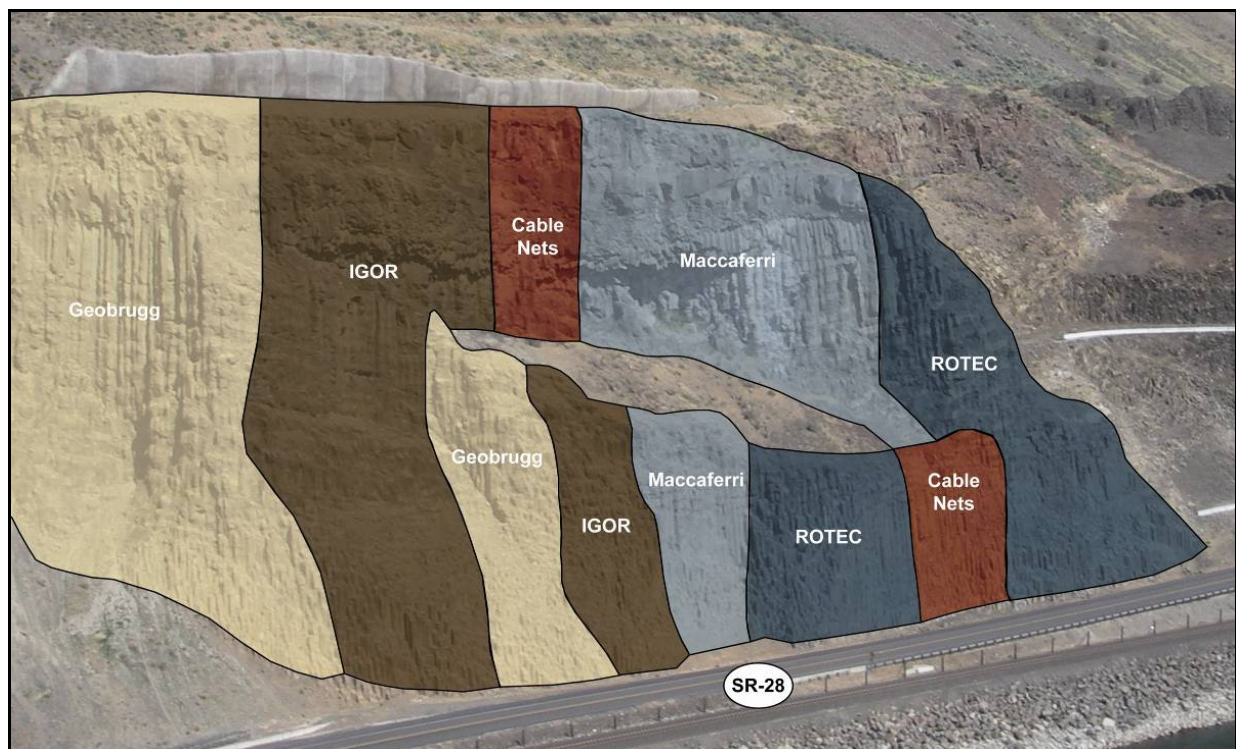
FIGURE 2. Design coverage for the specified ring nets for the sections of standard and modified (hybrid) slope protection, including two control sections of cable nets.

For the sections of standard slope protection, the top horizontal rope was specified to have a maximum segment length of 40 feet supported by cable anchors on 20-foot spacing. The modified section was designed with the top horizontal rope spanning a single 20-foot-wide section between two 10 ft posts and anchored on each end. All posts were inclined downslope at approximately 25 degrees from vertical.

The contract was advertized on November 13, 2007, and bids were opened December 13, 2007. Four pre-qualified contractors bid on the project with project bid costs that ranged from $2.39 to $4.10 million. The contact was awarded to Janod Incorporated of Champlain, New York for $2.39 million, which was about $848,000 less than WSDOT's engineers estimate.

The unit bid prices for installing the four ring nets and cable nets are summarized in Table 1. The unit bid prices for the fabrics are inclusive of all anchors, appurtenances, and installation costs; 19 steel posts for supporting the modified slope protection are not included in the unit bid prices. Scaling was completed during a long weekend highway closure in late March 2008. As specified in the contract, installation of the slope protection was delayed due to environmental restrictions until mid July 2008. The on-slope work was completed and Janod demobilized in late November 2008.

Table 1. Summary of ring net and cable net unit bid prices

Fabric	Plan Quantity (ft^2)	Contractor Bids ($/ft^2)
Geobrugg	52,248	5.55 – 10.25
IGOR Paramassi	52,596	6.74 – 12.00
Maccaferri	52,056	6.26 – 11.50
ROTEC International	51,972	8.22 – 13.75
Cable Nets	15,792	5.97 – 11.00

CONSTRUCTION SUMMARY

Prior to placing the nets, Janod utilized climbing gear, ropes, pneumatic pillows, and pry bars to hand scale large detached blocks from the upper portion of the slope that could potentially damage the ring/cable nets if they were to fall. Janod utilized a wagon drill to drill the anchor holes for the top

horizontal support ropes and for the posts along the intermediate bench. Three-inch-diameter anchor holes were drilled for the top horizontal rope anchors. Double, ¾-inch cable anchors were used to support the ¾-inch top horizontal support ropes. Janod elected to install anchors to a depth of 20 ft, which were then fully grouted with cement grout. For the modified installation, four 1-inch-diameter anchor bars and three, double ¾-inch cable tieback/lateral anchors were installed for each post to a depth of 10 ft and were fully grouted with cement grout.

The contract required submittals from the ring net manufacturers documenting unit weight of the fabric, 3-ring unrestrained tensile strength of not less than 7,000 lbf, mill certificates for the wire/wire rope, and galvanization information. A summary of product information is provided in Table 2. The 3-ring tensile test results in Table 2 are either the average value of the test reports provided by the manufacturer (Geobrugg, IGOR, Maccaferri) or the value of a single test (ROTEC). The contract was not specific about the number or basis of passing tests.

Table 2. Ring net and cable net technical data

Fabric	Ring Diameter in (mm)	Ring Weight lbs (g)	Approx. Unit Weight $lbs/ft^2 (kg/m^2)$	Wire Diameter in (mm)	3-Ring Tensile Test lbf (kN)
Geobrugg 4:1	11.8 (300)	0.70 (319)	0.55 (2.7)	0.12 (3.0)	8,990 (40.0)
IGOR 6:1	11.8 (300)	0.37 (168)	0.49 (2.35)	0.08 (2.0)	6,920 (30.8)
Maccaferri 4:1	13.4 (340)	1.22 (553)	0.84 (4.1)	0.13 (3.4)	22,900 (102)
ROTEC 6:1	12.4 (315)	0.59 (268)	0.60 (2.9)	0.31 (8.0)	13,000 (57.8)
Cable Nets	NA	NA	0.5 (2.4)	0.31 (8.0)	NA

Installation of Slope Protection

The contract specified for the double-twisted hexagonal mesh to be attached on the outside of the ring nets with high tensile steel hog rings at 1 ft intervals prior to placing the panels on the slope. Panels were fabricated offsite, and then transported to the top/base of the slope.

The contract specified both ring and cable net panels to be seamed with 5/16" wire rope. The wire rope seaming of the net panels was used initially, but Janod proposed to substitute shackles for wire rope as a superior seam for the ring net panels being much less prone to seam failure. WSDOT agreed to the proposal, and a ½-inch screw pin shackle with a minimum ultimate breaking strength of 24,000 lbf was selected and paid for by change order. Janod seamed the narrow panel side of either 2 or 3 panels, depending on the unit weight of the fabric and the size and weight of each type of ring net panel. The panels were then connected to a spreader bar and lifted into place on the slope. The panels were installed as they would hang, seaming the top of the lifted panels to the bottom of those already on the slope. A 50-ton crane mobilized to the top of the slope was used to place the upper portion of the ring and cable nets; the nets on the lower portion of the slope were installed with the crane set along the highway shoulder.

Janod started on the south end of the project area with the ROTEC and Maccaferri ring nets and worked primarily northward to the cable net, IGOR and Geobrugg ring net sections. During the initial placement of the ROTEC and Maccaferri ring nets, Janod noted large deformations in the ring net panels. Janod experienced increasing difficulty pulling the nets together as more were added, often requiring a come-along to move the nets and shackle the vertical seams together. Janod noted an extreme contrast in deformability between the stiff wire mesh and the deformable ring nets, with the wire mesh inhibiting conformance of the ring nets with the slope. The situation resulted in extreme tensioning in the wire mesh with stresses concentrating in the connections of the high tensile steel fasteners. With the addition of ring net panels, many fasteners began to fail. In attempt to reduce the rigidity of the panels, a modification was made at WSDOT's direction to increase the fastener spacing from 1 to 2 feet. Shortly after implementing this change, a mesh panel separated from one of the ring net sections and fell onto two workers below; fortunately, no serious injuries occurred. Janod temporarily suspended the placement of additional ring nets and secured all of the wire mesh to the top horizontal rope.

Janod had previously advocated for not connecting the wire mesh to the ring nets. Following this incident, WSDOT consented and allowed the remaining ring nets and wire mesh to be placed separately and not require subsequent connection. The remainder of the placement of the ring nets, cable nets, and wire mesh proceeded without significant problems.

The final coverage area of the different fabrics is approximately depicted in Figure 3. The areas changed somewhat from the coverage area shown in the plans for a number of reasons. Some additional coverage area was required on the south end of the project, which was covered with ROTEC ring nets and additional cable nets. Detailed survey locations of the different fabrics were not included in the plans. Placement of fabrics was made primarily by estimating their location from photographs. With the large slope heights, slope irregularities exacerbated modifications to the design layout. Additional nets were also added along the entire top, due to a modification in the anchoring and top horizontal support rope. These areas requiring additional fabric totaled about 22, 246 ft^2. The final installed

quantity was estimated to be 261,573 ft^2, representing a 36,723 ft^2 or about a 16% shortage on plan quantities. This shortage was accommodated by the installation of additional cable nets.

 FIGURE 3. As-built coverage for the ring nets and cable nets.

The following sections summarize the construction experiences of installing the four different ring nets and observations of their as-built condition.

Geobrugg Ring Nets

As specified, the Geobrugg rings were made of 5 loops of 3-mm-diameter wire with a 4:1 weave of interlocking rings. The wire loops are bound together with 3 pressed steel bands, with the wire ends commonly protruding 3 to 6 inches beyond the bands. These ring net panels are intermediate in weight as compared to the other specified ring nets.

Janod's crane was able to lift three Geobrugg ring net panels in a single pick, with each three-panel section measuring 12 feet wide by 75 feet long for a total area of 900 ft^2. Initial placement of the upper sections of Geobrugg rings occurred with the wire mesh pre-attached until this requirement was dropped. When the panel sections were lifted, both with and without the wire mesh backing, some contraction (necking) and elongation of the fabric occurred (Fig. 4). On the vertical portions of the slope where the nets had little to no slope contact and the dead load was carried entirely by the fabric, rings slightly deformed from a circular to an ellipsoid form. This ring deformation caused many of the wire ends to protrude (Fig. 5). Janod reported that the protruding wires caused the climbing ropes, wire

mesh, and workers' clothing to "hang up", and felt this increased the difficulty of this fabric installation. Janod also reported several occurrences of minor puncture wounds caused by the protruding wires. Despite the "necking" during lifting and initial placement, vertical seaming of the panel sections reportedly did not require excessive effort to place properly, as compared to some of the other fabrics.

FIGURE 4. Three panel section of Geobrugg ring nets with wire mesh; note contraction (necking) of panels.
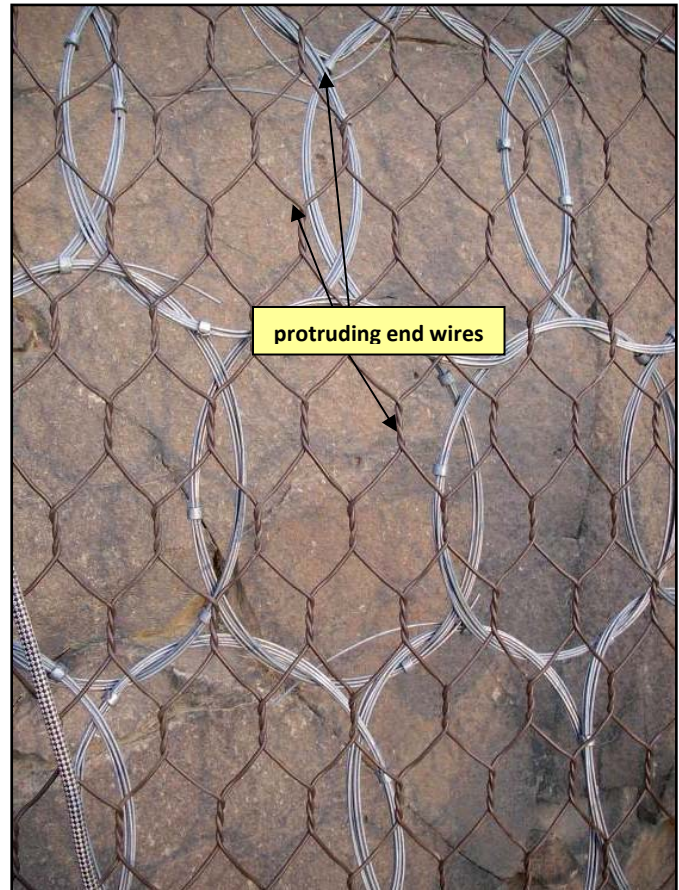
FIGURE 5. Elongation of individual rings caused wire ends to protrude on Geobrugg ring nets.

IGOR Paramassi Ring Nets

As specified, the IGOR rings were made of seven 2-mm-diameter wires with a right-hand spiral lay and a 6:1 weave of interlocking rings. The wire ends are finished by curling several loops over the ring. IGOR ring net panels are the lightest of the four specified ring nets.

Janod's crane was able to lift three IGOR ring net panels in a single pick, with each three-panel section measuring 14.5 feet wide by 111 feet long for a total area of 1614 ft^2. The panel sections were placed mostly without the wire mesh backing. When the panel sections were lifted, they maintained their

rectangular shape and contracted very little (Fig. 6). Similar to the other ring nets, the IGOR rings elongated somewhat where the nets had little to no slope contact and the dead load was carried entirely by the fabric (Figure 7). Janod reported that the ring net sections were relatively easy to move around on the slope and to seam.
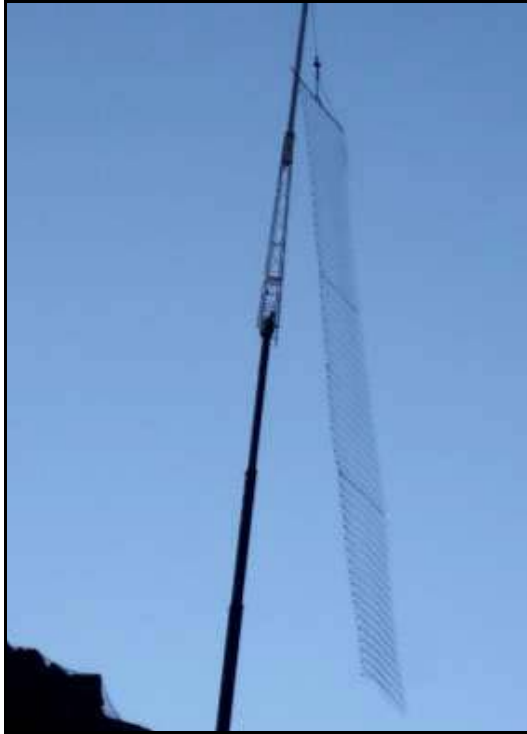
FIGURE 6. IGOR ring net panels without

wire mesh maintained their rectangular

shape when lifted.

FIGURE 7. Slight elongation noted in IGOR rings

where panels were heavily loaded

Maccaferri Ring Nets

As specified, the Maccaferri rings were made of six 3.5-mm-diameter wires with a right-hand spiral lay and a 4:1 weave of interlocking rings. The wire ends are turned into the ring. Maccaferri ring net panels are the heaviest of the specified ring nets. Janod's crane was able to lift only two Maccaferri ring net panels in a single pick, with each two-panel section measuring 13.5 feet wide by 67 feet long for a total area of 905 ft^2. Initially, the Maccaferri ring nets were placed with the wire mesh backing. During this phase of their installation, the ring net panels severely contracted in width as they were lifted by the crane and placed onto the slope (Fig. 8). The contraction of the ring net panels contributed to the wire mesh fasteners "popping-off" the mesh. Severe contraction persisted after the pre-attachment of wire mesh was discontinued (Fig. 9). Due to the heavy weight of these sections, Janod found that once placed on the slope it was extremely difficult to pull the rings apart and to shackle the adjacent panels together (Fig. 10).

FIGURE 8. Maccaferri ring net with wire mesh backing exhibited severe contraction within the panels

FIGURE 9. View of contracted panels without wire mesh backing

FIGURE 10. Seaming the contracted panels was difficult, often requiring the use of a come along to pull the seam together and secure the shackle

ROTEC Ring Nets

As specified, the ROTEC rings were made of a single 5/16-inch diameter wire rope joined with a pressed aluminum ferrule and a 6:1 weave of interlocking rings. Being fabricated of a wire rope rather than a bundle of stiff wire loops, ROTEC rings are highly deformable as compared to the other wire rings. ROTEC ring net panels are intermediate in weight as compared to the other specified ring nets.

Janod's crane was able to lift three ROTEC ring net panels in a single pick, with each three-panel section measuring 12 feet wide by 75 feet long for a total area of 900 ft^2. Initially, the ROTEC ring nets were placed with the wire mesh backing. When these panel sections were lifted, they generally maintained their rectangular form (Fig. 11A); without the backing mesh, the panels contracted severely (Fig. 11B). With subsequent placement and seaming of panels, significant ring deformation and tension developed in the upper portion of the installation, around slope protrusions, and along seams (Fig. 12). However, because the ROTEC ring is fabricated from wire rope, ring deformation is not permanent as it would be with a ring of bundled wire loops.
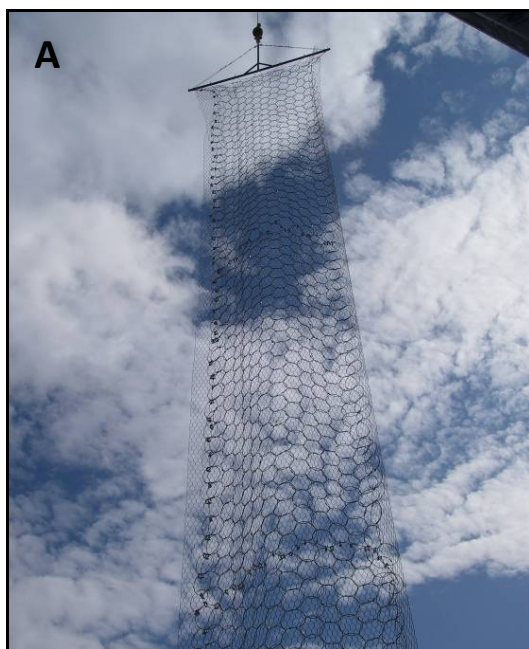
FIGURE 11. (A) ROTEC ring net panels with wire mesh and B) without wire mesh.

FIGURE 12. Deformation in upper backing portion of ROTEC ring nets.

The effort in pulling the heavy Maccaferri ring net panels together for seaming caused the adjacent ROTEC ring nets, which had been previously seamed to the Maccaferri ring nets, to be pulled laterally toward the Maccaferri nets (Fig. 13). Janod then had to try to pull the ROTEC rings back. This was only moderately successful, and additional material was required for the net loss in coverage area of the ROTEC ring nets.
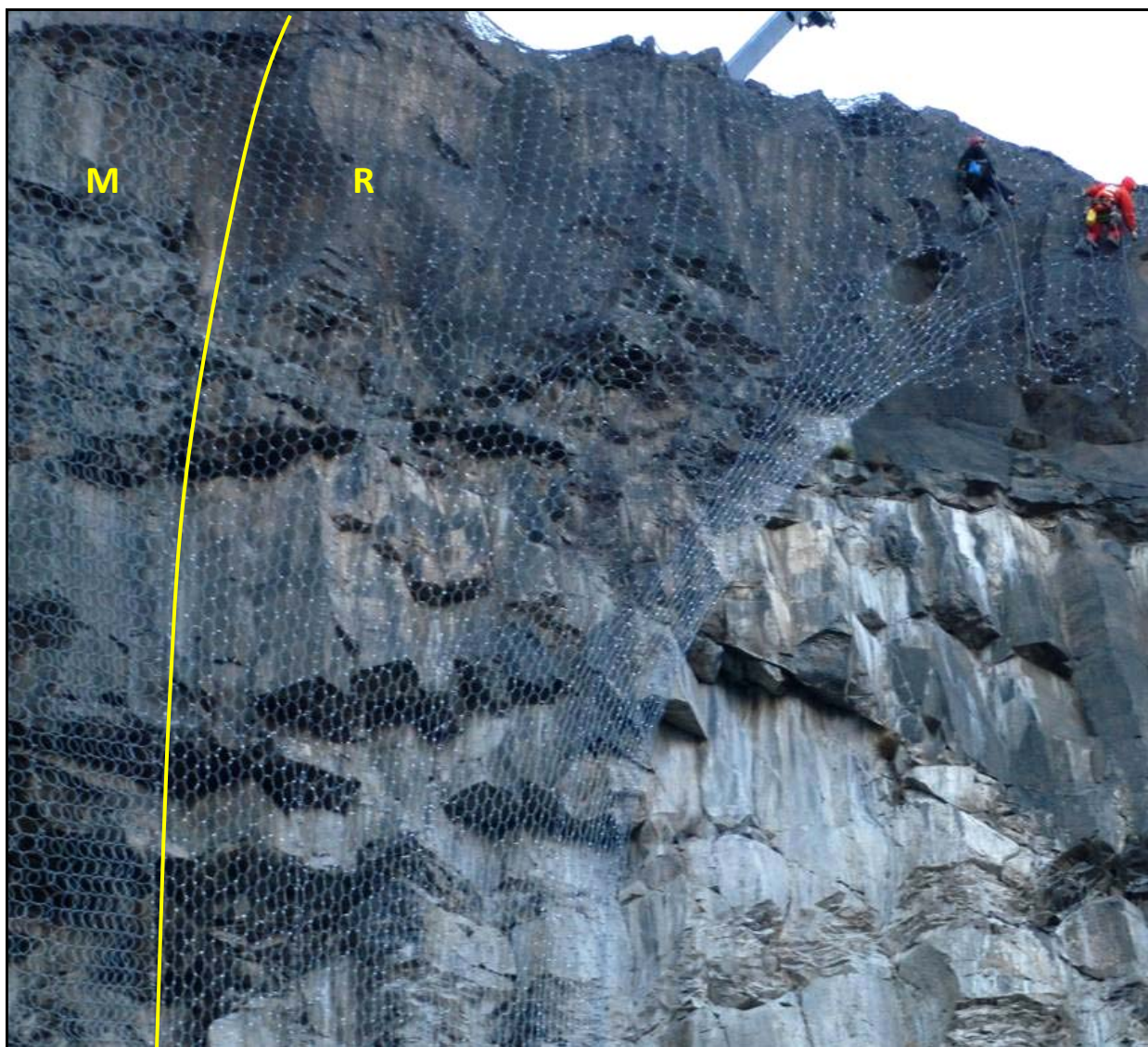
FIGURE 13. Yellow line denotes seam between Maccaferri nets (M) on the left and ROTEC rings (R) on the right. Note how the ROTEC rings have been pulled toward the Maccaferri nets.

Maccaferri Cable Nets

The wire rope cable nets were generically specified in the contract to be either square or diagonal grid with a 12-inch opening fabricated of 5/16-inch-diameter, galvanized wire rope with a 7x7 or 7x19 construction and minimum breaking strength of 9,200 lbf. The cable net panels were specified to include a perimeter rope with a minimum diameter of 5/16 inches. Janod selected Maccaferri cable net panels, which use a wire wrap to secure the cable junctions rather than a pressed steel clip. The cable nets provided also were diagonal weave rather than a square weave.

The panels were seamed with 5/16-inch-diameter wire rope, and later with shackles. Janod's crane was able to lift two Maccaferri cable net panels in a single pick, with each two-panel section measuring 21 ft

wide by 64 ft in height or 42 ft wide by 32 ft in height for a total area of 1344 ft^2. Initially, wire mesh was fastened to the cable nets prior to their hanging, but this requirement was eventually dropped and the wire mesh was added after placing and seaming the cable nets. As expected, the cable net panels kept their rectangular form with or without the wire mesh backing. Janod reported that the cable nets maintained their shape well and were relatively easy to handle and seam.

DISCUSSION AND CONCLUSIONS

This Experimental Features study provided an opportunity to compare the installation of different weaves, weights, and fabrication of ring nets for a large slope protection (drapery) installation.

Two fabrics (Geobrugg and Maccaferri) were specified to have a 4:1 weave, and two (IGOR and ROTEC) were to have a 6:1 weave. As would be expected, when unrestrained by wire mesh backing, a wire ring is much stiffer and less deformable than a wire rope ring. Because ROTEC was fabricated with wire rope, it is not easily compared to the other three wire rings when considering panel weaves and their associated deformation. The 6:1 IGOR ring, being the lightest of the wire rings, exhibited the least contraction or stretch. The 4:1 Geobrugg panels were intermediate in their weight and deformation, and the 4:1 Maccaferri were the heaviest and contracted the most. The Maccaferri section, however, had the greatest percentage of free-hanging length with no slope contact as compared to the other ring nets. While the reduced slope contact and considerable weight of the Maccaferri nets appeared to exacerbate their deformation, in general, the 6:1 weave experienced less ring and panel deformation than 4:1 weaves. Subsequent discussions with some of the manufacturers corroborated this observation. The weight of the ring nets also has a significant influence on their contraction. The lighter 4:1 Geobrugg nets deformed much less than the heavier 4:1 Maccaferri nets (Figs. 4 and 8). The heavy weight nets also reportedly made seaming much more difficult and labor intensive as compared to the lighter weight ring nets.

In preparation of the contract, WSDOT solicited input from several contractors experienced with ring net draperies about the need and means to control ring net deformations as additional panels were added. One method suggested by several contractors was to install support cables anchored at the top of the slope with their ends secured at multiple locations on the field of the mesh; these special support cables are referred to as "octopuses". A design basis for determining the number and spacing of octopuses could not be established prior to advertising the project, and they were not included in the contract. Examination of the different ring nets revealed that all four types experienced some ring elongation where large panel sections were free-hanging and/or had very limited slope contact. The area of ring elongation was not distributed throughout the panel but generally occurred near the middle of the free-hanging length. In our judgment, the extent of elongation was not severe enough to diminish performance with the possible exception of the ROTEC wire rope rings. As expected, the ROTEC rings were the most deformable, but also best conformed to slope irregularities. However, their conformance around numerous slope protrusions resulted in extreme localized tensioning in small numbers of rings with the addition of more panels or when seaming adjacent Maccaferri panels. In summary, the benefit

that octopuses would have provided for this project is judged to be minimal. Slopes with higher free-hanging lengths might possibly benefit from their inclusion.

For those ring nets that have a tendency to deform under their own weight, the attachment of the wire mesh can greatly reduce their deformation. This is well evidenced in the comparative photos of the ROTEC mesh (Figs. 11 A and B). This constraint on panel deformation, however, is limited to the strength of and stresses on the fasteners that secure the wire mesh to the ring nets. Even using high tensile steel fasteners on close spacing, the considerable weight of the Maccaferri ring nets and deformability of both the Maccaferri and ROTEC ring nets, especially after attaching additional panels, caused many of the fasteners to fail.

The contract requirement for pre-attaching the wire mesh to the ring nets was based on several decades of its successful practice for cable net installations. Because cable nets have fixed cable junctions and a perimeter cable, the rectangular panel shape as a whole is restricted in its ability to deform. Ring nets panels, however, have no perimeter rope or internal junctions of fixity, and, depending on their characteristics (i.e., weave, weight, deformability of each ring, etc.), the panels generally have greater ability to stretch and deform. Double-twisted hexagonal mesh has fixed wire junctions and is quite stiff. These differences in fabric deformability and stiffness were not fully appreciated in the design for this project.

With the wire mesh specified to be on the outside of the ring nets, Janod had advocated that the ring nets and wire mesh should act as two separate systems and not be connected. Janod started by placing the 6:1 ROTEC and the 4:1 Maccaferri panels, which were the most prone to deformation. After the fasteners started to fail on these ring net sections and a wire mesh panel detached, WSDOT agreed to drop the connection requirement. WSDOT concurred that by not attaching the wire mesh, it would likely still be effective in containing smaller sized rockfall debris that might pass through the ring nets. Possible installation methods that could have helped to control panel deformation include:

1.) Using a wider spreader bar to hang the panels in the short (horizontal) dimension to lessen the panel load per unit width, thus reducing panel contraction, and
2.) horizontally seam the bottom of the lifted panel to the bottom of a panel on the slope and then, as the panel is lowered, vertically seam adjacent panels. This second method might have lessened the dead load acting on the point of seaming, potentially making it easier to pull the seams together.
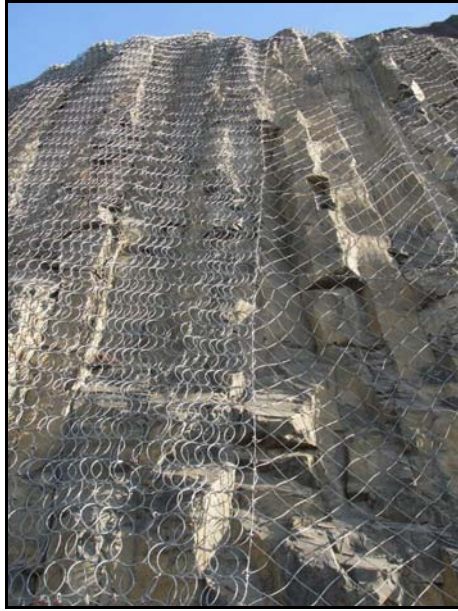
FIGURE 14. Photograph shows Maccaferri rings adjacent to Maccaferri cable nets. Note contraction in width of ring nets panels and less than optimal coverage area.

The contract quantity shortage in ring/cable nets was due to a number of factors. First, additional areas not specified in the contract (estimated to be about 22,246 ft^2) were added on the south end and along the slope crest. Second, most of the Maccaferri panels, and Geobrugg to a lesser extent, representing the 4:1 weaves, contracted when lifted and typically could not be fully stretched out once the ring nets were placed on the slope or after additional panels were added. This resulted in reduced coverage area from a number of the panels (Fig. 14). Third, the slope was large and irregular, which complicated estimating the contract plan quantities. Estimation of the coverage area using ground-based laser scanning and GIS was a newly employed method for WSDOT. To account for uncertainties with this estimating method and variable fabric conformance with the slope, a 20% contingency was provided for in the plan quantities. Subtracting the 22,246 ft^2 of additional coverage area and discounting the 20% contingency in planned quantities, the coverage area calculated with GIS underestimated the as-built quantities by about 28%. We assume that the percent loss of coverage area due to panel contraction would be less for shorter slope heights, for lower deformation ring nets (i.e., 6:1 rather than 4:1 weaves, lighter rather than heavier panels, etc.), and by tailoring installation methods to optimize coverage area. For future projects, consideration should be given to controlling panel deformation and loss of coverage area. This might include specifications on method of placement and using lower deformation ring net panels. While much of the slope was near vertical and the ring nets had little slope conformance, where the slope was more moderate in inclination, all of the rings nets and cable nets exhibited reasonably good conformance with the slope.

The final cost for completing this project was approximately $3.2 million. The additional $800,000 above the contract award price is attributed to acquiring about 7.5% more cable nets to cover the required area, the substitution of U.S. steel shackles for seam ropes, and some additional slope

stabilization measures. These additional costs lead to the project being approximately 25% over the original contract award amount of $2.39 million.

While no performance data are yet available, the installation phase provided useful information about the comparison of ring nets to cable nets for slope protection (drapery) systems. The unit bid prices for the installation of the ring nets from each of the contractors were competitive, but on the high end, with wire rope cable nets of comparable opening size (12 inches).

The ring net panel with the least amount of deformation (lightweight IGOR 6:1 weave) was reportedly comparable to the cable net panels in terms of ease and time of installation. With the use of heavier ring nets and those utilizing a 4:1 weave (both being factors that result in increased panel deformation), installation effort increased substantially over what would be typical for cable net installations. Janod provided data for the time required to install each of the fabrics, which is presented in Table 3. It is important to note that in addition to the specific properties of the ring nets, slope height and construction methods/access influence installation time. The reported differences of the installation rates may be significantly less for shorter slope heights or less challenging slope conditions. A qualitative assessment for evaluating panel deformation and ease of installation might include lifting a single panel in the long direction and noting the amount of contraction/deformation.

Table 3. Fabric installation rates

Fabric	Square Feet Installed	Installation Time (hrs)	Installation Rate ft^2/hr
Cable Nets	49,248	345	143
IGOR 6:1 Wire Ring Nets	54,896	439	125
Geobrugg 4:1 Wire Ring Nets	52,500	540	97
Maccaferri 4:1 Wire Ring Nets	52,461	688	76
ROTEC 6:1 Cable Ring Nets	52,200	902	58

Attaching the wire mesh to the ring nets, as WSDOT currently requires for cable nets, is likely not problematic for the installation of low-deformation ring nets. The necessity or benefit of this practice in terms of performance, however, has not yet been assessed for this project. If the wire mesh is pre-attached, its stiffness has the potential of limiting the desirable attribute of ring net deformability (and potentially increase damage) during rockfall impacts (up to the yield strength of the fasteners and wire

mesh). We assume that because cable nets do not have the capability to deform as much as ring nets, we have not observed any significant problems or damage on numerous WSDOT installations where the wire mesh has been attached to the cable nets. If this practice is found to be adverse or provides no discernable benefit, eliminating the requirement would result in substantial cost savings, both for ring nets and cable nets. Because of the differences in stiffness, the wire mesh placed on the outside of but not attached to the ring nets (or cable nets) would be expected not to conform as well to the slope and underlying ring (cable) nets without extra effort. This variance in slope conformance is likely to be more visible viewing from the side than from the front of the installation.

Lacking performance data, the specification and installation of low-deformation ring nets had no significant negative or positive attributes when compared to cable nets. One concern that we will be looking for in their future performance is the permanent deformation of wire rings due to rockfall impacts. A positive attribute of wire rope that is used for cable nets (and the ROTEC ring net) is that it does not experience significant permanent deformation within its yield strength. Wire rings, on the other hand, permanently deform within their yield strength. The extent to which this permanent deformation affects performance after repeated impacts is not known.

The ring nets included in the contract were explicitly specified by WSDOT so as to compare different attributes that included weave (4:1 and 6:1), weight, and element type (wire or wire rope). These comparisons do not fully represent the quality or range of product availability provided by the manufacturers, or the suitability of the evaluated products for other applications.

REFERENCES

WSDOT, Work Plan, Use of Ring Nets for Slope protection for Rockfall, SR 28/Rock Island-Rock Slope Netting, MP 11.83 to MP 11.96, WSDOT Geotechnical Division, October, 2007.

WSDOT, Geotechnical Report, Rock Island Slope Stabilization, Stage 3, SR 28, MP 11.83 to MP 11.96, Project OL-3422, WSDOT Geotechnical Division, August, 2007.

2.4

Protection from High Energy Rockfall Impacts Using Terramesh Embankments:

Design and Experiences

Ghislain Brunet
Maccaferri Inc.
10303 Governor Lane Boulevard
Williamsport MD 21795
Phone: 301-223-6910

gbrunet@maccaferri-usa.com

Giorgio Giacchetti

External Consultant - OFFICINE MACCAFERRI S.p.A.
Via degli Agresti 6, 40123, Bologna – Italy

giorgio.giacchetti@maccaferri.com

Paola Bertolo

OFFICINE MACCAFERRI S.p.A.
Via degli Agresti 6, 40123, Bologna - Italy

paola.bertolo@maccaferri.com

Daniele Peila

POLITECNICO DI TORINO - DITAG
Corso Duca Degli Abruzzi 24, 10129, Torino - Italy
daniele.peila@polito.it

ABSTRACT

The high energy impact embankment system represents an effective solution for rockfall protection that is relatively cost efficient in respect to price and maintenance in comparison with traditional rockfall barriers. The high energy impact embankments are designed to resist multiple impacts with negligible resultant deformation, and therefore, may be placed close to infrastructure. Additionally, this system may also have a vegetated façade to blend in with the surrounding environment.

The high energy impact embankments are sized with a statistical approach using rockfall simulation programs. Recent European findings, developed primarily in Italy, recommend applying partial safety coefficients to consider the uncertainty of the main input data when calculating barrier dimensions. While the embankment height is solely dependent upon trajectory height, the embankment width is dependent upon force of the impact, which is difficult to determine using common design applications. A procedure developed by Politecnico di Milano and Veneto Road Administration (Italy) presents a simple graph to facilitate the determination of the greatest expected impact penetration into the embankment and the minimum required embankment width. Using this approach, Maccaferri has designed embankments to accommodate up to 20,000 kJ (7375 ft-ton), with heights greater than 15 meters (49 feet) using their Green Terramesh system.

One of these embankments has been recently impacted with multiple rocks, which are up to 5 meters in diameter (15 feet). These events provided an opportunity to conduct a back analysis of the each event by modeling the rock trajectory and applying the Finite Element Method to reproduce the embankment behavior. As a result, valuable information was gained to contribute to the design methodology for sizing embankments for high energy rockfall impacts.

Introduction
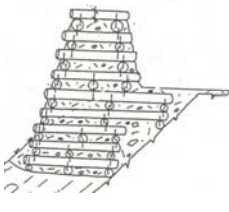
Rockfall protection embankments are usually built to stop rockfall events, both in civil and in mining applications, in order to protect roads, urban areas, quarry plants or workers. Different types of embankments (Table 1) constructed of compacted soil, large rocks, gabions or reinforced soil systems have been used in the past (Peckover and Kerr, 1977; Giani, 1992; Wyllie and Norrish, 1996; Oggeri and Peila, 2000; Nomura et al., 2002; Peila et al., 2007). Currently, the most commonly used system is reinforced embankment.

For an embankment to work effectively, the design assumptions should take into consideration the following aspects:

1. The embankment height shall be sufficient to intercept the rock trajectories.
2. The area directly upslope of the embankment must provide sufficient space to   accumulate fallen rocks.
3. The embankment must have sufficient thickness and density in order to prevent the rocks from penetrating the embankment.

A successful design should result in energy absorption capacity, trajectory interception, and financial commitment which are comparable to elasto-plastic rockfall fence barrier. In contrast to the rockfall fence barrier, the embankment will be able to absorb a larger number of high energy rockfall impacts under design energy levels and require little or no maintenance. Table II compares the main characteristics of the embankments with rockfall fence barriers.

Table 1. Embankment styles and characteristics

Embankment Style	Geometry	Example	Reference
Embankment composed of compacted soil	-Isosceles trapezoid -Faces dip ≈ 35° (with reference to horizontal) -Common maximum height ≈ 5-6 meters		- Paronuzzi (1989) - Del Greco et al. (1994) - Grasso and Morino (1991)
Embankment composed of large rocks	-Isosceles trapezoid -Both faces dip ≈ 35° (with reference to horizontal) -Maximum height ≈ 12 meters	 **Chatillon (Aosta Valley - Italy)**	- Pasqualotto et al. (2004)
Embankment composed of compacted soil with gabion facing	-Right-angle trapezoid -Downslope face dip ≈ 35° (with reference to horizontal) -Upslope face dip ≈ 90° (with reference to horizontal)	 **Paluzza (Udine – Italy)**	- Oggeri at al. (2004) - Lambertl et al. (2008)
Embankment composed of gabions	-Isosceles trapezoid or parallelepiped -Downslope face dip 70°- 90° (with reference to horizontal) -Upslope face dip 70°- 90° (with reference to horizontal)	 **(France)**	- Wyllie and Norrish (1996) - Lambert at al. (2007)
Embankment composed of compacted soil reinforced with wood and steel bars	-Isosceles trapezoid -Both faces dip ≈ 60-70° (with reference to horizontal)	 **Dorénaz (Vallis - Switzerland)**	- Tissieres (1999)
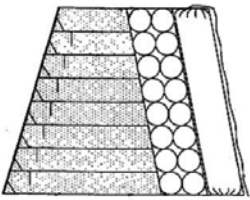
Embankment Style	Geometry	Example	Reference
Embankment composed of reinforced soil material with geotextiles, geogrids, and an energy absorbing mattress	-Isosceles trapezoid -Downslope face dip 70°- 90° (with reference to horizontal) -Upslope face dip 70°- 90° (with reference to horizontal) –Upslope facing of an energy absorbing sand filled mattress	 **Tyama (Japan)**	- Yoshida (1999) - www.proteng.co.jp
Embankment composed of reinforced soil material with geotextiles, geogrids, or steel wire mesh	-Isosceles trapezoid -Downslope face dip 70°- 90° (with reference to horizontal) -Upslope face dip 70°- 90° (with reference to horizontal)	 **Rhemes Saint-Georges (Aosta Valley- Italy)**	- Lazzari et al. (1996) - Burroughs et al. (1993) - Peila et al. (2007) - Pasqualotto et al. (2005)

Table 2 – Major differences between embankments and rockfall fence barriers.

Feature	Reinforced soil enbankment	Rockfall fence barrier
Energy absorption capacity	-Tests up to 5000 kJ -Numerical checks to more than 5000 kJ are possible to increase the size up to what is necessary	Up to 5000 kJ in products in the current market
Resistance to multiple maximum energy level impacts	-Yes	Variable depending on barrier type
Resistance in aggressive environments (fire, marine environment)	-Relatively high level of resistance due to lower overall level of exposure -Most parts are embedded within the embankment	Metal components have a much higher level of exposure to elements
Downslope deformation of structure from impact	-Negligible	Variable depending on barrier type and manufacturer
Downslope deformation of structure from maximum energy impact	-Minimum displacement of the structure	Variable depending on barrier type and manufacturer
Ability to intercept maximum velocity impacts	-Can withstand impact velocities up to 50 meter/second	Variable (25 to 30 meters/second maximum) depending on barrier type and manufacturer
Can be installed in a immediate proximity to the infrastructure of protection	-Yes, because the deformation is negligible	Space margins are required and based on barrier elongation, which varies between different barrier types and manufacturers
Maintenance required for low-energy impact	-Neglagable to none	Variable depending on impact, barrier type, and barrier manufacturer
Installation tolerances (geometric) of the structure	-There are no specific geometric requirements	Barrier must be installed within specific geometric requirements
Required slope topography for installation	-Suitable for slopes with medium to low gradient	Can be installed on any type of slope
Impairing wildlife, human, and vehicle passage on the hill slope	-Comparable to that of the barrier	Comparable to that of embankments
Cost of installation of the structure	-Cost efficient for energies greater than approximately 3000 kJ	Cost efficient for energies below approximately 4000 kJ
Environmental compliance	-Potential LEED compliance and blending with landscape by vegetating embankment facing	Structure is likely transparent to a distant observer
Certification and testing	-No certification -Tested in accordance with Italian standard UNI 11167	-Variable depending on manufacturer -Majority are tested and certified according to European standard certification ETAG 027
Requirements for verification of the project structure	-The designer is required to dimension the structure in accordance with the manufacturer design guideline and National Standards	The designer has to check the anchoring devices and foundation of the barrier according to National Standards

The information in Table 2 shows that there are significant differences between reinforced embankments and rockfall fence barriers. The reinforced embankments provide many advantages over the rockfall fence barriers; however, they do require a larger foundation and the geometry of the slope must be able to accommodate the embankment. If the slope geometry cannot be accommodated, it is more technically appropriate to install a rockfall barrier.

The rules that define testing procedures for dynamic impacts vary significantly between the different barrier systems. For the reinforced embankment, the only available testing standard is the Italian UNI 11167. The rockfall barrier has an advantage in that its testing methodology has been standardized by the European EOTA Group with the ETAG 027 testing guideline. However, because the behaviors of the rockfall fence barriers are derived from the relationship between the geometry of the structure and strength of the components, the designer cannot change the size of rockfall barriers tested, except for the tolerances allowed by the guidelines ETAG 027.

In respect to the design of reinforced embankment, the UNI 11167 standard has limited utility for the designer. It is limited because it describes the procedure for testing features such as the reinforcement structure geometry and filling, whereas the designer may require information regarding the energy capacity, which is in direct relation to the size of the embankment. As an alternative, the designer may instead oversize the embankment in order to ensure its technical efficiency, while also optimizing economic efficiency. The designer must be able to calculate the dynamic characteristics of the rockfall mass impact and deduce the best structural characteristics of the embankment structure.

Embankments have the flexibility of being reinforced with variable materials (wire mesh, geogrids, and geotextile). This document summarizes a detailed analysis of a Green Terramesh reinforced embankment that is manufactured by Maccaferri, Inc. This embankment is trapezoidal in shape, is reinforced with steel double twist mesh, and was built on a hillslope with an inclination of 60°- 70°.

The impact of the ROCK mass

The dynamic impact of the projectile mass is usually analyzed by statistical evaluation that is developed with numerical simulations of trajectories that must be evaluated in a case by case manner. The calculation of the kinetic energy of the blocks is done considering the translational velocity and the mass of the projectile rock mass, applying the usual formulations of classical physics.

The rotational velocity is usually neglected in the case of isodimensional falling blocks, because it is negligible in comparison with the translational velocity (Giani, 1997). By adopting the approach of the "Eurocodes" for designing rockfall mitigation structures, the falling block velocity corresponds to 95% of the calculated velocity (v_t) multiplied by an appropriate safety coefficient γ_F. Where γ_F is defined as $\gamma_F = \gamma_{Tr} \bullet \gamma_{Dp}\gamma_{Tr}$ = coefficient of reliability of the calculations of the trajectories that corresponds to the following:

- 1.04 for two dimensional or three dimensional calculations calibrated on the basis of back analysis;
- 1.07 for two dimensional calculations based only on the coefficients of restitution from published information.

γ_{Dp} = coefficient which takes into account the quality of the topographic profile of the slope that is equal to:

- 1.04 for slopes defined with high accuracy (to be defined case by case in relation to the characteristics of the site), but on the basis of an accurate topographic profile;
- 1.07 for slopes that are defined with low to medium accuracy.

The height of rock interceptions is defined as the bouncing height of blocks against the slope that corresponds to 95% of possible trajectories (ht) multiplied by a safety factor of: $h_d = h_t \bullet \gamma_F$ where the value of γ_F is established as above.

The design mass of the block is defined as the volume of the design block multiplied by the weight of volume of the rock type multiplied by a specific safety factor: $m_d = (Vol_b \bullet \gamma) \gamma_m$. Where γ is the unit weight per volume of rock in place, and γ_m is a safety factor expressed as:

$\gamma_m = \gamma_{VolF1} \bullet \gamma_\gamma$: coefficient related to the weight assessment of the rock volume could be equal to:

- γ_{VolF1} = coefficient related to the volumetric accuracy of the "Selected design block", which is suggested to be equal to 1.02 for accurate measurements of the slope face (for example with photogrammetric techniques or precise topographic surveys and measuring blocks in the debris at the base of the slope) or 1.10 per findings of lesser precision.

EMBANKMENT DESIGN PROCEDURE

The design of any embankment requires the consideration of the following parameters: (a) height of the embankment and its geometric characteristics; (b) stability of the slope on which the embankment is constructed (external stability); (c) internal stability of the embankment under static conditions (d) internal stability of the embankment under dynamic conditions (e) any other phenomena such as avalanches, debris flows that can generate a "dam effect" (f) construction and site accessibility considerations relating to the feasibility of the project (g) supply of structural fill materials and their geotechnical properties (h) and durability of the system for maintenance and repair (if necessary) as a result of one or more impacts. The static verification of internal and external stability of the embankment can be found in literature. For embankments that are reinforced with Green Terramesh (Figures 1 and 2), it is appropriate to use the design parameters developed specifically for Maccaferri products.
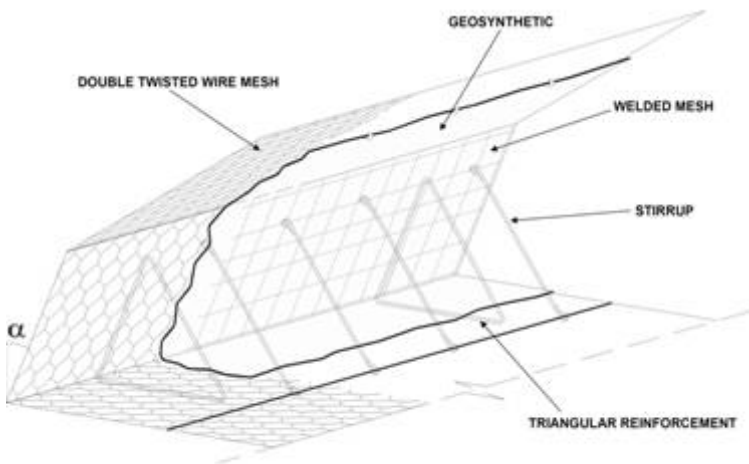
Fig. 1 – Typical configuration of the Green Terramesh reinforcement structure. The element is to be filled with selected proper grain size soil.

Fig. 2 – Trapezoidal Green Terramesh embankment structure (prior to establishment of vegetation on the facing). Horizontal Green Terramesh component structures are filled with soil and overlapped.

The structure must be designed to restrain the following phenomena during a dynamic impact: (a) the projection of fragments over the embankment after an impact

(b) the overtopping of the embankment by the blocks (c) penetration and passing of the block through the embankment (d) the collapse of the embankment due to geometrical deformation (e) development of instability within the soil foundation as a result of the dynamic forces. These parameters and the associated verifications are described below.

114

Overtopping of the embankment by post-impact projectile fragments

The projection of fragments occurs when the impacting block shatters because of the impulsive forces or when fragments of embankment material are projected downslope. This type of event is more likely in the case of embankments made with large blocks of rocks on the facing, or of embankments consisting of coarse material that is not properly contained. Therefore, the designer must consider the relationship between the impacting block of rock and the fill material of the embankment. For Green Terramesh embankments, this particular problem does not exist because the fill material is made with loose particles, and because the facing of the embankment is composed of wire mesh.

Overtopping of the embankment by rolling blocks that are released upslope of the structure

Impacting rocks that approach the embankment with a rotational motion may climb over the embankment (see Figure 3). The rotational kinetic energy of these blocks is an average of 10-15% of the total energy. If the slope facing of the embankment is not steep enough, there may be a risk that the rotating rock block may climb over the embankment. The Green Terramesh embankment system that is analyzed and discussed in this paper has an inclination 60° to 70° from the horizontal and is reinforced, which should be sufficient.
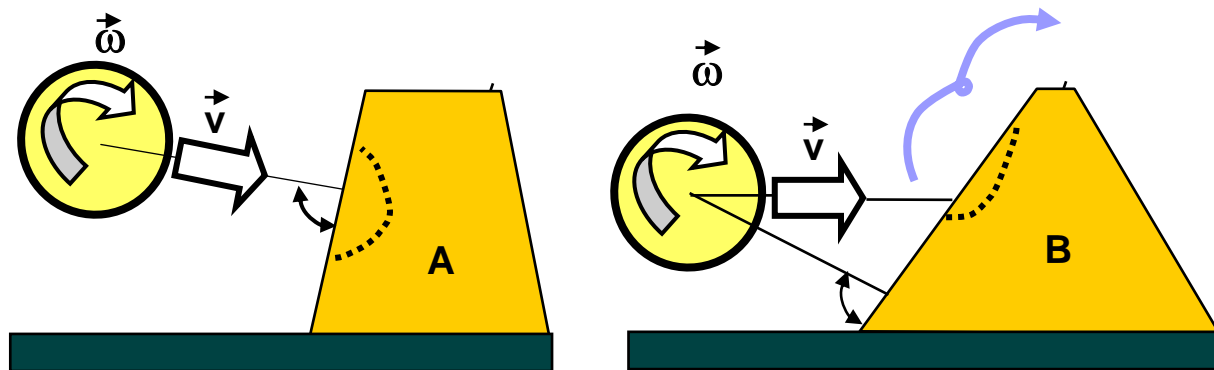
Fig. 3 – The slope facing of the embankment should be as perpendicular as possible to the direction of the impact (case A). If the direction is inclined (case B) the rotational speed of the boulder may allow the rock to climb over the structural embankment.

Impact stability test

Based on experimental observations of embankment barriers, it has been verified that the primary mechanisms of dissipation of the impact energy are the following (Figure 4):

1. The mutual movement of the layers (courses) of reinforced soil directly affected by the impact;
2. The plastic deformation of the soil related with the formation of impact crater.
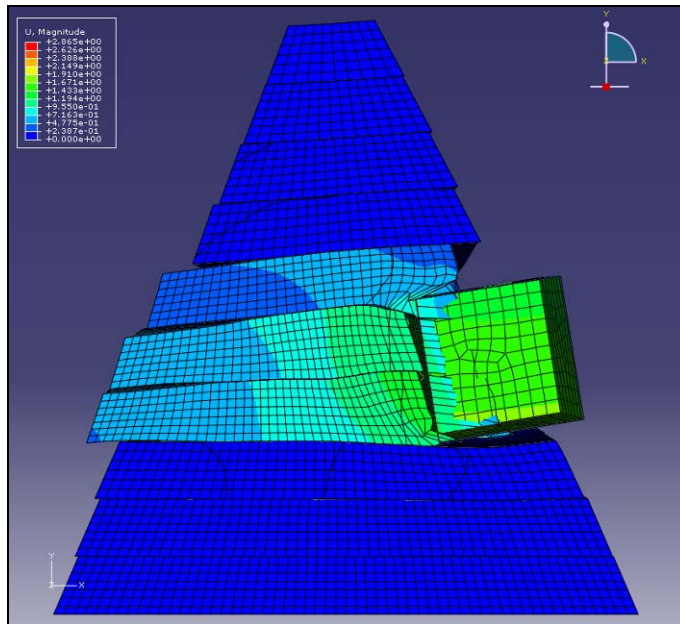
Figure 4 - Example of the contour plot of total displacements at the impact zone in an embankment computed using numerical modelling. The sliding effect of the impacted layers is quite evident, while the remaining part of the embankment appears to be relatively undisturbed by the impact.

The analysis of the two mechanisms is quite complicated because their magnitude depends on many factors related to each other, such as the following:

1. The penetration and stability of the embankment depend on the degree of density of the fill material (density of the soil).
2. Because the embankment has a trapezoidal section, the resistance to the impact varies with the height of the point of impact and consequently the depth of penetration.
3. The impact on the soil follows a theory of viscous behavior; given a constant level of energy impact, the filling reacts as a more compacted and resistant material if the velocity is higher. (Calvetti and Di Prisco 2007);
4. With a constant energy level of impact, the depth of penetration will depend on the area of impact.

However, if we adopt a pseudo static approach for calculation, we must transform the energies of the impact to equivalent forces acting on the embankment. And, these results are subject of many uncertainties. The problem can be solved by adopting a systematic numerical finite element model or equivalent. The successful application of these methods, however, requires the availability of appropriate tests for proper calibration of the model. Some solutions have been proposed to address these uncertainties and provide designers with a quick and simple tool for design practice. Recently, Calvetti and Di Prisco (2007) have improved calculation methods in order to estimate the penetration of boulders into the soil as part of an extensive study, including experimentation on a rockfall protection canopy (Figure 5).
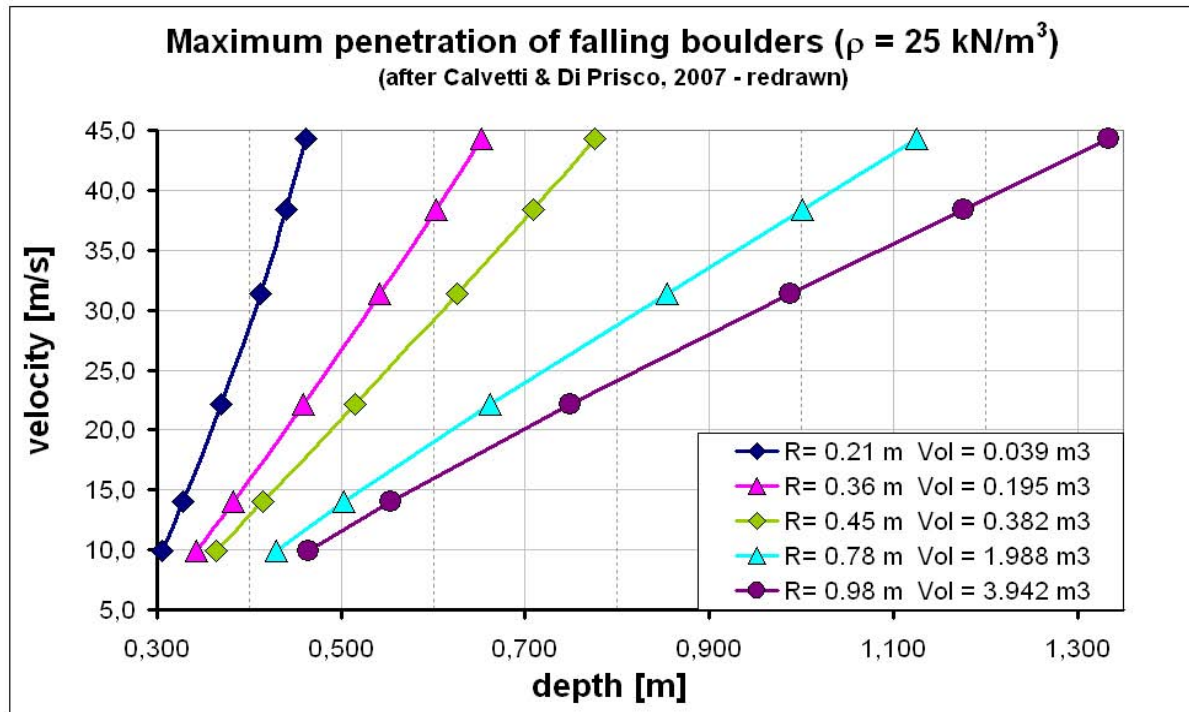
Fig. 5 – Maximum penetration of the block vs. velocity of impact
(after Calvetti and Di Prisco, 2007)

This approach is based on the following assumptions: (a) the impact occurs normal to the surface; (b) the impacting body is spherical with radius r density ρ 25 kN/m3; (c) the impacted fill material is made up of predominantly granular material, heterogeneous in size, properly mechanically compacted, which is in accordance with the construction of Green Terramesh embankments; and (d) the layer of soil has a thickness of at least 2 meters (6.6 ft) and lies on a rigid base.
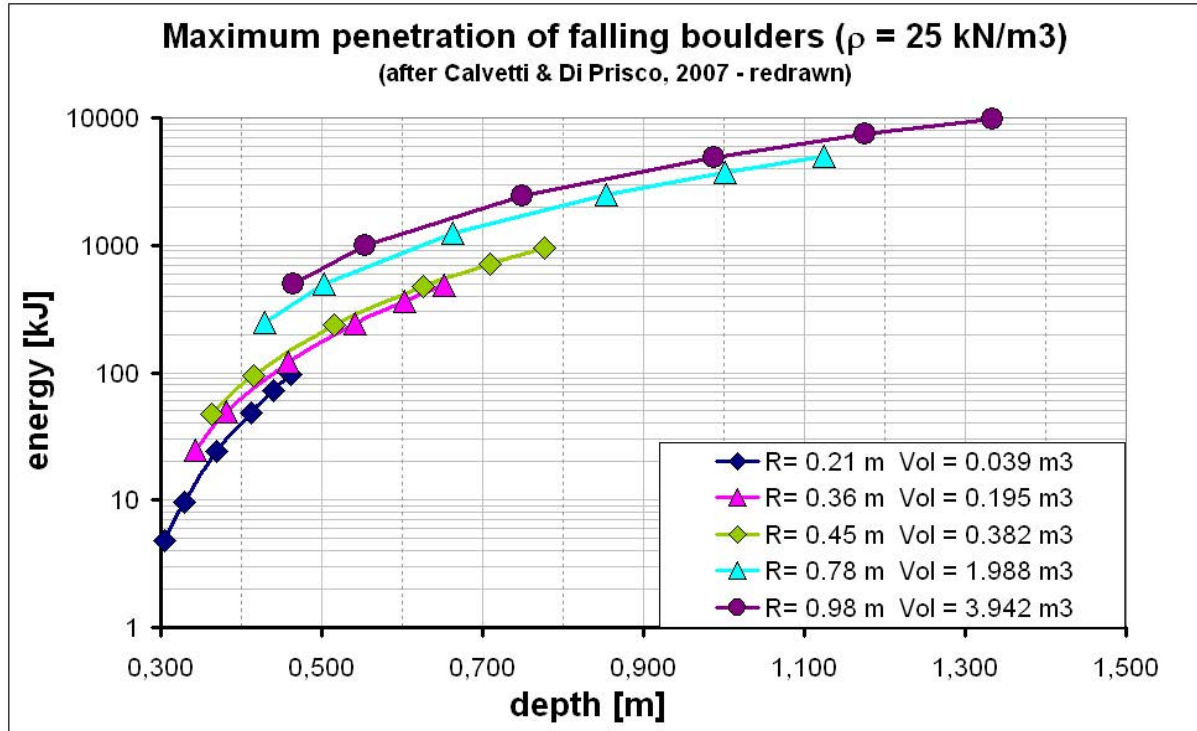
Fig. 6 – Maximum penetration of the block in relation to the impact energy (after Calvetti e Di Prisco, 2007)

boulders (Figure 6). This implies that at low speeds, the dept of penetration increases slightly for variations in the size of the block and therefore with variations in energy of impact. In light of this observation, it is obvious that the simulations of falling rocks in back analysis are valid only for the rocks of the size used in the simulation. The repetition of the simulation with different masses suggests that the coefficients of restitution of the fill material are changing with the masses. This concept confirms what has been noted by Pfeiffer & Bowen (1989) as the necessity to adjust the coefficient of restitution used in the normal R_N simulations of falling rocks to a function of impact speed or of the size of the boulder. The graph will then be able to directly estimate the penetration of rock once the size of the block and the energy level is known.

The penetration of the rock on the facing portion of the embankment can be determined by the aforementioned criteria; however, the estimation has been done without consideration of deformation of downslope side of the embankment. A higher position of the point of impact on the embankment could generate a less accurate estimation of the penetration of the block, and therefore be subject to error. Therefore, the graph should be used to determine the approximate thickness of the embankment at the point of its highest probable impact. Empirical assessment indicates that the minimum thickness of the reinforced embankment in its most unfavorable segment should be estimated to be a minimum of twice the maximum penetration achieved during the impact. The minimal thickness of the embankment t_w is obtained when:

$$t_W \geq 2\, p_B$$

where p_B is the penetration of the mass in the embankment, as determined on the chart.

Adoption of this proposed method along with consideration and integration of other parameters are particularly important in order to define the width of the top section t_E of the embankment. Additionally, the construction criteria, operational function and condition of internal stability of the structure must be taken into account.

In the case of the trapezoidal Green Terramesh, we obtain that:

$t_E \geq t_W - 2\, u_f / \tan \alpha$

where $\tan \alpha$ is the inclination of the uphill embankment from the horizontal and u_f is the upper free section of embankment. The upper section of the embankment where the impact should not occur (due to high potential deformation) is at least equal to the diameter of the projectile rock mass. The minimum height of the embankment h_E will be determined as:

$h_E \geq h_d + u_f = h_d + (t_W - t_E) / 2 * \tan \alpha$
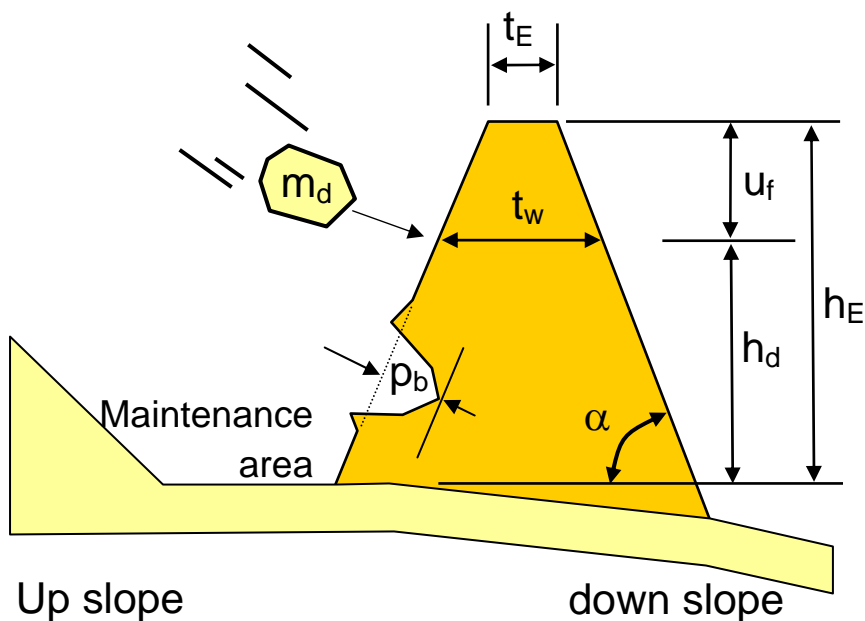
Figure 7 – Definition of the measures of the detected parameters.

Case history

The Green Terramesh embankments have been widely used to build embankments for protection of roads and infrastructure from falling rocks. Additionally, they have been used for the construction of deflection structures or for the construction of structures with the purpose of protecting urban areas from debris flow activity. A significant event occurred in Cogne (Valle d'Aosta - Italy), where a large embankment has been installed to protect highway SR 47 (Figure 8).

On the morning of June 5, 2007, there was a landslide with the collapse of large blocks, some of which were larger than 30 m³ (1000 ft³). The impact was along an embankment that is 50 meters (164 ft) in length and 11.5 meters (38 ft) in height above the ground surface. A boulder of about 6 m³ (211 ft³) (mass 15000 kg (33,000 lb)) impacted the embankment, at approximately mid-height (6 m (20 ft) from the base) and approximately 4 meters (13 ft) from the edge of the embankment, causing a deep crater of 0.60-0.70 meters (2 to 2.5 ft) in depth. The area surrounding the impact crater was deformed, but the adjacent area did not experience serious damage. The internal stability of the embankment was not compromised, and no maintenance was required. Only aesthetic repairs, easily executable with mesh patches or with an erosion control blanket, are planned. Impact craters must be filled with loose material where possible.

Figure 8 – Left: Green Terramesh embankment to protect SR 47 in Cogne (Valle d'Aosta). On June 5, 2007, several big boulders (30 m3) mobilized down the hillslope. Right: A rock block, approximately 6 m3 in volume, impacted the embankment at approximately mid- height (6 m from the base) on the embankment.

In this particular case, with the available data from the event, it was possible to determine the speed of the impact mass about 20 meters/second (44 miles/hr). It was also possible to estimate a penetration depth of 0.70-0.75 meters (2 to 2.5 ft) by assuming the rockfall volume (about 6 m³ (211 ft³) to a sphere of diameter 1.15 m (4 ft)), and using the chart proposed by Calvetti and Di Prisco (2007).

Numerical Analysis

The design procedure described above provides a method to quantify the size of the embankment, but this methodology does not allow predicting the deformation parameter of the embankment that can be expected during an impact at a given energy. When the impact of a rockfall event creates significant damage to the structure, it may be necessary to have the structure repaired to recover its functionality. In the event of an impact that creates significant damage, it may be necessary to demolish the structure and rebuild an entire portion of the embankment. In a scenario that could result in this last case, it would be necessary to develop a more complex analysis than the one described in this paper. A more comprehensive and rigorous analysis of the event would be required in order to be able to consider more precisely and effectively the mechanism that occurred during impact of this magnitude.

For this development we must use numerical models based on finite elements analysis with a dynamic impact range, which must be able to reproduce realistic scenarios. The "Politecnico di Torino" and Maccaferri are working in cooperation in order to develop a full set of models based on back-analyses of past events, for different embankment sizes and impacts. Their aim is to provide clear guidelines on energy absorption and on the deformation conditions after impacts for variable geometries of Terramesh system embankments, with a final goal of making it available to designers. This could provide guidance on optimizing the dimensions of the structures in order to effectively design for different energy level impacts.

Conclusion

Reinforced embankments for rockfall protection are a reliable solution primarily because they provide high energy level resistance and can withstand multiple impacts. Additionally, these structures require a relatively low level of maintenance in response to low energy impacts when compared to other rockfall barriers. A variety of full scale tests have demonstrated the effectiveness of these structures. Systematic numerical modeling defined with a back-analysis of full scale test results and past events can be used to provide a design chart for standardized structures. Alternatively, for design it is possible to use the proposed simplified analytical tool that allows evaluation of final embankment deformation after the impact, and verification of the embankment dynamic stability.

In the case of the Terramesh embankment, the approach is simplified with a graph and the result is consistent with numerical analyses as demonstrated in the case history cited above. The simplified method requires appropriate confirmation of certain parameter characteristics before its application to general embankments. Based on their long experience and the results of finite element modelling, Maccaferri has developed specific graphs to design Terramesh embankments in an efficient, economic, and immediate manner.

Bibliography

Azzoni, A., La Barbera, G., and Zaninetti, A.: Analysis and prediction or rockfalls using a mathematical model, Int. J. Rock Mech. Min., 32, 709-724, 1995.

Barrett, R. K. and White, J. L.: Rockfall prediction and control, in: Proceedings of National Symposium on Highway and Railway Slope Maintenance, Association of Engineering Geologists, Chicago, U.S.A, 23-40, 1991.

Bertrand, D., Nicot, F., Gotteland, P., and Lambert, S.: Modelling a geo-composite cell using discrete analysis, Computers and Geotechnics, 32 (8), 564-577, 2005.

Bertrand, D.: Modélisation du comportement mécanique d'une structure cellulaire soumise à une sollicitation dynamique localisée, Ph.D. thesis, Université Joseph Fourier, Grenoble, France, 2006 (unpublished).

Burroughs, D.K., Henson, H.H., and Jiang, S.S.: Full scale geotextile rock barrier wall testing, analysis and prediction, in: Proceedings of Geosynthetics 1993, Vancouver, Canada, 30 March- 1 April 1993, 959-970, 1993.

Calvetti F., Di Prisco C. Vecchiotti M., 2005 – Experimental and numerical study of rockfall impacts on granular soils, Rivista Italiana di Geotecnica, 39, 4, pp. 95-109.

Calvetti F., Di Prisco C., 2007 – Guideline for canopy design – Veneto Strade Research books – Starrylink Edition – Brescia (in Italian)

Carotti, A., Peila, D., Castiglia, C., and Rimoldi, P.: Mathematical modelling of geogrid reinforced embankments subject to high energy rock impact, in: Proceedings of Eurogeo, II European Geosynthetics Conference and Exhibition, Bologna, Italy, 15-18 October 2000, 305-310, 2000.

Castiglia, C.: Studio del comportamento di rilevati paramassi, M.S. thesis, Politecnico di Torino, Italy, 2000 (unpublished).

Del Greco, O. and Oggeri, C.: Caratteristiche di resistenza a taglio di geosintetici, in: Proceedings of XX Convegno Nazionale di Geotecnica, Parma, Italy, 22-25 September 1999, 79-86, 1999.

Di Prisco, C. and Vecchiotti, M.: A rheological model for the description of boulder impacts on granular strata, Géotechnique, 56 (7), 469-482, 2006.

Di Prisco, C. and Vecchiotti. M.: Impatti di blocchi di roccia su rilevati rinforzati: modellazione teorica e spunti progettuali, L'Ingegnere e l'Architetto, 10 (1), 62-69, 2003.

ETAG 027 - Guideline Falling Rock Protection Kits, EOTA, January 2008

Frey, R. P.: Swiss guideline: action on rockfall protection galleries, in: Proceedings of the Joint Japan-Swiss Scientific Seminar on Impact load by rockfall and design of protection structures, Kanazawa, Japan, 4-7 October 1999, 91-94, 1999.

Ghionna, V.N., 2002 : Analysis of the full scale experimental results on reinforced soil having different stiffness – First report– Numerical model of pullout tests using FLAC, reserved documentation MACCAFERRI.

Giani G.P. 1997. Caduta di massi, Hevelius edizioni, Benevento

Giani, G. P.: Rock Slope Stability Analysis, Rotterdam, Netherlands, 1992.

Grasso, P. and Morino, A.: Stabilità dei versanti ed interventi di protezione realizzati in Carema, Bollettino dell'associazione Mineraria Subalpina, XXVIII, 239-251, 1991.

Jacquemoud, J.: Swiss guideline for the design of rockfall protection galleries: background, safety concept and case histories, in: Proceedings of the Joint Japan-Swiss Scientific Seminar on Impact Load by rockfall and design of protection structures, Kanazawa, Japan, 4-7 October 1999, 95-102, 1999.

Labiouse, V., Descoeudres, F., and Montani, S.: Experimental study of rock sheds impacted by rock blocks, Structural Engineering International, 3, 171-175, 1996.

Lambert, S., Gotteland, P., Bertrand, D., and Nicot, F.: Comportement mécanique de géo-cellules soumises a impact, in: Proceedings of Congrés de Mécanique, Grenoble, France, 27-31 August 2007, 23-24, 2007.

Lambert, S., Nicot, F., and Gotteland, P.: Experimental study of the impact response of geo-cells as components of rockfall protections ditches, in: Proceedings of Interdisciplionary Workshop on Rockfall Protection, Morschach, Switzerland, 23-25 June 2008, 52-54, 2008.

Lazzari, A., Troisi, C., and Arcuri, G.: Protezione di nuclei abitati contro la caduta di massi mediante rilevati in terra rinforzata: esperienze della Regione Piemonte, in: Giornata di Studio su "La protezione contro la caduta di massi dai versanti rocciosi", Torino, Italy, 24 October 1996, 85-94, 1996.

Mayne, P. W. and Jones, S. J.: Impact stresses during dynamic compaction, Journal of Geotechnical Engineering, 109(10), 1511-1516, 1983.

Mayne, P. W., Jones, J. J., and Dumas, J. C.: Ground response to dynamic compaction, Journal of Geotechnical Engineering, 110 (6), 757-774, 1994.

Montani, S., Descoeudres, F., and Egger, P.: Impact de blocs rocheux sur des galeries de protection, in: Giornata di Studio "La protezione contro la caduta massi dai versanti rocciosi", Torino, Italy, 24 October 1996, 55-64, 1996.

Oggeri C., Peila D. & Recalcati P. 2004. Rilevati paramassi. Conferenza "Bonifica di versanti rocciosi per la protezione del territorio, Peila (ed), Trento, GEAM, Torino, pp.191-232

Oggeri C., Peila D., Ronco C., 2008 – Numerical analysis of embankments behaviour done with reinforced soil – Preliminary report – contract of research between DITAG Politecnico di Torino and Maccaferri SPA (in Italian).

Oggeri, C., Peila, D., and Recalcati, P.: Rilevati paramassi, in: Proceedings of Convegno su Bonifica di versanti rocciosi per la protezione del territorio, Trento, Italy, 11-12 March 2004, 191-232, 2004.

Paronuzzi, P.: Criteri di progettazione di rilevati paramassi, Geologia tecnica, 1, 23-41, 1989.

Pasqualotto, M., Hugonin, B., and Vagliasindi, B.: Rilevati in terra rinforzata a protezione dalla caduta massi in Val di Rhemes (AO), GEAM, 114 (1), 55-67, 2005.

Pasqualotto, M., Peila, D., and Oggeri, C.: Prestazioni di un sistema di rilevati a scogliera soggetti ad impatto di massi, in: Proceedings of Convegno "Bonifica di versanti rocciosi per la protezione del territorio", Trento, Italy, 11-12 March 2004, 435-442, 2004.

Peckover, F. L. and Kerr, W. G.: Treatment and maintenance of rock slopes on transportation routes, Canadian Geotechnical Journal, 14 (4), 487-507, 1977.

Peila D., Castiglia C., Oggeri C., Guasti G., Recalcati P. & Sassudelli F., 2000. Full scale tests on geogrid reinforced embankments for rockfall protection, II European Geosynthetics Conference and Exhibition, 1, Bologna. pp. 317-322

Peila D., Oggeri C., Castiglia C., Recalcati P. & Rimoldi P. 2002. Testing and Modelling geogrid reinforced soil embankments to high energy rock impacts, Geosyntetics - 7th I.C.G., Delmas, Gourc & Girard (eds), Swets & Zeitlinger, Nice, pp. 133-136

Peila, D., Oggeri, C., and Castiglia, C.: Ground reinforced embankments for rockfall protection: design and evaluation of full scale tests, Landslides Investigations and Mitigation, 4 (3), 255-265, 2007.

Pfeiffer, T.J., and Bowen, T.D., 1989. Computer Simulation of Rockfalls. Bulletin of the Association of Engineering Geologists Vol. XXVI, No. 1, 1989 p 135-146.

Technical data sheet MAC.RO System – Embankments, MACCAFERRI 2007

UNI 11167 – Structures for rockfall protection – Rockfall embankments; Procedure impact test and its realization – August 2006 (in Italian)

Wyllie D.C. & Mah C.W., 2004. Rock slope engineering civil and mining, Spon Press, pp. 313-315.

Plassiard, J. P., Donzé, F. V., Lorentz, J.: Simulations of rockfall impacts on embankments using a discrete element method, in: Proceedings of Interdisciplinary Workshop on Rockfall Protection, Morschach, Switzerland, 23-25 June 2008, 84-86, 2008.

Ronco, C.: Criteri di dimensionamento di rilevati paramassi in terra rinforzata, M.S. thesis, Politecnico di Torino, Italy, 2006 (unpublished).

Tissieres, P.: Ditches and reinforced ditches against falling rocks, in: Proceedings of the Joint Japan-Swiss Scientific Seminar on Impact load by rockfall and design of protection structures, Kanazawa, Japan, 4-7 October 1999, 65-68, 1999.

Yoshida, H.: Recent experimental studies on rockfall control in Japan, in: Proceedings of the Joint Japan-Swiss Scientific Seminar on Impact load by rockfall and design of protection structures, Kanazawa, Japan, 4-7 October 1999, 69-78, 1999.

2.5

Post Foundations for Flexible Rockfall Fences

by

Ryan Turner P.E.
California Department of Transportation
50 Higuera St, San Luis Obispo, CA 93401
(805) 748-1706
ryan_turner@dot.ca.gov

John D. Duffy P.G., C.E.G.,
California Department of Transportation
50 Higuera St, San Luis Obispo, CA 93401
(805) 549-3663
john_d_duffy@dot.ca.gov

John P. Turner, Ph.D, P.E.,
University of Wyoming
Civil & Architectural Engineering
1000 E. University Ave.
Laramie, WY 82071
(307) 766-4265
turner@uwyo.edu

ABSTRACT

The use of flexible rock nets to protect transportation infrastructure is gaining popularity with DOT's throughout the United States. As more of these structures are constructed and impacted by rockfall, design procedures and construction methods are adapting to more accurately and efficiently predict and resist the loads imparted to the structure via dynamic impacts from rockfall. This research paper will examine the design and construction of post foundations for flexible rock nets. Topics will include:

- Current industry standards for the design and construction of post assemblies and post foundations for flexible rock nets;
- Shear and axial demands and resistances of post assemblies and foundations; and
- Effects of dynamic loading on the passive and shear resistance of varying foundation soil and rock types.

The objective of this paper is to begin development of uniform standards for the design of post foundations for flexible rock nets, which will ensure the structural integrity and cost effectiveness of structures to be constructed in the future.

INTRODUCTION

Flexible rockfall fences used for the protection of highway facilities from rockfall has become a topic at the forefront of rockfall mitigation in the United States over the past two decades. Design and construction of flexible rockfall fences have undergone extensive theoretical research and field testing, leading to the development of more economical structures better suited to the unique conditions encountered at rockfall sites throughout the world. Observation and instrumentation of flexible rockfall fences with load cells and strain gauges impacted by rockfall under controlled conditions has allowed engineers and geologists to study the effects of dynamic impacts on the flexible structures and to calculate energy limits for given systems. Through the course of standardized testing procedures developed in Switzerland, The United States, and The European Union, a standardized system has been developed to rate the energy capacity of flexible rockfall fence systems.

Although much time and effort has been devoted to determining the energy dissipation path and loads imparted to the structural components of flexible rock nets, the post foundations are often designed by third party engineers unfamiliar with the systems. This paper will focus on the design of post foundations for flexible rockfall fences. In order to narrow the scope of the paper, flexible rockfall fence designs currently available from several major manufacturers rated for energy impacts of 500 to 1000 kilojoules are examined. [3]

A brief overview of the components of flexible rockfall fences and a description of the behavior of the systems under dynamic impact loads are presented. Data obtained from flexible rockfall fence manufacturers Isofer/Rotec and Maccaferri resulting from field testing and theoretical modeling of proprietary designs of flexible rockfall fences instrumented with load cells and strain gauges are presented and used to estimate the loads imparted to the post assemblies and post foundations under controlled energy impacts. Design of post foundations is examined for typical geomaterials encountered at rockfall sites. The goal of the paper is to characterize the design of post foundations for flexible rockfall fences, and ensure the structural integrity and cost-effectiveness of the systems.

FLEXIBLE ROCKFALL FENCES

Flexible rockfall fences consist of four major structural components: the cable mesh, the post assemblies, the anchors and friction brakes, and the cables attaching the net to the posts and anchors. Interlocking ring nets, cable ring nets, or cable nets hang on cable infrastructure, which is supported by posts founded on the post foundations at the base and supported at the top by upslope and end ground anchors (Figure 1). The flexible rockfall fence dissipates rockfall impact energy as the cable mesh elongates during impact, decelerating the rock. Simultaneously, energy is also dissipated through the elongation of the cable infrastructure and activation of the energy dissipaters (friction brakes). The primary function of the posts is to maintain the height of the fence and provide catchment. Each manufacturer's system contains the four major components with variations in the connections.

---

[3] English units used throughout paper. 500 kilojoules = 182 foot-tons and 1000 kilojoules = 364 foot-tons.
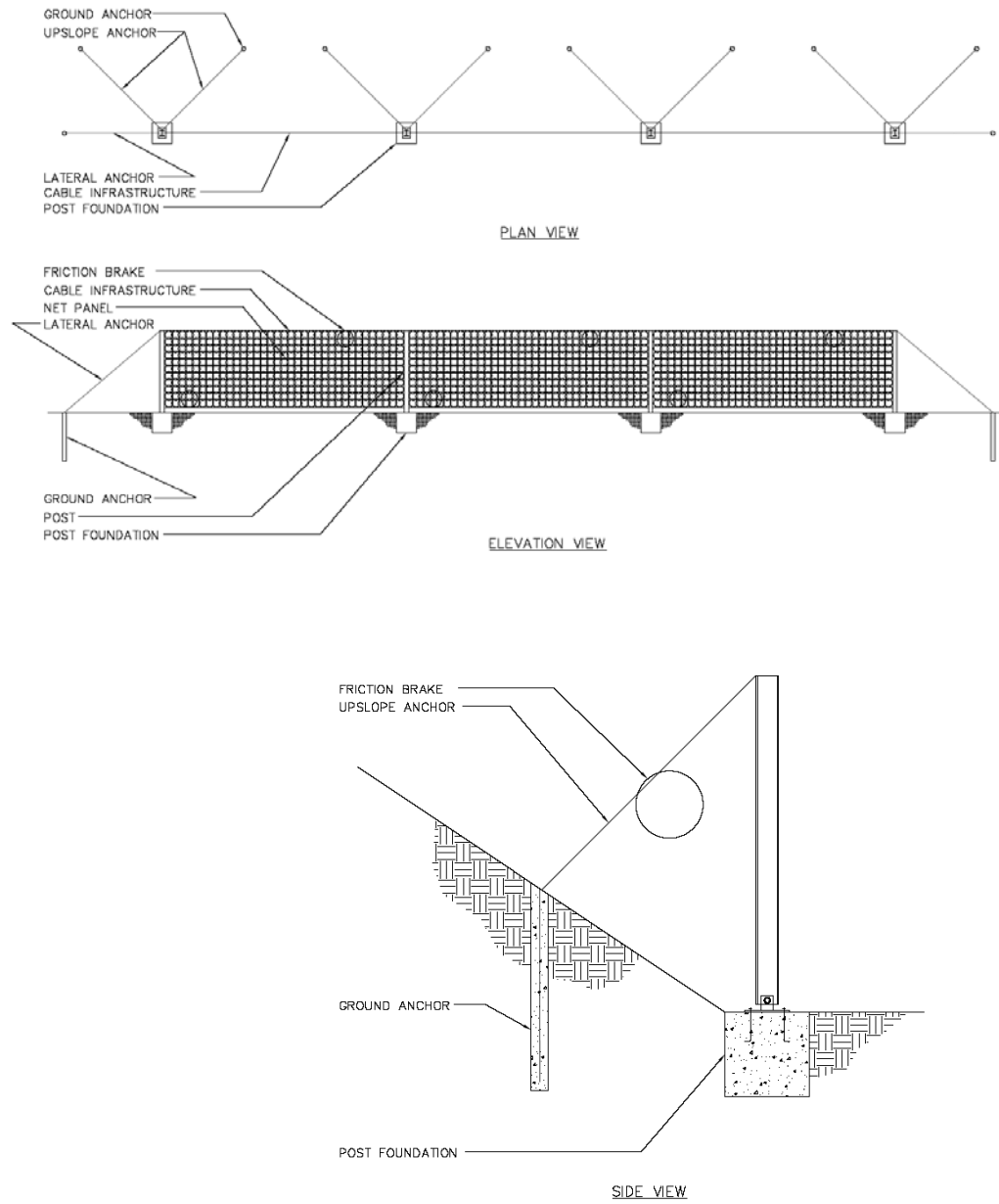
Figure 1: Flexible rockfall fence schematic

Figure 2: Constructed flexible rockfall fence

POSTS

Posts for the flexible rockfall nets are wide flange sections oriented with the major axis perpendicular to the plane of the fence. The posts used in the 500 and 1000 kilojoule systems examined in this paper are approximately 8-inch deep sections. The top rope of the cable infrastructure is looped through a welded bracket on the down-slope side of the top of the post, allowing the top rope to break free of the post in the event of a high-energy impact that induces deflection beyond the rotational capacity of the post. An upslope anchor with an energy dissipating friction brake is connected to the top of the post with a shackle through the web of the post. The use of shackles and replaceable connections designed to fail at or near the system energy capacity is intended to induce failure in the connections without damaging major structural and foundation elements. The base of the post is fastened to welded tabs on a rectangular base plate with a single steel bolt. Examination of constructed flexible rockfall nets and current specifications and plans from manufacturers indicate that the typical base connection is made with a single ¾-inch diameter A325 steel bolt through the web of the post section with welded steel plate tabs on either side of the web. The use of a single bolt at the post base results in a pinned condition, allowing the post to rotate freely about its base without imparting significant moment into the post foundation.
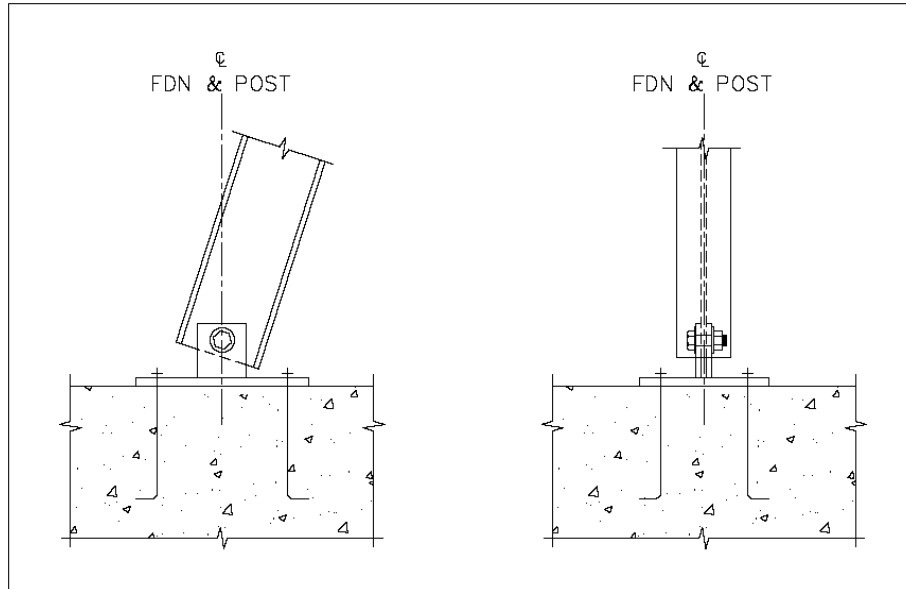
Figure 3: Side and front elevation views of typical pinned post to foundation connection

FOUNDATIONS

Determination of the soil or rock conditions and an understanding of the post foundation loads are critical elements in designing an economical and suitable post foundation. Budgetary constraints often eliminate the possibility of performing a foundation investigation, but a site reconnaissance and observation of the surrounding geology can often provide general information as to the nature of the foundation materials. Because flexible rock nets are used in active rockfall zones of exposed fractured rock, colluvium overlying country rock is a commonly encountered foundation material.

Due to the flexible nature of the systems and dynamic impact of the rock, accurately determining the foundation loads by theoretical modeling or field-testing is very difficult. Initial requests to flexible rock net manufacturers and designers for foundation loads were met with the reply that is was too difficult to instrument the post or foundation in such a way that the loads could be measured. Instrumentation of the upslope cable anchors with strain gauges is relatively simple because the cables are tension members and cannot transfer shear. Measuring the loads at the foundation level requires the ability to simultaneously measure the axial load and shear loads transferred to the pin. The only manufacturer able to provide field measured loads was Maccaferri. Maccaferri engineers had performed controlled testing of their MAC.RO. CTR-500-B System with a proprietary instrumentation device (Figure 4) able to measure the axial and shear loads at the post-to-foundation connection point. Isofer/Rotec submitted predicted foundation loads obtained from combining measured tensile loads in the upslope and end anchors and structurally modeling the post base to calculate theoretical foundation loads. The loads are presented in the Analysis Section.
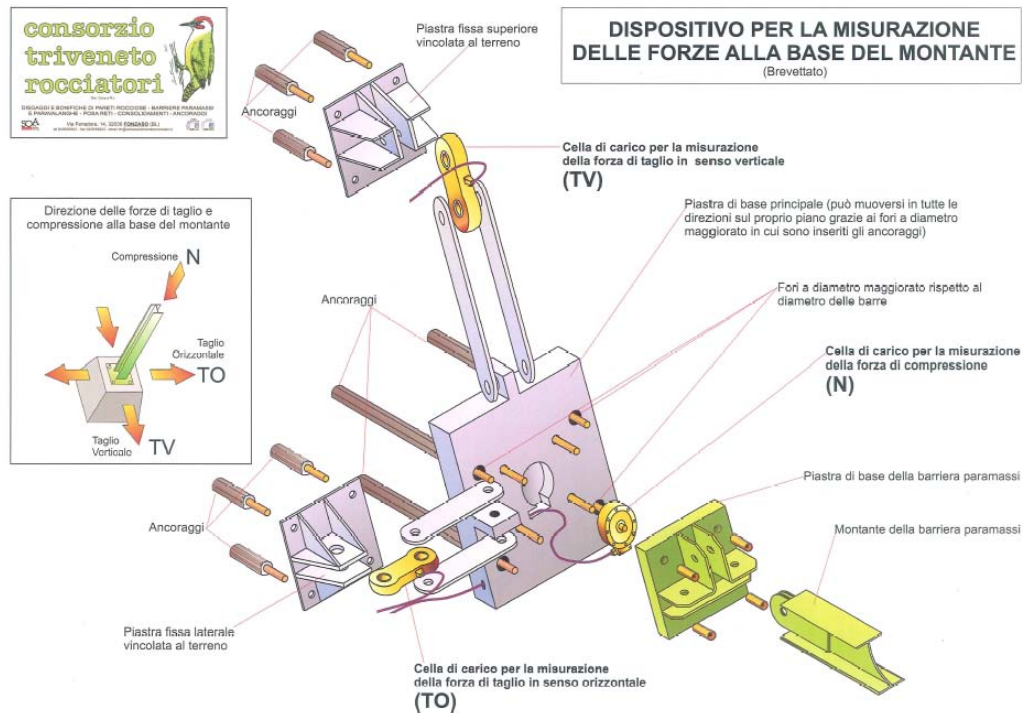
Figure 4: Diagram of the patented system used in CTR field test to evaluate loads at the base of the post. Evaluation of the forces transmitted by the post to the foundation during the impact of a block is a key value to be monitored according to the new ETAG 027 standard.

Since 1989, the design and construction of post foundations by The California Department of Transportation (Caltrans) has used three standard foundation designs for typically encountered foundation geomaterials including soil, rock overlain by a thin veneer of soil, and rock.

The standard soil foundation is a 2.5 x 2.5 x 2.5-foot concrete block poured against undisturbed native soils and typically excavated by hand or with a backhoe. The soil type most commonly found in fence installations is free draining colluvium. The colluvium can be described as silty, sandy, gravel with angular cobbles, generally loose at the surface with an increasing relative density as the depth of the footing increases. Similar to typical foundation construction methods, the excavation is filled with concrete and anchor bolts are wet-set in the concrete using a template or drilled and grouted after the concrete has cured.
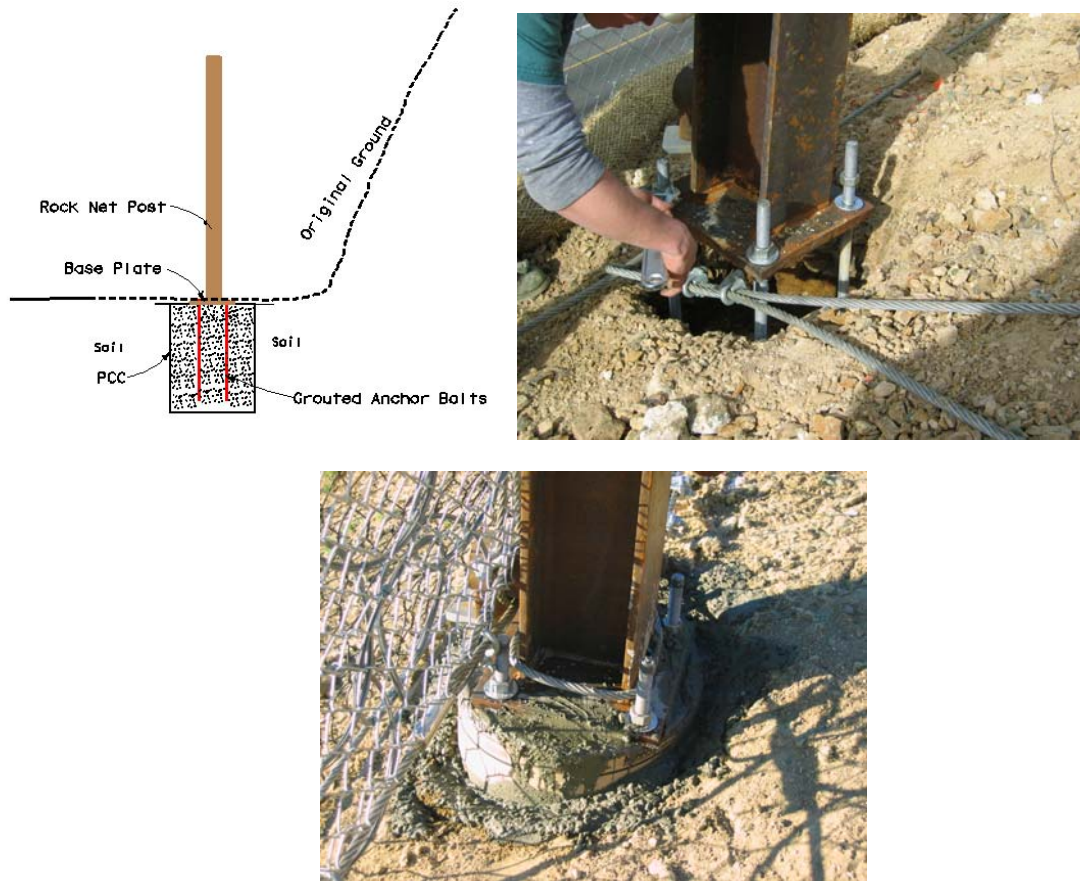
Figure 5: Typical post foundations in soil

The standard foundation for a geomaterial condition consisting of a thin veneer of soil overlying rock begins with an excavation though the soil extending in the bedrock. Two designs are used to anchor the post. One method is to install several grouted rock dowels into the rock beneath the bottom of the excavation. The rock dowels typically have a grouted length between 3 and 5 feet, depending on the strength and condition of the rock, and extend up into a concrete block that provides level bearing and anchorage for the post. The second design eliminates the dedicated anchor bolts and extends the rock bolts through the concrete block and bolts the base plate directly to the rock bolts. This method requires less material, but may be more difficult to maintain and replace in the event of failure of the rock bolts.
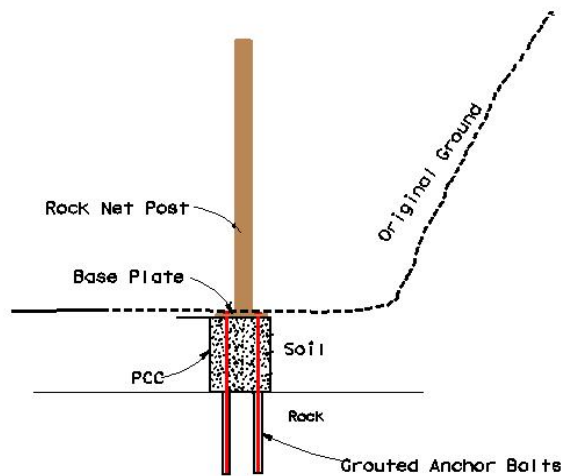
Figure 6: Typical post foundation in rock overlain by soil

Post foundations in rock are similar to the previous condition. Rock dowels are drilled in to the rock and serve as the anchor bolts connecting the base plate to the foundation. A concrete leveling pad is commonly hand placed around the dowels to provide a level surface for the post base plate. The dowels are typically grouted 3 to 5 feet into the bedrock depending on the rock strength and condition.
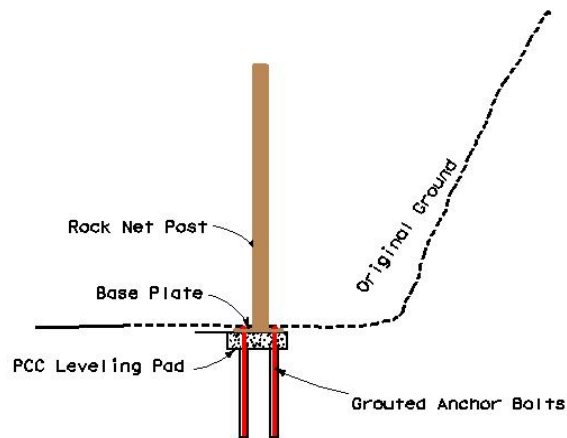
Figure 7: Typical post foundations in rock

MAINTENANCE

An important aspect of the design of flexible rockfall fences is the cost and ease of maintenance following a rockfall impact. Protecting the roadway and the travelling public (safety) is paramount when considering the performance and capacity of the systems, but reconstruction of the systems in a timely and economical fashion after a rockfall event is a practical consideration that should be incorporated into the design. The primary function of the posts is to maintain the fence catchment height. A rockfall impact that causes complete failure of the post and/or foundation, but which is stopped in the fence system, is successful. However, an acceptable level of maintenance must be established, especially if such events are frequent. Experience in California has shown that replacement of the posts, energy dissipating devices, and cable connections is less expensive and takes less effort and time than replacement of the foundation elements.

FLEXIBLE ROCKFALL FENCE FOUNDATIONS PRACTICE

Flexible rockfall fences designed to dissipate the dynamic impact energy of a falling rock have been in use on California highways since the early 1990's. To date Caltrans has installed 85 fences ranging in energy capacity from 70 kilojoules to 1500 kilojoules[4], totaling the construction of approximately 12,750 linear feet of fence and 731 posts and foundations. Prior to installing the fences on state highway corridors, Caltrans participated in extensive testing with the manufacturers and designers of the systems in 1989. These tests focused on two 200 kilojoule fence designs provided by Geobrugg (Switzerland) and L'Enterprise Industrielle (France). The two systems tested were similarly designed fences held upright by posts and supported by a system of cables. However, there was one notable difference: one design had the posts supported on a concrete footing, while the other design simply had the post base staked to the ground. Both systems successfully stopped the rocks. At the time, it was determined that the post supported on a concrete footing required less maintenance to restore the fence to full height and became the foundation design of choice.

---

[4] 70 kilojoules = 25 foot-tons and 1500 kilojoules = 550 foot-tons

(a)   (b)

Figure 8: Two different types of post foundations used during the 1989 California Department of Transportation flexible rockfall fence tests. (a) post founded on native material and secured with hand driven stakes and restraining cables and (b) post founded on concrete foundation.

Since the tests in 1989, five different manufacturers have supplied the 85 flexible rockfall fences installed by Caltrans. Foundations have been constructed in many varying geomaterials characterized generally in the Foundation Section. Many of these systems have been impacted multiple times, impacted with above design load impacts, replaced, rebuilt and reused. In 20 years of maintaining dozens of flexible rockfall barriers, a post foundation failure that required replacement of the foundation has never been observed.

Figure 9: Two rockfall events, the first illustrating a post failure maintained by replacing the post and utilizing the existing foundation and the second showing successful capture of rock later removed.

ANALYSIS

FORCES ACTING ON POST FOUNDATION

Third-party engineers often perform design of foundations supporting the posts.   The engineer responsible for the design is required to perform a basic check on the stability, taking into account the forces acting on the footing. For a pin connection between the base of the post and the top of the footing, the post is free to rotate and the moment is zero. The resultant force can be resolved into

vertical (P) and horizontal (H) components as shown in Figure 8. Note that within state transportation agency practice, it is common to specify a standardized footing size. For example, the standard Caltrans concrete footing used for soil sites consists of an equidimensional 2.5-foot concrete block. Although this design is not incorporated into Caltrans Standard Specifications, it is an informal standard utilized on most Caltrans rockfall barriers rated for 1,000 kJ or less.
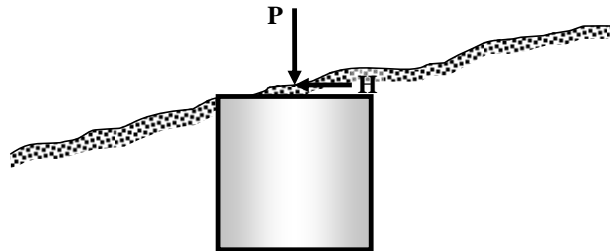

Figure 10. Forces acting on a post foundation

Information on the magnitude of forces P and H is provided (typically) by the supplier of the nets. This information is not site-specific, but is based on analytical and, in some cases, experimental data from full-scale load testing. The design forces are based on the assumption that a rock with kinetic energy equal to the rated energy capacity of the barrier impacts the net. A second type of loading, in which a rock impacts the post (direct hit) is not typically considered in design, but is discussed in a later section of this paper.

Results from a recent full-scale load test performed by Maccaferi on a barrier with a rated energy of 500 kilojoules are used to illustrate the force effects acting on intermediate post foundations. In this test, a block of weight = 3.55 kips was dropped from a height of 108 feet onto a net barrier supported by 9.8-foot high posts on 32.8-foot centers. The theoretical kinetic energy of the block at impact = 528 kJ (383 foot-tons). Load cells in the proprietary device at the base of the post were used to monitor axial and lateral forces during the impact. The forces vary as a function of time as the net deforms and energy is dissipated through the mechanisms described earlier. The peak values of axial compression and transverse shear measured at the post base were: P = 12,926 pounds force and H = 7,576 pounds force. Axial compression in the post is a direct result of the tensile force mobilized in the upslope anchor cable attached to the top of the post. For this test, the measured axial compressive force is approximately 3.6 times the weight of the block and the shear force is approximately 2.1 times the weight of the block.

Utilizing the results of tests such as the one described above, and numerical modeling of barrier systems under impact loading, manufacturers have established nominal force effects for their proprietary systems. For example, Table 1 below presents nominal post foundation forces for one vendor's 1,000 kJ system. Axial force varies with the height (H) of the posts and whether the post is an

end column or an intermediate column. Note that the horizontal force does not vary with post height or location.

TABLE 1. Example of Vendor-Supplied Nominal Force Effects on Barrier Post Foundations (Source: Rotec/Isofer International)

Energy Rating of Barrier	Vertical Compressive Force, P (lb-force)						Horizontal Force, H lb-force
	End Columns, Height			Intermediate Columns, Height			
	13.1 ft	16.4 ft	19.7 ft	13.1 ft	16.4 ft	19.7 ft	
363 ft-tons	35,519	39,341	43,163	11,690	12,139	13,263	21,356

RESISTANCE AND FOOTING STABILITY

Under the load combination described above, an individual footing can be checked for several potential failure modes, specifically (a) bearing capacity and (b) lateral stability. Bearing capacity analysis requires the nominal bearing capacity of the soil or rock beneath the footing to be calculated or presumed. Detailed information on the strength properties of the founding geomaterials typically is not available on rockfall barrier projects. Presumptive values of bearing capacity can be used to conduct rudimentary checks. Many state highway agencies use presumptive allowable bearing capacities for shallow footings on rock and soil. These values can typically be increased by 50% for short-duration loading such as impact. Bearing stress under impact load can be estimated as the nominal vertical compressive force P (provided by the vendor) divided by the bearing area. For example, for the Caltrans standard footing (A = 6.25 ft^2) and using the values of P in Table 1, the nominal bearing stress could range from 1.9 ksf to 6.9 ksf. For the most common material types encountered in rockfall environments (*e.g.*, colluvium and rock) these bearing stresses are usually within nominal values of allowable bearing capacity. Possible exceptions might include soft clayey colluvium derived from shale or other weak materials.

Lateral stability of the footing is derived from sliding resistance along the base and by development of passive resistance in front of the footing. In cases where strength properties of the supporting soil or rock are known or estimated, a simple model can be applied to check the lateral stability of a concrete footing under the force effects resulting from the design impact. Sliding resistance along the base of the footing develops as friction along the interface between the footing and underlying ground. The shear resistance (V) can be calculated as the product of the vertical force P, which acts as a normal force on the base of the footing, and the tangent of the interface angle of friction (δ), as illustrated in Figure 2. For concrete cast in place against soil, δ can be taken as the soil friction angle. Depending upon the underlying soil or rock type and condition, δ might typically range from 25 degrees to 40 degrees.
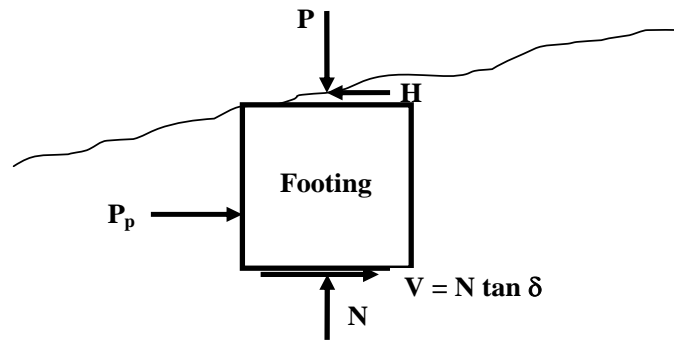
Figure 11. Free body diagram of force on post foundation

The resultant (P_p) of passive resistance in front of the footing can be approximated using relationships developed by Broms for laterally loaded piles and adopted by FHWA (Sabatini et al. 1999) for estimating the passive resistance of embedded soldier beams in anchored wall applications. As shown in Figure 10, passive resistance in cohesionless soils is assumed to develop over three times the footing width, B, with magnitude determined using the Rankine coefficient of passive earth pressure, K_p. In cohesive soils, passive resistance is assumed to develop over the width B and to be constant over the footing depth with a magnitude of nine times the soil undrained shear strength.

(a)   (b) Cohesionless soil   (c) Cohesive soil
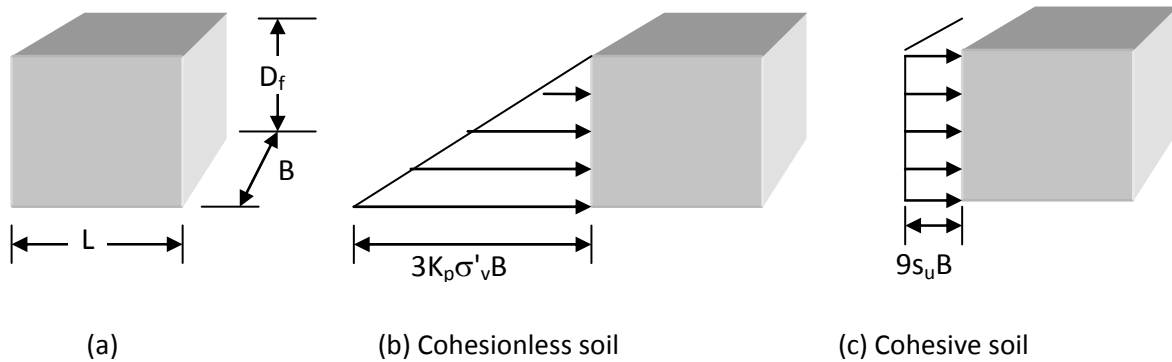
Figure 12. Broms method for approximating ultimate passive resistance

To illustrate this approach, the lateral stability of a standard Caltrans footing is evaluated under loads corresponding to the full-scale load test on a 500 kJ barrier described above. For illustrative purposes, it is assumed that the supporting material consists of coarse-grained colluvium with an estimated friction angle of 35 degrees and unit weight γ = 120 pcf. Footing dimensions are L = B = D_f = 2.5 feet.

Axial compressive force and shear force acting on the footing (measured):

P = 12.88 kips   H = 7.55 kips

Shear resistance at the base of footing:

V = P tanδ = 57.50 kN tan(35°) = 9.02 kips

Coefficient of passive earth pressure:

K_p = $tan^2(45^o + 35^o/2)$ = 3.69

Resultant of passive resistance:

P_p = ½ B [3 K_p σ'_v B]

P_p = ½ 2.5 ft x [3 (3.69) (2.5 ft) (120 pcf) (2.5 ft)] = 10.34 kips

Summation of resistances:

V + P_p = 9.02 + 10.34 = 19.36 kips > 7.55 kips

<u>Footing is stable</u>

If the stability is expressed in terms of a safety factor defined as the ratio of resisting to driving force, this footing has a factor of safety of 2.56. Similar calculations conducted for loads given in Table 1; for a 1,000 kJ fence show that the Caltrans standard footing in soil is stable under the vendor's nominal load values.

SUMMARY AND CONCLUSIONS

Design and construction of cost effective and serviceable flexible rockfall fences throughout the world is progressing as experience and technology provide engineers and contractors with tools to improve designs and construction methods. New methods for the determination and prediction of post foundation loads have emerged in recent years as part of manufacturer's efforts to improve performance and provide cost competitive designs in an increasingly competitive market. The information available at the time of this report is preliminary; more testing in the future should help

engineers determine accurate foundation load ranges for specific energy capacities and result in more economical structures.

Flexible rockfall fences consist of four components, as discussed in detail. The primary purpose of the posts is to maintain the catchment height of the fence. Stopping rocks from threatening the safety of the public is the measure of performance of the posts and post foundations. Experience has shown that the ease of maintenance of the systems after rockfall impacts is a practical aspect of the post and foundation designs, and led to the development and construction of systems with sacrificial connections designed to be replaced in the event of an impact exceeding the rated capacity of the system.

Observation of 85 flexible rockfall fences constructed in California and analysis of field-recorded loads and loads predicted by structural modeling demonstrates that the relatively small post foundations currently utilized are stable for rated system capacities up to 1000 kilojoules. Additional testing is required to more accurately determine the foundation loads for the full range of impact energies available from manufacturers.

REFERENCES

Broms, B.B., 1964. Lateral Resistance of Piles in Cohesive Soils. *Journal of the Soil Mechanics and Foundations Division*, ASCE, Vol. 90, No. SM2, pp. 27-63.

Broms, B.B., 1964. Lateral Resistance of Piles in Cohesionless Soils. *Journal of the Soil Mechanics and Foundations Division*, ASCE Vol. 90, No. SM3, pp. 123-156.

Brunet, G., Maccaferri Inc., Personal Communication, 2009.

Diotallevi, P., P., Gottardi, G., Govoni, L., High Resistance (Maccaferri) Rockfall

Barrier, (500kJoule) CTR/05/07/B, Full Scale Impact Test Certification, University Of Bologna, DISTART Department (Faculty of Engineering) and Consorzio Triveneto Rocciatori s.r.1 of Fonzaso, July 25, 2007.

Duffy, J, D., *Flexible Wire Rope Rockfall Nets,* Transportation Research Board, 71st Annual Meeting, Washington, D.C., January 1992.

Duffy, J, D., *Performance Review of Rockfall Mitigation Measures,* 49th Annual Highway Geology Symposium, Conference Proceedings, Prescott, Arizona, September 1998.

Giacchetti, G., Maccaferri, Inc., Personal Communication, 2009.

Paola, P., Ferraiolo, F., Documentation about the Patented System used in CTR Field Test to Evaluate the Loads at the Base of the Post, Consorzio Triveneto Rocciatori (CTR), 2009.

Sabatini, P.J., Pass, D.G., and Bachus, R.C. (1999). Ground Anchors and Anchored Systems. Geotechnical Engineering Circular No. 4, Publication No. FHWA-IF-99-015, *Federal Highway Administration, 281 p.*

Smith, D.W., Duffy, J.D. *Field Tests and Evaluation of Rockfall Restraining Nets*, 1989, California Department of Transportation Research Report No. CA/TL - 90/05.

Thommen, R., Rotec International., Personnel Communication, Structural Steel Columns Foundations for the Rotec/Isofer Rockfall Retaining Fence Systems, April 2009.

3.1

ROLE OF STRATIGRAPHY IN CUT SLOPE DESIGN FOR HORIZONTALLY-BEDDED SEQUENCES OF COMPETENT AND INCOMPETENT ROCKS OF EASTERN OHIO

Admassu, Yonathan and Shakoor, Abdul, Department of Geology, Kent State University, Kent, Ohio 44242; yonathanad@yahoo.com (330)672 2680; ashakoor@kent.edu (330) 672 2968.

Abstract

The geology in Ohio is characterized by horizontally-bedded sequences of competent and incompetent rock units (limestones, sandstones, siltstones, shales, claystones, and mudstones) that are highly prone to differential weathering and undercutting of the competent units by the incompetent units. Eighteen sites along eastern Ohio's highways were selected to investigate the factors that need to be considered for cut slope design aimed at minimizing undercutting-induced failures. The stratigraphy, slope geometry, and joint characteristics were investigated in the field, and slake durability index values for selected rock units from each site were determined in the laboratory. The stability of cut slopes subject to differential weathering was investigated with respect to three aspects: 1) the maximum amount of undercutting, 2) amount of rockfalls, and 3) fate and volume of rockfalls. Bi-variate statistical analysis shows that the factors influencing the maximum amount of undercutting include distance of the undercut rock from the slope crest, joint spacing within the undercut rock unit, and slake durability index of the undercutting rock unit. The amount of rockfalls is influenced by the joint spacing within the undercut unit. Bedding thickness and joint spacing, which depend on lithology, jointly affect the fate as well as the volume of rockfalls. Shale units have higher slake durability index values. These lithological associations suggest the need for basing the cut slope design on stratigraphic details of rock sequences.

Introduction

Road construction in mountainous areas involves the cutting of rock slopes at angles higher than their natural angles. Many of these cut slopes can fail due to unfavorable discontinuity orientations, low rock mass strength, or weathering of weak rocks causing hazards to motorists. Slopes in competent rocks (sandstones and limestones) fail mainly due to unfavorable orientation of discontinuities or low rock mass strength. Slopes consisting of incompetent rock units (shales, claystones, and mudstones), fail mostly as a result of weathering and subsequent surface creeping. Franklin (1983) recommends stable slope angles based on a rating system known as the Shale Rating System, which numerically rates incompetent rock units based on the slake durability index, point load strength index (estimate of unconfined compressive strength), and plasticity index .

The main purpose of design of rock cuts is to avoid or mitigate possible slope failures that are identified by the available stability analysis methods. Cut slope design involves the cutting of slopes at angles that can avoid slope failures, placing benches to facilitate construction and catch rockfalls, and providing drainage and catchment ditches to collect the failed materials.

In cases where slopes consist of inter-layered competent and incompetent rock units, differential weathering of incompetent rock units results in the generation of rockfalls from the overlying competent units (Shakoor and Weber, 1988) (Figure 1). These undercutting-induced slope failures are very common in Ohio, where the geology is characterized by horizontally-bedded sequences of competent and incompetent rock units.

The Ohio Department of Transportation designs cut slopes based on RQD (rock quality designation), slake durability index, and unconfined compressive strength. A close relationship has been shown between the rate of undercutting of competent rock units and the slake durability index of underlying incompetent rock units (Shakoor and Rogers, 1992). Ferguson and Hamel (1981) state the importance of valley stress relief joints to undercutting-induced rockfalls. This study investigates different geological and geotechnical parameters that influence undercutting-induced failures, shows the relationship of the important parameters with lithology, and finally suggests the use of stratigraphy for analysis and design of slopes subject to differential weathering.

Figure 1. Photograph showing a rockfall generated due to undercutting (US-7, Athens County, Ohio).

Research Methods

<u>Data Collection</u>

Eighteen sites from mainly the eastern part of Ohio were selected for the study (Figure 2). These sites included 59 competent rock units undercut by incompetent units. Slope profiles and accompanying stratigraphy of each site were established using a laser range finder. ARCGIS was used to generate cross-sections.

Orthogonal joints, valley stress relief joints, and bedding planes are the main discontinuities present in the area. Joint spacing and bedding thickness data were collected using the detailed line survey method developed by Piteau and Martin (1977). Window mapping and random measurements of discontinuities were also carried out. Due to the stress relief joints being parallel to the slope face, spacing measurements for these joints were very few.

Location Map
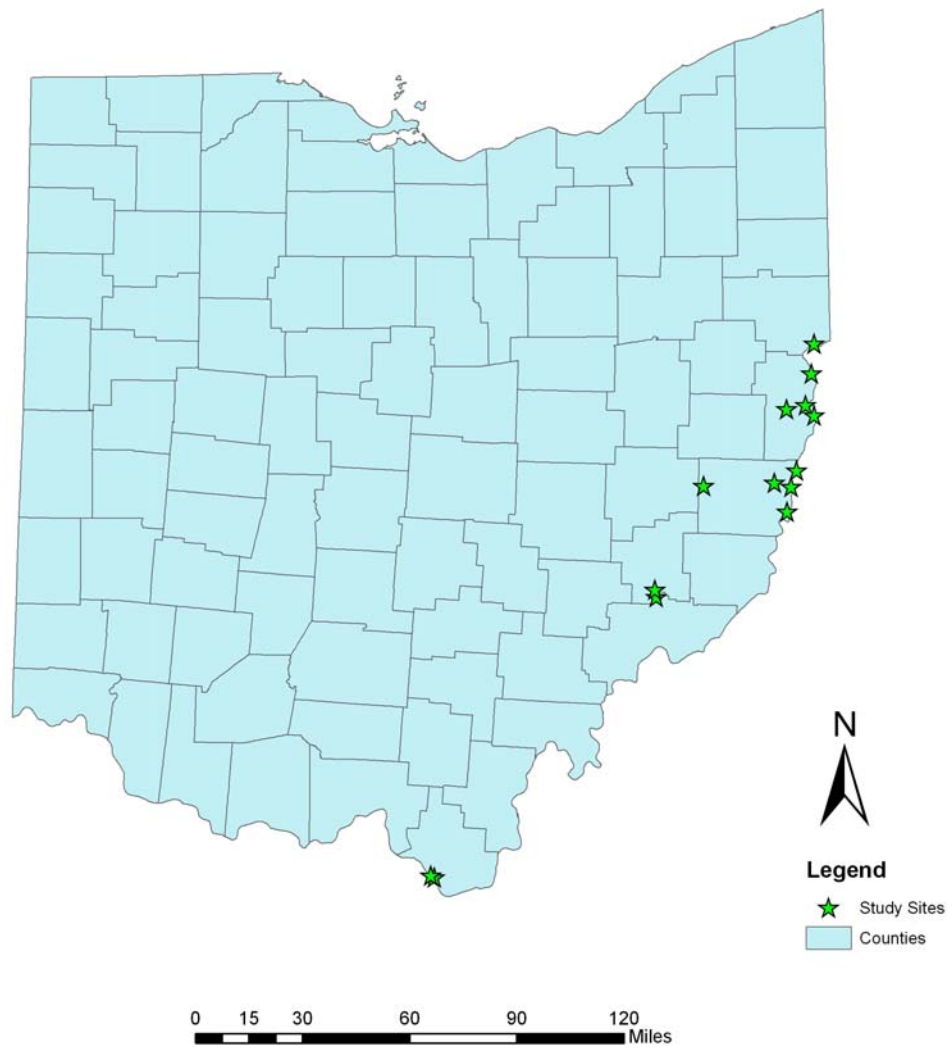
Figure 2. Location map of the study sites.

The depth of undercutting was measured using a scaled ruler, on accessible layers, and a laser range finder for inaccessible layers. Dimension of rockfalls found on slope faces and catchment ditches were measured using a scaled ruler. The longest dimension of a rockfall was denoted as A, the intermediate as B, and the shortest as C. The shortest dimension C is almost always the bedding thickness and the A dimension is dictated by the joint spacing. Slope angles of both undercut and undercutting rock units were measured using the clinometer on a transit compass. Profile sections were also used to determine slope angles .The slake durability test was conducted on undercutting incompetent rock units to evaluate the response of rock units to weathering. The test was performed in accordance with ASTM method D 4644 (ASTM, 1996).

Data Analysis

Three aspects of undercutting-induced failures were identified for investigation. The first aspect is the total amount of undercutting that has occurred since the construction of the slope (Figure 3). Deep undercutting generates more rockfalls than shallow undercutting. Based on field observations, different geological and geotechnical parameters that potentially affect the amount of undercutting were chosen. The selected parameters for the undercut units include distance of undercut rock unit from slope crest, distance of undercut rock unit from nearest bench, total thickness, and joint spacing. Relative position of the undercut layers from slope crest and nearest bench was also included. Relative positions are ratios of distances of an undercut rock unit from slope crest or nearest bench to total slope height or bench height measured from slope foot. These relative values which are in ratios were taken to check the role of the position of an undercut layer without the effect of slope height. The slake durability index was chosen as the parameter represents the undercutting potential of the incompetent rock unit. The slope angle of the undercutting unit was used to check if gentler angles reduce the total amount of undercutting. Ages of the cut slopes have also been considered to check if there is direct linear relationship with the total amount of undercutting. Bi-variate correlation of these parameters with the total amount of undercutting was investigated using SPSS.

The second aspect was the amount of rockfalls. It was observed that despite equal amounts of undercutting, the amount of rockfalls generated is variable. The amount of rockfalls was approximated by calculating the amount of recession of an undercut unit. The amount of recession was calculated by taking the difference between the total amount undercutting that
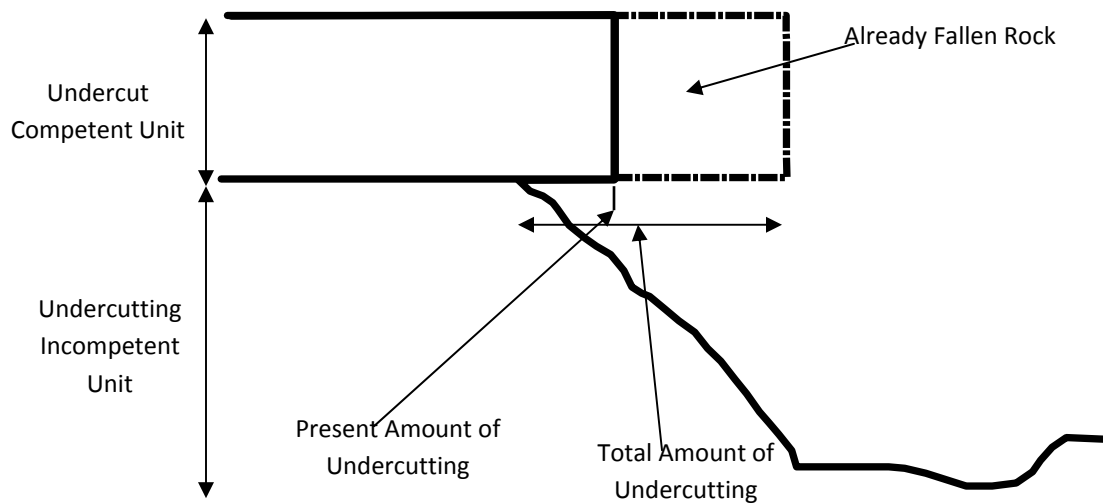
Figure 3. Diagram showing the total and the present amounts of undercutting.

took place since the construction of the cut and the present amount of undercutting (the amount of undercutting since the last rockfall) (Figure 3). If the difference is zero, then no rockfall has occurred and if it is more than zero, a certain amount of rockfalls have been released since the construction of the slope. Pre-split blast marks were used as references of original surface to calculate the total amount of undercutting. If pre-split marks were not found, original design plans in comparison with the slope profiles made for this study were used to determine the total amount of undercutting.

The third aspect is the fate and volume of rockfalls. The fate (landing site) of rockfalls is an important aspect to study since the ultimate concern of generation of rockfalls is their likelihood to cause accidents on the roadway. Field observations showed that the shape of rockfalls govern whether rockfalls stay on slope face, travel far into the catchment ditch, or possibly reach the roadway. Rounded rockfalls travel much farther than flat rockfalls which are usually held on the slope face and do not commonly make it to the road way. The effect of joint spacing and bedding thickness on fate and volume of rockfalls were investigated using Microsoft Excel's univariate statistics tool. The volume of rockfalls was also investigated since the hazard posed by bigger rockfalls is significantly different from smaller rockfalls.

Finally, univariate statistics was used to characterize the different lithologies (undercut and undercutting rock units) with respect to the geological and geotechnical parameters that play a major role on the three aspects described above.

Results

Bi-variate regression analysis was used to evaluate the relationships between selected parameters and the total amount of undercutting was carried out using SPSS statistical package (Table 1).

Table 1. Correlation coefficient values for the relationship between total amount of undercutting and the different geological/geotechnical parameters.

Geological and Geotechnical Parameters	Correlation Coefficient (r)
Distance of Undercut Rock Unit From Slope Crest (ft)	-0.59
Distance of Undercut Rock Unit From Nearest Bench (ft)	-0.28
Total Thickness of Undercut Rock Unit (ft)	-0.26
Relative Position of Undercut Rock Unit From Slope Crest (ratio)	-0.57
Relative Position of Undercut Rock Unit From Nearest Bench (ratio)	-0.30
Slake Durability Index of Undercutting Rock Unit (%)	-0.37
Spacing of Orthogonal Joints Within Undercut Rock Unit (in)	-0.47
Angle of Undercutting Rock Unit	-0.22
Age of Road Cut (yr)	0.25

Distance of undercut unit from slope crest, relative position of undercut layer from slope crest, joint spacing of undercut unit, and slake durability index of undercutting unit, show modest correlation with the total amount undercutting. According to the results of bi-variate analysis, it can be concluded that: 1) rock units closer to the crest are undercut deeper that the farthest layers, 2) undercut units with close spacing of joints undercut deeper than those with widely spaced joints, 3) underlying incompetent rock units with low slake durability cause deeper undercutting. Joint spacing of the undercut unit and slake durability index of the undercutting unit are, therefore, the most important parameters that need to be related to lithology.

Joint Spacing and Lithology

Joints spacing measurements were mainly taken on orthogonal joints. Joint spacing from the limestone units shows a left-skewed distribution (Figure 4), having an average value of 16.2 inches. The sandstone units show a normally distributed population (Figure 5), having an average value of 34.1 inches.
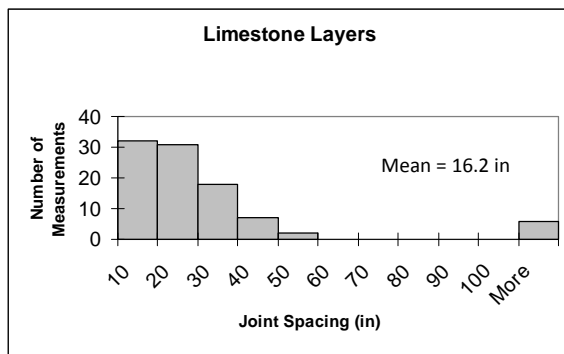

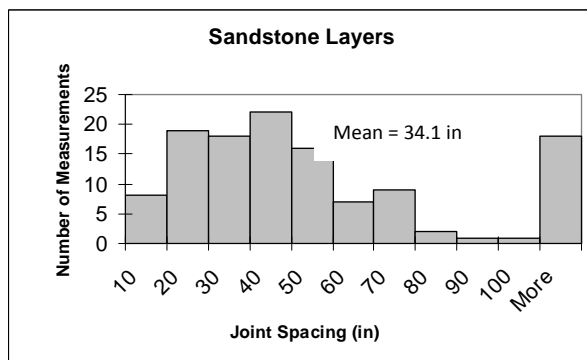Figure 4. Distribution of joint spacing for the limestone units.

Figure 5. Distribution o f joint spacing for the sandstone units.

Slake Durability Index and Lithology

There is a marked difference between the slake durability index values of shales and claystones/mudstones. Therefore, separate slake durability index histograms were made. The shale units have a right-skewed distribution with an average slake durability index value of 76 % (Figure 6). The claystone/ mudstone units show a left-skewed distribution, with an average value of 29 % (Figure 7).
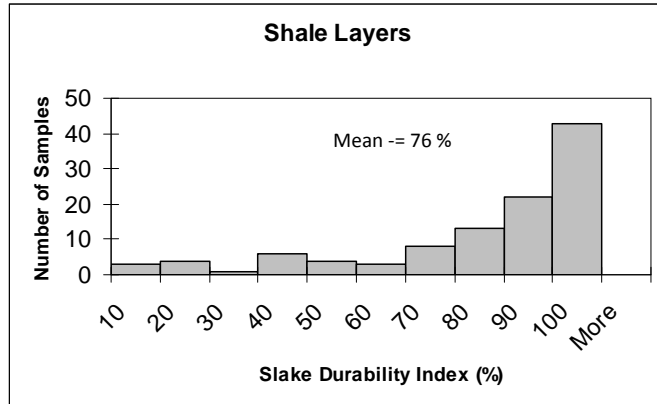
Figure 6. Distribution of slake durability for shale units.
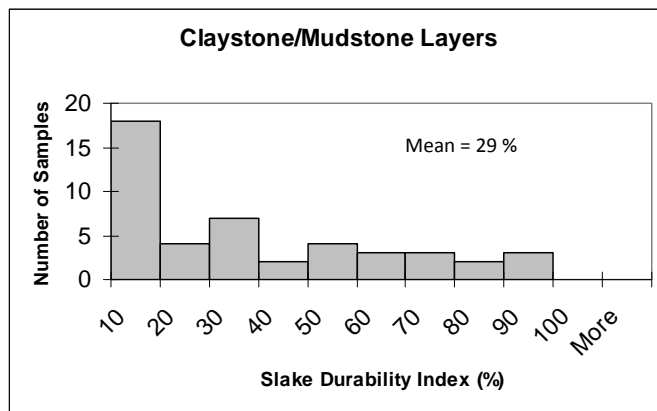
Figure 7. Distribution of slake durability for claystone/mudstone units.

The second aspect considered was the amount of rockfalls as estimated by the amount of recession of the undercut unit. The rate of recession (amount of recession/age of cut slope) was plotted against the rate of undercutting (total amount of undercutting /age of cut slope). The limestone units showed a positive relationship between the rate of undercutting and the rate of recession (Figure 8). The sandstone units on the other hand did not show any relationship (Figure 8).

Figure 8. Relationship between rate of undercutting and rate of recession.

Undercut rock units having close joint spacing have higher tendency to generate more rockfalls. The closer spacing of joints within the limestone units explains why there is a more direct relationship between the rate of undercutting and the rate of recession for the limestone units. However, there was no correlation found between the rate of recession and joint spacing.

The third aspect investigated was the effect of rockfall dimension on the fate and volume of rockfalls. Flat rockfalls were observed to travel less than the more rounded rockfalls. The ratio of the shortest dimension to the longest dimension was used to quantify rockfall shapes. The C/A value, which is basically bedding thickness (shortest dimension) to joint spacing (longest dimension) ratio, approaching to 1 indicates a rounded rockfall, whereas small C/A ratios indicate flat rockfalls. The distribution of C/A values for rockfalls on slope faces and catchment ditches were plotted. Rockfalls in catchment ditches (Figure 9) have higher mean C/A values than those caught on slope face (Figure 10).

Figure 9. Distribution of rockfalls of varying sizes in catchment ditches.
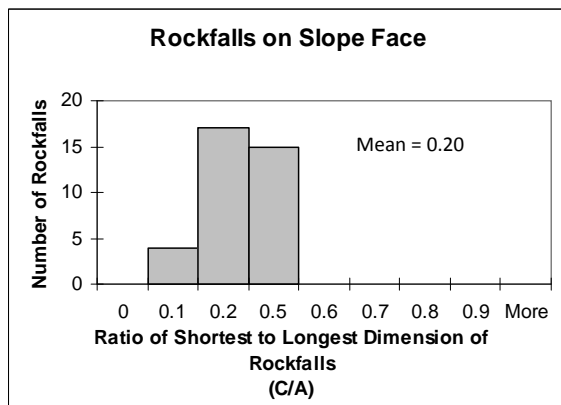
Figure 10 .Distribution of rockfalls of varying sizes on slope faces.

Volume of rockfalls was calculated by multiplying all dimensions (C*A*B). Distribution of rockfall volumes showed limestone units having a mean volume of 0.7 ft^3 (Figure 11) and sandstone units having a mean volume of 19.2 ft^3 (Figure 12).
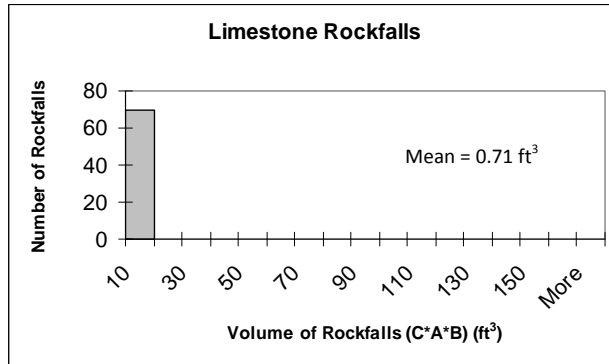
Figure 11. Distribution by volume in the limestone rockfalls.
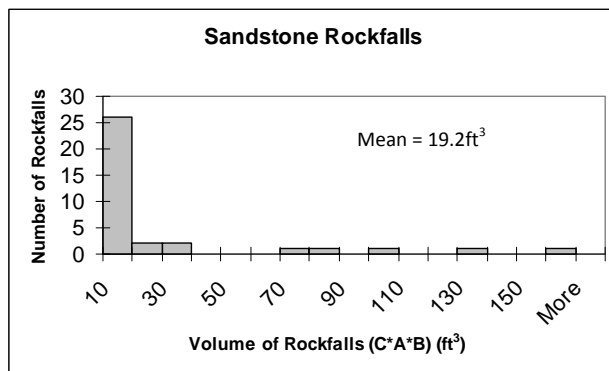
Figure 12. Distribution by volume in the sandstone rockfalls.

Rockfalls are bounded by bedding and joint planes. Therefore, bedding thickness and joint spacing of an undercut unit control the shape as well as the volume of rockfalls generated from it.

Bedding Thickness, Joint Spacing, and Lithology

The limestone units show a left-skewed distribution with respect to bedding thickness with an average thickness 10.3 inches (Figure 13). The sandstone units also show a left-skewed distribution with an average bedding thickness of 17.1 inches but have a wider range than the limestone units (Figure 14).
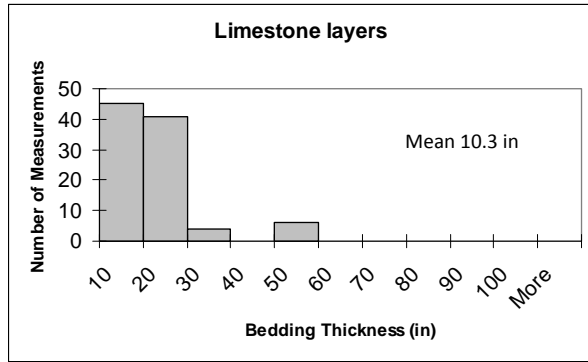
Figure 13.Distribution o f bedding thickness for the sandstone units.
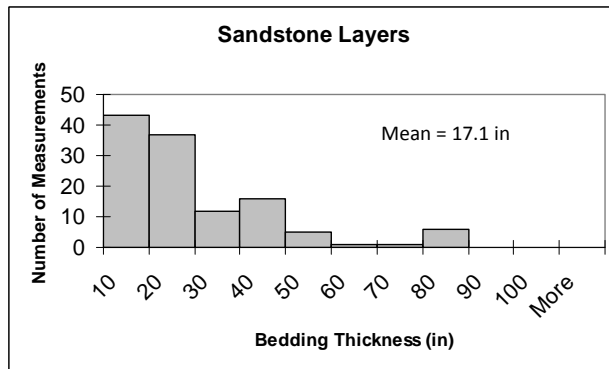
Figure 14. Distribution o f bedding thickness for the limestone units.

The shapes and volume of rockfalls produced from undercut competent units are governed by both bedding thickness and joint spacing. The ratio of bedding thickness to joint spacing is closely related to the shapes of rockfalls that are generated. Bedding thickness to joint ratios of close to 1 indicate that the rockfalls generated would be rounded, whereas rockfalls generated from rock units having small bedding thickness to joint spacing ratios would be flat in shape. The limestone units have higher average ratios of 0.96 (Figure 15) compared to the sandstone units of 0.53 (Figure 16).
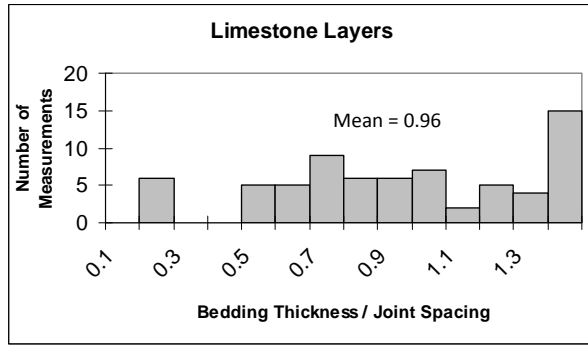
Figure 15. Distribution o f bedding thickness to joint spacing ratios for the limestone units.
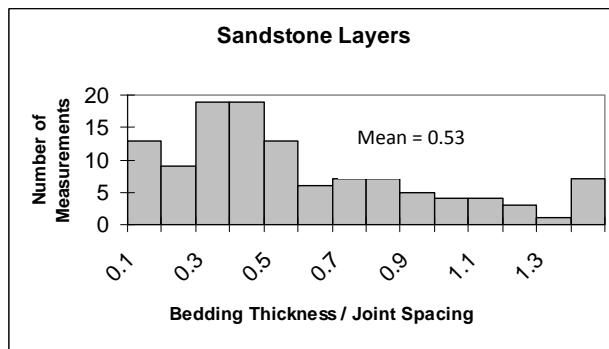
Figure 16. Distribution o f bedding thickness to joint spacing ratios for the limestone units

The product of bedding thickness and joint spacing of a rock unit is proportional to the volume of the rockfalls that would be generated from it. Large values of the product of joint spacing and bedding thickness indicate large–size rockfalls. The limestone units exhibit a much lower average value of the product of bedding thickness and joint spacing (1.56 ft^2), whereas, the sandstone units have a much higher value of 24.4 ft^2 (Figure 17 and 18).
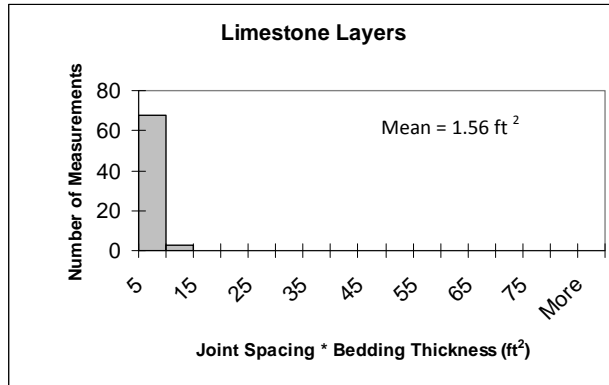
Figure 17. Distribution of product of joint spacing and bedding thickness for the limestone units.
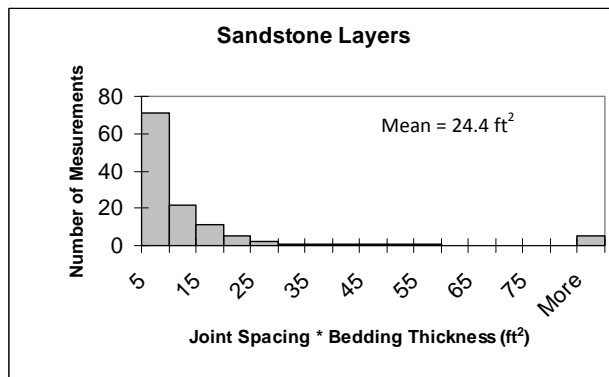
Figure 18. Distribution of product of joint spacing and bedding thickness for the sandstone units.

Stratigraphy and Design Considerations

Three types (Type 1, Type II, and Type III) of stratigraphic sequences were identified at the study sites:

Type I. This type of stratigraphy is characterized by thick (> 5ft) sandstone units underlain by shale, with coal and underclay usually marking the contact zone between the sandstone and shale. The underclay with zero slake durability index value promotes deep undercutting thereby causing rockfalls. Wide joint spacing of sandstone units, however, produces fewer rockfalls. The lower parts of the sandstones units are usually micaceous and thinly bedded, releasing flat shaped rockfalls that are easily caught on the slope face. The middle parts of the sandstone units, which are more massive can release heavy and rounded rockfalls that reach the catchment ditch and occasionally get onto the roadway.

The best design that can be suggested is the most widely used method of placement of a bench at the top of the shale unit to slow down undercutting of sandstone unit. The bench should be wide enough to contain rockfalls and must be properly drained.

Type II. The second type of stratigraphic assemblage is where thin (<1ft) to medium (1-5ft) layers of sandstone are inter-layered with shale or claystone/ mudstone. Such stratigraphy can produce more rockfalls if claystones/mudstones are the dominant incompetent rock units. Generally, due to the wide joint spacing, fewer but larger rockfalls are produced. Rockfalls from thin sandstone units are flat shaped, having very low joint spacing to bedding thickness ratios. However, there are cases where rockfalls from sandstone units in this type of stratigraphy can be rounded.

Slopes in Type II stratigraphy should be cut at angles equal to or less than 45 degrees to arrest flat-shaped rockfalls on the slope face and, at the same time, reduce the rate of undercutting. Sandstone units outcropping near the top third of the slope experience the deepest amount of undercutting. These top layers should be stabilized using rock bolts. Adequate catchment ditches should also be provided to catch rockfalls that might occur due to the presence un-stabilized layers in the lower portions of the slope.

Type III. The third type of stratigraphic sequence consists of limestone units inter-layered with claystone/ mudstone. The close joint spacing of limestone units and the low slake durability of claysones and mudstones makes the Type III stratigraphic sequence prone to deeper undercutting than Type I and Type II. The close joint spacing also results in Type III having the highest frequency of rockfalls. The high bedding thickness to joint spacing ratio causes the rockfalls to be rounded and travel far from their source.

Gentle slope angles (~45 degrees) could reduce the maximum amount of undercutting. Stabilization techniques such as rock bolts on these rock units may not be practical due the closeness of joints. Adequate catchment ditches with a barrier wall are needed to catch rockfalls, which have smaller sizes but have the potential to travel into the roadway.

Conclusions

Cut slopes within inter-layered sedimentary rocks are subject to undercutting-induced slope failures due to differential weathering. The most important geological and geotechnical parameters that should be considered to evaluate such slope failures are joint spacing and bedding thickness of undercut competent rock units, and slake durability index of undercutting incompetent rock unit. The position of the undercut unit on the slope also affects the amount of undercutting, with the units closer to the slope crest experiencing greater amount of undercutting.

Limestone and sandstone units underlain by claystones/mudstones are affected by severe amount of undercutting. Slopes consisting of undercut limestone units are likely to produce smaller but

rounded rockfalls that can travel into the road way. Sandstone units produce large but usually flat rockfalls which can be contained on the slope face or catchment ditch. Occasional rounded sandstone rockfalls can cause severe damage.

Based on the lithological associations of geological/geotechnical parameters discussed above, it is possible to design cut slopes prone to undercutting-induced failures on the basis of stratigraphy

References

American Society for Testing and Materials (ASTM), 1996, Annual Book of ASTM Standards, Soil and Rock (1): Volume 4.08, Section 4, 1000 p.

Ferguson, H.F., and Hamel, J.V., 1981, Valley stress relief in flat lying sedimentary rocks: Proceedings for the international Symposium on Weak Rock, September 21-24, Tokyo, Japan, pp. 1235-1240.

Franklin, J.A., 1983, Evaluation of shales for construction projects- an Ontario shale rating system: Research Report No. 229, Ministry of Transportation and Communications, Ontario, Canada, 99 p.

Piteau, D.R. and Martin, D.C., 1977, Description of detailed line engineering mapping method: Rock Slope Engineering, Part G, Federal Highway Administration, Reference Manual FHWA-13-97-208, Portland, Oregon, 29 p.

Shakoor, A. and Rogers, J.P., 1992, Predicting the rate of shale undercutting along highway cuts: Bulletin of the Association of Engineering Geologists, Vol. 29, No. 1, pp. 61-75.

Shakoor, A. and Weber, M.W., 1988, Role of shale undercutting in promoting rockfalls and wedge failures along Interstate 77: Bulletin of the Association of Engineering Geologists, Vol. 25, No. 2, pp. 219-234.

3.2

Green River Bridge Pier 1 Landslide, King County, Washington

T.C. Badger, E.L. Smith, S.M. Lowell, M. Frye, J. Cuthbertson, and T.M. Allen[5]

ABSTRACT

Early November 2008 storms caused the retrogression of a small landslide located below the south abutment of a 75-year-old, multi-pier highway bridge that spans the Green River gorge, located on State Route 169 about 30 miles southeast of Seattle, Washington. The landslide retrogression resulted in more than a half inch of movement of the abutment and a 220 day closure to construct remedial foundation support and drainage improvements. Interim stabilization efforts enacted before and after the movement of the abutment included soil nailing the undermined approach fill, installing horizontal drains, and, following the highway closure, unloading the upper slide mass by removing the 30-ft-high approach fill. Permanent measures involved a secant wall of 4-ft-diameter drilled shafts, tied-back with 300-kip ground anchors, and the installation of a 300-ft-long deep cut-off trench to intercept groundwater above the active slide limits.

BACKGROUND

The Green River – Dan Evans Bridge is located in rural King County on State Route 169 between the towns of Enumclaw and Black Diamond about 30 miles southeast of Seattle (Fig. 1). Constructed in 1932, the bridge is about 650 feet long with the deck located about 180 feet above the deeply incised Green River gorge (Fig. 2). The bridge consists of steel trusses supported on five piers. Piers 1 and 2 are located on the south valley wall in the area of the subject slide activity. While the bridge is functionally obsolete, it has not been scheduled for replacement. Prior to the detection of recent movement of the bridge in November 2008, it has never experienced any damage related to past landslide activity.
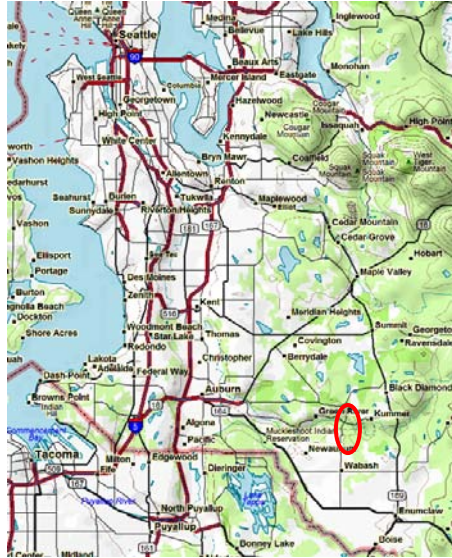
Figure 1. Location map of the State Route 169 Green River bridge (red ellipse in lower right).

Figure 2. Photograph of the bridge and the deeply incised Green River.

State Route 169 immediately south of the bridge crosses a very large, deep-seated landslide, known as the Kummer Slide, that has been episodically active since the highway was constructed (Fig. 3). Due to recurring movement and associated damage to the highway, a geotechnical investigation, involving deep borings and instrumentation, was performed by the WSDOT Geotechnical Division on the Kummer Slide in 1993. The investigation confirmed that its lateral extent was about 4000 feet wide and 3000 feet long, movement was occurring approximately 250 feet below the ground surface within the very weak sedimentary bedrock, and the landslide toe was located in the valley bottom. Very high hydrostatic pressures were encountered within/beneath the failure zone that produced artesian flow at the surface. The historical northern extent of movement (northern lateral scarp) of the Kummer Slide is located about 200 feet south of the bridge. The last movement on the Kummer Slide that significantly impacted the highway occurred in the early-mid 1990s.

In October 2006, the Geotechnical Division was notified of new landslide activity just north of the historic limits of the Kummer Slide, immediately downslope of the south bridge abutment (Fig. 3). We refer to this new slide as the Pier 1 landslide.
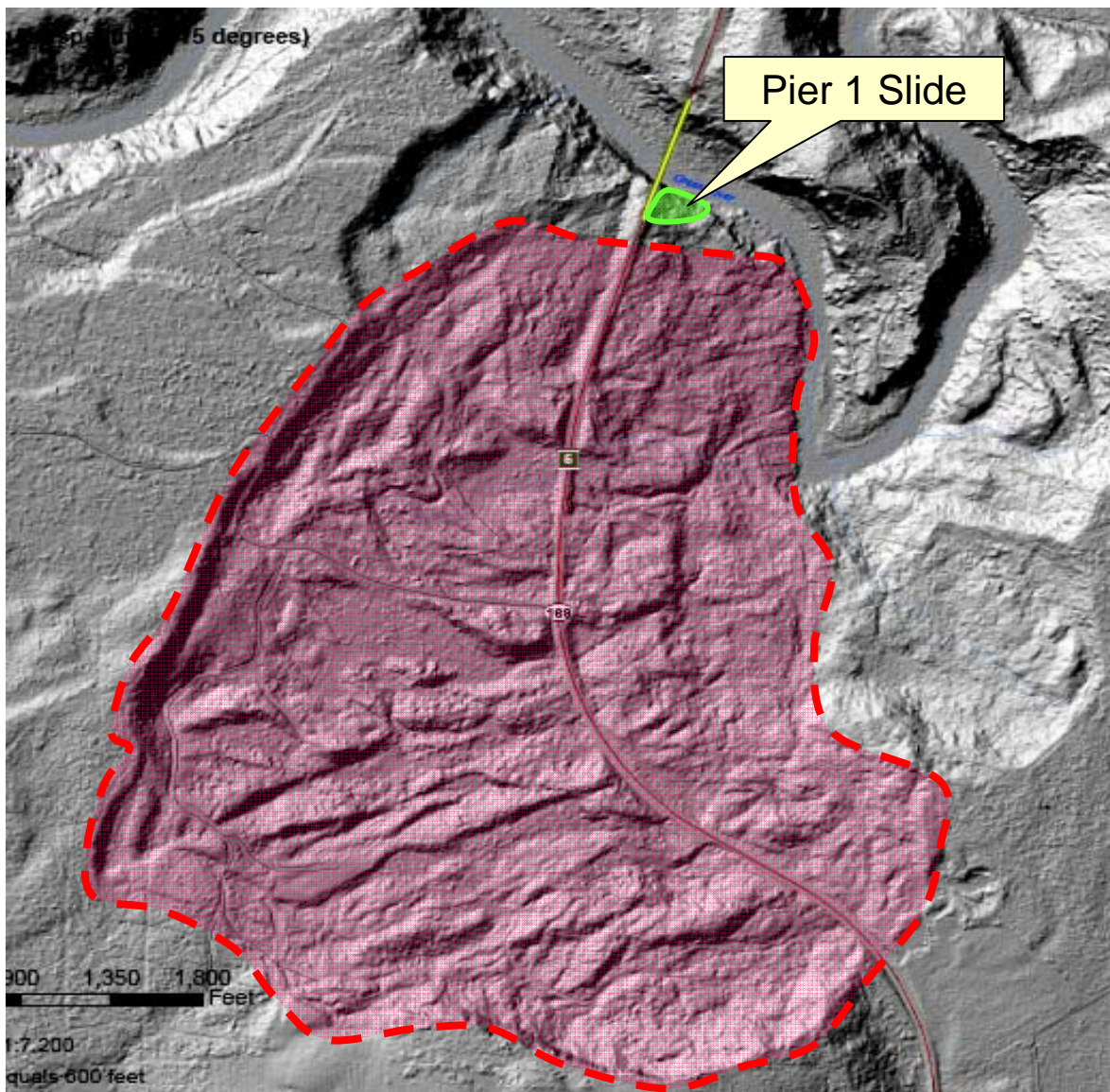

Figure 3. LiDAR image with limits of the Kummer Slide (red shaded area) and location relative to the bridge and Pier 1 landslide (green shaded area).

PIER 1 LANDSLIDE HISTORY

The timing of the initial movement of the Pier 1 landslide is not known. In October 2006 when the slide was first identified, its limits extended up to Pier 1 and southward into the approach embankment, undermining an old, concrete crib wall. The slide extended downslope about 200 feet to the toe, which was located near the top of a bedrock cliff forming the left bank of the river (Fig. 4). The northern slide limit skirted just east of Pier 2 located near the cliff edge.

Due to concerns of the slide undermining and threatening the southern piers, tiltmeters were installed on Piers 1 and 2 in Fall 2006. In addition, a seismic refraction survey was performed to investigate the foundation conditions beneath Pier 1 and the subsurface conditions within the slide mass. From bridge as-builts and the geophysical survey, it was determined that Pier 1 spread footing was likely founded in surficial deposits of glacial/alluvial origin and Pier 2 spread footing was founded on bedrock. Monitoring of the tiltmeters continued through June 2008, with no movement detected in the piers during this period.
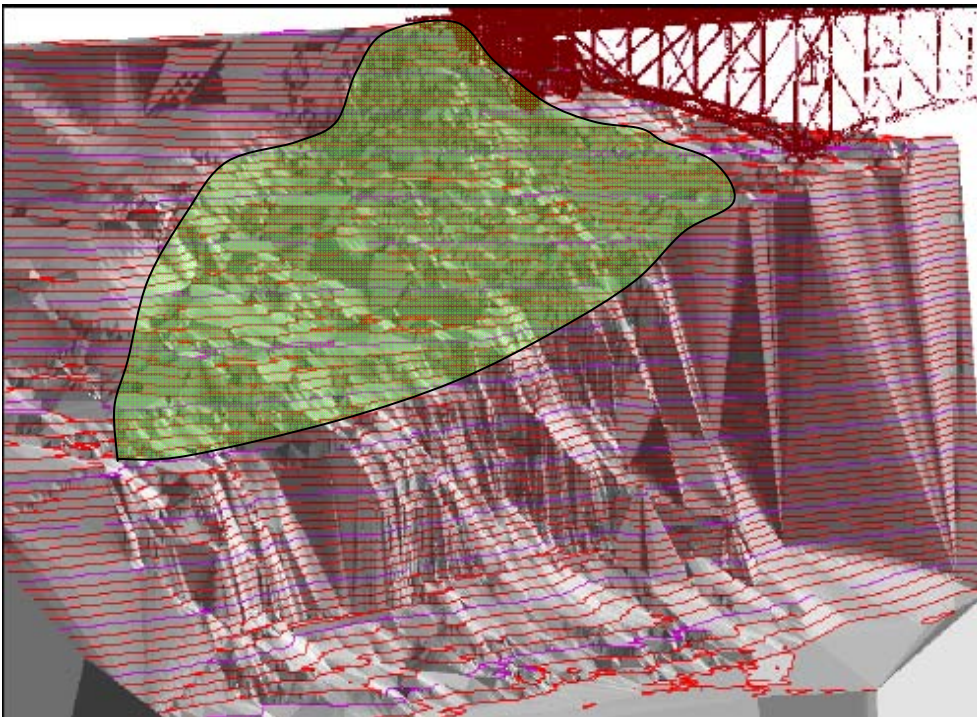
Figure 4. High-density-survey image of the Pier 1 landslide limits (green shaded area).

Additional movement of the Pier 1 Landslide was noticed in June 2008. This movement undermined guardrail posts on the approach embankment and further exposed Pier 1. An emergency declaration internal to WSDOT was made in June to address the developing problem. A second and more detailed geotechnical investigation was then initiated to better characterize the subsurface conditions of the slide, and to develop designs to protect the pier and approach embankment and improve stability of the downslope area (Fig. 5).
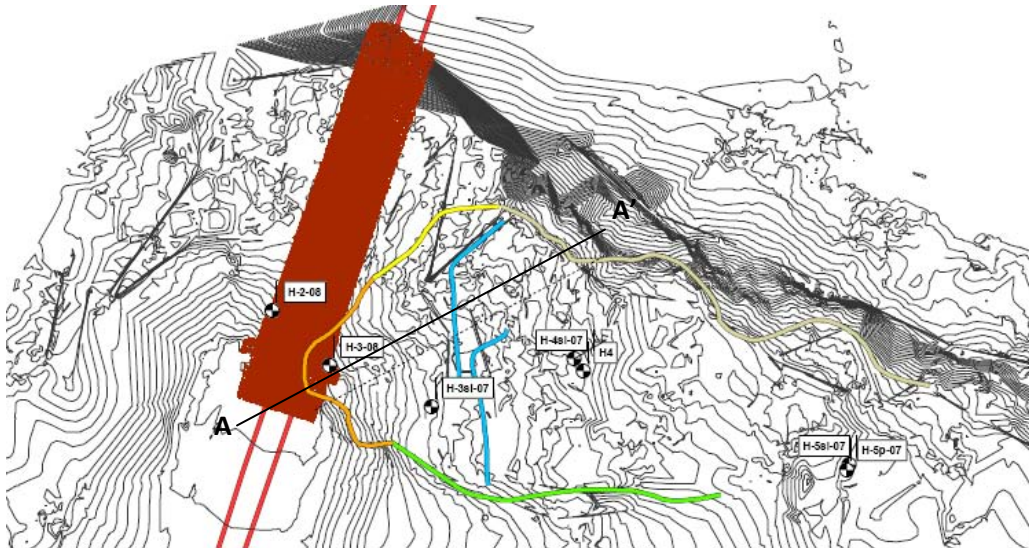
Figure 5. Site map showing active landslide limits, boring locations and critical cross section

Borings installed within the landslide encountered about 22 feet of silty sands and gravels of glacial-/alluvial-origin. This upper sand-gravel unit was underlain by a 6- to 10-ft-thick intermediate unit of clayey sand and gravel derived from weathered bedrock, which overlies bedrock consisting of interbedded claystone, sandstone, and coal (Fig. 6). Test boring H-3si-08 confirmed that the Pier 1 spread footing was founded in the upper sand-gravel unit approximately 28 feet above the bedrock surface. Groundwater was perched on the intermediate clay-rich and bedrock units and influences the upper sand-gravel unit. The failure zone occurred within the clay-rich unit, which dipped shallowly northeastward toward the river. Unlike the Kummer Slide, bedrock was not involved in the Pier 1 landslide with the failure confined within the surficial deposits.
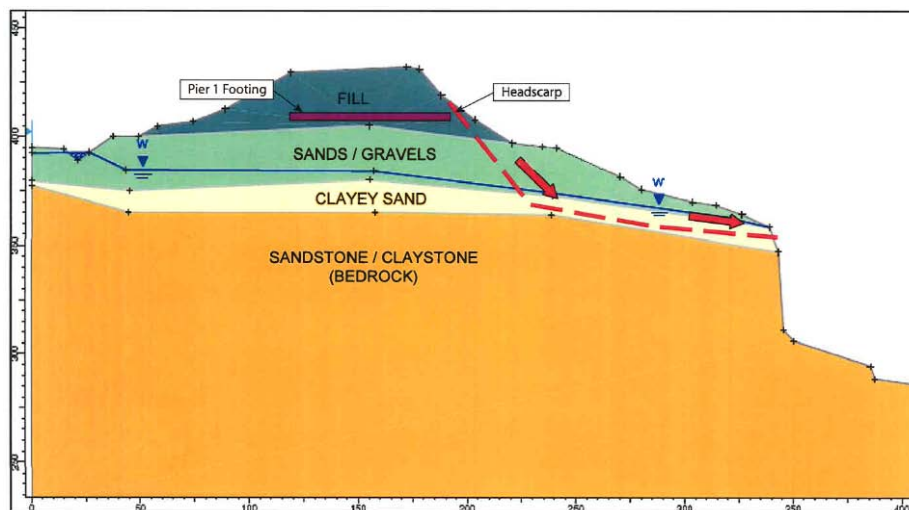

Figure 6. Interpreted cross section A-A' showing limits of failure as of October 2008.

Between July and October 2008, two phases of soil nailing with shotcrete facings were constructed on the approach embankment below Pier 1 under two separate contracts as interim measures to prevent further upslope enlargement (retrogression) of the slide (Fig. 7).

Figure 7. Soil nail reinforcement of approach embankment at Pier 1; note tiltmeter box on pier

In late October, a third contract was let to install horizontal drains into the Pier 1 landslide mass. During drilling of drain Array #1, which was located near the edge of the cliff and within the slide mass, slide movement accelerated. As a result, the Contractor moved off of Array #1 and commenced drilling the planned drains from Array #2, located just south of the lateral landslide scarp (Fig. 8). By the second week of November, eleven drains had been installed from Array #2. Due to the adverse impact that drilling fluids appeared to have on the stability of the Pier 1 slide, only four drains were installed into the slide mass. Drain yields were modest in the southern- and northernmost drains, and the middle drains produced very little to no yields. Surveying of the completed drains determined that few drains were successful in intersecting the narrow target zone. Little reduction in groundwater levels within the slide mass were realized, and the small number of drains were largely ineffective in averting increased groundwater levels during storms. Between June and November 6th, 2008, no movement was detected in the tiltmeters on Piers 1 and 2.
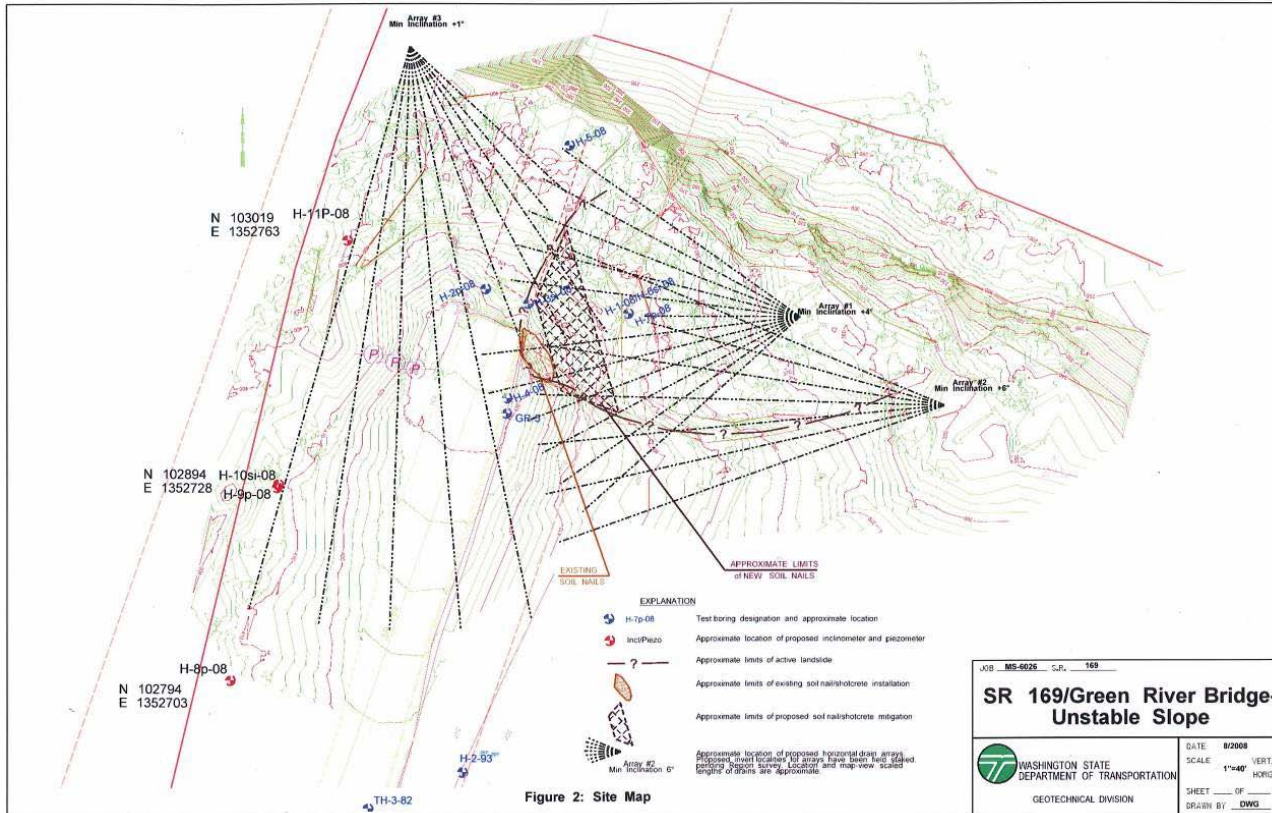
Figure 8. Site map showing planned distribution of drains; Array #3 was eliminated due to access difficulties

On November 6th to 7th and again on November 11th to 12th, two severe rain storms struck the region producing more than 3 and 4 inches of rainfall, respectively, estimated from nearby weather observation sites in Enumclaw and Black Diamond. While the quantity of rain resulting from each storm was not exceptional, severe flooding and associated damage occurred in Central Puget Sound as a result of these storms. In early December, the Governor signed an emergency declaration to gain Federal assistance for the widespread damages associated with these two storms.

Geotechnical instrumentation read on November 13th revealed an expanded area of movement around and beneath Pier 1 had developed during this wet period. Inclinometer H-3si-08, which was installed through the foundation of Pier 1, detected 0.6 inches of downslope movement, 20 feet beneath the footing, since the previous reading on November 6th (Fig. 9). Nearby inclinometers to the south and on the west side of the highway also detected new movement during this period. The zone of movement was located within the same clay-rich layer as observed in the slide mass downslope of the pier.
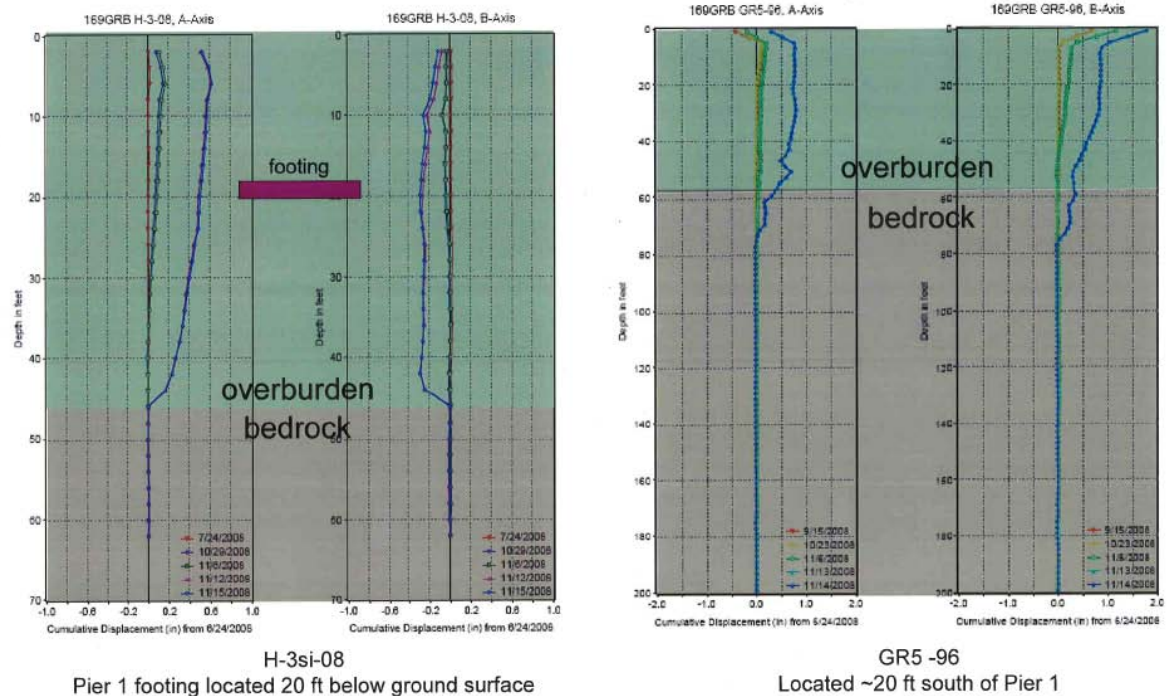
Figure 9. Inclinometer data from before and following the November 2008 storms depicting new movement 20 feet beneath the Pier 1 footing at contact between clayey residual soils (overburden) and bedrock.

In addition, titling of Pier 1 had occurred on November 6th, and again between the period of November 10th and 13th.   The expanded area of movement of the Pier 1 Landslide is shown on Figure 10, and was determined to be unrelated to the Kummer Slide.
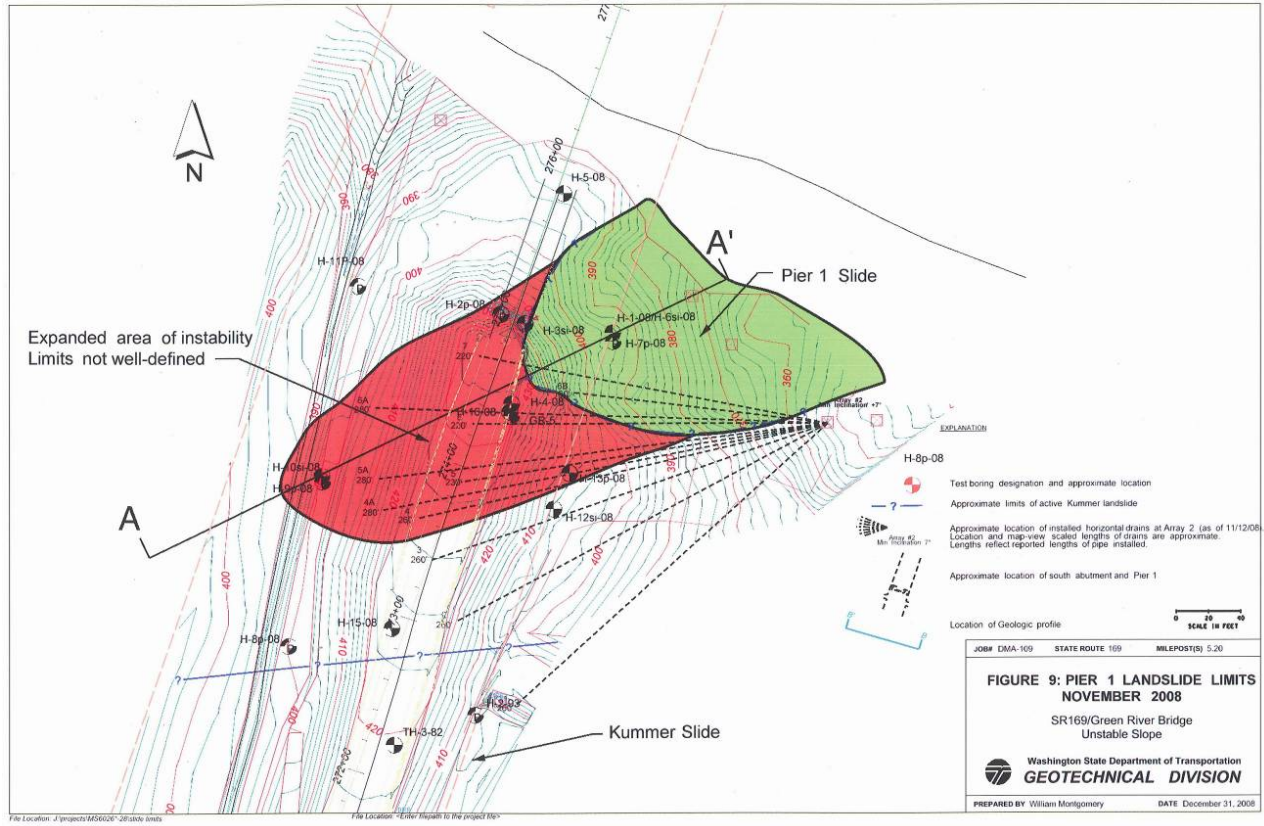
Figure 10. Expanded area of slope movement following November 2008 storms (red shading).

WSDOT closed the bridge on November 18th to protect public safety and to enact longer-term remedial measures to safeguard the structure. The closure affected nearly 8000 vehicles that daily use the highway and numerous businesses in nearby communities.

PIER 1 LANDSLIDE REMEDIATION

To address the immediate risk of further movement of the southern pier and damage to the bridge, a series of interim actions were rapidly implemented. These included:

- removal of the 30-ft-high approach embankment to unload the slide mass (Fig. 11);
- surface and subsurface drainage improvements to divert storm and groundwater away from the active area of slope instability;
- continuous pumping of an old and badly damaged drainage system on the uphill (west) side of the highway; and
- setup of a continuous monitoring and notification system for slide and bridge movements, groundwater levels, and precipitation.

166

Figure 11. Photo taken on December 12th, 2008 of nearly completed temporary removal of the approach embankment. Utility poles that carry high-voltage lines could not be de-energized and moved, limiting the extent of the embankment unloading.

Given that the stability around Pier 1 remained unacceptably low and vulnerable to renewed landslide activity from future storms and permanent bridge closure and rerouting of the highway was not considered a feasible alternative, a permanent solution was developed to protect the pier from further movement and improve overall slope stability.

The Geotechnical and Bridge & Structures Divisions collaborated on stabilization and protection alternatives. The preferred alternative consisted of a secant tie-back wall to isolate the lower slide mass from and provide additional lateral support for Piers 1 and 2 (Fig. 12). The wall consisted of 27, 4-ft-diameter steel-reinforced shafts and 26 unreinforced shafts ranging from 45 to 90 feet deep socketed approximately 20 feet into sandstone/siltstone bedrock. A grade beam connected the tops of the shafts through which 28, 300-kip tie-back anchors were installed. A 1500 ft^2 mechanically stabilized earth (MSE) wall was built on top of the secant wall to reestablish the roadway grade (Fig. 13A).   In addition, a 300-ft-long, deep cutoff trench was constructed to intercept groundwater on the uphill side of the approach embankment/bridge to restore a damaged subsurface drainage system located immediately to the south within the Kummer Slide limits. The trench was founded in the residual soils/bedrock, which involved shored excavation approaching 30 feet deep (Fig 13B).
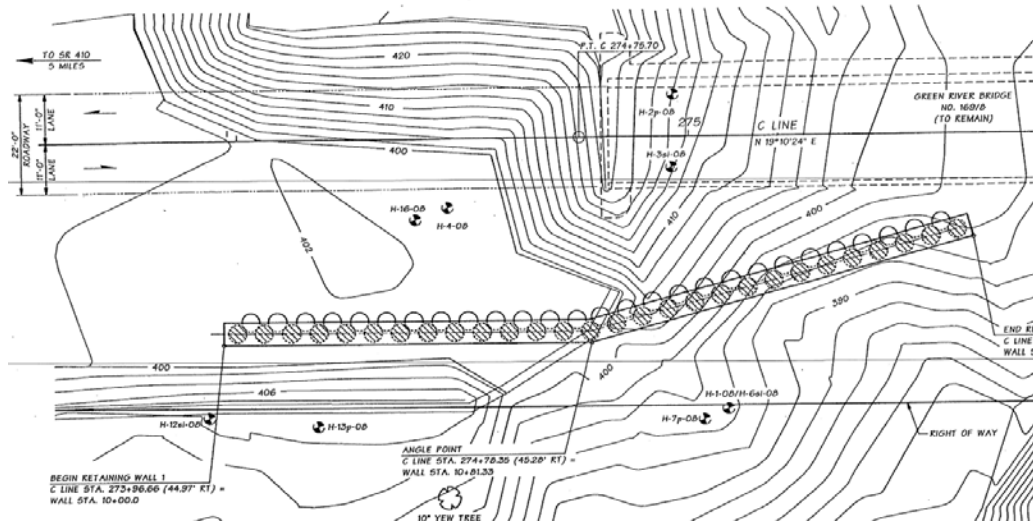
Figure 12. Plan view of secant tie-back wall located downslope of Pier 1.

Figure 13. (A) Completed secant wall with anchored grade beam and MSE wall downslope of Pier 1, and (B) cutoff trench on uphill side of the approach embankment.

The project was completed and reopened to traffic on June 26, 2009 after being closed for 220 days (Fig. 14). The direct costs for the emergency remediation of the slope were approximately $ 5.6 million.

Figure 14. The affected communities of Enumclaw and Black Diamond celebrate the completion of the remedial work and reopening of the highway.

3.3

Getting it Right the Third Time
Reconstruction of Interstate 476 over Unstable Karst in Plymouth Meeting, PA

Prepared by:

Bruce Shelly, P.E.
Regional Geotechnical Manager
AECOM USA, Inc.
260 South Broad Street
Suite 1500
Philadelphia, PA 19102
(215) 966-4827
Bruce.Shelly@aecom.com

Sarah McInnes, P.E.
District Geotechnical Engineer
Pennsylvania Department of Transportation
PENNDOT District 6-0
7000 Geerdes Blvd.
King of Prussia, PA 19406
(610) 205-6544
smcinnes@state.pa.us

Project Description

Interstate 476 is the primary north-south corridor in eastern Pennsylvania carrying traffic from the Philadelphia region to Scranton. This project is located on the Mid-County Expressway portion of Interstate 476 which is located in Philadelphia's western suburbs and links Interstate 95 to Interstate 276 (the east-west PA Turnpike). It is locally called the Blue Route and as one of the most controversial Interstate Highways in Pennsylvania, construction of I-476 began in 1967, but was not completed until 1991.

This project, designated 0476-RDC, includes complete reconstruction of 3.5 miles of 476 from Conshohocken north to the junction of the Pennsylvania Turnpike in Plymouth Meeting. This portion of the Blue Route was constructed in the 1970's and referred to as the "Built Section" because it was completed long before other portions of the roadway. According to the local regional planning commission, this section of I-476 now carries approximately 105,000 vehicles per day. The existing roadway consists of three 12' lanes with a 10 foot outside shoulder and a 4 foot inside shoulder in each direction separated by a grass median varying in width from 30 to 50 feet. In addition to reconstructing the roadway, PENNDOT will widen the left and right shoulders, upgrade acceleration-deceleration lanes, and replace drainage. The project also includes reconstruction of the I-476 bridge over the Schuylkill River, presently in construction. Construction of the project – for which costs have been estimated at $100M - is scheduled to begin in September 2009 and is anticipated to take approximately two years. Including original construction this will be the third attempt to construct the roadway properly, but this time undertaking an extensive and serious attempt to reinforce the subgrade, control surface water,

repair existing karst related problems, minimize future sinkhole development and significantly reduce future maintenance.

Geology and Site Characteristics

The project site crosses three carbonate formations, the Cambrian Elbrook Limestone and Ledger Dolomite, and the Ordovician Conestoga Limestone. The profile in this area consists of highly variable top of rock with pinnacles, voids and boulders.
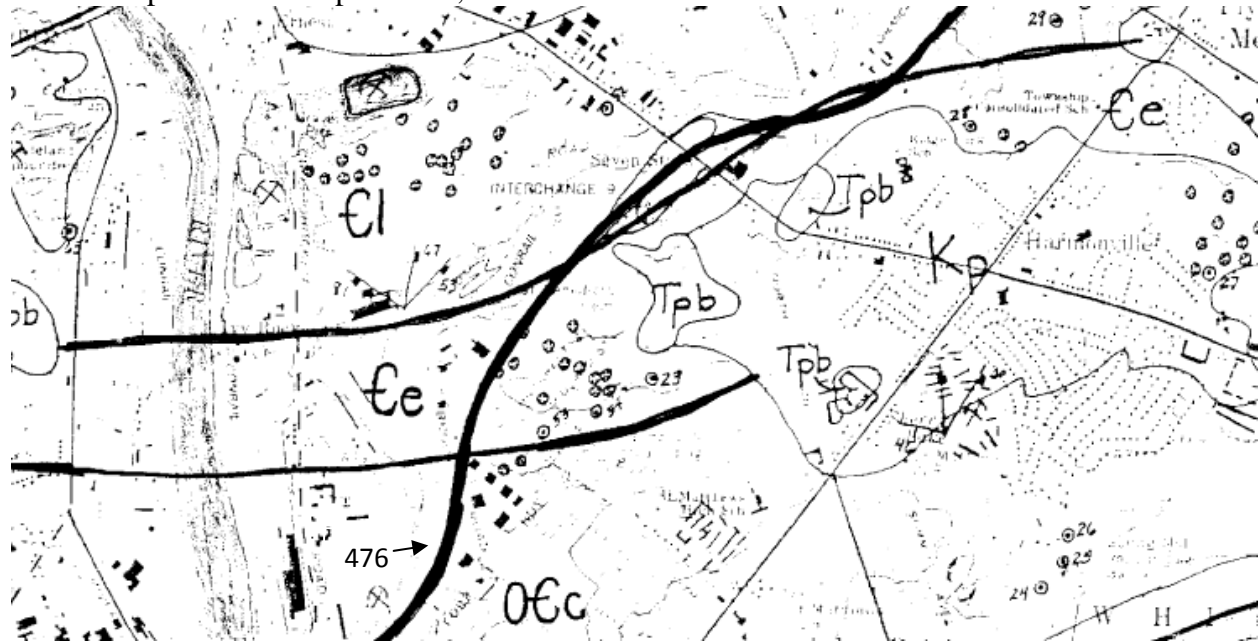
Since original construction, the area has experienced sinkhole development. Part of the project lies in a cut, which placed the roadway very close to the top of the epikarst, and has been one of the more active trouble spots for sinkhole formation post-construction. In addition to the irregular geologic profile, uncontrolled surface water has exacerbated the problem. After the road cut, surface water from an adjacent development was directed towards the roadway and as a result of improper construction was not directed to the inlets. Adding to the difficulty, nearby is the Schuylkill River, multiple quarries - which have changed (increased the gradient) the groundwater flow patterns over the years, and the infamous Plymouth Creek. Plymouth Creek is a losing stream which regularly disappears beneath the ground surface near the site.
The challenge for this project was accurately depicting the highly variable and unknown rock surface and using the data gathered to make appropriate construction recommendations that will ensure the longevity of this important corridor.

Built Section of the Blue Route, 1970s through 1980s

The original roadway was constructed of continuously reinforced concrete (CRC) pavement which immediately showed continuous cracking problems. It remains undetermined if the cracking, typical of CRC, was due only to the problems typical of this pavement type or if it had been exacerbated by karstic activity beneath the roadway. Although CRC is no longer used, we surmise that its strength "bridges" voids beneath the roadway. On the other side of the coin, due to the "bridging" effect, we therefore have virtually no information about karst activity and the

existence of voids beneath segments of the roadway, a challenge even for the most competent engineer.

During and after construction sinkholes developed early and often and have been a continuous maintenance headache. In addition to typical sinkhole occurrence due to solutioning of the carbonate bedrock and movement of groundwater, sinkholes began to form due to infiltration along the unlined drainage swales and in low spots, and in one area where a retail development completely cut of the drainage path of surface water. Contributing to the sinkhole formation is the corrugated metal pipe drainage system with poor seals, settlement of drainage pipes and poor grading near inlets.

Sinkhole repairs are performed by PENNDOT Maintenance crews using the "get 'er done" philosophy – get in, fill it, get out, FAST – which leaves no time for investigation. To fix sinkholes as quickly as possible they were often filled with concrete, flowable fill or worse, whatever material was available at the moment. Stone was often used which is excellent for conveying water exactly where we don't want it to go - down the sinkhole. Where the rock was shallow, a concrete plug in the throat with any material placed above often works. But where the rock is deep or the throat not found, the surface water that caused the sinkhole eventually finds its way around the plug and another hole surfaces adjacent to the repair, hence the continuous maintenance headache. Other typical problems with repair include - sinkholes adjacent to the roadway with a horizontal flow path beneath the travel lanes making it extremely difficult to find the throat; the inability to excavate deep enough, in the right direction, or at all; and the inability to direct water (for flushing) or concrete into the throat or void.

By the 1980s, the condition of the Built Section had deteriorated due to the poor design in combination with sinkhole problems. Reconstruction of this section was planned and test borings were taken in combination with some geophysical mapping. Complete reconstruction plans were complete but shelved due to lack of funds.

The bottom line: between standard construction methods, improper drainage considerations, poor quality repairs and lack of maintenance the roadway was not fixed right this time.

Built Section of the Blue Route, 1990s

In the mid 90s a construction project was undertaken to repair problem areas, essentially a temporary fix. The roadway portion of the project consisted of concrete patching and an asphalt overlay. During construction some existing sinkholes were fixed, but as mentioned previously, the true extent of subsurface problems was not known and many sinkholes were not properly repaired. At one point during construction, in the middle of rush hour, the center lane collapsed into a sinkhole leaving motorists to straddle the void on their commute. Temporary drainage repairs were installed in the cut section but ten years later these are inadequate.
The bottom line: complete reconstruction, not a temporary solution, was necessary; the roadway was not fixed right this time.

Subsurface Investigation

Initial Test Borings

Armed with this extensive history and related information, a preliminary test boring investigation plan was commenced. Boring spacings were typical for roadway reconstruction in a karst area. The proposed reconstruction includes pavement design, sliver fill, minor cuts and new infiltration basins. The investigation also included an innovative approach deemed "karst borings" where borings were added in specific problem areas. In addition to the standard delineation, any boring that specifically revealed voids or soft areas in or above the rock surface were tracked. Grout was pumped and grout quantity tracked during the traditional backfilling to provide a better idea of the extent of the problem. This idea was proposed by the District's Construction Unit after a similar project used significantly more grout than originally predicted. Traditional borings with split spoon sampling and recoverable core were not the most important aspect of these borings. This process was proposed to the interested drillers and the bids came in at good prices.

The karst borings were mainly taken next to and near the roadway where, as previously discussed, developers had changed the drainage. Another area where karst borings were located is an existing cut on the northbound side where numerous sinkholes have recurred. The drilling proceeded but unfortunately the drillers could not backfill with grout to any appreciable pressure. However, there was progress in the tracking of the grout backfill to obtain preliminary void estimates.
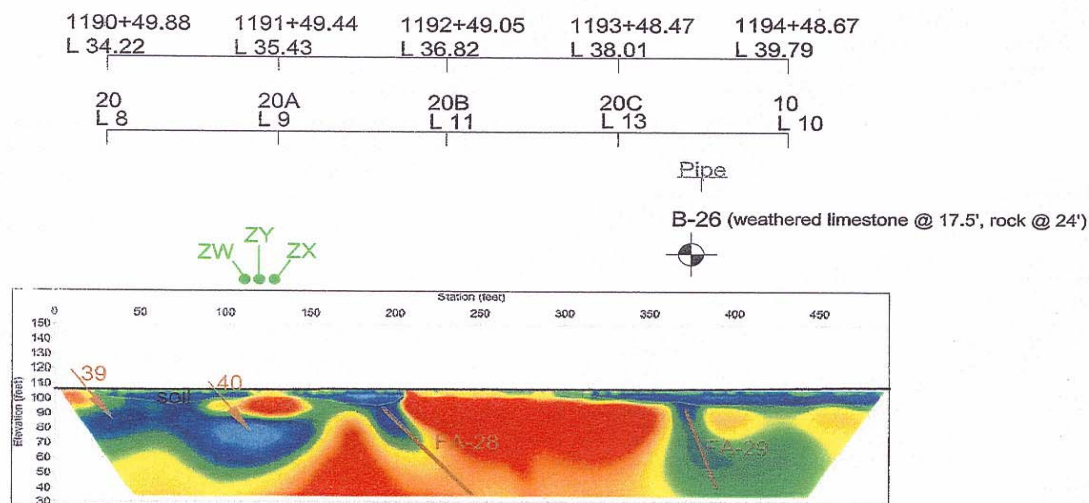
Geophysical

After the preliminary borings were taken, it quickly became apparent that additional investigation would be needed to effectively find sinkholes for such a large area. (Area of main concern spanned 7000 lf). After review of the many different types of geophysical testing available, it was decided that two-dimensional electrical resistivity imaging (ERI) would provide the best results for the specific situation. ERI measures earth resistivity by driving a direct current (DC) signal into the ground and measuring the resulting potential (voltage) created in the earth. From that data the electrical properties of the earth (the geoelectric section) can be derived and thereby the geologic properties inferred. Three lines off the roadway were chosen in an effort to view each line in cross-section across the most important area, the traveled roadway.

ERI Results

The 2-D ERI incorporated an electrical resistivity imaging system and 84-¼ inch diameter stainless steel stakes driven 8 to 10 inches into the ground. Data was acquired using dipole-dipole array with electrodes spaced 6.6' apart, rolling 42 electrodes forward at a time for continuous coverage. Three lines, one in the NB shoulder, one in the median toward the SB passing lane shoulder, and one in the SB shoulder, were taken. Emphasis using this method is placed on identifying potential voids and fractures within the bedrock. Using this method with the existing sinkhole information can determine underground channels and direction.
As can be seen, the data showed, along with the possible rock line, voids and fracture zones that seemed to line up with the surface activity. Plus this is a proven method that has been used for many years.

A problem with this method is the small horizontal scale with respect to which depth makes it difficult to locate the exact area of the problem. Also, the median line was located directly over corrugated metal drainage pipes and the lines were taken during a particularly wet time period. These elements in conjunction led to the finding that most of the line only picked up the pipe and

no subsurface (natural) information, the downside to using electrical currents as your main geophysical investigation. Discussion ensued about whether to run the median line again but further into the median away from the pipe. Due to the uncertainty of positive results, even moving as much as 20' away, it was decided to use other geophysical methods to fill in the gaps with respect to the other two lines.

Originally, seismic methods were ruled out due to the excessive traffic vibrations of such a busy highway. However, it was determined feasible to do the testing at night and the Department also allowed a traffic lane to be taken putting traffic even further from the line.

MASW Results

MASW, multi-channel analysis of surface waves, is a seismic method of geophysics which compares surface waves at different locations to estimate velocity variations with depth. The propagation velocity of surface waves is frequency dependent. The difference in soil density is determined by the vertical variation of shear wave velocity. By recording the fundamental mode Rayleigh Waves propagating from the source to the receiver, the dispersive properties directly beneath the seismic spread can be represented.

The MASW method utilizes pattern recognition techniques. Multiple receivers are equally spaced along a linear survey line and measure seismic waves generated by an implosive source (i.e. sledge hammer). MASW has been used to map top of rock, identify bedrock fractures, and evaluate sink activity, among other things. Some advantages are, unlike refraction, MASW does not require that velocities increase with depth. Also, because the near surface waves have stronger amplitude, there is less chance of vibration interference. I addition, it is not affected by buried pipes or reinforcement bars.

One MASW line was run just on the roadway next to the SB passing lane shoulder. An example of the results is depicted here:

Each triangle represents a single 1-D shear wave profile derived from a single shot record.
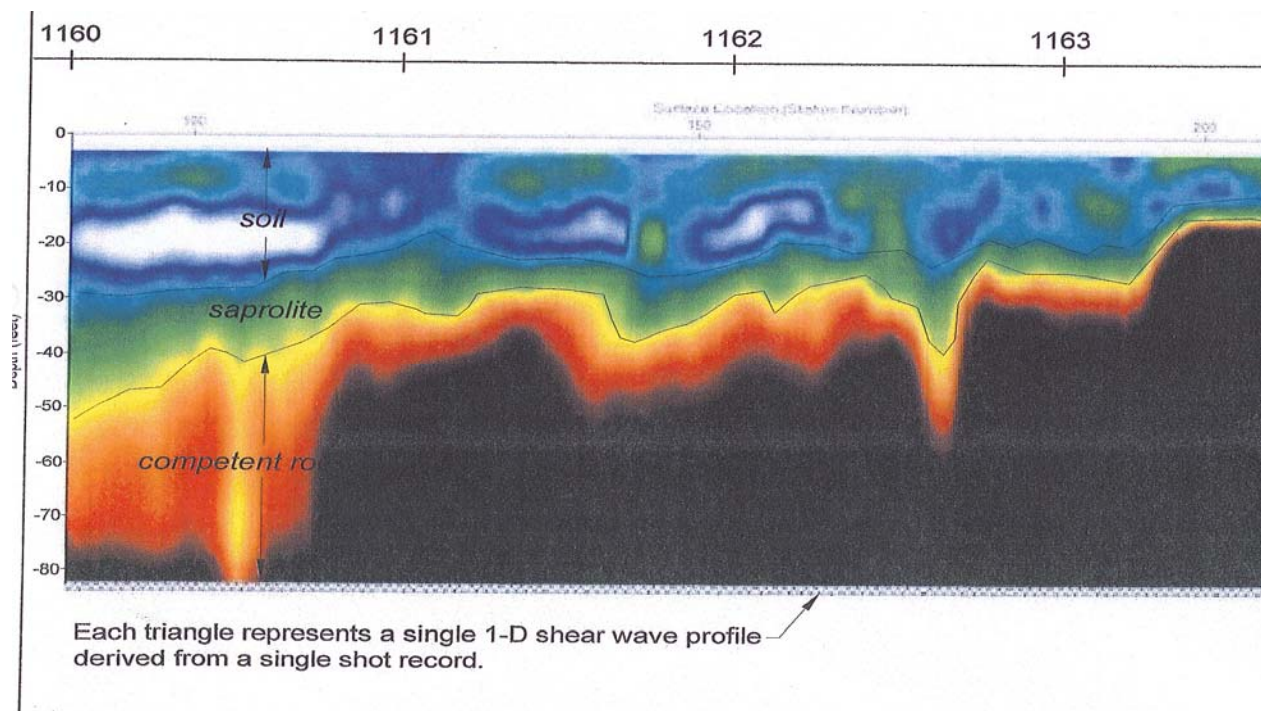
As shown, one can see the approximate rock surface along this entire line.

Comparing the two techniques, the 2D ERI data were more revealing of anomalies suggestive of voids and fractures within the rock, whereas the MASW data were more revealing of subsurface conditions related to top of rock surface and soil density.

Stimulus Package Saves the Project – Design Moves into Overdrive

Before this point, the project was moving along at a very slow pace. In fact the remediation of the roadway was never a high priority project and was opened and closed a number of times since 1991. AECOM acquired this portion of the project mainly to rehabilitate the bridges along this section. In 2007, due to a lack of funding for the entire project, it was determined to remove the highway portion and let a separate project for only the bridges rehabilitation. Naturally, it was felt that the roadway portion, although still with some design money left, would again be shelved without construction money. This explains the meticulous yet slow pace of the roadway design.

With the advent of stimulus package money, there was an indication from PENNDOT that the roadway portion would qualify with one condition: the project had to be let by July 20th. This being February and not yet official, we knew we needed to put it in overdrive.

Confirmation Test Borings

The final step of the investigation included confirmation borings to verify top of rock surface and soil consistency as well as confirm voids and weathered zones. Sixty four test borings were completed in early March 2009. This included groups of borings taken to find the drop in rock surface or key features observed along the geophysical lines. Due to the small window of time to obtain this information, drilling depths and number of contingent holes were sacrificed. But in the key areas of concern, significant confirmation of the geophysical work was accomplished. All of the information helped to develop focus areas along this project.

Creation of Investigation Super Map

It was always the purpose of the multifaceted investigation to gather all the information including geology, surface sinkholes past and present, mapped fracture traces, geophysical information, and test boring data, and use it to create a map. The map, along with the subsurface profile (PENNDOT requirement) which included selected cross sections across the roadway, explained the main areas of concern and gave a much better level of comfort with the recommendations.

Video Inspection of Drainage Pipes

Because many of the surface sinkholes over the years were related to surface drainage, it was felt one of the most important aspects of successful design would be to determine whether existing drainage pipes could be reused or replaced. An extensive video inspection was employed to investigate many of the drainage pipes in the area of concern. It was thought some of the pipes would be sagging and/or opening into a sinkhole but surprisingly most of the pipe lengths were clean and in good condition although one pipe appeared to be almost halfway filled with concrete and broken at one location. Any clogged pipe runs were identified and will be replaced and a main pipe that was cut off will be redirected to another pipe for proper outlet. The inlet to the underground corrugated metal pipe system has generally worked very well in this area.

Creating a Sinkhole Solution (no pun intended)

The most important aspect of roadway longevity in a karst area is to control the surface water. In addition to correcting the existing pipe system, all the drainage swales leading to and between the inlets will now be lined with a Geosynthetic Clay Liner (GCL). Because the GCL needs to be covered with topsoil and seeding for protection, the connection to the inlet is always a problem because some of the water will travel below the protective cover and sit next to or worse flow down along the inlet. A detail was developed to place weepholes in the inlet to drain water the GCL captured. In areas of concern with past sinkhole activity, a 2' overexcavation and proofrolling specification has been added to provide the necessary quality control.

The areas to be addressed with special construction recommendations were broken down based on geology and sinkhole history: 1) sinkhole prone areas with shallow bedrock, 2) slightly sinkhole prone areas with deep bedrock, and 3) highly sinkhole prone areas with deep bedrock. The term deep relates to whether the problem could be remediated with surface excavation. The depth agreed upon for constructability was 12'. There also is a large overlap between area 2 and 3 to be conservative on our delineation. For highly sinkhole prone areas with deep bedrock, cap grouting is recommended.

Two repair details are recommended for area 1 (below):
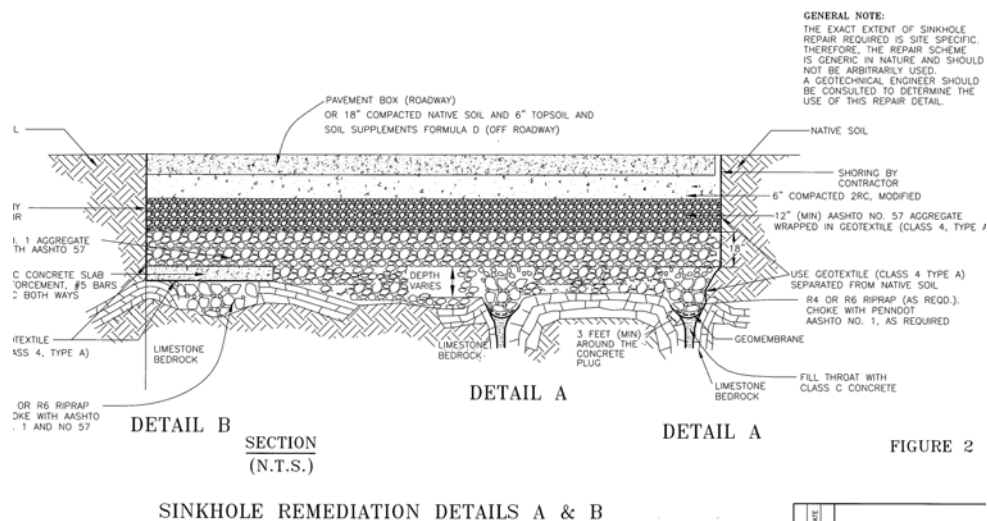
Area 2, where rock is too deep to excavate but there is less concern for sinkhole development:
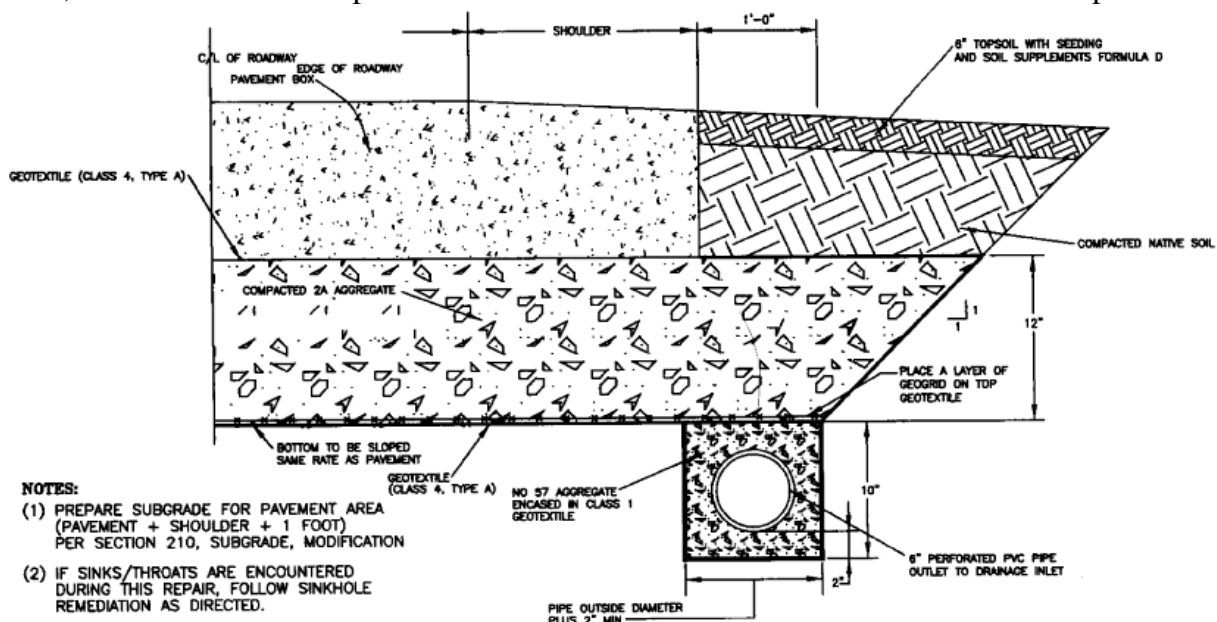
Notice the drainage pipe on the detail: because there was no cutoff to the permeable stone, the pipe was moved to below the geotextile reinforced mat. These pipes will be connected to the drainage system thanks to a lot of work from the plans unit.

Conclusion

Geophysics enhanced with confirmation test borings is fast becoming a reliable method to determine problems in karst areas over a large area. Government Transportation Agencies should provide additional funds to cover the additional investigation needed in these regions. Geotechnical engineers should be involved with project scoping to make sure this funding is placed into the project early. Armed with real data, sinkhole remediation recommendations for construction can be provided with a level of comfort, readiness and knowledge that the roadway will last its intended design life.

3.4

US-50 Big Horn Sheep Canyon, Fremont County, Colorado

A Rockfall Mitigation Case Study

Chad Lukkarila, Kleinfelder, 14710 87th Street NE, Suite 100, Redmond, WA 98052, 425-636-7900, clukkarila@kleinfelder.com

John Hunyadi, Kleinfelder, 4815 List Drive, Suite 115, Colorado Springs, CO 80919, 719-632-3593, jhunyadi@kleinfelder.com

William C.B. Gates, Kleinfelder, 14710 87th Street NE, Suite 100, Redmond, WA 98052, 425-636-7900, bgates@kleinfelder.com

ABSTRACT

US-50 extends west to east in Colorado from Grand Junction to Pueblo and beyond traversing through the rugged terrain of the Central Rocky Mountains and is lined with steep natural and constructed rock slopes. A rockfall mitigation analysis and design was requested by the Colorado Department of Transportation (CDOT) for an existing rock slope on US-50 between MP 242.2 and MP 242.6 near Coaldale in Central Colorado. The rock slope ranges in height from 100 to 300 feet and forms blind corners with limited rockfall catchment zones. The Arkansas River is immediately north of and parallels the road and rock slope.

In the spring of 2007, the authors conducted detailed geologic mapping of the rock slope using mountaineering techniques. Based on our mapping and mitigation analysis, blocks of concern and areas of rockfall were identified along the slope and recommendations for mitigation were developed. In conjunction with CDOT, detailed design plans and specifications for mitigation of the rockfall hazards were prepared. Mitigation began in September 2008 to stabilize the areas of concern. Because of the proximity of the Arkansas River, netting was suspended from a crane during scaling to reduce the potential for rockfall into the river. Modified rockfall nets were suspended in gullies and large rock blocks were anchored to the slope. Additionally, a joint team from CDOT and Kleinfelder engineers installed crack monitoring devices along the base and side of a large potentially unstable block to remotely monitor movement because of its size and location on the slope.

INTRODUCTION

Project Description

The project site is an existing rock cut slope on US-50 between MP 242.2 and MP 242.6 (approximately 2,100 feet long) in Central Rocky Mountains near Coaldale, Colorado (Figure 1). The rock cut is on the south side of the highway and forms a blind corner with a limited shoulder and rockfall catchment zone. The rock cut slope ranges in height from about 100 to 300 feet. In addition, the rock cut forms a compound slope with a ledge (bench) approximately midway between the shoulder of the road and the brow of the slope. The ledge dips towards the road and extends the full length of the rock cut. The Arkansas River parallels the road and rock cut on the north side.

Figure 1: Site Vicinity (Image Courtesy of Google Earth)

Local Geology

Precambrian granodiorite is exposed along this cut slope section of US-50. The regional geological map states that the main body of the granodiorite is characterized as pinkish-gray, massive to foliated, medium to coarse grained hornblende or biotite granodiorite. In localized areas, the granodiorite is altered to granitic gneiss (Scott et al, 1979). During our field investigation, we observed granitic gneiss with some localized areas of schist. The rock cut slope ranges in height from about 100 to 300 feet. The rock slope dips to the north at angles ranging from 60 to 90 degrees, overhanging in some locations. In addition, the rock cut forms a compound slope with a ledge (bench) approximately midway between the shoulder of the road and the brow of the slope. This area is known as Gobbler's Knob (Figure 2).

Design Challenges

In general, the overall rock quality is good and stabilization design was limited to isolated areas of rock fall or specific rock blocks. Challenges were present in developing a design to satisfy the road and environmental conditions. The roadway consists of two 12-foot wide lanes and minimal shoulders of less than six feet. The limited space reduced the potential for large crane support for rock anchoring. The limited road width and the height of the slope limited the potential design for stabilization of blocks on the upper section of the slope. Additionally, the proximity of the Arkansas River limited the design and recommendations for extensive scaling or blasting as part of the stabilization.

Figure 2: Aerial Photograph of Cut Slope (Provided By CDOT)

INVESTIGATION OVERVIEW

Rock Slope Mapping

As part of our field reconnaissance at rock cut slope locations, detailed geological and geomechanical mapping were completed (Figure 3). Much of the information collected during our outcrop mapping activities is attendant to the condition of discontinuities within the exposed rock masses including discontinuity information such as dip, dip direction, joint roughness and weathering characteristics. General rock mass information was collected to assess the quality of the rock mass and estimate the rock quality designation (RQD), Rock Mass Rating (Bieniawski, 1989) and Geological Strength Index (Hoek, 1997). Because of the height and inclination of the existing rock cut slopes, much of our field mapping was completed using mountaineering (climbing and rappelling) techniques (Figure 3).
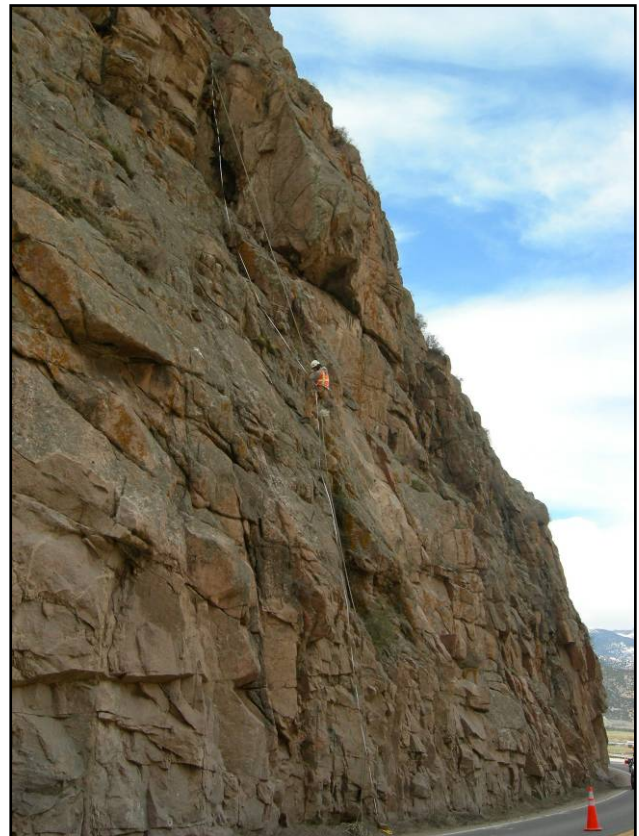

Figure 3: Rock Slope Mapping using

The rock slope mapping was completed along the road level, along the mid-height bench and in vertical traverses spaced across the cut slope. Three of the vertical traverses focused on specific large blocks we observed during the preliminary field visit. Two large blocks start at the bench height and extend 40 to 60 feet down towards the road (Figures 4 and 5). There are tension fractures present behind these large blocks indicating previous movement.

Figure 4: Rock Block 1 – Area of Concern

Figure 5: Rock Block 2 – Area of Concern

The third block is on the eastern end of the cut slope near the top of the slope approximately 300 feet above the road (Figure 6). Tension fractures are present along the side and base of this large block.

STABILIZATION DESIGN OVERVIEW

Rock Slope Stabilization Analysis
The development of recommended rock slope stabilization methods was based on three different analyses. These analyses included 1) kinematic evaluation, 2) global stability, and 3) rockfall hazard evaluation. Using the discontinuity data collected, we completed stereonet and Markland kinematic analyses (Watts, 2001) to establish if there is a potential for planar, wedge-, or toppling-type failures from the slope. The Markland analyses indicated the potential for toppling-type failures from the existing rock slope. Additionally, at the locations of Blocks 1 and 2 described above, there was a potential for planar-type failures. The potential for planar- and wedge-type failures was low in other locations based on the discontinuity data collected.

A global stability analysis of the existing rock slope was performed using the program Slide® by Rocscience. We utilized the Hoek-Brown Criterion (Hoek et al, 1997 and 2002) to estimate parameters for the rock mass. Based on the field mapping, we estimated average rock strength of 50 MPa (7,250 psi) and an average GSI of 60. The global stability analysis estimated a safety factor greater than 1.5 for the existing slope.

The slope stability of Block 1 and Block 2 was evaluated as planar failures from the slope. Cohesion was assumed to equal zero because the presence of

Figure 6: Rock Block 3 – Area of Concern

tension cracks which indicate that movement has occurred. We assumed a factor of safety of 1.0 for our analyses and applied a rock anchor force to achieve a factor of safety of 1.5. Hand calculations on the blocks were performed and the calculations checked using the computer program RocPlane V2® by Rocscience. Block 1 and Block 2 are located below the mid-height bench. The slide plane of the blocks is irregular and stepped from vertical to dipping towards the roadway at 55 to 65 degrees. To complete the stability analyses, a uniform slide plane was assumed at the angle observed during the field investigation. Based on our analyses for Blocks 1 and 2, we estimated that 15 to 20 25,000 pound tensioned rock anchors are required to achieve a factor of safety of greater than 1.5.

Stabilization Recommendations
Based on the analyses and field observations, we recommended stabilization methods for areas and potentially unstable blocks on the rock slope. Based on existing stationing along the roadway, the location of areas of concern and blocks were recorded and photographs were taken for figures and design specifications. Various potentially unstable rock blocks were observed along the length of the slope. Recommendations for the blocks included scaling and removal of the blocks if feasible and stabilization with rock anchors in scaling was not feasible.

Along the western end of the rock slope, chutes and gullies that extended to the road elevation were present with extensive loose rock. Stabilization recommendations for the chute and gullies included wire mesh drape rockfall system and a modified wire mesh drape system. The modified system included anchors and cables at the top of the system to hold the top of the drape three to four feet above the slope to allow rockfall to roll under the drape and be contained in the ditch.

Additionally, areas of highly fractured rock and blast damaged rock along the western end were recommended to be mitigated with a wire mesh drape system.

Along the eastern end of the rock slope, the mid-height bench slopes towards the roadway. Scaling was recommended along the mid-height bench to reduce the potential for rockfall. For the three large blocks, trim blasting was recommended to remove the unstable blocks. Because of the proximity of the Arkansas River, this option was not feasible. Based on the location and height on the slope of Block 3, stabilization or removal was not a feasible option. For Block 3, crack meter telemetry was recommended to monitor potential movement of the block on the rock slope.

Design and Construction Drawings and Specifications
Design and construction drawing specifications were prepared for the slope stabilization. The construction drawings package contained overview photographs of the slope with areas requiring stabilization highlighted (Figure 7). The photographs provided the contractor with a general picture and stationing of where the various stabilization methods would be installed. Details on the drawings summarized the rock anchor locations, quantities, geometries, loading requirements and testing requirements. Additionally, details summarized the wire mesh drape rockfall system installation specifications, wire mesh anchor installation, and approximate wire mesh quantities.
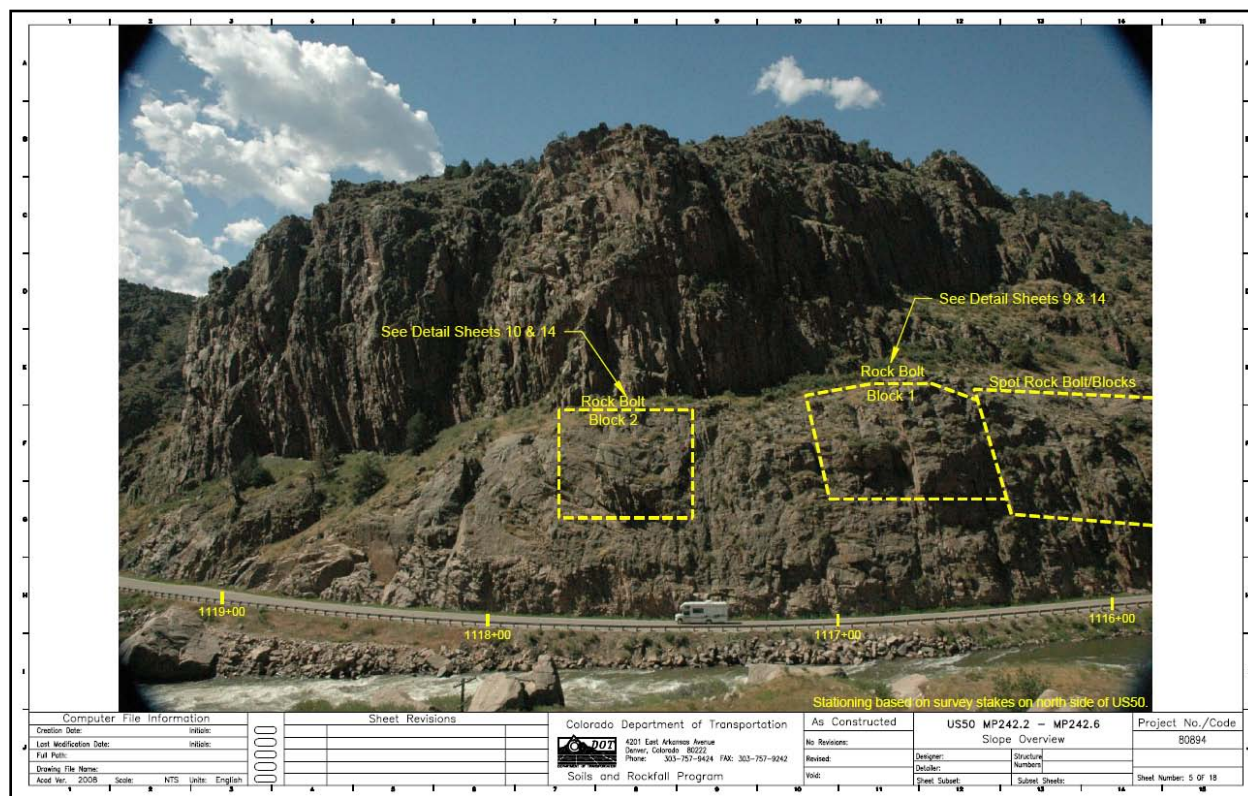
Figure 7: Typical Construction Plans Slope Overview Sheet

CONSTRUCTION OVERVIEW

Construction began in September 2008 at the close of summer to avoid the heavy use period of the Arkansas River. Slope stabilization was performed by AIS Construction. As described above,

stabilization included slope scaling in select areas, wire mesh and modified wire mesh installation, rock anchor installation, crack telemetry installation.

Slope stabilization presented environmental and technical construction challenges to the contractor. Slope scaling was closely monitored and a wire mesh was hung from a crane to reduce the potential for rockfall into the adjacent Arkansas River. To allow for traffic flow to continue, the road had to be cleared of debris and field work stopped on 20 to 30 minute intervals. Weather became a challenge as construction pushed into the late fall season in the Central Rocky Mountains. Because of safety concerns, icy roads often slowed construction. In addition, the steep inclination and height of the rock slope provided technical challenges. Stabilization efforts were completed with rope access or from a basket on the crane. Wire mesh placement was completed with the assistance of a helicopter (Figure 8).

Figure 8: Wire Mesh Installation with Helicopter Support

Slope stabilization progressed in phases. Phase 1 was slope scaling. Slope scaling was completed in specific areas of the slope and not the entire slope. Scaling was primarily completed on the western end of the rock slope where gullies were present and where more loose rock and blast damage was observed.

Phases 2 and 3 included wire mesh installation. During Phase 2, anchors to suspend the wire mesh were installed on the slope. Anchors were primarily installed using hand drilling methods with the contractor on rope access (Figure 9). Two types of wire mesh were installed to reduce rockfall onto the roadway. The standard wire mesh drape rockfall system was installed over areas with rockfall potential (Figure 10). A modified wire mesh drape rockfall system was installed in gullies and areas where

Figure 9: Wire Mesh Anchor Installation

rockfall may occur further up the slope. The modified system included anchors and cables at the top of the system to hold the top of the drape three to four feet above the slope to allow rockfall to roll under the drape and be contained (Figure 11). CDOT has utilized the modified wire mesh drape system in various locations in Colorado with success in containing rockfall.

Phase 4 of the slope stabilization was the installation of rock anchors in the unstable rock blocks identified during the field mapping and analyses. Rock anchors were installed from a basket supported by the crane and also by a drill rig installed on the boom of the crane with the driller supported with ropes using mountaineering techniques.   Rock anchors were installed and tensioned to 25,000 pounds. Rock anchor lengths ranged from 10 to 20 feet.

For Phase 5, telemetry was installed on Block 3 to remotely monitor movement of the block. Based on the location and height on the slope of Block 3, stabilization or removal was not a feasible option. In a joint effort with CDOT and Kleinfelder, three crack meters were installed at various locations along the tension crack behind Block 3 (Figure 12).   CDOT and Kleinfelder used mountaineering techniques (rappelling and climbing) to set-up at the desired locations. Hand drills were employed to install the anchors for the crack meters across the tension crack (Figure 13).

The crack meters are connected to a remote power source and can be monitored remotely. With real-time monitoring, the crack meters will detect the slightest movement in Block 3. If movement occurs, a signal will be transmitted to CDOT who will be able to close the road to protect the travelling public.
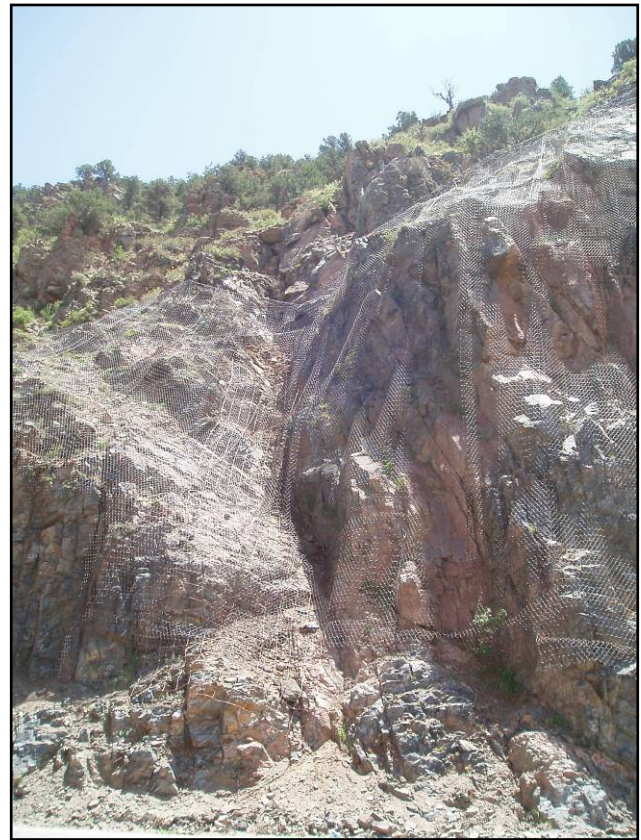

Figure 10: Installed Wire Mesh Drape Rockfall

Figure 11: Modified Wire Mesh Drape Rockfall System

186

CONCLUSIONS

The CDOT Rockfall Hazard Classification System identified a 2,100-foot long slope along US-50 in Central Colorado because of blind corners, limited rockfall catchment, high traffic volumes, and multiple objective hazards. Through discussions with CDOT, geologic mapping of the rock slope, and stability analyses, Kleinfelder provided a range of recommendations for stabilization and mitigation of rockfall hazards from the rock slope. During construction, Kleinfelder worked closely with CDOT to monitor construction and provide field engineering consultation where necessary.

Figure 12: Location of Crack Meters on Block 3

REFERENCES
Bieniawski, Z.T. (1989). Engineering Rock Mass Classifications. New York: Wiley.

FHWA. (1998). *Rock Slopes Reference Manual* (FWHA-HI-99-007). Wyllie, D., and Mah, C.W.

Hoek, E., and Brown, E.T. (1997). "Practical Estimates of Rock Mass Strength." International Journal of Rock Mechanics and Mineral Sciences, Vol. 34, No. 8, pp. 1165-1186.

Hoek, E., Carranza-Torres, C. and Corkum, B. (2002). Hoek-Brown criterion – 2002 edition. *Proc. NARMS-TAC Conference*, Toronto, 2002, 1, 267-273.

Rocplane Version 2.0 (2003). Stability Analysis Software for Translational Failures. RocScience Inc. Toronto, Canada.

Slide Version 5.0 (2003). Stability Analysis Software for Soil and Rock Slopes. RocScience Inc. Toronto, Canada.

Watts, C.F. (2001). Rockpack III, Slope Stability

Figure 13: Close-up of Crack Meter across Tension Crack on Block 3

Computerized Analysis Package Reference Manual, Radford University, 48pp. and
Appendices.

Wyllie, Duncan, C., Mah, C.W. (2004). <u>Rock Slope Engineering: Civil and Mining</u>, 4th Edition,
Spon Press, pp. 245-275

Acknowledgements

We would like to acknowledge the following personnel for their effort and support with this project: Mr.
Ty Ortiz and the engineers and geologists with the Colorado Department of Transportation (CDOT), for
the opportunity to be apart of this project and for their assistance during the investigation and design; and
the Kleinfelder staff who were involved in all aspects of this project from the initial investigation through
construction.

Disclaimer

Statements and views presented in this paper are strictly those of the author(s), and do not necessarily
reflect positions held by their affiliations, the Highway Geology Symposium (HGS), or others
acknowledged above. The mention of trade names for commercial products does not imply the approval
or endorsement by HGS.

Copyright

Copyright © 2009 Highway Geology Symposium (HGS)

3.5

Colorado Rockfall Simulation Program Version 5.0

Ryan Bartingale, E.I.T.
Yeh and Associates, Inc.
5700 East Evans Ave.
Denver, CO 80222
(rbartingale@yeh1.net)

Jerry Higgins, Ph.D., P.E.
Department of Geology and Geological Engineering Colorado School of Mines
1500 Illinois Street
Golden, CO 80401
(jhiggins@mines.edu)

Richard Andrew, P.G.
Yeh and Associates, Inc.
5700 East Evans Ave.
Denver, CO 80222
(randrew@yeh1.net)

Alan Rock
Summit Peak Technologies LLC
6121 N Powell Rd
Parker, CO 80134
(arock@summitpeak.net)

Runing Zhang
Department of Engineering Technology
Metropolitan State College of Denver
Campus Box 61, P.O. Box 173362
Denver, CO 80217
(rzhang@mscd.edu)

ABSTRACT

The Colorado Rockfall Simulation Program (CRSP) was developed in 1987 to estimate the velocity, energy, and bounce heights of rockfall, which in turn forms a basis for selection of designs for mitigation. Several revisions were issued in the following years, and the program has been widely used for rockfall design. A new version of CRSP (5.0) has been produced, and is based on a combination of Particle Flow Code and the Discrete Element Method for dynamic model simulation. This approach provides an accurate approximation to the equations of motion for rock and slope interaction and is an improvement on previous CRSP versions. CRSP 5.0 was calibrated with respect to rock velocity, energy, bounce height, and rollout. Program calibration was based on the results from previously completed

rock rolling experiments and new data collected from mapping natural slopes. Rock rolling experiments have been documented using high-speed cameras to estimate rock velocity and kinetic energy. Natural slopes with rockfall distributed on the slope were mapped to obtain information on runout. Where present, rockfall scar marks on trees were used as a source of bounce height information. Calibration experiments compared the experimental and observational measurements to CRSP output. The program accurately estimates the velocity and kinetic energy of rocks rolling on slope material varying from soft clay to hard rock. It accurately predicts bounce heights, but may overestimate runout distance because of the use of spherical rocks in the modeling.

INTRODUCTION

The purpose of this research and program update was to improve CRSP user friendliness and increase accuracy of predicted rockfall properties including rock velocity, kinetic energy, bounce height, and rock runout. User friendliness was improved by re-defining the roughness coefficient to simplify field measurements and reduce analysis time along with recreating the user interface to ease data input and program navigation. Also, slope hardness is represented using one numerical input value instead of two (tangential and normal coefficients of restitution) as in version 4.0. Program accuracy was improved by updating the algorithm to better simulate interaction between rock and slope, and by expanding the calibration data to include soft soil slopes, bounce height data, and runout data.

Calibration data includes existing rock rolling experiments used for calibration of CRSP version 4.0, two additional rock rolling experiments completed at a site near Rifle, Colorado, and runout and bounce height data from 15 natural rockfall areas in Colorado. The rock rolling experiments provided velocity and kinetic energy of rockfall calculated at an analysis point. Reference lines and a high speed camera were used to compute velocity, and estimated rock mass was used to calculate kinetic energy. Secondly, runout and bounce height data obtained from 15 slopes in Colorado were compared to CRSP output. Rockfall distribution on the slope was used to measure runout distance, and rockfall scar marks on trees were used to estimate bounce height. Calibrations of runout and bounce height were used to further define the reasonable hardness coefficient ranges established on the basis of rock rolling experiments. This research examines the new version's input parameters, algorithm, calibration, and finally discusses calibration results with program observations and limitations.

PREVIOUS WORK AND BACKGROUND

Two main versions of CRSP predate version 5.0. CRSP version 1.0 was created by Pfeiffer, 1989. Experimental verification and calibration of CRSP 1.0 was conducted in conjunction with the testing of rockfall fences at a test site near Rifle, Colorado. Version 1.0 underwent minor modifications over several years resulting in versions 2, 3, and 3a. A more complete discussion of the original CRSP calibration and verification efforts can be found in Pfeiffer (1989) or Pfeiffer et al. (1991, 1995).

Version 4.0, completed by Jones et al. (2001), was produced to be compatible with Windows 95 and Windows NT. It was reprogrammed using Visual Basic, and the input/text editor section

was modified to increase user friendliness. From version 1.0 to version 4.0 the CRSP algorithm did not change. The input coefficients (normal coefficient of restitution and tangential coefficient of frictional resistance) were recalibrated through the accumulation of six rock rolling experiments with data provided by Caltrans along with the original CRSP calibration effort. After program verification, CRSP predictions tended toward a worst case scenario in comparison to studied field tests, but the overall conclusions were similar.

CRSP 5.0 INPUT PARAMETERS

Input values include a slope profile (entered as a series of straight line segments known as cells), roughness measurement in each cell, slope hardness coefficient for each cell, plus the size, shape, density, starting location, and number of rocks comprising the simulated rockfall events.

The slope inclination and length (slope profile) is the most important factor in estimating rockfall behavior because it defines areas of rockfall acceleration and deceleration. The slope profile must be carefully constructed, starting new cells wherever the slope angle or surface material changes. Second in importance is the surface roughness. Irregularities on the slope surface account for most of the variability observed among rockfall events originating from a single source location. The surface roughness field measurement is defined as the greatest repeatable perpendicular variation of the slope surface from the average slope angle (within a single cell) over a distance of six feet (Figure 1). However, for the program to correctly model rockfall trajectory, the roughness value must be a function of the rock diameter, with a larger value used for a small rock and a smaller value for a larger rock. In an improvement over the old program, version 5.0 adjusts the surface roughness value according to the size of the simulated rockfall so that several different rock diameters can be run in a single simulation using one roughness input value.
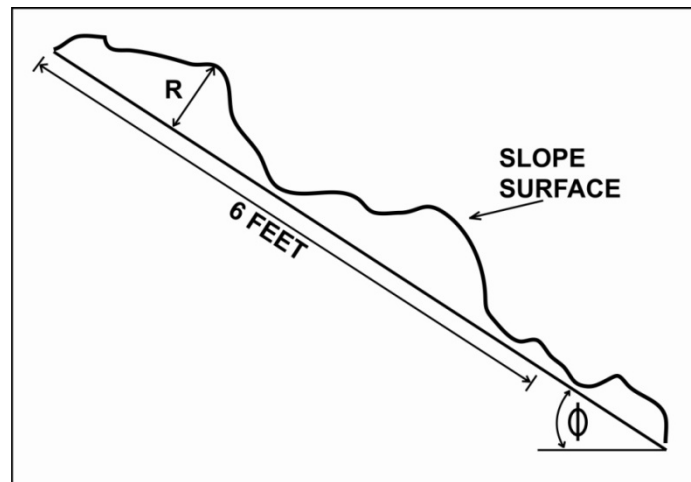

Figure 1. Surface roughness (R) established as the largest repeatable perpendicular variation of the slope surface from the average slope angle (Φ) over a distance of 6 feet.

Next, the slope hardness coefficient is a numerical representation of slope material properties used to estimate the amount of energy transferred from the rock to the ground surface upon impact. This is a subjective coefficient that normally requires site specific calibration to obtain proper values.

Finally, the size, shape, density, starting location, and number of rocks comprising the simulated rockfall event should be in accord with rockfall observed on the slope. Simulating the largest diameter rockfall possible will represent a worst case scenario and produce conservative results.

CRSP 5.0 ALGORITHM

The program algorithm was developed by Dr. Runing Zhang and Alan Rock (Summit Peak Technologies). The algorithm uses a combination of planar equations of motion and the Discrete Element Method (DEM) to simulate rock velocity and the contact forces between rock and slope. The DEM assumes a linear elastic contact force-displacement relationship between two impact bodies. The normal contact formulation is linear elastic with a viscous damping coefficient characterized by two parameters; normal stiffness and viscosity. The tangential force depends on the Coefficient of Restitution (COR) of the material and the relative tangential velocity of the two contact objects. The hardness coefficient is a function of the COR and damping coefficient.

The program had to first be set up by accurately selecting end values for the damping coefficient and COR. This was a one-time step, completed by the program developer. To relate the damping coefficient and the COR to material properties, a number of trial and error tests were performed. Maximum and minimum damping and COR values were assigned to maximum and minimum hardness coefficient values. The maximum and minimum hardness coefficient values were set at 1.0 and 0.1, respectively. The damping and COR have an inverse linear relationship. For example, a hard slope will have a relatively high COR and a low damping value while a soft soil slope will have a low COR and a high damping value. During the trial and error tests, different combinations of maximum and minimum COR and damping coefficients were run in CRSP until the simulated rocks behave similarly to field observations. The new algorithm is a more advanced and accurate representation of the interaction between rock and slope.

CALIBRATION

First, hardness coefficient calibration was completed for rock velocity and kinetic energy using the rock rolling experimental data. Hardness coefficients to represent various material types were selected on the basis of modeled velocities and kinetic energies that ranged from the average to upper bounds of observed values. This approach yields a moderately conservative yet reasonable model. The rock rolling experimental datasets were used to estimate new ranges of hardness coefficient values for the following three general slope types:

1. Smooth hard surfaces (Swiss Test).
2. Firm soil slopes (Brugg/Industrial Enterprise and Hi-Tech Tests).
3. Moderately firm soil with exposed rock and boulders (Rifle Test).

Secondly, the natural slope profiles were calibrated for rock runout and bounce height by adjusting the hardness coefficient until simulated output closely matched the measured field data. Of particular interest was the maximum runout distance of CRSP simulated rocks compared to that of the observed data. Maximum runout distance is often times used as a basis to determine if mitigation is needed to protect structures from rockfall. Therefore, the hardness coefficient used must produce runout distances that do not fall short of the actual maximum runout distance, nor do not consistently roll past the actual maximum runout distance. Figure 2 shows one slope on North Table Mountain near Golden, CO that was measured for runout distance.

Finally, bounce height was evaluated in the field by measuring the height of rockfall caused scar marks on trees. Figure 3 shows a tree that was hit by rockfall near Georgetown, CO. During bounce height calibration, hardness coefficient values that produced rock bounce heights equal to or slightly above the upper range of observed data were chosen to represent various material types. Output above the observed range was chosen because measured tree scars (used to estimate bounce height) may not represent the maximum bounce height seen in the field The natural slope profiles were used to further define the hardness coefficient ranges set during rock rolling experiment calibration for the general slope types listed below;

1. Moderately soft to firm soil. Talus covered in upper slope portions (Highway 149 profiles).
2. Moderately soft soil. Gravel to cobble talus in areas. Rockfall produces sandstone blocks up to 15ft in diameter (Minturn profiles).
3. Firm soil (North Table).
4. Very soft soil. Rockfall produces sandstone blocks up to 14ft in diameter (Trinidad Profiles).
5. Soft soil. Hard bedrock in upper cells. Abundant rockfall scar marks on trees (Marble profile).
6. Firm soil and cobble to boulder talus. Some rockfall scar marks on trees (Georgetown profile).

Figure 2. Large rockfall and source area on North Table Mountain near Golden, CO.

Figure 3. Tree broken off at 20ft by rockfall. Located near Georgetown, CO.

RESULTS

Select graphs used during program calibration of the rock rolling experiment and natural slope profile data are shown below. Graphs were chosen to show accurate estimates of the observed data and illustrate overall program trends.

Rock Rolling Experiments

Graphs showing different slope hardness values for two rock rolling experiments are shown in figure 4. Each graph includes measured velocity or kinetic energy data plotted with one set of CRSP output (associated with one hardness coefficient value); a linear trend line was fit to the velocity data while a second order polynomial trend line was fit to the kinetic energy data to help illustrate the overall trend.
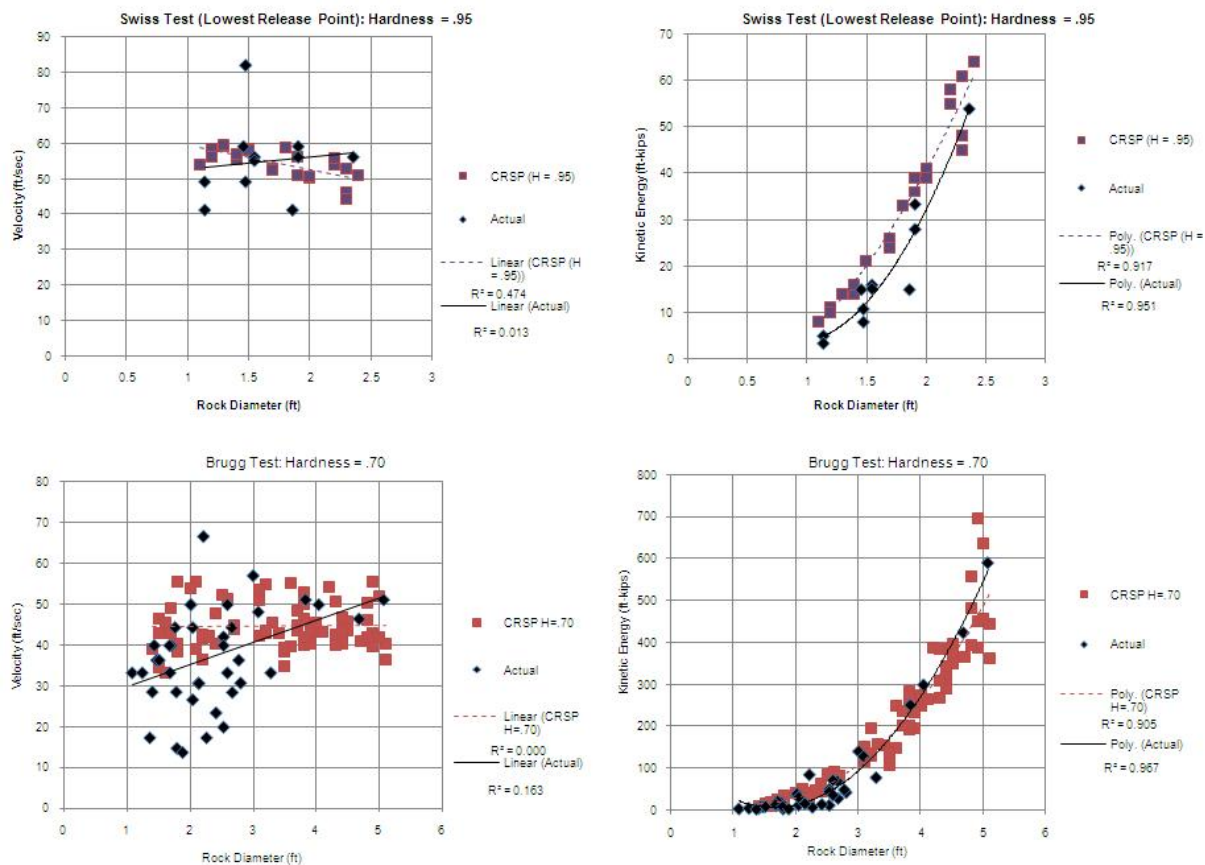
Figure 4. Velocity and kinetic energy calibration graphs relating observed and predicted data.

Natural Slope Profiles

Graphs from the runout and bounce height calibration are shown in figures 5 and 6. The runout graphs show "cumulative percentage of total rocks stopped" on the y-axis and "cell number" on the x-axis. The bounce height calibration graphs show "bounce height" on the y-axis and "analysis point" on the x-axis. The analysis point is anywhere a scar mark (or group of scars) was measured.

195
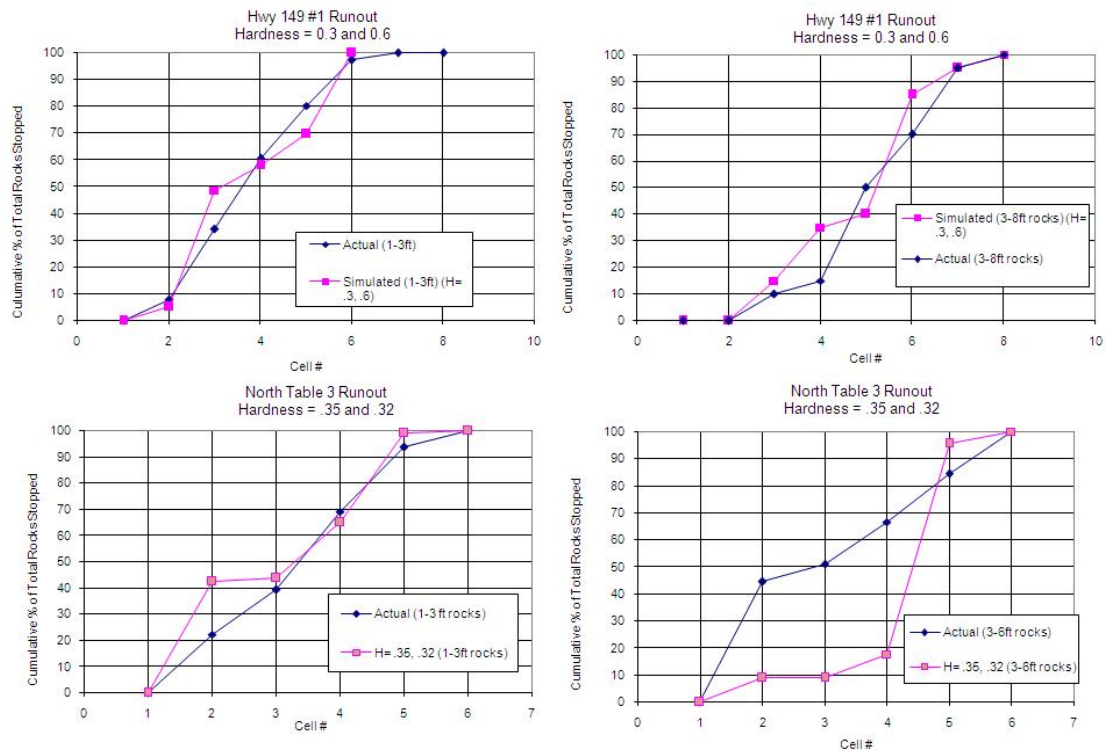
Figure 5. Rock runout calibration graphs relating observed and predicted data.
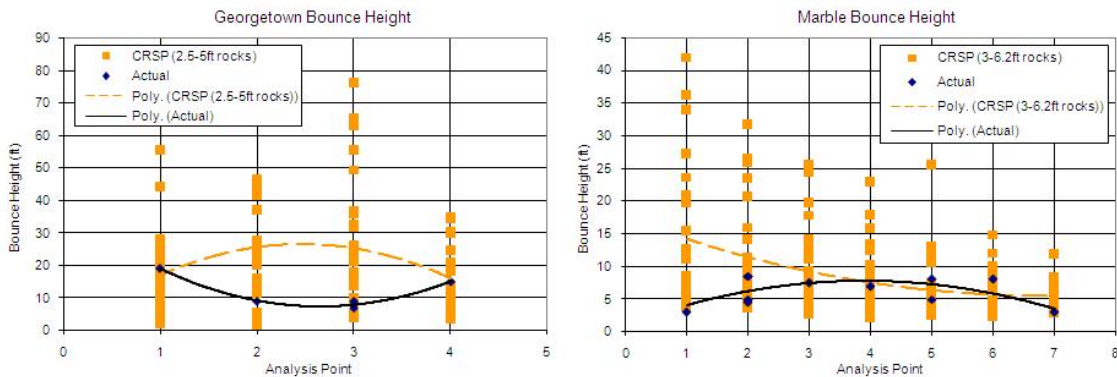
Figure 6. Bounce height calibration graphs relating observed and predicted data.

DISCUSSION OF THE CALIBRATION RESULTS

Extensive calibration was conducted on all rockfall data and the resulting calibration plots were evaluated to estimate sets of suggested hardness coefficient values for use with CRSP. Table 1 shows the hardness coefficient ranges found to produce accurate CRSP output when compared to observed data. The overlap in these hardness coefficient ranges for each material type was used to construct the coefficient ranges shown in Table 2. Table 2 is to be used by the program user as a starting point when choosing a hardness coefficient for a slope material. Further modification to the hardness coefficient

196

value can be accomplished by conducting site specific calibration of the program, if an existing slope has rockfall accumulation.

Table 1. This table shows all the hardness coefficient ranges set during calibration of the rock rolling experiment data and natural slope profiles.

Rock Rolling Experiment Data

Slope Type			Firm Soil		Hard Bedrock
Hardness Range			.60-.80		.90-1.0

Runout Data

Slope Type	Soft soil	Moderately soft soil	Firm soil:	Loose gravel to cobble talus	Boulder talus	Hard Bedrock
Hardness Range	.05-.30	.35-.50	.40-.70	.20-.55	.55-.80	

Bounce Height Data

Slope Type	Soft soil		Firm soil		Boulder talus	Hard bedrock surfaces
Hardness Range	.15-.35		.55-.75		.55-.80	

Table 2. Shows the recommended ranges of hardness coefficients for each slope material type. The ranges were set using the overlap from the ranges shown in Table 1.

Slope Type	Soft soil: > 100% rock pick penetration depth, footprints left in soil	Moderately soft soil: 75%-100% rock pick penetration depth	Firm soil. 50% - 75% rock pick penetration depth.	Gravel to cobble talus: covers >40% of slope.	Boulder Talus: covers >40% of the slope surface	Hard bedrock surfaces.

Hardness Range	.15-.30	.35-.50	.60-.70	.25-.55	.55-.80	.90-1.0

Site specific calibration can be used to establish rockfall distribution and rock size for the slope profile. The measurement described below is based on a method developed by Coe and others (2005). Rockfall distribution is measured by counting all the rocks (of rockfall origin) in a 15 ft wide section along the slope profile line (Figure 7). Each cell has a separate 15 ft wide section that extends the length of the cell. A rock of rockfall origin is defined as being at least 1 ft in diameter and lying entirely on top of the soil. Rocks that are partially buried are assumed to be deposited by processes other than rockfall. In many rockfall areas different sized rocks may stop in separate sections along the profile, so on slopes where there is a large range in rock diameters, rock sizes should be divided and counted separately.
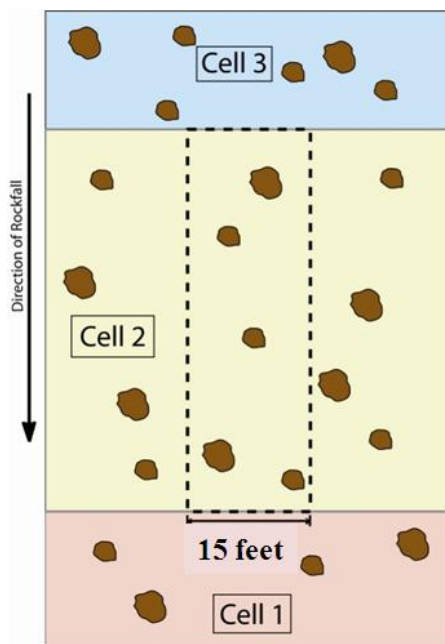
Figure 7. Rock distribution for each cell is measured by counting all the rocks in a 15 ft wide section (perpendicular to the rockfall path). Rocks at least 1 foot in diameter and located completely on top of the soil are considered to be from rockfall processes (After Coe et al., 2005).

Program Observations and Limitations

The runout and bounce height calibration charts along with the hardness coefficient ranges shown in Table 1 illustrate several observations. First, CRSP overestimates rock runout distance. Firm soil is the only common material between the natural slope profiles and the rock rolling experiments. For these firm soil slopes, the hardness coefficient range set from the rock rolling experiments was .60 to .80 while the coefficient range set from the runout data was .40 to .70. Runout estimates required a generally lower hardness coefficient to obtain accurate output compared to the rock rolling experiment data. For many of the runout profiles, increasing the hardness coefficient to a value between .60 and .80 resulted in rocks continually passing the observed maximum runout distance. To properly model rock runout, the user should choose a hardness coefficient in the lower part of the suggested coefficient range.

Overestimation is caused by CRSP modeling spherical rocks while rocks in field situations have many different shapes depending on weathering patterns, jointing, and bedding features. The shape of a rock has a large affect on its velocity as it travels down the slope. This is especially true in areas of rock deceleration. At high velocities, angular rocks act much like spherical rocks because their fast rotation causes the rock to contact the slope mostly on the high points of the rock. When an angular rock starts to decelerate, the high points on the rock slow it down because the rock contacts the slope more frequently on low points and must overcome the high points. During deceleration, angular rocks tend to tumble and fall while spherical rocks roll without needing to overcome any undulation in the rock surface, resulting in a longer runout distance.

During bounce height calibration, the predicted maximum bounce heights were much higher than the observed data. When a second order polynomial trend line was fit to the predicted and observed data, the CRSP predicted bounce height trend line was observed to accurately model the observed data. Therefore, the user should use an average bounce height when graphing CRSP predicted bounce heights and also when drawing conclusions from predicted bounce heights for mitigation design.

CONCLUSIONS

The new version of CRSP has been written based on a combination of Particle Flow Code and the Discrete Element Method for dynamic model simulation. This approach provides a more accurate approximation to the equations of motion for rock and slope interaction than employed by previous CRSP versions.

The new user interface has made this version more user friendly than previous CRSP versions by easing data input and program navigation. Also, changing the definition of the roughness coefficient so that one input value can be used for a variety of rock sizes decreases the time required for field measurement, along with time in the office conducting rockfall simulations. Finally, replacing the normal and tangential coefficients (CRSP 4.0) with one hardness coefficient increases the program's user friendliness and decreases time spent conducting rockfall simulations.

The calibration of CRSP Version 5.0 to include soft soil slopes, runout, and bounce height is a substantial expansion over prior calibration efforts that were based only on rock rolling experiments on a narrow range of slope types. Program calibration to rock runout and bounce height using a range in slope material types provides a sense of the hardness coefficient sensitivity and accuracy of runout and bounce height estimates. This provides the user a basis for judgment of simulation results.

The user needs to be aware that CRSP overestimates runout and when modeling runout, should use a hardness coefficient in the lower part of the suggested range set for the particular slope material. Also, using the average CRSP estimated bounce height results in a more accurate approximation of the actual bounce heights along the slope profile.

CRSP 5.0 represents an improvement to a well known and proven rockfall modeling program. Updates to the user interface and input parameters increase the user friendliness: while an expansion in calibration data and an advanced algorithm improves the programs accuracy.

REFERENCES

Coe, J.A., Harp, E.L., Tarr, A.C., and Michael, J.A., 2005, Rock-Fall Hazard Assessment of Little Mill Campground, American Fork Canyon, Uinta National Forest, Utah. U.S. Geological Survey Open-File Report 2005-1229, U.S. Department of Interior, 48p.

Jones, C.L, Higgins, J. D., Andrew, R. D., 2001, Colorado Rockfall Simulation Program Version 4.0 Users Manual: Colorado Department of Transportation, Denver, CO, 127 p.

Pfeiffer, T.J., 1989, Rockfall Hazard Analysis Using Computer Simulation of Rockfalls, Thesis, Colorado School of Mines, 103p.

Pfeiffer, T.J., Higgins, J.D., Andrew, R.D., Schultz, R.J., and Beck, R.B., 1995, Colorado Rockfall Simulation Program Version 3.0a User's Manual: Colorado Department of   Transportation, Denver, CO, 60 p.

Pfeiffer, T.J., Higgins, J.D., Schultz, R., and Andrew, R.D., 1991, Colorado Rockfall Simulation Program

User's Manual for Version 2.1: Colorado Department of Transportation, Denver, CO, 127 p.

4.1

A Proactive Approach To Limit Potential Impacts from Blasting to Drinking Water Supply Wells, Windham, New Hampshire

Krystle Pelham and Dick Lane, P.G.

New Hampshire Department of Transportation
Bureau of Research and Materials
P.O. Box 483
5 Hazen Drive
Concord, NH 03302-0483
(603) 271-1657
KPelham@dot.state.nh.us   DLane@dot.state.nh.us

Jay R. Smerekanicz, P.G.
Golder Associates Inc.
670 North Commercial Street, Suite 103
Manchester, NH 03101
(603) 668-0880
jay_smerekanicz@golder.com

William J. Miller, III, R.P.G.
Continental Placer, Inc.
II Winners Circle
Albany, NY 12205
(518) 458-9203
wmiller@continentalplacer.com

ABSTRACT

The New Hampshire Department of Transportation (NHDOT) is widening and improving Interstate 93 (I-93) from Salem to Manchester. This project includes reconfiguration of Exit 3 in Windham to improve safety and traffic flow. The Exit 3 reconfiguration requires blasting to remove about two million cubic yards of bedrock over a seven year period. Blasting for rock removal at recent private developments and municipal construction projects in Windham has allegedly caused environmental impacts to residential drinking water wells. As a result the NHDOT has implemented a proactive approach to limit potential impacts from blasting for the Exit 3 project. As part of this approach, NHDOT conducted a drinking water baseline monitoring program in May and June 2008 to measure background and pre-blasting groundwater and surface water conditions prior to the initiation of blasting activities in December 2008. Part of the monitoring program included development of a conceptual hydrogeologic model of the project area to locate new monitoring wells. Key portions of NHDOT's proactive approach to reducing potential environmental impacts from blasting include implementation of best management practices (BMPs) for the handling, use, and detonation of explosive materials; and

implementation of an ambitious biweekly groundwater monitoring program to detect potential impacts prior to reaching drinking water resources. This paper presents the preliminary findings from this ongoing program intended to protect the environment and the public. An overview of the programmatic implementation, day-to-day and corrective action BMPs, and groundwater monitoring results are included.

INTRODUCTION

As part of the I-93 widening project, the NHDOT will be improving the roadway alignment, and exit and entry ramp configuration of Exit 3 in Windham (Figure 1). This portion of the project lies roughly between mileposts 5 and 7 of I-93, and will include:

- Construction of detention basins

- Realignment of the north- and south-bound barrels

- Construction of new on- and off-ramps

- Relocation of a portion of NH Route 111

- Construction of a new Park-n-Ride facility

The NHDOT estimates that about 1.5 million cubic yards (cy) of rock will be removed via blasting for the roadway and detention basin construction, and another 0.5 million cy of rock will be removed for the Park-n-Ride facility. The NHDOT plans to let the blasting portions of this work through four contracts over a seven year period, which started in November 2008.

In the Town of Windham (the Town), recent blasting projects for a commercial development project and a school have allegedly caused impacts to groundwater, including elevated nitrate concentrations and turbidity. The NHDOT is sensitive to the potential for blasting to impact drinking water resources. Therefore, the NHDOT requested Golder Associates' (Golder) assistance in developing and implementing a plan to monitor water resources in the project area and to recommend Best Management Practices (BMP) to reduce the potential for impact.

In June of 2008 Golder completed a drinking water baseline study for the Exit 3 area in Windham NH (Golder, 2008). This study included developing a conceptual hydrologic model,
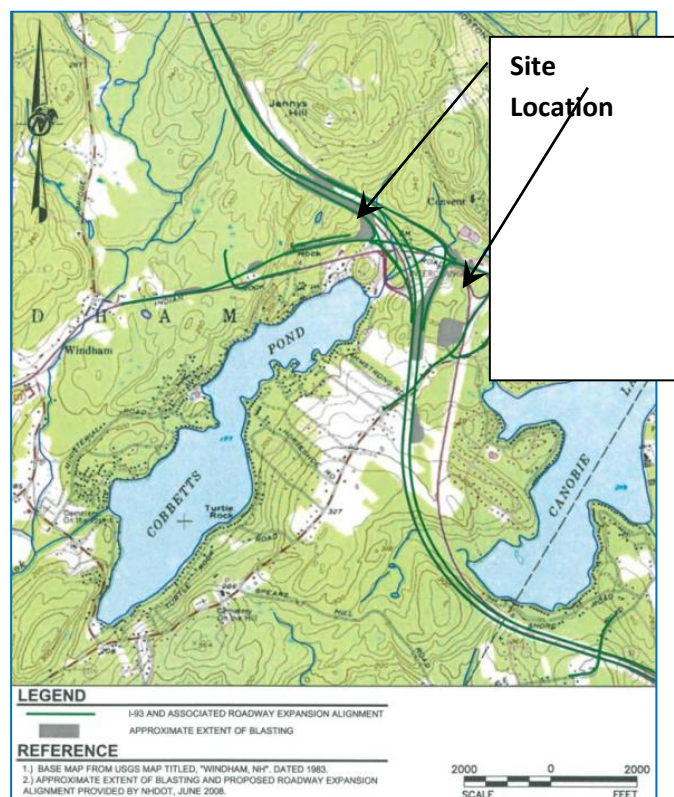

Figure 2 - Site location map. New interchange roadways in green, and blasting areas in gray.

developing and implementing a plan to monitor water resources in the project area, and recommendations for BMPs to reduce the potential for impact.

CONCEPTUAL HYDROGEOLOGIC MODEL

The local topography in the Exit 3 area is hummocky with elevations ranging between approximately 175 and 500 feet above mean sea level (ft msl) (USGS 1985) (Figure 1). There are two large surface water bodies in the project area. Canobie Lake exists at an elevation of 219 ft msl and is located to the east of I-93. Canobie Lake's shoreline is developed with residential homes and an amusement park. Canobie Lake is used for recreational purposes, and also serves as the primary drinking water supply for the town of Salem, New Hampshire during the summer. Groundwater recharge for Canobie Lake is primarily by groundwater infiltration and surface water runoff. Cobbetts Pond at an elevation of 177 ft msl is located to the west of I-93. Cobbetts Pond's shoreline is also developed with residential homes and is used for recreation. The pond's primary recharge is derived from Dinsmore Brook located on the northern shoreline of the pond. Currently, surface water runoff from I-93 Exit 3 and the associated ramps drains into Dinsmore Brook and ultimately into Cobbetts Pond. The pond discharges into Golden Brook along the southwestern shoreline.
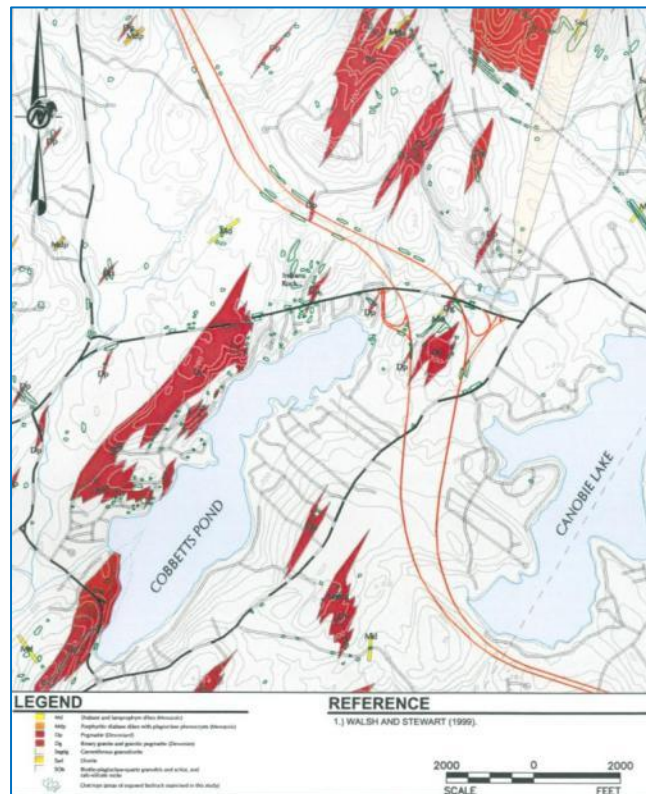
Figure 3 - Bedrock geologic map of the Windham, NH project area.

The surficial geology in the vicinity of I-93 Exit 3 consists of late Pleistocene glacial till containing a poorly sorted mixture of clay, silt, sand, pebbles, cobbles and boulders. Lesser amounts of gravel were deposited over the till by the melt waters of retreating glaciers approximately 13,000 to 20,000 years ago (Larson, 1984; VHB, 2004). The overburden varies in thickness between 1 and 40 ft (Golder, 2005; VHB, 2004). The project area also contains Holocene-age peat deposits mainly located along the eastern shoreline of Cobbetts Pond. The peat deposits range between 1 to 5 ft thick and overlie the glacial till deposits in low lying areas (VHB, 2004).

The bedrock underlying the unconsolidated overburden in the project area consists of the Ordovician and Silurian (about 500 million years old) Berwick Formation, one of several formations comprising the northeast trending Merrimack Trough (Lyons et al., 1997; Walsh and Clark, 1999). Figure 2 contains a bedrock geologic map of the project area. The Berwick Formation consists of interbedded biotite-plagioclase-quartz granofels and schist, with interbeds or lenses of calc-silicate granofels and minor metapelites.
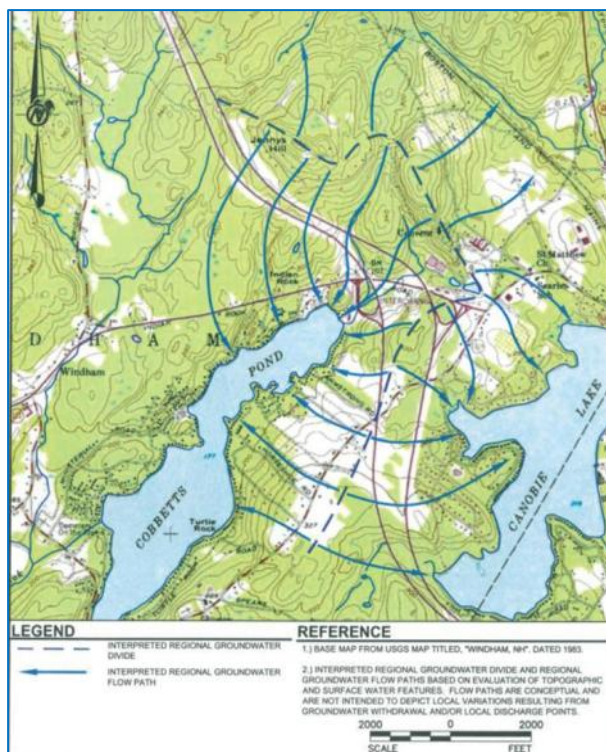

Figure 4 - Groundwater flow paths.

In addition to the metasedimentary rocks, granitic rocks of the New Hampshire Plutonic Suite occur as dikes and plutons in the bedrock, and these features are observed in outcrop in the project area (Walsh and Clark, 1999). The igneous rocks present in the I-93 Exit 3 vicinity are identified as granitic pegmatite, consisting of coarse-grained intrusive igneous rock, possibly of Devonian age (about 400 million years old). Minor occurrences of Devonian age binary granitic pegmatite have also been identified in the I-93 Exit 3 area. Much of the pegmatite has been metamorphosed to a garnet zone grade, as defined by the presence of garnet, quartz, and calc-silicate minerals.

The bedrock is strongly foliated, with the foliation trending northeast, and dipping steeply to the southeast or northwest. Minor folding and discontinuous quartz veins and pegmatite are common. Steeply dipping, northwest trending joints are the most common brittle fabric (Walsh and Clark, 1999).

The hydrogeologic system is fracture-dominated. To get a better understanding of horizontal groundwater flow, we reviewed regional topography, surface water features and borehole/monitoring well data. Regional groundwater divides were identified and the interpretation of groundwater flow was consistent with work completed by others in areas at nearby New Hampshire Department of Environmental Services (NHDES) listed remediation sites. It was assumed that groundwater flows from areas of high topography to areas of low topography (Figure 3).

Two hydrogeologic cross sections were generated using United States Geological Survey (USGS) topographic information, borehole and well information collected for the roadway realignment design (NHDOT), and well data from the Town (Figure 4). Cross section A-A' (Figure 5), oriented east-west, was generated to understand the groundwater-surface water relationship relative to I-93. This cross section determined the location of the groundwater divide between Cobbetts Pond and Canobie Lake. The groundwater flows from the divide to the east and west toward the surface water bodies. The north-south oriented cross section B-B'

(Figure 6) was generated to understand the upgradient conditions. This cross section depicts groundwater flow to be southerly towards Cobbetts Pond. Residential wells in the area are on average 400 ft deep, and have a 40 ft surface casing.

We reviewed a number of resources to estimate bedrock hydraulic conductivity and porosity and to calculate representative horizontal hydraulic gradients. This information was used to estimate groundwater flow velocities and hence potential blasting impacts.

Data was obtained from NHDES on a public water supply located near Canobie Lake indicating a bedrock average hydraulic conductivity value between 0.1 ft/day and 0.27 ft/day. Porosity was estimated by using data from optical/acoustic televiewer logs of 10 geotechnical borings conducted by the NHDOT (Golder 2005). Porosity of the rock mass was estimated by summing the fracture apertures and dividing the total by the length of the corehole surveyed. By that approach the porosity was estimated to be 0.25%.

Horizontal hydraulic gradients based on the inferred groundwater surface depicted on conceptual hydrogeologic cross sections A-A' and B-B' were estimated along with gradients between rock blast areas and potential downgradient receptors (i.e. residential or commercial water supplies). Calculated horizontal hydraulic gradients ranged from approximately 0.05 ft/ft to just under 0.09 ft/ft.

Using the highest hydraulic conductivity estimate, highest horizontal gradient, and lowest porosity value, the highest linear flow velocity was estimated at 25 ft/day. The conservative approach of not including dispersion or attenuation of blasting related compounds was taken since the goal of calculating the linear flow was to determine how soon after blasting monitoring should occur.
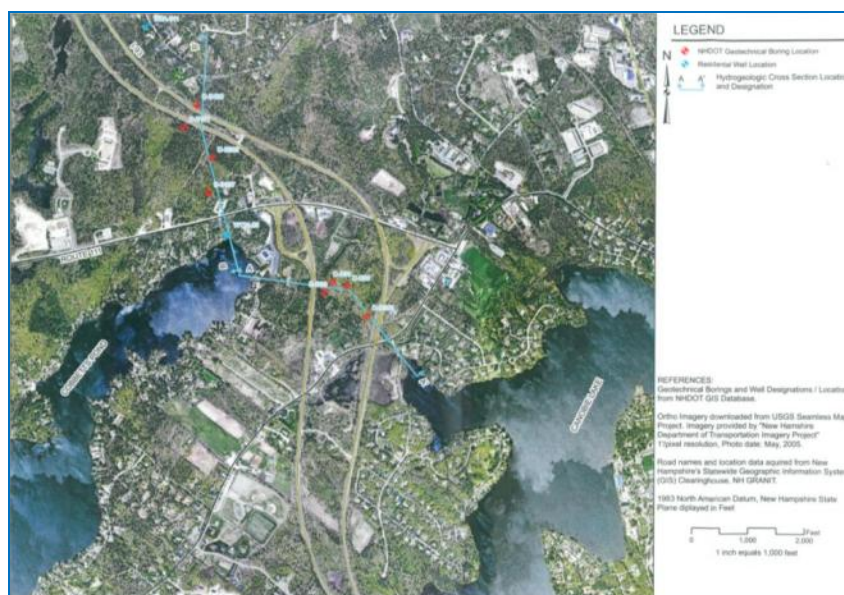
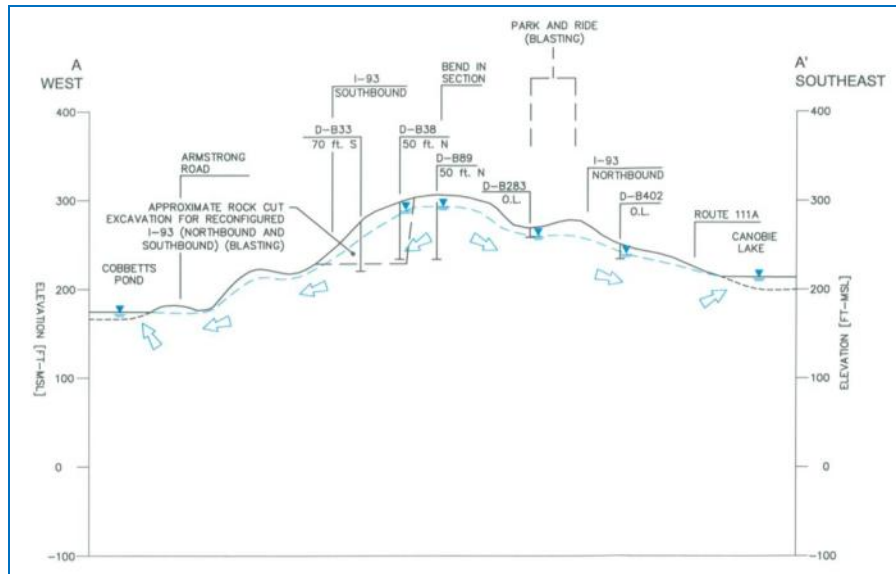

Figure 5 - Cross section location map.
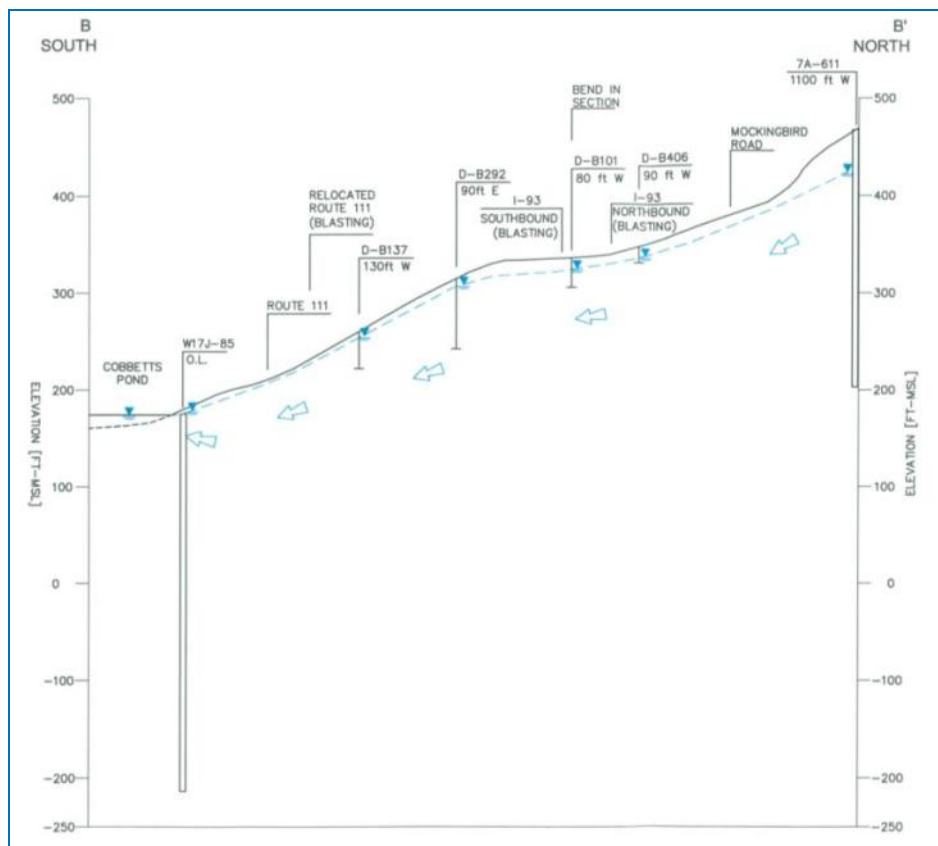
205

Figure 6 - Cross section A-A'.

Figure 7 - Cross section B-B'.

BASELINE MONITORING PROGRAM

A baseline water quality monitoring program was designed and implemented to establish a baseline (pre-blasting) groundwater and surface water quality database. Prior to sample collection, we conducted a study area reconnaissance to determine surface water, public and private water supplies in the project area. Groundwater sampling data available at the Town of Windham (2008) were reviewed for wells that were targeted for sampling during the project. Data showed evidence that elevated levels of arsenic were prevalent in Windham as is typical in southern New Hampshire.

We utilized the site conceptual hydrogeologic model to target locations downgradient that could be impacted by blasting effects, and upgradient background locations to establish baseline or preconstruction water quality conditions. We requested consent from the well owners to conduct the water sampling. Request letters were sent to 139 potential sampling targets and we received 53 consent forms. Of the 53 consenting well owners 41 were selected to be sampled, with preference given to those wells closest to the project blasting areas. Between May 14 and June 6, 2008 we collected the groundwater samples from the groundwater wells, two surface water samples from Cobbetts Pond, and one surface water sample from Canobie Lake. Samples were collected from outside spigots at houses, and treatment systems were noted if present.

Prior to the sampling, we recorded field measurements of pH, dissolved oxygen (DO), specific conductance (SC), reduction/oxidation potential (ORP or Eh), temperature, and turbidity. The samples were divided into two suites of parameters: a baseline list (44 samples), and an extended list (15 of the 44 samples). The baseline list of parameters contains the following:

- pH
- Total Alkalinity
- Iron
- Manganese
- Arsenic
- Chloride

- Calcium
- Sulfate
- Radon
- Magnesium
- Total Hardness
- Total Dissolved Solids

- Nitrate
- Nitrite
- Ammonia
- Turbidity

These baseline parameters are commonly associated with blasting impacts, either directly due to byproducts or the explosives (e.g., nitrates), or indirectly due to the blasting vibrations (e.g., iron).

The extended list of parameters included the above, with the addition of:

- Polyaromatic Hydrocarbons (PAH EPA 8270)
- Diesel Range Organics (DRO, TPH EPA 8015B)
- Methyl-tertiary-Butyl Ether (MtBE)
- Perchlorate

These extended parameters may be present as byproducts from explosive materials (e.g., DRO) or may be liberated by blasting vibrations from other environmental action sites such as closed gasoline stations (e.g., MtBE). As the four additional parameters on the extended list are not often associated with blasting, we limited the analysis of these to only 15 of the 44 sampling points. We selected both upgradient and downgradient locations for the extended list.

We compared the groundwater and surface water laboratory analytical results with United States Environmental Protection Agency (USEPA, 2003) maximum contaminant levels (MCLs) and secondary maximum contaminant levels (SMCLs), and with newly-proposed NHDES ambient groundwater quality standards (AGQS, NHDES, 2008). MCLs have been established for select radiological, microbiological, organic, and inorganic contaminants in public drinking water supplies. SMCLs apply to contaminants in drinking water that primarily affect the aesthetic qualities relating to the public acceptance of drinking water; although at considerably higher concentrations of these constituents, health implications may also exist. AGQS apply to all regulated contaminants that result from human operations or activities as set forth in Table 600-1 of New Hampshire Code of Administrative Rules Part Env-Or 603.03

Results of the laboratory analyses indicated that concentrations of arsenic, iron, manganese, nitrite, pH, radon, total dissolved solids, and/or turbidity exist above either USEPA or NHDES standards or both, and were reported in all but four water supply wells and two surface water samples. The fifteen samples that were analyzed for the extended parameter list detected MtBE in two wells below the AGQS along with PAH, DRO, and perchlorate below respective detection limits.

Figure 7 - Typical bedrock monitoring well.

PROPOSED CONSTRUCTION PHASE MONITORING PROGRAM

We recommended the installation of a groundwater monitoring well network downgradient of the blasting areas to monitor groundwater level and groundwater quality before, during and after blasting activities. Our estimates of bedrock linear groundwater flow velocities were as high as 25 ft/day. Assuming no degradation or transformation effects (e.g., dispersion, advection, sorption, etc.), compounds released into groundwater due to blasting could be transported by groundwater downgradient of blasting areas at this velocity. Our recommended monitoring well network was designed to detect potential blast-related impacts between the blast areas and potential impacts before they affect downgradient receptors (i.e., residential and public water supply wells).

It was also recommended that the monitoring wells be constructed in a similar manner as most of the residential and public supply wells to mimic residential and public groundwater use in the Windham area. These wells usually consists of a 6-inch diameter black iron steel casing driven through the overburden and seated into bedrock (Figure 7). This casing seals off the loose overburden, preventing the borehole from collapsing, and sealing off near-surface groundwater, which can have unpleasant aesthetic or environmental qualities. Once the overburden is sealed, a rotary drill bit (hammer drill or roller cone) is used to drill an open borehole into the bedrock. Open fractures within the bedrock provide groundwater to the well. Often these wells are drilled as deep as 500 or more ft below ground surface (bgs), in an effort to increase well yield. With increasing depth, fractures are usually closed, and the well bore largely acts as a storage reservoir. Fractures below 100 to 200 ft bgs are usually non-productive due to the overlying weight of bedrock. Due to the lack of fractures with depth, we recommended the monitoring wells be drilled to 75 ft within bedrock, the zone most likely to be impacted by blasting activities. The surface steel casing should be either left as a stick-up or cut as a flush-mount, and a lockable lid should be used to prevent tampering. The groundwater level measuring point, ground surface and well should be located by precise survey methods.

It was recommended that the monitoring wells be installed in a phased program, with wells installed as needed as the Exit 3 project progresses. The four phases of the project, or contracts that will include blasting are, in order: K, G, I and L. The monitoring wells should include the contract letter in the designation. The drilling and installation of the monitoring wells should be observed by the contractor's hydrogeologic consultant (a New Hampshire Professional Geologist), who should also prepare geologic and well logs of the monitoring wells.

Since residential and public supply wells contain pumps which remove groundwater from the wells drawing the water levels down as the pumps cycle, accurate static groundwater levels will be difficult to obtain from these wells. The new monitoring wells will not have high flow pumps, and can be used to obtain static groundwater levels. Once installed, the static groundwater levels should be obtained two

weeks prior to blasting, weekly during blasting, and once per month for the first three months following the end of blasting. Changes in groundwater level trends may indicate permanent lowering of the static groundwater level as new rock cuts drain cause dewatering of the aquifer. This may affect downgradient or upgradient wells.

A round of the extended parameter list previously described should be analyzed from samples obtained from the monitoring wells at least two weeks after installation and development but at least two weeks prior to blasting. One week after the start of blasting, groundwater samples should be collected from each well and analyzed for parameters on the baseline list. Groundwater samples should be obtained every two weeks following the start of blasting until blasting is complete. If blasted rock (i.e., the muckpile) is left in-place, sampling of the groundwater wells should occur monthly after blasting is finished, with analysis of parameters on the baseline list. One month after the muckpile is processed and removed, a final round of sampling should be conducted, and the samples should be analyzed for parameters on the extended list.

If blasting impacts are detected at the monitoring wells, downgradient residential/public supply wells should be sampled for the extended parameter list within two weeks initially, and pending the results, for the reduced parameter list once every two weeks or as determined by the NHDOT. The exception for this will be if impacts are found at monitoring wells located 250 ft or less upgradient of potential receptors. For this condition, the receptor wells should be sampled within one week following detection of impacts at the monitoring wells, and a one week turn-around time of analysis results should be requested.

One month after completion of all blasting and removal of all muckpiles, a final round of sampling for the extended parameter list should be conducted on the downgradient monitoring wells. This round will be the final closing round on the project.

For all sampling, baseline or extended, field parameters should be obtained. These are at a minimum: dissolved oxygen (DO), temperature, pH, specific conductance, turbidity and reduction-oxidation potential (redox). The sampling team should use field-calibrated meters to obtain these readings. Samples should be obtained from the monitoring wells using low-flow purge methods (USEPA, 1996).

As groundwater discharging to the surface water bodies (i.e., Canobie Lake and Cobbetts Pond) will rapidly diffuse, sampling of pond and lake surface water will likely not determine if impacts from blasting have occurred. However, background samples should be obtained from these water bodies at least once a year and be analyzed for the baseline list of parameters to identify if any long-term trends in surface water quality occur.

BLASTING BEST MANAGEMENT PROCEDURES (BMPs)

The potential for introducing nitrogen-based compounds from explosives into the natural groundwater and surface water systems depends on the following (Forsyth et al., 1995):

- specific types of explosives used

- hydrogeologic conditions

- handling and management of the explosives

- efficiency of the blasting operations

The amount of available nitrogen, the potential rate of release, and the ease of release into the groundwater are functions of the specific explosive chosen. Commonly used explosives include ammonium nitrate/fuel oil (ANFO), which has a high nitrogen content and low water resistance (i.e., resistance to being dissolved in water), and film-wrapped emulsions, which have a lower nitrogen content and high water resistance.

Hydrogeologic conditions determine the volume and flow of water that contacts explosives or explosive residues in the ground which in turn will also influence the post-blasting concentration of nitrogen that develops in groundwater.

The handling of the explosive product has the most significant influence on the quantity of nitrogen entering the groundwater system. In the case of ANFO, losses can occur as spillage when explosives-loading equipment is filled, when blastholes are loaded, and during disposal of excess product. Previous studies (Wiber et al., 1991) report that these losses can amount to between 5% and 15% of the total ANFO used. Golder Associates (1993, unpublished) found that, for a particular mine, approximately 5% of the total ANFO used was entering the water system. Explosive losses due to spillage are not limited to the use of ANFO. Pommen (1983) reports that 6% of the total nitrogen from a slurry-based explosive used at a coal mine operation entered the surface water and groundwater. Cameron et al. (2007) report that with good housekeeping practices at the Diavik diamond mine in Northwest Territories, Canada, estimated losses from spillage of slurry-based explosives is low.

The efficiency of the blasting operation determines the amount of nitrogen available from undetonated explosives. Advanced blast monitoring routinely shows that 10% to 20% of blastholes misfire in a given blast. Blastholes can fail to detonate (misfire) due to proximity effects such as dislodgment or desensitization. However, poor blast design and execution are the most common causes of misfires, resulting in a single blasthole, portion of the blast, or the entire blast failing to detonate. The ultimate result of a misfire is undetonated explosive mixed into the muckpile which is then available to leach into surface water and groundwater.

A substantial reduction in the concentration of nitrate in surface water and groundwater can be achieved through proper management of the explosive material and education of operating personnel. All personnel handling explosives should be made aware of the potential magnitude and severity of nitrate problems and should be trained in

explosives handling and loading procedures designed to reduce nitrate exposures (Figure 8). Case studies have shown significant reductions in total dissolved nitrate levels after implementing employee education programs. Wiber et al. (1991) shows a greater than 30% decrease in total ammonia as nitrogen in mine discharge water at two large gold mines after implementation of an education program.

BMPs to reduce the effects of nitrates in groundwater and surface water systems related to blasting include: third-party observation of the entire blasting procedures; preparing, reviewing and following an approved blasting plan; proper drilling, explosive handing and loading procedures; evaluating blasting performance; proper handling and storage of blasted rock; and treating of surface water runoff from blasting areas. The following paragraphs provide descriptions of these BMPs.

Figure 8 - Use of tarp beneath pump of bulk emulsion truck to contain spills.

Blasting should be observed by a third-party blasting consultant to review submittals, observe test/production blasting, and evaluate/modify blasting methods. It is preferable to retain a consultant with a hydrogeologic background. They should observe all aspects of the blasting program including the blasting pattern layout, drilling, loading, matting, detonation, and muckpile excavation. The observer should also verify that the blasting plan is adhered to and consult with the blaster. The consultant should have the authority to advise a halt to blasting activities if adverse environmental impacts are anticipated.

Adherence to the blasting plan can reduce environmental effects simply by enabling a blast to perform as designed. BMPs to include in a blasting plan are: descriptions of explosives and detonation systems to be used in dry and in wet conditions; groundwater removal procedures; misfire prevention/mitigation; procedures for handling, loading, and detonation of explosives; spill prevention and a spill mitigation plan; and an explosives workers education plan.

An accurate drilling pattern and an understanding of rock conditions are vital for blasts to perform as designed, including minimization of environmental effects. Blast holes should be drilled within one foot of the intended blast pattern. The orientation of the blasthole should be within five degrees of the intended orientation

Figure 9 - Typical production blast log.

and blast hole boring logs should be recorded (Figure 9). Unpackaged explosive should not be used if artesian/flowing groundwater conditions are present. Additionally explosives should be detonated as soon as possible.
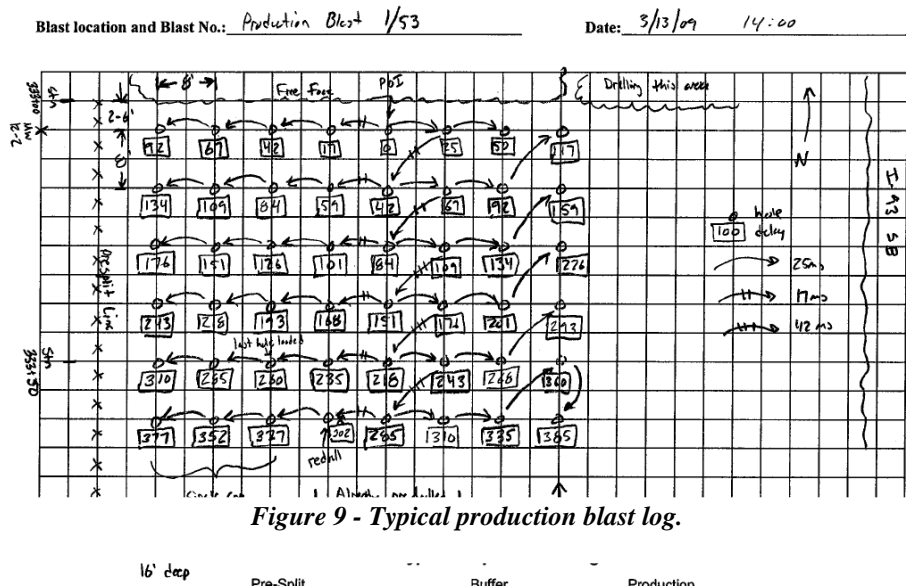
ANFO is the most commonly used explosive, and the most common source of nitrates in surface water and groundwater downgradient of rock blasting sites. BMPs that should be followed when ANFO is utilized are the following: standing water in the blasthole should be removed prior to loading; water resistant ANFO-WR should be used in wet holes; spills should be cleaned up around blasthole collars; and reduce "blow-back" if loading ANFO pneumatically (Figure 10). Loading equipment should be cleaned in the proper area and the product shouldn't be stored on site.

Figure 10 - Dewatering blastholes prior to loading explosives.

Bulk emulsions and slurry/water gel explosives have high water resistance, but also must be handled with care to minimize environmental impacts. The BMPs for bulk emulsions and slurry/water gel explosives BMPs include: cleaning up spills promptly; extruding the bulk product into itself from the bottom of the blasthole; and use packaged explosive if groundwater flow conditions are severe.

Contamination of the explosive products can occur during loading from drill cuttings. Similarly, stemming placed too forcefully can dilute the upper portion of water based emulsion explosives. The blast holes should be cleaned out thoroughly using compressed air from the drill. Drill cuttings should not be used as stemming material. The stemming should be placed with care to prevent bridging and be placed completely. The drill logs should be detailed to enable the stemming to be placed appropriately as decks in weak zones, voids and cavities.

Misfires can leave undetonated explosive products in the muckpile, which in most cases cannot be recovered and will leach into the surface water and/or groundwater. Most blasting in developed areas utilize blasting mats to contain flyrock. Shifting blasting mats or other conditions could cause cut-offs. Redundant surface delays between blastholes can reduce the potential for cut-offs to occur. The blastholes can be double or triple primed to prevent cut-offs down the hole. Electric detonating systems can be checked for continuity prior to detonation. Programmable electronic detonating systems can be used to not only reduce vibrations but to check the circuits after mats are placed.

Evaluation of blasting performance should be an integral part of the BMPs. The blast performance evaluation should include videotaping blasts, analyzing the videotapes for flyrock, rifling, fumes, and other indications of poor blast performance. Also velocity of detonation (VOD) measurements may be used to determine explosive performance. Fragmentation analysis of the muckpile may also indicate underperforming explosives.

Large rock excavation projects usually include processing blasted rock on site for reuse in construction. Residues from explosive byproducts and undetonated explosive product can coat the surfaces of the broken rock fragments in the muckpile. The residues can migrate to groundwater from infiltrating precipitation. The muckpile should be removed from the blast area as soon as possible. Water should be used to control dust during primary and secondary crushing and the processed rock should be stored over low permeability areas. The runoff from muckpiles can be directed to stormwater structures. Also, the stockpiles of processed rock can be distributed widely throughout the project.

Treatment of nitrate-containing surface water or groundwater at large mining or construction sites using explosives is largely an effort of last resort to mitigate nitrate impacts. The treatment methods are similar to those employed in municipal water systems and can be grouped into three categories: ion exchange, electrochemical ion

exchange, and biological denitrification. The most logical approach to minimize impacts to groundwater is proper management.

IMPLEMENTATION OF CONSTRUCTION PHASE MONITORING

The recommendations provided to the NHDOT by Golder in 2008 have been implemented for the first construction contract ("K") that was awarded in the fall of 2008. NHDOT developed specifications for the contract which required the contractor to retain the services of a hydrogeologic or environmental consultant to implement the groundwater monitoring plan. Additionally, specifications were developed based on blasting BMP's regarding the storage, handling, loading of explosive products.

For the K-contract nine monitoring wells have been installed at locations determined to be downgradient of the blasting operations. The monitoring wells were installed to depths ranging from 75-100 ft into bedrock. Groundwater samples have been collected throughout construction since two weeks prior to blasting in late November 2008. Analytical results are indicating an increase in nitrate concentrations at a limited number of monitoring wells over time. Currently the detections of potentially blasting related contaminants in groundwater appear to correlate with the proximity to muckpiles that remained in place. Amendments to the contractors blasting plan including an evaluation of appropriate blasting products for conditions at the site have been mandated to minimize the potential for further groundwater impacts. Continued groundwater sampling from the monitoring well network will assist in the determination of the extent of the impact to groundwater as a result from blasting.

CONCLUSIONS

A well designed and implemented blasting plan provides the best chance of reducing groundwater impacts from blasting. The adherence and monitoring of the implementation of the blasting plan is also vital. Properly selected blasting products for the site conditions are vital to minimize groundwater impacts. Packaged explosives reduce potential spills and minimize exposure of explosive products to groundwater. A solid understanding of the hydrogeologic model is also

Figure 11 - Typical production blast.

crucial to develop an effective sentinel well network that can provide warning of potential impacts from blasting (water quality and quantity).

REFERENCES:

Cameron, A., Corkery, D., MacDonald, G., Forsyth, B., and Gong, T., 2007. *An Investigation of Ammonium Nitrate Loss to Mine Discharge Water at Diavik Diamond Mines*, Proceedings: Explo Conferences, Wollongong, NSW Australia, September 3-4, 2007.

Golder Associates Inc., June 30, 2008. *Baseline Drinking Water Study, Interstate 93 Widening Project, Exit 3, Windham, New Hampshire.* Prepared for the New Hampshire Department of Transportation, Bureau of Research and Materials.

Forsyth, B., Cameron, A. and Miller, S., 1995. *Explosives and Water Quality.* Proceedings, of Sudbury 1995 Mining and the Environment (Hynes, T.P. and Blanchett, M.C., ed.), Volume II: Ground and Surface Water, Canmet, Ottawa, p. 795-803.

Golder Associates Inc., July 25, 2005. *Borehole Geophysical Logging, Exit 3 Rockcut, Interstate 93 Widening, Salem-Manchester 10418, Windham, New Hampshire*. Prepared for New Hampshire Department of Transportation, Bureau of Materials and Research.

Larson, G.J., 1984. *Surficial Geologic Map of the Windham Quadrangle, Rockingham & Hillsborough Counties, New Hampshire*. State of New Hampshire, Department of Resources and Economic Development, Office of State Geologist. Concord, NH. 1984.

Lyons, J.B., Bothner, W.A., Moench, R.H., and Thompson, J.B., 1997. *Bedrock Geologic Map of New Hampshire.* United States Geological Survey, Scale 1:250,000.

New Hampshire Department of Environmental Services (NHDES), June 16, 2008. *Ambient Groundwater Quality Standards (AGQS),* Env-Or 603.03, Table 600-1.

Pommen, L.W., 1983. *The Effect on Water Quality of Explosives Use in Surface Mining*. British Columbia MOE Technical Report 4.

Town of Windham, 2008. *Well Log Records*, Obtained in May 2008 from Mr. Al Turner, Director of Planning and Development.

United States Environmental Protection Agency (USEPA), June 2003 (updated 1/23/06). *National Primary and Secondary Drinking Water Standards*, Office of Water (4606M), EPA 816-F-03-016.

United States Environmental Protection Agency (USEPA), 1996. *Low Stress (low-flow) Purging and Sampling Procedure for the collection of Ground Water Samples From Monitoring Wells*. USEPA Region 1, July 30, 1996, Revision 2, 13 p.

United States Geological Survey (USGS), 1985. *Windham Quadrangle, New Hampshire 7.5 Minute Series (topographic), SE/4 Manchester 15' Quadrangle 42071-G3-TF-024*. Topography by photogrammetric methods from aerial photographs taken 1947 and 1952. Field checked 1953, photorevised 1985.

Vanasse Hangen Brustlin, Inc. (VHB), 2004. *Final Environmental Impact Statement, Interstate 93 Improvements, Salem to Manchester, IM-IR-93-1(174)0, 10418-C*. Prepared for New Hampshire Department of Transportation and the Federal Highway Administration. April 2004.

Walsh, G.J. and Clark, S.F., 1999. *Bedrock Geologic Map of the Windham Quadrangle, Rockingham and Hillsborough Counties, New Hampshire*. U.S. Department of the Interior, U.S. Geological Survey, Open File Report 99-8.

Wiber, M., Connel, R., Michelutti, B., Bell, B., Joyce, D.K. and Luinsta, W., 1991. *Environmental Aspects of Explosives Use*, Northwest Mining Association Short Course, Spokane, Washington.

Acknowledgements

Disclaimer

4.2

Remediation of Soft Clay Utilizing the "Dry Mix Method"

Introduction

Tonawanda Creek meanders as it flows in a generally westerly direction from its headwaters east of Batavia, New York to its discharge into the Niagara River at Tonawanda, New York. The geologic conditions along Tonawanda Creek have historically contributed to a number of bank failures that have damaged pavements and threatened homes constructed along the creek. The western portion of the creek flows through soft lacustrine clay soils that extend to a depth of about 30 to 50 feet. Subsequent glacial deposition resulted in a layer of sand and silt above the soft clay along the banks of Tonawanda Creek. The meandering creek causes erosion that eventually results in a loss of support for the creek banks. This effect, coupled with saturation of the upper silty soils due to rain events and poor drainage, is the cause for many of the slope failures along Tonawanda Creek.

Two slope failures along Tonawanda Creek have been investigated; one in Niagara County by the US Army Corps of Engineers and one in Erie County by the Erie County Department of Public Works. Site investigations included borings with in-situ strength testing, and installation of instruments including vibrating wire piezometers and inclinometers. The investigations revealed that the soft clay soils are sensitive, losing strength as they deform. Research into remedial methods revealed that soft sensitive clays have been remediated in Scandinavia for the past 25 years by mixing dry cement or lime with the soft clay to depths of 50 feet or more. This process, known as the "dry mix" method, has been used on a few projects in the United States and was selected for remediation at these two sites. This paper describes the testing and engineering analysis that led to the selection of the "dry mix" process and the use of this approach to remediate these two sites in 2008 and 2009.

Geologic Conditions along Tonawanda Creek
Tonawanda Creek flows in a generally westerly direction from its headwaters east of Batavia to its discharge into the Niagara River at Tonawanda, New York. Figure 1 is a plan showing a section of the western portion of Tonawanda Creek near Transit Road. Tonawanda Creek Road exists on both sides of Tonawanda Creek, one in Erie County and one in Niagara County.
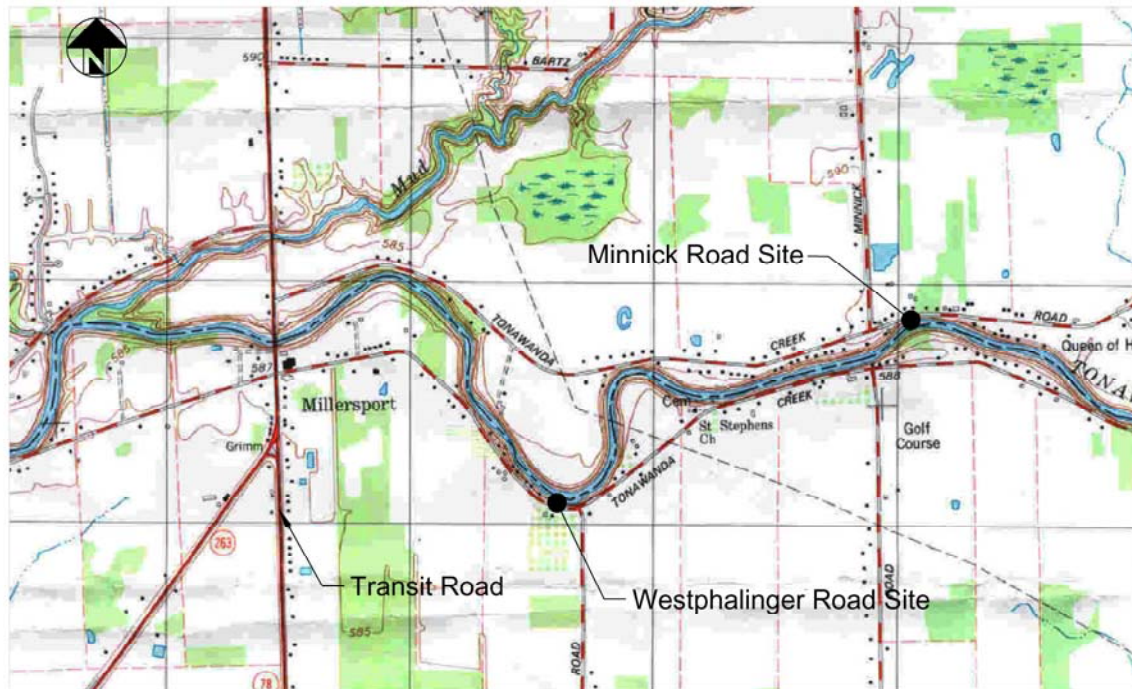
FIGURE 1 - USGS 7.5 minute quadrangle map of Clarence Center, New York, dated 1980.

Figure 1

The western portion of Tonawanda Creek flows through soft clay soils that were deposited during the last glacial period. As the glacial ice retreated, a lake (Lake Tonawanda) was impounded between the glacial ice and higher ground to the south. Soft clay was deposited on the bottom of the lake and remained after the glacial ice and lake waters receded. Subsequent deposits resulted in a layer of sand and silt above the soft clay along the banks of Tonawanda Creek.

<u>Site Conditions</u>

This paper discusses two slope failures along Tonawanda Creek; one in Niagara County investigated by the US Army Corps of Engineers and one in Erie County investigated by the Erie County Department of Public Works.

In 2004, a slope failure along the south bank of Tonawanda Creek in Erie County damaged a portion of Tonawanda Creek Road between Transit Road and Westphalinger Road in the Town of Clarence (see Figure 1). A section of Tonawanda Creek Road, approximately 250 feet long dropped about 10 feet and pushed soil into Tonawanda Creek as shown on Figure 2.

Figure 2

Beginning in 1994, a continual failing slope along the north bank of Tonawanda Creek in Niagara County damaged a portion of Tonawanda Creek Road near Minnick Road in the Town of Lockport (see Figure 1). A section of Tonawanda Creek Road approximately 100 feet long continued to drop damaging an existing culvert underneath the roadway.

Subsurface explorations indicate similar subsurface conditions at the two sites. Explorations included collecting Standard Penetration Test (SPT) split spoon samples and thin walled tube samples (Shelby tubes) of the overburden soils and core samples of the rock. Testing included in-situ vane shear tests (VST's) to estimate the shear strength of the soils and laboratory tests, including grain size distribution, unit weight, strength testing, moisture content tests and Atterberg Limits.

Figures 3 and 4 are logs of two borings that illustrate the typical subsurface conditions and the test results at the sites. The figures summarize the SPT-N-value with depth, moisture content profile, VST results (peak and residual), Atterberg limit data and a generalized soil description.

In general, a few feet of fill is present at each site. Beneath the fill, a silty sand deposit extends to a depth of about 10 feet. Boring logs from the two sites describe this soil as either sand, silty sand or silt depending on location. Because of the relatively high silt and fine sand percentage, the silty sand drains slowly, contributing to the unstable slope conditions along the creek.

Beneath the silty sand is a deposit of soft to very soft clay that extends to about 35 feet deep. The soft clay covers a glacial till deposit, a mixture of gravel, sand, silt and clay with boulders and cobbles. The glacial till deposit is relatively loose for about the upper 5 feet, and then becomes dense or hard, based on the SPT N-values that generally range from about 40 to more than 100. The top of bedrock was observed at a depth of about 68 feet at the Westphalinger site and at a depth of 59 feet at the Minnick Road site. Bedrock is of the Camillus Formation and is a medium hard to hard dolomitic shale with gypsum deposits.

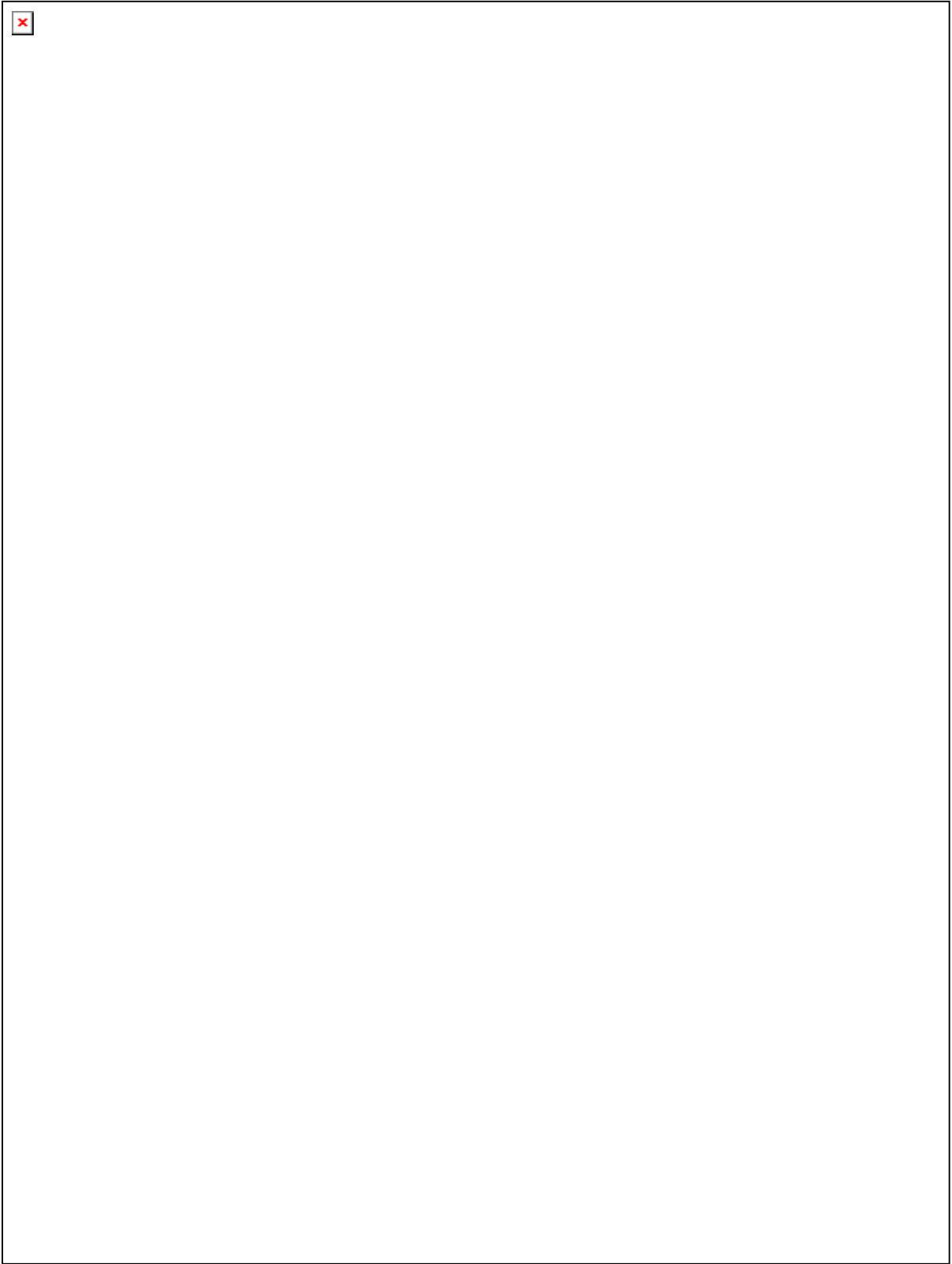**Figure 3 – Typical Westphalinger Road Boring**

Figure 4 – Typical Minnick Road Boring

The thickness and consistency of the soft clay layer are important factors in the stability of slopes along Tonawanda Creek. The SPT N-values range from WR (weight of rods) to WH (weight of hammer), signifying that the weight of the drilling rods or the weight of rods and hammer in the borehole was sufficient to advance the split spoon sampler the specified 24-inch distance. VST measurements of the peak shear strength of the soft clay ranges from 228 to 608 pounds per square foot (psf) with a remolded strength between 35 and 186 psf. The ratio of the peak to the remolded strength varies from about 2.5 to 10 indicating that the soft silty clay is slightly to moderately sensitive. The moisture content of samples of the soft silty clay layer are close to or greater than the liquid limit, a characteristic that is common to sensitive soils. The groundwater level in the soft clay soil coincides with the top of the soft clay deposit. Perched groundwater is present in the sand and silts above the soft clay.

The Problem

Tonawanda Creek's meandering flow pattern results in erosion of the stream bank on the outer bend in the creek and deposition on inside bends of the creek. Erosion of the outer creek banks over time results in a loss of support for the banks. During wet times of the year, the upper silty soils become saturated due to rain events and poor drainage. Failures occur where the soft clay soils are too weak to support the increased weight of the saturated soil, especially where there has been a loss of toe support. This is the reason that most of the failures occur during the spring or early summer along bends in the creek. The result is a failure through the soft clay with the soft soil pushing up and out into the creek as shown on Figure 5 (stream bank located in upper right hand corner).

Figure 5

Consideration of Remedial Options

Stabilizing this condition requires creating a stable base upon which to reconstruct the road embankment. In general, the stability of slopes can be improved in four ways:

- modifying the slope geometry,
- providing or improving surface and or subsurface drainage,
- providing internal slope strengthening/reinforcement and,
- constructing a retaining structure.

Modification of Slope Geometry

Modification of slope geometry to improve stability may include flattening the slope, adding weight to the toe of slope or removal of weight from the top. Removing weight from the top of the slope would require lowering the road and was not a feasible option at either site. Removing weight from the top of slope and replacing it with light weight fill would improve the slope stability but does not provide a sufficient margin of safety against future failures. Similarly, adding weight to the toe would require constructing a berm that extends into the creek, also not a feasible option. Because the clay has such low strength, stability calculations indicate that flattening the slope to 10 horizontal to 1 vertical is necessary for a factor of safety of about 1.5. Due to the limited area between the roadway and stream channel, and the vicinity of nearby residents, this option is not realistic at either site.

Surface and Subsurface Drainage

Improving the stability of both sites by improving the surface drainage and providing subsurface drainage for the upper sandy silt deposit is an important part of the remedial plan for each site. High groundwater levels in the upper sandy soil is a contributing factor to the slope failures therefore, improving the surface drainage to limit infiltration into the sandy soil and providing subsurface drainage to keep it drained are important components of the remedial design. Stability calculations indicate that providing better drainage improves the slope stability but does not provide a sufficient margin of safety against future failures. Therefore, the drainage improvements must be done in conjunction with other measures to improve the slope stability.

Internal Slope Strengthening

Internal slope strengthening involves improving the shear strength and reducing the compressibility of the soil within the failure zone. Examples of this include installing stone columns through the failure zone, injecting dry cement or grout (i.e. dry or wet soil mixing) into the failure zone or using reaction blocks and anchors to compress the soil and increase its strength and resistance.

Stone columns were evaluated but the number of columns required would be prohibitive at this site. We also rejected reaction blocks and anchors because the soil is too weak to provide sufficient reaction and extending the anchors to rock would require 100-foot long anchors.

Wet and dry soil mixing was considered. The wet mixing involves mixing cement grout with the in-situ soil. The resulting column strengths are on the order of several hundred pounds per square inch (psi), however there is a significant amount of waste associated with this process. Dry mixing yields a column that is not as strong as wet mixing, (typically on the order of 50 to 60 psi) but there is virtually no waste. Considering that the columns must be spaced closely enough to provide uniform support for the road embankment, the higher strength columns afforded by the wet process are not necessary. Because the dry columns provide sufficient strength with no waste, we selected this method for further evaluation as described in the following section.

Retaining Structures

Retaining walls can be used to provide lateral resistance against slope movement. At both sites the wall would have to be approximately 35 feet deep to provide the necessary resistance. Driven sheet piles or

drilled in soldier piles and lagging are the two types of walls considered feasible. This would involve driving sheet piles or drilling soldier piles through the soft silty clay and into the glacial till. Due to the low strength of the very soft silty clay, the top of the wall would have to be restrained with anchors that extend diagonally to rock, making them approximately 100 feet long.

Pile driving induces vibrations that can weaken the sensitive silty clay soils leading to instability and movement of the wall during installation. Figure 6 shows a wall under construction on Tonawanda Creek where the top of the sheetpiles moved and the slope behind the wall dropped during installation. Because of concerns about stability during construction and the length and expense associated with the anchors, the wall was not considered a viable alternative.

Figure 6

Slope Stabilization Approach

The approach selected for remediation involves providing additional subsurface and surface drainage and strengthening the soft soils with soil cement columns. Drainage improvements are incorporated into the design to limit the build-up of groundwater in the silty sand soils that overlie the soft clay. The soil cement columns extend through the soft clay to the hard glacial till providing support for the road embankment.

The soil cement columns are constructed using the "dry mixing" method. This method was developed in and is used throughout Northern Europe and Japan to improve the engineering properties of soft clays, peats and other weak soils. The process uses cementitious powders to bond soil particles, thereby increasing the shear strength and reducing the compressibility of the soil. Dry mixing is often used in high groundwater conditions and has the advantage of producing no spoil for disposal. Using specialized mixing equipment; the soil is mixed during penetration, until the mixing tool reaches the maximum treatment depth. Dry binder agents are injected into and mixed with the soil during withdrawal of the mixing tool, leaving behind a dry soil mix column. The general process is shown on Figure 7.
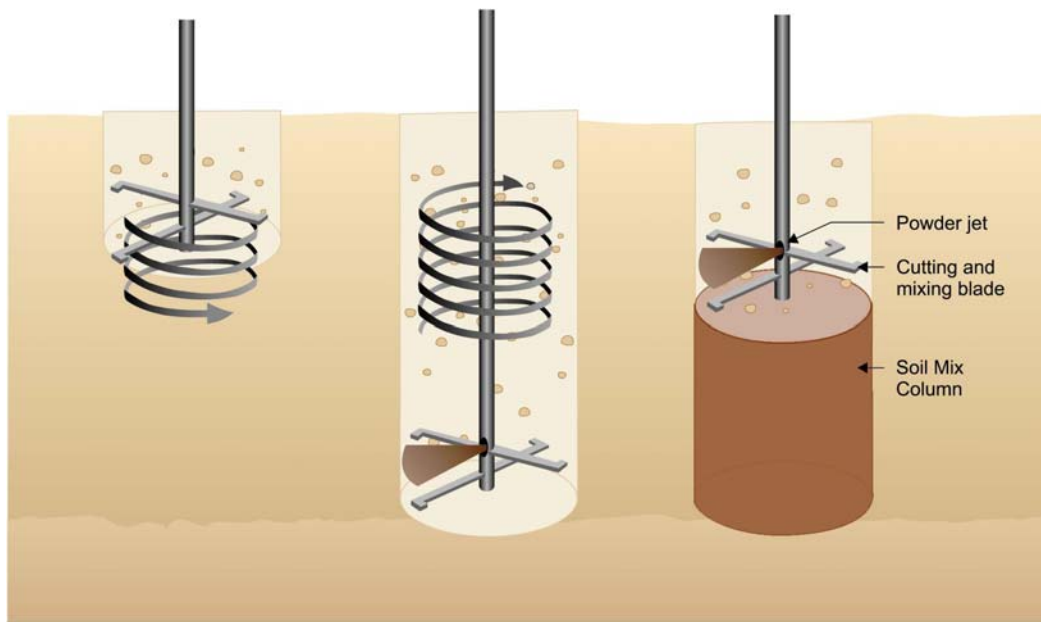
Figure 7

The strength of the soil cement column is dependent on the type of soil and the amount and type of binder used. Typical binder agents include cement, lime, gypsum, slag or a combination. The strength and stiffness of the soil cement column generally increases with increasing binder dosage. The binder dosage rate typically ranges between 80 pounds per cubic yard (lb/yd^3) (50 kilograms per cubic meter (kg/m^3)) in soft clays to as high as 450 lb/yd^3 (270 kg/m^3) in peat. Shear strengths in different types of soils and binder dosage rates are shown on Figure 8.
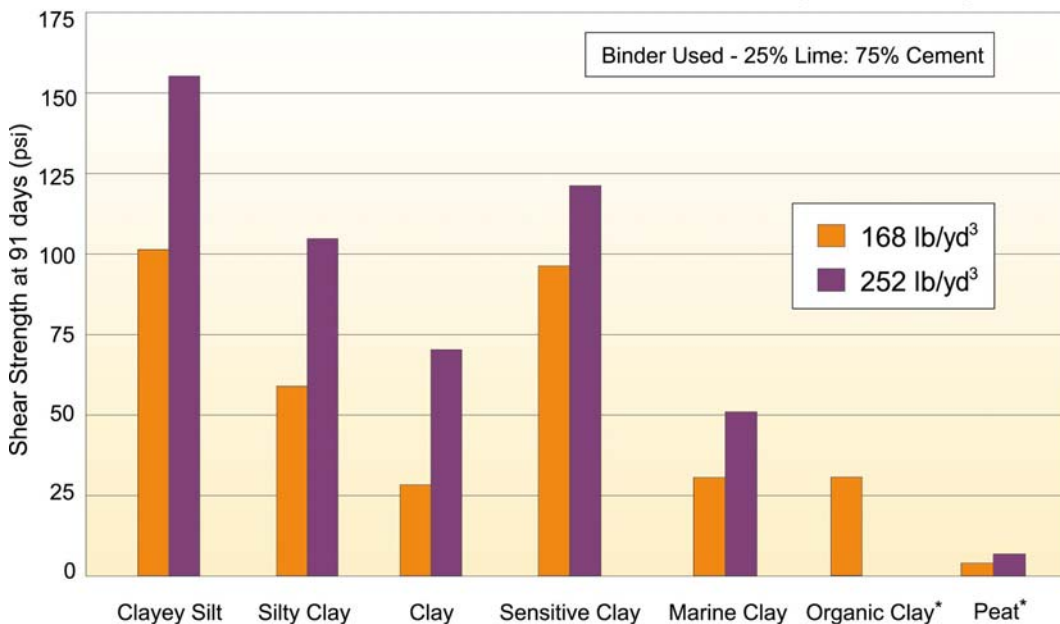

Figure 8

Soil mix column diameters of 2 to 3 feet can be constructed to depths of 60 feet. Soil mix column strengths typically are 10 to 50 times stronger and much stiffer than the native soils. Figure 9 shows the interaction between the native soils and dry mix columns (shown as springs). The columns transfer most of the embankment load to the stiffer underlying layer.
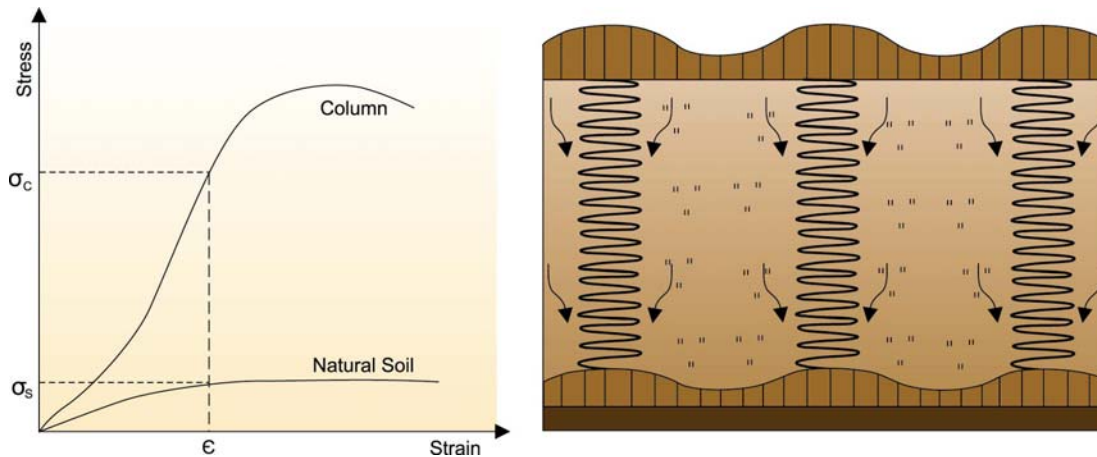
Figure 9

Cost comparisons indicate that the dry mix method is less expensive than either stone columns or wet soil mixing and is comparable to the cost of a tie-back sheet pile wall.

Laboratory Testing and Test Pad

Laboratory tests and a test pad were completed to evaluate the column strength that could be achieved using soil from the Minnick Road and Westphalinger sites. We collected Shelby tube samples of the soft clay and shipped them to Geotesting Services, Inc. (Geotesting) for testing. Geotesting added dry cement and a combination of dry cement and lime at various addition rates to the soft clay, allowed the mixture to cure and then measured the compressive strength of the mixture at 7, 14, 28 and 57 days. The following table is a summary of the mix proportions and strength results obtained during the laboratory investigations completed for the Westphalinger Road site. The laboratory results indicate that a cement addition rate of 75 kg/m^3 (125 lb/cy) would provide a soil-cement column shear strength between 6,000 and 8,000 psf.

| SAMPLE NO. | SOIL ADDITIVES | | | POUR DATE | CURING PERIOD | WATER CONTENT | TOTAL UNIT WGT. | DRY UNIT WGT. | PEAK COMPRESSIVE STRESS |
	Additive Rate (kg/m3)	Cement (%additive)	QuickLime (%additive)		(days)	(%)	(pcf)	(pcf)	(psi)
Mix 1	75	75	25	10/05/04	7	43.5	110.0	76.7	42.1
Mix 1	75	75	25	10/05/04	14	43.5	109.0	76.0	55.2
Mix 1	75	75	25	10/05/04	28	42.6	108.8	76.3	62.7
Mix 1	75	75	25	10/05/04	57	43.9	108.1	75.2	84.1
Mix 2	75	100	0	10/05/04	7	43.9	109.4	76.1	52.8
Mix 2	75	100	0	10/05/04	14	43.6	109.4	76.2	63.6
Mix 2	75	100	0	10/05/04	28	43.1	109.8	76.7	83.9
Mix 2	75	100	0	10/05/04	57	43.0	109.2	76.4	121.5
Mix 3	50	75	25	10/06/04	7	44.8	109.6	75.7	36.4
Mix 3	50	75	25	10/06/04	14	44.1	109.3	75.9	49.2
Mix 3	50	75	25	10/06/04	28	44.1	110.0	76.4	60.0
Mix 3	50	75	25	10/06/04	57	43.9	110.1	76.5	74.5
Mix 4	50	100	0	10/06/04	7	43.4	110.4	77.0	47.5
Mix 4	50	100	0	10/06/04	14	43.8	111.2	77.4	54.5
Mix 4	50	100	0	10/06/04	28	43.4	109.8	76.6	66.1
Mix 4	50	100	0	10/06/04	57	43.7	109.3	76.1	83.1

To verify the suitability of the dry mix method, Hayward Baker Inc. (Hayward Baker) was retained to mobilize its dry mix equipment and install 12 test columns at the Westphalinger Road site. We monitored the column installation and the cement addition rate, drilled borings into the completed columns and collected Shelby tube samples for strength testing. The test results indicate shear strengths between about 2,000 and 4,000 psf (28-day), which are lower than indicated by the tests on the laboratory mixes. The lower values could be due to the difficulty in collecting undisturbed samples of the completed columns or actual differences between the strength achieved in the field compared with that in the laboratory.

To provide another means of measuring the strength of the completed columns, Hayward Baker installed vanes in several columns. A metal vane is attached to a steel cable that is inserted during the initial penetration of the mixing apparatus. The steel cable extends from the vane at the bottom of the column to the ground surface. Several days after installation, the vane is pulled up through the center of the soil-cement column. The column shear strength is estimated based on the force required to pull the vane, the vane area and a bearing capacity factor. A schematic of the vane test is shown in Figure 10. The vane results indicated column shear strength values in excess of 8,000 psf.
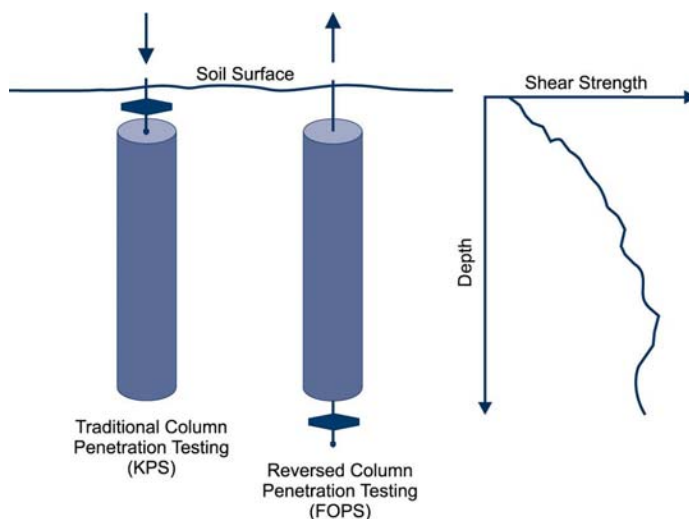

Figure 10
<u>**Design Plan**</u>

The spacing of the soil-cement columns and the appropriate mixture of cement and soil are dependent on the site soil conditions. The lab results did not show a benefit of using quicklime, therefore the design considers adding only cement. Based on the laboratory and test pad results, we selected a cement addition rate of 75 kg/m^3 (125 lb/cy), which is equivalent to mixing 8 to 10 bags of dry cement (Type I cement) with the soft clay in a hole that is 30 inches in diameter and 30 feet deep.

We based the column layout on a weighted strength using a conservative estimate of shear strength for the treated area of 2,000 to 3,000 psf and the in-situ vane shear strengths for the untreated area. We completed slope stability analysis using the estimated weighted average strength and varied the column layout to achieve a calculated factor of safety of 1.5.

The following table is a summary of the design layout for each site and Figure 11 is a plan and section of the column layout for each site. As indicated, the percentage of area treated at the Westphalinger site is significantly greater than at the Minnick site. This is because the remolded strength was factored into the design at the Westphalinger Road site since the slope had experienced substantial movement. The Minnick site did not experience movement of the magnitude that occurred at the Westphalinger site, therefore, we based the design on the peak shear strength. This resulted in a lower treatment percentage at the Minnick site.

Parameter	Minnick Road Site	Westphalinger Road Site
Diameter of Soil-Cement Column (inches)	30	30
Number of Columns	651	2,227
Roadway Length (ft)	200	570
Area Treated with soil-cement columns (%)	38	58
Blade Rotation Number[1]	400	400

Table Note: 1. The blade rotation number is the total number of mixing blades passing during 3.28 feet (1 meter) of mixing tool extraction.
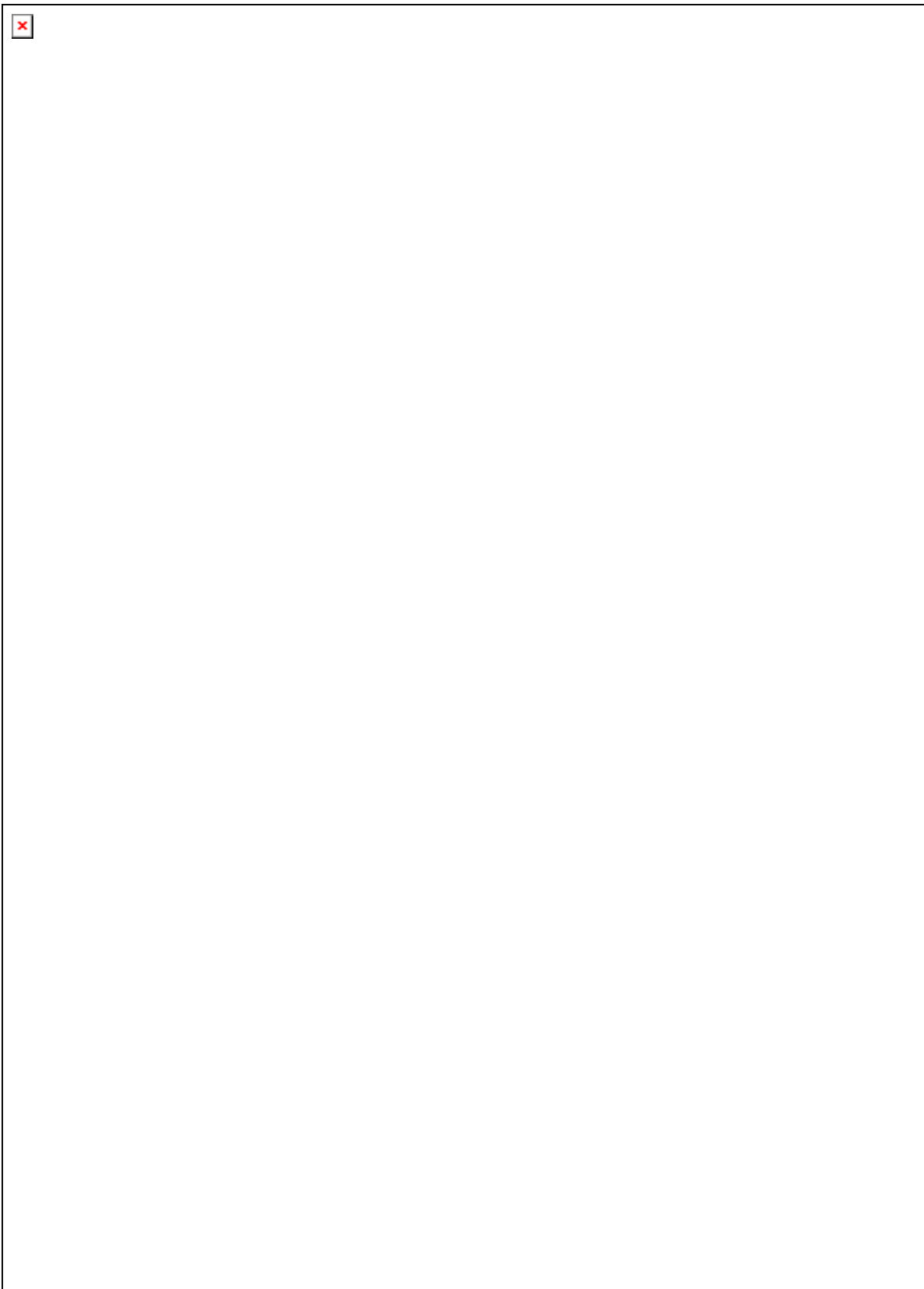
Figure 11

As shown on Figure 11, the columns extend from the top of the soft clay layer to the top of the glacial till. The majority of the columns are directly beneath the roadway to transfer the embankment load to the glacial till layer. The soil-cement columns are effective when under compressive loading but not effective when placed in shear or bending configurations. Therefore, the layout has the columns in a continuous wall pattern, perpendicular to the direction of the road. This puts the columns primarily in compression and limits bending and shear stresses on the columns. Additionally, a strength reduction factor is applied to columns outside the embankment (between the roadway and creek).

The Westphalinger design also includes a mechanically stabilized earth wall through the failure area. The wall limits the aerial extent of the road embankment, reducing the required treatment area. Under drains and improved surface drainage are included in both designs to limit groundwater build-up in the silty sand.

Construction

Hayward Baker, as a subcontractor to Nichols Long and Moore Construction Corp., completed column installation at the Minnick Road site in the summer and fall of 2008. Hayward Baker completed column installation as a subcontractor to Accadia Site Contracting, Inc. at the Westphalinger Road site in the winter and spring of 2009, when construction activities are normally prohibited by weather.

At each site, a precut was made to offset the weight of the proposed dry mixing equipment. Figure 12 shows a picture of the dry mixing apparatus consisting of a mixing rig, concrete storage shuttle and a compressor. Figure 13 shows a picture of the dry mixing rig and mixing apparatus.

The dry soil mixing process induces air pressure into the soil that creates an increase in pore pressure and corresponding loss in soil strength. If not controlled, this can lead to slope failure during construction. Dissipation of the induced pore pressures takes several days, therefore the work must be sequenced to allow the pressure to dissipate before continuing work in an area. Inclinometers and vibrating wire piezometers were installed at the Westphalinger site to monitor the pore pressure build-up and provide information necessary to develop an appropriate work sequence. Additionally, the slope at each site was monitored for movement using a series of survey hubs between the treated area and Tonawanda Creek. At the Minnick Road site more than 2 feet of lateral movement occurred on the slope between the work area and the creek during the column installation. Movement was not observed on the work platform or on the backside of the road. Therefore, no impact was suspected on the design/performance of the dry mix columns.

Figure 12 – Minnick Road Site

Figure 13 – Westphalinger Road Site

Soil-Cement Column Results

Three sampling methods were employed to estimate the strength of the soil-cement columns. Earth Dimensions, Inc. drilled borings in completed columns and collected Shelby tube samples for unconsolidated undrained (UU) triaxial testing. Difficulties in maintaining the hole within the column for its entire depth and in retrieving the Shelby tubes of the hard brittle soil-cement resulted in a wide variation in the strength results, with peak shear strengths ranging from 500 psf to 5,000 psf.

Hayward Baker installed vanes in several columns and pulled them out of the columns after approximately 7 to 10 days of curing. A typical vane testing report is shown as Figure 14. The vane results indicated a column shear strength in excess of 10,000 psf.

The third method consisted of continuous SPT's and visual logging of samples in completed columns. Figure 15 shows photos taken of samples of the soft clay collected before treatment and from a completed column showing the dramatic difference in the soil consistency. The SPT N-values also show a dramatic difference, as indicated on Figure 16. As indicated on the figure, the N-values before improvement are less than 5 and in many cases "weight of hammer" or "weight of rods" as described previously. In the completed columns, the N-values vary from Figure 14 about 25 to more than 100.

Photo from Pre-Improvement Sampling
Photo from Post-Improvement Sampling

Figure 15

Minnick Road
Vane Testing Report
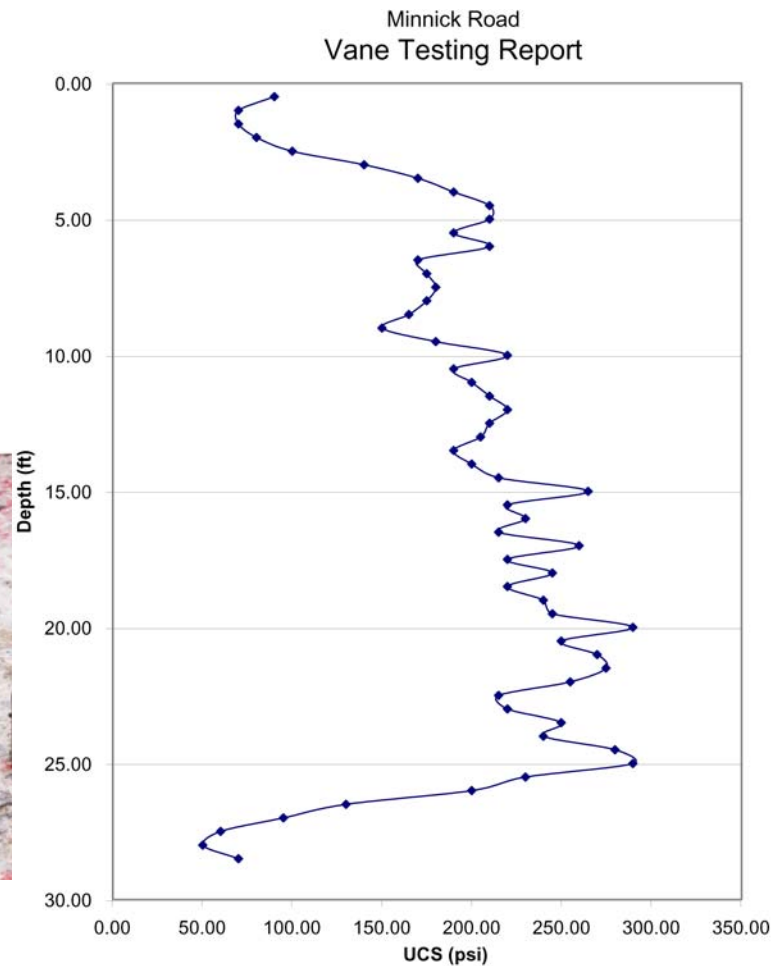
Column No. C-58 (Installed 3/9/09)
Boring C-58-09 (Drilled 4/8/09)
30 Days Old

Figure 16

Figures 17 and 18 show photos taken following completion of construction at each of the sites.
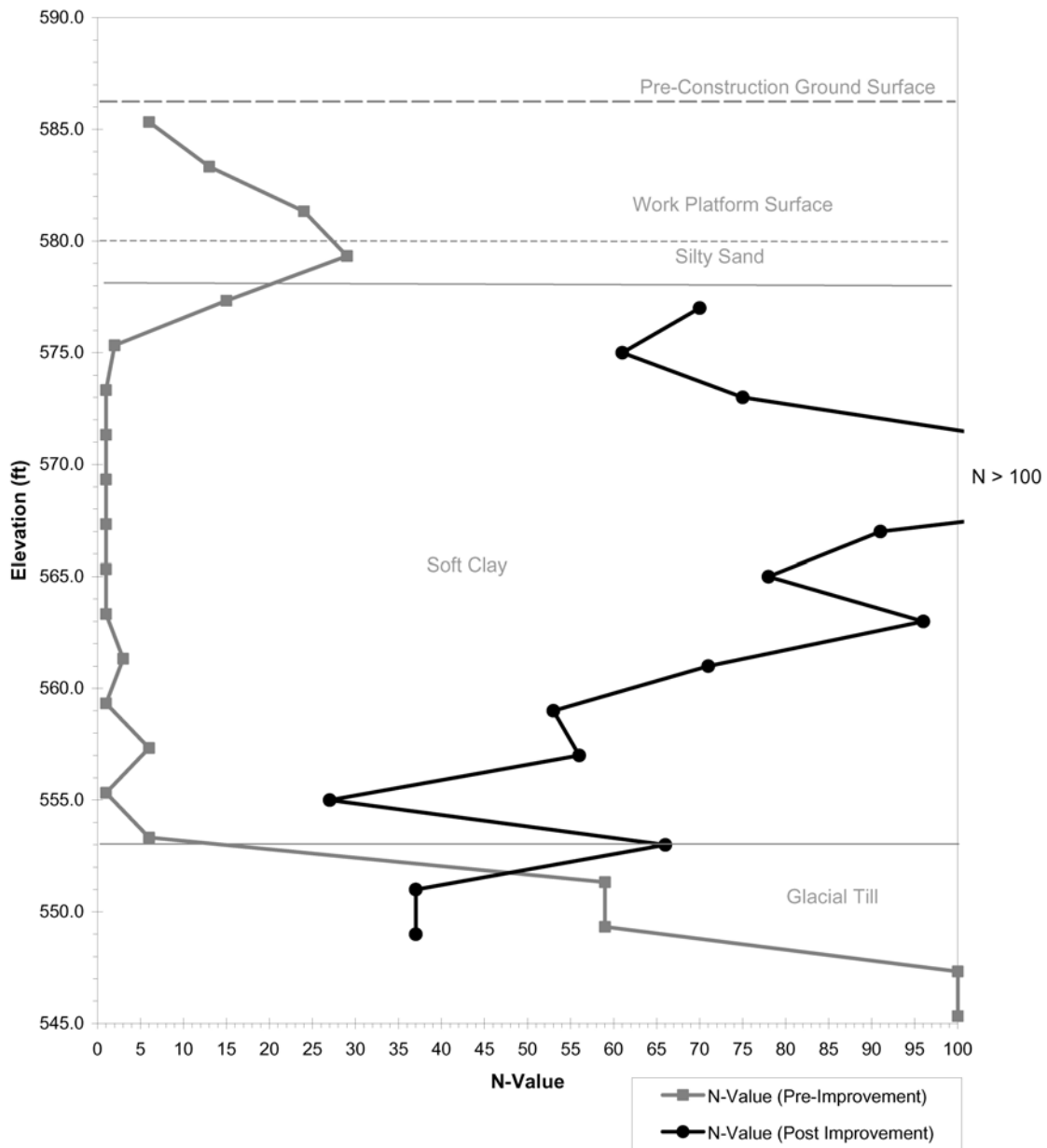
Figure 17 - Westphalinger Road Site

Figure 18 - Minnick Road Site

Summary

Numerous slope failures occur along Tonawanda Creek. Saturation of the upper silty soil combined with loss of support for the stream bank caused by erosion create a condition where the thick deposit of soft clay cannot support the slope resulting in numerous stream bank failures.

Two projects, one in Niagara County by the US Army Corps of Engineers and one in Erie County by the Erie County Department of Public Works utilized a technique common in Scandinavia called "dry mixing" to remediate slope failures that affected Tonawanda Creek Road. The process involves mixing dry cement with the soft clay to form soil-cement columns. The results show that mixing the equivalent of 8 to 10 bags of dry cement with the soft clay in a hole that is 30 inches in diameter and 30 feet deep, results in a soil cement column that is 10 to 20 times stronger than the in-situ clay. The stronger, stiffer soil-cement columns support the road embankment and alleviate instability of the creek bank.

Paper Authors:

Shawn W. Logan, P.E.
Project Engineer
McMahon & Mann Consulting Engineers, P.C.
2495 Main St., Suite 432
Buffalo, New York 14214
(716) 834-8932
slogan@mmce.net

Brian Rose
Erie County Department of Public Works – Division of Highways
95 Franklin Street, 14th Floor
Buffalo, New York 14202
(716) 858-2079
brian.rose@erie.gov

Michael L. Grant, P.E.
Hayward Baker Inc.
16 Drumlin Drive
Weedsport, NY 13166
(315) 834-6603
mlgrant@haywardbaker.com

Michael J. Mann, P.E.
Project Engineer
McMahon & Mann Consulting Engineers, P.C.
2495 Main St., Suite 432
Buffalo, New York 14214
(716) 834-8932
mmann@mmce.net

Jonathan Kolber
US Army Corps of Engineers, Buffalo District
1776 Niagara Street
Buffalo, New York 14207-3199
716-879-4242
Jonathan.E.Kolber@lrb01.usace.army.mil

Load-Settlement Model of Rock Sockets from O-Cell Testing

John P. Turner, Ph.D., P.E.
Professor
University of Wyoming
Civil & Architectural Engrg.
Laramie, WY 82070
(307) 766-4265
turner@uwyo.edu

Reid Buell, R.G., C.H.G., C.E.G.
Senior Engineering Geologist
Caltrans
5900 Folsom Blvd.
Sacramento, CA 95819-4612
(916) 227-1012
reid_buell@dot.ca.gov

Xing Zheng
Engineering Geologist
Caltrans
5900 Folsom Blvd.
Sacramento, CA 95819
(916) 227-1036
xing_zheng@dot.ca.gov

INTRODUCTION

Design of drilled shaft foundations to satisfy Service I limit state criteria requires the load-settlement behavior to be predicted. Very little guidance is available to design engineers for predicting load-displacement behavior of rock-socketed drilled shafts. Field load testing of drilled shaft foundations by the Osterberg load cell method (O-cell) is being used increasingly by many transportation agencies. Typically, the O-cell measurements are used to construct an "equivalent top load-displacement curve" by adding the measured side and base resistance values at common values of displacement. The resulting load-settlement curve can be applied directly to production shafts having the same dimensions and constructed in rock profiles very close to that of the test shaft. This paper demonstrates how the load-settlement curve obtained from an O-cell load test can be interpreted within the framework of an analytical model based on a procedure developed by Randolph and Wroth (1978) for elastic analysis of piles and later adapted to the interpretation of rock-socketed shafts by Kulhawy and Carter (1992). Once a model is developed that exhibits reasonably good agreement between the predicted and measured load-settlement response, it can then be used to predict the response of drilled shaft trial designs with geometries different than those of the test shaft, if it can be assumed that the characteristics of the rock mass are generally similar. A bridge project in which the authors are involved is used to illustrate the application of this approach to service limit state evaluation of drilled shafts.

OSTERBERG LOAD CELL FOR AXIAL LOAD TESTING

The Osterberg Cell (O-cell) is a hydraulically operated jacking device that can be embedded in a drilled shaft by attachment to the reinforcing cage (Figure 1). After concrete placement and curing a load test is conducted by expanding the cell against the portions of the shaft above and below it. The load is applied through hydraulic piston-type jacks acting against the top and bottom cylindrical plates of the cell. The maximum test load is limited to the ultimate capacity

of either the section of shaft below the cell, the section above the cell, or the capacity of the cell.
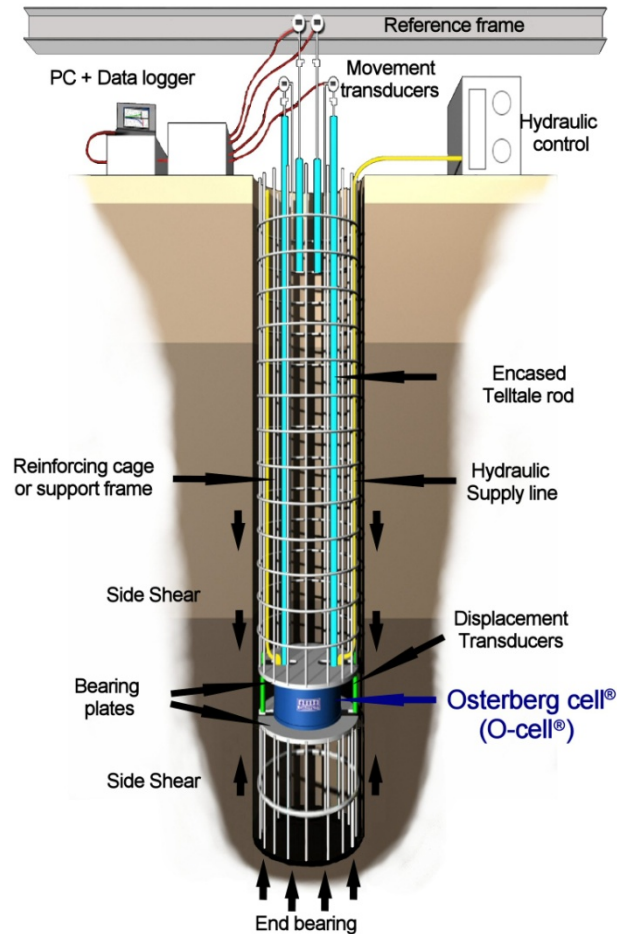

Figure 1. Bi-Directional (O-cell) Testing Schematic (courtesy Loadtest, Inc.)

Pressure transducers are used to monitoring hydraulic jack pressures and converted to load. Linear vibrating wire displacement transducers (LVWDT's) between the two plates measure total expansion of the cell and telltales are installed to measure vertical movements at the top and bottom of the test sections. The downward movement of the bottom plate is obtained by subtracting the upward movement of the top test section from the total extension of the O-cell as determined by the LVWDT's. Telltale deformations are monitored with digital gages mounted on a reference beam. All of the instrumentation is electronic and readings are collected by a data acquisition unit. The O-cell device is patented and under exclusive license to LOADTEST, Inc.

Interpretation of O-cell tests in rock sockets is typically based on the assumption that total applied load at the ultimate condition is distributed uniformly over the shaft/rock side interface, and used to calculate an average unit side resistance by:

$$f_s = \frac{Q_{oc}}{\pi BD}$$

where f_s = average unit side resistance (stress), Q_{OC} = O-cell test load, B = shaft diameter, and D = socket length. The degree to which this average unit side resistance is valid for design of rock sockets loaded at the head depends upon the degree to which side load transfer under O-cell test conditions is similar to conditions under head loading. Detailed knowledge of site stratigraphy is needed to interpret side load transfer. Base resistance is computed from the downward-acting O-cell load minus the side resistance mobilized over the depth interval between the O-cell and the base of the shaft.

O-cell test results typically are used to construct an equivalent top-loaded settlement curve. The measured upward and downward loads determined for each value of displacement are added to obtain the equivalent top load for a given value of downward displacement and plotted on a load-displacement curve. This procedure is used to obtain points on the load-displacement curve up to a displacement corresponding to the least of the two values (side or base displacement) at the maximum test load. A correction is made to account for the elastic compression of the shaft which would occur under conditions of axial load applied at the head of the shaft in order to approximate the final equivalent top load-displacement curve.

The maximum test load is limited to the maximum axial resistance of the shaft above or below the cell, or the maximum capacity of the cell. It is therefore important that the O-cell be located at or near the point in the shaft where the axial resistance above and below the cell are approximately equal. If the side shearing resistance exceeds the base resistance, then the O-cell should be located at the point at which the base plus a portion of the side near the bottom of the shaft are approximately equal to the side shear above. If the base resistance exceeds the side shearing resistance, then the magnitude of the base resistance that can be mobilized during the test is limited to the maximum side resistance.

MODEL FOR AXIAL LOAD-DISPLACEMENT BEHAVIOR OF ROCK SOCKETS

An approximate method given by Kulhawy and Carter (1992), and also included in the current FHWA Drilled Shaft Manual (O'Neill and Reese 1999), provides simple closed-form expressions that compare reasonably well to more sophisticated nonlinear finite element analyses of drilled shaft axial load-displacement response. The basic problem is depicted in Figure 2 (a) and involves predicting the relationship between an axial compression load (Q_c) applied to the top of a socketed shaft and the resulting axial displacement at the top of the socket (w_c). The concrete shaft is modeled as an elastic cylindrical inclusion embedded within an elastic rock mass. The cylinder of depth L and diameter B has Young's modulus E_c and Poisson's ratio v_c. The rock mass surrounding the cylinder is homogeneous with Young's modulus E_r and Poisson's
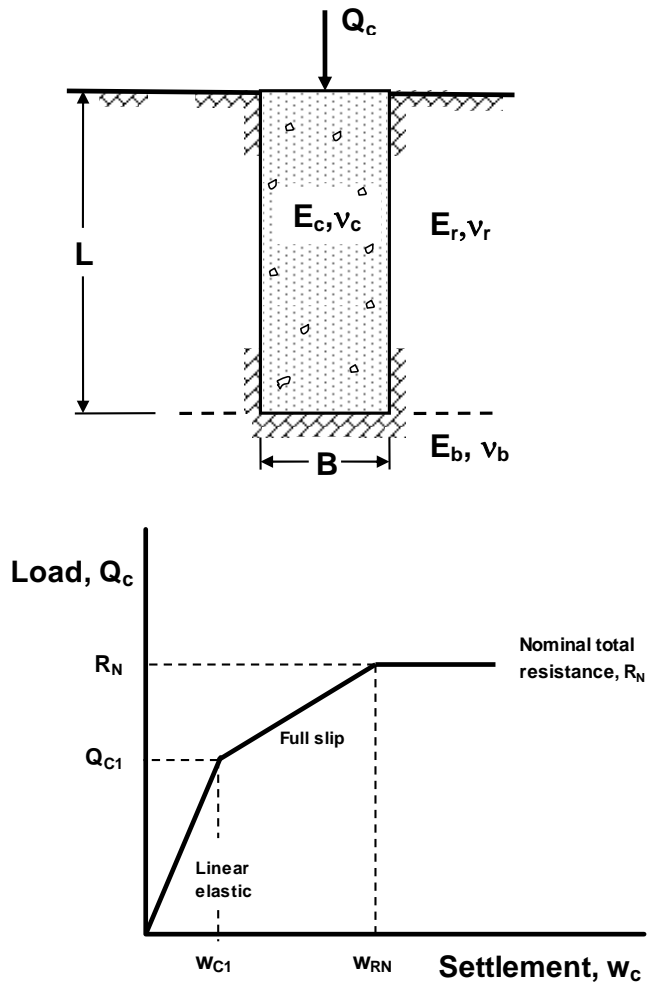
(a) elastic model of rock socket   (b) computed bilinear load-settlement curve

Figure 2. Simplified Model of Axial Load-Deformation Behavior, Drilled Shaft in Rock

(after Kulhawy and Carter 1992)

ratio ν_r while the rock mass beneath the base of the shaft has Young's modulus E_b and Poisson's ratio ν_b. The solution (Figure 2b) approximates the actual nonlinear load-deformation response of an axially loaded rock socket as consisting of two linear segments: (1) the initial linear elastic response and (2) the full slip condition. The maximum load is limited to the nominal axial resistance.

The complete analytical solution for modeling the load-displacement curve as described above is presented in Appendix A. The equations have been implemented into a spreadsheet by

the authors and used to analyze the O-cell test results and to predict axial load-displacement behavior of trial designs.

The above method is best applied in conjunction with load testing of rock sockets, and is one of the ways to take maximum advantage of load test results (Turner 2006). The analytical solution is fit to the measured axial load displacement curve from the load test through trial values of the rock mass elastic and strength properties (E_r, E_b, c, ϕ, and ψ; see Appendix A for all symbol definitions). Where borings verify that the rock mass has similar lithology, strength, and discontinuity characteristics, the analysis can then be used to evaluate load-deformation behavior of trial designs. The authors recently employed this approach by applying it to results of a load test conducted by the California Department of Transportation at the site of a proposed bridge (Pitkins Curve Bridge, Monterey County).

LOAD TEST AT PITKINS CURVE

Site and Test Conditions

This project serves to illustrate the potential benefits of performing the type of enhanced analyses described above. At the site of a proposed bridge at Pitkins Curve on Highway 1 in central California, a high degree of uncertainty existed as to whether drilled shaft foundations were a feasible option. Rock at this site belongs to the Franciscan Formation and consists of metamorphosed siltstone and sandstone with inclusions of metabasalt. The rock is highly folded and fractured, difficult to sample in some locations, and exhibits wide variations in strength and quality. Design for strength limit states required knowledge of side and base resistances, while design for service limit states required a reliable method to predict the load-deformation response. A bi-directional O-cell load test was proposed as a means to provide this information.

A boring was made at the exact location of the test shaft and carefully logged to provide a detailed profile of the rock. Core samples that were sufficiently intact were tested for uniaxial compressive strength. In general, the material to a depth of 18 ft was highly fractured and weathered, with moderate recovery and very low RQD values (zero in most cases). Over this depth interval, no intact specimens suitable for uniaxial compression testing were obtained. Rock strength was evaluated on the basis of point load tests on eleven specimens, yielding an average compressive strength of q_u = 574 psi. Below a depth of 18 ft the rock becomes harder and less fractured, with higher recoveries and RQD values ranging from zero to 25 percent. Figure 3 is a photo of core samples over the depth interval between 10 ft and 22 ft. The transition described above at approximately 18 ft is visible. Two intact specimens were obtained over the depth interval between 21 ft and 23 ft and tested in uniaxial compression, yielding values of q_u = 4,800 psi and 9,770 psi, respectively. At a depth corresponding to the tip of the test shaft (35.5 ft) the rock is described as very hard metabasalt.

Figure 3. Core Specimens at Test Shaft Location, Depth Interval = 10 – 22 ft.

The test shaft was 42-inches in diameter, 35.4 ft deep. Figure 4 shows the O-cell attached to its frame and ready for placement into the drilled shaft excavation. The O-cell was placed at a distance of approximately 3 ft above the base of the shaft. The test shaft was drilled using a rock auger without casing or other support (Figure 5). Seepage of water into the excavation was observed during drilling. Water at the base was mixed with cement and re-excavated just prior

Figure 4. O-Cell and Frame Ready for Placement in the Test Shaft.

Figure 5. Construction of Test Shaft at Pitkins Curve.

to the final concrete pour in order to minimize potential adverse base conditions. Strain gages placed at a depth of 20 ft were used to determine the magnitude of load transfer over the depth intervals from 0 – 20 ft, 20-ft to the O-cell, and O-cell to the base of the shaft.

Analysis of Results

Full results of the O-cell test are presented in a report prepared by Loadtest Inc. (2007). The maximum load applied to the test shaft was 5,200 kips.   At this maximum load, axial displacements above and below the O-cell were 1.02 and 0.76 inches, respectively.   Table 1 presents values of unit side resistance measured at the maximum test load. In addition, the mobilized base resistance was calculated to be 396 ksf.

Figure 6 shows the equivalent top load-displacement curve from the O-cell test (Loadtest, Inc. 2007) and the modeled load-displacement curve. The modeled curve was established by

fitting to the equations given in Appendix A and carried out using a spreadsheet solution developed by the authors. Values of rock mass modulus (E_r and E_b) were adjusted to obtain close agreement between the measured curve and the modeled curve. These values of modulus are within the range expected for rock mass with the characteristics observed in boring logs and with strength values cited previously.

Table 1. SUMMARY OF UNIT SIDE RESISTANCES FROM O-CELL TEST

Depth Interval	General Material Description	Unit side resistance (ksf)
1.6 – 20.0	top 2-3 ft pavement base course underlain by interbedded metasediments/metabasalt rock	5.51
20.0 – 32.3	metasediment and metabasalt	29.43
32.3 – 37.0	metabasalt	27.0
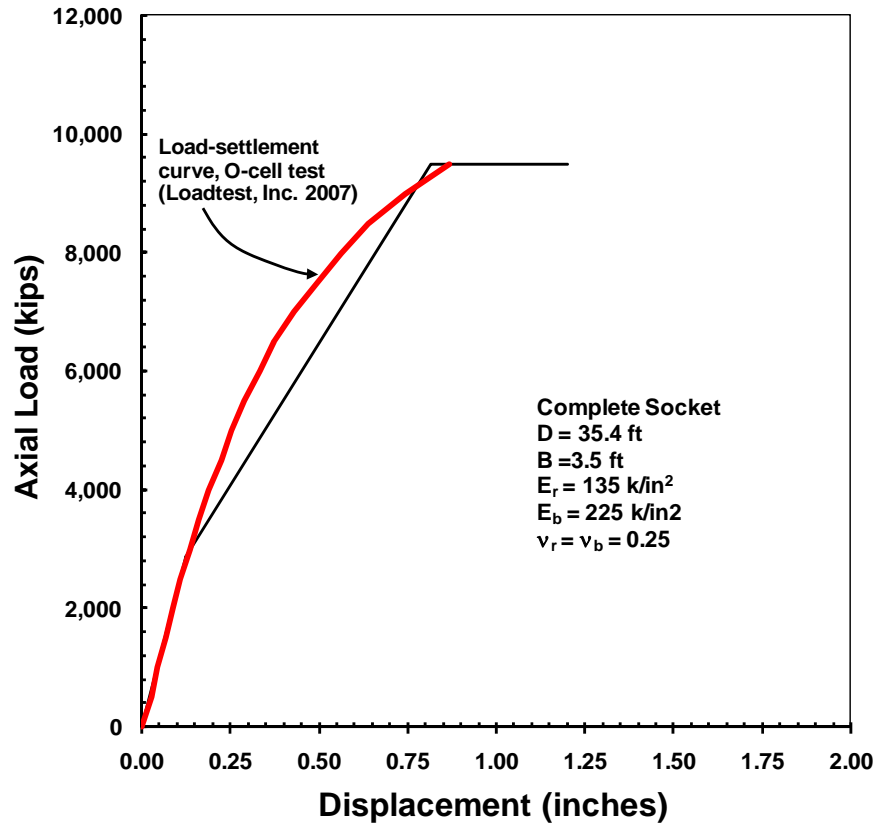
Figure 6. O-Cell Equivalent Top-Load Settlement Curve and Modeled Curve.

Trial designs were evaluated for their ability to satisfy appropriate strength and service limit states for the bridge at Pitkins Curve. The final design consists of two piers supported by four drilled shafts at each pier, with shaft diameter B = 5 ft and depth D = 60 ft. The bridge structural engineer established a tolerable settlement for individual shafts of ½ inch under a nominal axial force of 2,300 kips. The load-displacement model was used to analyze this service limit state for axial settlement by changing the shaft dimensions to those of the trial design (B = 5 ft, D = 60 ft), with the material properties held constant.   The predicted load-displacement curve for the trial shafts is shown in Figure 7. As indicated in the figure, for an axial compression load of 2,300 kips, the predicted displacement is approximately 0.07 inches and the shaft response is in
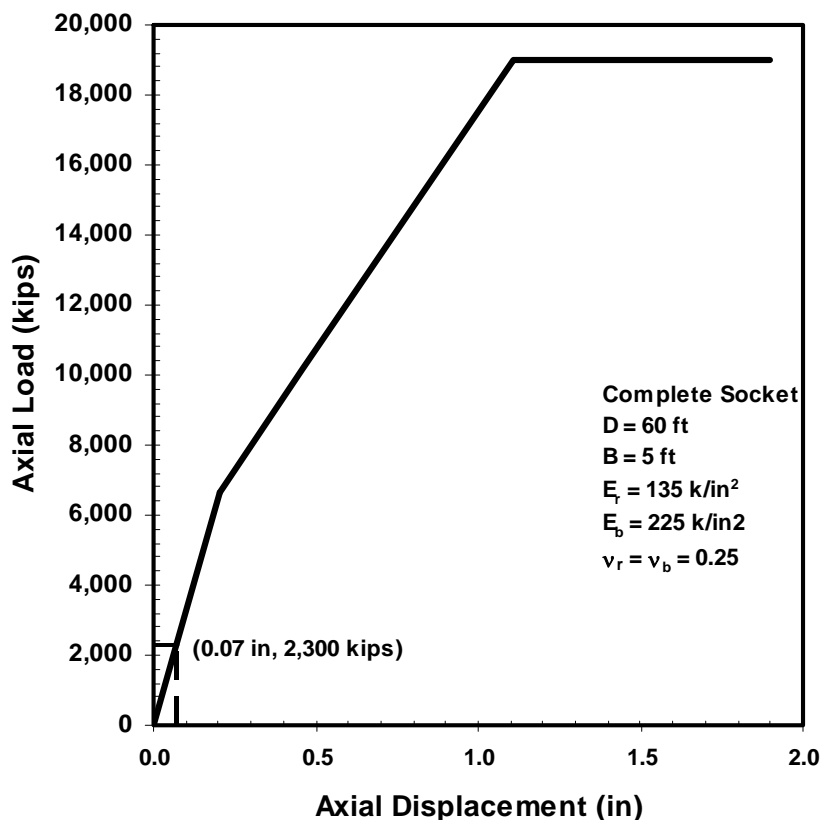
Figure 7. Predicted Load-Settlement Curve for Trial Design, Single CIDH Pile.

the linear elastic range. By this analysis, the proposed trial design easily satisfies the service limit state criterion that limits settlement to ½ inch. Furthermore, the nominal resistance corresponding to the limiting settlement (½ inch) is approximately 10,750 kips, which exceeds the nominal loading of 2,300 kips, thus satisfying the LRFD service limit state criterion. The final shaft dimensions are governed by lateral loading considerations and not by the axial settlement criterion.

DISCUSSION AND LIMITATIONS

The most important limitation of the analysis presented above is that it is based on the assumption that the engineering characteristics of the subsurface materials at the bridge pier locations are generally similar to those at the location of the O-cell test shaft. Comparison of the boring logs from the three locations suggest that they are underlain by the same rock unit,

but all show high degrees of variability in rock mass characteristics such as percent recovery, RQD, degree of weathering, foliation, and degree of fracturing. More refined analyses are possible by conducting more detailed evaluations of rock mass properties at the pier sites for comparison with properties at the test shaft site. Once a model is fitted to load test results, sensitivity studies can be carried out by varying the rock mass properties (*e.g.* rock mass modulus) and evaluating the resulting settlement under expected loads. In this particular case, properties averaged over the depths of the proposed productions shafts are quite similar to those at the test site. The analysis presented above serves to illustrate the application of an appropriate load-displacement model to an O-cell load test in order to provide a tool for service limit state analyses.

It is further assumed in the above analyses that the shafts to be constructed at the pier locations will be capable of developing unit base resistance values at least equal to that measured by the O-cell test. For the pier locations, a more detailed analysis of the rock mass over a depth of 5 to 10 ft (one to two shaft diameters) below the proposed tip elevations is recommended in order to verify that the drilled shafts will bear on rock that is as competent as the rock at the test location. If it is determined that highly fractured zones exist within 5 to 10 ft below the tips, consideration should be given to modifying the tip elevations to more competent rock or to reducing nominal base resistance values.

SUMMARY AND CONCLUSIONS

A method is presented for modeling the load-displacement behavior of rock-socketed drilled shafts, which is needed when designing for service limit states. The method is best applied in conjunction with a field load test conducted on a shaft that may have smaller dimensions than the productions shafts, but is embedded in rock mass with similar engineering characteristics. The method fills a need for appropriate design for service limit states according to AASHTO LRFD Specifications (AASHTO 2007). A case history in which the authors are involved is presented in order to illustrate the application of this method to the design of a highway bridge to be supported on rock-socketed drilled shafts.

REFERENCES

AASHTO (2007), *AASHTO LRFD Bridge Design Specifications*, Customary U.S. Units, 4th Ed., 1510 p.

Kulhawy, F.H. and Carter, J.P. (1992). "Settlement and Bearing Capacity of Foundations on Rock Masses," Ch. 12, *Engineering in Rock Masses*, F.G. Bell, Editor, Butterworth-Heinemann, Oxford, pp. 231-245.

O'Neill, M.W., and Reese, L.C. (1999). "Drilled Shafts: Construction Procedures and Design Methods," *Publication No. FHWA-IF-99-025*, Federal Highway Administration, Washington, D.C., 758 p.

Randolph, M.F., and C.P. Wroth, "Analysis and Deformation of Vertically Loaded Piles," *Journal of the Geotechnical Engineering Division*, ASCE, Vol. 104, No. GT12, 1978, pp. 1465-1488.

Turner, J.P. (2006). *NCHRP Synthesis 360: Rock-Socketed Shafts for Highway Structure Foundations*, Transportation Research Board, National Research Council, Washington, D.C., 148 p.

Turner, J.P. (2007). Analysis of Osterberg Cell Load Test at Pitkins Curve, unpublished report to California Department of Transportation, 12 p.

Yang., K. (2006). "Analysis of Laterally Loaded Drilled Shafts in Rock," Ph.D. Dissertation, University of Akron, Akron, OH, 291 p.

APPENDIX A: Closed-Form Solution for Axial Load-Settlement Response of Rock Sockets

For compression loading, two cases are treated by Kulhawy and Carter: (1) a "complete socket", for which full contact is assumed between the base of the concrete shaft and the underlying rock, and: (2) a shear socket, for which a void is assumed to exist beneath the base. The shear socket solution would be useful in analyzing a load test in which base resistance is eliminated by creating a void beneath the base of the drilled shaft. Only the complete socket case is treated here.

1. For the linearly elastic portion of the load-displacement curve (see Figure 2b).

$$w_c = \frac{2Q_c}{G_r \, B} \; \frac{1 + \left(\dfrac{4}{1-v_b}\right)\left(\dfrac{1}{\pi\lambda\xi}\right)\left(\dfrac{2L}{B}\right)\left(\dfrac{\tanh[\mu L]}{\mu L}\right)}{\left(\dfrac{4}{1-v_b}\right)\left(\dfrac{1}{\xi}\right) + \left(\dfrac{2\pi}{\zeta}\right)\left(\dfrac{2L}{B}\right)\left(\dfrac{\tanh[\mu L]}{\mu L}\right)} \qquad \text{A-1}$$

in which:

$$(\mu L)^2 = \left(\frac{2}{\zeta \lambda}\right)\left(\frac{2L}{B}\right)^2 \qquad \text{A-2}$$

$$\zeta \quad = \ln\left[5(1 - \nu_r)L/B\right] \qquad \text{A-3}$$

$$\lambda \quad = E_c/G_r \qquad \text{A-4}$$

$$G_r = E_r/\left[2(1 + \nu_r)\right] = \text{elastic shear modulus of rock mass} \qquad \text{A-5}$$

$$\xi = G_r/G_b \qquad \text{A-6}$$

$$G_b = E_b/\left[2(1 + \nu_b)\right] \qquad \text{A-7}$$

The magnitude of load transferred to the base of the shaft (Q_b) is given by:

$$\frac{Q_b}{Q_c} = \frac{\left(\dfrac{4}{1-\nu_b}\right)\left(\dfrac{1}{\xi}\right)\left(\dfrac{1}{\cosh[\mu D]}\right)}{\left(\dfrac{4}{1-\nu_b}\right)\left(\dfrac{1}{\xi}\right) + \left(\dfrac{2\pi}{\zeta}\right)\left(\dfrac{2D}{B}\right)\left(\dfrac{\tanh[\mu D]}{\mu D}\right)} \qquad \text{A-8}$$

2. For the full slip portion of the load–displacement curve.

$$w_c = F_3\left(\frac{Q_c}{\pi E_r B}\right) - F_4 B \qquad \text{A-9}$$

in which:

$$F_3 = a_1(\lambda_1 BC_3 - \lambda_2 BC_4) - 4a_3 \qquad \text{A-10}$$

$$F_4 = \left[1 - a_1 \left(\frac{\lambda_1 - \lambda_2}{D_4 - D_3}\right) B\right] a_2 \left(\frac{c}{E_r}\right) \qquad \text{A-11}$$

$$C_{3,4} = \frac{D_{3,4}}{D_4 - D_3} \qquad \text{A-12}$$

$$D_{3,4} = \left[\pi\left(1 - v_b^2\right)\left(\frac{E_r}{E_b}\right) + 4a_3 + a_1\lambda_{2,1}B\right]\exp[\lambda_{2,1}D] \qquad \text{A-13}$$

$$\lambda_{1,2} = \frac{-\beta \pm \left(\beta^2 + 4\alpha\right)^{1/2}}{2\alpha} \qquad \text{A-14}$$

$$\alpha = a_1\left(\frac{E_c}{E_r}\right)\left(\frac{B^2}{4}\right) \qquad \text{A-15}$$

$$\beta = a_3\left(\frac{E_c}{E_r}\right)B \qquad \text{A-16}$$

$$a_1 = (1 + v_r)\zeta + a_2 \qquad \text{A-17}$$

$$a_2 = \left[(1 - v_c) \left(\frac{E_r}{E_c} \right) + (1 + v_r) \right] \left(\frac{1}{2 \tan \phi \tan \psi} \right) \qquad \text{A-18}$$

$$a_3 = \left(\frac{v_c}{2 \tan \psi} \right) \left(\frac{E_r}{E_c} \right) \qquad \text{A-19}$$

The magnitude of load transferred to the base of the shaft (Q_b) is given by:

$$\frac{Q_b}{Q_c} = P_3 + P_4 \left(\frac{\pi B^2 c}{Q_c} \right) \qquad \text{A-20}$$

in which:

$$P_3 = a_1(\lambda_1 - \lambda_2) B \exp[(\lambda_1 + \lambda_2)D] / (D_4 - D_3) \qquad \text{A-21}$$

$$P_4 = a_2(\exp[\lambda_2 D] - \exp[\lambda_1 D]) / (D_4 - D_3) \qquad \text{A-22}$$

Note that the point of intersection between the linear elastic portion of the curve and the full slip segment, defined by point (Q_{C1}, w_{C1}) in Figure 2b, can be calculated by setting Equation A-1 equal to Equation A-9, solving for the resulting value of axial load (Q_{C1}) and using this value to compute the corresponding displacement w_{C1}.

Numerical solutions to Equations A-1 through A-22 are implemented easily by spreadsheet, thus providing designers a simple analytical tool for assessing the likely ranges of behavior for trial designs. The user of this method should be familiar with the assumptions made in its development. The modulus of the rock mass is assumed to be constant over the depth of shaft embedment and beneath the base. Rock mass modulus and its variation with depth must, therefore, be assessed carefully and determined to satisfy the assumption of uniformity. Strength of the rock mass is required in terms of its Mohr-Coulomb parameters (c, ϕ, and ψ) where ψ = angle of dilatancy. In the absence of laboratory testing of the rock-concrete

interface, Kulhawy and Carter (1992) suggest the following correlations between the Mohr-Coulomb strength parameters and uniaxial compressive strength (q_u) of intact rock:

$$\frac{c}{p_a} = 0.1 \left(\frac{q_u}{p_a} \right)^{2/3}$$

D-23

$$\tan\phi \tan\psi = 0.001 \left(\frac{q_u}{p_a} \right)^{2/3}$$

D-24

where p_a = atmospheric pressure in the same units as cohesion (c) and uniaxial compressive strength (q_u).

253

4.4

SCOBY HILL LANDSLIDE – ROUTE 219 (SECTION V) – SPRINGVILLE, NY

Brent A. Black, C.E.G., R.G.
Landslide Technology
10250 S.W. Greenburg Road, Suite 111
Portland, Oregon 97223
PH: 503-452-1200
FAX: 503-452-1528
email: brentb@landslidetechnology.com

George Machan, P.E.
Landslide Technology
10250 S.W. Greenburg Road, Suite 111
Portland, Oregon 97223
PH: 503-452-1200
FAX: 503-452-1528
email: georgem@landslidetechnology.com

ABSTRACT

Highway construction discovered the presence of a very large ancient landslide within the Cattaraugus Creek valley in western New York State. The active landslide is contained within this ancient landslide complex. The depth of the slide is about 30 m (100 ft). The landslide is 1,000 m (3,300 ft) wide, 500 m (1,600 ft) long and up to 30 m (100 ft) deep. The Route 219 landslide is complex and very expensive to stabilize completely, and therefore a "Balanced Approach" has been developed to best manage slide forces and movements. The landslide was first identified during initial earthwork in 2007. Subsequently, several measures were implemented in late 2007 and during 2008 to slow down the slide movements. The observational approach was used to monitor landslide conditions and to adjust or supplement the mitigation measures. Periodic site reconnaissances were performed to look for other landslide clues and changes in ground distress and relative performance of constructed mitigations. Based on these observations, landslide mitigations were adjusted to minimize long-term highway distress.

INTRODUCTION

Highway construction in the summer of 2007 discovered the presence of a very large ancient landslide complex within the Cattaraugus Creek valley in western New York State. An active landslide is contained within this ancient landslide complex. The ground within the landslide area is gently sloped (typically 5 to 10 degrees), and is generally hummocky and incised with springs and drainage channels. The active landslide is approximately 1,000 m (3,300 ft) wide and 400 m (1,300 ft) long. The depth of the slide is about 30 m (100 ft) under the highway corridor. An oblique airphoto of this area showing the interpreted ancient landslide limits and the cleared

embankment footprint is presented on Figure 1. The active scarps and interpreted ancient headscarps are superimposed on the oblique air photograph.

GEOLOGY

The geology at the project area has been heavily affected by glaciation and subsequent incision and erosion. It is located within a late Wisconsinan till complex that overlies shales and sandstone of the Upper Devonian Canadaway and Conneaut Groups.

The main unit consists of Lavery Till, which is a thick, overconsolidated deposit of hard gray clayey silt, with scattered gravel. This unit is an interfingered complex comprised of pebble and cobble till with clayey silt matrix. Typically, the amount of gravel is about 10 to 20 % by volume. The geological literature describes silt stringers and possible concentrated zones of sand and gravel within this unit. LaFleur (1979) described the Lavery Till as highly susceptible to slumps and shallow-seated rotational slides due to its clayey silty texture, thickness, and deep post-glacial dissection. The disturbed zones are reworked and softened lacustrines with deformed silt and sand stringers.

Bedrock was not encountered in the exploratory borings drilled within the slide limits of the project. Geophysical surveys indicate that bedrock could be as deep as 30 to 45m to 60m (100 to 150 ft) below the basal shear plane of the landslide.

Numerous springs and ponds exist throughout the site, related to groundwater discharging from the upper glacial outwash deposit and from the underlying Lavery Till. It is not clear how the rather homogeneous and low-permeability Lavery Till unit is transmitting concentrations of groundwater. The geological literature describes silt stringers and possible concentrated zones of sand and gravel within the till, which may explain the springs. In addition, studies performed for a nearby project to the southeast identified fracture patterns that developed in the Lavery Till that may be the result of stresses related to post-glacial drift, or volumetric changes resulting from isometric processes (Dames and Moore, 1997). Groundwater in an upper more permeable unit is perched and the clayey silt acts as an aquitard. This perched water likely infiltrates slowly into the underlying clayey silt and provides the source of groundwater for this lower unit.

SUBSURFACE CONDITIONS

The near surface material consists of a water-bearing, upper sand and gravel unit (glacial outwash). This unit is underlain by the less permeable Lavery Till. The upper 10 to 35 m (30 to 115 ft) of silty clay and clayey silt in the slide area is disturbed, very soft to medium stiff with SPT values typically 2 to 10 blows per 0.3 m (1 ft), with occasional stiffer zones with SPT up to 20 blows per 0.3 m (1 ft). The underlying undisturbed silty clay appears to be stiff to hard, with SPT values generally greater than 10 blows per 0.3 m (1 ft), increasing to over 40 blows per 0.3 m (1 ft) with depth.

The clayey soil has natural moisture content close to its liquid limit (based on liquid limits of about 22 to 42 % and natural moisture contents of 20 to 35 %). These tested values signify clay with a high sensitivity and excess moisture, indicating the material can experience significant shear strength reduction when remolded. The plasticity index (PI) ranges from 4 to 20 %. The soil exhibits plasticity and has a high dry strength.

Permeability of the silty clay is about 10^{-8} to 10^{-9} cm/sec, based on the results of triaxial and consolidation tests. The permeability of sandy silt stringers and layers could be about 10^{-4} to 10^{-6} cm/sec.

Ring shear tests were performed to determine a range of softened and residual (remolded) shear strengths in the upper slide mass and at the basal shear zone. Based on a ring shear test, the softened shear strength of the clayey silt soil in the upper portions of the slide mass had a result of $\phi_r' = 26°$. However, the ring shear tests performed on the remolded silty clay in the deeper basal shear zone resulted in low residual shear strengths in the range of $\phi_r' = 12°$ to $14°$.

The soils at the failure plane were similar in appearance and moisture content to the other soils in the area. The basal shear zone only revealed itself through ground movement, and its location was determined by using slope inclinometers installed after the cracks appeared on the grade.

Instruments to measure subsurface movement and ground water pressure were installed across the slide area to detect the depth and magnitudes of landslide shear displacement and the levels of groundwater. Perched and regional groundwater levels were measured, and the instruments verified that artesian groundwater does not exist at this site.

LANDSLIDE EVALUATION

The movement instruments (slope inclinometers) verified that basal landslide movement was deep and translational (see Figure 2). Initial rates of slide movement were on the order of 2 meters (80 inches) per year. The water pressure instruments (vibrating wire piezometers and standpipe observation wells) indicated high groundwater levels, typically within 2 meters (6 ft) of the ground surface. This data, coupled with information obtained from geologic/landslide mapping and laboratory testing, was used to evaluate the landslide. The presence of low residual shear strength clay and high pore-water pressures at the site indicated that the area was marginally unstable prior to construction. Fill placement during construction of the highway in the summer of 2007 was a contributing factor to the reactivation of the ancient landslide. Up to 6 meters (20 feet) of the placed fill and existing native soil was removed from the slide in the fall of 2007 in an effort to minimize further movement. This resulted in the dissipation of excess pore pressures, which resulted in the lowering of the piezometric elevations of up to 3 meters (~10 feet) within the slide. The net effect of unloading was a reduction in the rate of slide movement, particularly in the middle of the new highway corridor. However, cut slopes made earlier in the summer still experienced cracking and slumping, and the deep basal shear plane continued to show signs of movement at a rate of 0.20 meters (8 inches) per year (see Figure 3).

Observations made during construction have shown the delicate balance that currently exists at the site. Any changes to the geometry that reduced the resisting forces or increased the driving forces in the slide area (or elevated pore-pressure levels) resulted in increased movements. Other complicating factors included: i) the potential for multiple failure planes (localized nested slides) above the basal shear plane, and ii) Right-of-Way (R-O-W) concerns where the head scarp and toe of the ancient slide complex were outside the highway corridor. These issues made designing a mitigation solution especially complex.

HORIZONTAL DRAIN TEST PROGRAM

Initial stability analyses indicated that excess pore-water pressures within the clay stratum comprising the basal shear zone were a significant factor contributing to ground movement. Horizontal drains could be a way of reducing these pore-water pressures. Installing deep horizontal drains in clay soils is not commonly done due to low permeability and siltation issues and was therefore considered challenging. The potential benefit of improving stability at relatively low cost prompted the implementation of a test program to investigate the effectiveness of horizontal drains.

The field test program consisted of 19 horizontal drains that were installed in 2007. Drilling was conducted from four pit locations downslope of the highway corridor: three pits were near the landslide toe and the other pit was about midway between the slide toe and the highway corridor. The intent was to install the horizontal drains in fan arrays within the center of the most active portion of the slide at elevations just above the basal shear zone where they can influence the groundwater acting on the shear zone. The horizontal drains typically ranged in length from 134 to 230 m (440 to 750 ft). Three borings were terminated short (between 30 and 108 m) due to drilling issues. The drill holes were inclined are various slopes, ranging from horizontal to +7 degrees. A few drains angled slightly down to improve drilling operations and to try to penetrate more-permeable zones/fissures of silt/sand within the clay unit.

Initially, drawdown was not observed in the piezometers in the vicinity of the test horizontal drains (see Figure 4). Several months following the installation of Horizontal Drain Pad No. 4, it become apparent that the deep piezometers within the drains' influence area were experiencing reductions in water pressure, as indicated in Figure 5. Stability analyses showed that potential increases in the slide's Factor of Safety (FS) would result if moderate groundwater level drawdowns were achieved. It is possible that a 2 to 5% increase in FS could be achieved with about 1.5 m (5 ft) of drawdown. The results of this test program confirmed the feasibility and effectiveness and supported the decision to install a broad system of horizontal drains across the landslide to help mitigate the landslide.

LANDSLIDE MITIGATION

The selection of appropriate mitigation measures was based on an assessment of the probability and consequences of continued landslide movement, impacts to various nested slide configurations, constructability, roadway and ditch geometries, environmental impacts, Right-of-Way issues, and cost. Several mitigation options were evaluated. Stabilization methods to achieve standard Factors of Safety (FOS) levels were determined to be prohibitively expensive. Therefore, options with greater risk were considered in order to reduce slide impacts, movements, and potential damage. Eventually, an option termed the "Balanced Approach" was selected, which improves the FOS slightly but is still considered "marginally stable" and includes provisions for dealing with more slide movements. This mitigation option constructs the highway at-grade to minimize and balance cuts and fill placement on the landslide (see Figure 6). Horizontal drains were used to lower groundwater levels and reduce excess pore-water pressures. Mitigation also included strengthening the subgrade using crushed stone reinforced with biaxial geogrid to bridge across slide cracks and differential slide subsidence. The bluff in the upper portion of the slide was excavated to unload some of the driving force. A buttress was constructed near the toe of the bluff cut slope to provide stability where shallower nested slides exist. This "Balanced Approach" option would reduce, but not completely eliminate the slide movement. In addition, there is a risk that the active headscarp could retrogress upslope (to the east) or a nested slide may occur in the eastern cut slope.

Construction resumed on the north end of the slide area using the at-grade "Balanced Approach" in the summer of 2008. Horizontal drain work did not start at this time due to R-O-W acquisitions. During the construction of the north bound roadway alignment, some excavations were required. These excavations inadvertently removed resisting forces along the toe of the eastern slopes which resulted in the activation of localized nested slides (see Figures 7). To improve stability, the north bound (NB) roadway was raised and an adjacent rockfill buttress was added to support the toe of the eastern cut slopes and provide additional resisting forces for the nested slide condition (see Figure 8). A cross-section of the modified approach and the design details are shown on Figure 9.

The horizontal drain drilling began on October 1, 2008 and was completed on May 20, 2009. A total of 173 horizontal drains were drilled at ten separate pad (fan array) locations (see Figure 10). The drain lengths range between 125 meters (410 feet) and 271 meters (890 feet). The combined length of the drains is 29,307 meters (96,151 feet, or 18 miles). After the drains were installed, they were jetted to clean the screens and remove sediment in the pipes. Groundwater drawdown has been developing slowly but surely. A site plan with interpretations of groundwater drawdown, based on July 2009 piezometer readings, is shown on Figure 10. Approximate drawdown contours (for 5-ft, 10-ft, and 15-ft drawdown zones) are given. Trends show areas with roughly 2 to 4 meters (5 to 15 feet) of drawdown in the west portion of the slide area, with a few localized zones with more drawdown. Drawdown levels are currently still dropping. Flow rates from each drain and the relative suspended sediment were measured to evaluate drain conditions and for indications of possible siltation. Flow rate measurements in May 2009 recorded a combined flow of 4 to 5 gpm, which represents an average of 0.03 gpm per drain. The flows are relatively small because of the low permeability of the silt and clay in the Lavery Till. Flows are expected to decrease as groundwater levels are lowered. Water from the horizontal drains discharges downslope of the pads were it benefits wetlands and stream flows.

Landslide movements accelerated during construction when pits were excavated for the horizontal drain drilling, which reduced slide resistance in the lower third of the deep seated landslide. In addition, groundwater pressures temporarily increased due to drilling where water was used to facilitate removal of the drill cuttings. Following completion of the horizontal drains, the pits were backfilled with shale buttresses which regained stability and helped to slow the global slide movements.

Earthwork will continue through 2009 to finish the NB roadway, median, and east cut slopes along the bluff (headscarp area of the global landslide). Instrument monitoring will continue over the next few years to guide decisions for completing the project and to identify long-term performance and maintenance needs. Paving is planned for 2010. Currently, asphalt concrete pavement is recommended since it would require less maintenance as landslide movements continue. At this time, it appears that long term slide movements could be reduced to less than 1-inch per year, and possibly less than 0.1-inch per year. However, predicting future movement rates is difficult due to the nature and complexity of this very large ancient landslide.

SUMMARY AND CONCLUSIONS

DOTs are occasionally faced with significant challenges or problems that unexpectedly occur during construction. The common approach is to stabilize a landslide to provide acceptable long-term roadway performance. However, landslides can be very expensive to stabilize, and therefore DOTs examine alternative approaches to find reasonable cost solutions. At the Route 219 site, the cost of full stabilization could have exceeded $100 million, far more than the initial cost of the new 5-mile highway and bridge project.

A thorough geotechnical investigation was conducted by NYSDOT, along with input from Landslide Technology. Over 100 borings have been drilled, along with installation of inclinometers and piezometers. Many series of stability analyses and engineering studies were conducted to evaluate various mitigation options. FHWA assembled a team of landslide experts to provide a peer review. Ultimately, the DOT decided that managing the landslide using a "Balanced Approach" would be more cost effective than conventional but exorbitantly expensive stabilization options. Implementing lower-cost construction methods to achieve small improvements in stability FS can result in slowing slide movements. This case history demonstrates the application of marginal mitigation, with successful slowing of slide movements.

Geotechnical challenges during construction of the "Balanced Approach" included:

- Development of horizontal drains in low permeability clay, including issues with hydraulic fracturing and siltation of the drain pipes,

- Finding methods to control erosion of the soil within the slide in drainage mitigation methods; such as horizontal drains, aggregate trench drains, ditch lining, and slope blankets,

- Iterative evaluations with the highway designer to develop "landslide-balanced" grading, by checking closely-spaced cross-sections, ditch geometry, and verifying that localized cut/fill quantities are balanced in all subareas of the kilometer-wide landslide,

- Complexity of nested slides that conflicted with behavior and mechanisms of the global slide. Discovering localized responses of the landslide and nested slides and then reacting to adjust alignment grades and buttress dimensions,

- Competing project needs that made landslide mitigation more difficult, such as sediment basin excavations within the landslide, maintaining/protecting ponds and streams next to the highway, protecting groundwater resources while dewatering is used to reduce pore pressures on the slide shear zone,

- Sequencing construction to minimize exacerbating landslide conditions and movements,

- Construction scheduling to optimize excavation/disposal of clay materials, development of borrow pits to obtain rockfill for buttresses and subgrade stabilization, and backfilling of borrow pits.

REFERENCES

Black, B.A., Machan, G., and Poelma, M., *Horizontal Drains in Clay – Landslide Stabilization Test Program,* 2009 TRB Annual Meeting presentation (final paper in process of being published in the Journal of the Transportation Research Board).

Cornforth, D.H. *Landslides in Practice: Investigation, Analysis, and Remedial/Preventative Options in Soils*, John Wiley & Sons, Inc., New Jersey, 2005.

Dames and Moore, *RCRA Facility Investigation Report, Volume 1*, West Valley Demonstration Project, 1997.

LaFleur, R.G., *Glacial Geology and Stratigraphy of Western New York Nuclear Service Center and Vicinity, Cattaraugus and Erie Counties, New York*, US Geological Survey Open-file Report 79-989, 1979.

Martin, R.P., Siu, K.L. mad Premchitt, J. *Performance of Horizontal Drains in Hong Kong,* GEO Report No. 42, GEO Special Project Report No. SPR 11/94, Hong Kong, 1994.

Smith, D.D. *The Effectiveness of Horizontal Drains*, Publication Final Report FHWA-CA-TL-80-16, 1980.

Turner, K.A. and R.L. Schuster. *Landsides: Investigation and Mitigation*, TRB Special Report 247, Transportation Research Board, National Research Council, National Academy Press, Washington D.C., 1996.
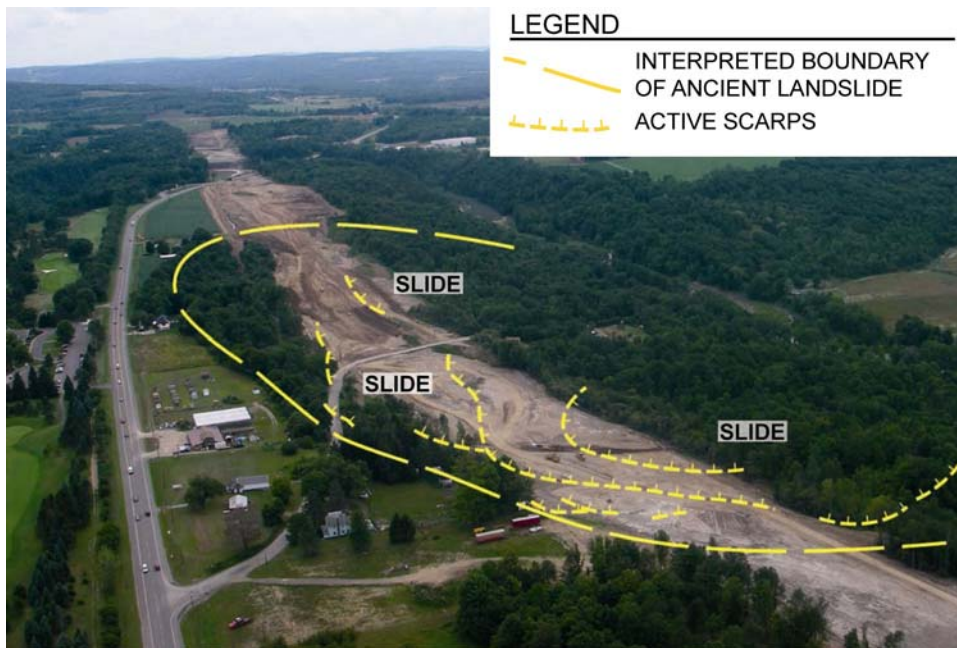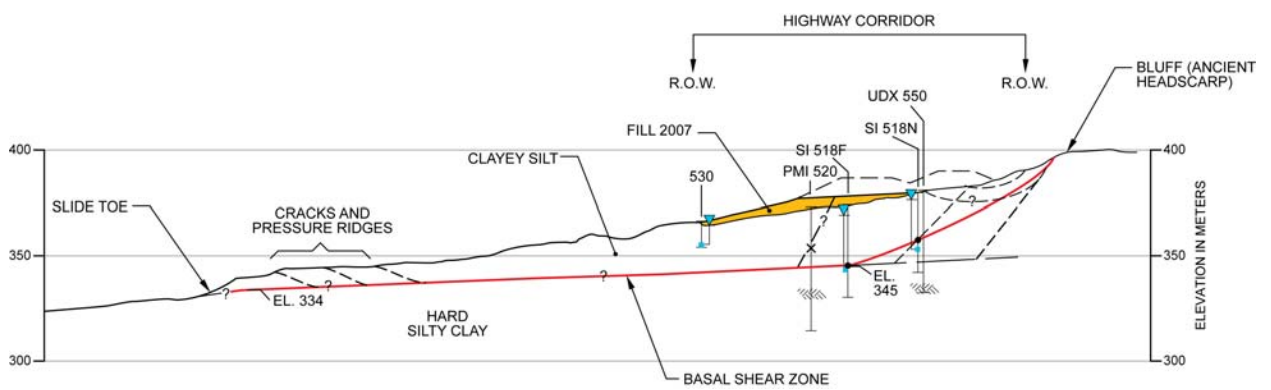
FIGURE 1 Oblique Air Photo of Landslide.

FIGURE 2 Cross Section STA. SB 51+450.

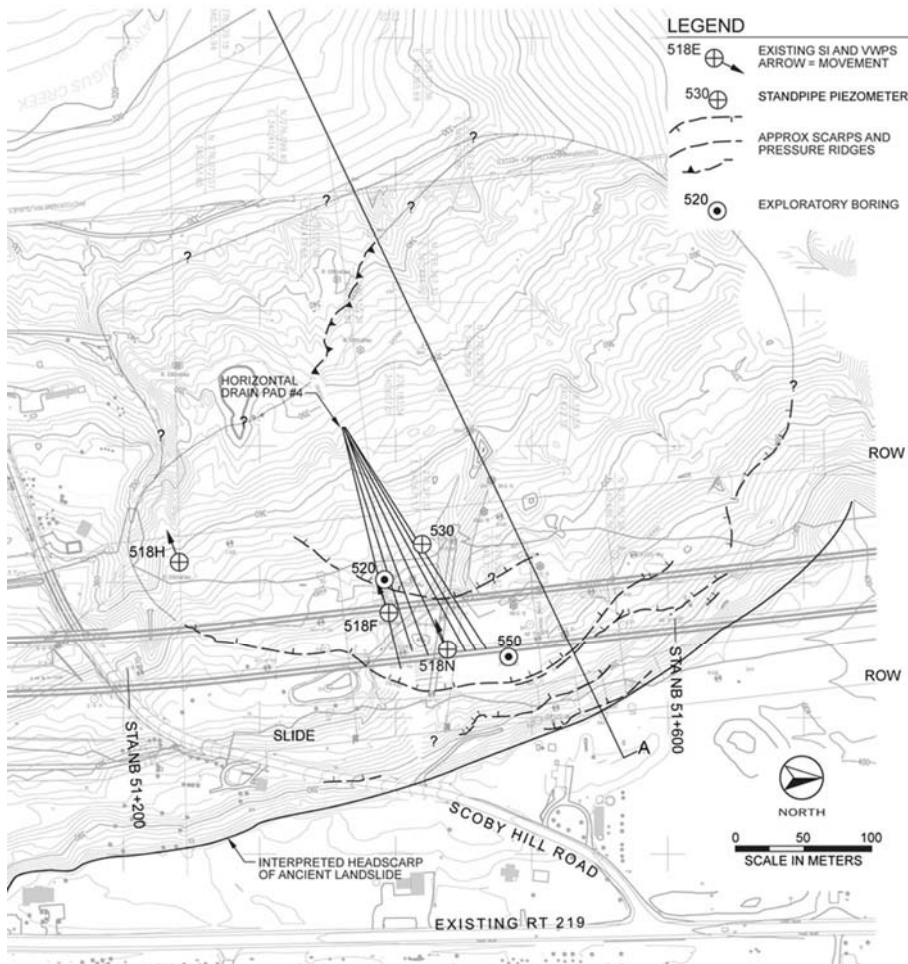| Rate of Slide Movement	
Summer '07	60-100 "/yr
Fall '07	10-20 "/yr
Nov '07 unload	2-8 "/yr
Early '08 after HDs	1-4 "/yr

FIGURE 3 Rates of Slide Movement.

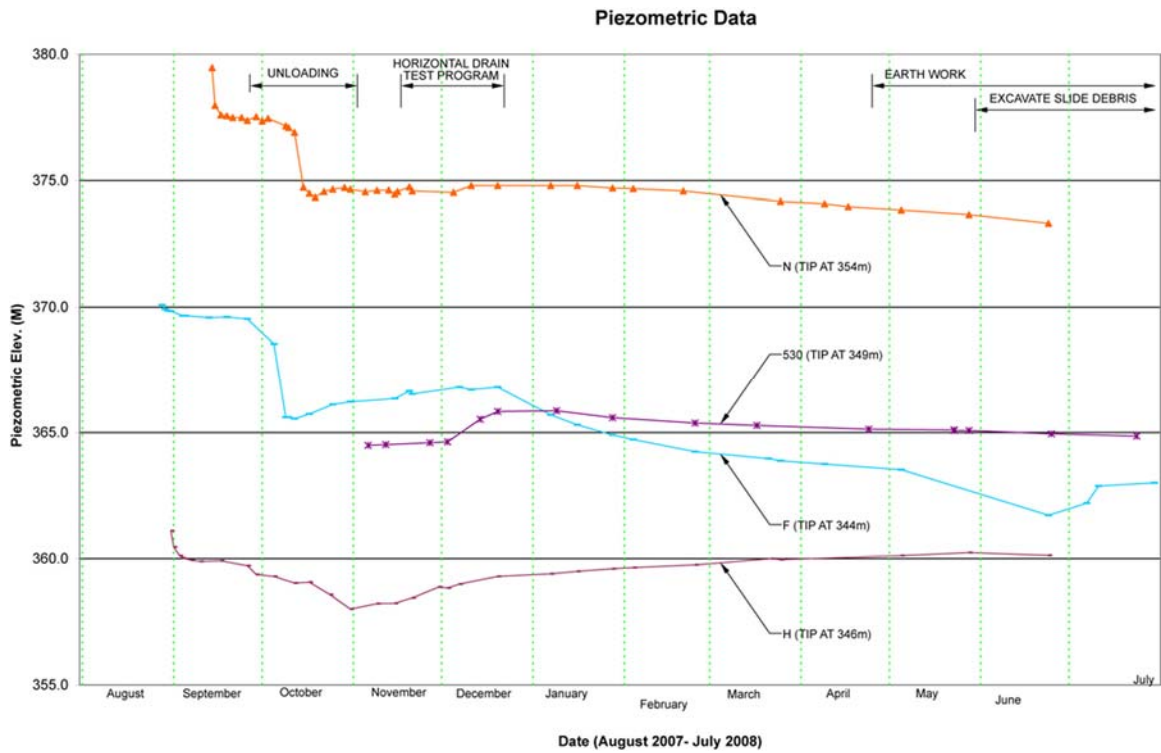**FIGURE 4 Site Plan – Test Horizontal Drains at Pad 4.**
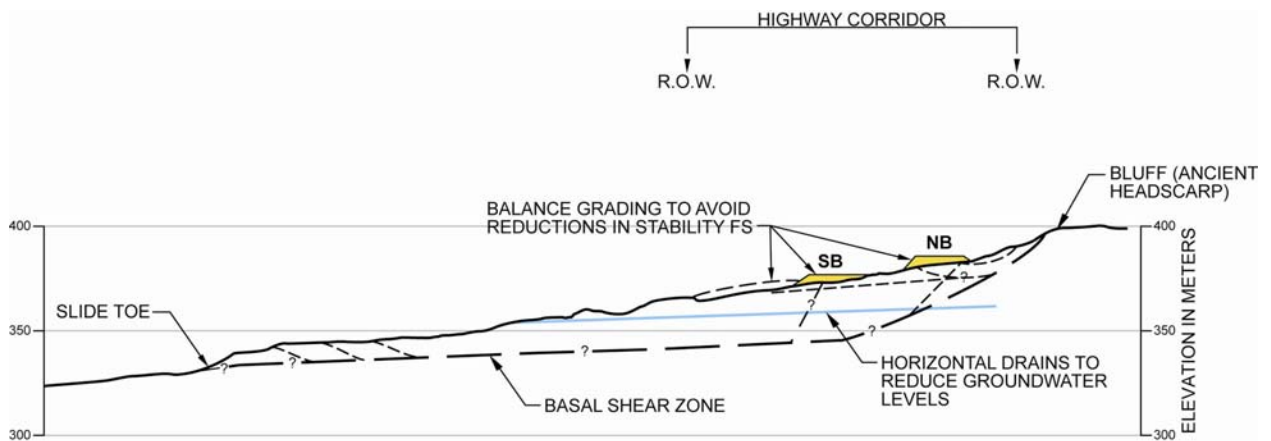
FIGURE 5 Piezometer Data (Test Horizontal Drains).

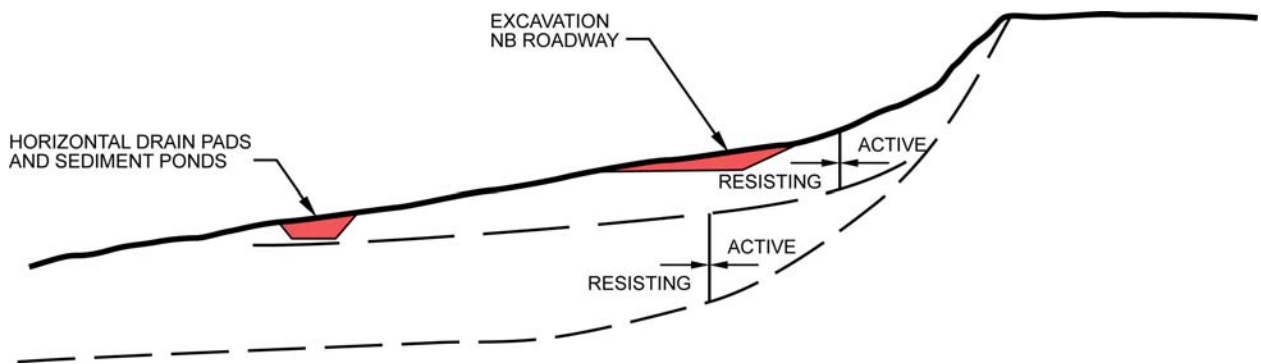**FIGURE 6 Cross Section Showing Balanced Approach (STA. SB 51+450).**

FIGURE 7 Excavation of Northbound Roadway Resulted in the Activation of Localized Nested Slides. Excavation for Sediment Ponds and Pads for Horizontal Drains Destabilized Both Global and Nested Slides.
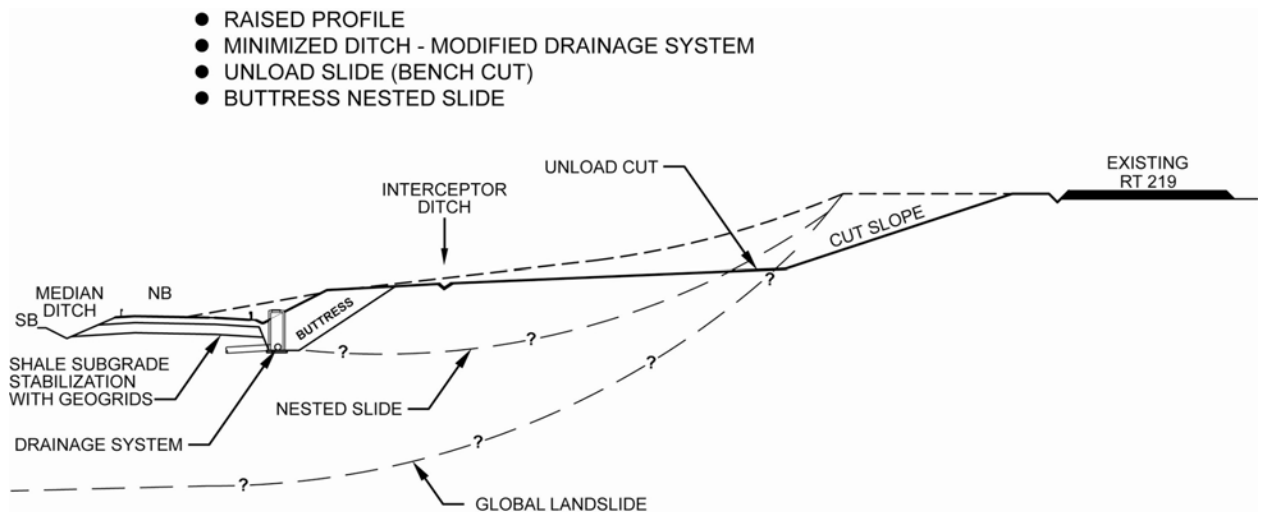
FIGURE 8 Mitigation Details for the Localized Nested Slides in the East Cut Slope.
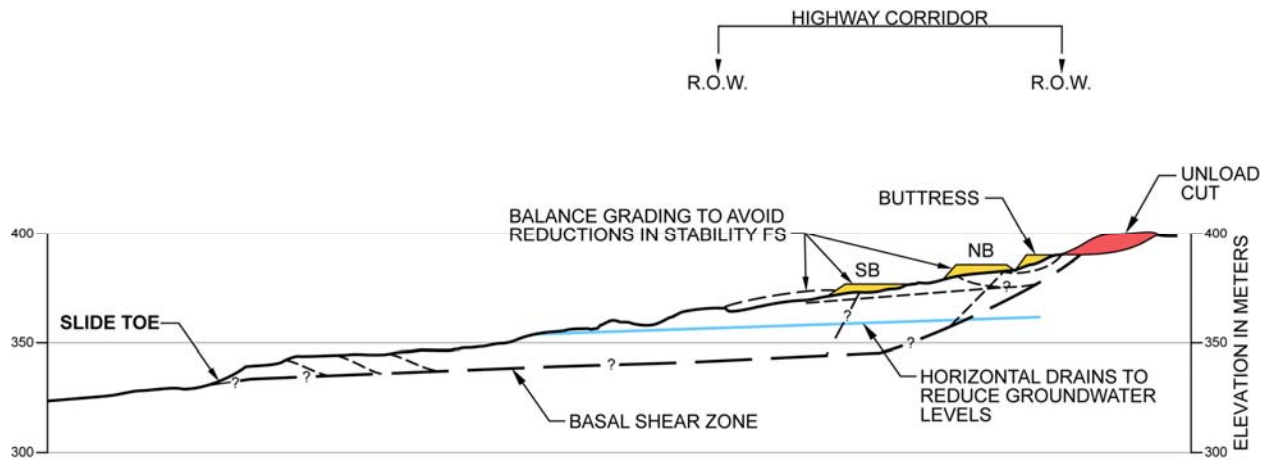
FIGURE 9 Cross Section Showing the Modified Balanced Approach (STA. SB 51+450).
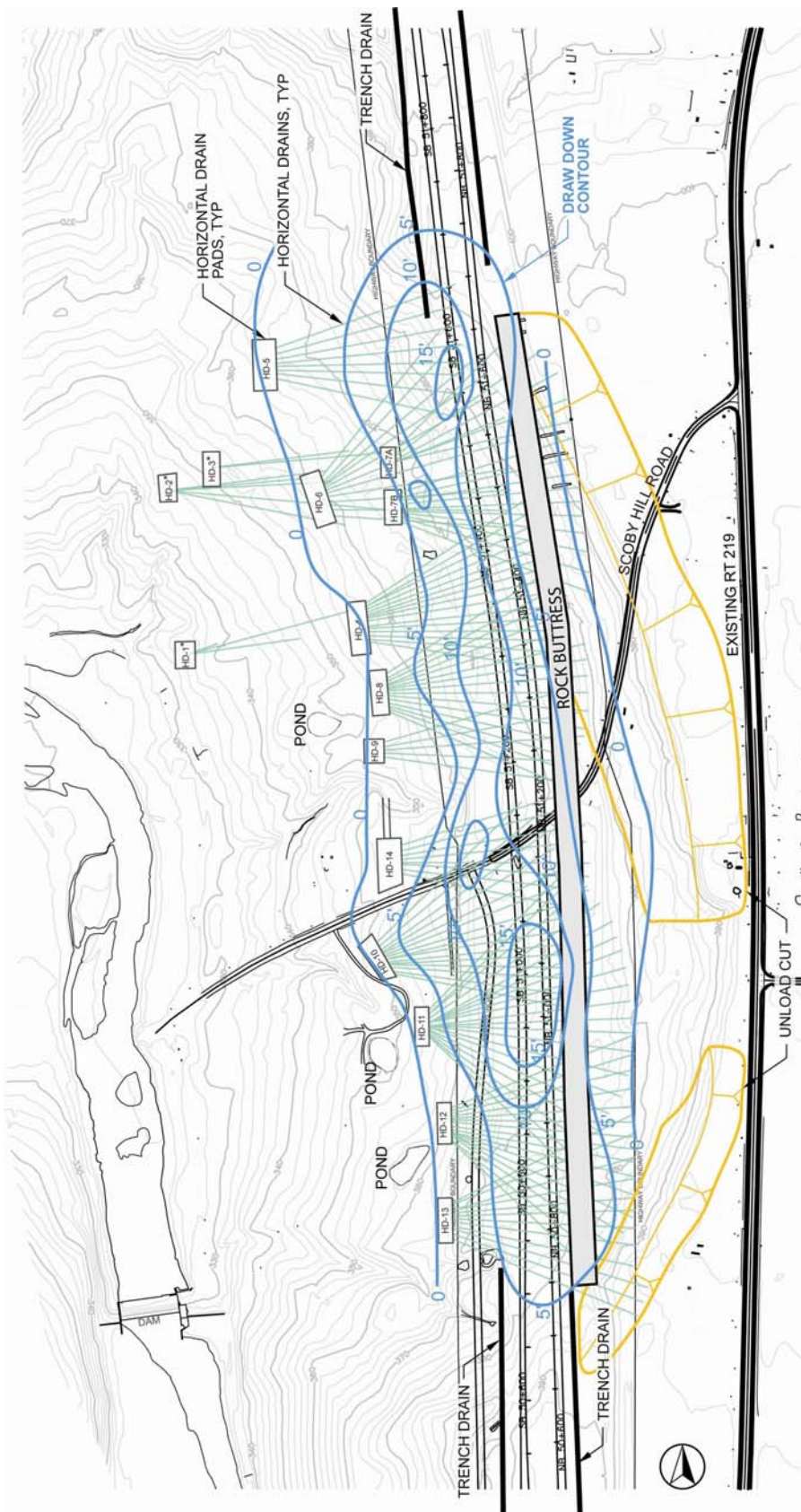
FIGURE 10 View of Horizontal Drain Arrays, Drawdown Contours, and the Extent of the Rockfill Buttress and East Cut Slope Unloading within the Landslide.

5.1

The Practical Solution for a Cave Located on a School Campus in Central Kentucky

Richard Wilson, P.G.

QORE, Inc.

Abstract

A school system in Central Kentucky found it necessary to address their expanding population of school age children by developing a new middle school campus. This campus is on property formerly of agricultural use. It consists of multiple buildings, miles of streets, acres of parking lots and thousands of feet of buried utilities. During construction of the middle school site and the related facilities, numerous sinkholes and karst features were encountered. It was during the construction of a sewer main adjacent to one of the roadways that a 2 foot by 2 foot sinkhole in rock was uncovered. Subsequent excavation for remediation of the sinkhole uncovered a large multi-level cave with flowing water. The cave trends under the road and toward the new school. Remediation consisted of excavation of the cave and karst features under the roadway and toward the school until sufficient roof strata thickness was obtained. Overflow relief from the cave was provided via a detention basin. Support for the roadway and forced sewer was achieved mainly with a combination of crushed stone, filter fabric and structural concrete.

The Jessamine Board of Education determined it was necessary to construct a new middle school east of Nicholasville, KY to address the increase in school age children in their growing community. From this idea was created the East Jessamine Middle School (EJMS). Jessamine County, being one of the fastest growth areas of Kentucky, decided to take a longer term view than just a school. They elected to go with a long range plan of developing a campus for future expansion as the need arose.   The selected site is located east of Nicholasville, KY on KY 169 (Richmond Ave). The campus site was previously a farm with few structures.

After site selection was made, the Architect - Sherman Carter Barnhart, along with Site Civil Engineer – Horne Engineering, developed the master plan for the new campus and the initial East Jessamine Middle School. The first building constructed at the site was a 122, 000 square foot facility, designed to address the immediate needs for grade 6 through 8. The geotechnical consultant retained for the design focused their recommendations at the initial facility and not the overall campus site.


In the spring of 2008 the Jessamine Board of education accepted a bid of 23 million dollars from general contractor DW Wilburn for the initial construction, some site grading on future building sites, Access Road No. 1 and utilities to support the campus. The general contractor subcontracted the site grading to Philpot Enterprises and the utility construction to Flynn Brothers Construction. QORE was contracted by the Jessamine Board of Education to provide

construction inspection and special inspection of the project. The project is on schedule for a summer 2009 completion.

Topography and Geology

The campus site is located in the Inter-bluegrass physiographic region which is characterized by gentle rolling terrain. Specifically this site, being a farm, was largely open fields with mostly grass cover with a few ponds and sinkholes.
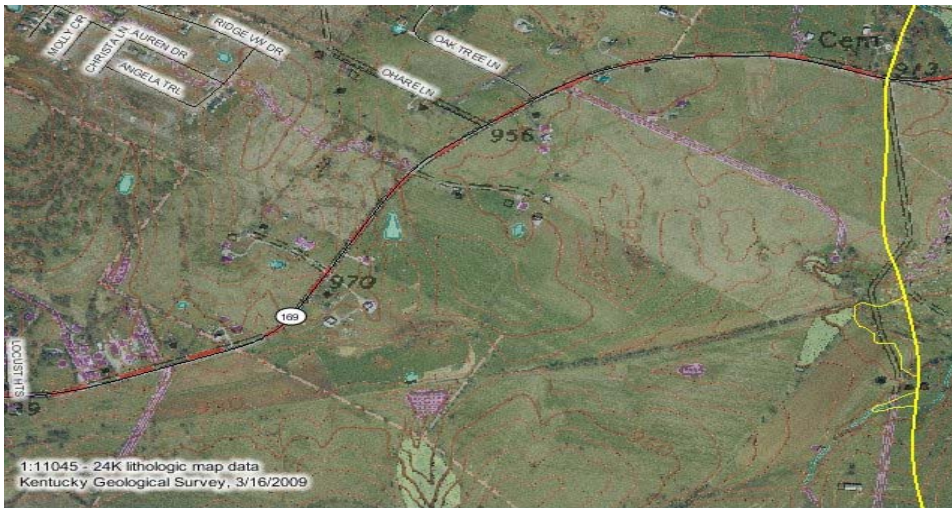
Geologically the campus site is underlain by Middle to Lower Ordovician Age Limestone. The rock unit is referred to as the Lower part of the Lexington Limestone (Ollr) or Grier Limestone (Olg). The unit is composed of limestone (80 percent), bluish-gray in fresh outcrop to brownish-gray where weathered. Shales occur in irregular beds. Where the overlying Brannon Member (50 percent limestone and 50 percent shale) is missing karst features may develop. Karst may also develop in the limestones of the Lexington between the shale beds resulting in karst on multiple levels.

1:11045 - 24K original GQ map image lithologic map data
Kentucky Geological Survey, 3/16/2009
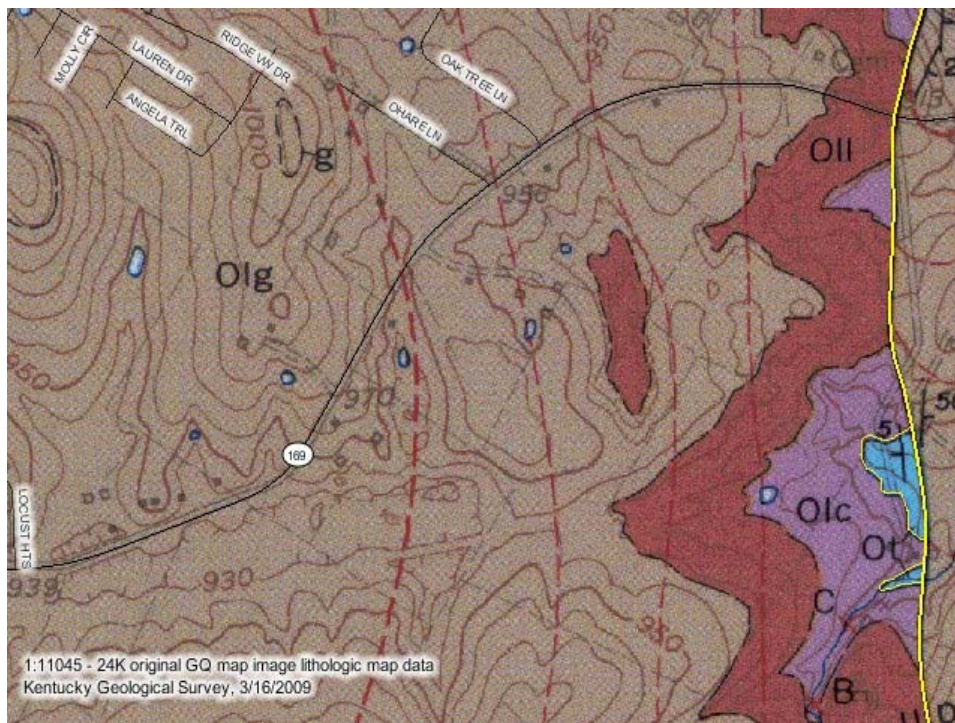
The farm's lower elevations contain no surface streams, while adjacent drainage basins have surface steams and springs in them. It is reported by local residents that water has been observed rising in the basin while no rainfall or surface flow is occurring into the basin. The conclusion is a highly mature karst system is located below the valley floor that has the ability to accept surface runoff until it becomes flooded at which point standing water in the valley occurs. The karst system also has the ability to flood from water originating outside of the school's surface drainage basin which results in surface flooding on the school site. Therefore, this is highly active karst operating on multiple levels.
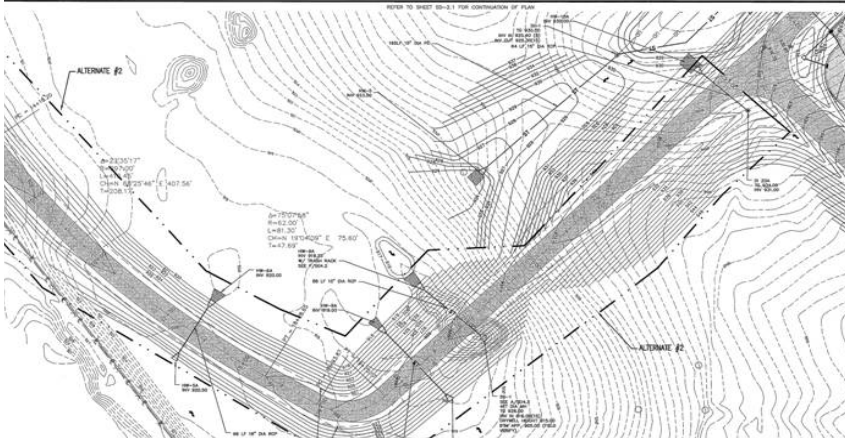
Access Road Number 1

Access Road No. 1 is located along the south side of this highly developed karst and crosses the karst near the middle of this basin. An eight (8) inch sewer line is located beside Access Road Number 1.

Karst Conditions

Karst conditions addressed in the geotechnical report concerning the building and parking areas included two open sinkholes located in the parking area.

Sinkhole in Parking Lot Looking toward Detention Basin

Other well developed karst was noted to the southwest of the building in the area of the access road, and it was recommended future investigation address this area. Treatments of sinkholes located near the access road and in the detention basin were not addressed at the time of initial design.

With the large surface disturbance created by the site grading for the school campus there was a need to address surface runoff. This site presents a challenge because it has a large closed drainage basin with numerous sinkholes and dropouts. A decision was made to construct a detention basin and dry well to address the surface flow. It was pointed out the potential problems with this type of solution (such as sediment transport to the underground, creation of new drop outs resulting in damage to other areas both on and offsite, and the capacity of the dry well) were largely unknown.

The detention basin is located to the west of the access road and the dry well is located to the east. Water is proposed to enter the dry well via a cross drain from the detention basin.

Construction Begins

QORE Property Sciences was selected to provide construction and special inspection for the new school campus. After a smooth 2008 construction season, in January 2009, QORE Inc. was requested by Sherman Carter Barnhart Architects to visit the site and make an initial evaluation of a depression (sinkhole) which had developed recently near the toe of the slope between the proposed future parking area and the Access Road No. 1.

Sinkhole in Slope

It did not appear to be located close enough to the school to cause any damage. No immediate threat to the roadway was likely although it was considered a possibility that an underground cavity may extend below the proposed sanitary sewer line and roadway requiring mitigation measures before the sewer line is installed and roadway paved.

QORE issued a field report on January 22, 2009 that recommended assessing the "sinkhole" when the nearby sanitary sewer trenches were excavated and the feature became exposed.

Another sinkhole was encountered during excavation for the sanitary sewer line parallel to Access Road No. 1, about 60 feet south of the one described above. QORE issued a letter dated February 25, 2009 "East Jessamine Middle School Sinkholes" that provided mitigation alternatives for these sinkholes as they were understood at that time. During excavation to mitigate the sinkholes an underground cave was discovered connecting the two sinkholes which necessitated the revision of QORE's recommendations.

Cave Looking toward School Complex

A site meeting was held on February 27, 2009, to discuss the remediation of this large unearthed karst feature (i.e. cave). Present at the meeting were Jessamine County School Board Superintendent and Board Members, the Architect, General Contractor, Site grading Contractor, Utility Contractor, Site Civil Engineer, Design Geotechnical Consultant and QORE Property Sciences.

A solution feature approximately 125 feet long, 26 feet deep, and 20 to 25 feet wide with cave openings at the end nearest the school was exposed while excavating the sinkholes   The cave extends 60 feet in the general direction of the school and branches in three directions. Water can be seen running down one wall and into holes in the floor of the cave. Rubble is present in the base of the excavation; therefore, it is unknown how deep this channel extends. The sides of the channel are composed of limestone bedrock. The end of the excavation closest to Access Road No. 1 contains broken bedrock which, in our opinion, appears to have collapsed into the cave system. QORE concluded based on the trend of the karst feature, that the solutioned conduit likely continues in this same trend into the detention basin located on the west side of Access Road No. 1.

At the cave opening, there is an undetermined amount of loose roof fall and soil lying on the cave floor. Above the cave debris is a cave opening estimated to be about 3 to 5 feet tall between the roof rock and the top of the debris. In-place bedrock located above the roof of the cave creates additional roof stability issues.

Cave Entrance

Collapsed Cave under Access Road No. 1 and Sewer Line

The following additional karst conditions were either observed or commented on by others:

- A karst slot feature at a higher elevation in an area designated as future development. This one trends at approximately 90 degrees and toward the cave.

- We noted that no standing water was present in the detention basin located on the opposite side of Access Road No. 1. This is significant because of the heavy rainfall event within the previous 24 hours leaving soil washouts and no evidence of water exiting through a culvert leading to a newly constructed dry well. In QORE's opinion, this is evidence of another level of karst located below the cave.

- It was reported by others that they observed both standing water and resurging water in the general area of the drainage basin located adjacent to Access Road No. 1 and the area frequently floods after heavy rains.

QORE concludes there are at least three levels of interconnected karst present on this site with each one flowing with water at different times as each lower level fills. Water levels are dependent on rainfall not only within the immediate property footprint but also within the entire karst drainage basin which is likely much larger than the surface drainage basin.

Therefore any correction must take into account this larger subsurface drainage area. Surcharging of upper level open conduits in the rock can occur when the lower levels fill and flood. Changing the subsurface water flow pattern can impede the established flow patterns. This change in flow conditions can increase the subsurface water pressure as the water backs up in the system of open conduits. This significantly increases the likelihood of creating new drop-outs along the conduits as water pressure builds up in the conduits and the flushing action increases.

QORE developed two options for treatment of the cave. Those options are outlined below:

Cave and Karst Remediation

Option Number 1

Excavate roof rock over cave entrance until 4 to 8 feet of stable rock is found.

- Remove weathered roof rock shelf located between the two excavated karst features to allow for more positive control of refill.

- Excavate all soil and rock debris from the opened cave until either solid rock floor is exposed or the opening in floor narrows to 24 inches. This is recommended to extend from the cave opening toward the detention basin.

- Line the walls of the excavated rock channel with filter fabric, and then place clean rock (KY #2 size stone) in the solutioned trench to within 2 feet of the intact rock rim of the excavation. The stockpiled stone from the on-site crushing operation appears sufficient. QORE defines the rock rim of the excavation as the interface between the in-place bedrock and the shot rock overburden. After the No. 2 stone is placed, the filter fabric will be overlapped to enclose the rock refill. A layer of soil about 2 feet thick will be "padded" on top of the filter fabric to protect the filter fabric. Once the pad lift of soil has been placed, construction equipment can then place compacted soil fill to the required finished grades.

- Because this is an active karst feature with a large amount of groundwater flowing on multiple levels, provisions must be provided to allow the continuation of this groundwater flow. The following scenario should be implemented at the cave entrance. Filter fabric (type IV geotextile fabric) should be placed from above the top of the cave roof, draped into the cave opening providing an angle of repose for the rock refill and onto the excavated cave floor. Approximately 2 feet (thickness) of No. 2 crushed stone

276

should be placed on top of the filter fabric into the excavation. This should protect the filter fabric from the clean rock refill, allow water to flow through the rock refill, and prevent soil migration out of the cave.

- While the base flow of the system is likely confined to the lower level conduits, we believe is it prudent to incorporate some provision for handling water that may surcharge into the cave and backup into the "upstream" conduits. We recommend installing a 36-inch diameter equalization pipe (HDPE) into the cave opening and through the filter fabric into the rock refill in the excavated solution feature. Extend this equalization pipe to the detention basin. Install a headwall on the discharge end of the equalization pipe and install a grate to prevent access to the pipe. This equalization pipe will allow water flow from the cave into the basin during periods of high flow conditions reducing the likelihood of surcharging the open conduits "upstream" of the cave and aggravating the unknown conditions nearer the school.

- The exact elevation or grade of the 36-inch equalization pipe is unknown at this time. However it is our intent that the outlet end elevation in the basin be at or near the base of the headwall going to the existing drywell. The equalization pipe will have positive drainage from the cave to the basin. After the equalization pipe is installed, continue refilling with No. 2 crushed stone as described above.

Sanitary Sewer Line

A sanitary sewer line crosses this cave at a skew to the centerline of the cave for an approximate 20 foot span, and QORE felt it was necessary to address the long term stability of this sewer line. We recommend constructing a concrete slab extending from bed rock to the sewer pipe bedding elevation. A recommended method to accomplish this follows:

- After excavation of the solution feature is completed begin installation of filter fabric and No. 2 Crushed Stone refill as described above.

- Continue with compacted No. 2 crush stone refill to the base of the 36 inch equalization pipe installation grade.

- Install equalization pipe in accordance with the manufacturer's recommendation.

- After installation of equalization pipe is complete, continue with the crushed stone refill from the top of the 36-inch equalization pipe to the base elevation of the concrete support mat for the sanitary sewer line. Install the reinforced concrete mat on the compacted crushed stone refill. The concrete mat should extend from one side of the

karst feature to the other to provide continuous support of the sewer line.   Coordinate with Civil Engineering consultant to determine the thickness of the pipe bedding required between the mat and the sanitary sewer pipe and between the top of the sanitary sewer pipe and the subsequent No. 2 stone refill.

- An alternative to the concrete mat is to support the sanitary sewer pipe on the web (between the flanges) of a horizontal steel H-beam.   Place the H-beam horizontally so that it rests on the intact rock on both sides of the solution feature. Hoe-ram out a rock seat and grout the H-beam to the rock so that it is firmly held in place. The sanitary sewer pipe can then be laid along the beam, between the flanges, and secured with galvanized pipe clamps. Seat the H-beam in the crushed stone as a bed. This alternate must be approved by Horne Engineering but may be cheaper than the concrete mat.

- After installation of the sanitary sewer pipe continue placement of No. 2 crushed stone refill as recommended. Once this elevation is achieved closure of the rock refill as described above is recommended.

A drawing indicating the typical repair cross section is shown below along with details on the treatment of the cave entrance, and backfilling at the sanitary sewer line.

Option Number 2

The cost of Option Number 1 will be expensive. As an alternate, the Jessamine County Schools could clean out the feature and leave it open. From a geotechnical perspective, this would be equivalent to remediating the feature. We understand that other considerations are involved such as safety and final form of the area affected. But a "do-nothing" alternative is viable from the geotechnical perspective. To that end the support of the sanitary sewer line and re-grading around the feature are the main technical issues.

- Support sanitary sewer line by means of a reinforced concrete beam, a steel beam, or pillars to provide adequate support (design by others).
- Install steel grate across the cave entrance to prevent entrance into the cave. This can be attached to the rock face.
- Install a perimeter fence around the excavation and cave to prevent entrance into the area.

Summary

 The decision was made by the Board of Education to construct Option Number 1 with concrete mat to support the sanitary sewer line. Construction took 10 days to complete and the overall project schedule was maintained.

Installation of Filter Fabric

Pipe Installation

Rock Refill over Pipe

Filter Fabric Closure

Forced Sewer Main Structural Pad

Completed Remediation

5.2

Some Notes on the Geotechnical Investigation Process

Verne C. McGuffey

New York State Dept of Transportation (retired)
22 Lombard St.
Schenectady, New York 12304
518-393-3565
Geo96pop@aol.com

Introduction

This discussion is an attempt to document some of the lessons we learned through the "Interstate years" in hopes the messages can be used by today's practitioners.

We have learned much over the years about which investigative processes work best for different problems and sites. However, many of today's Engineers & Geologists never were exposed to the numerous learning experiences (failures) of the early practitioners. I have seen many mistakes repeated. Some are site and soil specific, some are process specific, and many are major goofs.

I have been there & done that. I had my chance to make many mistakes, so why should I deny others that joy? (No one needs to make as many mistakes as I did.) I hope this collection of examples of mistakes, and examples of directions to solutions will help others. There are too many issues which can influence the outcome of any one decision that this collection can only be a beginning reality check for those starting a new job in an unfamiliar setting.

Problems with the Start of Investigation Process

Some examples of what can go wrong:

A) Example 1: Urban area

Dozens of borings in streets of a built-up city area showed no problems for construction of new road. After construction started , settlements occurred and walls moved laterally. A review of old (1800's & 1700's) USGS Topographic sheets showed old salt water inlets had been buried & houses built over them. They found

lots of buried organic and lots of differential settlement, resulting in major repair expenses.

Note: *Some very old data is very difficult to find. Talking with locals & historians may give clues to existence and possible locations for old data. Reliance on new boring data may often be very misleading. Borings are never taken through occupied homes. Few borings are taken after site demolition. Knowledge of geologic history is essential to understanding how the present site data should be evaluated. (http://docs.unh.edu/nhtopos/nhtopos.htm)   Is believed to have NY and New England topographic maps.*

B) Example 2: Rural Interstate highway

I received a call that there was a shear failure on the mainline of an Interstate Highway during fill placement. A quick review of the USGS Topo sheets showed that there was an old meander channel in the area and no borings were taken in that area. Sure enough, there was buried organic in the old meander channel. This cost a lot to correct, but would have been very cheap to fix if it had been identified in advance. This resulted in setting up a training session for site investigators so simple clues, like old stream meanders, would not be overlooked.

C) Example 3: Urban Interstate

Undisturbed samples at a structure site indicated that the approach fill could not be safely built. However, there was an existing railroad embankment on the same soils only 100 feet away. The designer decided that the existing railroad fill was better evidence than the samples and lab tests. However, a persistent investigator dug into old records & found that the original railroad embankment had problems when built. The problems were solved by building hollow concrete boxes in the fill and burying them with a thin cover so it looked like regular fill when in effect it was a very light weight approach fill. This information gave the investigators & designers enough confidence to include expensive light weight fill in the roadway design to prevent very costly remedial treatment if nothing was done.

More examples: Not recognizing the story the ground is showing

A) Example 1: Moving Wall

An old concrete crib wall about 20 feet high was bulging and showing signs of distress. The investigators had borings & field measurements and decided that the backfill was pushing out the wall. They then rebuilt the wall and were surprised to see the new wall starting to show signs of distress. A look at old airphotos showed that the problem was bigger than the investigators had considered. There were patches in the pavement at the edges of what turned out to be an extremely large landslide. There were signs of sliding nearly 1000 feet up the slope and the investigators had never looked that far. The investigators were structure oriented

284

and the only geotechnical Engineers involved were young and inexperienced and had missed the key elements related to the wall movement. (Patches in the old pavement and a circular shape to the topography on the hill above the wall.) The wall movement was stopped by installing long horizontal drains into the shear plane of the large landslide.

B)   Example 2: Moving railroad tracks and house

A new roadway was being constructed 500 plus feet uphill from a railroad track, a river on a bend, and a house near the railroad. The railroad company had cut out sections of tracks because they had slid off the ties, or moved the ties. After weeks of cutting out sections they went to the highway office to see if they might know what was going on. At the same time, a homeowner went to them with the complaint that he kept having to cut off his doors to be able to open them. Both the railroad and the house were sitting on the toe of a very old landslide and the small amount of construction of the new road set the old slide into slow movement. The original investigators had not reviewed the old air photos, so had overlooked the existence of the old landslide. It is also unusual that more attention was not paid to the outside of a bend in a river in mountainous terrain.

C)   Missed sheeting under old railroad bed

A new roadway was constructed over an abandoned railroad bed and as construction started, unusual settlements and movements occurred. The railroad bed was across a long, deep swamp. No one looked into why the rail bed was so good over a deep swamp. Old records showed that the railroad had installed steel sheet piles along both edges of the railroad bed and tied them together with tie bars. The new road was wider than the old tracks so new fill was placed over the deep swamp. Also, the road preparation had damaged some of the tie bars, so strange vertical and lateral movements took place.

More examples of mistakes:

Relying on "industry standards", or "common practice"

Example 1: (1960's practice)

Soil borings were taken at the proposed structure site and one taken every 200 feet back until the grade was low enough to not present a problem for stability or settlement. When equipment tried to prepare the area for construction, some got stuck in the middle of the fields.

The site had been used as a waste disposal site and 50 ft. strips of stiff clay had been removed to 15 feet depth starting from the property line (at railroad ROW and structure location,). The strips had been filled with miscellaneous garbage and loose cover. The excavation had removed the very strong surface clay and

left the very soft clay, so there was a stability and settlement problem not foreseen by designers. The borings (taken at uniform spacing equal to a function of the constructed garbage strip spacing) were taken through the natural soils remaining between the strips so they did not show any problems. The result was extra cost and delays and reduced performance. The process problems that caused this mistake included the following:

- o Locals weren't contacted but were aware of the garbage placement activities.

- o The site walk and drilling were done in winter with snow cover so no surface evidence was visible.

- o Old air photos used in site study were taken before the waste site was developed.

- o New photos showed the waste site evidence, but were not reviewed because they were not readily available (they were at a different Government office).

Example 2: (1940's Standards)

Borings were taken every 500 feet and at structures and all were taken to 51.5 feet depth. Here are some of the results:

Swamps with peat deposits were missed as well as old clay landslides. Rock was cored to 51.5 ft. for low fills. Groundwater was not noted in borings, so cut and trafficability problems were missed. Settlement took place from soft soils below 51.5 feet where no samples were taken.

The problems were made worse by a poor construction inspection engineer and inexperienced contractor. Construction was tried across the swamps so failures and major long term settlement occurred. Excavation was done into the toes of landslides causing major slide movements. Lots of other bad decisions were made, and the resulting pavement was not rideable after completion. A second contract was let to try to correct as many problems as possible. However, it took major rebuilding to get good rideability.

Problems in planning exploration programs:

Planning the exploration program requires much input about the proposed project construction actions. Here are a couple of items needing review:

- Construction plan or expected actions

- Likely time of year and weather expected

- Likely construction methods and schedules

- Details of the final product including water control

- Expected maintenance practices

- A look at possible changes

A couple of examples:

Project changes:

Good example - warning of problem near site. My preliminary site report said to immediately take a boring if the road was moved to the north. Five years later, I received a boring. They had read and used my report. The site was near a landslide and the new location required fill to be placed on the top of the old slide. After negotiations and further studies, the road was moved off the slide and a wall was put in a stable uphill slope. If I had not noted the problem next to the proposed construction, a major, costly failure would likely have occurred.

A bad example occurred when the designer's & construction staff made a field change and neglected the note on the plans of an old slide next to the road. When they tried to build it, it slid and destroyed the water supply to a small city.

Some problems effecting outcome of the drilling program:

Equipment Problems

Drill rigs:
1) Don't use "Walking beam", or well drilling rigs. Often excessive blow counts were observed because the operator couldn't, or wouldn't allow enough slack in the cable. The weight did not free fall.

2) Plugs in Continuous flight auger rigs: Using a plug to eliminate clean-out between sample intervals may miss important changes in soil strata. Also, the plug pushes the natural soil away from the tip of the auger and disturbs the soil for the next sample. This gives misleading strata information as well as blow counts and moisture contents. It also may destroy integrity of an undisturbed sample if taken.

Problems with Drilling Methods

Here is a partial list of common problems: Overdrive of samples is common. Large chopping bit clean-out drives course material ahead of casing into next sample. Withdrawal of the chopping bit drops the water level in the hole. This causes negative pressure in the casing and often causes uplift or flowing into the casing. Samples obtained often will be totally disturbed and may not be representative of the natural material. (blows, MC, PI, type, etc.) Since the flow-in may leave the soil above the planned sample depth with no resistance, the sampler often is full of flowed material and therefore the blow count will be off as well as having non representative sample material. Often the casing and rods are not even lengths and assuming it to be 5 or 10 feet long is not correct. Also, the coupling changes the length. Accurate measurements from tip of drive shoe to

top of each section of casing are needed to prevent major disturbance to the soil. This is especially important for undisturbed sampling. If the casing is longer than the drill rod string, then the casing doesn't get properly cleaned and the sample obtained (from inside the driven casing) bears little resemblance to the natural soil. (Note: often accurate measurements of drill rod string are taken, but no measurements of the casing string are taken,). Using small diameter clean-out rods, or using a weak wash pump can give poor results. Insufficient up-flow velocity will not allow the water to carry the coarser particles up to the surface and out of the casing. The result is "fall back" after the pump is shut off, the material in suspension falls back into the casing and appears to be "flow in". Rapid dropping of the drill string (surging) may increase the velocity sufficiently to clean most of the material out, but it is better to get a bigger pump and use larger diameter rods.

Some special drilling issues:

Bent rods, or poor connectors. When using drilling mud instead of pipe casing, any small deviation from straight rods will cause the open sample spoon to hit the hole sides and be full of erratic soils during deep explorations. Poor sampling equipment or lumpy mud. The ball check valve my not seal because of wear or because of lumpy drill mud allowing the full head of fluid in the drill stem to push out the sample during retrieval. Use of salt water (or contaminated water) can change the character of the dill mud, so fresh, non chemical water should be used. When drill mud is used, separate observation wells may be needed to identify at least the surface ground water.

Laboratory problems

Transcription errors (similar names & numbers):

Borings & samples are usually given similar identification numbers. There can be dozens of "boring # 1" and "sample # 1" on each project. Often taken at different times and with different reference systems. This can lead to transcription errors. My staff transposed I-550 to I-505 & it took months to find and correct all potential errors. One project had structure numbers that changed as the project developed over many years, so it took much effort to find where the data should really be used. Errors of transcription can be found in any step of the design & construction activities.

Sample containers:

Cardboard containers allow the samples to dry quickly & change character & moisture. Plastic containers can slowly allow moisture changes & can introduce volatiles. Glass works best if there is a good rubber seal for the lid & it is put on tightly. Small opening into the jar (lids) can lead to mashed & damaged samples that are hard to get out of the jar. Too small containers do not provide space for representative samples. Transit vibrations can completely change the character of the samples as can exposure to heat or freezing. Sometimes it is good to run field moisture and characteristics tests on parts of the samples that won't fit into the jars.

Here are a couple more potential problems: Mishandled undisturbed samples; Sample preparation; Equipment calibration; Inadequate data review and correlation

Some guiding principles:

- Each site needs different approach to evaluate the potential problems of any planned construction.

- Each construction option has different evaluation needs.

- The evaluation process therefore must be a continuing process with changes made as information is gained from the designers and as information is gained from the Geotechnical investigation team.

- The quality of the data obtained in the investigation process must be continually evaluated as new information is gathered. There should be no conflicts unresolved between original data and later data.

*Final Note:

The most important boring is one never taken & the most important test is the one never run.

5.3

High Energy Rock Fall Embankment Constructed Using a Freestanding Woven Wire Mesh Reinforced Soil Structure

-Recent Experience in British Columbia, Canada

Michael Simons, P.Eng.
Technical Manager
Maccaferri Canada Ltd.
400 Collier MacMillan Drive, Unit B
Cambridge, ON N1R 7H7
Phone: 519-623-9990
Email: msimons@maccaferri-canada.com

Steve Pollak, P.Eng.
Rockwork Engineer
BC Ministry of Transportation and Infrastructure
Geotechnical and Materials Engineering
South Coast Region
7818-6th Street
Burnaby, BC V3N 4N8
Phone: 604-660-8047
Email: steve.pollak@gov.bc.ca

Barth Peirone, P.Eng.
Western Regional Manager
Maccaferri Canada Ltd.
736 Granville Street, Suite 612
Vancouver, BC V6Z 1G3
Phone: 604-683-4824
Email : bpeirone@maccaferri-canada.com

ABSTRACT

This paper discusses the site history, design, installation, and recent post-construction experiences with an 8m high rock fall embankment built on BC Highway #1 (Trans-Canada Highway) near Boston Bar, British Columbia.

There have been over 60 recorded rock fall events at the site since the highway was constructed in 1958. Numerous attempts have been made since 1958 to mitigate the rock fall hazard using different techniques with limited success.

The new rock fall embankment was built using a double sided, woven wire mesh, gabion-faced, mechanically stabilized earth system. The structure was designed to withstand a maximum rock fall impact energy of 10,000kJ. The reinforced soil embankment has a maximum height of 8m, with a maximum base width of 7m.

INTRODUCTION

Posted rock fall hazard zones are common throughout the highways of central British Columbia. Since the construction of the Trans Canada Highway through the Fraser Canyon in the late 1950's, there have been numerous areas along this highway that have required some form of rock fall hazard mitigation.

The section of the Trans Canada Highway, Highway #1 from Hope to Lytton is one of the most scenic drives in Canada. It contains numerous areas that have been identified by the British Columbia Ministry of Transportation (BC MoT) as rock fall hazards. Many different methods to mitigate these hazards have been implemented over the years, with varying degrees of success. The section of Highway #1 from 53.3km to 53.6km east of Hope is one of these areas.

The site, referred to as Slide 5, is located south of the Hells Gate Rapids (Fig 1.).

This section of highway was originally constructed in 1958. Shortly after the highway was opened, indications of slope instability were observed and rock fall events were recorded. Between 1960 and 2008, over 60 rock fall events have been recorded where material reached the highway. Some of these rock falls have resulted in damage to highway infrastructure, vehicle damage and personal injury.

There have been a number of attempts made to mitigate the risks due to rock falls at this site. In 1961, a concrete wall was constructed. The concrete wall, known as the Ferrabee Wall, is 255m long and 2.4m high (Fig. 2). Behind the wall, there is a rock fall catchment area that varies between 8m and 22m in width. A diversion trench was excavated into the slope in 1975 in an attempt to re-direct rock falls away from the highway. In 1976, the highway was relocated westward 10m in an attempt to create additional catchment width. This catchment area is routinely filled with over 1000m^3 of debris, resulting in rocks bouncing over or breaking through the concrete wall.
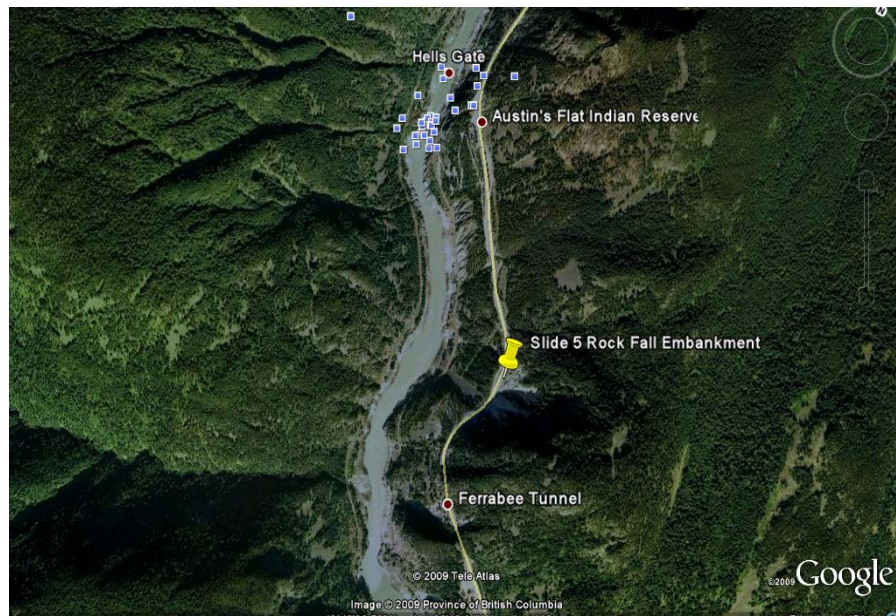
Fig.1 – Site Location

Fig. 2 – Highway #1 looking northward at Ferrabee Wall and rock fall slope

292

SITE GEOLOGY

Slope stability studies conducted for BC MoT have summarized that the site was formed in a postglacial rock slide that resulted from a wedge failure along two major faults. Sliding was probably initiated by glacial scour and river erosion at the toe of the slope resulting in removal of support. Slopes in this area were probably marginally stable before highway and railway construction. This slide debris is continually sloughing and ravelling. The underlying bedrock consists of Late Eocene to Early Oligocene (Tertiary) rocks of the Hells Gate Pluton (dated 35 Ma at the southern edge) on the western Coast Belt. The Hells Gate Pluton consists of variably fractured biotite hornblende granodiorite, locally porphyritic with feldspar phenocrysts, its eastern boundary apparently faulted on the Hope Fault (Monger and Journeay, 1994).

Surficial soil and talus rock material consists of silt to boulder sized material in varying proportions. Overburden or talus thicknesses may exceed 12m in some areas.

The rock cut and eroding portions of the talus slope generally appear unvegetated. Vegetation within unexposed talus areas consist of shrubs, trees with diameters that may be over 200mm and other ground cover.

The dominant problem at this site appears to be a post-glacial slide that has resulted in rock falls from the talus or colluvium raveling due to the steep slope. Ongoing erosion in the talus/ colluvium soils has resulted in the slide scarp experiencing a regression of approximately 200m in 40 years.

DEVELOPMENT OF DESIGN CRITERIA

During the 1970's and 1980's, BC MoT conducted numerous engineering studies in an attempt to develop rock fall mitigation structures for this site. In 1977, BC MoT conducted 350 rolling rock tests at the site to determine path and measured bounce heights of the rock falls. Steel cable rock fall catch fences were proposed based upon these studies, but were ultimately rejected due to the required strength of the protection structure exceeding the strength of the catch fences available.

Mechanically Stabilized Earth (MSE) structures have been in active use in transportation related infrastructure for over 30 years. The ability to construct two MSE structures back to back has resulted in the development of narrow embankments that have been successfully used as noise and rock fall structures around the world. A narrow embankment can be defined as a stable structure that has a base width less than the height of the structure. These structures can be vertical/near-vertical berms, reinforced steep vegetated slopes, or a combination. BC MoT began a review of the Slide 5 site in late 2005 in order to determine the suitability of an MSE-style structure for use as a rock fall embankment.

Based upon computer simulations using the RocFall program from Rocscience and the results of the rolling rock tests conducted BC MoT, it was determined that any embankment structure would be required to withstand a design impact of 10,000kJ. The rocks would range in size from 0.6m to 3.0m in diameter. The structure was required to start at 6m in height, with a maximum height of 8m. The proposed rock fall embankment was required to fit into the existing roadway platform, consisting of a 10m wide shoulder in front of the Ferrabee Wall. A 3m shoulder was required in front of the proposed embankment, so the maximum design width of the structure was set at 7m. The length of the proposed structure was set at 96m. The structure was required to have a maximum vertical batter of no more than 10 degrees.

BC MoT contacted Washington State Department of Transportation (WSDOT) to learn about their experience using a rock and wire mesh faced embankment as a rock fall embankment on SR20, North
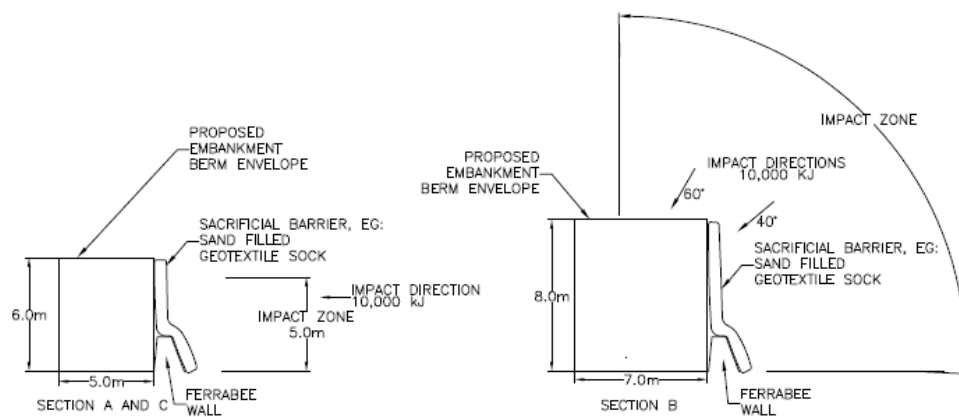
Cascade Highway, between Newhalem and Diablo.

To reduce maintenance requirements on an exposed woven wire mesh facing, BC MoT decided to include a sacrificial barrier on the impact side of the proposed embankment.

The design concept is illustrated in Fig. 3.

In January 2006, BC MoT contacted Maccaferri Canada Ltd. regarding the feasibility of their embankment concept and to discuss the detailed design of the embankment using double twisted woven wire mesh materials. Double twisted woven wire mesh materials are used extensive in BC for rock fall drapery systems and soil retaining structures.

TERRAMESH® SYSTEM DESIGN

Detailed design of the rock fall embankment began in February 2006. In order to minimize the cost of the structure, it was decided to investigate the use of an MSE system in lieu of a conventional solid woven wire gabion gravity structure. The use of the MSE system would allow for the construction of an engineered dense core of compacted sand and gravel material with a flexible gabion basket facing. Constructing the core of the structure with engineered fill was more economical than using rock filled gabion baskets. The Maccaferri Terramesh® System was proposed as an efficient combination of flexible facing and reinforced engineered backfill core.

The Terramesh® System is a modular system that is similar in concept to woven wire gabion basket with an integral soil anchor. It is manufactured from soft tensile, heavily galvanized and PVC coated double twisted steel wire mesh. The wire mesh used to manufacture the Terramesh® System is manufactured in accordance with ASTM A975-97. The facing and the tail are made from the same mesh panel. The unit is formed by connecting the back panel and a diaphragm to the main unit, creating rectangular shaped cells. Granular backfill is placed and compacted on the mesh tail unit, thereby reinforcing it. Terramesh® System units are typically supplied as 2m wide units with a single layer of woven wire mesh reinforcement having a length determined for the individual structure design. The units can be either 0.5m or 1.0m in height. These units are intended for use in structures that are of a traditional nature in that there is a reinforced soil mass holding a retained soil mass in behind.

Double-sided reinforced soil structures have been constructed in Europe for use as rock fall embankments. These structures allow for the construction of tall embankments that are capable of withstanding very high rock fall impacts in areas that are unsuitable for the use of traditional rock fall catch fences. The Italian head office of Maccaferri (Officine Maccaferri) has developed experience in the design of rock fall embankments. This experience was utilized in the design of the Slide 5 embankment.

The design concept provided by BC MoT set the physical envelope into which the proposed structure must fit. Given the design constraints, it was necessary to determine that the structure would:

1. Be sufficiently robust to survive the impact of the design rock fall event.
2. Be structurally stable as a free-standing embankment.
3. Constructible

In order to determine the structural dynamic response of the embankment to the design impact rock fall, it was necessary to determine the penetration depth of an impacting rock fall. There are currently various methods in Europe that are used for this determination (Kars 1978; Calvetti 1998; Peila 2004). The design rock fall event was assumed to be a single boulder, approximately 5m³ in size and traveling at 30m/s. The depth of penetration of this boulder into the embankment was determined to range from 1.0 -1.5m. Based on the depth of penetration, the structure was required to be a minimum width from outside face of embankment to outside face of embankment of 2 times the maximum penetration depth.

295

Based upon the site constraints, the base of the embankment was set at 7m (face to face of embankment). Using this initial base width and a maximum vertical batter of 10°, a model was created using the program MacSTARS 2000 in order to check the static stability of the proposed embankment structure. MacSTARS 2000 is a program developed for Maccaferri that is used to perform slope stability analysis using different types of reinforcement and complex design scenarios. Stability checks are performed using conventional Limit Equilibrium Method methods (Bishop or Jambu); either with or without the presence of a reinforcement configuration.

Figure 4 shows the overall configuration of the 8m section of the embankment. The reinforced soil core of the embankment was 5m at the base plus 2 -1m wide woven wire gabion baskets facing elements (7m total width). The structure was segmented into 4 - 2m high vertical blocks. Each block was set back 0.25m at the face from the underlying block. At the highest part of the embankment, the reinforced core was 3.5m plus 2 -1m gabion units (5.5m total width).

The Slide 5 embankment could have been constructed using typical Terramesh® System units. Using typical units would have had reinforcing mesh being overlapped at each layer of reinforcement, resulting in
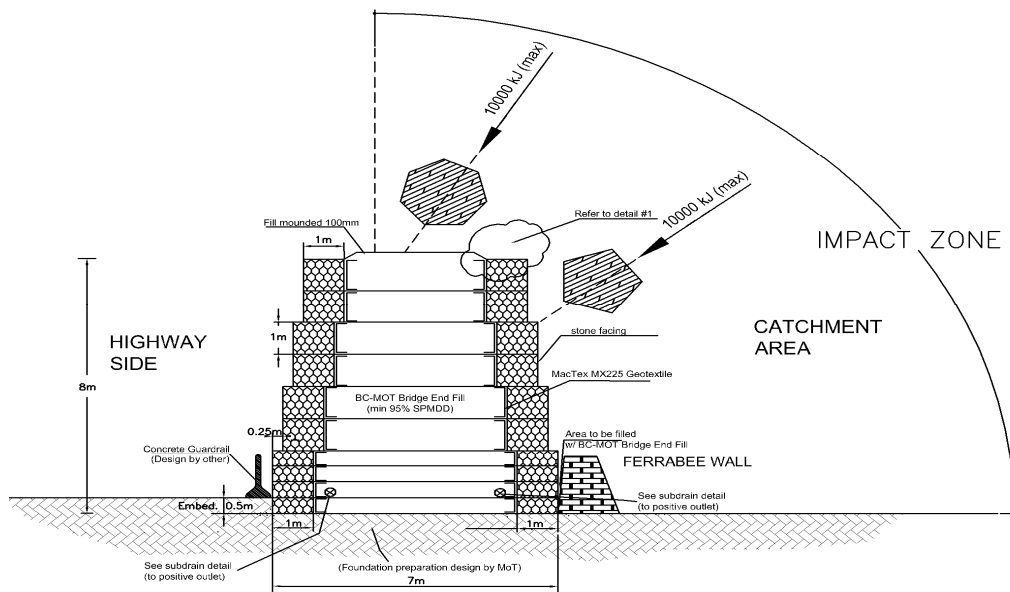
Fig. 4 – Terramesh® Embankment Section

a significant amount of mesh wastage compared to the overall size of the structure. Given the narrow configuration of the reinforced embankment, it was determined that it would be easier to custom manufacture single, double faced Terramesh® System units that would have a series of variable lengths (distance from unit face to unit face) with a standard 2m width and heights of either 0.5m or 1.0m (Fig. 5). Each unit was individual identified in order that it would be assembled and positioned correctly within the embankment.

The location of the embankment is on the outside edge of a slight horizontal curve in Highway #1. The layout of the new embankment was required to follow the curve of the existing Ferrabee Wall.
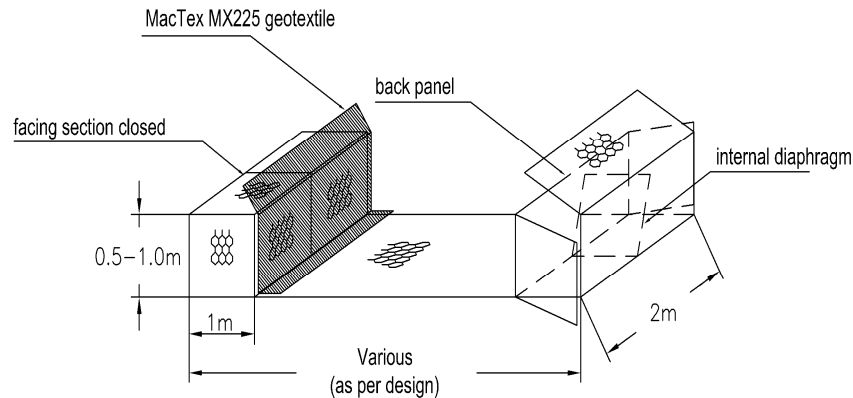
CONSTRUCTION

Construction was originally scheduled for fall 2007. Due to emergency road works elsewhere in the province, much of the funding for the project was diverted to repair projects. Sufficient funding was retained to allow for the tendering of a material supply contract in October 2007. Maccaferri was awarded the supply contract with delivery of the Terramesh® System scheduled for April 2008. The value of the contract was approximately $179,000 (CDN)

The material used for the gabion stone fill and for the reinforced soil backfill (BC MoT Bridge End Fill) was provided to the General Contractor by BC MoT from a roadside borrow pit located approximately 10km south of the project site.

A public tendering process in the spring of 2008 resulted in a contract being awarded to Gable Construction of Kamloops, BC for the installation of the Terramesh® System embankment and associated road works. The installation of the Terramesh® System was sub-contracted to a specialist gabion installer, Gabion Wall Systems of Barriere, BC. The total value of the project, including contractor mobilization/demobilization, supply of Terramesh System and granular materials was approximately $879,000 (CDN). Construction began in July 2008 and the installation of 1,374m^2 of total wall surface was completed by the end of August 2008.

Highway #1 is a two lane highway through the project site. In order to maintain access on this section of highway during clean up operations from past rock fall events, traffic diversion lanes had been previously

constructed around the work area. This diversion was easily configured to carry a single lane of southbound traffic. Northbound traffic was directed into the old southbound lane, thereby freeing up the original northbound lane for construction operations related to the installation of the rock fall embankment.

Due to the extreme constraints posed by limited access to the structure at heights exceeding 3m, the Contractor decided to build the Terramesh® System by constructing access ramps at the both ends of the structure and using one-way equipment travel in order to construct the gabion basket facing units and to place and compact the engineered fill. At the uppermost layer, the back of gabion to back of gabion clearance was only 3.5m

Fig. 6 – Looking southward prior to placing backfill

Access to the centre portion of embankment was achieved via the ramps at the north and south ends of the structure. Once the centre portion of the embankment exceeded 6m in height, work began to complete the north end of the structure. This required that access was then further restricted to the southern ramp only and all equipment was required to travel backwards up the ramp. The final step was to remove the southern ramp and complete the embankment.

Fig. 7 – Northern end of embankment

Fig. 8

The sacrificial barrier on the impact side of the embankment was originally conceived as a geotextile sock or similar type of system. Recycled 5/8" thick fibre reinforced rubber conveyer belting was installed as the sacrificial barrier. As an additional layer of sacrificial protection, a single layer of woven wire mesh was draped and secured over the conveyer belting. An unintended benefit of using the layer of double twisted wire mesh is that all rock falls that impact on the structure are now recorded, thus providing an empirical method of tracking the actual number of rock fall events.

The size and impact energy requirements of the structure renders a comparison of projects costs to other forms of rock fall protection structures difficult. The closest comparison the Owner could develop was against a 7m catch fence rated at 3,000kJ that was constructed for a railway line located in the general area of the Slide 5 site at a cost of approximately $8,000/lin.m. The Terramesh® structure for Slide 5 was constructed for just over $9,100/lin.m. When compared as cost per kJ per linear metre of structure, the Terramesh® System embankment was approximately one third the cost of catch fence. The use of an MSE embankment allowed for the construction of a taller structure with three times the energy rating at cost that compared very favourably to a more traditional method.

Fig. 9 – Completed embankment, September 15, 2008

CONCLUSIONS

Less than one month after completion of the Terramesh® System rock fall embankment, the structure started to receive rock falls (Fig. 10). The embankment has performed in a manner that has fully satisfied the Owner, from both an operational perspective and from a cost perspective.

As it is now possible to quantify in greater detail the number of rock falls at the site, a greater understanding of the nature of the rock fall hazard risk at this site is being developed. Rock falls that previously cleared the concrete wall and traveled over Highway #1 are now being intercepted by the Terramesh® System.

Double sided or back-to-back MSE structures have been used successfully through Europe for rock fall embankments. This is the first use of a double sided MSE structure along a highway in British Columbia as a rock fall embankment. This concept has allowed for the construction of a robust, high impact strength structure within very limited physical constraints in a cost effective manner.

Although a specialist gabion installer was used by the General Contractor on this project, it was not a requirement to install the Terramesh® System. It is possible for these types of structures to be built using general labour and equipment, thus allowing for the possibility that government public works crews or maintenance contractor crews can be used to build these structures.

ACKNOWLEDGEMENTS

REFERENCES

1. Calvetti F. (1998) - Distinct Element evaluation of the rock-fall design load for shelters. Rivista Italiana di Geotecnica No. 3, 1998.
2. Departement federal de l'environnement, des transports, de l'energie et de la communication – Office federal des routes – Direction des travaux CFF – Directive (1998): "Actions sur les galeries de protection contre les chutes de pierres" (Berne - Edition 1998).
3. Kar A.K. (1978), Projectile pentration into buried structures, Journal of Structures Division ASCE 104: 125-139
4. Maccaferri Canada Ltd., Terramesh® System Technical Data Sheet, 2005
5. Maccaferri , Inc. Roadworks Problems and Solutions Rockfall Protection, 2007, 16 pages
6. Peila D. (editor) (2004) - Bonifica di versanti rocciosi per la protezione del territorio, Trento, 11 ÷ 12 marzo 2004. – Proceedings
7. Monger, J.W.H. and Journeay, J.M. (1994), Guide to the Geology and Tectonic Evolution of the Southern Coast Mountains, Geological Survey of Canada, Open File 2490, p. 31.
8. Monger, J.W.H. and Journeay, J.M. (1994), Geology of the Southern Coast and Intermontane Belts, Preliminary Map 1152A, Geological Survey of Canada, Scale 1:500,000.

Fig. 10 – Rock fall

5.4

SH 20 Keetonville Hill Landslide Repair

Rogers County, Oklahoma

Vincent G. Reidenbach[1] and James B. Nevels, Jr.[2]

1. Vincent G. Reidenbach, Ph.D., P.E., Geotechnical Engineer Materials Division, Oklahoma Department of Transportation, 200 N.E. 21st Street, Oklahoma City, OK 73105; PH (405) 522-4998; FAX (405) 521-0522; email: vreidenbach@odot.org.
2. James B. Nevels, Jr., Ph.D., P.E., Geotechnical Engineering Consultant, PH (405)-818-2897, email: jnevels1@cox.net.

Abstract. This paper presents the concluding remarks of a landslide repair project that was completed in May 2008. The scope of the repair project involves the Oklahoma Department of Transportation (ODOT) history dealing with this site, a limited site investigation, the development of a repair solution, construction details and changes, and a detailed post slope stability analysis. The landslide occurred on a heavily traveled (20,000 ADT), narrow, widening alignment of SH 20 between Claremore and Owasso, which is located in northeastern Oklahoma. The project was let as a highway emergency project funded 100 percent by the Federal Highway Administration. The project was to be completed as quickly as possible per the instruction of the ODOT Director. The final project construction time totaled 55 days.

There was no time allotted for a proper geotechnical investigation and slope stability analysis again per the instruction of the ODOT administration staff and Director. The site investigation consisted of an afternoon walkout of the landslide on April 10, 2008, and repair solution was to be presented the next morning to the emergency scoping team. The scoping team included key personnel from the field Division 8 Construction Division and central Oklahoma City Survey, Roadway Design, Bridge, and Materials Divisions. A total of twelve borings were allowed with the essential effort of assisting the contractor. No inclinometers to monitor the repair performance were authorized. ODOT had investigated this landslide in 1983, 1994, and 1995 through the ODOT Geotechnical Branch in the central office Materials Division. Division 8 had elected to make only temporary maintenance following these previous slope failures. The Geotechnical Branch had experience with the site soils and geology from their previous studies.

The landslide repair solution consisted of originally three rows of driven Z-section sheet pile walls supported by rakers and wales that were anchored to 30 inch diameter steel pipes filled

with concrete and centered with a 10 inch H-pile. The lower sheet pile wall was later replaced with a rock buttress, and as a compromise during field discussion with scoping team the spacing of the 30 inch diameter steel pipes filled with concrete for the middle sheet pile wall was decreased. This is an example of a forced over-design in the remediation emergency repair that turned out to just be safe enough based on a thorough back-calculated slope stability analysis. The critical factor for ODOT was the immediate placement of the road back into service as quickly as possible. The initial estimated cost was 5 million, and the final cost was 9.47 million dollars.

Introduction. The SH 20 Keetonville Hill landslide occurred on April 10, 2008, and a scoping meeting on the repair through an emergency contract was held on site on April 11, 2008 with Department staff. The scope of work covered in this report includes the following: location description, a review of the soil and geology of the landslide site, borings, assessment of the probable causes of this landslide, and remedial repair recommendations.

A review of the history of this site indicates that the landslide has failed in previous years at approximately the same location in each case in 1983, 1994, and 1995. In these previous landslide events Division 8 maintenance forces enacted temporary slide repairs. In these cases the Materials Division was called in to make borings; however, no formal reports or boring logs were available.

The landslide occurred on a heavily traveled (20,000 ADT), narrow, widening alignment of SH 20 between Claremore and Owasso, which is located in northeastern Oklahoma. This alignment was an essential corridor for commuter traffic to the Tulsa area. The project was planned to be let as a highway emergency project funded 100 percent by the Federal Highway Administration. The project was to be completed as quickly as possible per the instruction of the ODOT Director

There was no time allotted for a proper geotechnical investigation and slope stability analysis including the installation of inclinometers again as per the instruction of the ODOT administration staff and Director. The site investigation consisted of an afternoon walkout of the landslide on April 10, 2008, and repair solution was to be presented the next morning to the emergency scoping team. An impressive effort was made by all Divisions of the Oklahoma Department of Transportation (ODOT) in order to put together a set of construction plans and notes for an emergency contract in approximately a week and a half time frame following the April 11, 2008 landslide occurrence.

The overall project included the repair of a large landslide with braced sheet pile walls (Walls A and B) and rock buttress at the toe and two smaller landslides with drilled shaft walls (Walls C and D). Walls C and D were located approximately 800 feet (244.0 m) and 1062 feet (323.91 m) respectively east of the larger landslide centerline station of 121+58. This paper presents the work done on the large landslide which was stabilized with Walls A and B and the rock toe buttress.

Site Description. The site is located approximately 5.75 miles east of the junction of SH 20 and US169 on SH 20 near Keetonville and this highway route is a major connector between Owasso and Claremore. SH 20 transitions from the Claremore Cuesta Plains (upland) topography to the Verdigris River floodplain, and in this transition SH 20 follows a very old, steep grade, and winding county road alignment. The ODOT right of way is highly restricted through this grade transition. The Claremore Cuesta geomorphic province consists of resistant Pennsylvanian sandstones and limestones dipping gently westward, forming cuestas between shale plains. The site location is shown in a section of the 7.5 minute Sageeyah Quadrangle in Figure 1. Note specifically in Figure 1 that the SH 20 alignment crosses a drainage path (circled) that is in the immediate vicinity of the landslide. The landslide site condition is presented in Figures 2 through 5.

Site Soil and Geology. The surface soil series mapped at the site by the Natural Resources and Conservation Service (NRCS) in the Rogers County Soil Survey on sheet 36 is the rough stony land unit (Rs). According to the USDA Natural Resources Conservation Service (NRCS) May 22, 2001 recorrelation the Rs soil unit has been recorrelated to the Hector-Endsaw complex, 20 to 35 percent slopes soil unit. The Endsaw clay is the predominant soil series at this site location, and it can be characterized as yellowish red, blocky, high plasticity, shallow residual soil with fragments of sandstone developed from shale of Pennsylvanian geologic age. The pedon depth is approximately equal to or less than 60 inches.

The site geology according to the Oklahoma Department of Transportation (ODOT) Engineering Classification of Geologic Materials, Division Eight, 1965 (Red Book), is the Oologah unit underlain by the Labette unit. The Oologah unit (IPo) consists of limestone lensed with shale and some sandstone. The limestone is described as hard, gray to dark gray, mostly massive bedded and locally contains some chert. The shale is dark gray to black, flaky, fissile, and calcareous. The limestone ranges in thickness up to about 50 feet but are mostly less than 10 feet. The Labette unit (IPlb) consists of gray shale containing some lenses of sandstone. The shale is silty, clayey, and sandy. Qualifying this geologic description on site indicates that the Oologah is highly jointed and contains several springs at the base contact with the Labette shale. At the initial site visit on April 11, 2008 significant spring water was observed flowing in the roadway ditch being

emitting from two sources between approximate stations 109+00 and110+40. The Labette shale grades in color from an olive or yellowish gray to gray.

According to the Oklahoma Geological Survey Hydrological Atlas 2 by Melvin V. Marcher and Roy H. Bingham, 1971, the geology is also recorded as the Oologah formation underlain by the Labette formation. There are more recent geologic publications by the Oklahoma Geologic Survey that cover this site such as Bulletin 144 and Special Publication 97-2; however, these are specialty reports that have only limited geologic descriptions of the Oologah and Lebette formations.

Borings. A total of 5 borings were made along the landslide centerline at station 121+58 according to the ASTM D 6151 utilizing the logging of the soil profile with hollow-stem (HS) augers at. A limited number of Standard Penetration Tests (SPT) was also performed. The most significant aspect of the HS logging was watching the pull-down pressure required to advance the augers with depth in which weak and/or stiff layers within olive gray or yellowish gray and gray shales were observed at pull-down pressures ranging from 200 to 600 psi. All borings except one indicated zones of water with depth. The water appears to under a significant head.

Assessment of Probable Cause. The causes of this landslide appear to follow the classical precepts in landslide occurrence in that there has been a decrease in shear strength due to increased pore water and along with other factors affecting the landslide occurrence such as cracking of the slope surface and orientation of the Labette shale structure, and failure following a significant rainfall event. From past experience with the Labette shales we knew that it was highly plastic soil material. Perhaps the most significant fact observed from this current failure is that the landslide appears to be very similar to past failures (essentially in the same location) and that the slope failure most likely was a progressive one. The judgment at the time based on a walkout and through site inspection was that the critical slip surface most probably was that of a wedge failure near the boundary of olive gray or yellowish gray and underlying gray zones of the Labette shale based on the slope geometry. The operating shear strength parameters at the time of failure were reasoned to be residual based on the recorded history of the site. However, these assumptions were our best estimate of what the soil and water conditions were at the time of failure.

A post rigorous slope stability analysis was planned some time after the construction completed. That being said without a well done and proper detailed geotechnical investigation the only choice in this case was to be extraordinary very conservative in the remedial recommendation.

Remedial Recommendation. The solution was worked out in the field on April 11 and 14 based on estimates of passive earth pressure resistance and slide perimeter measurements for three braced sheet pile retaining walls. The elements of the walls consist of a driven Z-section sheet pile wall supported by rakers and wales that are anchored to 30 inch diameter concrete filled shafts with a centered H-pile. The purpose of the three walls was to have redundancy in the solution as well to break the slide mass up into thirds. The third wall (C) nearer to the toe was later substituted by a rock filled berm based upon the analysis and design of Mr. Jeff Dean of the Roadway Design Division with walls B being substantially strengthened by spacing the drilled piers at a16 foot spacing. Key plan components of the slope repair are shown in Figures 6 through 9.

Construction. On the strength of ODOT's Materials Division past experience at this landslide site location, the field formulated repair solution as described above was implemented. The construction was handled by two bridge contractors who had long and considerable experience in pile and pier construction (Muskogee Bridge Company and M.J. Lee Construction) with ODOT. The construction was intense with two contractors in a small construction area as seen by Figure 10 which represents multiple contract pay functions on going at the same time. An on-site inspection of the clearing and grubbing on May 02, 2008, it was observed that the contractor had uncovered a partially collapsed old corrugated metal pipe at the base of the scarp between stations approximate 120+00 and 121+00 that had been the covered in the previous Division 8 maintenance repairs. The project was completed in 55 days from the time of the award of the contract.

Slope Stability Analysis. An initial slope stability analysis was made at the plan centerline of the landslide cross-section station at station 121+58 before construction to determine the probable operating residual soil parameters (c_r and Φ_r) that correlate with a factor of safety equal to 1.000. After several trial runs a critical slip surface was found that reasonably matches the surface slope geometry at the time of failure with estimated shale profile depths, and water table, see critical slip failure plot in Figure 10. The slope stability analysis was performed using the GSTABL7 with STEDwin version 2.005, software by Garry H. Gregory, September 2006. This software uses an iterative approach where the soil property data, slope geometry, water table, and analysis technique is inputted into the GSTABL7 program using the Block2 analysis. These assumptions are the best estimate of what the soil and water conditions were at the time of failure, and they are considered as such.

A more rigorous slope stability analysis was performed months after the completion of the project taking into account a more accurate surface survey and careful estimate soil layer, water table, and residual soil parameters. The location of the sheet pile walls, drilled piers, and rock to buttress is also shown in the slope stability analysis, see Figure 11. The factor of safety of 1.525 was lower than expected; but marginally sufficient based on very conservative soil parameter, soil profile, and water table estimates.

Conclusion. The proposed solution was intended to provide a fix that would serve ODOT until such time that a realignment of SH 20 could be constructed. The landslide repair was constructed in a record time of 55 days. However, the total cost was a staggering 9.47 million dollars compared to the original construction estimate of 5 million dollars. The finished project is seen in Figures 12 through 14. The overall plan view of Walls A and B, and the rock buttress are shown in Figure 15. The most significant conclusion following the post slope stability analysis was that ODOT was very fortunate not to have built in a potential continued slope failure. Finally this project should point to the absolute necessity of performing quality up front geotechnical engineering.
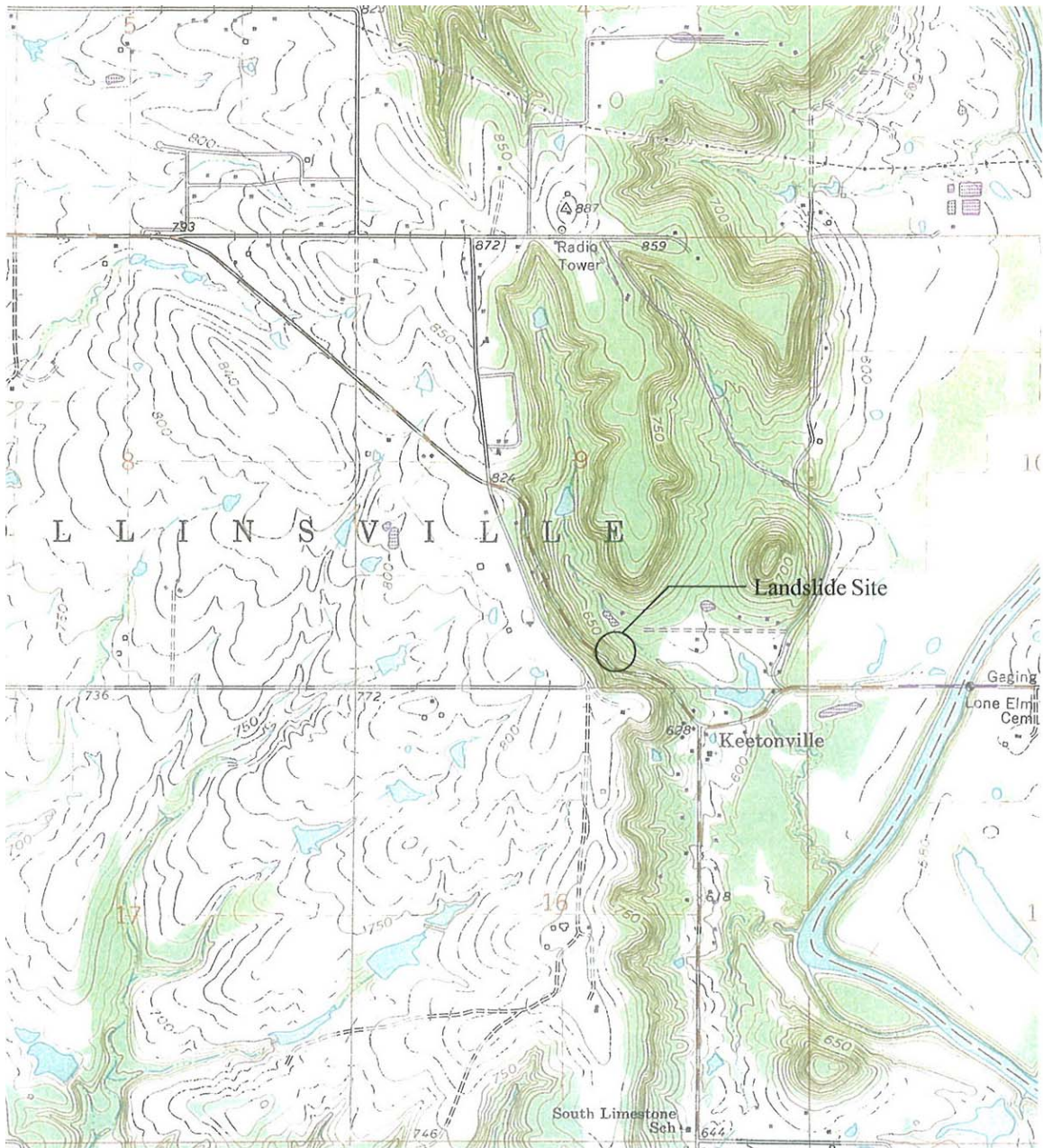
Figure 1. Landslide Site.

Figure 2. Landslide scarp looking west.

Figure 3. Close-up of scarp.

Figure 4. Break-up of of local road.

Figure 5. Toe of the landslide near an abandoned house.

variable slope

Place 4" Perforated Pipe in void, as shown. Backfill with Crushed Rock

4'-0"

2'-0"

DETAIL OF MINIMAL FILL AT SHEET PILE WALL
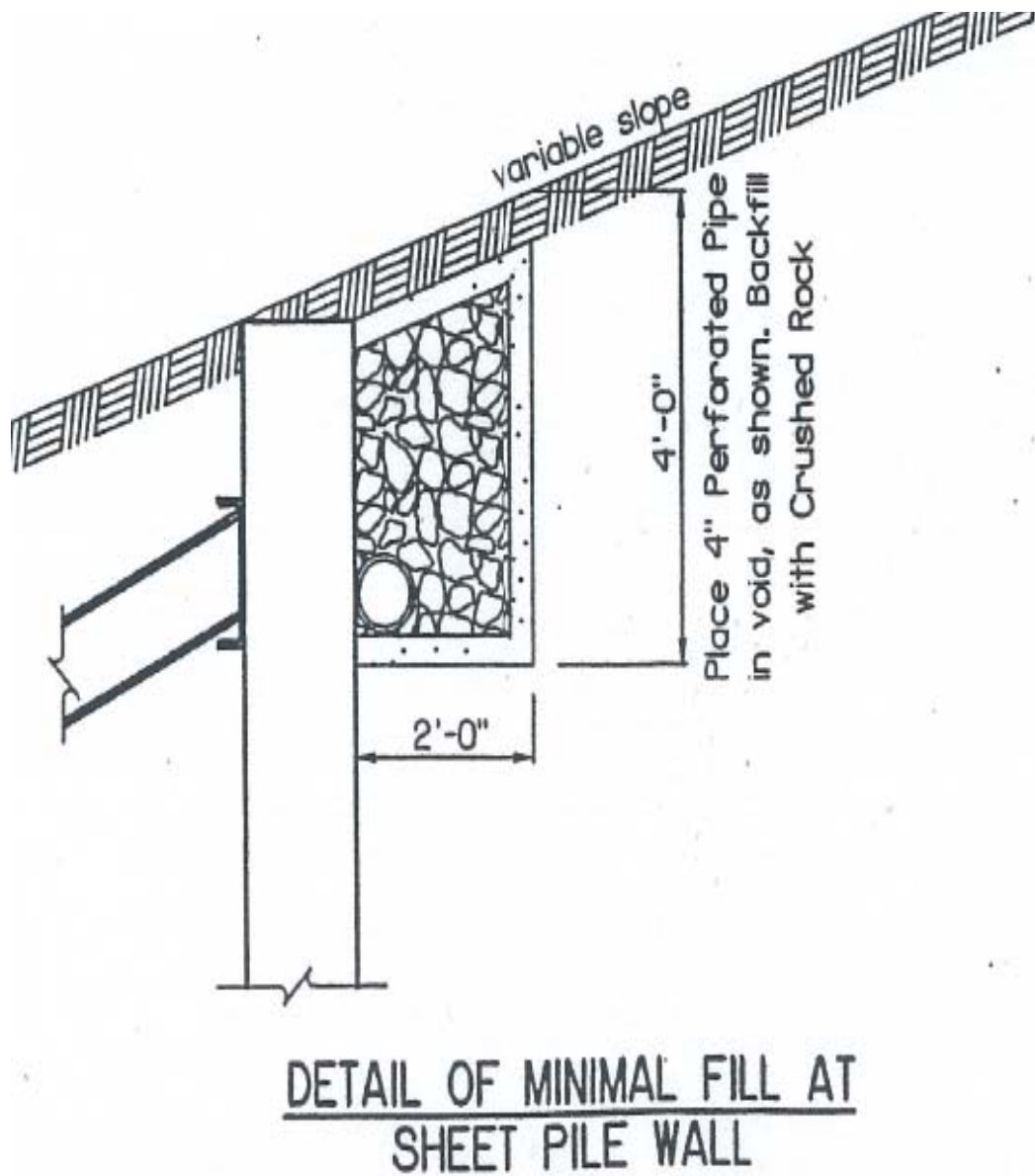
Figure 6.   Wall B plan detail.
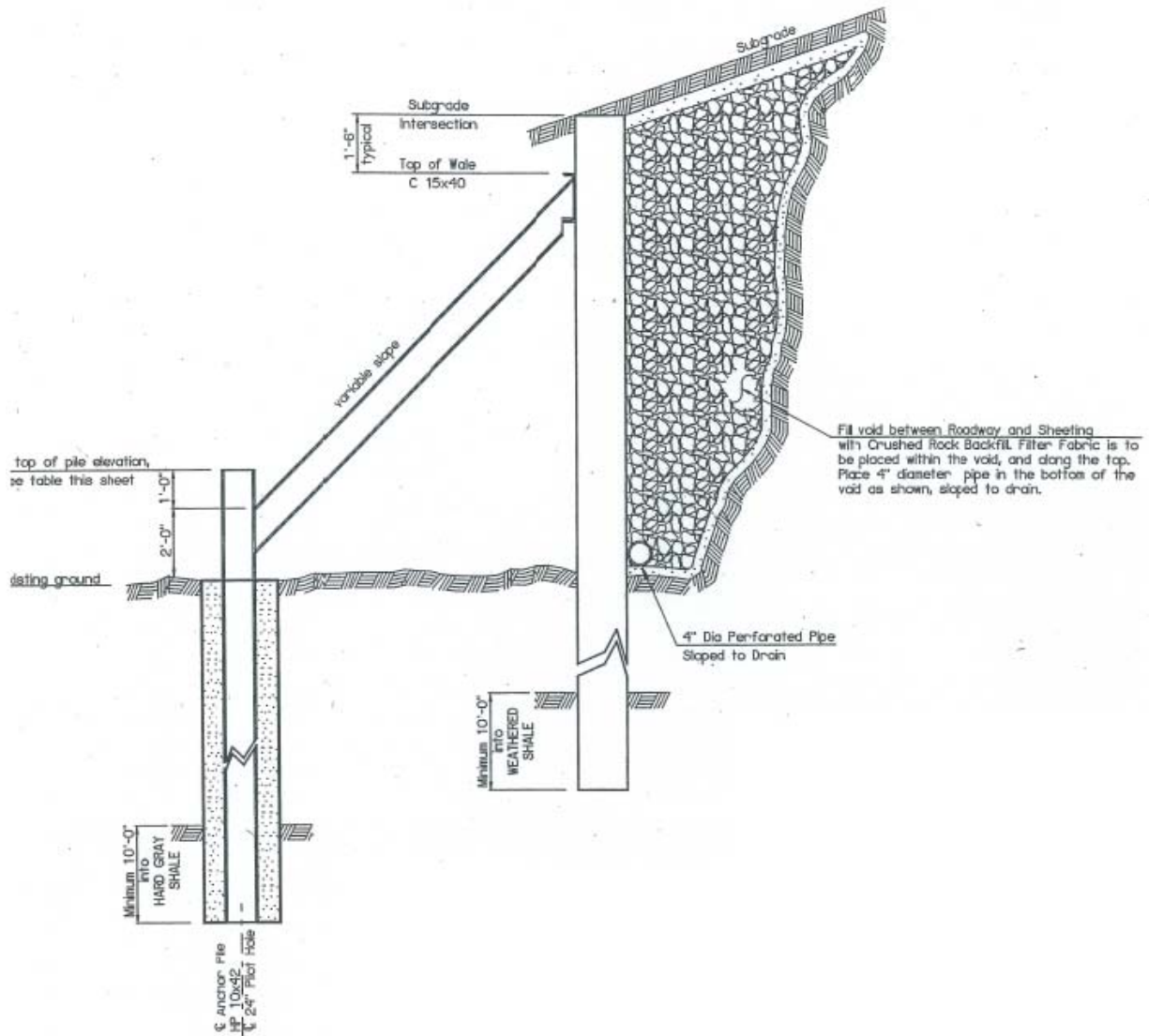
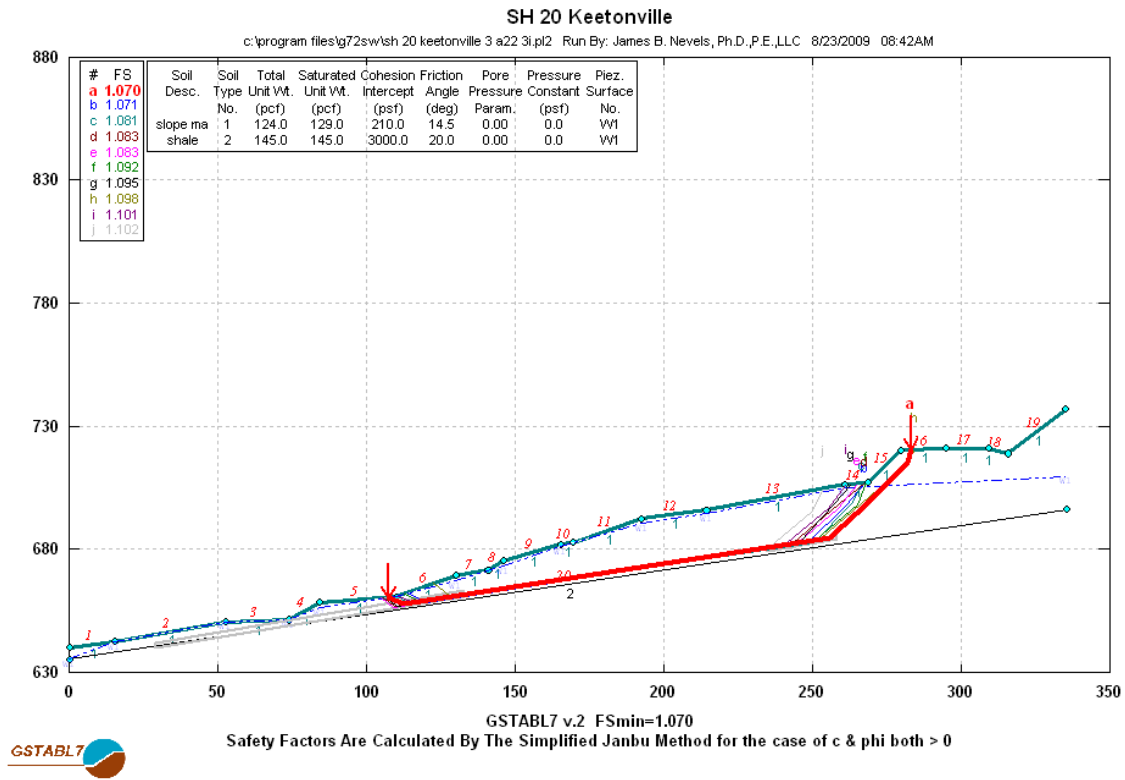Figure 7. Wall A plan detail.
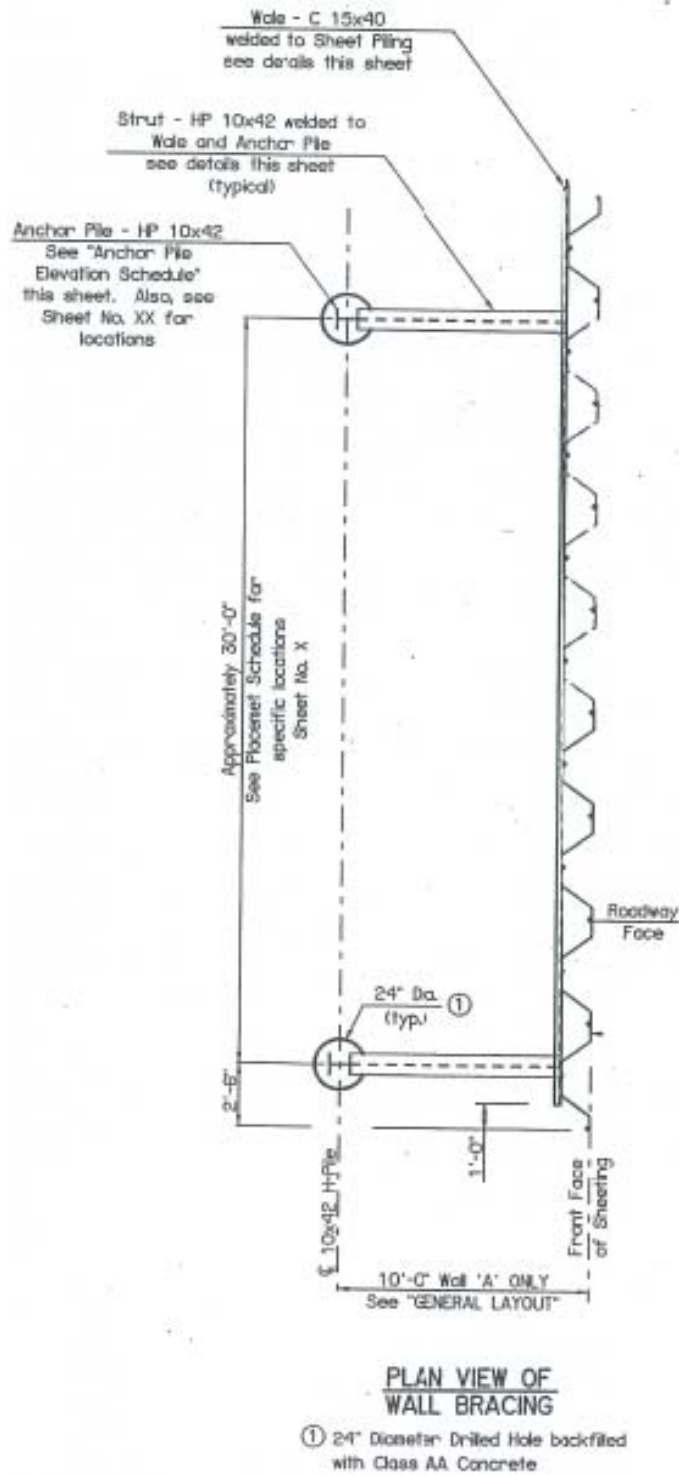
Figure 8. Wall A plan detail.
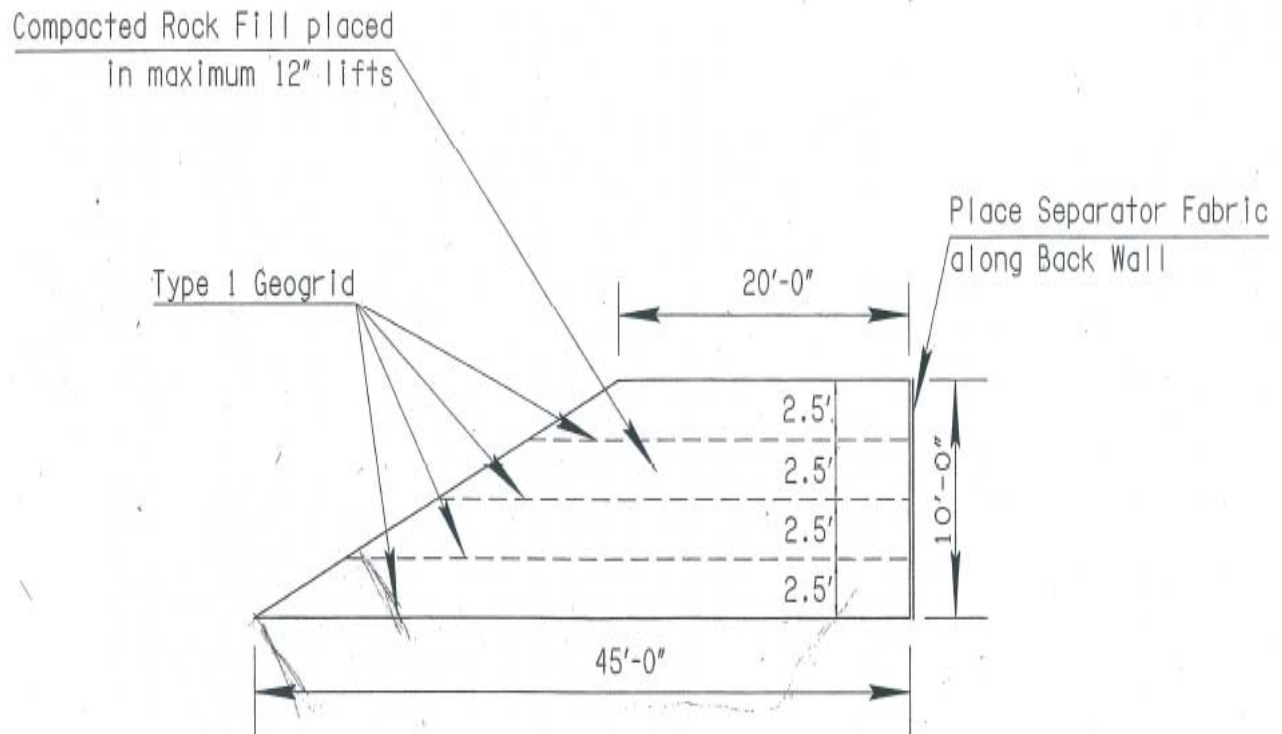
Figure 9. Rock buttress detail at the toe.

Note: Horizontal and Vertical Scale in feet (ft).

Figure 10. Back-calculation of shear strength parameters.

43 33

c:\program files\g72sw\final station 121+58 keetonville sh 20.pl0   Geometry Preview 8/23/2009   8:47 PM

Soil Desc.	Soil Type No.	Total Unit Wt. (pcf)	Saturated Unit Wt. (pcf)	Cohesion Intercept (psf)	Friction Angle (deg)	Pore Pressure Param.	Pressure Constant (psf)	Piez. Surface No.
resdiual	1	120.	126.	150.	15.	0.	0.	W1
rock but	2	140.	145.	0.	30.	0.	0.	W1
brn shal	3	124.	129.	210.	14.5	0.	0.	W1
gr shale	4	145.	145.	3000.	20.	0.	0.	W1

GSTABL7
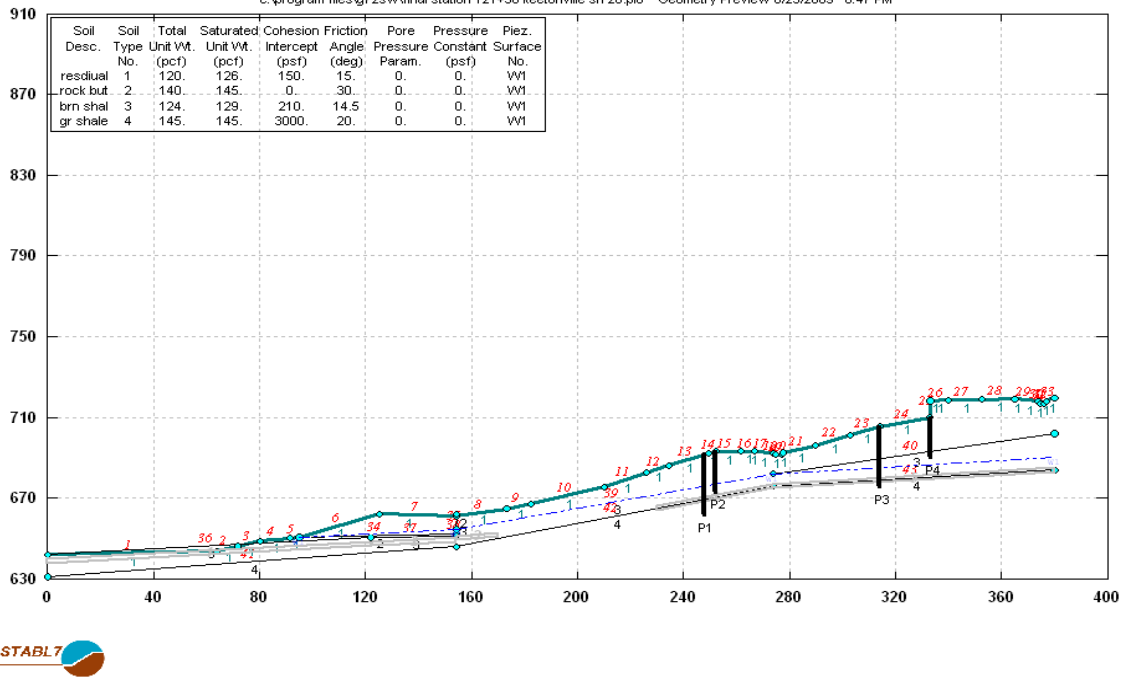
Note: Horizontal and Vertical Scale in feet (ft).

Figure 1. Slope stability of completed project.

Figure 12. Completed Wall A looking west.

Figure 13. Local road and Wall B on the left looking east.

Figure 14. Rock buttress at the toe of the landslide.
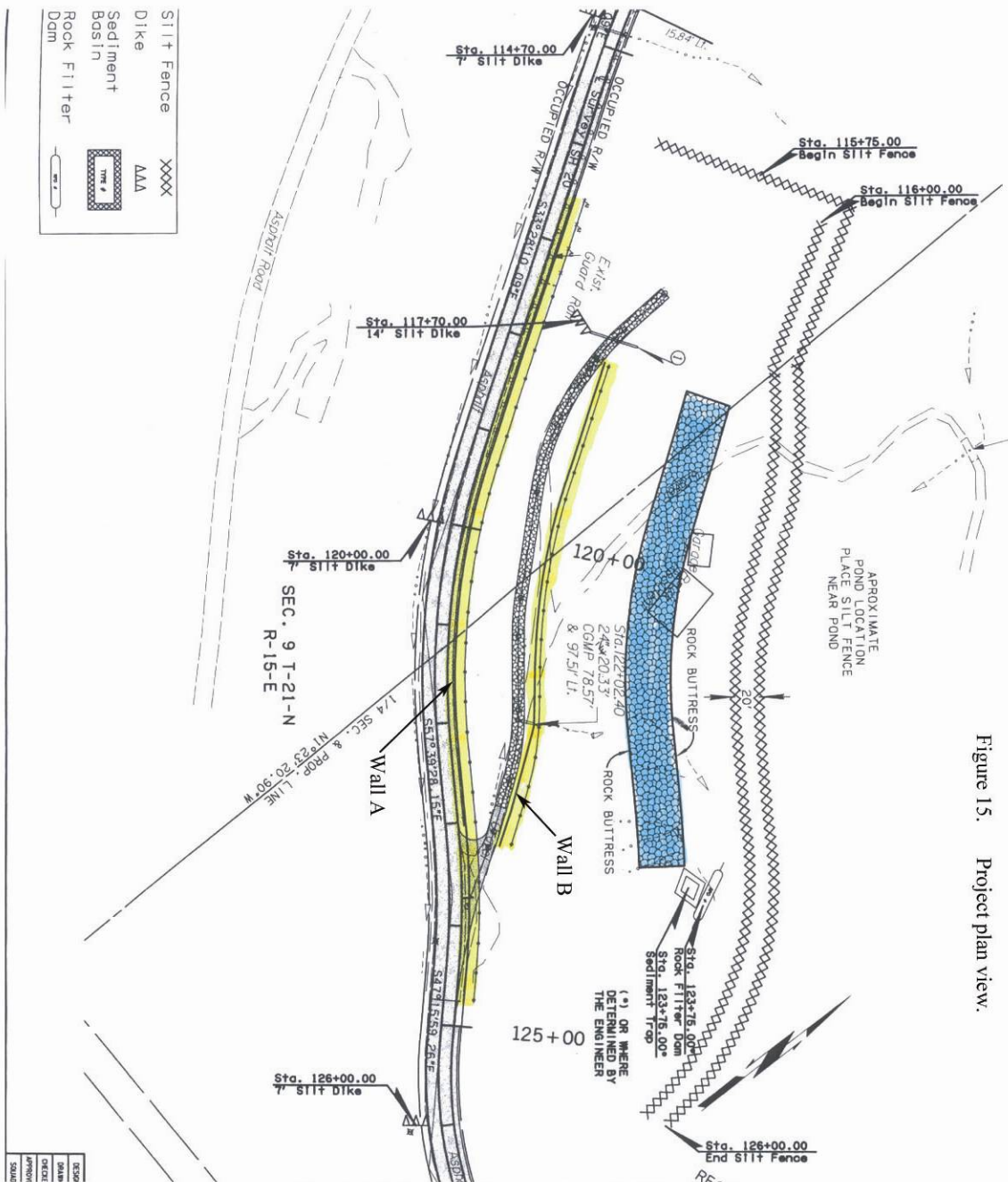
Figure 15. Project plan view.

5.5

REVIEW OF BRIDGE SITES VISITED

FOR NCHRP PROJECT 24-29:

SCOUR AT BRIDGE FOUNDATIONS ON ROCK

Jeffrey R. Keaton
MACTEC Engineering and Consulting, Inc.
5628 East Slauson Avenue
Los Angeles, CA 90040
323-889-5316; jrkeaton@mactec.com

Su K. Mishra
Ayres Associates, Inc.
2150 River Plaza Drive, Suite 330
Sacramento, CA 95833-4129
916.563.7700; MishraS@AyresAssociates.com

ABSTRACT

Five bridge sites were visited in 2008 as part of National Cooperative Highway Research Program (NCHRP) Project 24-29: Scour at Bridge Foundations on Rock. I- 10 Chipola River Bridges, Jackson County, Florida, are founded on thick bedded Oligocene marine limestone that shows geologic evidence of dissolution. SR-22 Mill Creek Bridge, Polk County, Oregon, is founded on widely fractured Oligocene marine siltstone prone to slaking in air. I-90 Schoharie Creek Bridge, Montgomery County, New York, that failed in 1987 was founded on Quaternary ice-contact stratified drift armored by hard sandstone boulders and cobbles. The armor layer of boulders over the glacial till in New York provided a threshold control for scour and was used for evaluating excess stream power. Paleozoic marine sandstone is present across the channel at a US Geological Survey stream gage on Schoharie Creek. SR-262 Montezuma Creek Bridge, San Juan County, Utah, is founded on stratified Jurassic sandstone and claystone excavated in 1955 to create a channel which cut off a meander loop. Cavitation pits were observed on sculpted sandstone in Utah, but the primary control on scour was plunge pool excavation of fractured claystone interbedded with the sandstone. SR-273 Sacramento River Bridge, Shasta County, California, is founded on thinly bedded Cretaceous siltstone that slakes in water. Laboratory tests

included slake durability, continuous abrasion, Rotating Erosions Test Apparatus (RETA), point load, and specific gravity. Reliable channel cross section data were available for bridges in Oregon, New York, and California for at least two dates several years apart.

INTRODUCTION

National Cooperative Highway Research Program (NCHRP) Project 24-29, Scour at Bridge Foundations on Rock, began in 2006 with objectives of developing a methodology for determining design scour depth and time-rate of scour in rock, and creating design and construction guidelines for application of the methodology. The status of this research in the spring of 2008 was described by Keaton and Mishra (2008), before field visits had been made to bridge sites. The objective of the current paper is to review some geologic and hydraulic conditions of the five sites visited during the summer and fall of 2008 and laboratory test results.

The bridge sites were identified from key reports (OEA, 2001; Dickenson and Baillie, 1999; Resource Consultants and Colorado State University, 1987; Wyss, Janney, Elstner and Mueser Rutledge Consulting Engineers, 1987) and personal information provided by Utah Department of Transportation, California Department of Transportation. Assistance from Florida Department of Transportation, Oregon Department of Transportation, New York State Thruway Authority, and New York State Department of Transportation was instrumental in the success of the research. The field sites visited for NCHRP Project 24-29 are listed in Table 1 and shown on Figure 1. Flood frequency data for the five sites are summarized on Figure 2.

Table 1. List of bridges visited for NCHRP Project 24-29.

River or Stream	Highway	County and State	Drainage Area
Chipola River	Interstate 10	Jackson County, Florida	587 mi^2
Mill Creek	State Route 22	Polk County, Oregon	33 mi^2
Schoharie Creek	Interstate 90	Montgomery County, New York	935 mi^2
Montezuma Creek	State Route 262	San Juan County, Utah	1,153 mi^2
Sacramento River	State Route 273	Shasta County, California	7,560 mi^2
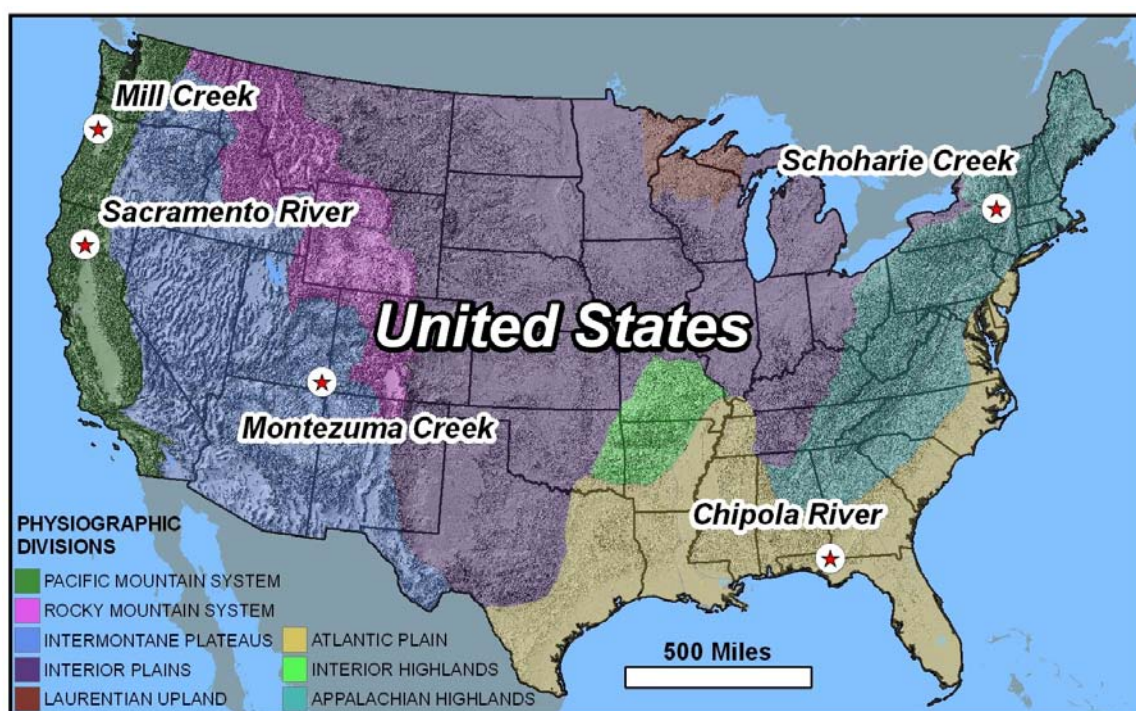
Figure 1. Locations of NCHRP 24-29 field sites. Physiographic divisions from ESRI.
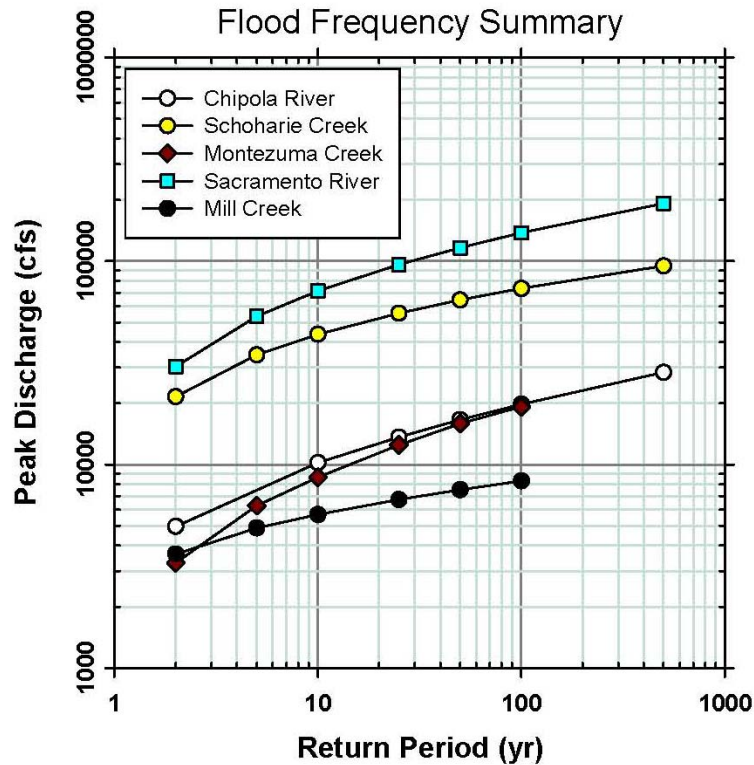
Figure 2. Flood frequency summary. Data from OEA (2001) for Chipola River and from HDR (2004) for Montezuma Creek; other data from nearby USGS stream gages.

SELECTED FIELD DATA FOR BRIDGE SITES

General geologic information and site conditions for the bridge sites are summarized below:

Chipola River – Interstate 10

Interstate 10 crosses Chipola River in the panhandle of Florida approximately 60 miles west of Tallahassee. The drainage basin extends into Alabama, near the Georgia state line (Figure 3). The bridge (Figure 4) is founded on Oligocene Marianna Limestone, white to gray marine limestone that ranges from argillaceous limestone to argillaceous dolostone. The formation contains

dissolution features (Figure 5) along the Chipola River. Bedload in this low-gradient stream is fine to medium sand.
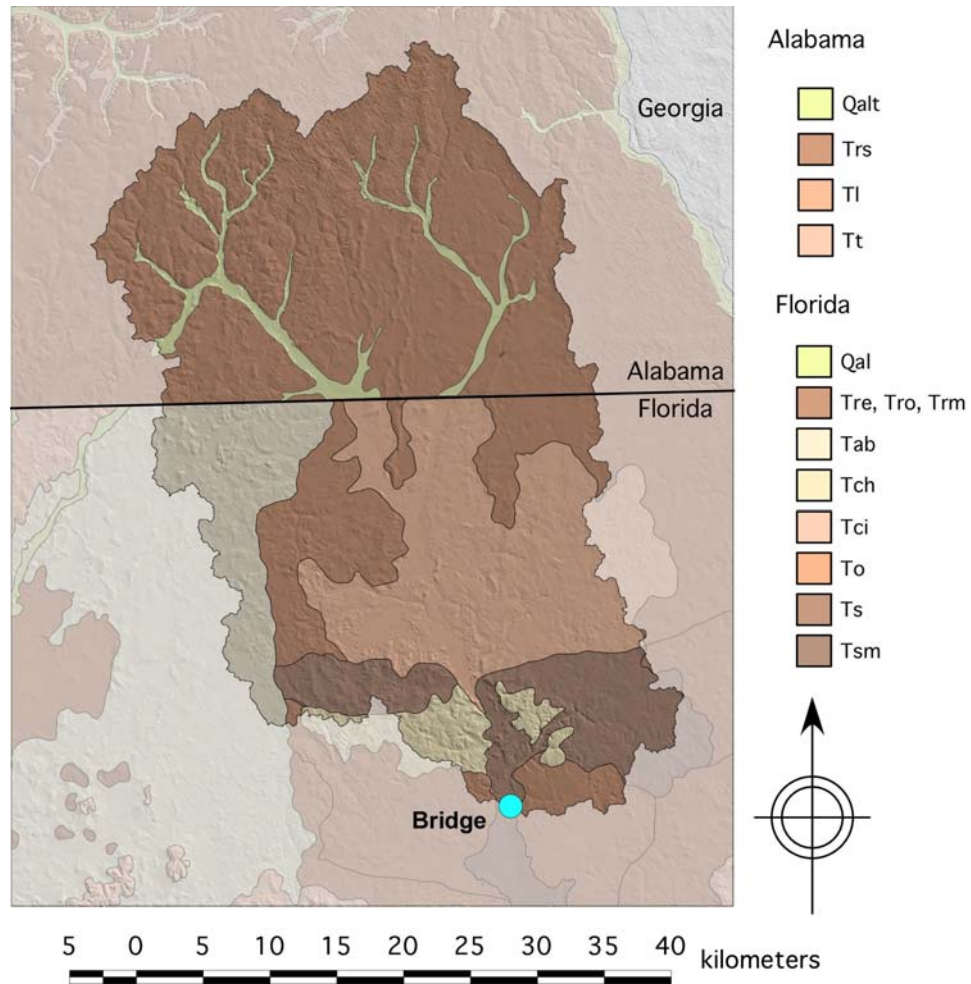
Figure 3. General geologic map of Chipola River drainage basin; geology from Dicken et al., 2007. Map prepared by William C. Haneberg.

Figure 4. I-10 bridges over Chipola River. View is upstream; sample location is in lower right.

Figure 5. Dissolution features on left bank about 1000 feet downstream of bridge.

Mill Creek – State Route 22

State Route 22 crosses Mill Creek in northwest Oregon approximately 20 miles west of Salem. The drainage basin outline and general geologic formations are shown on Figure 6. The bridge (Figure 7) is founded on Eocene Yamhill Formation, gray marine siltstone that ranges from massive to thinly bedded and locally contains interlayered basalt lava flows. The siltstone formation at the bridge site is massive, but it erodes along fractures into cobble- and boulder-

sized fragments which, along with basalt boulders, form the bedload (Figure 8); the siltstone

slakes in air, as evidenced by boulder-sized mounds of slaked siltstone on the stream bar

upstream of the bridge. The Yamhill Formation is sculpted in the rock-bed channel under the

bridge (Figure 9).
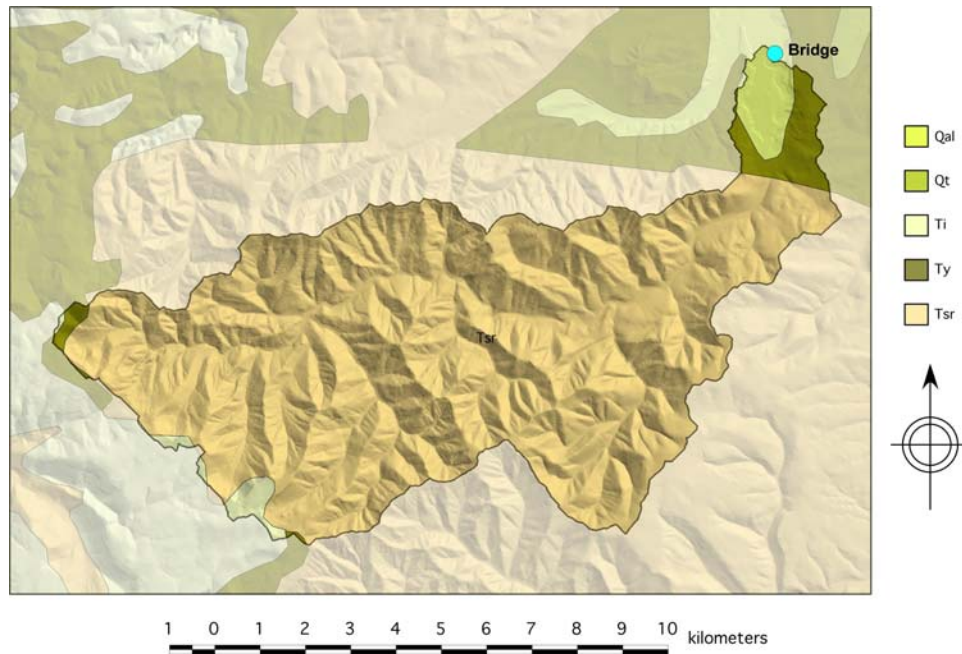
Figure 6. General geologic map of Mill Creek drainage basin; geology
from Ludington et al., 2007. Map prepared by William C. Haneberg.

Figure 7. State Route 22 Bridge over Mill Creek.

329

Figure 8. Boulder bar upstream of bridge.

Figure 9. Sculpted siltstone in rock-bed
channel under bridge. View is toward left
abutment; flow is left to right.

Schoharie Creek – Interstate 90

Interstate 90 crosses Schoharie Creek in east-central New York about 35 miles northwest of
Albany. The drainage basin outline and general geologic formations are shown on Figure 10. The
bridge built in 1954 was founded on Quaternary ice-contact stratified glacial till. It failed during a
flood in 1987 and was replaced with a bridge (Figure 11) that was founded on bedrock below the
glacial till. The Burtonsville gage on Schoharie Creek (USGS 01351500) is about 12 miles
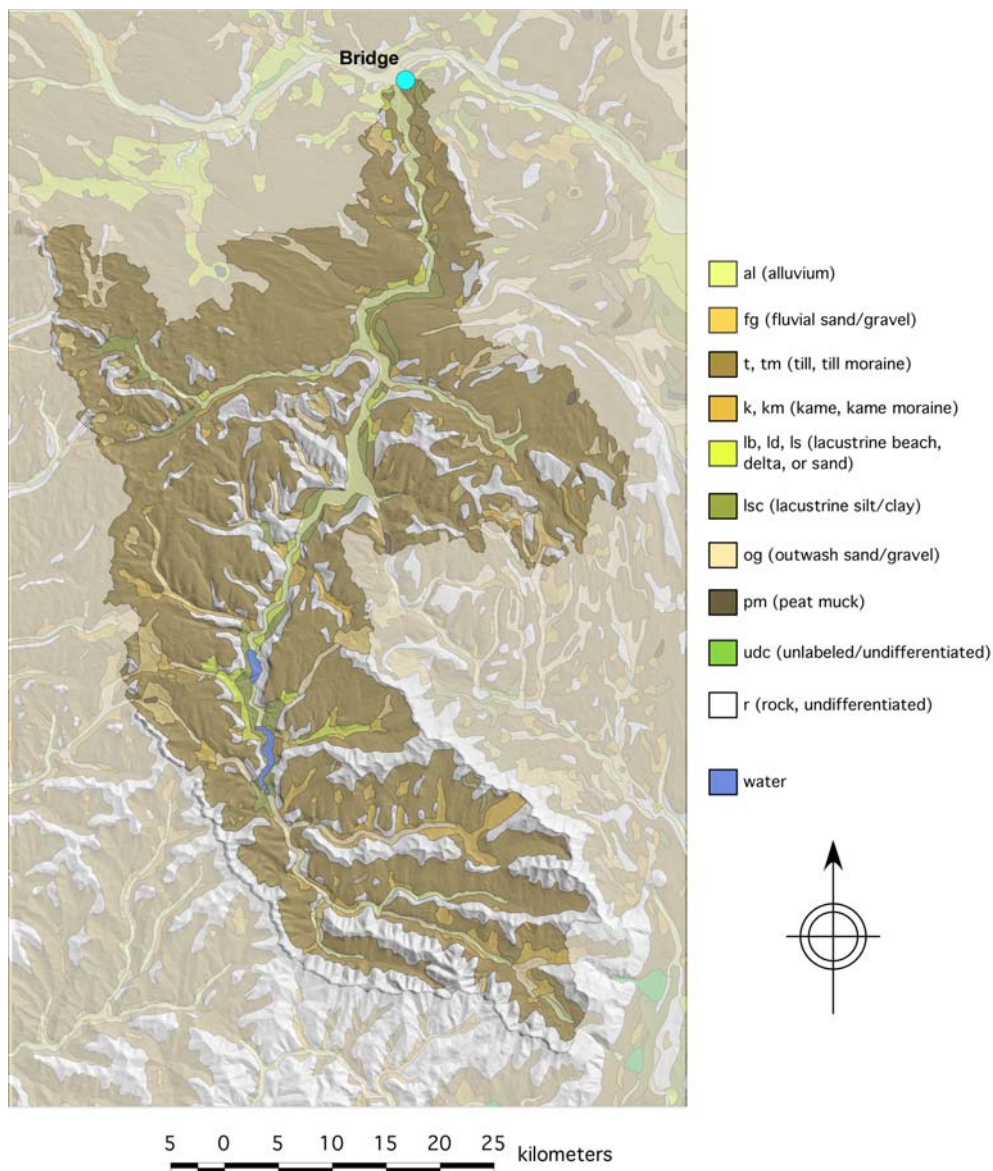
Figure 10. General geologic map of Schoharie Creek drainage basin; geology
from Dicken et al., 2008. Map prepared by William C. Haneberg.

upstream of the bridge; bedrock at the gage site is thick-bedded Paleozoic (Devonian) marine

sandstone (Figure 12) that is jointed into tabular boulder-size blocks (> 12 inches). The sandstone

boulders formed an armor layer on Schoharie Creek (Figure 13), protecting it from exposure to

scour at peak discharges less than 20,000 cubic feet per second (cfs) (Resource Consultants and

Colorado State University, 1987). Figure 13 shows the August 2008 condition at State Route 161

approximately 4 miles upstream from the I-90 Bridge.

Figure 11. Interstate 90 Bridge over Schoharie Creek rebuilt after 1987 flood. View looking upstream. No samples obtained from bridge site; data from forensic report used.

Figure 12. Thin- to thick-bedded sandstone on left bank of Schoharie Creek at the USGS Burtonsville gage site. Samples taken from the camera position on the right bank.

Figure 13. Schoharie Creek at State Route 161 about 4 miles upstream from I-90. Boulder armor layer here is similar to the channel at I-90 before the bridge failed in 1987.

Montezuma Creek – State Route 262

State Route 262 crosses Montezuma Creek in southeast Utah about 275 miles southeast of Salt Lake City. The drainage basin outline and general geologic formations are shown on Figure 14; the drainage basin extends into Colorado. The bridge (Figure 15) is founded on Jurassic fluvial sandstone with claystone interbeds. Before the bridge was built in about 1960, Montezuma Creek consisted of a large meander bend that defined a narrow peninsula of sandstone and claystone (Figure 16). A narrow channel about 50 feet wide was excavated across the peninsula and an embankment with a culvert was placed across the meander bend. The excavated channel effectively is an unlined spillway; it appears that the initial construction created a knickpoint in the sandstone nearly 200 feet downstream from the bridge. By 2003, the knickpoint had migrated to a point about 15 feet upstream from the bridge (HDR, 2004). In September 2008, the knickpoint was nearly 8 feet high and exposed friable claystone under hard sandstone (Figure 17). Concrete retaining walls were constructed in 2004 to protect exposed claystone interbeds under the bridge foundations from further erosion. Sculpted forms in hard sandstone within about 10 feet of the crest of the knickpoint have pits in downstream-facing sides (Figure 18) that are best explained as cavitation features. Gravel fragments are wedged tightly into vertical joints (Figure 19) and bedding planes. Circular holes with radial fractures in hard sandstone (Figure 20) mark blast holes used for initial excavation of the channel.
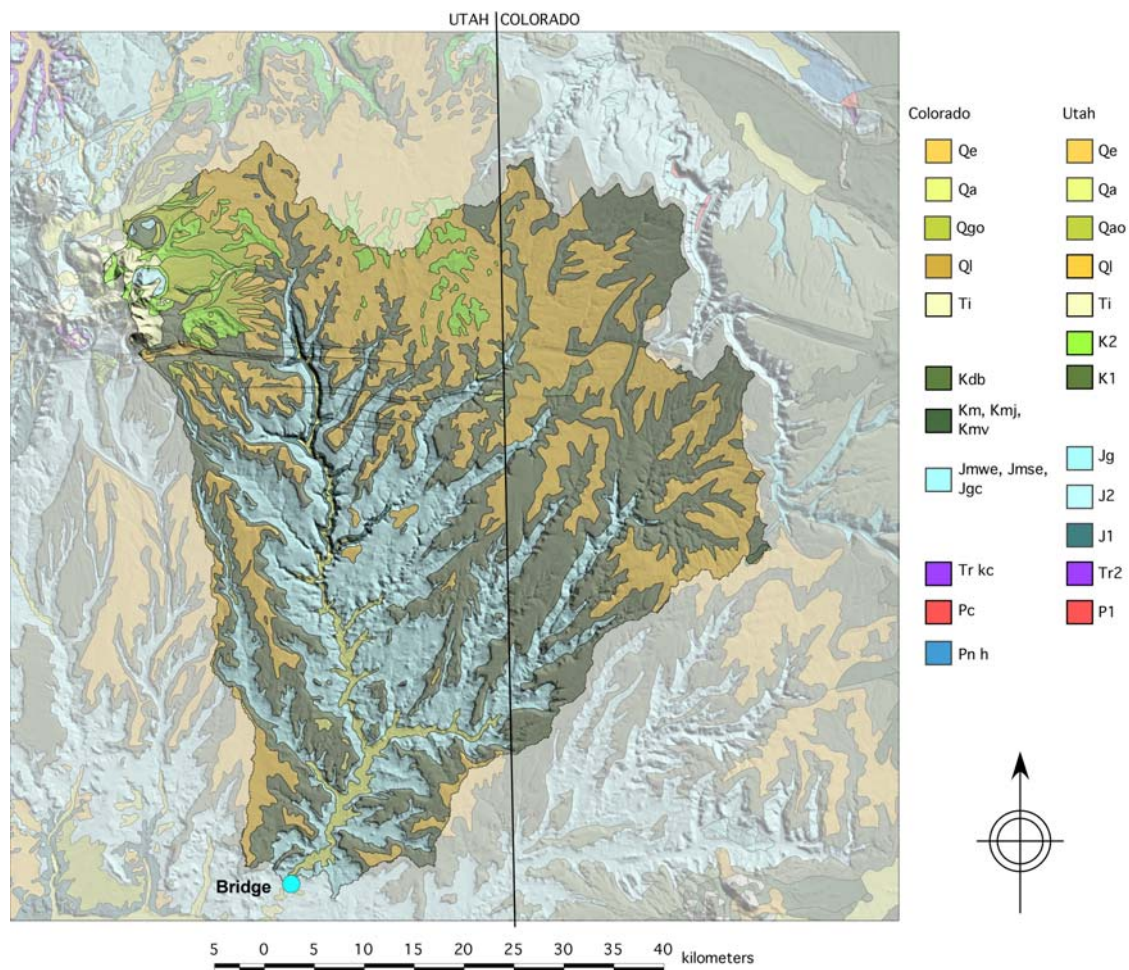
Figure 14. General geologic map of Montezuma Creek drainage basin; geology from Ludington et al., 2007. Map prepared by William C. Haneberg.

Figure 15. State Route 262 Bridge over channel constructed through narrow ridge which became the main channel of Montezuma Creek. View is looking upstream at knickpoint.

Figure 16. Topographic map showing Montezuma Creek channel and cutoff.

Figure 17. Sandstone and claystone exposed in
knickpoint about 15 feet upstream from bridge.
Orange circles are 1.35m apart on vertical pole.

Figure 18. Sculpted and pitted sandstone
within 10 feet from crest of knickpoint
Water flow is right to left.

Figure 19. Gravel fragments wedged tightly into vertical joint in hard sandstone indicating turbulence-induced opening during flood flow.

Figure 20. Blast hole with radial fractures in hard sandstone. White spots on board are 20 cm and 30 cm apart.

Sacramento River – State Route 273

State Route 273 crosses Sacramento River at Redding in north-central California about 150 miles north of Sacramento. The drainage basin extends into Oregon; the outline and general geologic formations are shown on Figure 21. The bridge (Figure 22) is founded on soft, dark gray,

Cretaceous marine siltstone that is thinly bedded and locally fractured (Figure 23). Beds are

locally folded and dip toward the left abutment (north) at about 17°; some beds are harder than

others (Figure 24). Cobble-sized fragments of hard igneous rocks form the bedload (Figure 25).

Shasta Dam, located approximately 10 miles upstream, was closed in 1945.
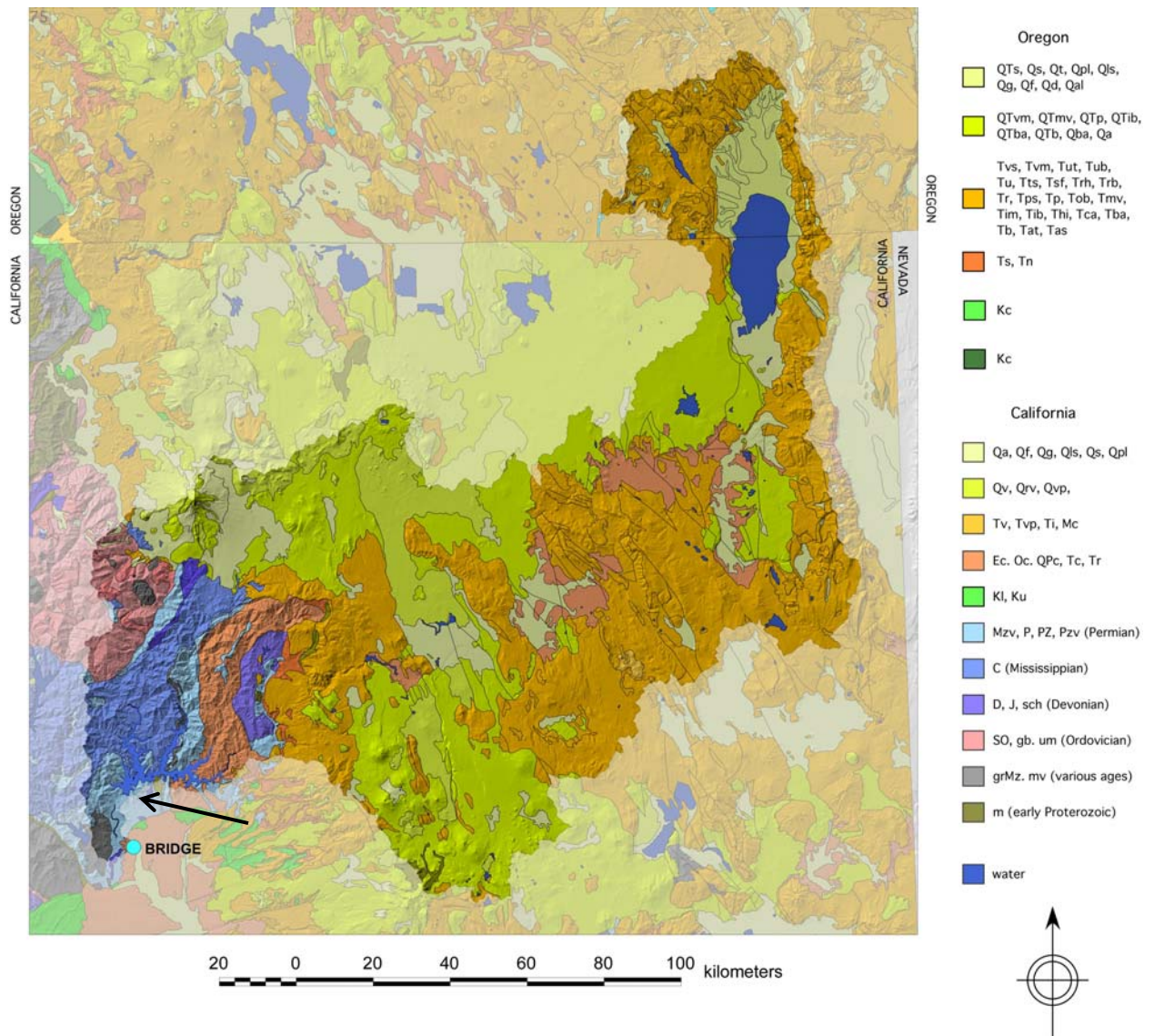
Figure 21. General geologic map of Sacramento River drainage basin; geology from
Ludington et al., 2007. Arrow points to Shasta Dam. Map prepared by William C. Haneberg.

Figure 22. State Route 273 Bridge over Sacramento River. View looking toward right abutment.
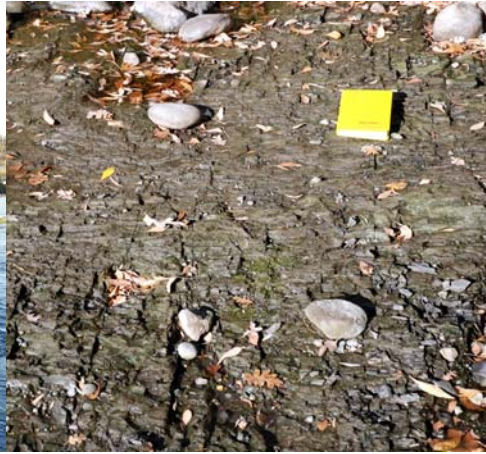
Figure 23. Thinly bedded and locally fractured siltstone. Notebook is 140 mm wide by 192 mm long.

Figure 24. Harder layers in siltstone mark local fold exposed in Sacramento River upstream of SR-273 Bridge. View looking about 45° right of directly upstream; photo taken from bridge.

Figure 25. Rounded cobble-size bed load fragments on bank of Sacramento River near left abutment of SR-273 Bridge. Orange targets are 1.0 m apart.

SELECTED PHYSICAL PROPERTIES FROM LABORATORY TESTS

Laboratory tests included specific gravity, moisture, point load, slake durability, continuous

abrasion, and Rotating Erosions Test Apparatus (RETA) tests. Samples collected from bridge

sites were supplemented by samples of dolostone from a local quarry (Chipola River), rounded

gravel-sized fragments of basalt from a terrace deposit in southwest Utah, and samples of

geotechnical grout produced by Moore & Taber Geotechnical Constructors. Selected laboratory

test results are summarized in Table 2.

Table 2. Summary of laboratory test results. Test results in the Unconfined

Compressive Strength column followed by (T) indicate splitting tension in psi.

Location	Sample	Rock Type	Specific Gravity	Unit Weight (pcf)	Moisture (%)	Point Load Is(50) MPa	Unconfined Compressive Strength (psi)	Slake Durability Index Id(2)	Abrasion Number
Chipola River	Bank	Limestone	2.16	134.8	11.0	1.097	3500	93.1	27.2
	Quarry	Dolostone 1	2.02	125.7	16.0	1.149	3650	98.8	31.4
	Quarry	Dolostone 2	2.31	144.1	3.9	4.736	15100	92.9	8.2
Mill Creek	Bank	Siltstone	2.26	141.1	16.8	0.264	850	2.4	27.4
	Core (OSU)	Siltstone	2.27	141.5	6.0	2.627	8380	23.4	23.7
	Core (RETA)	Siltstone	2.23	139.3	13.1	---	203, 67 (T)	---	---
Schoharie Gage	Bank	Sandstone	2.66	166.0	1.0	14.090	44950	---	4.6
Montezuma Creek	Head Cut	Sandstone	2.60	161.9	1.4	10.629	33900	---	13.6
	Head Cut	Claystone 1	2.50	156.3	14.3	1.176	3750	35.8	23.8
	Head Cut	Claystone 2	2.30	143.7	16.7	---	---	---	63.5
Sacramento River	Bank	Siltstone	2.31	144.1	7.2	4.202	13400	0.7	43.1
	Core	Siltstone	2.36	147.2	13.5	0.690	2200	5.3	33.3
Basalt gravel	Terrace	Basalt	2.54	158.6	1.5	---	---	---	8.9
Grout	1 sack mix	Sand-cement	2.10	130.9	16.2	1.299	4150	88.3	51.2
	1/2 sack mix	Sand-cement	2.06	128.7	17.0	0.169	540	22.3	> 51.2
	1/2 (RETA)	Sand-cement	1.92	119.8	12.3	---	40 (T)	---	---

Specific gravity tests were performed on bulk samples using ASTM method C127-07. Point load

index tests were performed using ASTM method D5731-08. Continuous abrasion tests were

modified from the Slake Durability Test, ASTM method D4644-08, using the general procedure

described by Dickenson and Baillie (1999). The ASTM slake durability procedure calls for oven

drying and two 10-minute-long cycles of tumbling; the Slake Durability Index $(Id_{(2)})$ is the

percentage of initial sample mass retained in the basket after the second cycle. The modified

procedure eliminates the oven drying part and changes the tumbling and weighing increments to

30 minutes or 60 minutes for a number of hours. Weighing is done on 'drip dry' samples that

have most of the free water off of the sample fragments, but without letting them dry for

substantial amounts of time. The sample fragments are left in the basket during weighing.

The 'continuous abrasion' test of Dickenson and Baillie (1999) expresses sample loss as a

function of accumulated time during the test (Figure 26). The abrasion number is defined as the

slope of the abrasion loss rate curve for that part of the test beyond 120 minutes on a semi log plot

of the data (lower graph on Figure 26). The first 60 to 120 minutes of the test display a sample

loss rate that is controlled by rounding of angular fragments, whereas sample abrasion is

occurring after rounding is complete (Figure 27). The samples demonstrate a wide range of

results.
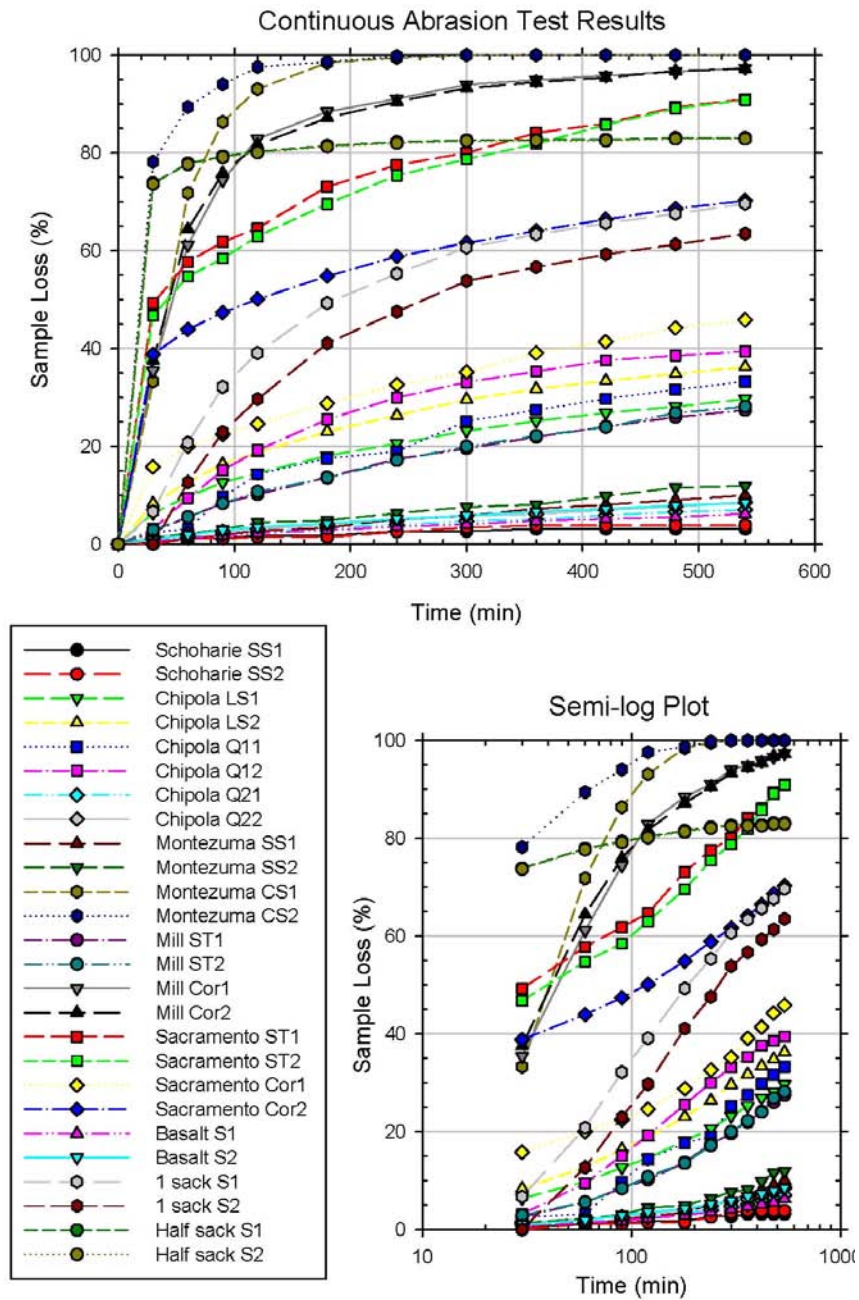
Figure 26. Continuous abrasion test results. Notations: SS – sandstone;

LS – limestone; Q1, Q2 – quarry; CS – claystone; Cor- Core; S - sample.

Sacramento River
Siltstone Core Sample

Geotechnical Grout
1-Sack Mix Sample

Figure 27. Comparative photographs showing two samples at
0, 60, and 300 minutes during the continuous abrasion test

The wide range of sample loss (very little loss of resistant samples compared to complete loss of

nonresistant samples) suggested that the continuous abrasion test results might not be directly

comparable. At some degree of sample loss, nonresistant sample fragments are abrading only

against the wire mesh of the basket, whereas resistant sample fragments are abrading against each

other as well as the wire basket. Therefore, energy was calculated as sample mass × distance

traveled (Newton-meters or Joules) and plotted against the equivalent cumulative distance that the

samples traveled during the test. The distance was calculated from the rate of basket rotation (20

rpm) and the basket circumference (0.44 m). The equivalent relative velocity of the sample is

0.1467 m/s. The samples travel an equivalent distance of 4752 m during a 9-hr test. Resistant

samples exhibit more constant energy during the continuous abrasion test than nonresistant

samples. Figure 28 shows cumulative energy for eight samples with resistant samples plotting as

straight lines and nonresistant samples exhibiting nonlinear behavior.
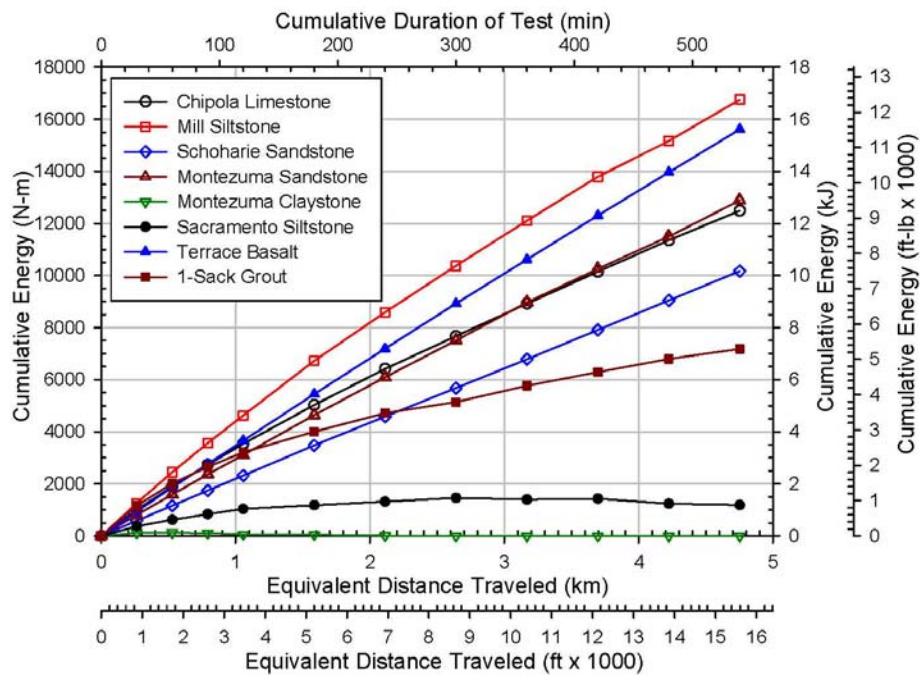
Figure 28. Cumulative energy plotted against equivalent distance traveled during

a 9-hr continuous abrasion test using standard slake durability test equipment.

Energy dissipation can be expressed in terms of Newton-meters per second or foot-pound per

second, which are the units of stream power (1 N-m/s = 1 J/s = 1 W). Unit stream power is stream

power normalized per area of channel cross section, expressed as W/m^2. The continuous abrasion

test results were converted to equivalent power or unit energy dissipation by dividing the

incremental energy by the number of seconds between measurements and assuming that the

sample fragments remain in the lower 45° of the slake durability basket during the test. The

basket circumference is 0.44 m and its length is 0.10 m; therefore, the area of a 45° sector of the

basket is 0.0055 m^2. Figure 29 shows the first 3 hours of the test data plotted in Figure 28 with the

results normalized as percentages of initial sample mass and initial equivalent power. The values

progress from right to left, starting with 100% of the equivalent power.
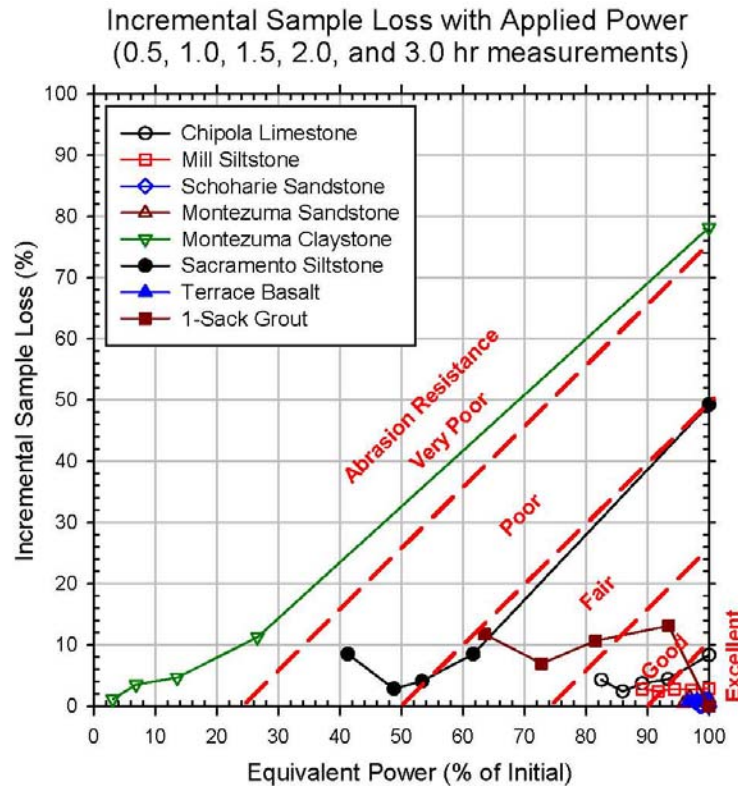
Figure 29. Incremental sample loss plotted against equivalent power.

Abrasion resistance field boundaries are arbitrary.

It can be seen in Figure 29 that samples with linear trends in Figure 28 retain at least 95% of the

initial power during the first 3 hours of the continuous abrasion test. Samples with strongly

nonlinear trends in Figure 28 (Montezuma claystone and Sacramento siltstone) exhibit large

sample loss in the initial test increment. Samples with mild nonlinear trends in Figure 28 (Chipola

limestone, Mill siltstone, and 1-sack grout) exhibit modest sample loss in the initial test

increment, with continuing loss in subsequent test increments. Samples with linear trends in

Figure 28 exhibit high equivalent power (>95%) and low incremental sample loss (<5%) during

the 3 hours of test data plotted on Figure 29. It should be noted in Figure 27 that coarse sand

grains (>2 mm) abrading from the 1-sack grout sample are retained in the basket and contribute to

incremental sample mass; therefore, the continuous abrasion test results for the geotechnical grout samples do not represent actual abrasion loss.

Florida DOT tested four samples in their Rotating Erosion Test Apparatus (RETA) (Figure 30): Siltstone core samples from Mill Creek obtained with drilling donated by Oregon DOT and geotechnical grout samples donated by Moore & Taber. Siltstone samples were tested at field moisture and saturated. Grout samples were sand-cement slurry mixed with ½ sack of cement per 8 cubic feet of grout and cast in standard plastic tubes 3 inches in diameter and 6 inches long. The exterior surface of the grout cylinders were as smooth as the inside of the plastic tube in which they were cast. The RETA results show negligible erosion rate on the smooth sample, but a rough sample showed a higher erosion rate. Testing of several other samples was attempted, but the samples were too fragile to survive handling during preparation.
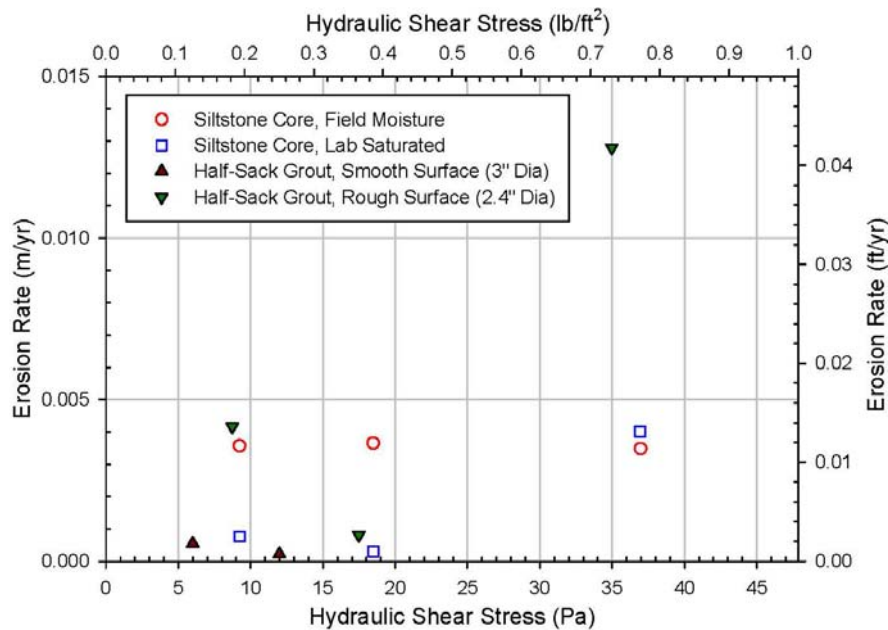
Figure 30. Rotating Erosion Test Apparatus (RETA) test results

CONCLUSIONS

The five bridge sites described above demonstrate a wide range of field conditions (e.g., drainage basin area, geologic setting, elevation, and climate) and tests results. Using test results to predict scour depths and rates continues to be a challenge. Bridge sites for which multiple cross sections are available provide a basis for determining scour rates empirically if stream flow data are available or can be estimated. Sites of proposed bridges and existing bridges for which repeated cross sections are not available require geotechnical characterization as well as stream flow data for predicting scour depth and time rate of scour.

REFERENCES

Dicken, C.L., Nicholson, S.W., Horton, J.D., Kinney, S.A., Gunther, G., Foose, M.P., and Mueller, J.A.L., 2008, Preliminary integrated geologic map databases for the United States; Delaware, Maryland, New York, Pennsylvania, and Virginia: U.S. Geological Survey Open-File Report 2005-1323, version 1.1.

Dicken, C.L., Nicholson, S.W., Horton, J.D., Foose, M.P., and Mueller, J.A.L., 2007, Preliminary integrated geologic map databases for the United States; Alabama, Florida, Georgia, Mississippi, North Carolina, and South Carolina: U.S. Geological Survey Open-File Report 2005-1323, version 1.3.

Dickenson, S.E., and Baillie, M.W., 1999, Predicting Scour in Weak Rock of the Oregon Coast Range: Department of Civil, Construction, and Environmental Engineering, Oregon State University, Corvallis, OR, Final Report SPR 382, Oregon Department of Transportation and Report No. FHWA-OR-RD-00-04.

HDR Engineering, 2004, Montezuma Creek Bridge Scour Technical Memorandum: Unpublished consulting report submitted to Utah Department of Transportation, 14 p. plus appendices.

Keaton, J.R., and Mishra, S.K., 2008, Status of NCHRP Rock Scour Project, in Proceedings of the 59th Highway Geology Symposium: Santa Fe, NM, CD ROM, 18 p.

Ludington, S., Moring, B.C., Miller, R.J., Stone, P.A., Bookstrom, A.A., Bedford, D.R., Evans, J.G., Haxel, G.A., Nutt, C.J., Flyn, K.S. and Hopkins, M.J., 2007, Preliminary integrated geologic map databases for the United States; Western States: California, Nevada, Arizona, Washington, Oregon, Idaho, and Utah: U.S. Geological Survey Open-File Report 2005-1323, version 1.3.

OEA, 2001, Final Report, Rock Scour Analysis for the I-10 Bridge Crossing of the Chipola River, Bridge No. 530052 (Westbound) and Bridge No. 530053 (Eastbound): Unpublished consulting report submitted to E.C. Driver and Associates, Tallahassee, FL, and Florida Department of Transportation, District 3, Chipley FL, by OEA, Inc., 5329 NW 33rd Place, Gainesville, FL, 32606, 77 p.

Resource Consultants, Inc. and Colorado State University, 1987, Hydraulic, Erosion, and Channel Stability Analysis of the Schoharie Creek Bridge Failure, New York: Consulting report repared for National Transportation Safety Board and New York State Thruway Authority, paginated by section.

Wyss, Janney, Elstner Associates and Mueser Rutledge Consulting Engineers, 1987, Collapse of the Thruway Bridge at Schoharie Creek: Consulting report prepared for the New York State Thruway Authority, Albany, NY, paginated by section.

<div align="center">**6.1**</div>

Condition Assessment of Earth Reinforcements

for Asset Management

Kenneth L. Fishman, Ph.D., P.E.[6], Robert A. Gladstone, P.E.[7], John J. Wheeler, Jr., P.E.[8]

Abstract

Mechanically Stabilized Earth (MSE) structures have been constructed in the United States since 1971 using galvanized steel soil reinforcements. Currently there are more than 45,000 MSE structures with steel reinforcements in service throughout the United States. These critical components of the surface transportation network should be included in a Transportation Asset Management (TAM) program, and this paper briefly describes techniques and data tools to collect and analyze data and measure performance of MSE structures.

Introduction

As part of a TAM strategy, data are collected to document the performance of MSE structures including the condition of metallic reinforcements and corresponding rates of metal loss. Performance data make an important contribution to asset management as a means to quantify service life, including the effects of alternative materials, climate and site conditions, and the benefits of maintenance and rehabilitation. This paper describes the framework of a performance database useful for asset management, test techniques and protocols that are being employed to collect performance data for earth reinforcements, data interpretation, and preliminary information available from data that has been collected to date worldwide.

The New York State Department of Transportation (NYSDOT) has routinely collected data from selected sites as part of an MSE corrosion-monitoring program initiated in 1998. Selected sites in New York State (NYS) include use of alternative lightweight fill materials for which the corrosion resistance is suspect, and conventional fills that meet

---

[6] President, Earth Reinforcement Testing, Inc., c/o McMahon & Mann Consulting Engineers, P.C., 2495 Main St., Suite 432, Buffalo, NY 14214, (716) 834-8932 (v), kfishman@mmce.net.

[7] Executive Director, Association for Metallically Stabilized Earth, McLean, VA, bobgladstone@amsewalls.org

[8] Senior Civil Engineer, New York State Department of Transportation, Office of Structures, Metal Engineering Unit, 50 Wolf Rd., Albany, NY, (518) 457-4525, jwheeler@dot.state.ny.us

specific criteria for corrosion resistance. Data from these sites are discussed and compared with trends observed from an analysis of the worldwide data.

Description of MSE

Mechanically Stabilized Earth (MSE) structures have been constructed in the United States since 1971 using steel soil reinforcements. The technology quickly became known for its economy, its ease and speed of construction, its adaptability to varying and/or poor foundation conditions and, with time, for its durability. Within the civil works infrastructure, MSE retaining walls and bridge abutments have become standard construction for highway, mass transit and railroad, airport, port, waterfront, industrial, commercial and residential projects.

Concept

The concept of Mechanically Stabilized Earth is a simple one. A material with substantial compressive strength – compacted granular fill – is reinforced by a material with significant tensile capacity – steel, with each component being used in its most efficient manner. The resulting composite material has both great strength and structural flexibility, is easy to construct, and has a predictable design life. In structural concept, a Mechanically Stabilized Earth wall is a gravity structure, having a cross sectional width typically at least 70% of its height as shown in Figure 1. MSE walls often support a traffic barrier or other protection system.
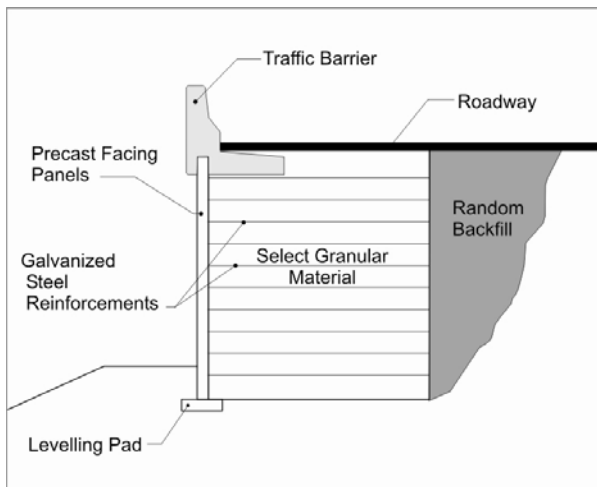

Figure 1. Schematic Illustration of MSE Construction

MATERIALS

The principal elements of MSE construction, also depicted in Figure 1, are wall facing, galvanized or plain steel reinforcements and granular backfill. The anticipated service lives of MSE structures are most dependent on the durability of the earth reinforcements although, in some circumstances, foundation conditions and construction-related problems may also play an important role. Most steel reinforcements for MSE structures are hot-rolled steel strips or welded wire or bar-mat grids, manufactured, respectively,

from steel bars or cold-drawn wire as depicted in Figure 2. Most often the reinforcements include hot-dip galvanizing for corrosion protection. Durability of the reinforcements is controlled by backfill characteristics, site conditions, climate, steel type (galvanized or not), and several details of project construction and in-service operations.

a) bar mat reinforcements
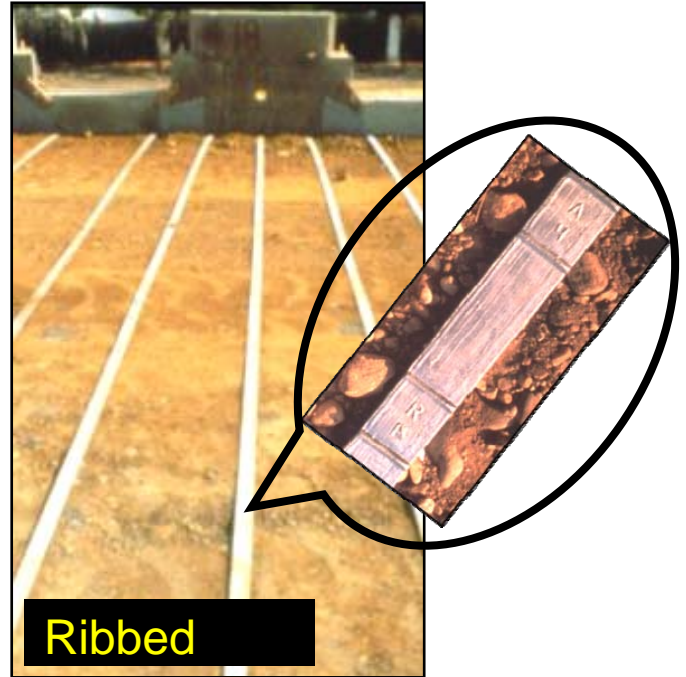
b) hot-rolled steel strip reinforcements

c) welded wire grid reinforcements

Figure 2. Examples of Metallic Reinforcements Used in MSE Construction

Design Considerations

Most of these MSE walls are owned by state departments of transportation and are, therefore, designed and constructed using some form of the AASHTO specifications as a guide. The approach to metal loss has been to calculate the expected loss of both zinc and steel during the design life, then add sufficient sacrificial steel to the reinforcement cross section to ensure the end-of-design-life allowable stress condition. Table 1 describes the AASHTO-recommended metal loss model for design of MSE structures (AASHTO, 2007) and the corresponding backfill requirements. Significant efforts have been devoted to documenting the performance of in-service reinforcements and to verifying the reliability of the AASHTO (and other) models used in MSE structure design.

Table 1. AASHTO Metal Loss Model and Backfill Requirements

Metal Loss Model		Backfill Requirements	
Component Type (age)	Loss (μm/yr)	pH	5 to 10
		Resistivity	≥ 3000 Ω-cm
Zinc (< 2 yrs)	15	Chlorides	< 100 ppm
Zinc (> 2 yrs)	4	Sulfates	< 200 ppm
Steel (after zinc)	12	Organic Content	< 1%

Construction Inspection, Maintenance & Performance

While we presume that every MSE structure is to be properly designed and designs are thoroughly checked, construction inspection is critical to achieving long-term performance and durability. First, all manufactured and natural materials must meet the specifications, especially the backfill, which is contractor-supplied and differs from project to project. As noted earlier, backfill characteristics – both mechanical and electrochemical – are critical to achieving the expected service life. Second, structure longevity and performance depend on good construction practices such as proper storage, handling and installation of manufactured MSE components, careful attention to all installation details, placement and compaction of backfill to proper elevation, grade, density and moisture content, site grading to control runoff, and correct installation of all drainage features. Third, active involvement of a trained, knowledgeable inspector can assure that the first and second conditions listed above are met, providing the owner with professionally-prepared records that will both inform and simplify the task of managing and maintaining this MSE asset.

MSI Inventory

The Association for Metallically Stabilized Earth (AMSE) has compiled an inventory documenting details of MSE walls constructed in the United States over the past 35 years (AMSE, 2006). The majority of walls constructed with grid reinforcements serve as retaining walls, but approximately one third of the walls with strip reinforcements serve as part of a bridge structure (abutment or wing walls). Approximately half of the walls in the AMSE inventory are located in the Western Region of the United States, within an arid climate where backfill sources are alkaline. Compared to steel grid type reinforcements, which are used predominantly within the Western Region, use of strip reinforcements is more uniformly distributed geographically. Approximately 40 percent of the walls constructed with strip reinforcements are located in the more temperate Southern climates, where soils are normally slightly acidic.

Asset Management for MSE

Asset management is an important issue facing highway owners, and forecasting the need for maintenance, retrofit or replacement of existing facilities is an important component of Transportation Asset Management (TAM). MSE structures should be included in a TAM program along with pavements, bridges, ancillary structures, etc., to help ensure optimal usage of limited available funding (FHWA, 2008). Properly defining the existing inventory and development of a performance database are important components of asset management.

Well-designed and constructed MSE structures are expected to have service lives of 75 years (in some cases 100 years), but service life is uncertain and should be monitored for confirmation or to enable remediation. Therefore, relatively rapid, non-intrusive, and nondestructive test techniques are needed to collect data necessary for corrosion monitoring and condition assessment of MSE structures. Results from corrosion monitoring indicate if, or when, accelerated corrosion is occurring, while condition assessment can help transportation agencies decide on the most appropriate course of action when drainage, environmental and/or subsurface conditions are unfavorable. Agencies can also use these data to evaluate the variance associated with the performance of an inventory; this is valuable information for those with an interest in making reliability-based decisions.

Service-Life and Durability of Reinforcements

Data on metal loss for buried elements, collected by the National Bureau of Standards (Romanoff, 1957), involved direct physical measurements including weight loss measurements and measurements of corrosion pit depth and section loss. Metal loss may be estimated from remaining weight and thickness measurements, provided the original thickness, or weight, of the steel and zinc components of the element are known. Similarly, early corrosion monitoring practices for MSE structures (Darbin, et al. 1978; Frondistou-Yannis, 1985; McGee, 1985; Ramaswamy and DiMillio, 1986; Whiting, 1986*)* involved exhuming and examining samples of reinforcements for evidence of corrosion, including loss of cross section. This technique is limited to reinforcements

that are accessible, and usually near the surface of the structure. The process is costly and time consuming such that only a limited number of reinforcements are sampled. Therefore, a good statistical sampling of the reinforcements is difficult to achieve with this technique.

Several studies (e.g., Anderson and Sankey, 2002) involve exhuming reinforcements from in-service facilities, but the original dimensions of the elements are uncertain because corrosion monitoring was not anticipated during installation. In these cases, the original dimensions or weights of the elements must be estimated to compute metal loss from observations of remaining thickness or weight. Nominal dimensions may be used with confidence for the steel thickness, but the original thickness of the galvanized layer is more uncertain. A minimum thickness of zinc coating is specified, however the hot dipped galvanization process specified by ASTM A123 (ASTM, 2007) results in galvanized layer thickness that may exceed the minimum by a wide margin. Rossi (1996) reports thickness measurements as high as 280 μm from elements with a specified minimum zinc coating thickness of 86 μm. Various estimates of initial zinc thickness are used as a basis to evaluate zinc loss of exhumed reinforcements in the absence of initial measurements, including (1) observing the zinc thickness from a sample retrieved from the connection to the wall face where the (strip-type) reinforcement is sandwiched between two plates and assuming that zinc loss is negligible because the portion of the reinforcement sandwiched within the connection is not in direct contact with the backfill, and (2) assuming that zinc oxide adhered to the surface is equivalent to the loss of zinc. Both of these assumptions can lead to large errors, and uncertainty with respect to initial conditions remains. However, often one or both of these methods may be used to obtain an estimate of zinc loss.

Alternatively, electrochemical test techniques may be applied for monitoring earth reinforcements (Stern and Geary, 1957; Lawson et al., 1993; Berkovitz, 1999) as shown in Figure 3. With these techniques, a large number of samples may be obtained. Because the tests are nondestructive, reinforcements remain intact and in service after testing and are, therefore, available for future monitoring. Electrochemical measurement techniques may be used to monitor the presence and/or rate of corrosion. Results from electrochemical tests are useful for indicating if the corrosion process is currently active and, if it is, at what rate.

Figure 3. Electrochemical Testing of MSE Reinforcements Showing Core Holes Used to Access Reinforcements and Field Unit for making Measurements

Several nondestructive tests are available for corrosion monitoring including measurements of half-cell potential (E_{corr}), linear polarization resistance (LPR), electrochemical impedance spectrometry (EIS), and electrochemical noise (Fontana, 1986; Tait, 1994). The EIS and LPR techniques monitor the instantaneous rate of metal loss. Because loss history cannot be established from individual instantaneous measurements, reinforcement condition is difficult to determine from isolated LPR or EIS measurements. In older structures, discrete measurements may be particularly difficult to interpret, especially if the existing condition of the reinforcements is unknown. In addition, metal loss rate may vary throughout the year due to transient temperature and moisture conditions, so LPR or EIS measurements should be performed during different seasons to estimate the average rate of metal loss. When measurements are taken throughout the service life of a wall, however, these techniques can quantify the relationship between rate of metal loss and time. Ideally, protocols for condition assessment and corrosion monitoring should include both direct physical observations (i.e., weight loss, remaining thickness, pit depth) and electrochemical tests such as LPR and half-cell potential measurements. However, very few of the documented studies include such complete data.

Table 2 is a summary of statewide practice and MSE corrosion monitoring programs that have been implemented by various state DOT's to date and is an update to that described by Berkovitz (1999). Many of these programs have produced data that has been collected and archived into a performance database.

Database/Inventory

TAM programs are data driven and require databases that (a) identify and name components, (b) describe locations, (c) define and describe data, and (d) explain performance. A performance database has been compiled as part of NCHRP Project 24-28 and includes data from 170 sites located throughout the United States and Europe. Databases that have been developed by several state transportation agencies and industry (Wheeler, 2002(a); Hearn et al., 2004; AMSE, 2006, Beckham et al., 2005; and Timmerman, 1990) were considered and used as a basis to develop the framework for the NCHRP Project 24-28 database. In general, these databases follow a format and protocol consistent with that employed by the FHWA mandated Bridge Management System (Hearn, et al., 2004).

The NCHRP Project 24-28 database is self-contained yet structured such that it can be ported to other existing databases**.** The database is formatted using Microsoft Access®, which is linked to a GIS (ArcView) platform to provide visual and spatial recognition of data. The organization and structure of the various tables and data fields are updated, as necessary, to accommodate different types of information that are identified from available data sets. For example, observations of reinforcement performance/condition may be based on NDT, direct physical measurement, or visual observations, and these data types are archived accordingly. Drop down lists and check boxes are implemented to facilitate mining/querying of the database. Information within the shell of the database is distributed amongst seven distinct tables comprising a total of 150 data fields. The tables are divided into categories of information similar to that employed in other databases that are based on the FHWA Bridge Management Inventory.

Table 2. Summary of State DOT MSEW Corrosion Assessment Programs

State	Description	References
California	Have been installing inspection elements with new construction since 1987, and performing tensile strength tests on extracted elements. Some electrochemical testing of in service reinforcements and coupons has also been performed. LPR and EIS tests were performed on inspection elements at selected sites as part of NCHRP Project 24-28 and results compared with direct physical observations on extracted elements.	Jackura et al. (1987), Elias (1990), Coats et al. (1990), Coats et al. (2003- Draft Report)
Florida	Program focused on evaluating the impact of salt-water intrusion, including laboratory testing and field studies. Coupons were installed and reinforcements were wired for electrochemical testing and corrosion monitoring at 10 MSE walls. Monitoring has continued since 1996.	Sagues et al. (1998, 1999, and 2000), Berke and Saques (2009)
Georgia	Began evaluating MSE walls in 1979 in response to observations of poor performance at one site located in a very aggressive marine environment incorporating an early application of MSE technology. Exhumed reinforcement samples for visual examination and laboratory testing. Some in situ corrosion monitoring of in service reinforcements and coupons at twelve selected sites using electrochemical test techniques was also performed.	McGee (1985), Deaver (1992)
Kentucky	Developed an inventory and performance database for MSE walls. Performed corrosion monitoring including electrochemical testing of in service reinforcements and coupons at five selected sites.	Beckham et al. (2005)
Nevada	Conditions assessment and corrosion monitoring of three walls at a site with aggressive reinforced fill and site conditions. Exhumed reinforcements for visual examination and laboratory testing; performed electrochemical testing on in service reinforcements and coupons. A total of 12 monitoring stations were dispersed throughout the site providing a very good sample distribution.	Fishman et al. (2006)
New York	Screened inventory and established priorities for condition assessment and corrosion monitoring based on suspect reinforced fills. Two walls with reinforced fill known to meet department specifications for MSE construction are also included in program as a basis for comparison. Corrosion monitoring uses electrochemical tests on coupons and in service reinforcements.	Wheeler (1999, 2000, 2001, 2002a and 2002b)
North Carolina	Initiated a corrosion evaluation program for MSE structures in 1992. Screened inventory and six walls were selected for electrochemical testing including measurement of half-cell potential and LPR. This initial study included in service reinforcements but coupons were not installed. Subsequent to the initial study, NCDOT has installed coupons and wired in-service reinforcements for measurement of half-cell potential on MSE walls and embankments constructed since 1992. LPR testing was also performed at approximately 30 sites in cooperation with NCHRP Project 24-28.	Medford (1999)
Ohio	Concerned about the impact of their highway and bridge deicing programs on the service life of metal reinforcements. Performed laboratory testing on samples of reinforced fill but did not sample reinforcements or make insitu corrosion rate measurements	Timmerman (1990)

| Oregon | Preliminary study including 1) a review of methods for estimating and measuring deterioration of structural reinforcing elements, 2) a selected history of design specifications and utilization of metallic reinforcements and 3) listing of MSE walls that can be identified in the ODOT system. | Raeburn et al. (2008) |

The database includes the following tables:

- Project
- Walls/Structure
- Reinforcements
- Backfill/Subsurface
- Observation Points
- NDT Results
- Direct Observations

Microsoft Access data forms were created to facilitate data entry. Tables are related using a one to many relationship using "project number" as a key parameter. Relationships are also defined among backfill, wall, reinforcements, monitoring stations and results tables.

Each project is associated with a point that is displayed on a map within ArcView. ArcView mapped points are also linked to the Microsoft Access tables so pertinent information for each project can be displayed next to each point when selected by the user. In this way, the geographic distribution of performance data, as well as specific attributes for each site can be displayed within a GIS platform. Thus, the user may associate the data with geographic location and view all of the performance data and pertinent information associated with that point.

Figure 4 is a summary of analysis of data from the database grouping measurements of corrosion rates with respect to backfill character, age, and reinforcement type. Figure 4 demonstrates that if the quality of the reinforced fill meets electrochemical requirements as described in Table 1, then relatively low rates of corrosion are observed. However, for poor quality fill materials, e.g. resistivity < 3000 Ω-cm, relatively high rates of corrosion can be observed compared to those that are recommended for design and depicted in Table 1. These corrosion rates can be 20 to 30 times higher than those observed with good quality fill materials.

NEW YORK STATE Experience

Baseline Measurements

The NYSDOT selected two sites for corrosion monitoring where the backfill parameters meet the requirements relative to corrosion control as specified by NYSDOT, including

one in Marcy-Utica-Deerfield (SR 49). The Marcy-Utica-Deerfield Project was constructed during the spring of 2000 and initial readings were obtained shortly thereafter. The wall system includes galvanized, ribbed, steel strips and cruciform precast concrete wall facing units. Results from electrochemical tests performed on 62 backfill samples include minimum resistivity data ranging between 9000 to 15, 000 Ω-cm, pH ranging from 7.5 to 8.9, and sulfate and chloride concentrations less than 10 ppm. Therefore, the backfill at this site satisfies NYSDOT and AASHTO criteria, and is not considered aggressive relative to corrosion.
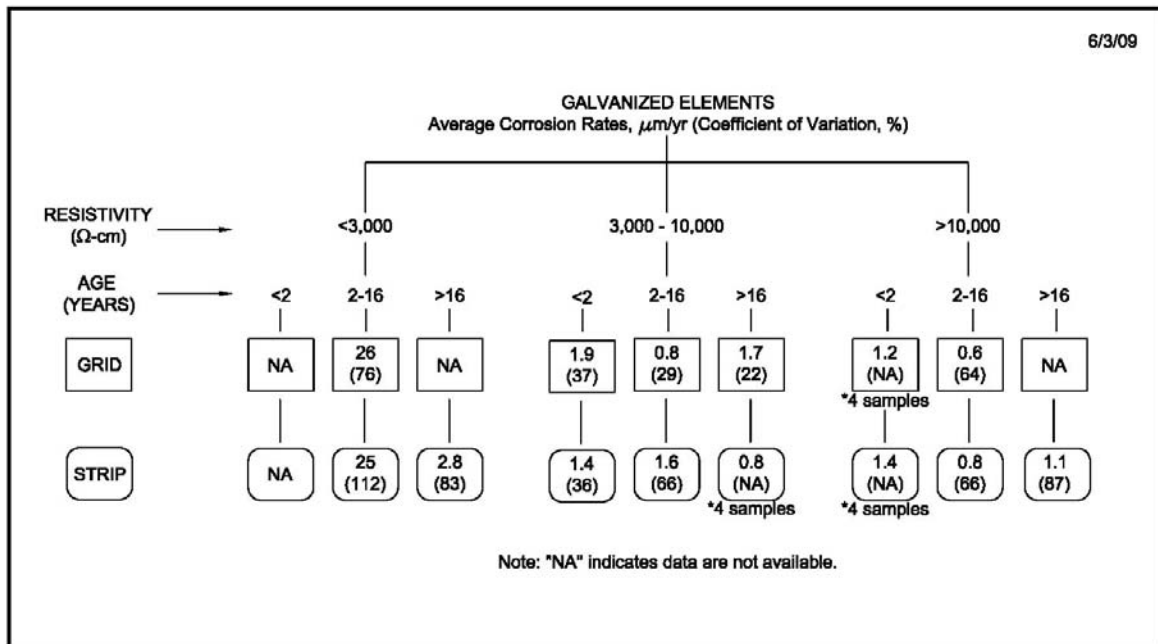
Figure 4. Summary of Corrosion Rate Measurements f rom NCHRP Project 24-28 Database

Measurements were collected shortly after construction in 2000 and eight years after construction on May 29, 2008. Figure 5 presents a comparison of results from measurements made in 2000 and 2008. In general, the soil resistance measured as part of the LPR test was much lower in 2008 compared to 2000. Figure 5(a) depicts the trends with respect to half-cell potential measurements, and Figure 5(b) shows the corrosion rates measured for galvanized elements including galvanized coupons and in service reinforcements.

 The half-cell potential measurements from 2000 (horizontal scale in Figure 5(a)) show that, generally, the range of potentials for the galvanized elements overlapped with the range of potentials for the zinc coupons. Half-cell potential measurements from 2008 (vertical scale in Figure 5(a)) show that the half-cell potentials of the galvanized elements have shifted away from the half-cell potential of the zinc elements, and there is some overlap with the lower range of potentials measured for the steel coupons and the galvanized elements. These trends are as expected, and the data serve to expand the

database and enhance our ability to evaluate the condition of reinforcements with respect to time.
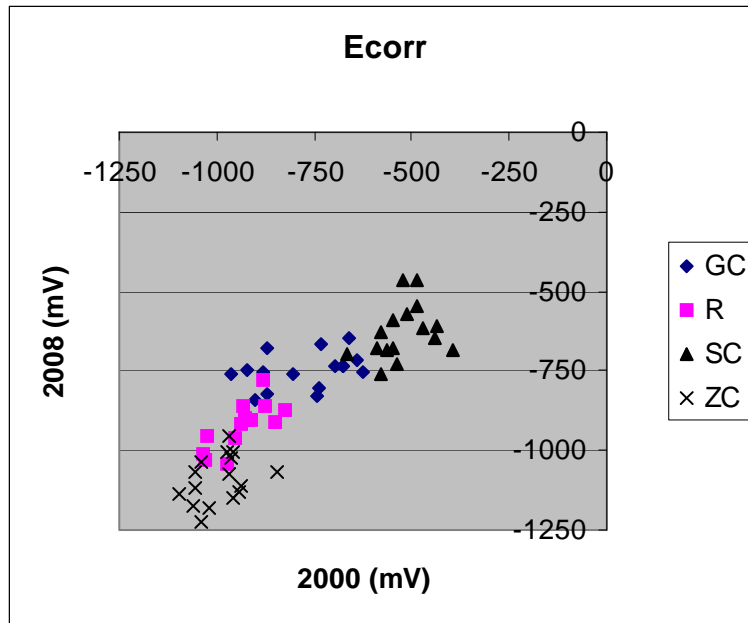
a) Half-Cell Potentials (mV); GC – Galvanized coupons, R – Reinforcements (galvanized), SC- steel coupons, ZC – zinc coupons
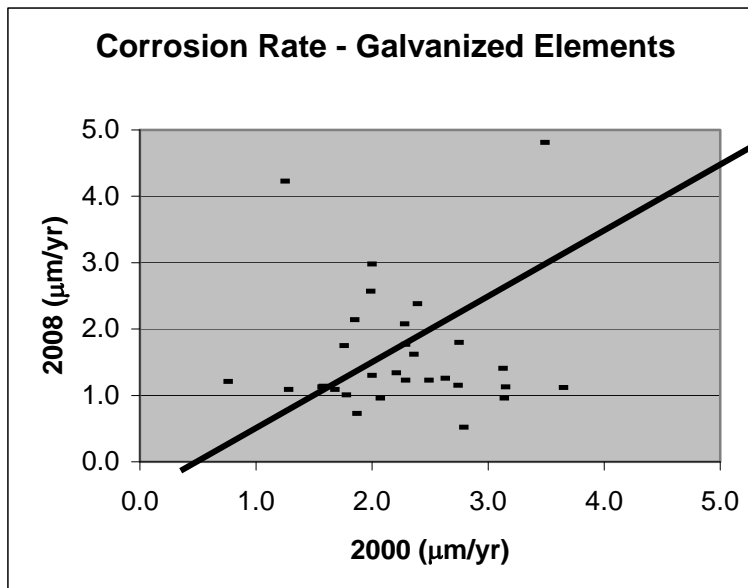
b) Corrosion Rates (μm/yr) for Galvanized Coupons and In Service Reinforcements
Figure 5. Mary-Utica Wall Results from Monitoring After Construction in 2000 and After Eight Years in Service in 2008.

Figure 5(b) shows that corrosion rates for galvanized elements are generally lower in 2008 compared to 2000. The mean corrosion rate for galvanized elements in 2000 was 2.2 μm/yr with standard deviation equal to 0.67. In 2008 the mean corrosion rate for galvanized elements was 1.6 μm/yr with standard deviation equal to 0.96.

Backfill Issues

In 1998, The New York State Department of Transportation established corrosion-monitoring stations at two walls in Amherst, NY as part of its MSE wall corrosion assessment program. The walls included embankment walls for the Lockport Expressway (I-990) over Sweet Home Road and I-990 over Dodge Road. These MSE walls were constructed in 1980 and 1981, respectively, and were backfilled with a mixture of lightweight fill containing blast furnace slag and cinder ash. Due to the nature of the reinforced fill, and the fact that other MSE walls backfilled with a lightweight industrial waste product in the area had to be replaced due to severely corroded metal reinforcing strips, the occurrence of accelerated corrosion was suspected at these sites. Results from chemical testing indicated that the reinforced fill provided an aggressive corrosive environment. Table 3 presents a summary of the chemical properties of the slag/cinder ash reinforced fill. All of the reinforced fill parameters described in Table 3 are outside the limits recommended by AASHTO.

Table 3. Electrochemical Properties of Slag/Cinder Ash Reinforced Fill at I990 over Dodge and

Sweethome Road Sites in Buffalo, NY

Test	Results	AASHTO Specified Limits
Resistivity	426 to 963 Ω-cm	> 3000 Ω-cm
pH	10.9 to 11.4	5 to 10
Chlorides	6 to 499 ppm with 4 of 8 samples >100ppm	< 100 ppm
Sulfates	523 to 742 ppm	< 200 ppm

Each site includes four monitoring stations, similar to the on depicted in Figure 3, that are at least 100 ft (30 m) apart. Each station includes measurements from five in service reinforcements that are within 2 to 3 feet (0.6 to 1 m) of each other, and from steel, zinc and galvanized coupons. NYSDOT collected corrosion-monitoring data from these sites subsequent to installation of corrosion monitoring stations in 1998 (Wheeler, 2002(a)); and then in May 2002 and November 2005. Corrosion monitoring includes measurements of half-cell potential and corrosion rates from LPR. Observations from coupons and reinforcements support the following conclusions:

1. The corrosion rates of the zinc coupons are significantly higher than those of the steel and galvanized coupons and of the in-service galvanized reinforcements. This may be due to the fact that the reinforced fill at this site includes slag and cinder ash that is relatively alkaline (pH > 11), and the corrosion rate of zinc is adversely affected by high alkalinity.

2. In general, the observed temporal variations of corrosion rates are negatively correlated to the temporal variation in measured soil resistance.

3. In general, the half-cell potentials of the steel and galvanized coupons and the in-service reinforcements are in the same range of -400 mV to –500 mV, but the zinc coupons exhibit a distinctly different range of –800 mV to –900 mV. This indicates that the zinc is nearly consumed on the galvanized coupons and in-service reinforcements.

4. In general, corrosion rates observed for galvanized coupons and in-service reinforcements are similar, and less than the corrosion rates for the plain steel coupons.

As part of NCHRP Project 24-28, readings were taken at approximately monthly intervals between June 2007 and December 2008 in an effort to document the seasonal variations of corrosion rate. Results from these monthly measurements are summarized in Figure 6 including a comparison between corrosion rates and monthly precipitation; and measurements of soil resistance (R_s). The data in Figure 6 represent the means of the measured corrosion rates from reinforcements at the respective sites. These means are associated with coefficients of variance between 10 and 40 percent. These data indicate that corrosion rates appear to correlate well with monthly precipitation and corrosion rate measurements at this site vary by a factor of 1.5 considering seasonal fluctuations.
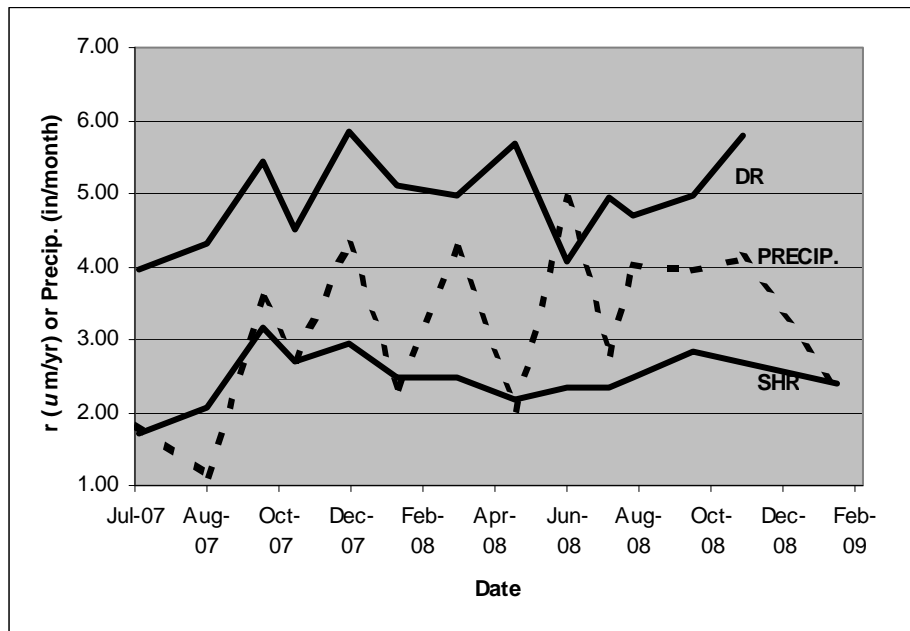
a) Mean Monthly Corrosion Rates Compared to Monthly Precipitation
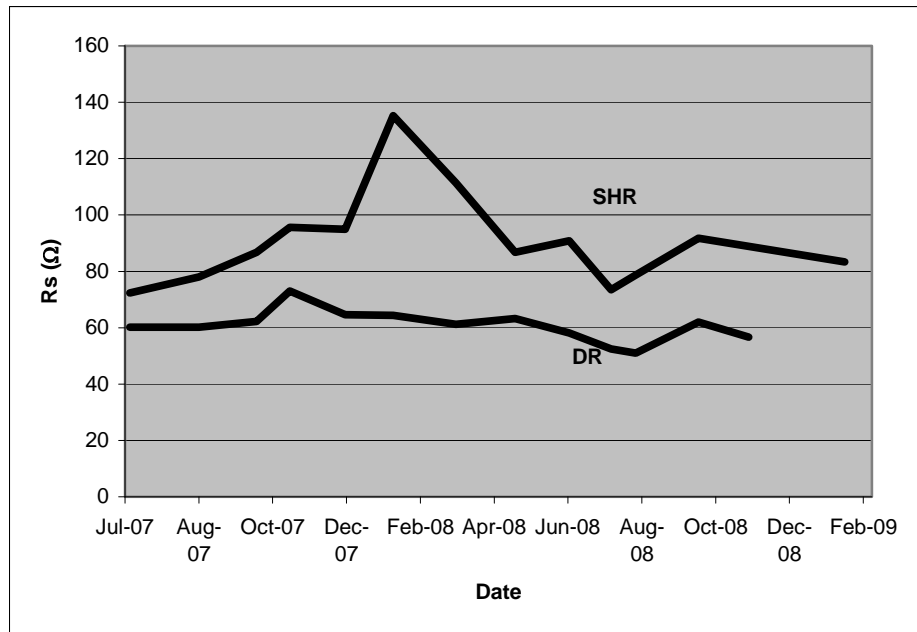
b) Mean Monthly Soil Resistance

Figure 6. Transient Response of Reinforcements at Dodge and Sweet Home Road Sites

Comparison with Database and TAM

Interpretation of data collected in NYS is greatly facilitated by comparison with trends apparent from the much larger data set that has been archived in the MSE performance database. The means and standard deviations of the Marcy-Utica data are consistent with data shown in Figure 4 for steel strip type reinforcements with reinforced fill having minimum resistivity (ρ_{min}) between 3000 Ω-cm and 10,000 Ω-cm, and ages less than 2 years and between 2 and 16 years, respectively. Therefore, data collected at the Marcy-Utica site are consistent with trends observed for the case of reinforced fill that meet current AASHTO criteria. This indicates that the NYS experience is similar to other regions in the US in terms of the magnitudes and distributions of corrosion rates.

Data from the sites in Amherst, New York, are from MSE walls that were constructed with reinforced fill that does not meet current AASHTO criteria for electrochemical parameters. Corresponding corrosion rates are higher, by approximately a factor of three, compared to those documented by Figure 4 for good quality backfill (ρ_{min}> 3000 Ω-cm). Thus, the quality of backfill has a significant effect on performance. However, in this case the observed corrosion rates of approximately 6 μm/yr are not significantly higher than those normally used in design (see Table 1for fill materials that meet AASHTO criteria and reinforcement age > 2 yrs). Also, the corrosion rates observed at the Amherst sites are much less than the relatively high rates of corrosion that have been documented from a number of other sites where fill materials that do not meet AAASHTO criteria (ρ< 3000 Ω-cm) have been used. These data are associated with a high degree of dispersion

362

(COV 76%-112%), some of which may be attributed to effects from other site conditions, in addition to electrochemical properties of reinforced fill, that contribute to a corrosive environment (e.g., poor drainage conditions, high moisture content).

Based on these data, NYSDOT is better able to manage its MSE wall assets and has decided to keep these walls in service and continue corrosion monitoring and observing performance. Without corrosion monitoring or the database to serve as a reference, the course of action for these structures would be more uncertain. It is apparent that, in the absence of performance monitoring and archived data, such uncertainty often leads to a decision for rehabilitation or replacement that may not be necessary.

CONCLUSIONS

MSE retaining walls are common features of highway and bridge construction and should be included in a TAM program. Basic concepts and design and construction details of MSE are described as well as techniques for performance monitoring and archiving performance in a MSE performance database. Performance data collected in New York State provide an opportunity to explore the benefits and utility of archiving performance data and the utility of the MSE performance database within the context of TAM. These data include one site where good quality reinforced fill material was used (Marcy-Utica) and a second set of sites where poor quality reinforced fill materials were used in construction (Amherst sites).

Corrosion monitoring and comparison with existing data as part of a TAM strategy indicate that the service life of reinforcements at the Amherst sites may not be as long compared to sites with good quality fill material (Marcy-Utica), but there is no immediate cause for alarm. This case study demonstrates how experience, documented in a comprehensive database, can be used to broaden the interpretation and utility of site-specific data. Thus, a TAM strategy can save money and allow agencies to make informed decisions relative to the need to replace or rehabilitate MSE structures, especially when the material used in construction may be suspect. In this sense, the performance database itself is also an important asset that needs to be maintained.

References

1. AASHTO, 2007, *LRFD Bridge Design Specifications,* 4th Ed., American Association of State Highway and Transportation Officials, Washington, D.C.

2. American Society for Testing and Materials (ASTM), 2007, ASTM A 123, "Standard Specification for Zinc (Hot-Dip Galvanized) Coatings on Iron and Steel Products," *Volume 01.06, Steel – Plate, Sheet, Strip, Wire, Stainless Steel Bar,* American Society for Testing and Materials, West Conshohocken, PA.

3. Anderson and Sankey, 2002, "The Performance of Buried Galvanized Steel Earth Reinforcements After 20 Years in Service," *Earth Reinforcement Practice: Proceedings of the International Symposium of Earth Reinforcement Practice*, H. Ochiai, S. Hayasashi, and J. Otani, (Eds.), Balkema, Rotterdam.

4. Association for Metallically Stabilized Earth (AMSE), 2006, "Reduced Zinc Loss Rate for Design of MSE Structures", White Paper, AMSE, McLean, VA, http://www.amsewalls.org.

5. Beckham, T.L., Sun, L., and Hopkins, T.C., 2005, "Corrosion Evaluation of Mechanically Stabilized Earth Walls", Report No. KTC-05-28/SPR 239-02-1F, Kentucky Transportation Cabinet, Frankfort, Kentucky.

6. Berke, B.S, and Saques, A.A., 2009, Update on Condition of Reinforced Earthwall Straps, Report No, BD544-32, Florida Department of Transportation, Tallahassee, FL http://www.dot.state.fl.us/research-center/Completed_StateMaterials.shtm, as BD544-32* [PDF - 11,209 KB].

7. Berkovitz, B.C., 1999, "Field Monitoring for Corrosion of Metallic Reinforcements in MSE Structures," Presented to Transportation Research Board, July, 12, 1999, Denver, CO.

8. Coats, D.M., Castanon, D.R., and Parks, D.M., 2003 , "Needs Assessment for Maintenance Monitoring Program for Mechanically Stabilized Embankment Structures*," Draft Report*, State of California, Department of Transportation, Division of Engineering Services, Materials Engineering and Testing Services, Corrosion Technology Branch, 251 pp.

9. Darbin, M., Jailloux, J.M. and Montuelle, J., 1978, "Performance and Research on the Durability of Reinforced Earth Reinforcing Strips," *Proceedings of the ASCE Symposium on Earth Reinforcement,* Pittsburgh, PA.

10. Deaver, R., 1992, "Mechanically Stabilized Earth Wall Study," *Final Report, GDOT Research Project No.9001*, Office of Materials and Research, Georgia Department of Transportation, Forest Park, GA.

11. Elias, V., 1990, *Durability/Corrosion of Soil Reinforced Structures*, Report No. FHWA-RD-89-186, Office of Engineering and Highway Operations, R&D, McLean, VA, 173p.

12. Fantana, M. G., 1986, *Corrosion Engineering*, McGraw Hill.

13. FHWA, 2008, *Earth Retaining Structures and Asset Management,* Publication No. FHWA-IF-08-014, Federal Highway Administration, Washington D.C.

14. Fishman, K.L., Salazar, J.M., and Hilfiker, H.K., 2006, *Corrosion in an Arid Environment and Condition Assessment of a 20-Year Old MSEW,* CD-ROM, Transportation Research Board, National Research Council, Washington, D.C.

15. Frondistou-Yannis, S., 1985, *Corrosion Susceptibility of Internally Reinforced Soil Retaining Structures,* Report No. FHWA/RD-83/105, National Technical Information Service, Springfield, VA.

16. Hearn, G., Abu-Hejleh, N., and Koucherik, J., 2004, "Inventory System for Retaining Walls and Sound Barriers", CD-ROM, Transportation Research Board, 2004 Annual Meeting.

17. Jackura, J.A., Garofalo, G. and Beddard, D., 1987, *Investigation of Corrosion at 14 Mechanically Stabilized Embankment Sites,* Report No. CA/TL-87/12, California Department of Transportation, Sacramento, CA.

18. Lawson, K.M., Thompson, N.G., Islam, M., Schofield, M.J., 1993, "Monitoring Corrosion of Reinforced Soil Structures," *British Journal of NDT,* British Institute of Nondestructive Testing, Liverpool, England, 35(6), pp. 319-324.

19. McGee, P., 1985, *Reinforced Earth Wall Strip Serviceability Study*, Final Report: Study No. 8405, Georgia Department of Transportation, Atlanta, GA, 24p.

20. Medford, W.M., 1999, *Monitoring the Corrosion of Galvanized Earth Wall Reinforcement,* North Carolina Department of Transportation Field Investigation, presented at 78th Annual Meeting of TRB, January 13, 1999, Washington, D.C. (preprint).

21. Ramaswamy, S.D. and DiMillio, A.F., 1986, "Corrosion in Reinforced Soil Structures," *Public Roads,* Federal Highway Administration Office of R&D, Washington, D.C., pp.43-48.

22. Raeburn, C.L., Monkul, M.M. and Pyles, M.R., 2008, "Evaluation of Corrosion of Metallic Reinforcements and Connections in MSE Retaining Walls," *Report No. FHWA-OR-RD-08-10,* Oregon Department of Transportation, Salem, OR, http://www.oregon.gov/ODOT/TD/TP_ERS/, 24 pp.

23. Romanoff, M., 1957, Underground Corrosion, *National Bureau of Standards, Circular 579*, U.S. Department of Commerce, Washington, D.C.

24. Rossi, J.P., 1996, *The Corrosion Behavior of Galvanized Steel in Mechanically Stabilized Earth Structures*, MS Thesis, Department of Civil and Environmental Engineering, University of South Florida, Tampa, FL.

25. Sagues, A.A., Rossi, J., Scott, R.J., Pena, J.A. and Simmons, T., 1998. "Influence of Corrosive Inundation on the Corrosion Rates of Galvanized Tie Straps in Mechanically Stabilized Earth Walls", Final Report WPI0510686, Florida Department of Transportation Research Center, Tallahassee, FL.

26. Sagues, A., Scott, R., Rossi, J., Pena, J.A., and Powers, R., 1999, "Corrosion Performance of Galvanized Strips in Florida Mechanically Stabilized Earth Walls", Preprint CD-ROM, Transportation Research Board 78th Annual Meeting, TRB, Washington, D.C.

27. Sagues, A.A., Scott, R., Rossi, J., Pena, J.A., and Powers, R., 2000, "Corrosion of Galvanized Strips in Florida Reinforced Earth Walls", Journal of Materials in Civil Engineering, ASCE, Reston, VA.

28. Stern, M. and Geary, A.L., 1957, "Electrochemical Polarization," *Journal of the Electrochemical Society,* 104(1), p.56.

29. Tait, S.W., 1994, *An Introduction to Electrochemical Corrosion Testing for Practicing Engineers and Scientists,* Pair-O-Docs Publications, Racine, WI, 138 pp.

30. Timmerman, D.H., 1990. Evaluation of Mechanically Stabilized Embankments as Support for Bridge Structures, Ohio Department of Transportation Interim Research Report.

31. Wheeler, J.J., 1999, *NYSDOT, MSES Corrosion Evaluation Program, End of the Year Report for 1998*, NYSDOT Geotechnical Engineering Bureau, Albany, NY.

32. Wheeler, J.J., 2000, *NYSDOT, MSES Corrosion Evaluation Program, End of the Year Report for 1999*, NYSDOT Geotechnical Engineering Bureau, Albany, NY.

33. Wheeler, J.J., 2001, *NYSDOT, MSES Corrosion Evaluation Program, End of the Year Report for 2000*, NYSDOT Geotechnical Engineering Bureau, Albany, NY.

34. Wheeler, J.J., 2002(a), *New York's Mechanically Stabilized Earth Corrosion Evaluation Program*, TRB 81st Annual Meeting CD-ROM, TRB, Washington, D.C.

35. Wheeler, J.J., 2002(b), *NYSDOT, MSES Corrosion Evaluation Program, End of the Year Report for 2001*, NYSDOT Geotechnical Engineering Bureau, Albany, NY.

36. Whiting, D., 1986, "Corrosion Susceptibility of Reinforced Earth Systems: Field Surveys," *Corrosion Effect of Stray Currents and the Techniques for Evaluating Corrosion of Rebars in Concrete*, ASTM STP 906, V. Chaker, Ed., American Society for Testing and materials, Philadelphia, pp. 64-77.

<center>**6.2**</center>

<center># ROCK SLOPE STABILIZATION PROJECTS</center>
<center>## LETCHWORTH STATE PARK</center>
<center>**PORTAGEVILLE, NEW YORK**</center>

INTRODUCTION

The New York State Office of Parks, Recreation and Historic Preservation (OPRHP) operates

Letchworth State Park in Wyoming and Livingston Counties, New York. The park is located along

the Genesee River, which traverses a deep rock gorge. At two locations along the gorge, the

instability of the soil and rock on the gorge face created concerns for OPRHP (see Figure 1 for

location plan).

A section of the rock face adjacent to the Middle Falls was undermined creating safety concerns

for those viewing the Falls. Additionally, a section of the gorge face beneath the park road had

fallen into the gorge undermining the road and threatening its stability. The OPRHP retained

TVGA Consultants (TVGA) and McMahon & Mann Consulting Engineers, P.C. (MMCE) to develop

plans to stabilize and instrument the rock slope at these locations. This paper describes the

subsurface explorations, engineering evaluation and the methods employed to stabilize the

gorge face at these sites.

The paper presents the gorge road project first, followed by the Middle Falls project. The

stabilization methods at the gorge road site included rock scaling, installing soil nails and

shotcrete, along with rock anchors and horizontal drains. At the Middle Falls site, loose

rock was scaled and high strength bar anchors were installed 40 feet into the slope to

improve its stability. Because of access restrictions, much of the work had to be completed from ropes. The rock anchors are equipped with strain gauges that provide measurements of slope movement with time, allowing OPRHP to plan slope maintenance work.
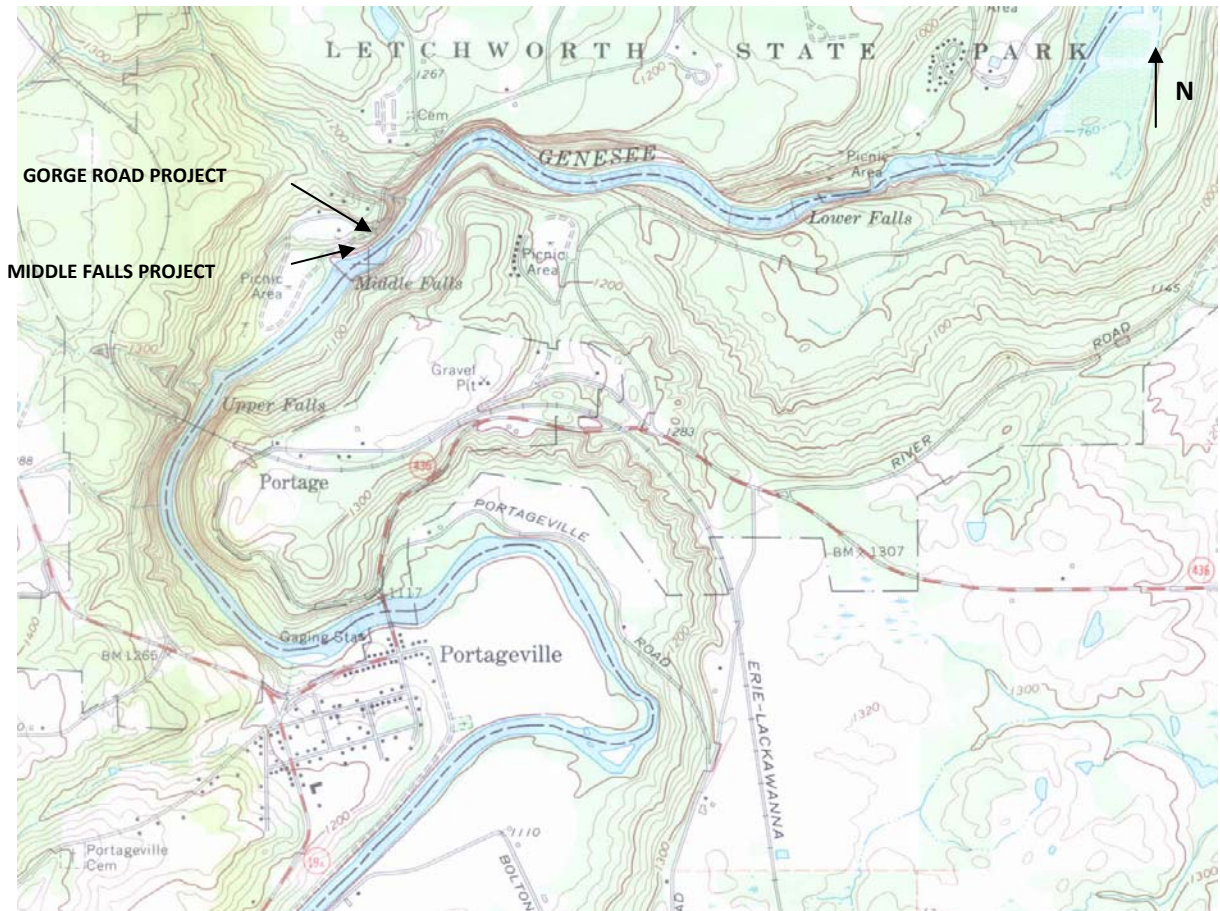

Figure 1 Location Plan

GORGE ROAD PROJECT

Background

In 2005, OPRHP workers noticed an unusual absence of trees and brush along the west edge of the gorge, north of the Glen Iris Inn and the Middle Falls. The gorge in this area has nearly vertical walls and the edge of the road is within a few feet of the gorge wall, making it impossible to observe the gorge wall beneath the road. OPRHP personnel photographed the area from the opposite (east) side of the gorge (Figure 2) and noted some apparent irregularities in the gorge wall at this location.

Figure 2 - Photo by OPRHP personnel of west side of gorge.

OPRHP retained TVGA and MMCE and Earth Dimensions, Inc. (EDI) to visit the site and observe the gorge conditions using a crane and a man basket.

Observations and Site Conditions

MMCE, EDI and OPRHP personnel observed the site conditions in May 2005 with the assistance of a crane and operator provided by Clark Rigging Company. The crane operator lowered personnel over the side of the gorge using a man basket (Figure 3).

A rock outcrop was observed extending to about 7 feet above the road on the west side of the road at the location being studied. Based on the "Geologic Map of New York, Niagara Sheet," by Fisher and Rickard (1970), the rock is shale, sandstone and siltstone of the West Falls Group. Our observations confirmed that the rock is alternating layers of shale, sandstone and siltstone.

Figure 3 Man Basket Used for Observations

The rock jointing pattern was observed in the Genesee River and on the east gorge wall (opposite side of the river – Figure 4). Two sets of near vertical joints are evident, one

approximately perpendicular to the river (estimated to be about N 55˚W) and another

approximately parallel to the river and alignment of the gorge walls. This nearly right angle joint

pattern is common in the exposed sedimentary bedrock in Letchworth Park.

Figure 4 - Looking east across gorge at rock joint pattern

The area immediately beneath the road is not intact rock but is comprised of loose rock, soil and

concrete. It appears that this area was a natural swale that workers who constructed the road

filled in with stacked stones and concrete. Both the stones and concrete are disturbed and have

fallen out of place for a distance of about 40 feet along the gorge wall. A concrete grade beam

could be seen spanning the area where stones have fallen out (Figure 5). Support had been lost

for approximately 10 to 15 feet of the wall and road.

Figure 5 – View (looking west) showing undermined area.

Two rock blocks or columns, one at each end of the approximate 40-foot disturbed section, were observed to be separating from the gorge wall (Figures 6 and 7).

The rock column at the south end (Figure 6) appeared to be separating from the gorge face along a nearly vertical joint parallel to the gorge face. The rock column at the north end of the disturbed area (Figure 7) appeared to also be separated along a near vertical joint but had moved slightly less laterally. Each column appeared to be composed of more competent rock at the bottom and loose rubble near the top.

Figure 6

Figure 7 - Rock Block on north side of undermined area separating from gorge face
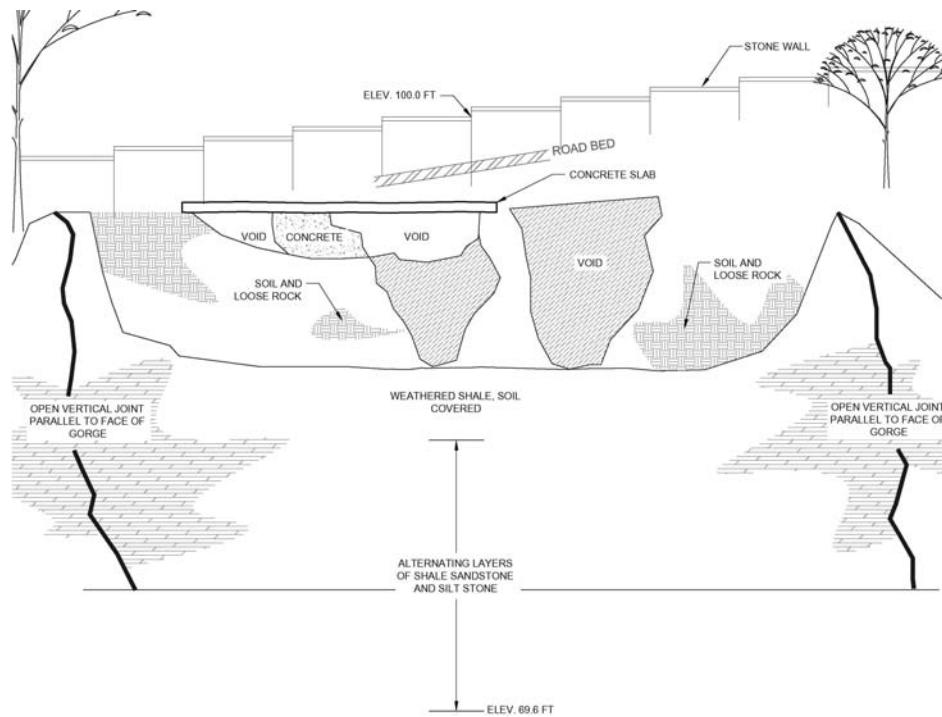
Figure 8 – **Schematic elevation view of the gorge face prior to remediation, looking west.**

Remedial Design and Construction

OPRHP closed the road to traffic and requested that MMCE and TVGA prepare plans to remediate the undermining. EDI drilled borings in the roadway to define the subsurface conditions. Figure 9 is a cross section of the road and gorge face based on our observations and the borings.
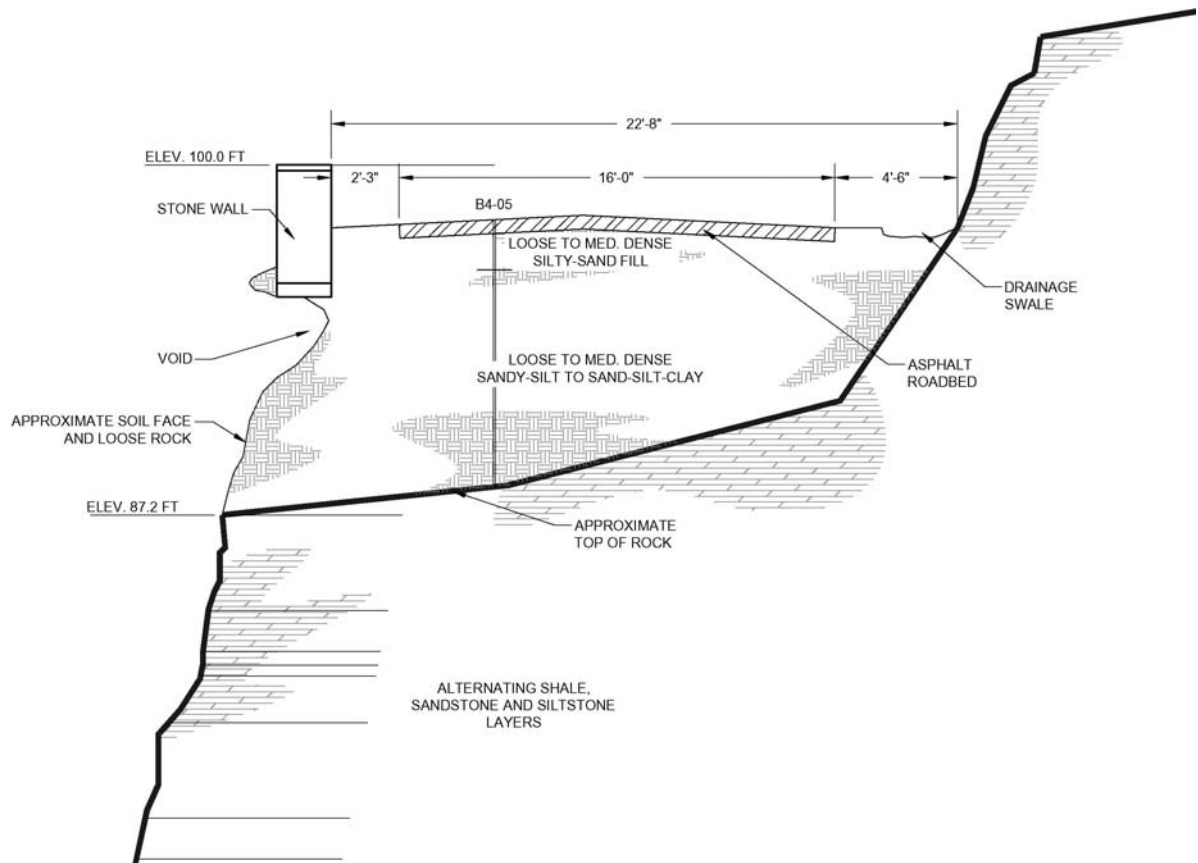
Figure 9 – Typical Section Prior to Construction

Because the road was undermined it was not feasible to complete the remedial work from a crane located on the roadway. It was necessary to develop a design that was constructible considering the site access restrictions. We contacted Janod Inc. (Janod), a specialty subcontractor for rock scaling, shotcreting and rock nail and anchor installation, for design consultation relative to the feasibility of constructing various remedial features. We developed the design based on discussions with the Janod regarding what was feasible and stability calculations for the roadway. Figure 10 is a cross section illustrating the components of the remedial design.
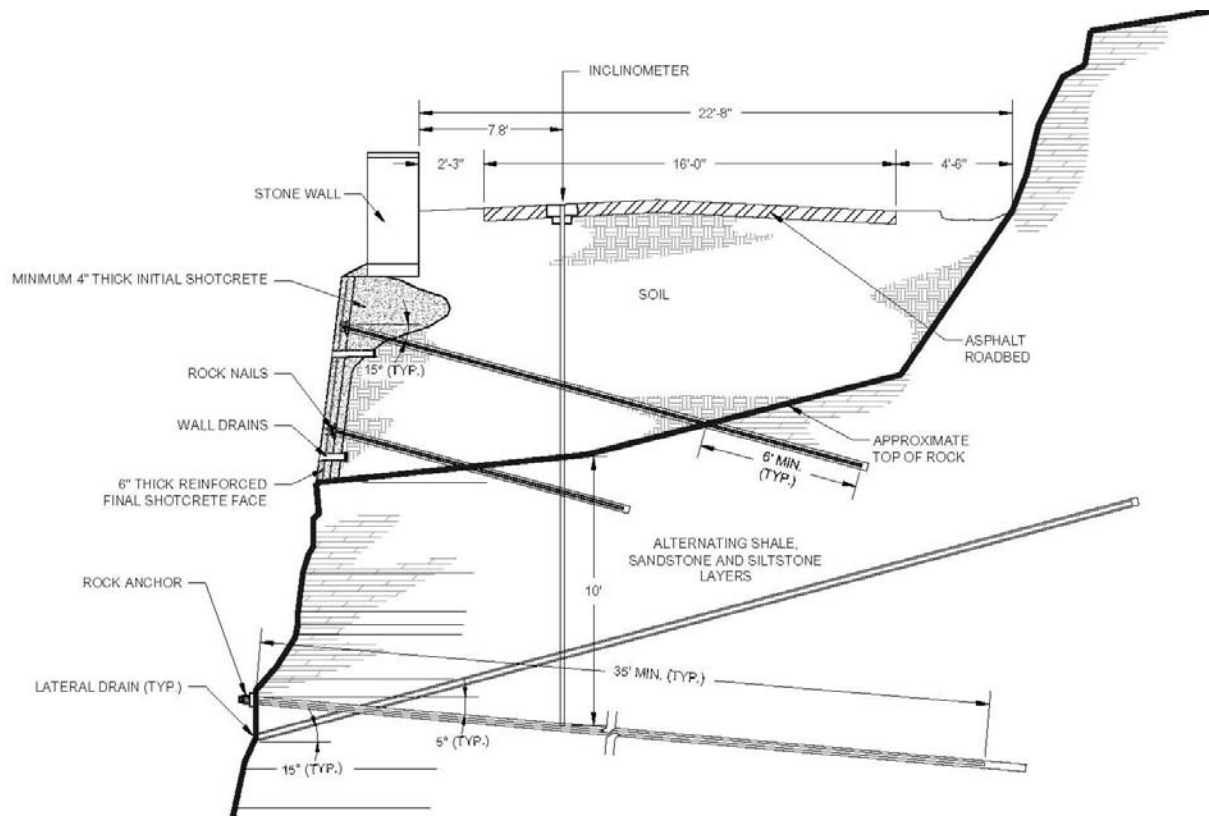
Figure 10 - Typical Design Cross Section

The remedial design included scaling loose rock from the face then installing shotcrete to fill the voids and stabilize the gorge face. The shotcrete facing is reinforced and secured to the gorge face by rock nails. The nails are 1-inch diameter, Grade 95 kips per square inch (ksi), reinforcing bars, drilled at least 6 feet into rock and grouted. Plastic pipes extend through the shotcrete to provide drainage and limit groundwater buildup behind the shotcrete.

The design also includes rock anchors and drains installed in the rock below the void area. Observations of the joint spacing in the gorge indicate that joints tend to be spaced about 20 feet apart. The rock anchors are designed to extend 35 feet into the gorge face with a 20 foot unbonded zone. The anchors are specified to be tensioned to stabilize joints that may exist parallel to the gorge face along the road. The anchors consist of 1¼ inch, Grade 150 ksi, high strength steel bars.

Drains are also included in the design to drain groundwater seeping from the gorge face. The drains consist of 2-inch diameter slotted PVC pipe installed 35 feet into the gorge face.

374

OPRHP contracted with C.P. Ward Inc. to complete the work with Janod as the specialty subcontractor for rock scaling and rock nail and anchor installations. Construction began in the Fall of 2005 with Janod scaling loose soil and rock from the gorge face and initial filling of the void with shotcrete. Janod placed a rubber bladder into the open joints on the north and south sides of the undermined area and inflated the bladder to remove loose material. Once the loose material was removed they began initial filling of the void with shotcrete as shown in Figure 11.

Figure 11 – Janod Filling Void with Shotcrete

Figure 12 shows the shotcrete work in progress. Once the void was partially filled, Janod lowered a drill rig over the side for use in installing the rock anchors, drains and rock nails. Figure 13 shows the rock nail installation and Figure 14 shows the rock anchor installation.

Figure 12

Figure 13 – Rock Nail Installation

Figure 14 – Rock Anchor Installation

Janod completed performance and proof testing on rock anchors and nails. A
performance test, which is a cyclic test of loading and unloading, was completed on a
sacrificial rock nail. Proof tests (single cycle tests) were performed on each of the three
rock anchors and on selected production rock nails. The performance and proof test
results met or exceeded the acceptance criteria defined in the project specifications.

EDI installed two inclinometers within the roadway area after construction was complete.
These devices allow measurements of lateral movement with depth. MMCE has
monitored the inclinometers since 2006 and to date have not observed lateral movement
of the remediated area.

MIDDLE FALLS PROJECT

Background

The Middle Falls at Letchworth State Park (see Figure 1 for location) offers dramatic views of the rock gorge and the Falls. OPRHP personnel requested that MMCE and EDI inspect an area near the Middle Falls viewer platform requiring remediation. MMCE and EDI along with the Gorge Road contractor Janod, observed the conditions and found a loss of rock on the gorge walls along with a large, block of rock at this location, separated from the gorge face by an open joint. The joint was also visible on the river side of the block. The open joint and loose rock is of concern relative to the stability of the overhang, a prominent location for pedestrians to view the Middle Falls (Figure 15). This poses a significant safety threat to those viewing the Falls.

Figure 15 – Middle Falls Prior to Construction – Note Open Joint

OPRHP requested that EDI collect subsurface information for design and MMCE and

TVGA develop a remedial plan for the Middle Falls.

Site Studies

TVGA completed a three dimensional laser survey of the gorge face and prepared a

topographic contour map. The map shows elevation contours of the gorge face from top

to bottom. This map provided the orientation of the gorge face at the Middle Falls and

demonstrated that it follows the joint pattern that is generally perpendicular to the flow of

the river.

EDI drilled a boring approximately 20 feet back from the face of the gorge and collected rock core samples. The rock core consists of alternating layers of siltstone and shale and revealed a vertical joint. MMCE selected several rock samples for unconfined compressive strength testing. The results indicate that the unconfined strength of the core samples varied from 8,000 to 17,000 pounds per square inch (psi).

Remedial Design and Construction

The remedial design included scaling and removing the overhang and removing loose rock from the gorge face. The design included installing seven rock anchors in the rock block next to the Falls and eight rock anchors in the gorge face next to the rock block (i.e., the "overhang area"). Figure 16 is a schematic diagram of the design components.
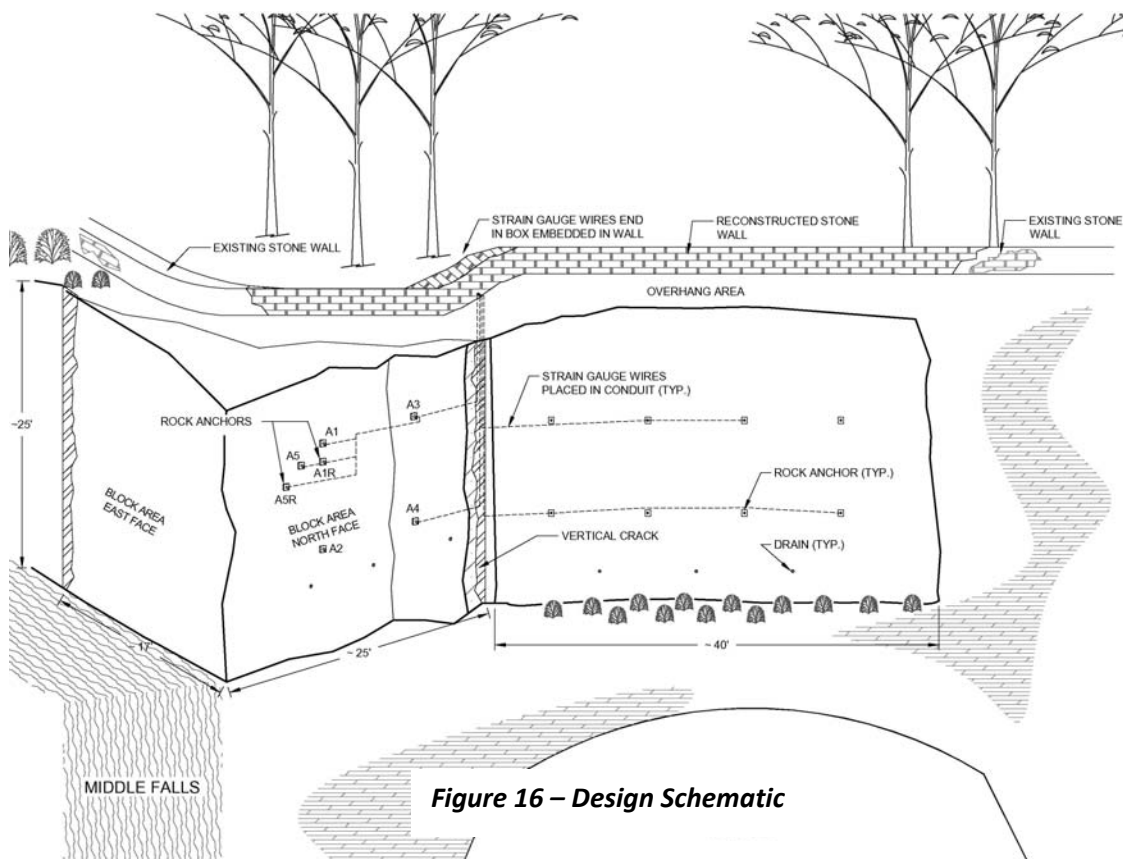
Figure 16 – Design Schematic

Drains were included in the design to provide a drainage path to the gorge face, particularly for water that accumulates in the open joint. Figure 17 is a plan of the anchors and drains in the block and Figure 18 is a typical section through the block.
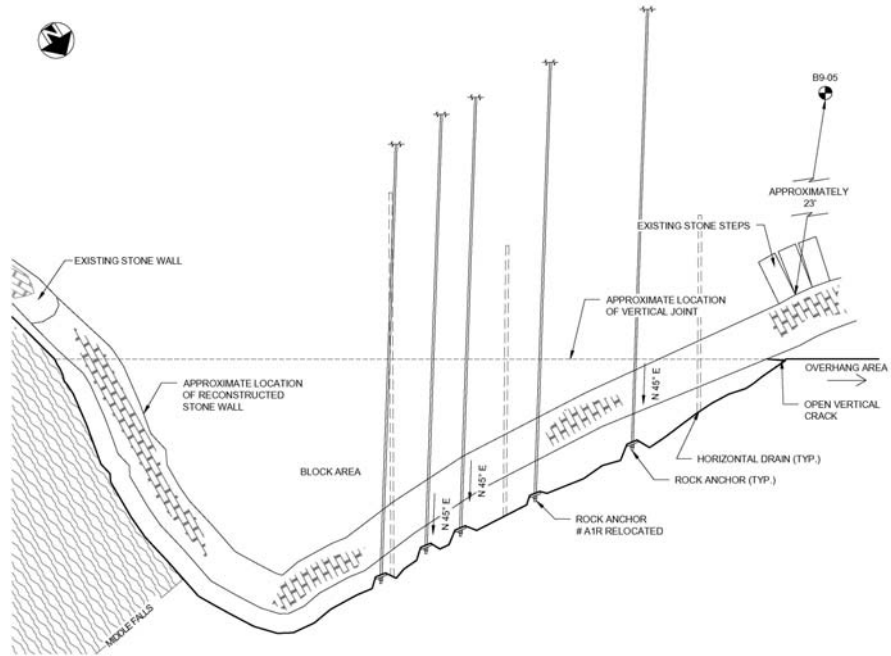
Figure 17 – Plan of Block Area
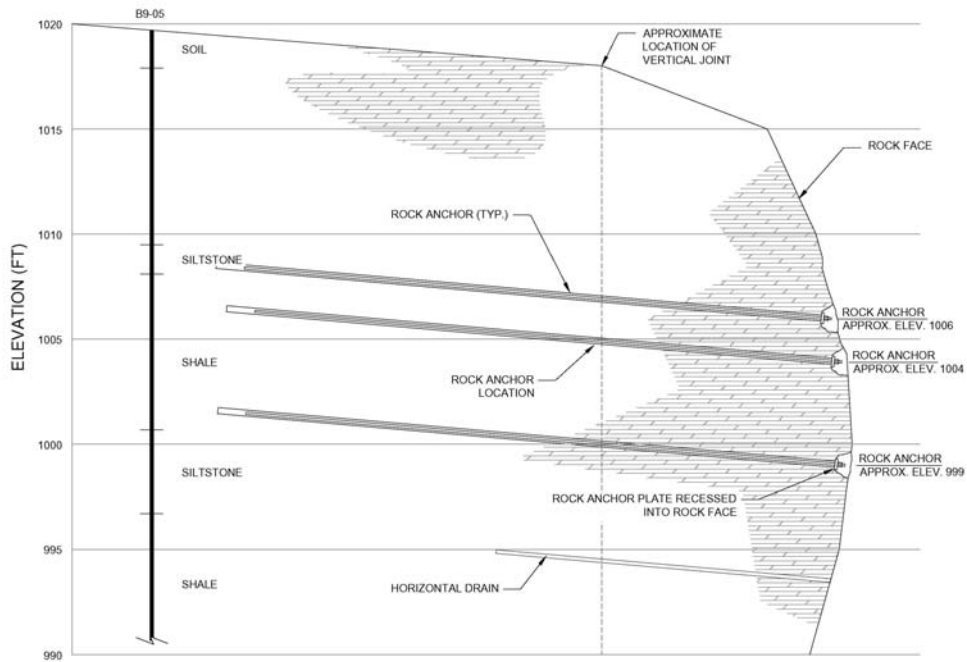
Figure 18 – Section of Block Area

The anchors consist of 1¼ inch, Grade 150 ksi, high strength steel bars. Grout socks are specified around the bars to limit grout loss, especially in the open joint.

Observations of the joint spacing in the gorge indicate that joints tend to be spaced about 20 feet apart. The rock anchors are designed to extend 40 feet into the gorge face with a 23 foot unbonded zone. This is specified so that the bond zone is behind the next vertical joint. The anchor heads are recessed into the gorge face and covered with grout to blend into the gorge face.

The anchors in the block are not tensioned because of concerns that high tension forces could cause the block to rotate and or crack. Rather, the block anchors provide a stabilizing force to limit future movements of the block. The anchors installed in the gorge face are specified to be tensioned to stabilize joints parallel to the gorge face.

The design includes strain gauges attached to rock anchors in the block and the overhang area. The strain gauges are intended to provide an indication of future movement and the need for additional scaling or other remedial work. It is expected that eventually the rock supporting the block along the gorge face will erode potentially destabilizing a portion of the block.

The instrumented rock anchors serve as transducers to monitor performance of the loose block and reflect changing rock conditions. As the block begins to move, load will be

transferred to the rock anchors and will be reflected in the strain gauge measurements, allowing time to plan and implement future actions.

Construction began in the Fall of 2005 with Janod removing the overhang and scaling loose soil and rock from the gorge face. Once the loose material was removed, they began installing drains and rock anchors in the loose block as shown in Figures 19 and 20. As for the Gorge Roadway, all of the work by Janod was completed from ropes.

Figure 19 – Janod Installing Anchors in Block

Figure 20 – Janod Installing Rock Anchors on a Rainy Day

Due to the onset of winter work was suspended until the Spring of 2006.

The remaining work at the Middle Falls included installing anchors and drains in the overhang area. OPRHP solicited bids for the work in the Spring of 2006 and contracted with Patterson-Stevens Inc. to complete the outstanding work. Nothnagle, Inc. subcontracted with Patterson-Stevens as the specialty subcontractor for rock scaling and rock anchor installations.

Instead of working from ropes, Nothnagle constructed a work platform as shown on Figure 21. The platform was suspended from a crane and attached to the gorge face with wedge bolts.

Figure 21 Nothnagle Installing Rock Anchors in the Overhang Area.

Nothnagle completed performance and proof testing on rock anchors and nails. Figure 22 shows an anchor test setup.

Figure 22

Strain gauges were installed on several rock anchors to provide a means of monitoring stress in the anchor rods and rock movement. Figure 23 shows a typical strain gauge installation.

Figure 23 Strain Gauge Installation

Wires from the strain gauges lead to a central readout box installed into the newly construction portion of the viewing platform wall. MMCE has monitored the gauges since construction was completed. The data do not indicate an increase in stress in the anchors.

Nothnagle recessed the anchor heads into the rock face as shown on Figure 24. Figure 25 shows the completed project. Although the anchor locations are evident in Figure 25, as the grout has set, it blends with the rock color making the anchor locations imperceptible to those viewing the gorge face.

Figure 24 Recessed Anchors in Overhang Area

Figure 25 – Completed Project

Paper Authors:

Michael J. Mann, P.E.
Project Engineer
McMahon & Mann Consulting Engineers, P.C.
2495 Main St., Suite 432
Buffalo, New York 14214
(716) 834-8932
mmann@mmce.net

Mr. Ken Wojtkowski, P.E.
TVGA Consultants
One Thousand Maple Road
Elma, New York 14059-9530
(716) 655-8842
kwojtkowski@tvga.com

Mr. Donald Owens
Earth Dimensions, Inc.
1091 Jamison Rd.
Elma, NY 14059
(716) 655-1717
edi@earthdimensions.com

Mr. David Herring
Capital Facilities Regional Manager 1
OPRHP
1 Letchworth State Park
Castile, New York 14427
(585) 493-3602
david.herring@oprhp.state.ny.us

6.3

ROCK SLOPE STABILIZATION USING SPIDER SYSTEM

Joseph C. Bigger
Geobrugg North America, LLC
New London, Connecticut 06357 USA
Telephone: 860-442-9945
Email: joseph.bigger@geobrugg.com

ABSTRACT

The technique of stabilizing rock formations or blocks using cable lashing or nets with rock bolts has been used for a number of years. Geobrugg developed the TECCO Slope Stabilization System using the Ruvolum Dimensioning Program to stabilize soil and highly weathered rock slopes. The recent development of the SPIDER System using the Ruvolum Rock Dimensioning Program to stabilize rock slopes is another tool for engineers and designers to use. The program allows the user to analyze sliding and toppling mechanisms and based on Mohr-Coulomb Equilibrium theory it establishes the relationship between driving and stabilizing forces. The result is the number of required anchors and their relative positions is optimized. The design concept was modeled and tested to verify the program. The system has been successfully used for several applications to hold blocks or overhanging rock in place in Europe and Asia.

BACKGROUND

Over the years, conventional solutions were developed and used to hold rock ledges, rock

overhangs or individual loose rock areas in place and they include:

- Anchor beams

- Shotcrete

- Wire rope nets

- Wire rope nets with rope restraints

The various conventional solutions are outlined in the following paragraphs:

1) Anchor beams

This method often required comprehensive, difficult and intensive construction to place

anchor beams directly on the rock slope. This often required closing roads or highways

during construction. The installed anchor beams were highly visibility and did not

enhance the natural scenery of the slope.

2) Shotcrete

In order to achieve sufficient stiffness, the supporting nails or anchors are in a tight grid

and the shotcrete needs to have a minimum thickness. The combination of anchors on a

tight grid and thick layer of shotcrete make the solution expensive. Plus, shotcrete is

often not very aesthetically pleasing and it can be damaged by water and weather which leads to chipped and cracked surfaces.

3) Wire rope nets

In the past, wire rope nets were often used with rock bolts or anchors. Due to the given geometry of the square or rectangular nets, the nail grid was inflexible and it did not adapt well to the local rock shapes or configurations. It was not possible to optimize the installation. A further disadvantage is that each individual net panel can only cover a few square meters and to connect the nets together to cover a larger area was time consuming. Wire net ropes are generally made using 5/16-inch diameter, 7x7 construction, wire rope and the individual wires have a diameter of ≤ 1.0 mm. The result is a smaller amount of zinc galvanizing and reduced life expectancy of the rope.

4) Wire rope nets and rope restraints

The addition of wire ropes with wire rope nets has only have a limited effect on improving system capabilities. Because the components are not coordinated, the stability of each utilized part is not equally distributed. Also, adequate protective methods can be difficult to dimension. This is especially problematic for rock areas with irregular surfaces. Ropes can only work locally. Over time the rope tension is reduced which impacts the protection level.

TECCO® SLOPE STABILIZATION SYSTEM

Several years ago, Geobrugg developed TECCO® Mesh which is a high-tensile steel wire mesh featuring elongated diamond shape openings. The mesh provides the strength of a wire rope net and it easier to handle. This innovation has opened up new possibilities including:

• nail pattern optimized to meet the local conditions (slope, ground, topography)

• offsetting of nails in horizontal rows to avoid the crossing of pathways in the slope line

• tensioning of the system against the ground using spike plates

In the process of development it became clear that the transmission of force to the nails or anchors played an important role in improving the bearing resistance of the slope stabilization system. Because of this, the further advancement of flexible slope stabilization systems required that spike plates be adapted and optimized in terms of size, geometrical layout and bending resistance.

THE SPIDER NET INNOVATION

The SPIDER® rock protection system was designed to secure rock slopes where the rock is not prone to decomposition or weathering, where the surface is irregular and where rocks that come loose tend to be large. There are currently two concepts regarding the potential risks and maintenance requirements:

• Concept (I): If the critical area is to be secured in a proactive manner and deformation and maintenance work is to be kept to a minimum, the solution is to utilize nailing in the critical area with a net cover system including spike plates. The type and arrangement of nails as well as its lengths are to be adapted to meet the requirements for static loads.

• Concept (II): Should it not be possible to drill through the critical areas or should the requirements regarding deformation and maintenance be less, the nails could be arranged around the critical area (e.g. around an unstable boulder). The protective measure in this instance is rather passive. Larger deformations must be anticipated should pieces of rocks or even a mass come loose under the protection of the net drapery. The concept is applied to limited areas only.

System Components

The innovative rock protection system has been developed by Geobrugg AG and consists of the following elements: SPIDER® net, nails, spike plates, shackles, boundary ropes, wire rope anchors and a secondary mesh (optional) as shown in Figure 1.

The SPIDER® net features an elongated diamond shaped mesh and the openings are 19.75 inches/500 mm x 11.5 inches/292 mm. The rope used to make the nets consists of (3) 0.157 inch/4mm diameter high-tensile strength galvanized wires twisted together. The wires have a tensile strength of at least 256,000 psi/1,770 N/mm2.

Similar to the TECCO® Mesh, the rope is first crisscrossed to form the spiral shape and then twisted together to form a net. The ends of the rope are knotted to one another to permit the full transmission of force to the adjoining panels. Protection from corrosion consists of a coating of 95% zinc and 5% aluminum. The net can also be made with stainless steel if exacting requirements concerning the protection from corrosion have to be met. The basic dimensions of the net rolls are 11.5 feet/3.5 meters x 65.6 feet/20 meters; one roll weighs approximately 418 pounds/190 kilograms.

Commercially available nails are used to fix the net cover which has to fulfill the static requirements. Plain or galvanized or epoxy coated nails can be used and grouted with at least 0.75 inches/20 mm of concrete gout or cement. With plain nail used for permanent protection, an allowance for corrosion of 0.157 inches/4.0 mm in reference to the nail diameter is often taken into account. Contrary to earlier cable net covers where so-called ear heads were utilized for fastening the cable nets to the nails, elongated diamond shaped spike plates are now used to simply tension the net against the rock. The shape, size and bending resistance of the plates have been optimized based on various puncturing and bending tests and adapted to the system requirements. For the connection of the net panels, 3/8 inch shackles are used normally. The result is the loss due to overlapping is kept to a minimum.

In order to achieve an ideal load transfer in adjoining areas and to reinforce the edges, boundary ropes, 1/2 inch/14 mm in diameter, are used all the way around and they are

attached to the wire rope anchors laterally. The boundary ropes can be pulled directly

through the mesh openings from the top, bottom or sides. Seam ropes or boundary

shackles or compression claws are not needed to attach the net to the boundary ropes.

The shackles may be fixed with glue to prevent possible vandalism. In the event of

overhangs, it may be wise to attach additional cables under the overhangs to optimize the
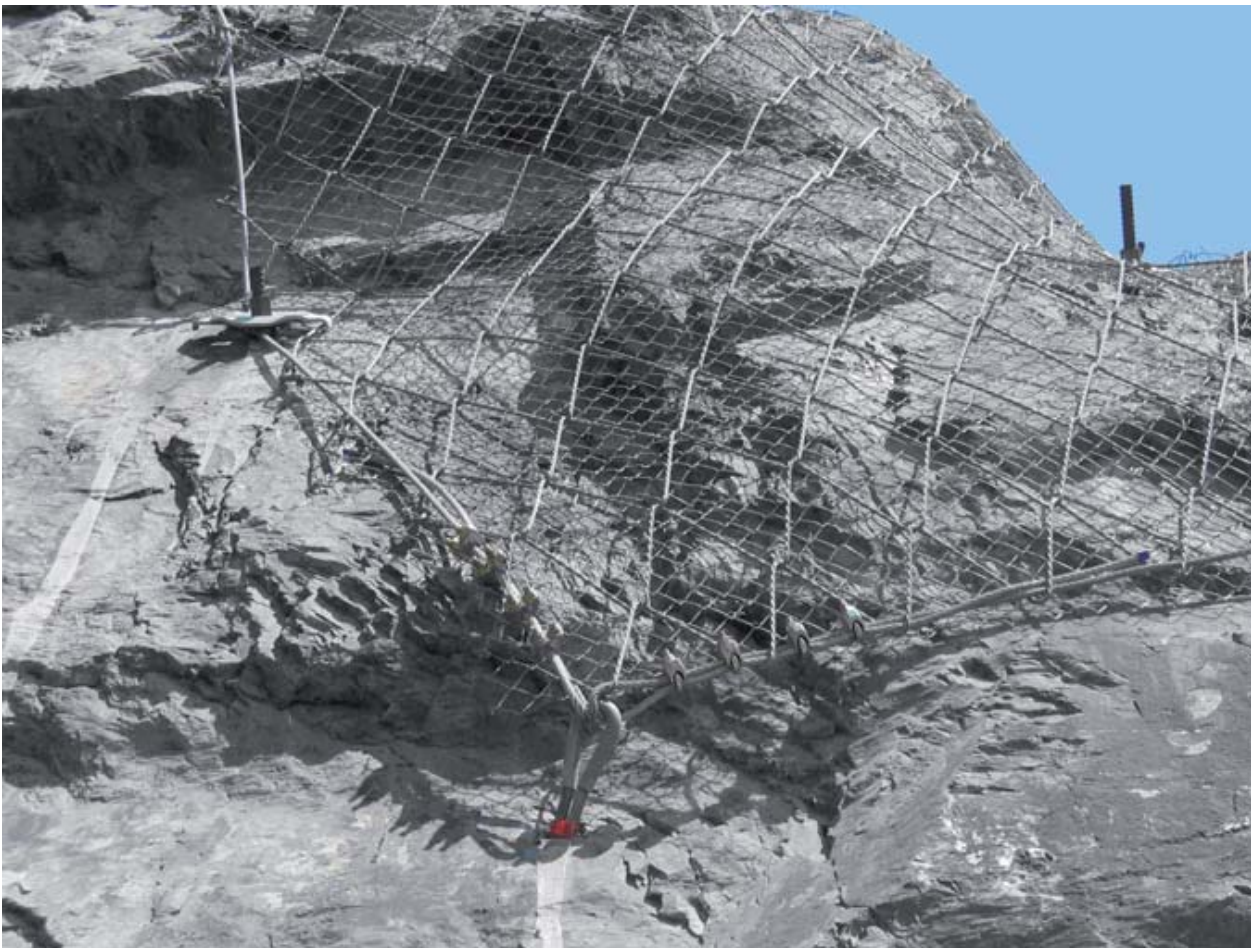
bearing behavior of the system.

Figure 1: SPIDER® Net Installation

As an option, a secondary steel wire mesh could be placed underneath the SPIDER® net if there is a risk of rocks coming loose that might fall through the mesh openings. Intermediate nails or pins can be provided to ensure the net is adequately pinned against the rock using a simple spike plate to do the job.

Design Approach

In order to secure an individual boulder, an external stabilizing force (P) is required to hold the boulder against the stable ground. This force depends predominantly on the following:

• dead weight (G) of the block-shaped boulder

• inclination of the sliding surface to horizontal (β)

• friction angle (φ) between the stable ground and the block

• cohesion (c) or interlocking force along the slide plane and its size (A)

• direction (ϑo) and (ϑu) of the forces (Zo) and (Zu) in the net cover
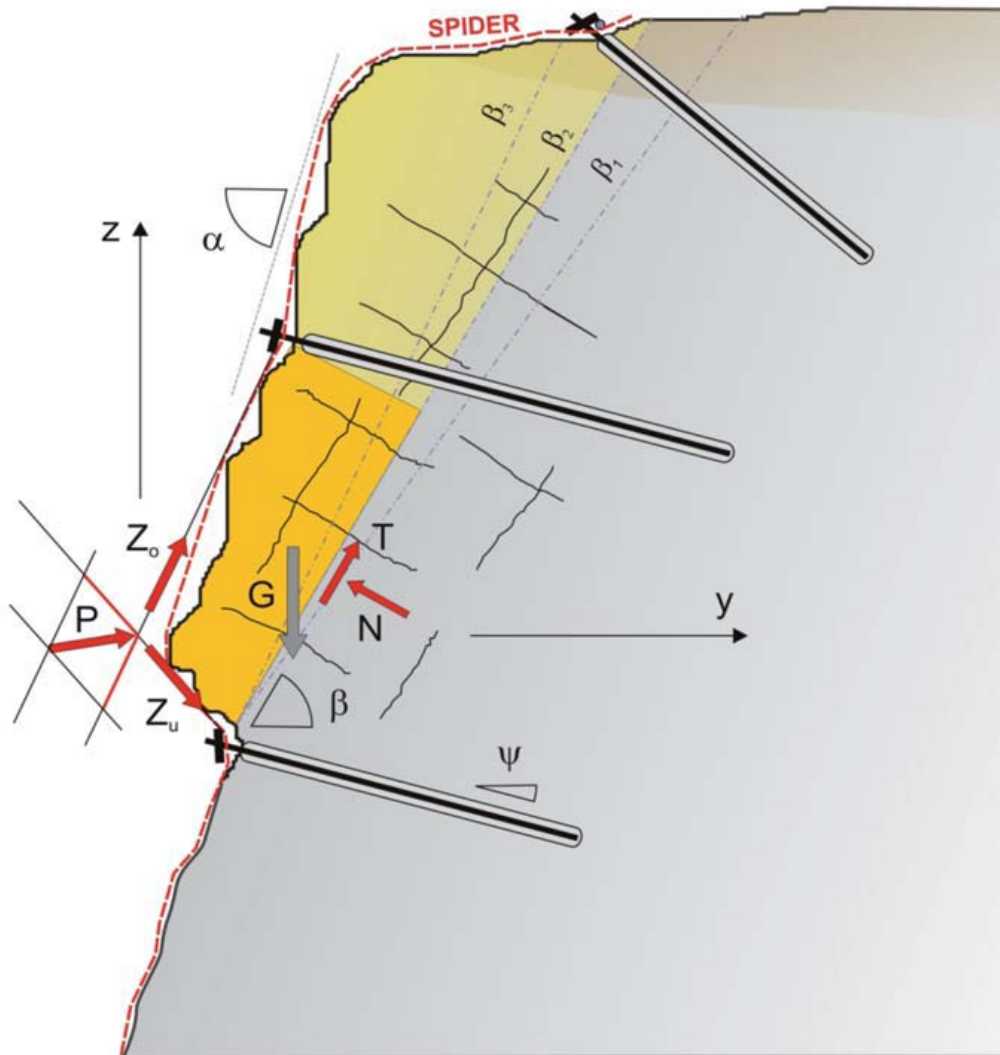
Figure 2: Retention Forces

The external stabilizing force (P) can be calculated as follows and takes into account the stabilization issues relevant to an individual block-shaped boulder as well as the model uncertainty correction value (γmod).

$$P \, [kN] = \quad \gamma mod \cdot \cos (\beta - \omega) + \sin (\beta - \omega) \cdot \tan\phi / G \cdot (\gamma mod \cdot \sin \beta - \cos \beta \cdot \tan\phi) - c \cdot A$$

The force (P) is a vector and can be applied in a two-dimensional model where it is divided into the vectors Zo and Zu. These are the forces which will be transferred from the net to the nails and into the stable subsurface. The direction (ω) of the force (P) to horizontal (upwards = positive) or the relation factor η, respectively, depends on various factors such as the interlocking action and/or friction between the surface of the block and the net restraint and the surface irregularities/roughness of the block as shown in figure 3a.
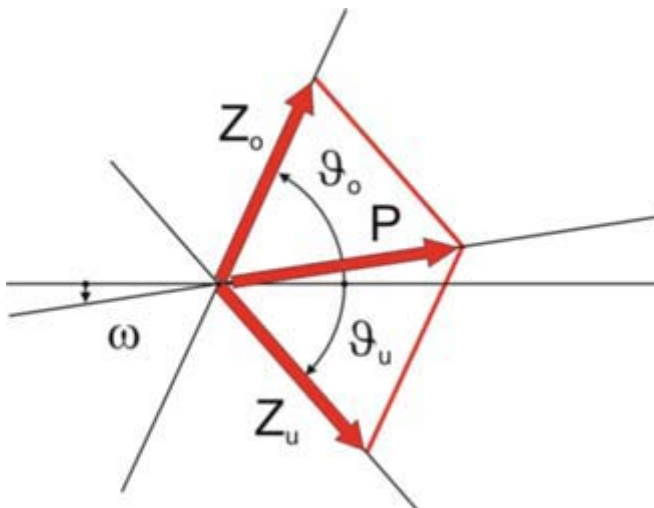
Figure 3a.

The stronger the interlocking action between the net cover and the boulder, the more favorable is the direction of action of the force (P) and the tensile force on the lower restraint is smaller. In general, the force at the lower restraint is always smaller than or equal to the force at the upper restraint as shown in figure 3b.
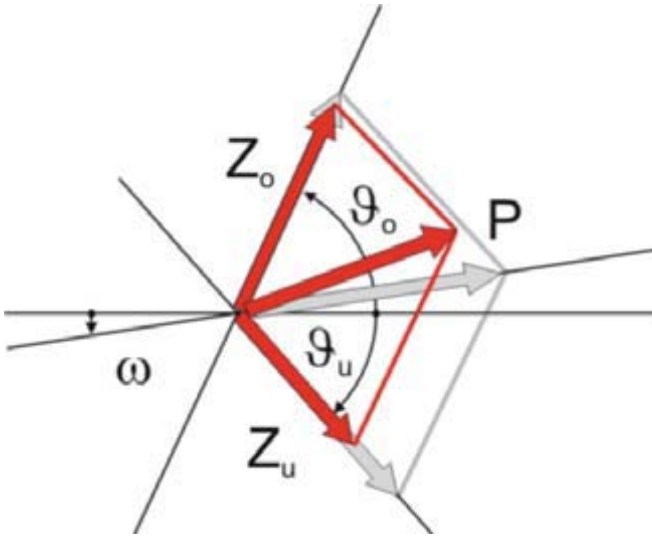
Figure 3b.

The forces (Zo) and (Zu) significantly depend on their orientation to each other. If the opening angle ($\vartheta = \vartheta o + \vartheta u$) tends towards 180 degress, the forces (Zo) and (Zu) tends theoretically towards infinite when keeping force (P) constant and not equal to 0. Figure 3c clarifies this. The result is the arrangement of the SPIDER net on the slope plays an important role in securing a boulder.
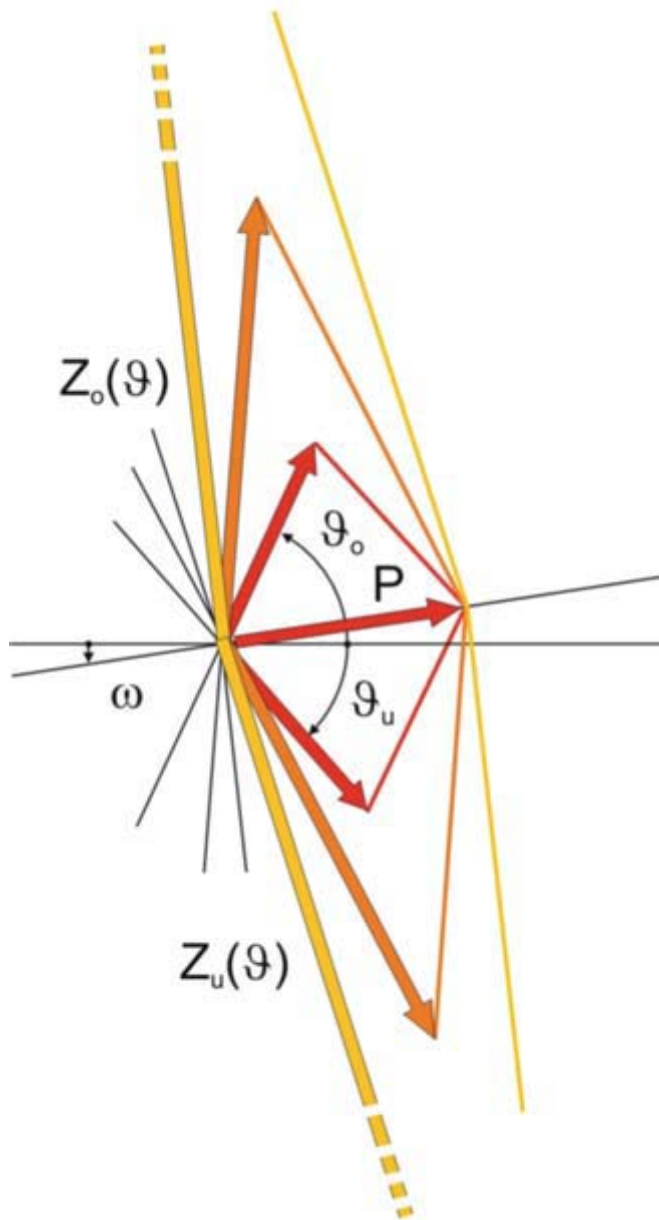
Figure 3c.

Since the SPIDER® protection system has a certain degree of elasticity, it is unavoidable for the boulder to be displaced along the slide face in the event of a failure. The stress on the restraint is reduced as a result of this boulder movement. The opening angle ($\vartheta = \vartheta o$

+ ϑu) becomes smaller with an increasing displacement and the upper and lower

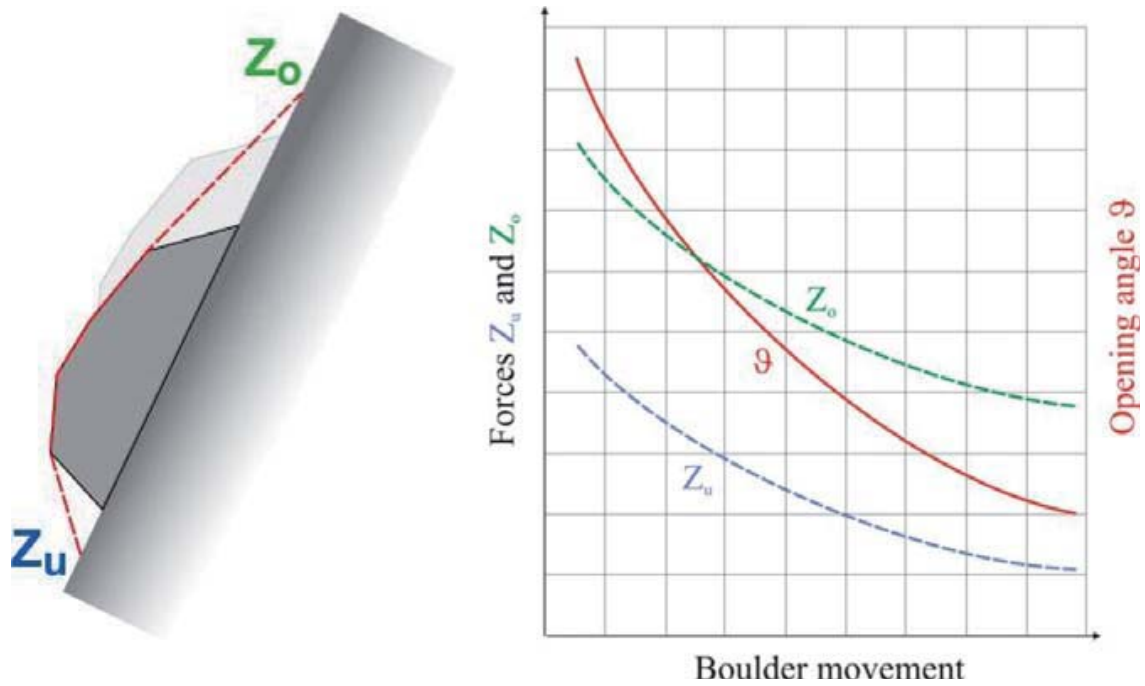retention forces consequently decrease. Figure 4 shows the qualitative presentation of the

parameter interdependence.

Figure 4: Parameter Interdependence

PROCEDURE FOR DIMENSIONING

In order to dimension the systems, the following input quantities have to be determined

through field investigation:

• Weight, geometrical dimension of the block-shaped boulder

• Inclination of the sliding surface (β)

• Shear parameters along the sliding surface (friction angle and possibly cohesion)

• Angle of the net restraint to horizontal (ϑo) on top of the boulder

• Angle of the net restraint to horizontal (ϑu) at the bottom of the boulder

• Angle of the lateral net restraint to horizontal (δ)

• Accelerations due to earthquake horizontal (εh) and vertical (εv)

Experiments conducted on models so far allow the following qualitative conclusions in terms of the distribution of forces. These conclusions will have to be refined by means of different anchorage arrangements and by utilizing different block-shaped boulders.

• The friction between the net and the block-shaped boulder can increase the calculated upper retention force by 10% - 20 % and reduce the lower retention force accordingly.

• The influence of the lateral retention forces may reduce the longitudinal retention forces by approx. 15% - 30 %.

• The lateral retention forces may exceed 50% of the upper retention force, depending on the arrangement and deflection of the net in the restrained section.

Ruvolum Rock Program

The program was originally developed for applications involving the TECCO Mesh G65. With the development of the SPIDER® net, the program was changed and will be available for use as an online application.

The first step is to determine the relevant input parameters for the slope or block and they are:

• Weight, geometrical dimension of the block-shaped boulder

• Inclination of the sliding surface (β)

• Shear parameters along the sliding surface (friction angle and possibly cohesion)

• Angle of the net restraint to horizontal (ϑ_o) on top of the boulder

• Angle of the net restraint to horizontal (ϑ_u) at the bottom of the boulder

• Angle of the lateral net restraint to horizontal (δ)

• Accelerations due to earthquake horizontal (ε_h) and vertical (ε_v)

When the program is opened there are preset input quantities already in place and the determined input quantities are entered in their place as shown in figure 5.

Figure 5: Program Input Quantities

As the input quantities are changed, a graphical presentation of the forces is shown and it shows the relationship between Pd, Zod, Zud and Sd as shown in figure 6.
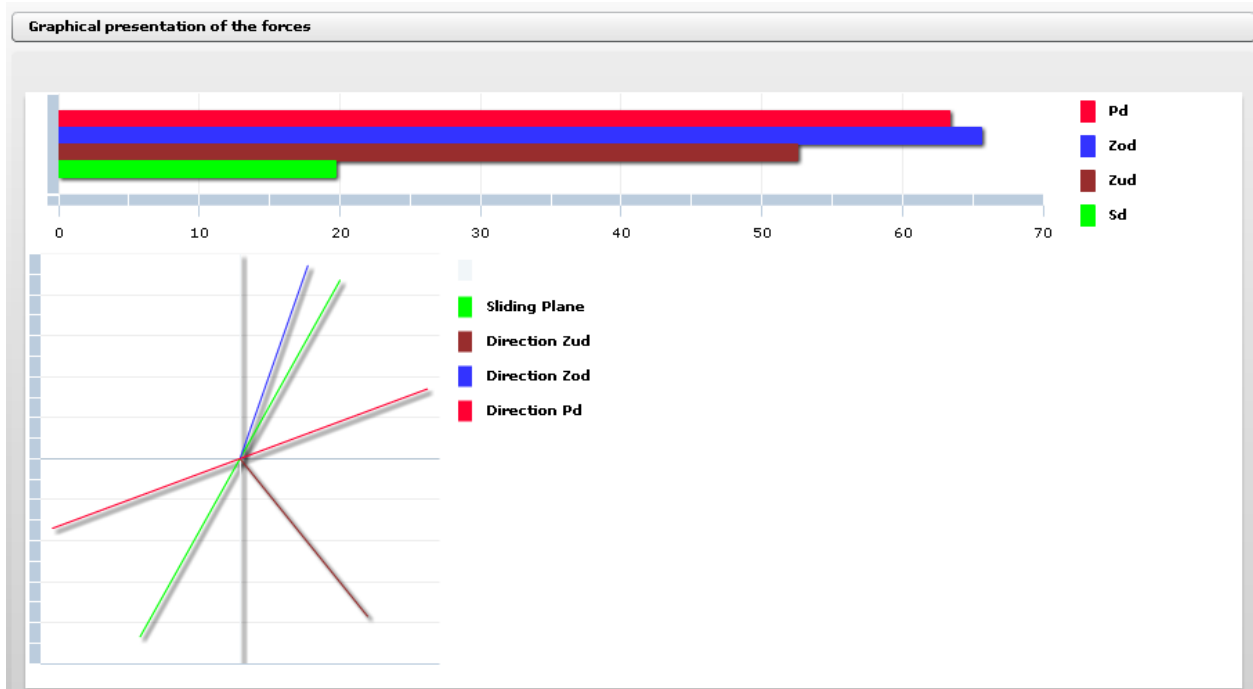

Figure 6: Graphical Presentation of Forces

Additional parameters change be changed and they include geotechnical parameters, safety factors, number of anchors, earthquake and water pressure acting on the block. In additional to balancing the load, a key consideration is to fulfill (1) Proofs of bearing resistance of the net and (2) Proofs of bearing safety of the nails. There are a total of 7 individual proofs that need to be fulfilled and they are listed below:

1.   Proof of local force transmission in the net to the top nails

2.   Proof of local force transmission in the net to the bottom nails

3.   Proof of local force transmission laterally in the net to the nails

4.   Proof of shear stress in nails at the top

5.   Proof of combined stress in the nails at the top

6.   Proof of shear stress in nails at the bottom

7.   Proof of combined stress in the nails at the bottom

The key is to optimize the anchors arrangement so all the forces are in equilibrium and forces at the anchors are not unbalanced.

CONCLUSION

The SPIDER® net along with the SPIDER® rock protection system was developed specifically for rock slopes where it is not practical to remove loose rock. The net is supplied in 11.5 feet/3.5 meter wide x 65.6 feet/20 meter long rolls which facilitates an

easier and faster installation. Plus, it is possible to optimize the net and anchors so the loads are balanced which was not possible using other techniques The Ruvloum Rock Dimensioning Program is a new tool designers and engineers can use to optimize their applications.

6.4

Terrain Reconnaissance at New York State

Department of Transportation

Douglas Hadjin
New York State Department of Transportation
50 Wolf Road
Albany, NY 12232
(518)-457-4728
dhadjin@dot.state.ny.us

ABSTRACT

Terrain reconnaisance (TR) for highway construction in New York State was initiated in 1947 by the New York State Department of Public Works (DPW). In 1956, the Interstate System was authorized by Congress, and for the next thirty plus years New York State was involved in major interstate highway construction. When the New York State Department of Transportation (NYSDOT) was organized in 1967, terrain reconnaissance was a well established and documented process and was utilized for all new highway alignments. Following completion of the interstate highways a period of little or no new highway construction ensued. Procedures and processes for producing terrain reconnaissance reports (TRRs) remained the same, concurrent with the loss of experienced personnel. Previously produced terrain reconnaissance reports for unconstructed, "shelved" projects were recycled for new projects in the same area without revision.

Following a recent landslide at a highway construction project, the FHWA reviewed NYSDOT's terrain reconnaissance procedures and made recommendations. Implementing these recommendations, and incorporating new Geographic Information Systems (GIS) based analysis, the NYSDOT has refined and improved its terrain reconnaissance procedures. This paper will give a brief history and the current practices for terrain reconnaissance at NYSDOT, its use, and its value to highway design.

GEOLOGIC HISTORY

New York State is composed of a great variety of bedrock ages and types: the Precambrian metamorphic rocks of the Adirondacks; Cambrian slates of the Lake Champlain Region; Silurian metasedimentary rocks of the Taconics; Devonian sedimentary rocks of the Catskill Delta; Triassic sandstones and diabase of the Palisades; and the Creataceous sands, silts and clays of Long Island. With the exception of a small part of Cattaraugus County south of Buffalo, the entire State was covered by continental glaciers. The glaciers were over a mile thick during the Pleistocene and greatly altered the geomorpology of New York landscape to its present day configuration. This includes such glacially produced features as the Finger Lakes, the classic drumlin fields of Weedsport, the gorges and waterfalls surrounding Ithaca, and the terminal moraines that formed Long Island.

HIGHWAY CONSTRUCTION HISTORY

New York State has some of the oldest highways in the country. "The Bronx River Parkway Reservation, in Westchester County, was the first public parkway designed explicitly for automobile use," in 1925. *(1)* Numerous parkways were constructed in Westchester County and on Long Island during this period. Robert Moses began his thirty nine year tenure with the Long Island State Park Commission in 1924 where he directed construction of parkways and bridges

into New York City.   In the 1950's construction of the New York State Thruway was financed by the sale of $972 million in bonds. The passage of the Federal-Aid Highway Act of 1956, led to the construction of major Interstates such as I-87(Northway); I-81; I-84; I-287 (Cross Westchester Expressway); and I-495 (Long Island Expressway). During this time, State funds were used to construct Route 17, Sunrise Highway and the extension of the Taconic Parkway. Today the New York State Department of Transportation maintains over 113,000 State and local highway miles and more than 16,000 bridges. *(2)*

Figure 1- N.Y. S. Thruway under Construction

DEVELOPMENT OF ENGINEERING SOIL MAPS

New York State DPW engineers realized that an understanding of the geologic history would be beneficial to highway design; however, they had almost exclusively relied on detailed boring information to develop soil and rock profiles. In 1948, Bulletin No. 13 of the Highway Research Board written by the Bureau of Soil Mechanics, (now the Geotechnical Engineering Bureau), documented the first formal attempt at classifying New York State soils into engineering groups

and creation of engineering soil maps to aid in the engineering of highways. The engineering

soil map was defined as: "a grouping of the soils on the basis of their deposition, parent

material, soil and rock profile, land form and drainage characteristics as these factors affect

highway problems". *(3)*

A total of twenty different depositional units were identified by the Bureau (4). The units were:

Table 1- Depositional Units	
1. Thick till	11. Esker deposits
2. Thin till	12. Old alluvial deposits
3. Variable till	13. Organic deposits
4. Bedrock	14. Alluvial fan deposits
5. Outwash deposits	15. Man-made fills
6. Kame field deposits	16. Windblown sands
7. Lacustrine bottom sediments	17. Marine bottom sediments
8. Delta deposits	18. Coastal plain sediments
9. Beach and bar deposits	19. Tidal marsh deposits
10. Recent alluvial deposits	20. Undifferentiated urban areas

PROCEDURE

The first step in any terrain reconnaissance effort is to research the available scientific literature related to the area. This includes geologic reports from the USGS and the New York State Geological Survey, available aerial photographs, and soils survey reports prepared by the USDA. "The pedological series boundaries and characteristics can usually be readily translated into areas of different geologic origins and, consequently, different soil characteristics."*(4)*

At the NYSDOT Bureau of Soil Mechanics, the development of these engineering soils maps was done using a team including an agronomist, a soils engineer, and a geologist. Each terrain reconnaissance report (TRR) included: an engineering soil map, a complete description of each depositional unit involved, and the general engineering significance of each depositional unit in tabular form. A field inspection to examine the topography, rock and soil conditions, vegetation and performance of existing highways and structures was conducted. The Bureau has always had the policy that a field inspection would be performed to evaluate and confirm all the aspects of the TRR.

USE OF ENGINEERING SOIL MAPS

The engineering soil map was used to evaluate the proposed highway alignments to design a highway "that will include the best utilization of soils in the area." This work was performed "during the early preliminary planning stages of design for a major project, for it is during these stages that adjustments in line and grade can most easily be made to adapt the route to the actual terrain conditions."*(4)*

This information would go to the district head and district Soils Engineer and a "line" conference would be held. The purpose of the line conference was to review preliminary alignments and profiles to select the best highway alignment based upon the terrain. The report would serve as a guide to indicate problem locations, suitable areas, and areas that required additional subsurface information.

I-87 THE ADIRONDACK NORTHWAY

The first major road construction projects in which the Department utilized the TRR were the Adirondack Northway I-87, Route 17 Expressway, and the NYS Thruway.   Two general alignments were proposed for a 100 mile stretch of the Adirondack Northway between Glens Falls and Keeseville (See Figure 2). The Bureau evaluated both routes for the relative costs associated with the earthwork.

One alignment was called the Adirondack Route, cutting through the mountains of the Adirondacks. The other route, the Champlain Route, was further to the east and traversed through the Hudson-Champlain Lowland Province. Following the creation of the generalized terrain class map, a cost factor was applied to each terrain class, based upon the costs associated with the construction of the then recently completed NYS Thruway. (The estimated earthwork costs per mile were averaged for each mapped depositional unit).. Despite what was first assumed, based upon the relative earthwork cost estimate for the mapped terrains, the Adirondack route was estimated to be 7% cheaper than the water-level route.   The Champlain route crossed large areas of highly sensitive marine clay deposits and major swamp and muck deposits. Based upon the construction cost estimates and the anticipated maintenance costs, the mountainous Adirondack Route was chosen.
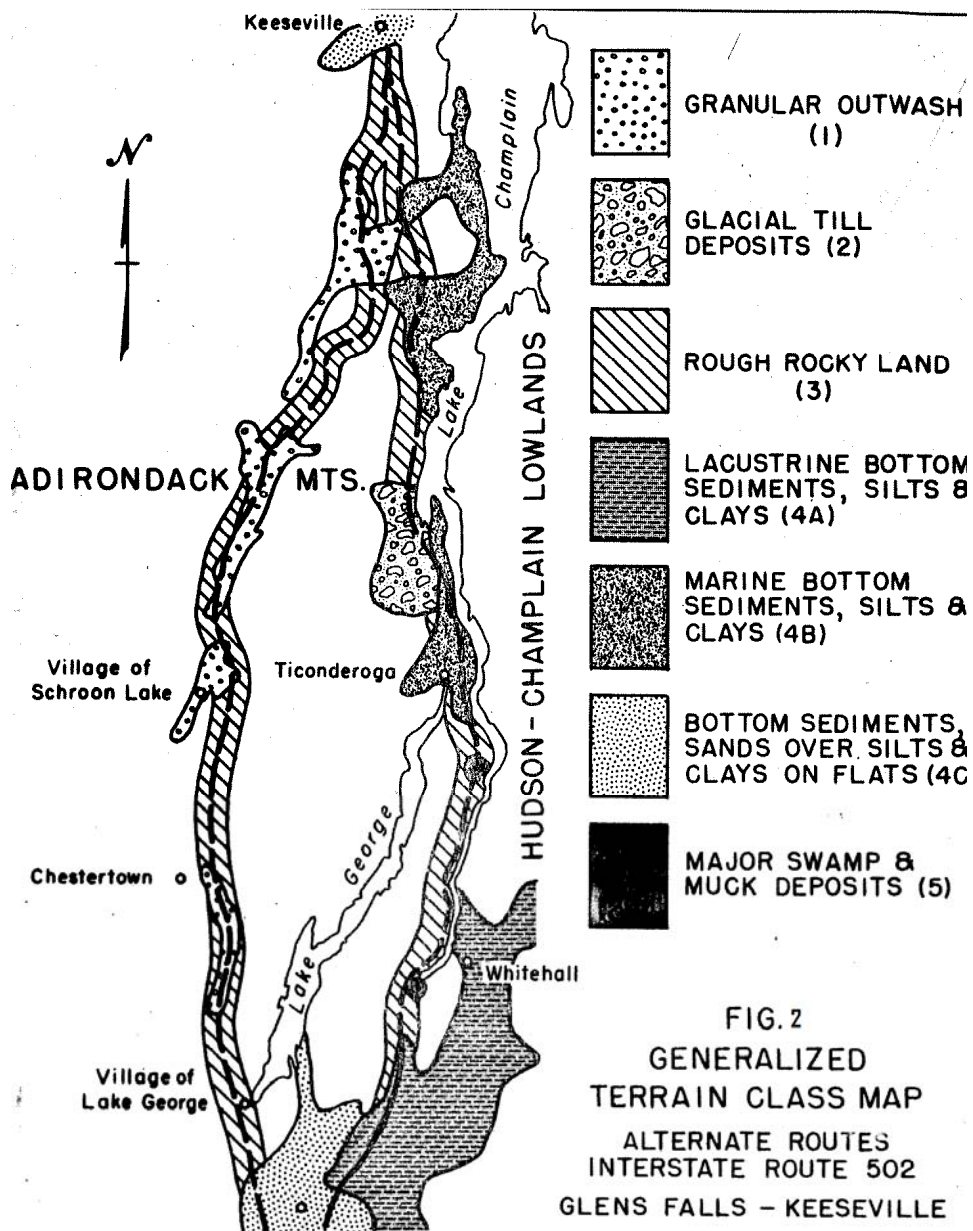
Figure 2- Route 502 (I-87) Terrain Map *(5)*

POST INTERSTATE CONSTRUCTION YEARS

Through the years the TRR became standardized in procedure and purpose for the Department. A TRR was also generated for major slope failures. In 1974 a comprehensive manual entitled: "Engineering Guide to Soil Series of New York" was written. *(6)* This manual became the definitive source for production of all the subsequent TRRs. Each soil unit mapped by the USDA soil survey in New York State is described in terms of its depositional unit, occurrence and topography, soil profile, drainage characteristics, and engineering properties. Terrain reconnaissance became a separate section of the Bureau. However over the years the TR section lost experienced personnel due to attrition. The emphasis on the depositional landforms or terrain features faded and the terrain map became a direct translation of the soil map to a terrain depositional unit. The background research, air photo interpretation and interdisciplinary team analysis skills were diminished due to lack of practice and experienced personnel, as no new major highways were constructed and TRRs were not developed for re-alignments and reconstruction projects.

The emphasis of the terrain report as being the essential factor in determining new alignments became secondary to other factors such as right of way and property acquisition costs, environmental considerations, and public input, as new alignments went through more populated and developed areas. Line conferences, to pick the best highway alignment based solely upon the terrain, were eliminated. Construction material resource reports and maps were eliminated as permits were required for sand and gravel mining. The computations of the

estimated earthwork costs were not considered as important since the above mentioned factors were frequently overriding.

As the emphasis and use of the TR for designing highways was decreasing, the scope of the reports was increasing (7). As of 1981 a checklist of suggested maps and tables included:

Table 2- Tables and Maps	
Generalized Terrain Unit Classification Table	Slope Map
General Earth Engineering Consideration Table	Bedrock Map
Soil Engineering Classification Map	Unconsolidated Aquifer Situation Map
Soil Erodibility Map	Climatological Data Chart
Soil Runoff Map	Flood Plain Map
Soil Wetness and Ponding Map	Stream Classification and Watershed Map
Wetland Food and Cover Map	Project Location Map
Hypsographic Map	Project Study Area Map

The time and effort required preparing these maps and the TRR by hand was extensive. The first use of Geographic Information Systems (GIS) for the construction of these maps was in 1991. The use of GIS for map generation greatly improved the accuracy, speed, appearance, continuity and consistency of the maps in the reports.   Since then GIS has been used extensively for

presentation as well as interpretation and analysis of all the data collected for a reconnaissance

report.

The Department produced TRRs at the initial design scoping and preliminary alignment stage.

Based upon the analysis of the TRR, a subsurface investigation program, that could include drill

holes, probes, and seismic refraction surveys was designed and data assembled by the Regional

Soils Engineer. This subsurface information would be used for final design of the highway.   As

the TRR was used for initial scoping only, a thorough review of the project and final geotechnical

reports was not performed even when large new construction projects were shelved for years

before contract lettings.

This was the case on the Scoby Hill Road was determined to be caused by a reactivation of a

previous landslide. In May 2008, at the recent State Route 219 (Section 5) reconstruction

project, where movement of the fill placed on a new alignment near Department's request, the

Federal Highway Administration (FHWA) led a review of their project development process and

evaluated whether a change in process could have identified the potential instability earlier and

possibly prevented the costs and complications associated with redesign.(*8*

FHWA EXECUTIVE SUMMARY-EXCERPTS

"The review team found that the project development process resulted in missed

opportunities to identify the Scoby Hill Road landslide hazard and discuss the associated

risk, especially with others outside the NYSDOT Geotechnical Engineering Bureau. The

missed opportunities are the use of engineering geologists in the terrain reconnaissance phase of project development and the use of geotechnical reports as a way to inform others of geohazards, risks, and ways to mitigate them… NYSDOT should routinely produce a comprehensive project geotechnical report. It is recommended by the Federal Highway Administration (FHWA) and is becoming a standard practice among State Departments of Transportation (DOTs) to produce a geotechnical report that brings together in a single document all the geologic and geotechnical information for a project, and discusses how that information impacts soil and rock stability, structures, roadway features and pavements." *(8)*

NYSDOT RESPONSE

Following the review process the GEB has revamped the TR team to include Engineering Geologists and added increased the focus on landforms and potential geohazards. In addition, previously prepared TRRs for projects that have not yet been constructed have been re-examined and new project geotechnical reports prepared. These efforts have included literature searches which are greatly enhanced by use of the Internet. GIS layers, including digital elevation models overlain by new orthophotos and soil survey polygons, have greatly added to the ease of identifying terrain features by enabling computer assisted 3-D analysis. The plotting and analysis of the project borings and other subsurface information can verify the mapping and identify potential problem areas. This data is all included in the appendix of the final project geotechnical report that is produced prior to final design phase. The project geotechnical reports provide a good review of the original TR with all the additional subsurface information such that the final road and bridge designs can be re-examined with all the terrain and subsurface information available.

GIS MAPPING

With GIS software, a large number of map layers can be simultaneously examined and evaluated. Many of these map layers are immediately available on the Internet or on the DOT servers with coverage of the entire State. The main soil polygon layer is generated for each county by the United States Department of Agriculture Natural Resources Conservation Service (NRCS). These polygons are generated from the "SSURGO" database (Soil Survey Geographic Database) and can be downloaded from the Soil Data Mart http://soildatamart.nrcs.usda.gov/. *(9)* Other Statewide geologic or environmental layers that are incorporated into a GIS terrain map include:

Table 3- GIS layer with Mapping Scale	
GIS Layer	**Mapping Scale**
Orthophotos- Natural Color, Infared, and B&W	2 foot to 0.5 foot per pixel
USGS plainimetric and topographic quadrangles and Digital Elevation Models (DEM's)s	1:24,000
Geologic bedrock , surficial and structural features	1:250,000
National Wetlands Inventory (NWI)	1:24,000
Linear, Areal, General and Floodplain Hydrography	1:24,000- 1:100,000
National Hydrography Dataset (NHD) Aquifers	1:100,000
New York Aquifers USGS	1:24,000

National Land Cover Dataset (NLCD)	30m pixel resolution
National Landslide Incidence and Susceptibility New York State Geological Survey Landslide Inventory	varies

MAPPING SUBSURFACE INFORMATION

NYSDOT has incorporated boreholes for highway design since its inception. Most locations have previous borings and since 1993 the borings have been entered into BLAP, (Boring Log Automation Program), a custom built MsAccess™ program (connected to GiNT™ for automated printing). Along with an extensive subsurface drilling program, the Bureau's Engineering Geology Section has conducted seismic refraction surveys to determine depth to bedrock. During the Interstate construction era, up to three seismic crews worked full time to determine bedrock depth for new highways.

Bedrock outcrop is mapped in the field using GPS receivers, then uploaded and converted into a GIS layer. New and old borings as well as the seismic data and bedrock outcrop are plotted onto the project map and can be analyzed in GIS. Using an extension for plotting boring stick diagrams in ArcGis™, the boring profile can be plotted and analyzed in 3D to aid in subsurface visualization.
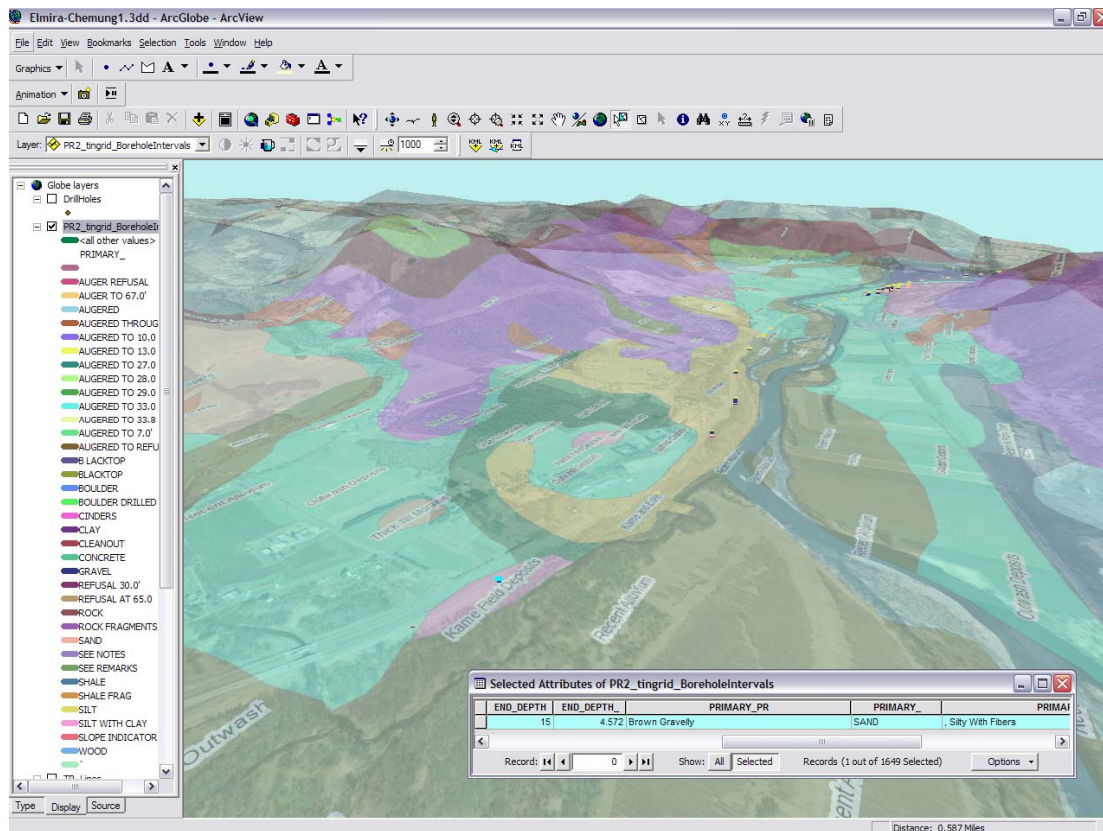
Figure 3- Screenshot of a 3D terrain with drill holes displayed in ArcGlobe ™-   The blue highlighted point is a drill hole with a brown gravelly sand layer to a depth of 15 ft depth, mapped in a kame deposit.

CONCLUSION

The focus of the TRR remains to be identifying landforms and earth conditions expected to be encountered during construction of new highways. The report is prepared early in the design phase of construction to aid in developing an alignment. Over the years, additional considerations have been given precedent in the final alignment decision process but the value of the TRR is still important to highlight potential problem areas and to refine the subsurface investigation program. Following a peer review of the GEB's procedures by FHWA, the GEB has

included engineering geologists on the TR team, and refocused the mapping to look at the geologic landforms and identify potential geohazards. The use of the internet for conducting a literature search and the use of GIS to for assembling a large quantity of high quality data and incorporate the data into maps and the report has greatly improved the TRR. Producing a final geotechnical report summarizes all the geotechnical data available and provides the most recent geotechnical data to the project designers.

REFERENCES:

1. *A Short History of the Origin and Development of The Public Works Concept in the State of New York* , New York State Department of Public Works, 1966.

2. History of New York State Department of Transportation and Interstate Construction: *Website.* New York State Department of Transportation, https://www.nysdot.gov/about-nysdot/history/, Accessed June 18, 2009.

3. Bennett, Earl F., McAlpin, George W., *An Engineering Grouping of New York State Soils, Highway Research Board Bulletin No. 13*, pp 55-65, 1948.

4. Hoffmann, William P., Fleckenstein, John B., *Terrain Reconnaissance and Mapping Methods in New York State,* Highway Research Board Bulletin*,* No. 299, pp 56-63, 1961.

5. Hoffmann, William P., Fleckenstein, John B., *The Comparison of General Routes by Terrain Appraisal Methods in New York State,* Highway Research Board Proceedings, No. 39, pp 640-649, 1960*.*

6. Fleckenstein, John B., *Engineering Guide to Soil Series of New York Volume I and II -* New York State Department of Transportation, Bureau 1974.

7. *Procedural Manual- Subsurface Exploration Section -Soil Survey and Mapping Unit*, New York State Department of Transportation, 1981.

8. Anderson, Scott A., Seil, Barry D., Lowell, Steve M., Process *and Peer Review of Route 219 (Section 5) Scoby Hill Road Landslide- New York State Department of Transportation,* Federal Highway Administration, July 2008.

9. Soil Data Mart*: Website.* United States Department of Agriculture-Natural Resource Conservation Service (NRCS)*.* http://soildatamart.nrcs.usda.gov/, Accessed June 23, 2009.

Disclaimer

Copyright Notice

THE USE OF TIME DOMAIN REFLECTOMETRY (TDR) TO MONITOR AN ACTIVE LANDSLIDE

S. D. NEELY, P.E. (TERRACON)[9]
A.M. VIEIRA, PH. D. (TERRACON) [10]

Abstract: The northernmost ½ mile of the 1999 realignment of SR 87 (approx. MP 224) has experienced slope and retaining wall failures that were initiated during the 2004/2005 winter storms. Subsequently, on March 21, 2008, a landslide closed SR 87. Arizona Department of Transportation (ADOT) addressed the 2008 landslide with an emergency remediation project, and is now evaluating the potential impacts of the recent and ancient landslide complex with an extensive investigation and monitoring program. The monitoring program consists of multiple Inclinometers, TDR cables and VWP. The TDR cables have been monitored with automatic data acquisition and data transfer. The monitoring system was also set up to alert multiple personnel once threshold values had been exceeded. Measurement of displacement using the TDR could be obtained for approximately 4 to 8 times greater displacements than were measured by the inclinometers. Results suggest the TDR can be used to determine rate of ground movement provided calibration curves are obtained for each location. The cost of the TDR system was very inexpensive when added to the inclinometer installation. Some of our lessons learned will be enumerated.

INTRODUCTION

A landslide occurred on March 21, 2008 that partially blocked the southbound lanes of

State Route 87 (SR-87). The landslide resulted from excavation activities associated with

---

[9] S. D. Neely, P.E.. Principal/Geotechnical Services
Manager Terracon Consultants, Inc.: Phoenix Office.
4685 S. Ash Avenue, Suite H-4, Tempe, AZ
85282.
[10] A. M. Vieira, Ph.D.. Staff Engineer
Terracon Consultants, Inc.: Phoenix Office.
4685 S. Ash Avenue, Suite H-4, Tempe, AZ
85282.

creating the highway through-cut for the re-alignment of SR-87. The Arizona

Department of Transportation (ADOT) contracted with AECOM to conduct explorations

and perform engineering analyses to develop mitigation measures relative to the

landslide. The Arizona Department of Transportation also contracted with Terracon to

perform measurements of the landslide area using Time Domain Reflectometry (TDR) to

supplement inclinometer and vibrating wire piezometer (VWP) data collected during the

on-site monitoring program. The TDR monitoring system also included a telemetry

station with an automated alert system that contacted ADOT and Terracon personnel

when threshold values were exceeded.

This paper will describe the geology comprising the SR-87 landslide, the TDR

equipment, the technology of TDR, the analyses and interpretation of the data, and

present a comparison of TDR data with that of inclinometer data obtained from the same

boring locations.

PROJECT DESCRIPTION

The material used to describe the landslide and surrounding geology was provided by

AECOM [11] in their initial report to ADOT.

Landslide: For purposes of mapping landslide units, the paleoslide and recent slides are

each given the same unit name, Qls, regardless of age of first sliding. In this paper

---

[11] AECOM
2777 East Camelback Road, Suite 200
Phoenix, AZ 85016.

"ancient" or "paleo-" refers to the large ancient slide and "recent" or "March 2008 slide" refers to the smaller slide that occurred on March 21, 2008, and failed into the roadway resulting in the temporary road closures.

The ancient slide occurs as a subtle landform mainly unrecognizable to the layperson and subtle enough to be overlooked even by some professional geologists. Slides of this size and scale are rarely encountered in Arizona. However, it is not uncommon in general for ancient slides in similarly soft sedimentary rock to go unnoticed and unmapped on regional geologic maps. To the untrained eye, this paleoslide is relatively indistinguishable from the surrounding hilly and mountainous terrain.

The following aerial photograph depicts the relationship of the landslide and the SR87 highway cut passing through it, and covers the overall geomorphic character of the slide mass.

Figure 1: May 2008 Aerial Stereo Photo Pair Showing Current SR 87 Alignment and the Ancient Landslide Extending from Bottom Left to Upper Right of Photo

The geomorphic characteristics of the large paleoslide, as previously stated, are subtle. From the clearly demarcated headscarp in the southern portion of the picture one can observe the blocky nature of the slide mass. The upper portion of the slide mass appears to consist of relatively coherent rock blocks translated and rafted downward northeast in the main direction of sliding. Back rotation of these blocks on the upper portion of the slide mass has created sag basins, or grabens, resulting in closed depressions that seasonally collect and pond water after heavy precipitation events. Some conspicuous drainages were also observed in this area, where the break in slope at the top of the slide mass meets the lower edge of the headscarp, and are suspected to be tension or other landslide related ground cracks.

The stability of the ancient slide is presently being monitored.   From a perspective of gross stability, based on months of monitoring and observations, the ancient paleoslide appears to be dormant. However, localized areas of the highway through cut near the northbound (NB) and southbound (SB) walls have begun to show some slow creep-type movement (an approximate rate of ⅛ inch per year). Yet, no indications of movement have been observed in the slope inclinometers or TDR cable measurements that monitor deep within the upper central portion of the large paleoslide above (southwest) the roadway.

Geologic and Geotechnical Profile: The site area is predominated by minor basalt flows capping Miocene-age sedimentary rock. The sedimentary rock is generally characterized as a fining upwards basin fill sequence with thicknesses greater than 400 feet. The basin is underlain by a Foliated Paleozoic schist basement rock.

Qls, Landslide (Pleistocene-Holocene): – The landslide is composed of chaotic masses of rock that have been transported down and away from their bedrock source on the order of tens to hundreds of feet. The ancient landslide appears to have occurred entirely within the Tga unit primarily along shears in the bedded claystone in the upper Tga section, and includes boulders of units Tbp and Tbb. Movement is along a basal slide plane and along numerous internal breaks of great complexity. A maximum slide thickness of 237 feet has been observed in the drill core.

Tga, Gravel with arkosic matrix (Miocene) – The Tga unit is a major basin-filling unit at this locale and is a generally fining upwards fluvial sequence (and possibly lacustrine due to the fine-grained claystone and clayey siltstone facies). The unit Tga is the primary geologic unit involved in both the paleo and March 2008 landslides. The unit Tga is comprised of interstratified sandstone and claystone with minor discrete layers of low shear strength clayey siltstone (10 degree residual shear strength) prone to bedding plane failure and cut slope instability. Approximately the upper 200 feet (thickness varies) encountered in the drill core is comprised of translated and slightly tilted, relatively coherent blocks of weak sedimentary rock involved in the ancient slide, with approximately 80 to 100 feet of sandstone overlying approximately 100 to 110 feet of claystone with numerous slickensided, highly sheared zones of great complexity. Clast content in the sandstone member varies from about 10 percent to 50 percent. The material is moderately well-bedded; poorly to moderately sorted and generally poorly consolidated, but with local moderately indurated beds, becoming more indurated with depth. Throughout most of the map area this unit is the basal Tertiary unit resting directly on the Proterozoic basement.

Shear plane frequency observed in drill core decreases significantly below the elevation of the bottom of the interpreted ancient slide plane. Occasional shears (mostly high angle dip and rake) occur below the ancient slide and are interpreted to be an imprint of millions of years tectonic faulting preserved in the deeper more indurated sandstone member. Estimated thicknesses in the areas outside the landslide may be in excess of 450 feet.

Xasu, Schistose rocks, undivided – Wide variety of felsic schist, shale, siltstone, sandstone, conglomerate and minor mafic volcanic rocks, which exhibited grey to light purple in color as encountered in drill core. The schist unit forms the Paleozoic basement for the site area, and locally underlies the Tgm and Tga units separated by unconformity representing a billion and half years of missing rock record at this site, likely the result of regional uplift and erosion or non-deposition. The structure and stratigraphy of these greenschist facies metamorphic rocks are controversial among research geologists that study the early formation of the western North American continental crust. Less frequent occasional shears or faults observed in the drill core present at elevations well below the ancient slide within the schist are interpreted to be an imprint of many millions of years of tectonic faulting preserved in the upper weathered schist of the Paleozoic basement.

Monitoring System: The monitoring system for the landslide has consisted of the following:

- Inclinometers placed to depths of 30 to 400 feet;
- TDR cables placed to similar depths; and,
- Vibrating Wire Piezometers.

Most of the inclinometers were installed with TDR cables and the top of the cable was exposed within a vault. The research for this paper has focused on three specific Inclinometer/TDR locations, namely, B-25, B-30 and B-31. It should be noted that B-25 was installed in May 2008, as part of the immediate investigation after the March 2008

failure, and B-30 and B-31 were installed in September, approximately 4 months after B-25 during a separate exploration. The locations relative to the roadway and the recent landslide are shown on the following geologic map.
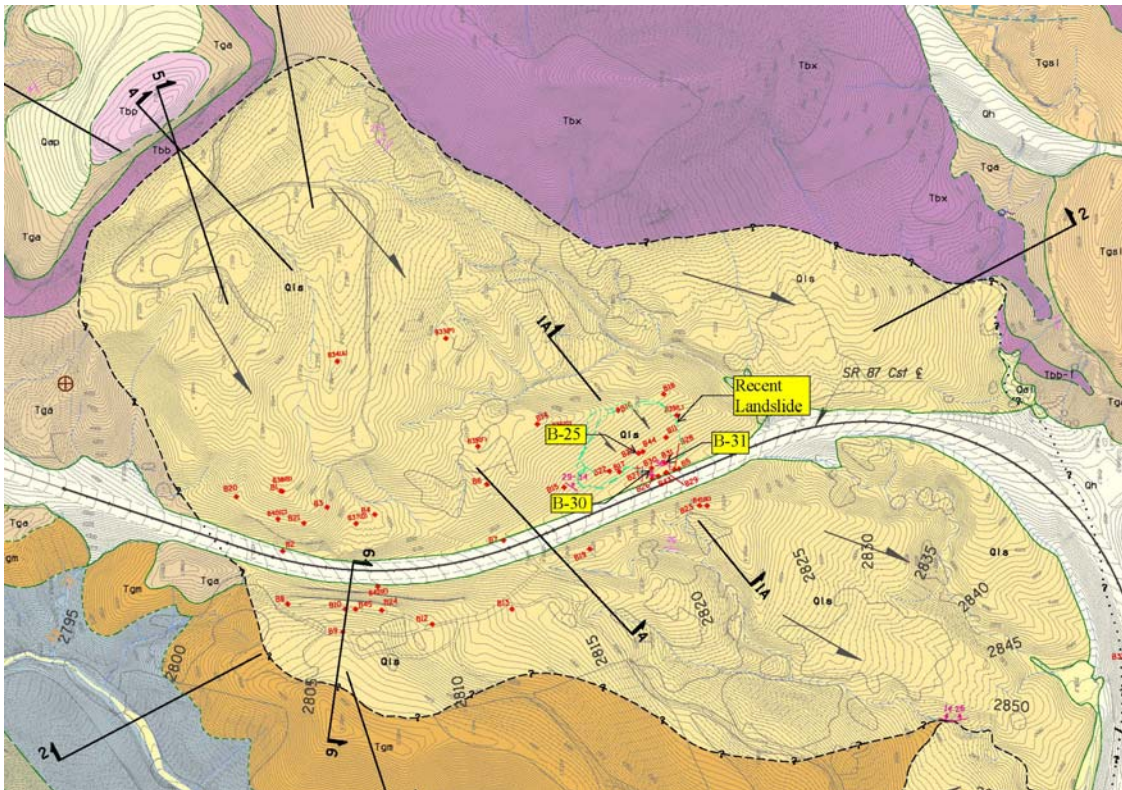
Figure 2: Geology Map showing locations of borings
(Original Scale 1:3600, North is to the Right, courtesy of AECOM)

Telemetry and TDR Equipment:

The TDR cables were installed when the inclinometers were constructed in May and September 2008. The cable type installed was a ½-inch diameter superflexible 50 ohm Foam Coaxial Cable, Heliax Coaxial Cable (FSJ4-50B), manufactured by Andrew Inc..

Cable connectors were installed that permit the TDR data reader to communicate with the coaxial cable. One connector was installed at each cable location.
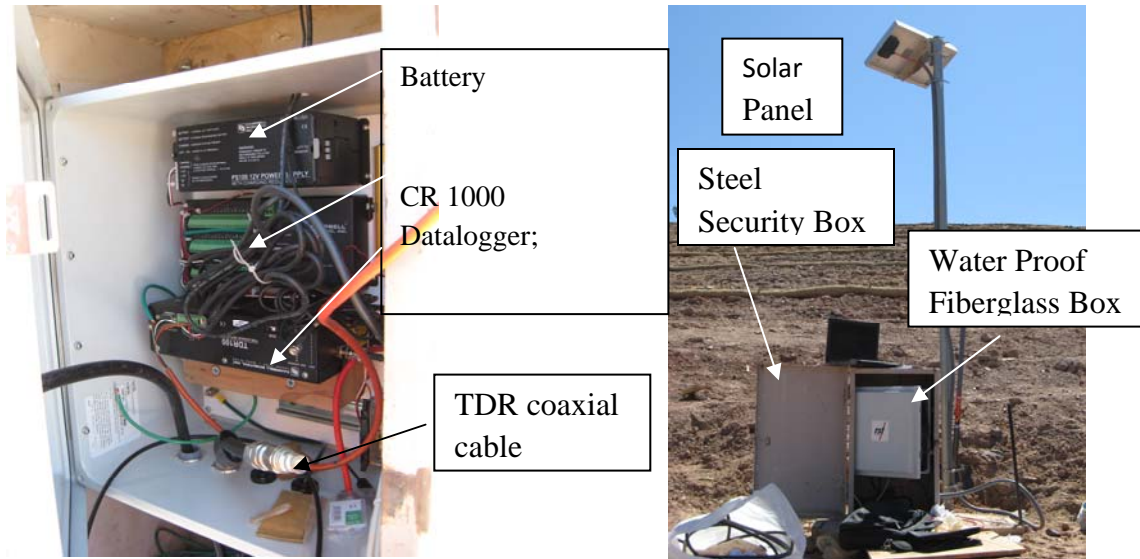

Figure 3: Equipment at the Telemetry Station

A telemetry station was constructed within 300 feet of the three TDR locations. The telemetry station consisted of a TDR 100 Pulser, CR1000 datalogger, multiplexer, cell phone, modem, battery, and solar panel. The equipment, except for the solar panel, was housed inside a water proof fiberglass box. This box was secured inside a steel box that was bolted to a concrete pad and locked on the outside.

The TDR data from boring B-25 was remotely collected and recorded once every hour. The data was retrieved and stored once a day on a central computer located in Terracon's Phoenix office. An alarm program was created that analyzed the data and trigger levels were adjusted based on the collected data. When the trigger levels were exceeded, an email message was sent to designated personnel (one person at ADOT, and two people at Terracon's Phoenix, Arizona office).

In addition to the telemetry station, a manual TDR cable fault locator was used during the monitoring program. The fault locator equipment used was a Riser Bond TDR model 1270A. This manual TDR was used to obtain the data for borings B-30 and B-31.

Technology of TDR: The TDR pulser generates an electric pulse that is propagated down the coaxial cable. A receiver records a signal reflection. Many pulses are read over time, which creates a scan that generates a waveform. The waveform shows the variation of signal amplitude with time. The signal amplitude can be normalized in the form of a reflection coefficient, which is a ratio of the signal amplitude sent down the cable compared with the signal amplitude measured at the receiver. The time delay between the pulse and the reflection, and the change in the signal amplitude (reflection coefficient) uniquely determine a cable fault. The cable fault location is determined by a relationship between the velocity of propagation of the signal, cable properties and time. A schematic drawing showing the key elements of the TDR system is presented on Figure 4.
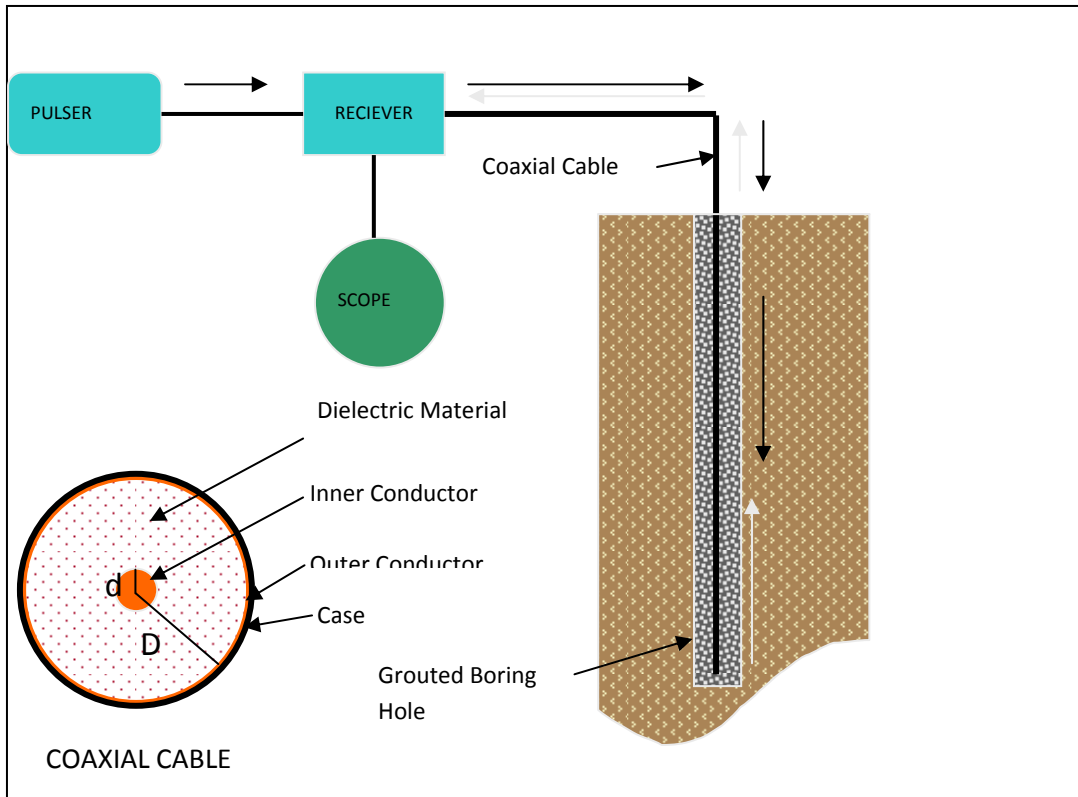
Figure 4: Schematic of Basic Physics

ANALYSES AND INTERPRETATION OF TDR RESULTS:

At each inclinometer/TDR location, cumulative displacement data with depth was plotted, as well as TDR data. The TDR data was plotted on a graph as reflection coefficient versus depth. The data for both plots have been plotted adjacent to each other for ease of comparison. Plots of the three locations are presented as Figures 5, 6, and 7.
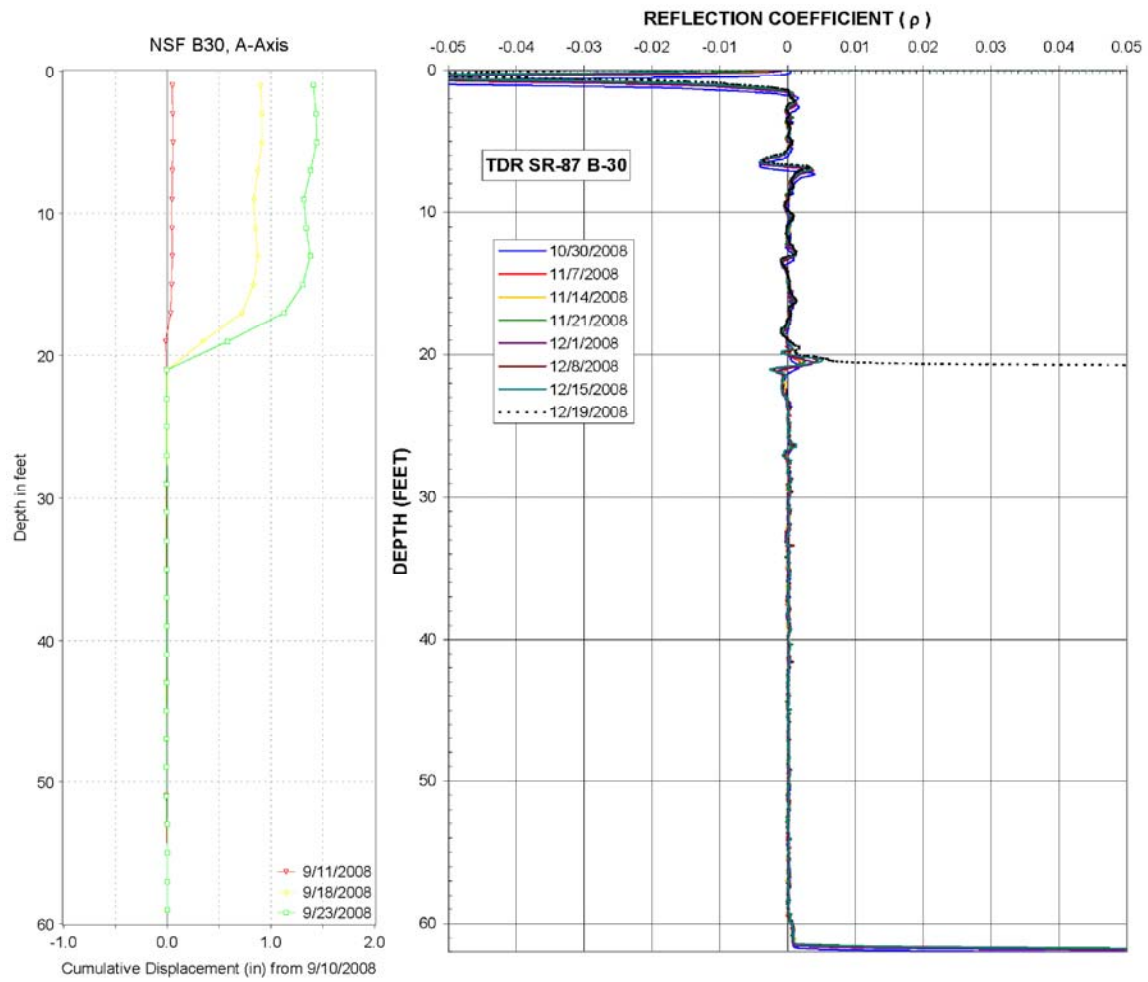
**Figure 5: Graph of Depth vs. Cumulative Displacement
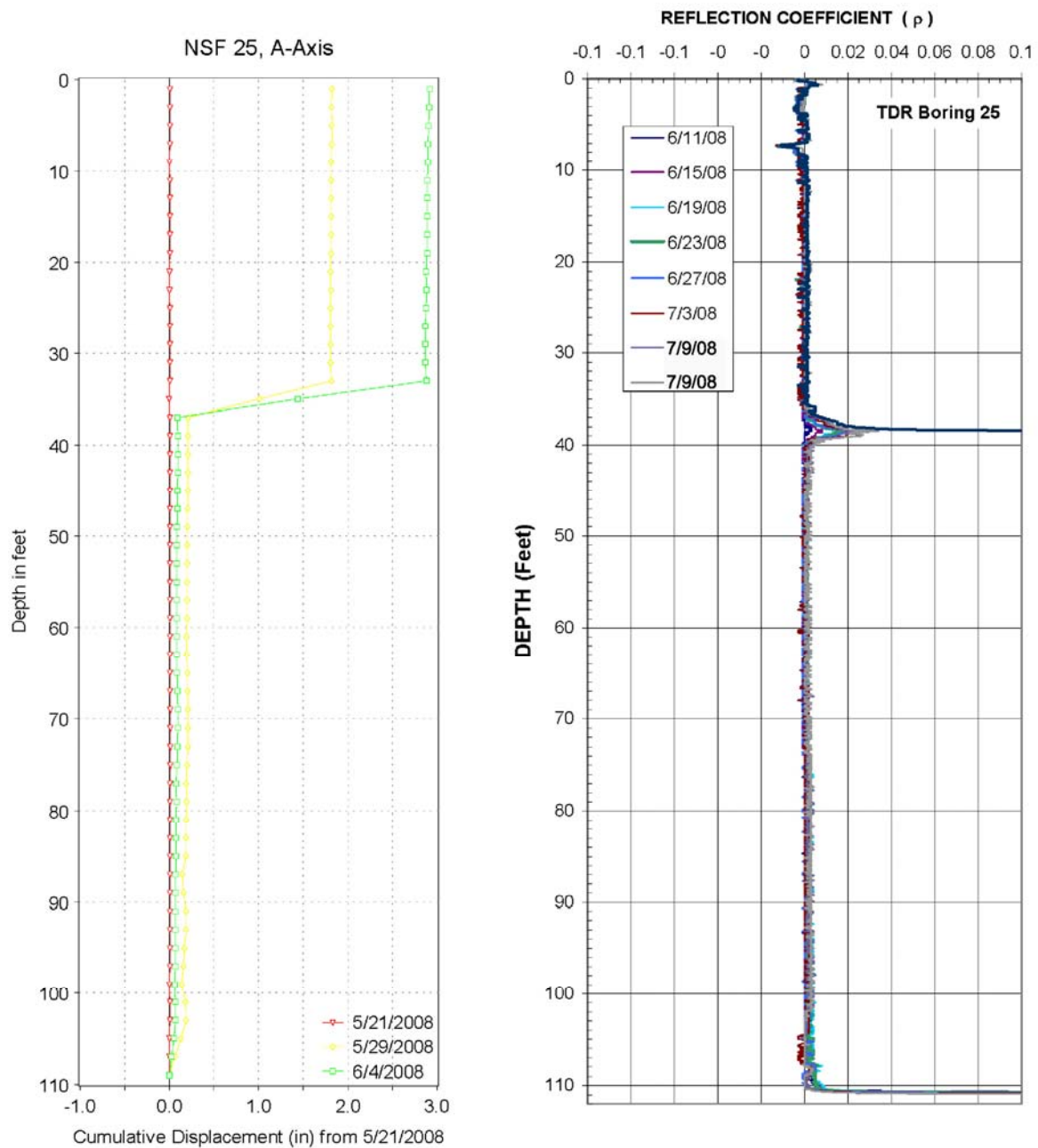and Depth vs. Reflection Coefficient for B-30**

Figure 6: Graph of Depth vs. Cumulative Displacement and Depth vs. Reflection Coefficient for B-25
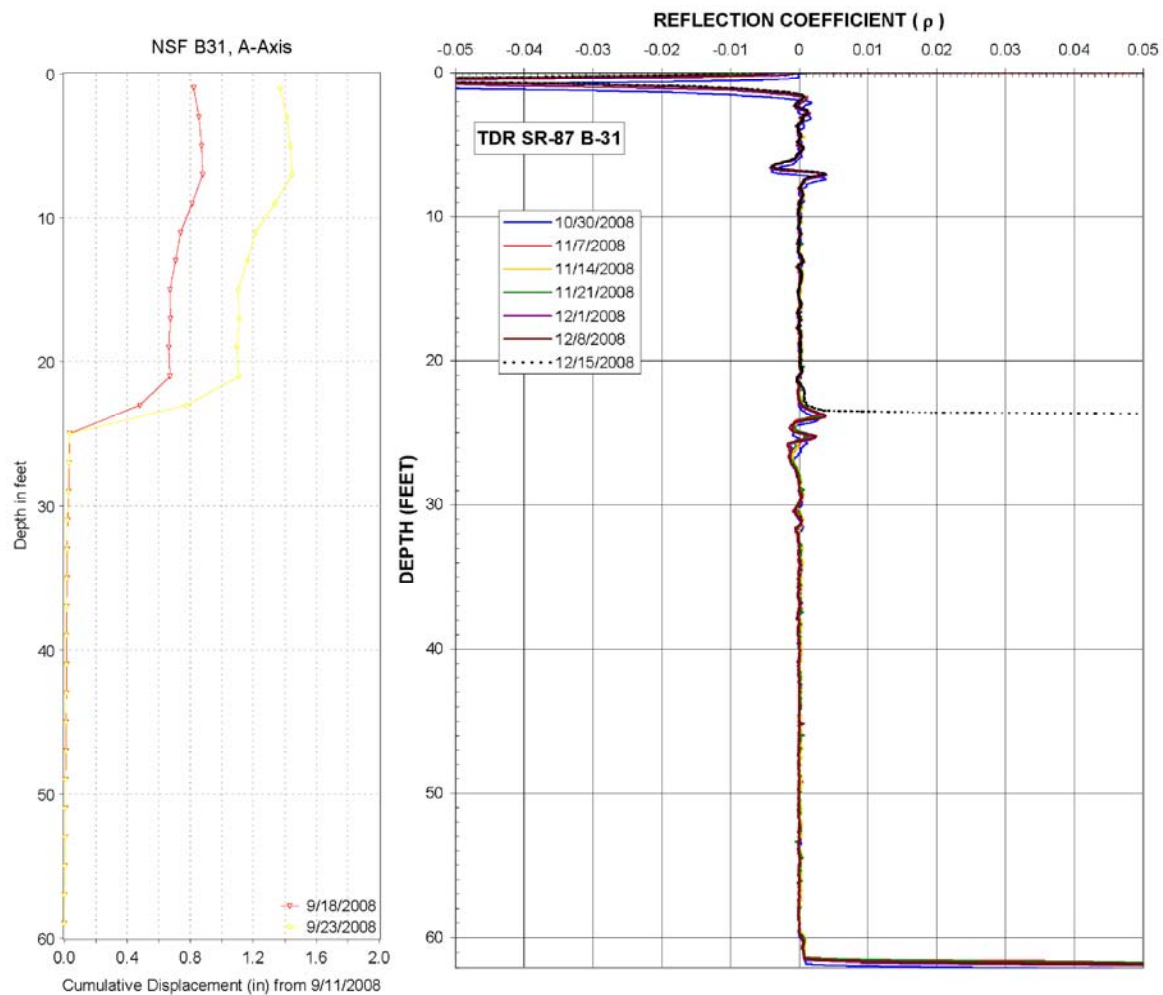
**Figure 7: Graph of Depth vs. Cumulative Displacement
and Depth vs. Reflection Coefficient for B-31**

Analyses: The TDR data portion of Figures 5 through 7 show development of spikes

with various amplitudes and at various depths. Each spike represents a potential

development of a shear plane at the depth shown. These spikes are caused by changes in

the reflection coefficient (cable impedance) and are directly related to the reflection

coefficient measured by the receiver. The reflection coefficient (cable impedance)

changes when there are changes in the cable dimensions, material property changes along

the cable system, or changes in material properties surrounding the cable. The following

is a list of potential causes of reflection coefficient (cable impedance) change:

- Connection between the lead cable and the ½-inch cable (material properties along the cable system),

- Noise during data collection (material properties along the cable system or surrounding materials),

- Cable damage during installation (cable dimension change), and

- Ground movement (cable dimension change).

The first spike observed on the graphs at the beginning of the plotted TDR data is caused by the connection between the lead cable and the main cable, and is generally of high amplitude. In general, subsequent spikes of low amplitude are caused by noise and minor cable damage occurring during cable installation. The resulting spikes from these two causes will not grow in amplitude with time. The fourth cause of spikes (i.e. ground movement) will show an increase in amplitude with time as the ground continues to move and subsequently reducing the cross sectional area of the coaxial cable. Spike amplitudes caused by ground movement can increase up to a point where the cable is sheared or pinched-off at the failure plane causing the ground movement.

Low and medium amplitude data caused by noise or dented cable can appear as a potential shear plane and may lead to incorrect conclusions by inexperienced end users. Careful, reproducible, methodology should be employed when collecting, downloading and reducing the TDR data. Depth errors may be caused by changes in the signal velocity of propagation in the cable, a change in cable reference, or interpretation error. It is important when reading TDR data to have the correct cable depth and if possible reference marks.

The reference marks are used to calibrate the TDR readings with the known distance between the marks. Usually the top of the TDR cable serves as the zero depth reference.

Data Interpretation: Based on the TDR data graphics, in each of the three locations, the high amplitude spike at the beginning of each cable is caused by changes in reflection coefficient (impedance) between the lead cable and the beginning of the ½-inch cable. The high amplitude spike shown at the end of the cable indicates a very high degree of reflection or near "infinite" impedance.

The data results for B-25 show various low amplitude (reflection coefficient, $\rho<0.004$) and high amplitude (reflection coefficient, $\rho>0.02$) spikes along the cable. Similar low and high amplitude spikes are observed on the graphs for B-30 and B-31.

At the B-25 TDR cable location, a high amplitude spike along the cable is shown on the figure. The high amplitude spike at a depth of 38 feet is a shear plane along which ground movement has occurred. This shear plane is in close agreement with the ground movement depth recorded by the B-25 inclinometer (approximate depth of 32 to 36 feet). The medium amplitude spike that occurs at a depth of approximately 7 feet, is assumed to be an indication of cable deformation during installation of the TDR. Note that the amplitude of this spike at 7 feet does not change with time.

Data Comparison: Figure No. 8 shows a graph of the cumulative displacement vs. time, and the reflection coefficient vs. time for each inclinometer/TDR location. The initial readings for B-25 and B-31 were removed to better define the slope of the line defining the rate of change of the reflection coefficient for these two locations.

The following are observations and analyses of the graphed data.

- The plot of cumulative displacement vs. time is linear for the three inclinometers. The time is of such a short duration due to the amount of movement occurring and the inability of the inclinometer to be used after nearly 3 inches of displacement had occurred. There was a potential to not retrieve the equipment below the shear plane depth if excessive movement, beyond the 3-inch displacement, had developed.

- The TDR reflection coefficient varies through time, but is generally linear. Statistically, the coefficient of determination (R^2) has values of 0.887, 0.978 and 0.998 indicating that representing the data as linear is reasonable. Other published data (e.g. O'Connor and Dowding, 1999) concurs with this linear behavior.

- The inclinometer data was obtained prior to acquiring of the initial TDR data. Because of the excessive casing deformation as mentioned before, the acquisition of inclinometer data ceased prior to collection of the initial TDR data.

- The rate of slope movement immediately after installation of the inclinometers would appear to be constant based on the cumulative displacement data. Based on this inclinometer data, one can conclude the rate of movement of the active landslide is constant in the area where the borings are located. Based on assuming a constant rate of slope movement and the rate of change for the reflection coefficient with time is also linear, the results strongly suggest the TDR could be used to

determine the total differential movement at the shear plane prior to shearing of the TDR cable.

■ Based on the inclinometer data presented in Figure 8, the rate of slope movement was constant over the small strains measured by the inclinometers. The TDR reflection coefficient data indicates the rate of slope movement/displacement continued to be constant. Measurement of displacement using the TDR could be obtained for approximately 4 to 8 times greater displacements than were measured by the inclinometer.
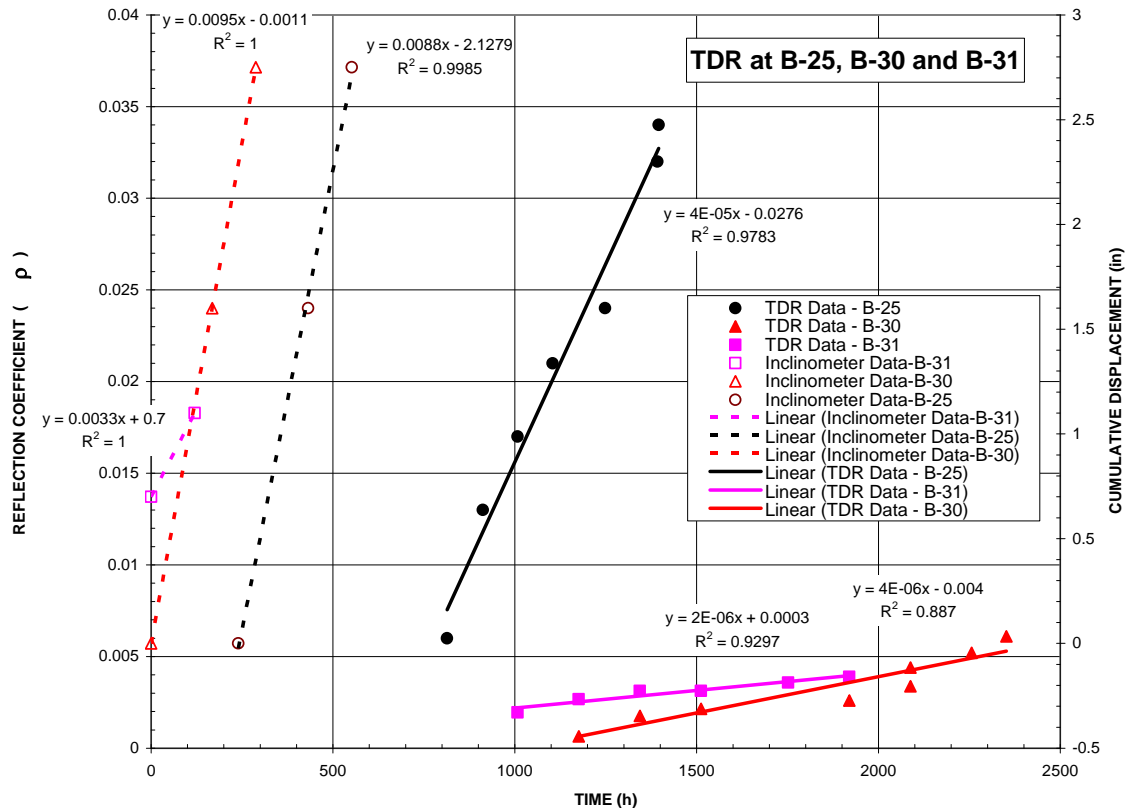

Figure 8: Graph of Cumulative Displacement vs. Time and Reflection Coefficient vs. Time for B-25, B-30 & B-31

Conclusions: Based on the results presented herein, the TDR reflection coefficient data indicates the rate slope movement/displacement continued to be constant. Measurement of displacement using the TDR could be obtained for approximately 4 to 8 times greater displacements than were measured by the inclinometer. Therefore, the cost-benefit of the borings can be prolonged by using a TDR system.

Based on this assumed constant rate and on the rate of change for the reflection coefficient with time is also linear, the results strongly suggest the TDR can be used to determine the rate of ground movement of the landslide at the TDR cable locations, provided calibration curves are obtained for each location. More inclinometers installed with TDR cables and simultaneous readings are needed to confirm the findings of this paper.

The use of TDR at very small strains is not sensitive enough to accurately quantify the amount of movement that is occurring. It is our opinion that this is due to the inclinometer casing, which acts as a tensile member immediately adjacent to the TDR cable.

Benefits of TDR monitoring:

- The TDR cable is capable of undergoing much greater deformation than an inclinometer, with a significantly reduced initial capital cost ($2.50/ft. installed for the TDR cable vs. $21.00/ft. installed for inclinometer casing). The potential loss of equipment is also removed since with the TDR method there is no equipment down the hole except for the cable.

This is a cost savings of approximately $5,000 per inclinometer probe should the probe be lost down the hole.

- The TDR remote monitoring system is a reliable system to identify and locate slope surface failure.

- It is easy to set up the telemetry system up for continuous monitoring at remote locations provided cell phone coverage is available. This allows for a reliable alarm system if properly installed.

- The telemetry system can also be used to monitor additional instrumentation such as VWP, inclinometers, extensometers, etc. The telemetry system will reduce numerous man hours in travel to and from the site and allows for continuous monitoring.

Short Comings of TDR Technology/Monitoring:

- The TDR requires calibration graphics, as shown on Figure 8, or historical data development in order to provide quantitative data.

- Requires careful analysis of data in order to identify and differentiate real shear from cable noise.

- The data is not distinctive with regard to direction of movement.

- Initial cost is high for telemetry equipment.

Lesson Learned:

- Grout strength and inclinometer casing can influence the deflection of the coaxial cable at very small strains, and the reflected signal in the TDR cable.

- Uniform crimps equally spaced along the cable during the cable installation assists immensely in determining the rate of wave propagation along the cable.

REFERENCES

O'Conner, Kevin M., Dowding, Charles H., 1999, "**GeoMeasurements by Pulsing TDR Cables and Probes**."CRC Press, Boca Raton, Florida, pp. 15-22.